Proceedings of the 6th ENIGMA Meeting

22 - 25 November 2005
Kinsale, Ireland

The European Network for the Investigation of Galactic nuclei through Multifrequency Analysis (ENIGMA)
is a Research Training Network funded within the FP5 program of the European Community

List of Talks

Niall Smith - Irish Team update
Alan Giltinan - L3CCD Performance Analysis
Dylan Loughnan - Fast, two-channel Photometer
Vladislavs Bezrukovs - High-frequency, multi-wavelength VLBI observations of BL Lac objects
Andreas Papageorgiou - VSOP polarization observation of 3C 380
Jochen Heidt - The OJ 287 polarization monitoring programme at Calar Alto
Ivan Agudo - NRAO 150: A powerful quasar hidden by the Milky Way
Denise Gabuzda - Surprising Correlations between the optical and VLBI Polarizations of Blazars
Mirko Tröller - Analysis of 22GHz and 37GHz observations
Krzyzstof Katarzynski - The cyclo-synchrotron process and particle heating through absorption of photons
Nektarios Vlahakis - Magnetic Driving of AGN Jets: Observational Implications
Jose Gracia - Hard TeV spectra of blazars and the constraints to the IR intergalactic background
Manolis Angelakis - The 6000-source survey
Stefan Wagner - Variations of the high energy cutoff in Blazars
Dimitris Emmanoulopoulos - MKN421 Final Chapter
Stefano Ciprini - OJ 287, PKS 2155-304, PKS 0735+178: Multifrequency Campaigns and Variability Monitoring
Luisa Ostorero - The colour of 0716+714 during the ENIGMA-WEBT core campaign
Uwe Bach - Structural variations in the jet of BL Lacertae and their effect on radio light curves
Claudia Raiteri - The WEBT campaign on 3C 454.3
Lars Fuhrmann - A rapid and dramatic outburst in Blazar 3C 454.3 during May 2005
Lucasz Stawarz - High Energy Emission in the jets of M87 and CenA
Nicola Marchili - Variability analysis of the IDV source 0954+658
Jochen Heidt - The QSO HE1013-2136 (z = 0.785): Tracing the ULRIG-QSO connection towards large look-back times?

Irish Team Update

Niall Smith

Cork Institute of Technology

Steps in the Data?

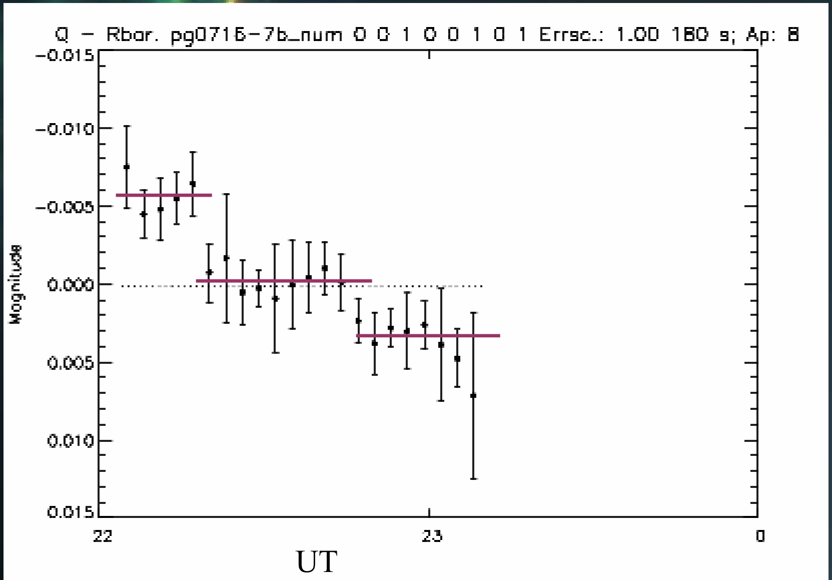

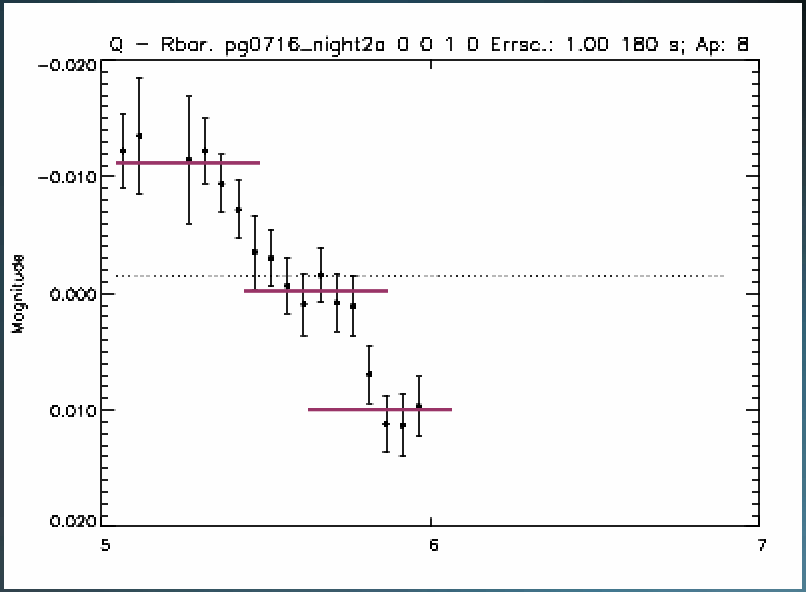

NO STATISTICALY SIGNIFICANT EVIDENCE FOR STEPS

Watcher

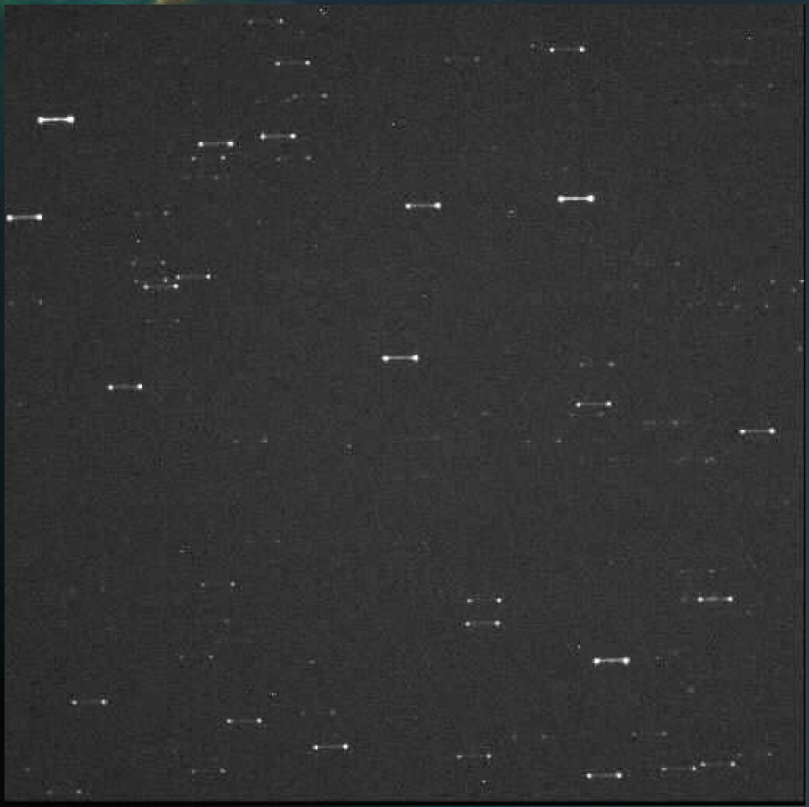

First Light

ENIGMA Paper

- E.M. Xilouris, I.E. Papadakis, P. Boumis, A. Dapergolas, J. Alikakos, J. Papamastorakis, N.Smith, and C.D. Goudis (astro-ph/0511130)
- Observed S5 2007+777 and 3C371 in the *B* and *I* bands for 13 and 8 nights, respectively, in 2001, 2002 and 2004.
- When the flux decays, we observe significant delays, with the *B* band flux decaying faster than the flux in the *I* band.
- As a result, we also observe significant, flux related spectral variations as well.
- The flux-spectral relation is rather complicated, with loop-like structures forming during the flux evolution.
- The presence of spectral variations imply that the observed variability is not caused by geometric effects.

Distributed Data Reduction Pipeline

"The network is the computer …" Sun Microsystems.

What we are trying to do…

Develop a fast, robust data reduction pipeline which utilises a distributed processing model.

How we are doing it …

Project is using rapid prototyping and development principles with development being undertaken in the Windows environment

•Development platform is MATLAB …

- Industry Standard
- Scripting – platform independent (Windows and Linux)
- *Toolboxes* to expand functionality – artificial intelligence/image processing/instrument control
- Code can be compiled (.exe)

Distributed Computing (Phase I)

Large numbers of images to process / sophisticated analysis / archiving

- •Uses dynamic allocation of resources – recipe concept
- •Recipe – describes the data reduction process, what images must be analysed, what routines will be applied and what nodes perform analysis.
- •Later will facilitate communication between nodes.
- •Recipes written in XML (communication over WWW possible)

I. Server Initialises by determining the Nodes involved, the Images to process & the Script to use.

II. Server divides work, creates XML “Recipes” + Sends to appropriate Nod

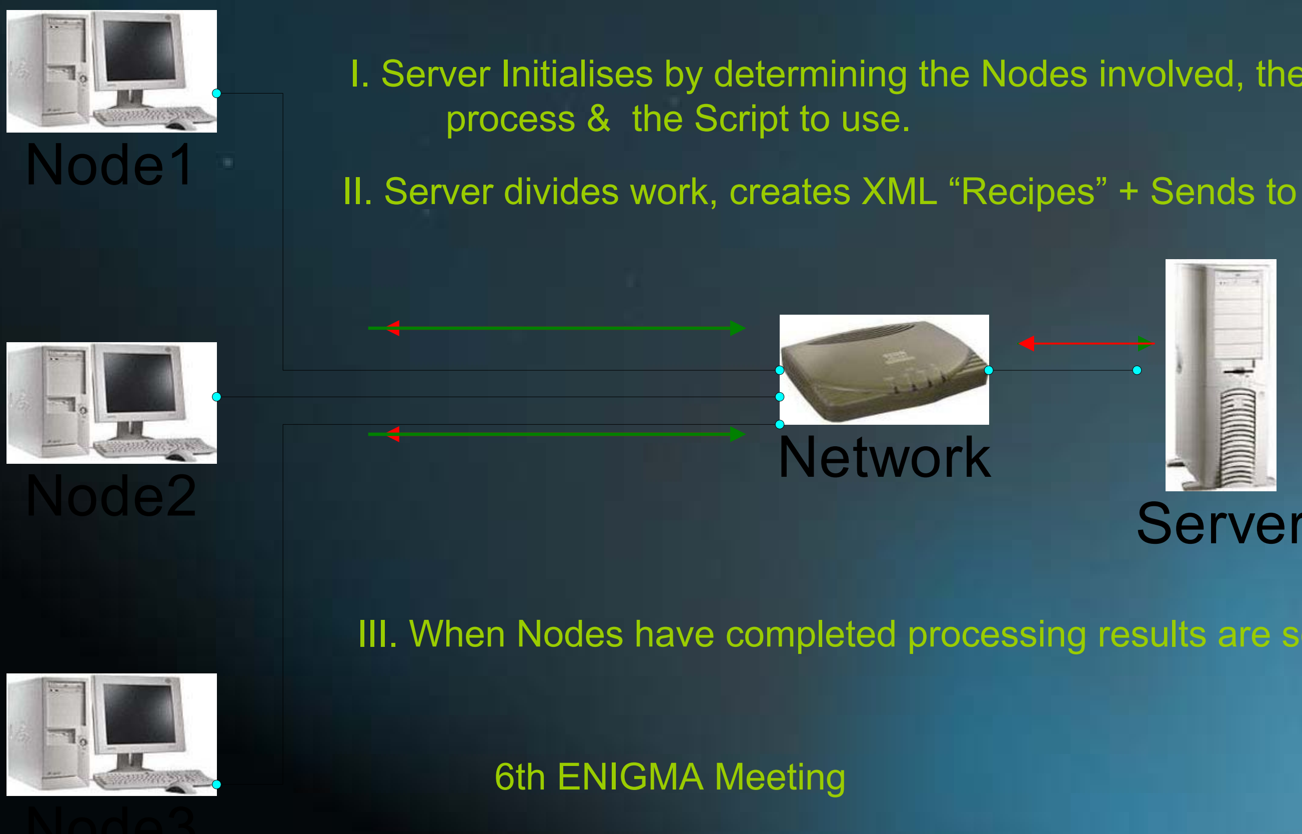

III. When Nodes have completed processing results are sent back to Serve

Near Future Development

Milestones

- Two Channel Fast Photometer – SFI Funded Project.
- 15th IEEE International Symposium on High Performance Distributed Computing, Paris, France.

Further Development

- Integration of artificial intelligence (AI) to process data.
  - Automatic Image Quality Determination.
  - Optimum Apertures.
  - Plate Solve.
- Communication with telescope to provide feedback.
- Further development of Distributed Computing to a true Peer-to-Peer System.

Blackrock Castle Robotic Observatory

Cork City Council

Cork Institute of Technology

History of Blackrock Castle

- Late 16th century the citizens of Cork appealed to Queen Elizabeth 1st to construct a fort at Blackrock to "repel pirates and other invaders".
- Castle was twice destroyed by fire (1722 and 1827).
- Subsequently used for many purposes including offices, a restaurant and as a private residence.
- The building was purchased by Cork Corporation in 2001 and refurbished.
- In 2004 the City Council agreed to our proposal to convert it to a Robotic Observatory and Astronomy Centre.

Castle Layout

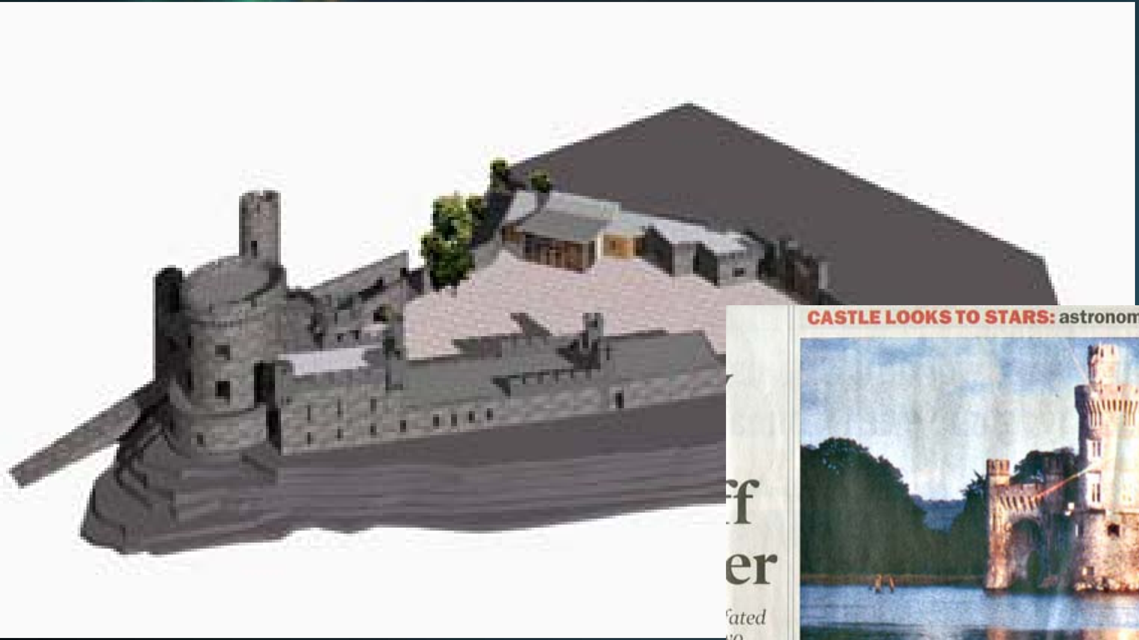

CASTLE LOOKS TO STARS: astronomy centre planned for Cork landmark

Blackrock Castle, Cork: city council to seek tenders for astronomy centre, restaurant and pub following €4 million restoration programme.

Castle restoration nearly complete

BARRY ROCHE,
SOUTHERN CORRESPONDENT

Work on the €4 million restoration of Blackrock Castle in Cork is nearing completion. Cork City Council has confirmed it is shortly to seek tenders for a franchise operator to run an astronomy centre and a restaurant and pub at the site.

The council has engaged specialists to advise on the most appropriate layout for an exhibition area in the castle which will feature the astronomy centre.

Blackrock Castle was originally built ... build a fort in Blackrock "to repel pirates and other invaders". It is on the southern side of the River Lee and is one of Cork's landmark buildings.

The current neo-Gothic building dates from about 1830.

After many years in private ownership it had lain idle for three years and had fallen into disrepair when Cork city councillors agreed to buy the castle.

The council paid £825,000 for the property and now, three years on, following extensive work by conservation architects Murray O'Laoire, the project is nearing ...

The castle will house a high-tech robotic observatory operated by Cork Institute of Technology. It will feature two high-power telescopes, an optical telescope which will be placed on the castle's top tower and a radio telescope which will be located over the gallery room.

A fully-equipped operations room will also be set up where experts can download and interpret the telescope data, while the observatory will be linked with other observatories around the world.

It is expected that the astronomy ... schools who will be able to visit the centre, as well as link up with the observatory through the internet.

Cork city manager Joe Gavin confirmed that Cork City Council has applied to the Department of Communications, Marine and Natural Resources for a foreshore licence to fill in an area near the castle to create a car park and amenity area.

He said there is an area of slobland there which the council hopes to develop as a car park and an amenity area so the Loughmahon Walk can be brought up to the castle. It is hoped that a boardwalk ...

Reviews

Access All Beckett season:
Texts for Nothing
Masonic Lodge, Cork
Enough
The Other Place, Cork

MARY LELAND

Determined to find venues unfamiliar to the public for the "Access All Beckett" programm[e] in Cork until April 16th, Gare S[t] Lazare Players Ireland outran their aspirations in the choice [of] the Masonic Lodge for the performance of *Texts for Nothing*.

Here the location itself is the performance, or would be, wer[e] it not that Conor Lovett's monologue is delivered with such detachment that its very ironies echo like a commentary on the meeting room.

Marvellously dramatic with black-panelled walls draped with heraldry and embossed with insignia and armorial bearings, the room, nonetheles[s] succumbs first to the shaft of light through which Lovett passes to the Master's pedimented seat and then to th[e] confiding, conversational style in which texts III, VIII and XII are given. But it is ownership, rather than mastery, that Lovet[t] exudes; these memorised readings, in performances directed by Judy Hegarty Lovet[t] dwell on the contradictions of thought, on matters stopping and starting, leaving and departing, or places of high depression, the adjacent extremes of human experience.

Unforced because there is no need to project, the sardonic implications of self-referral are touched lightly, but very accurately.

Again it is externals that see[m] most striking in *Enough* at The Other Place: here Allie Ní Chiaráin's high, Elizabethan forehead seems to signal a physical as well as an ...

Side View - Outside

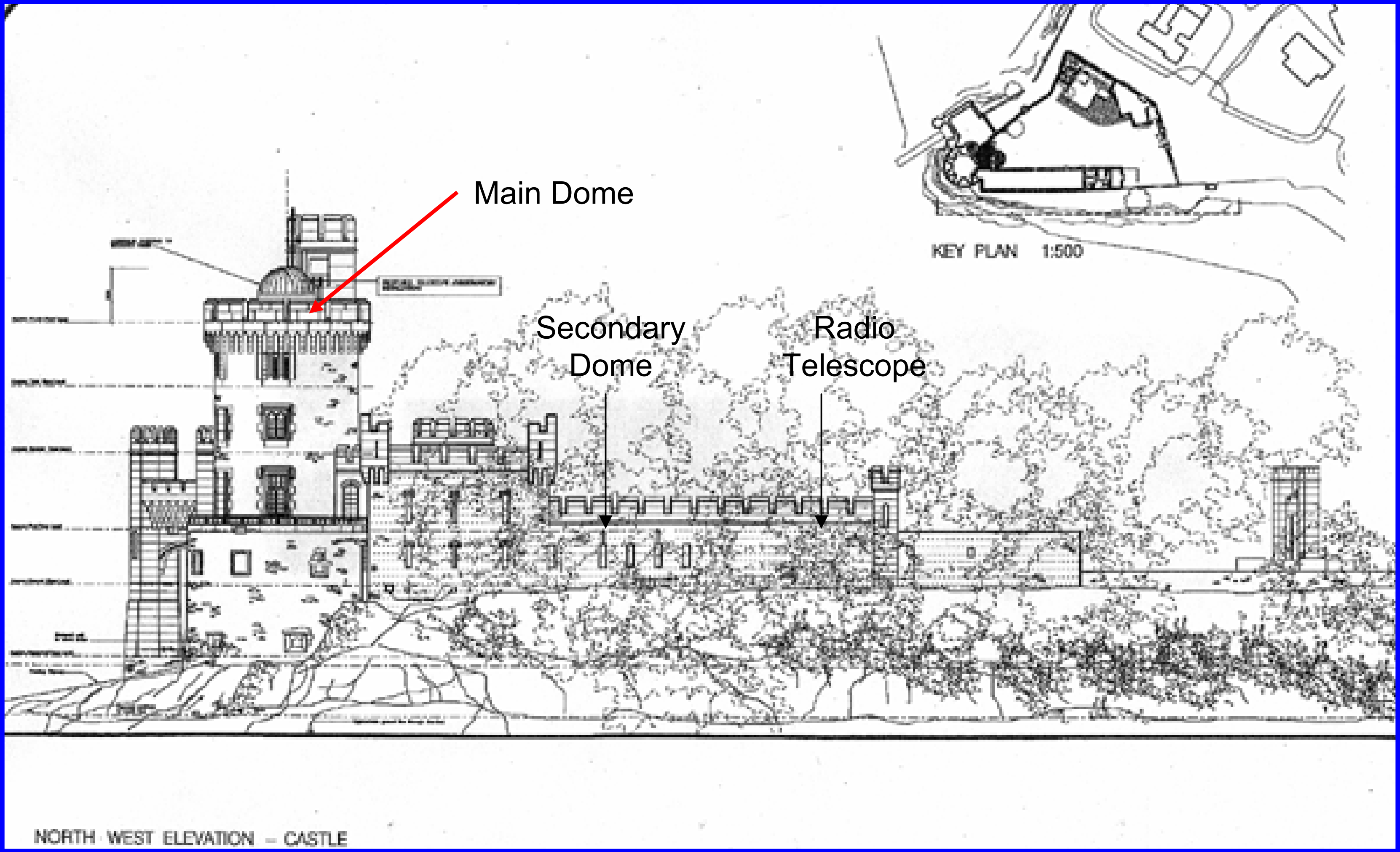

Cutaway View

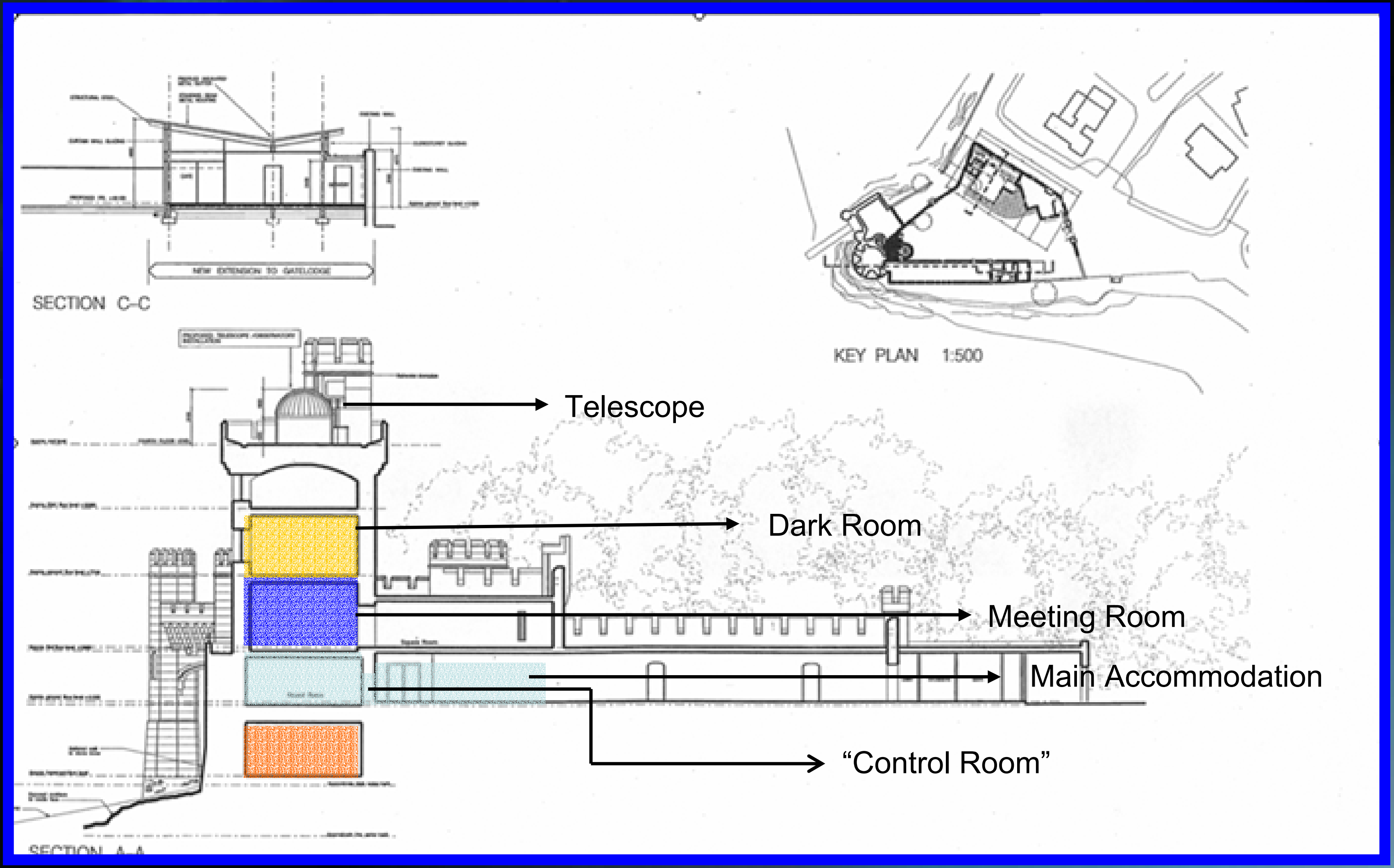

Exhibition and Restaurant

Kryoneri Telescope Project

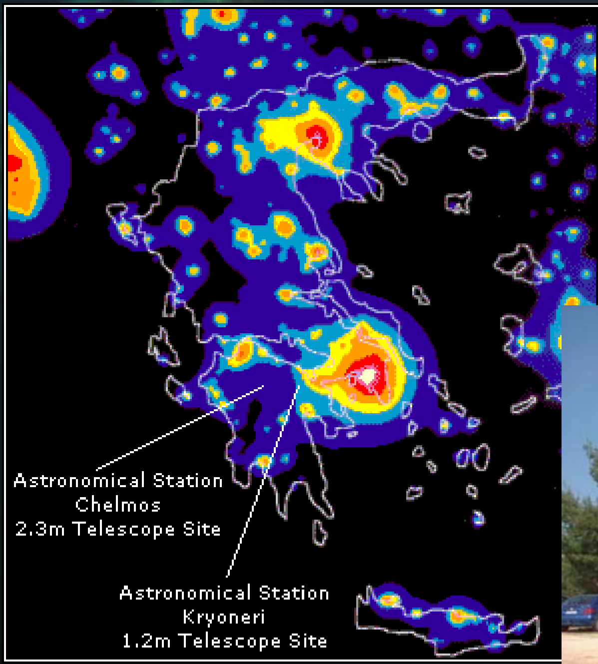

- Agreement in place with Institute of Astronomy & Astrophysics, Athens
- Now seeking funding to match small percentage of resources already secured (€4m) to robotise the 1.2m Kryoneri Telescope

Faulkes Telescopes

http://www.faulkes-telescope.com/

The Faulkes Project aims to make a number of telescopes around the world accessible to students and researchers with the goal of increasing awareness in science, engineering and technology.

Currently, two Faulkes Telescopes (2 metre class) at sites in Hawaii and Australia.

Also “Liverpool Telescope” coming online soon: 2 metre fully robotic telescope, associated with Faulkes project located in La Palma.

Plans to develop a network of ~20 telescopes all over the world.

Recently, the Irish Faulkes Telescope Project was launched – free access to Irish researchers

Students in Armagh were first in world to confirm Deep Impact using Faulkes Telescope in Hawaii.

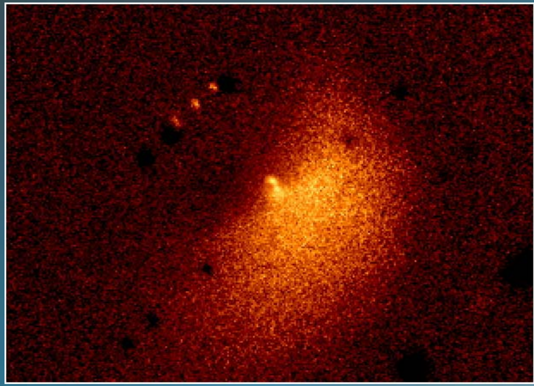

blackrockcastleobservatory
A Cork City Council / Cork Institute of Technology Partnership

L3CCD Performance & Analysis

Alan Giltinan, Niall Smith, Aidan O’Connor, Stephen O’Driscoll

Sixth ENIGMA meeting

Cork, Ireland

November 2005

- Quick L3CCD architecture review
- Experimental Setup
- Data acquisition
- Analysis
  - Photometric Performance
  - Clock Induced Charge
  - Gain
  - Dynamic Range

L3CCD Architecture

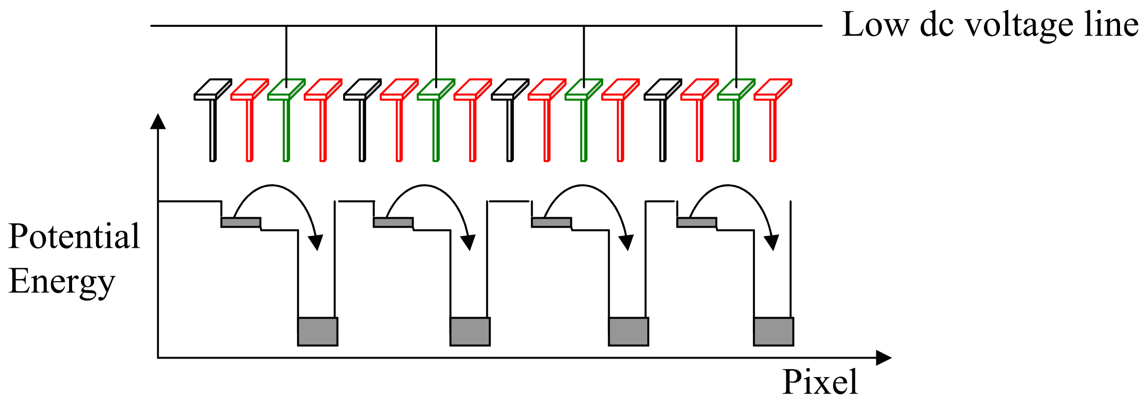

- Large voltage drop across low DC voltage line
- Impact ionization
- Gain, **G = (p+1)ⁿ**, where p = probability

  and n = number of pixels

So, **SNR** $= \dfrac{Q.I.t.F}{\sqrt{Q.t.F(I + B_{sky}) + \left(\dfrac{N_R}{G}\right)^2}}$

Multiplication Noise

Gain

Setup

blackrockcastleobservatory
A Cork City Council / Cork Institute of Technology Partnership

- Light Tight container
- Water cooled to -79ºC
- Simulated star field consisting of 5 stars
- Single light source

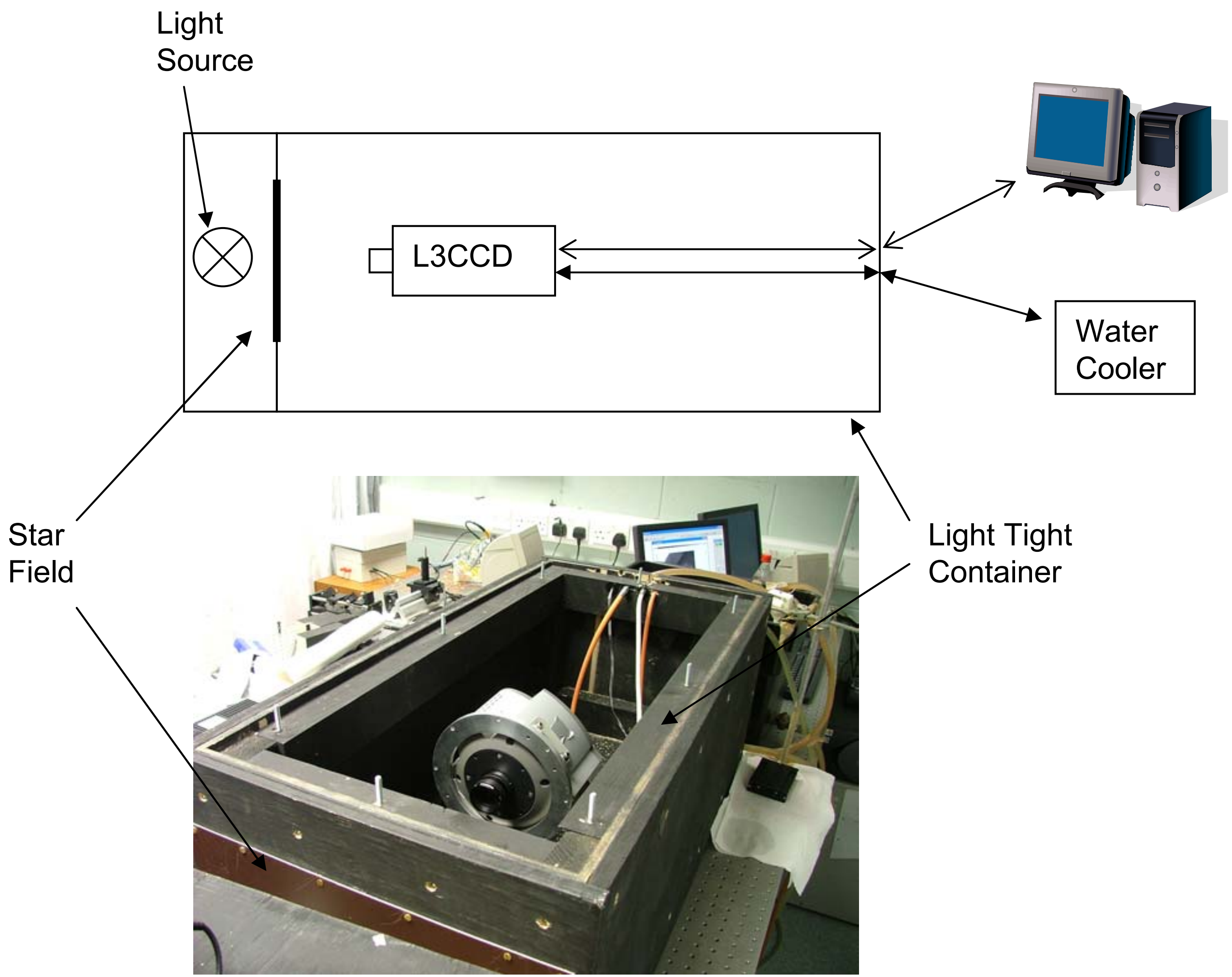

Data Acquisition

~90GB data in 2 days

~90,000 images

Modes of operation

- Photometric accuracy using simulated star field
- Clock Induced Charge
- Gain
- Dynamic Range

Photometric Analysis

blackrockcastleobservatory
A Cork City Council / Cork Institute of Technology Partnership

Photometric accuracy based upon scatter in data

Increasing number of averaged data points decreases scatter

Scatter in single star = 0.02%

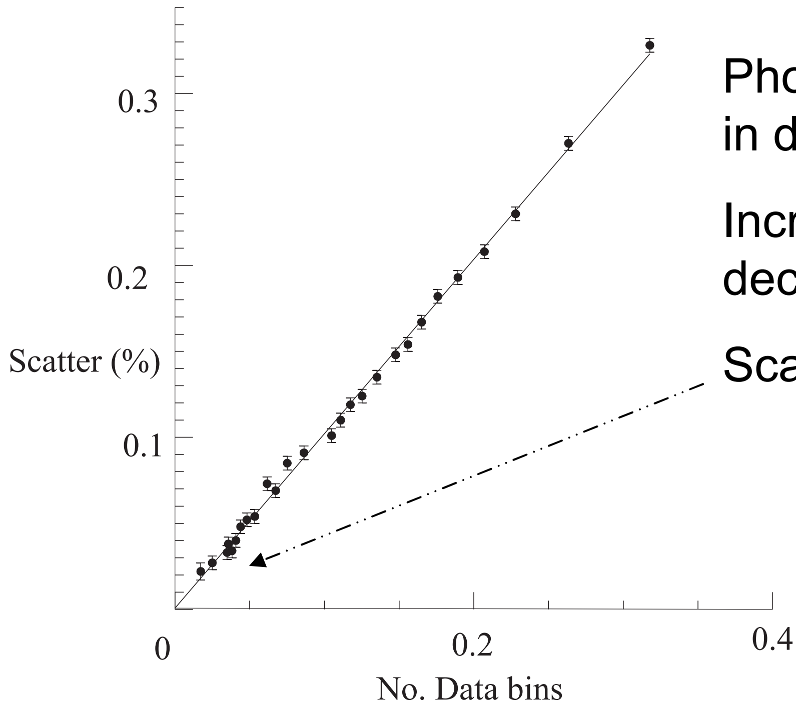

√N statistics -> straight line through origin

Including all stars, scatter = 0.075%±0.02

0.075% corresponds to ~0.75mmag accuracy

Large number of averaged data points means poorer time resolved but better accuracy

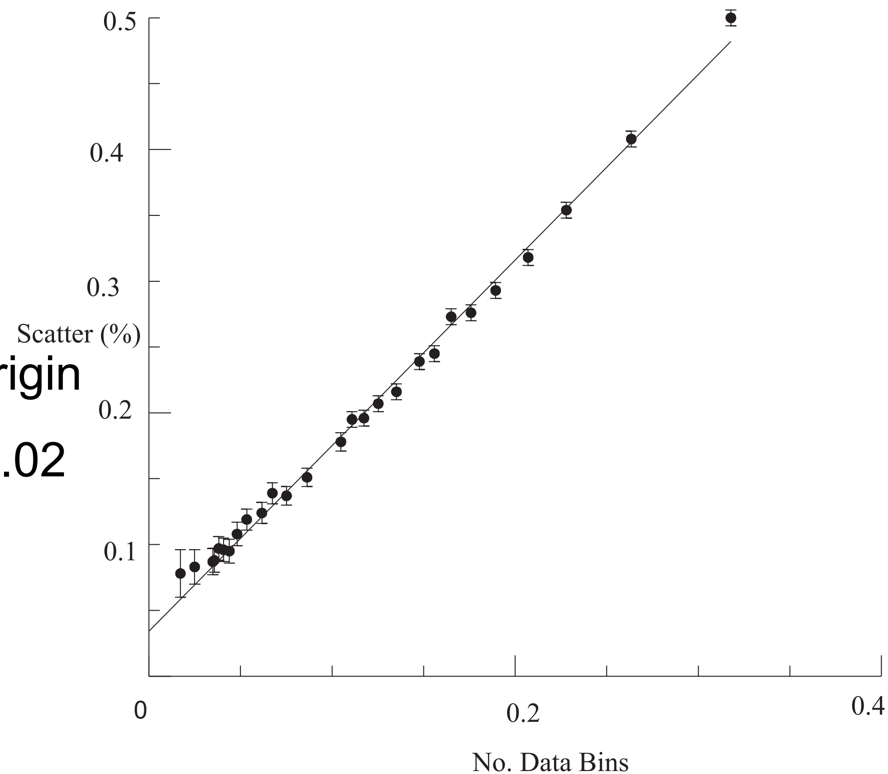

Clock Induced Charge

Threshold results

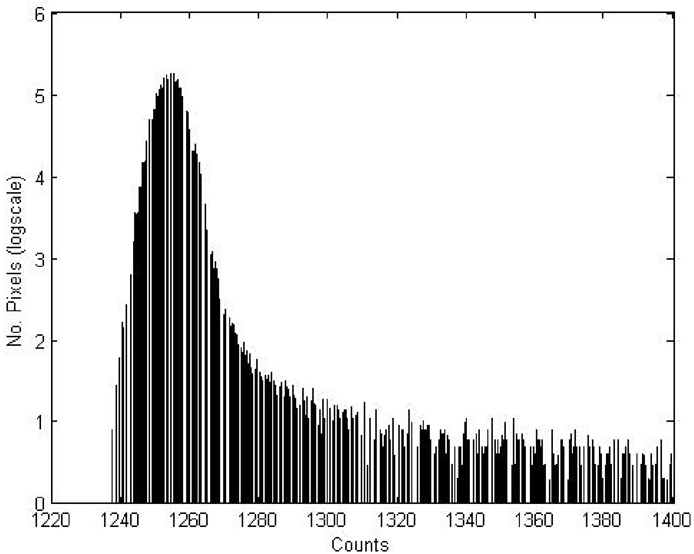

0.0006% CIC detectable above 3σ

Thresholding under estimates actual CIC value

Different method applied for CIC calculation.

Fit to line, extrapolate to zero and integrate. Area Shown corresponds to 0.77%

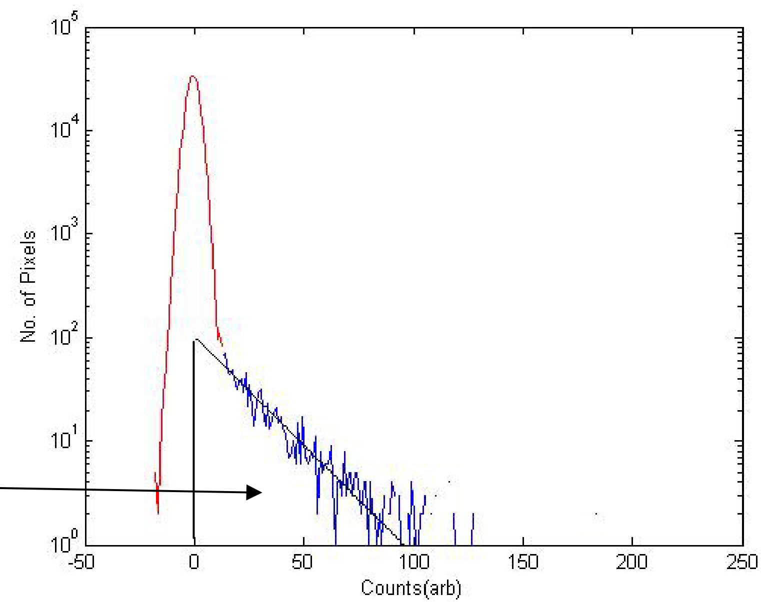

Clock Induced Charge

blackrockcastleobservatory
A Cork City Council / Cork Institute of Technology Partnership

CIC independent of gain

Compared to previous L3CCD which was found to contain ~5.5% CIC, new CCD ~5 times better

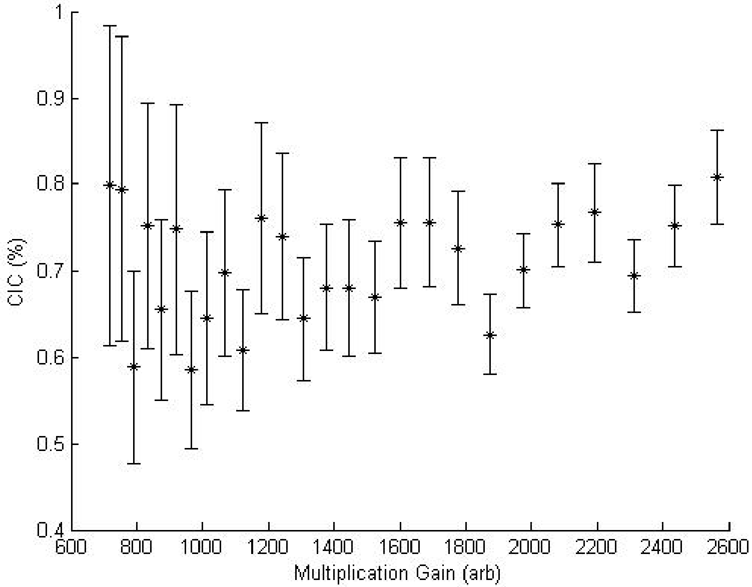

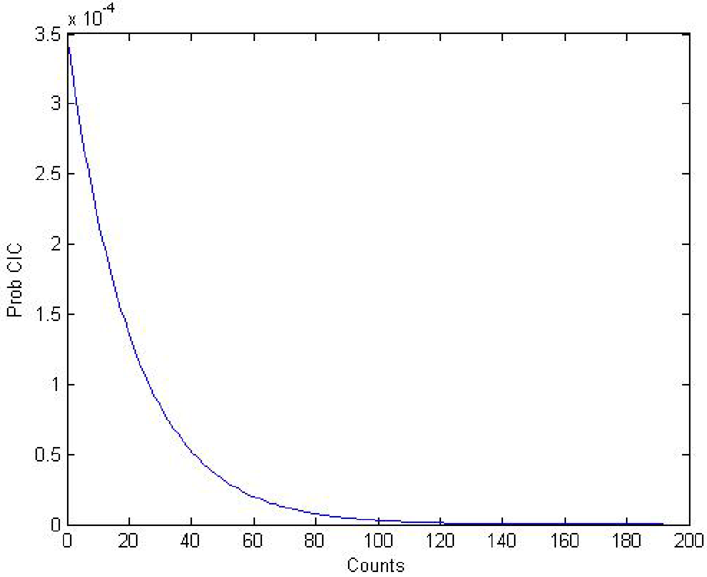

Probability of CIC in a pixel with X counts.

Could be used to test if single photon detection is possible

Gain

Calculation performed using the standard Gain calculation of Signal Vs. Variance used.

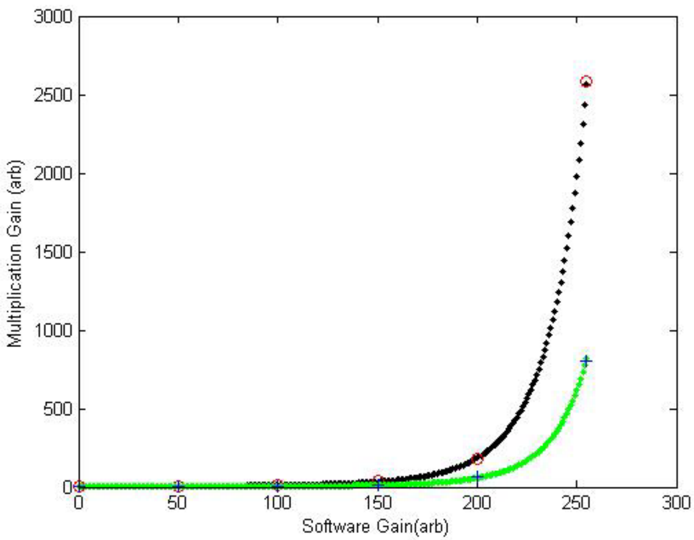

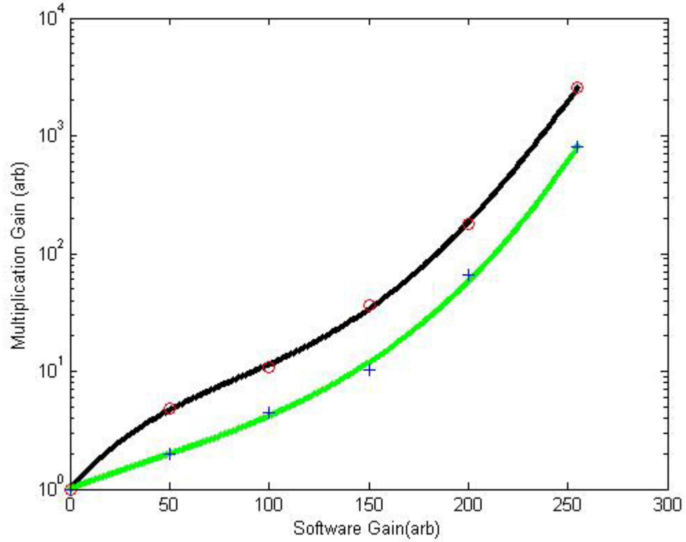

Similar trend to Andor Specifications. Offset due to specifications stated at different temperature.

Dynamic Range

Dynamic Range is defined as ratio of full well capacity to readout noise. For L3CCD this becomes

$$\frac{\mathbf{FullWellCapacity}}{\mathbf{Readnoise \times gain}}$$

Readnoise reduces to 0.01e$^-$ with increasing gain. This results in decreasing Dynamic Range at high gain.

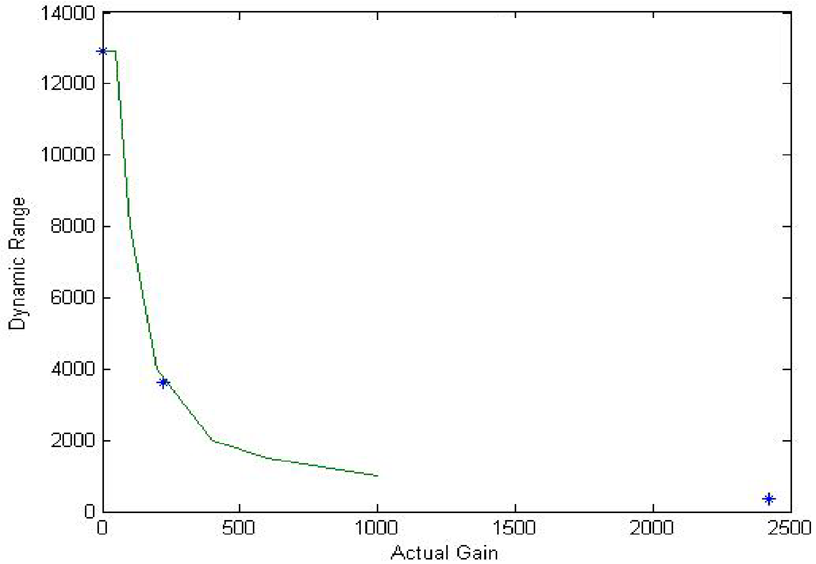

Conclusion

~90,000 images acquired for L3CCD performance analysis

- Photometric Accuracy
  - <0.1% photometric accuracy achievable
  - Very large data sets
- CIC
  - Clock Induced Charge present but <1% in total
  - Preliminary analysis suggests single photon detection maybe possible
- Gain
  - Gain of 2500 achievable at very low temperature

AIG Fast Two Channel Photometer

CIT, Ireland

LSW, Germany

Boyden Observatory, South Africa

Kryoneri Observatory, Greece

Introduction

blackrockcastleobservatory
A Cork City Council / Cork Institute of Technology Partnership

- Funded by Science Foundation Ireland
  - €200,000 over 3 years

- 160 Nights Observation
  - Greece – Kryoneri (1.2m)
  - Greece – Aristarchos (2.3m)
  - South Africa – Boyden (1.5m)
  - Spain – Calar Alto (2.2m)
  - Other?

- First light summer 2006

Why?

To address the following questions

- What is the duration of the most rapid events that can be reliably observed?
- How frequent are they?
- What temporal shape do they have?
- How does their spectrum evolve with flare amplitude?
- On what timescale does acceleration/cooling dominate over geometric effects?
- How is flare behavior in different objects influenced by the Lorentz factor, total luminosities and long-term variability properties?
- These questions can be addressed by dense optical monitoring in two or more colour simultaneously.
- Even future space-borne mm-interferometry would fall short in angular resolution by three orders of magnitude.

System Overview

blackrockcastleobservatory
A Cork City Council / Cork Institute of Technology Partnership

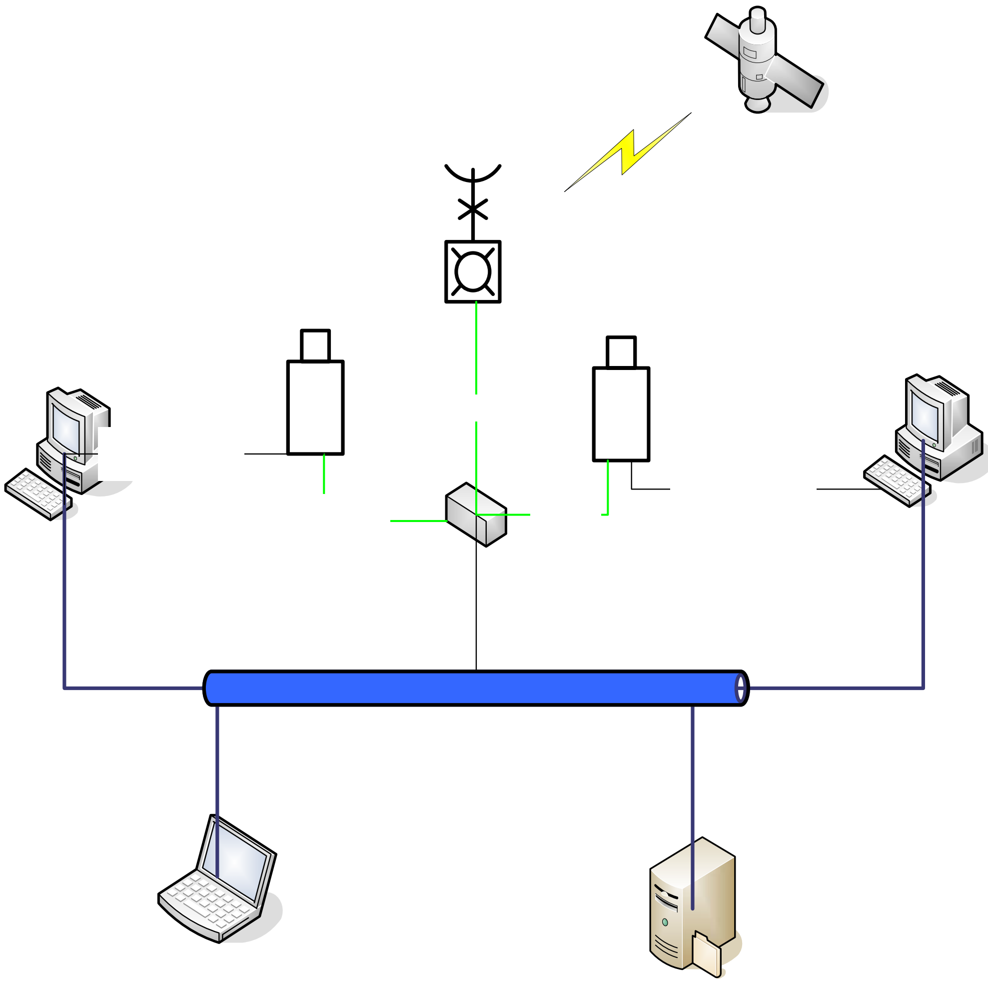

- Timing
  - GPS
  - 1PPS
  - ms resolution
  - PC104 controlling triggering and logging timestamps
- 2 camera control PCs
  - P4, 2 GB RAM
  - Raid 0 SATA HDs
  - 2 x 200 GB drives
  - Data stream to disk
  - Removable HDs
- Control PC (GUI)
  - TCP/IP over Ethernet communication
- Live Photometry

Optical

blackrockcastleobservatory
A Cork City Council / Cork Institute of Technology Partnership

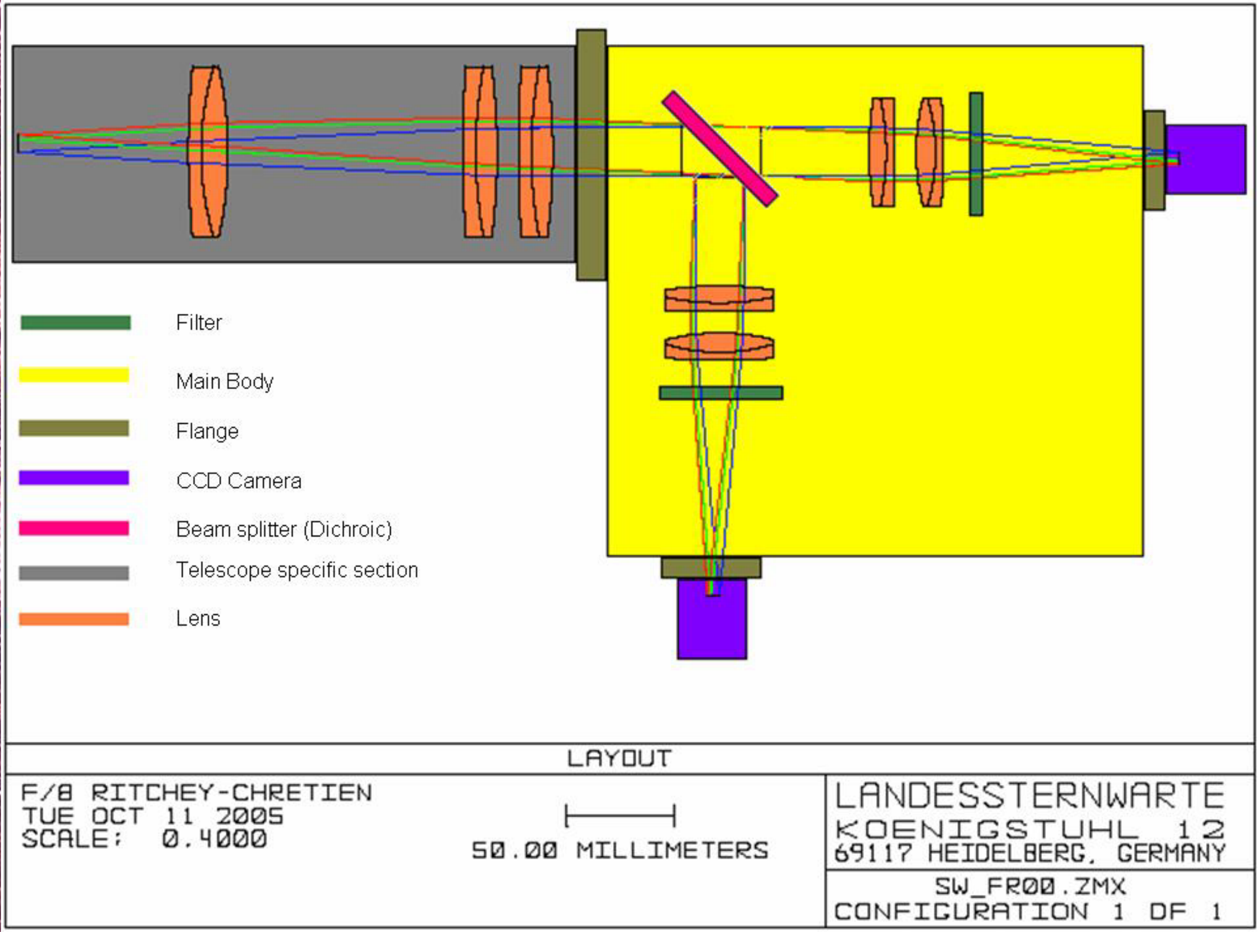

- Optical design by our colleagues at the LSW, Heidelberg, Germany
- f/8 Optical ratio
- Plate scale 0.3''/pixel
- B,V,R bands
- One filter fixed, other changeable
- Changeable collimator section
- Optics better than likely seeing (1.0'')

Mechanical

- Design and Fabrication - Mechanical Engineering Dept in CIT
- Project to be split in 3 sections
  - Photometer body:
    - Compact, lightweight, simple (no moving parts)
    - Rigid temperature tolerant chassis
    - Optics fixed, except one changeable filter
    - Collimator optics fitted per telescope
    - Approximately 8 hrs to make changes, no need for quick release/easy access
  - Control PC housings:
    - Attached to photometer body
    - Easy access to hard drives
    - Data/Control cabling
    - Temperature control/monitoring, Air movement
    - Able to withstand harsh conditions
  - Transport system:
    - Logistics: System protection and Shock Logging
- Design to be finalised by 9th December

Control Software Data Acquisition

- Andor MCD
  - Biotech oriented – Short quick acquisitions
  - Single camera, no remote control
  - Inflexible, recourse hungry

- Andor BASIC
  - Scripting language for MCD
  - More flexible but still limited control

- SDK/Linux and Windows
  - Andor provides libraries - can be accessed using most higher level languages such as LabView, Visual Basic and C/C++
  - Windows – In house expertise, off the shell applications – rapid development, most devices come with Windows drivers
  - Will experiment with Linux – Hardware/driver issues

  - ANSI C/C++ Will give us control at a lower level
    - Relatively easy to port to other operating systems
    - System lends itself to object oriented idea – Encapsulation, inheritance etc
    - Greater control over application timing – multithread, driver events,
    - No GUI waste on control PCs

- MySql database
  - Group information – Exposure, Target, filters, camera settings, number of frames
  - Assist data archiving

ENIGMA 6th meeting
22 – 25 November, 2005
Kinsale

High-frequency, multi-wavelength VLBI observations of BL Lac objects *(Task 4)*

Vladislavs Bezrukovs
Cork Institute of Technology,
Irish team

•My project:

To analyze VLBA data from Kuhr and Schmidt sample of BL Lac objects > 1 Jy at 43 GHz, 22 GHz and 15 GHz (May 2002, August 2002, November 2004)

BG121A May 2002	BG121B August 2002	BG121C November 2004
0003-066	0119+115	0814+453
0235+164	0454+844	0828+453
0745+241	0954+658	**0851+202(OJ287)**
1147+245	1308+326	1156+245
1334+127	1803+784	
1749+096	1807-698	
2155-152	2007+777	

- Preliminary calibration and D-term calibration finished for all epoch (May 2002, August 2002, November 2004) at all 3 frequencies;
- Polarization angle calibration made for all sources;
- Maps made for all sources at 15, 22 and 43 GHz;
- Fractional polarization made for all sources at all frequencies;
- Spectral indexes made for all sources, combined from 15 and 22 Ghz and 22 and 43 Ghz intensity maps;
- Rotation measure made for all sources, combined all three frequencies.

CORK INSTITUTE OF TECHNOLOGY

Intensity maps with polarization sticks

15285.459 MHZ (May 2002)

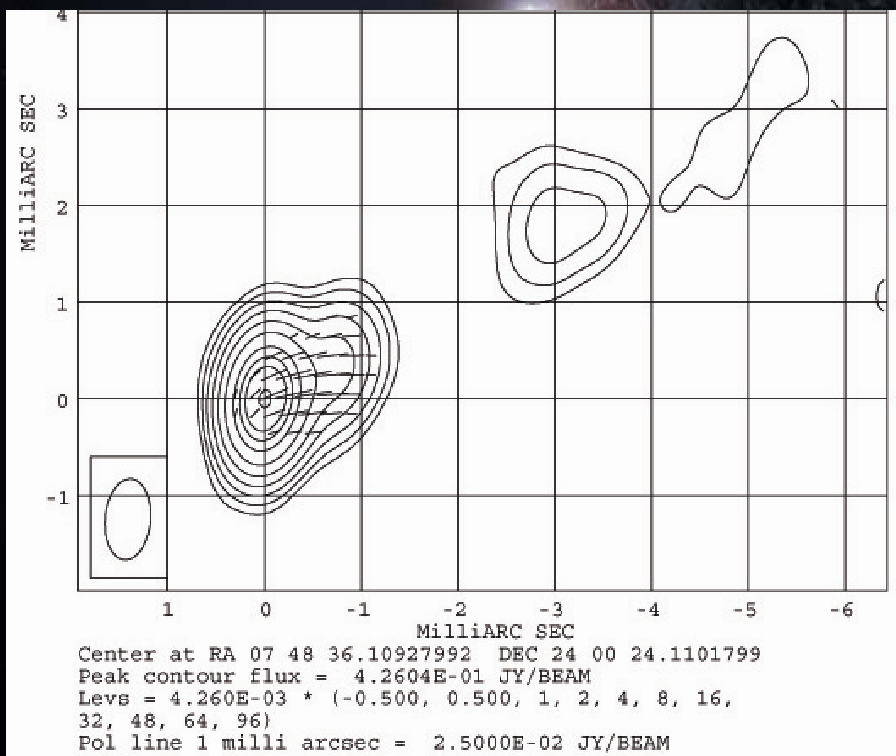

22235.459 MHZ (May 2002)

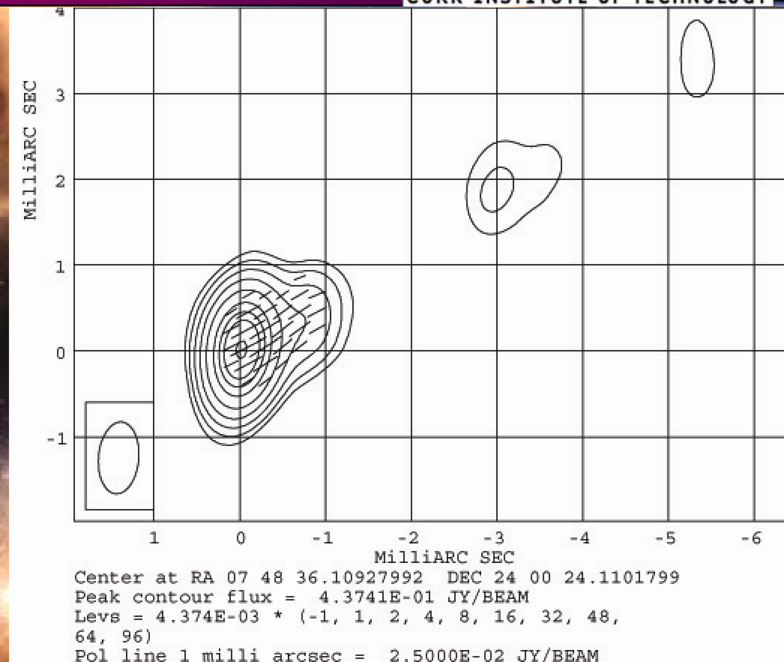

43135.459 MHZ (May 2002)

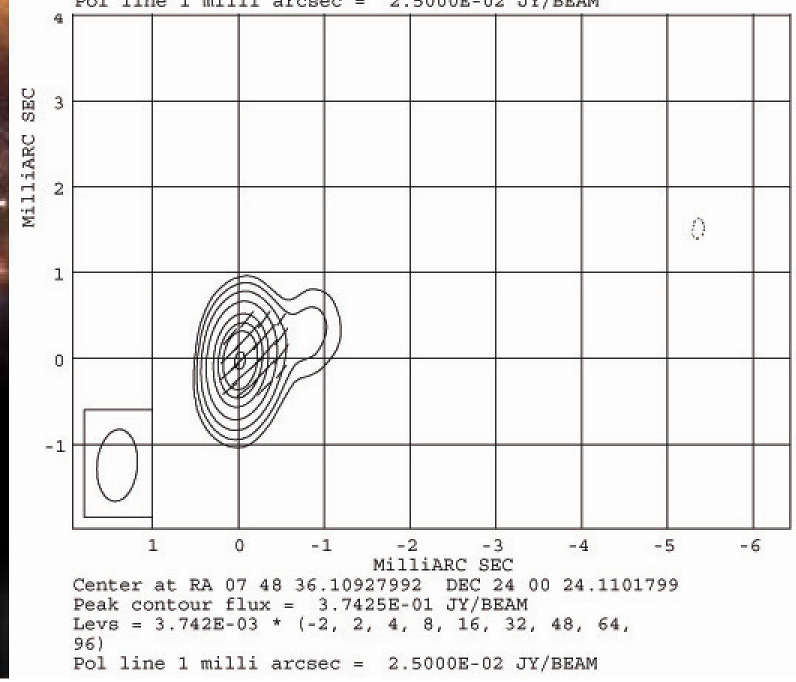

0745+241 (May 2002)

Fractional polarization maps

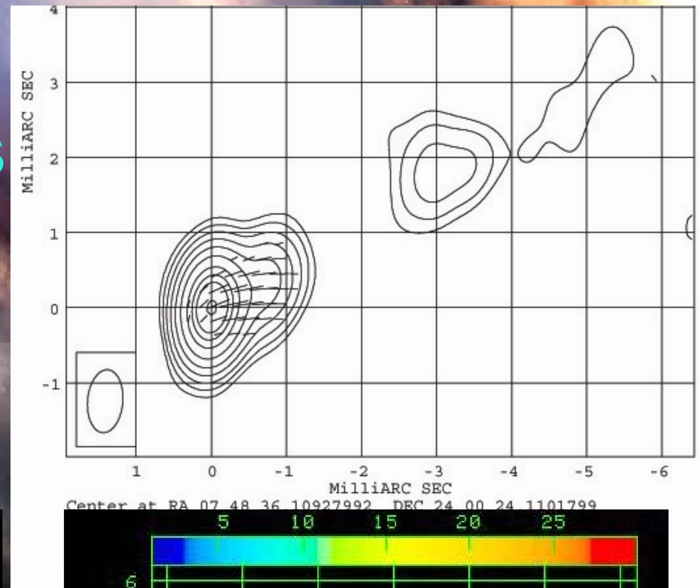

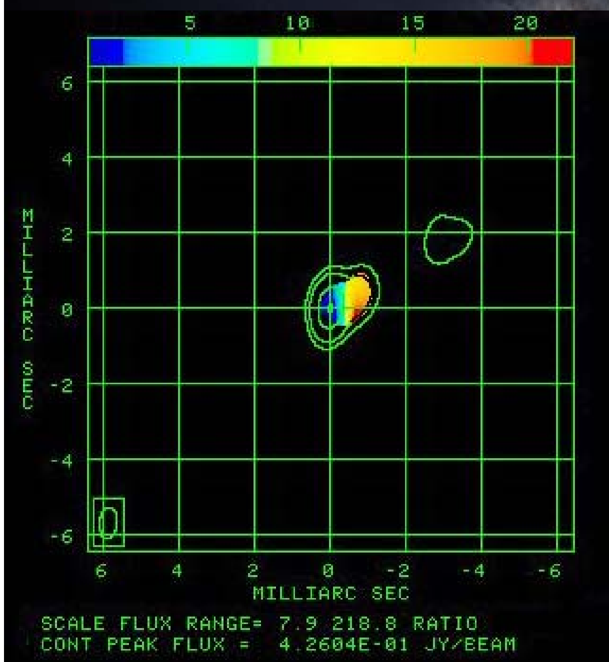

15285.459 MHZ
map cut off at 0.004 Jy

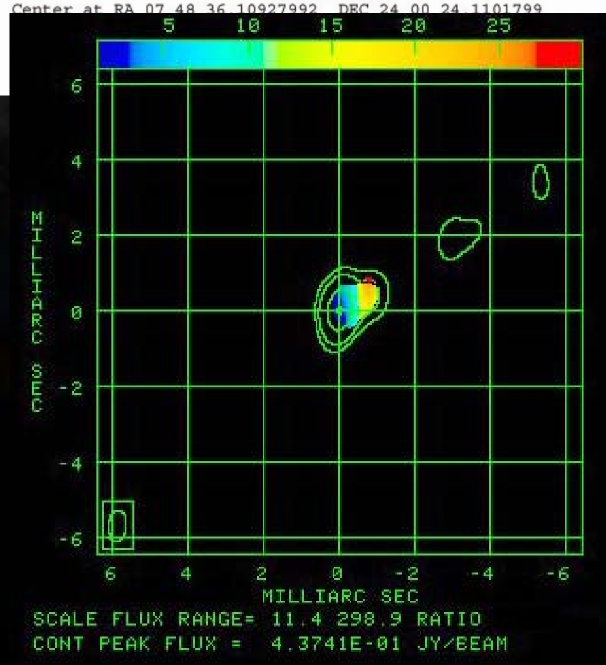

22235.459 MHZ
map cut off at 0.006 Jy

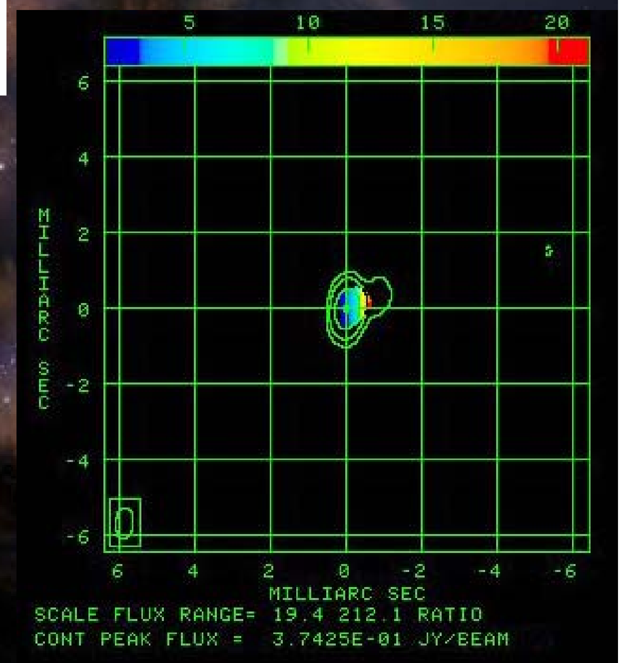

43135.459 MHZ
map cut off at 0.008 Jy

0745+241 (May 2002)

Spectral index maps

Combined from
15Ghz and 22Ghz
intensity maps

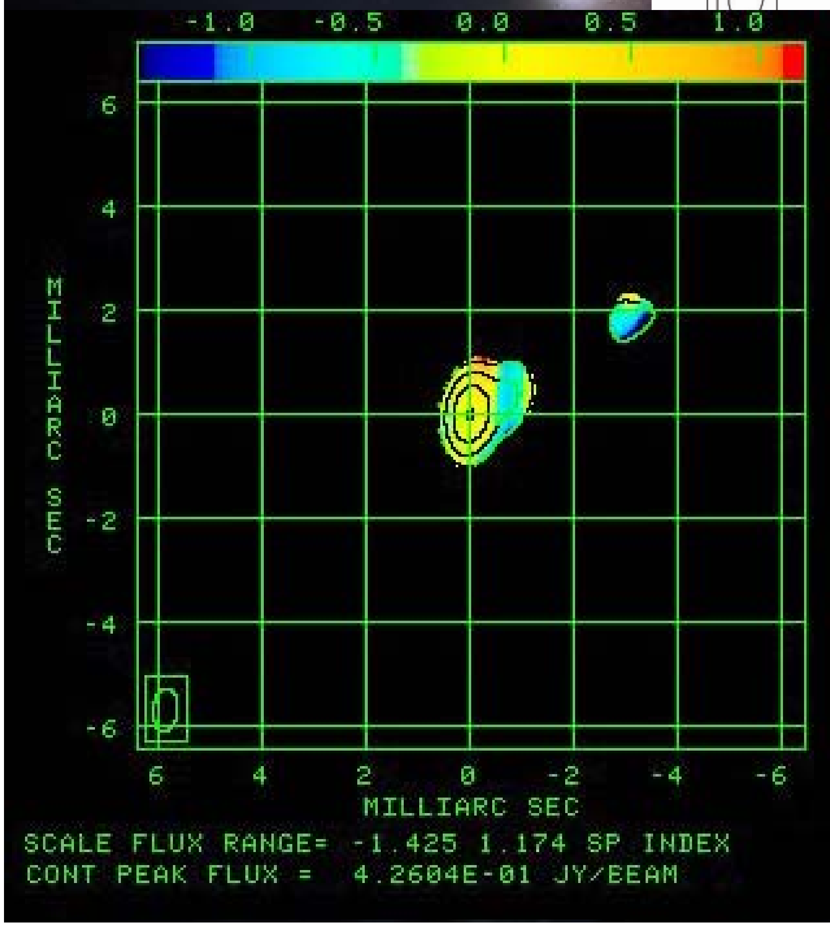

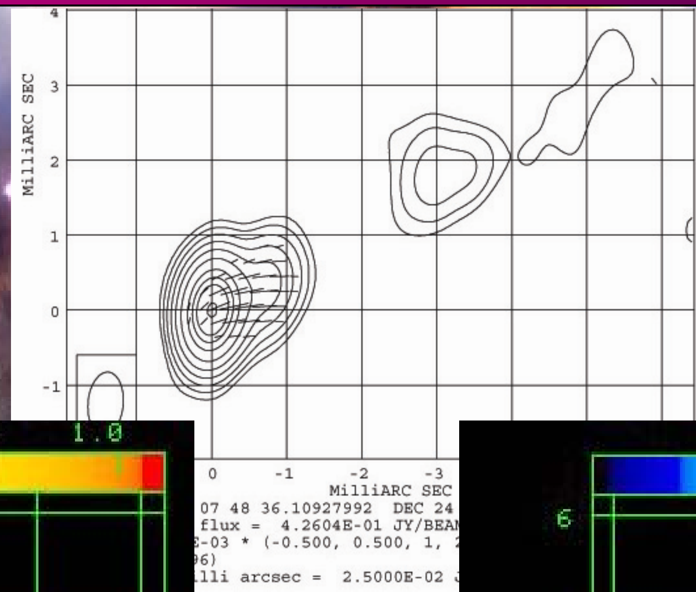

Combined from
22Ghz and 43Ghz
intensity maps

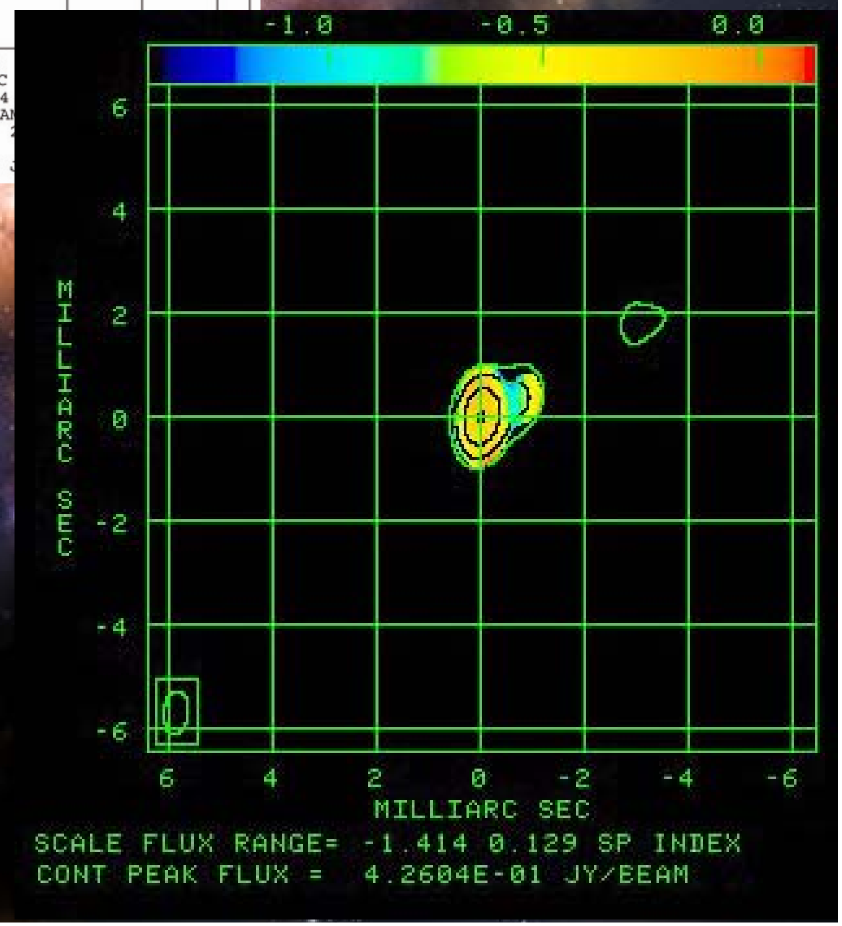

Rotation measure map

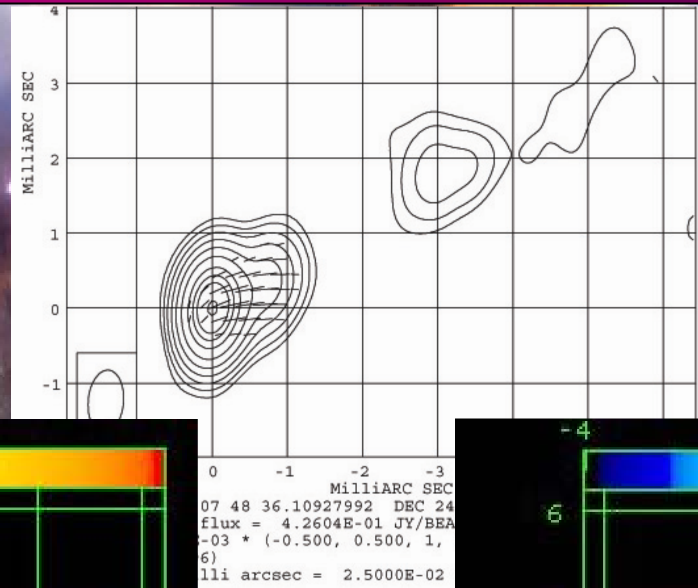

Made from
15Ghz, 22Ghz and 43Ghz

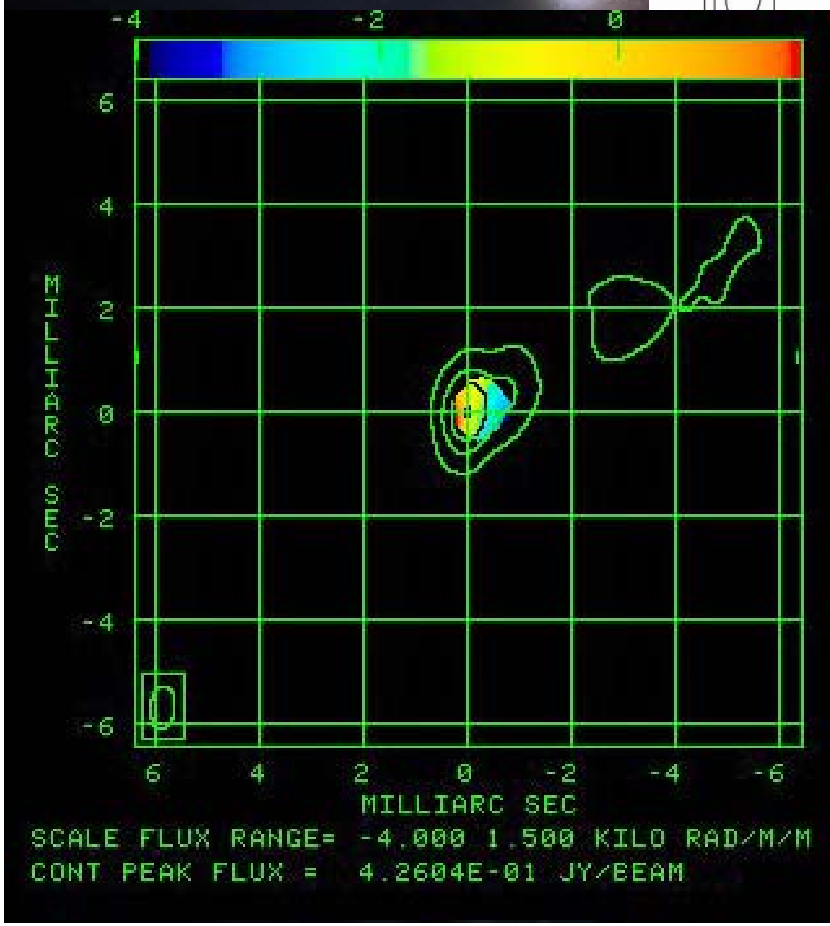

Made from
15Ghz and 22Ghz

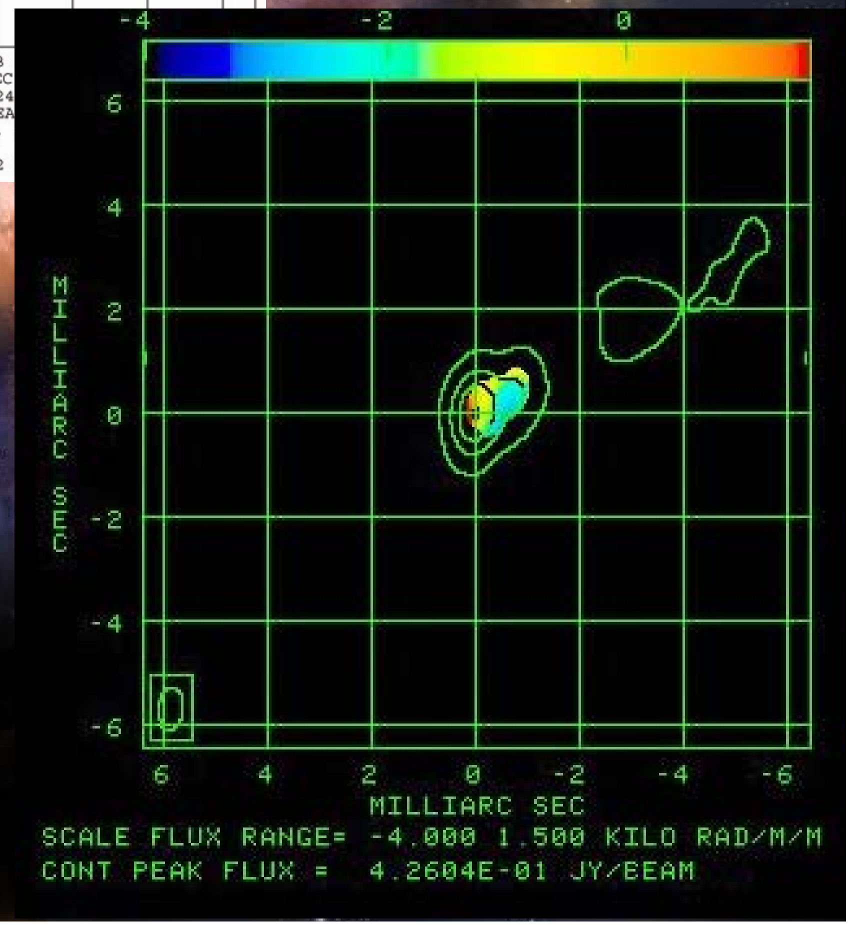

OJ287 (0851+202, August 2002)

Intensity maps with polarization sticks

15285.459 MHZ

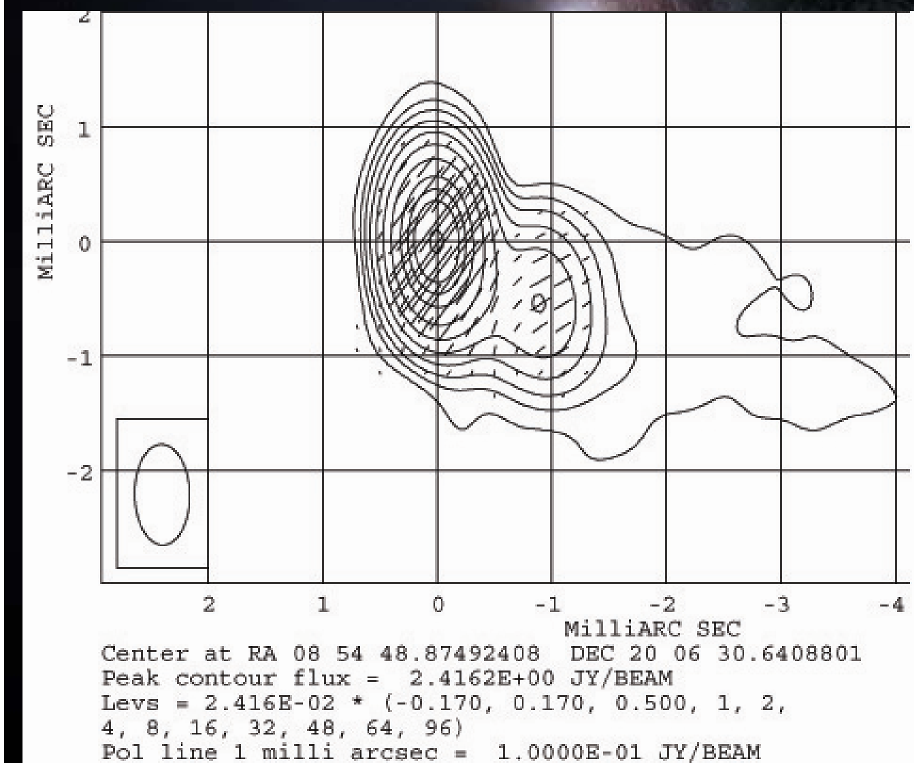

22235.459 MHZ

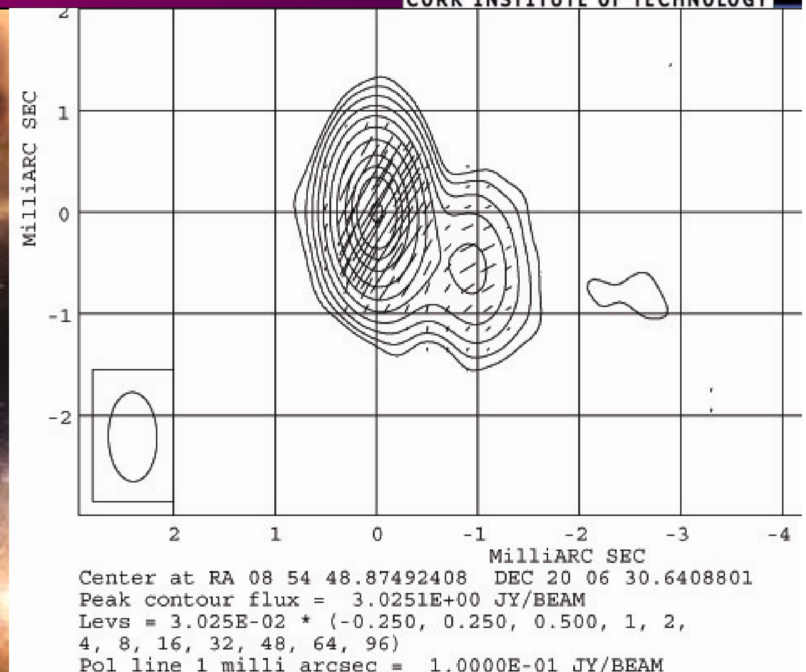

43135.459 MHZ

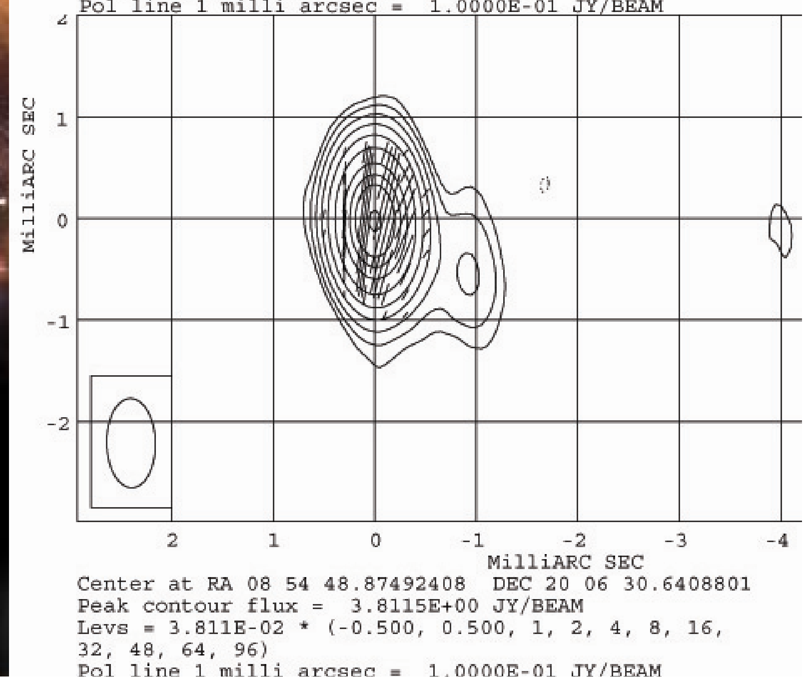

OJ287 (0851+202, August 2002)

CORK INSTITUTE OF TECHNOLOGY

Fractional polarization maps

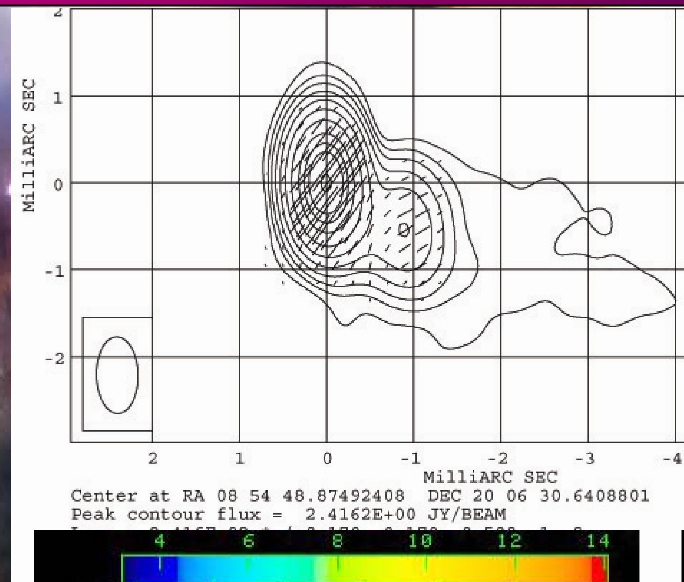

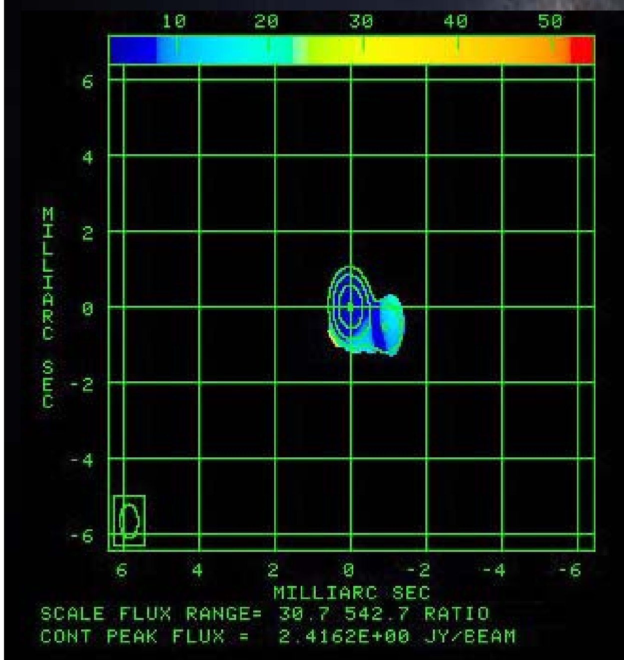

15285.459 MHZ
map cut off at 0.012 Jy

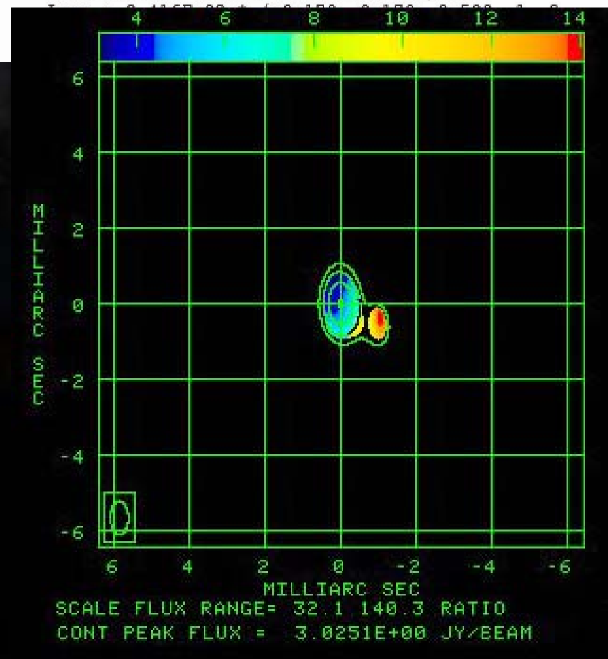

22235.459 MHZ
map cut off at 0.015 Jy

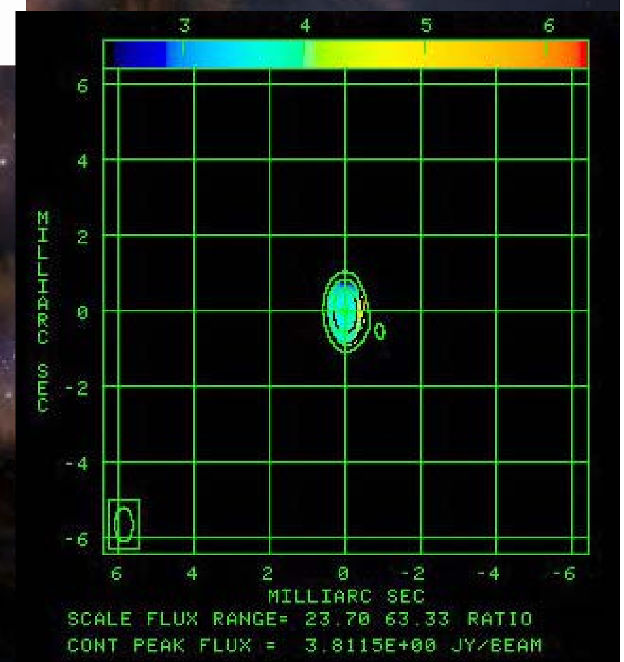

43135.459 MHZ
map cut off at 0.019 Jy

OJ287 (0851+202, August 2002)

Spectral index maps

Combined from
15Ghz and 22Ghz
intensity maps

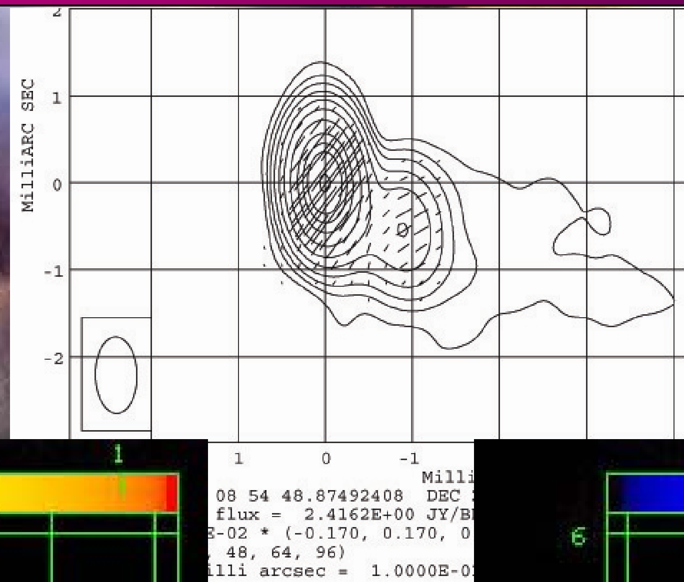

Combined from
22Ghz and 43Ghz
intensity maps

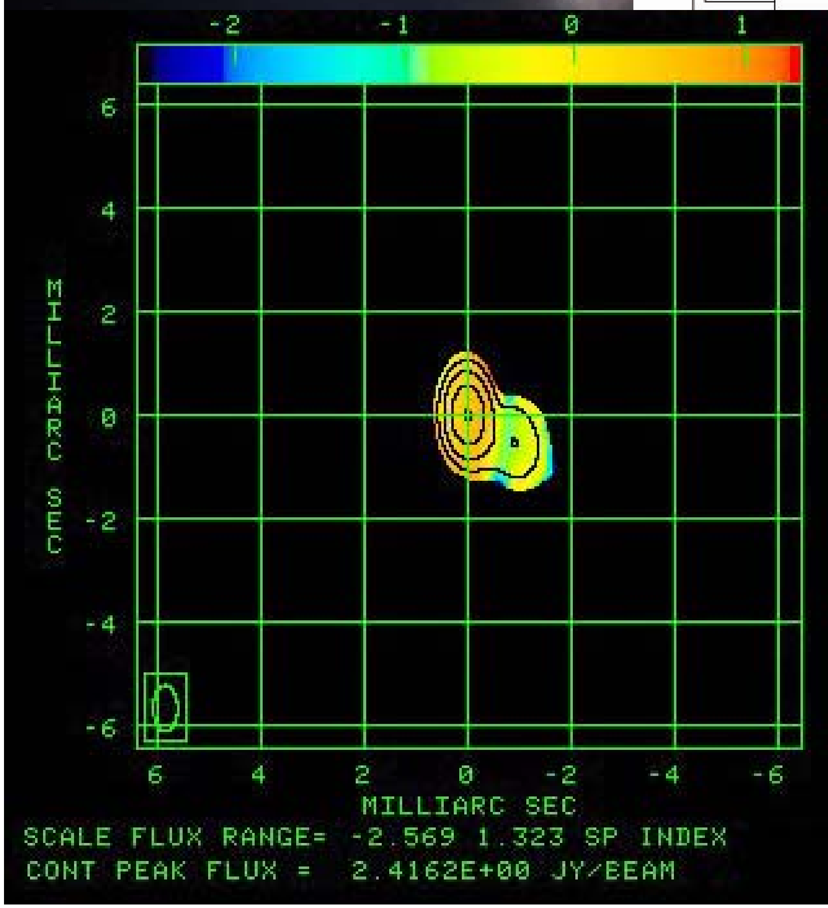

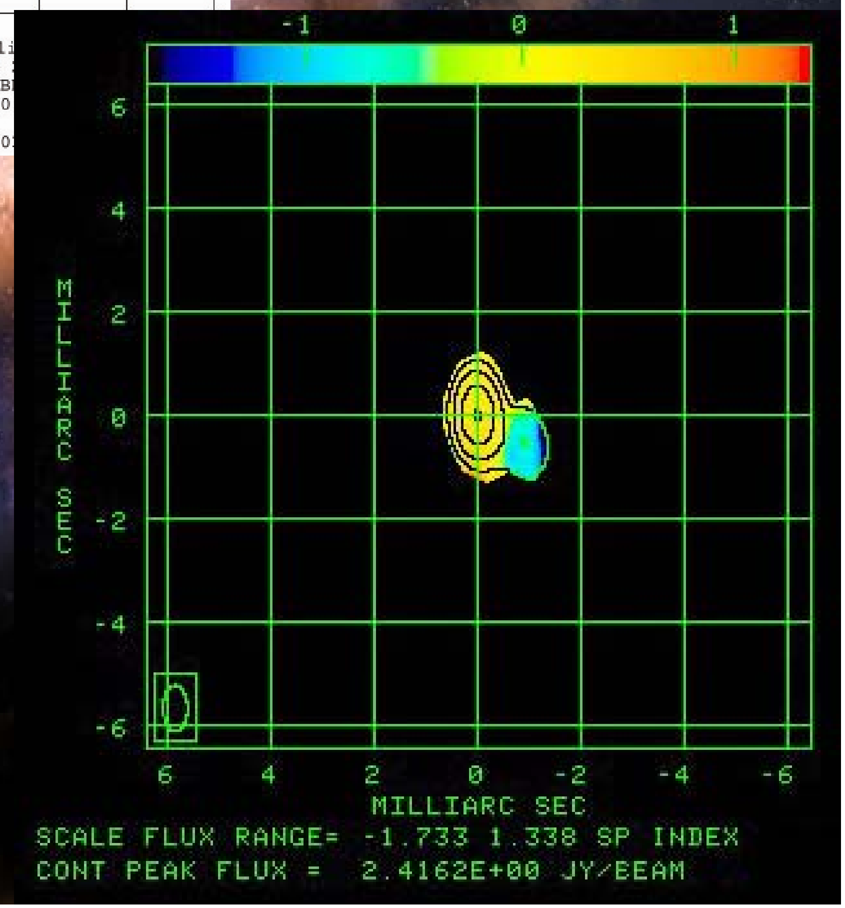

CORK INSTITUTE OF TECHNOLOGY
Institiúid Teicneolaíochta Chorcaí

Rotation measure map

Made from
15Ghz, 22Ghz and 43Ghz

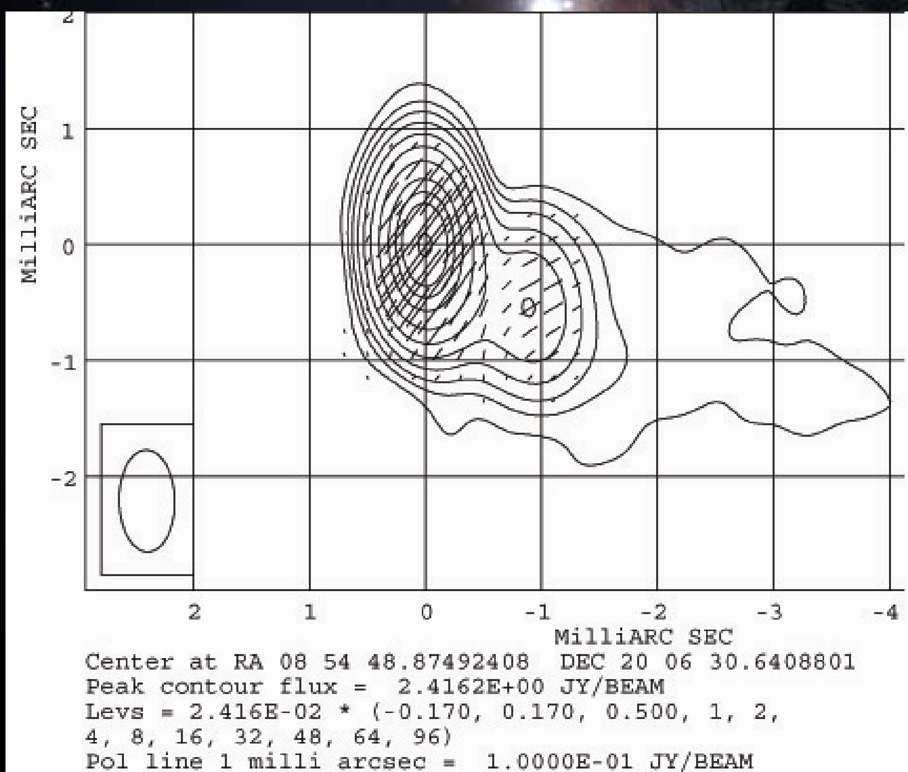

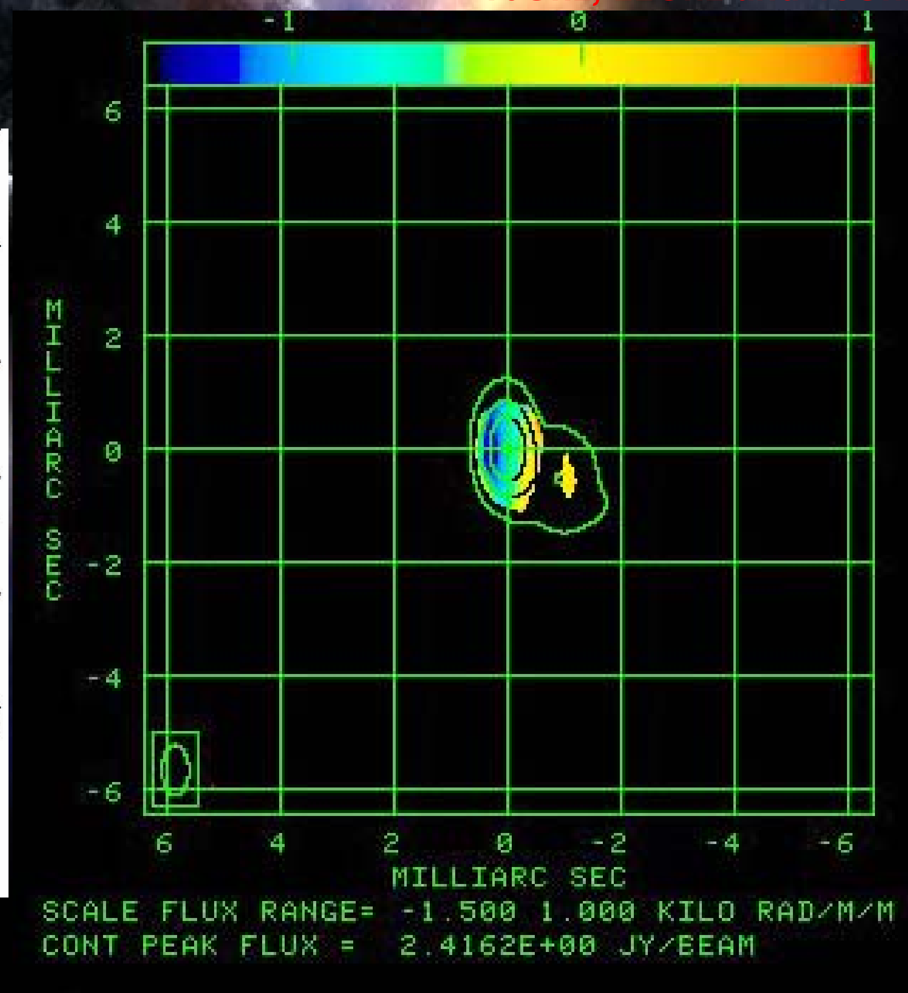

2155-152 (November 2004)

Intensity maps with polarization sticks

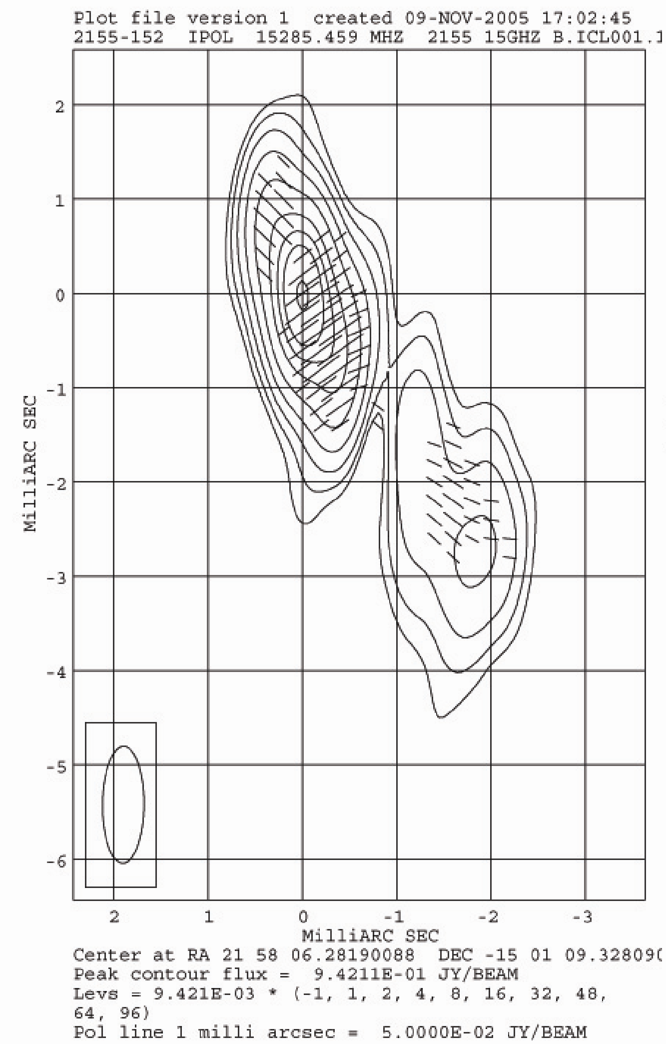

15285.459 MHZ

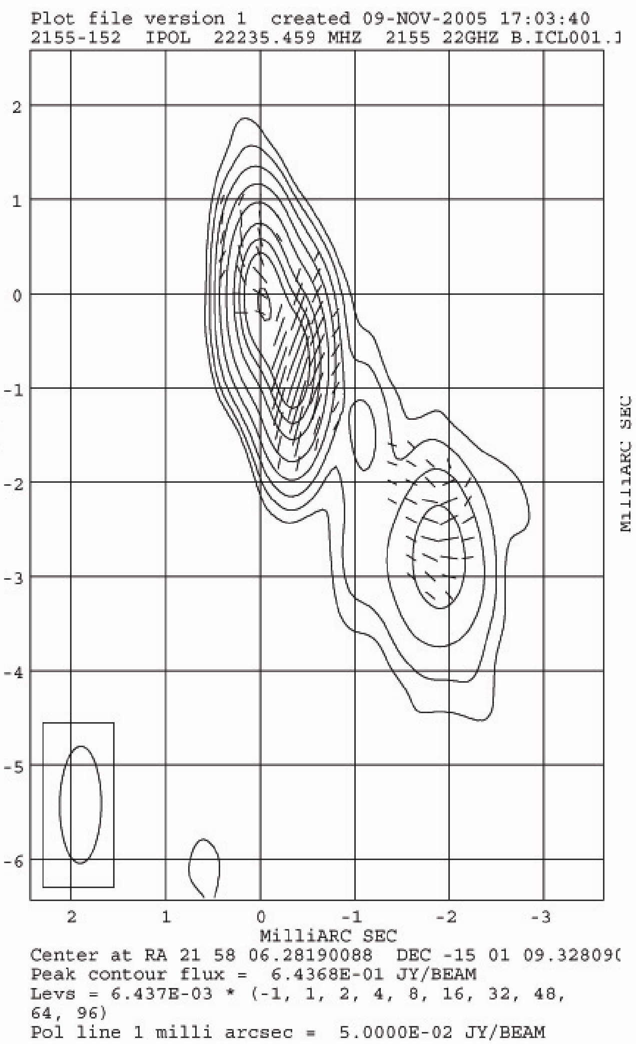

22235.459 MHZ

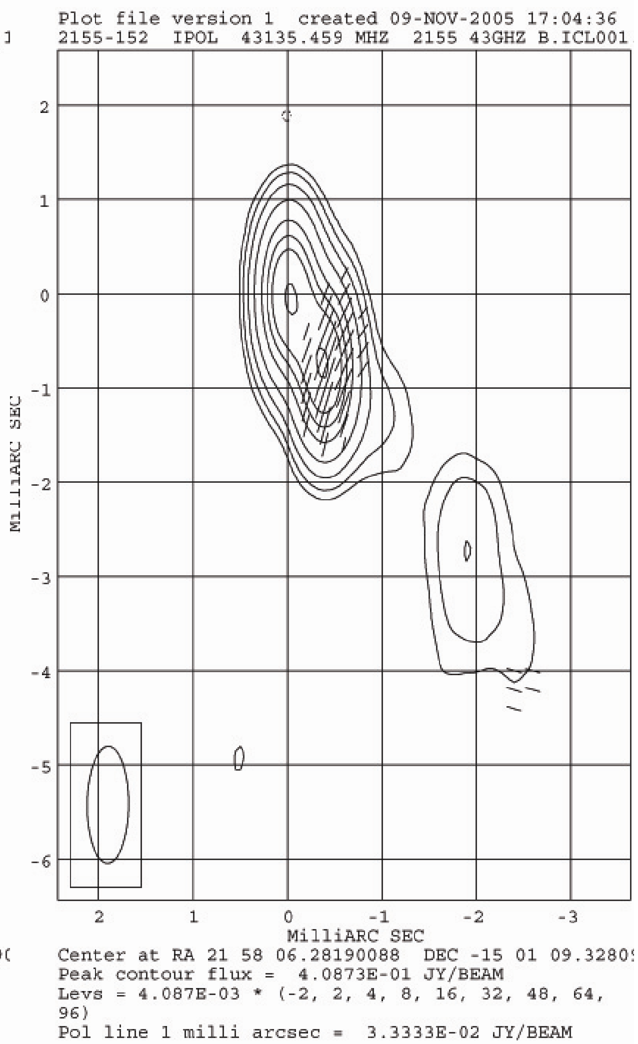

43135.459 MHZ

Fractional polarization maps

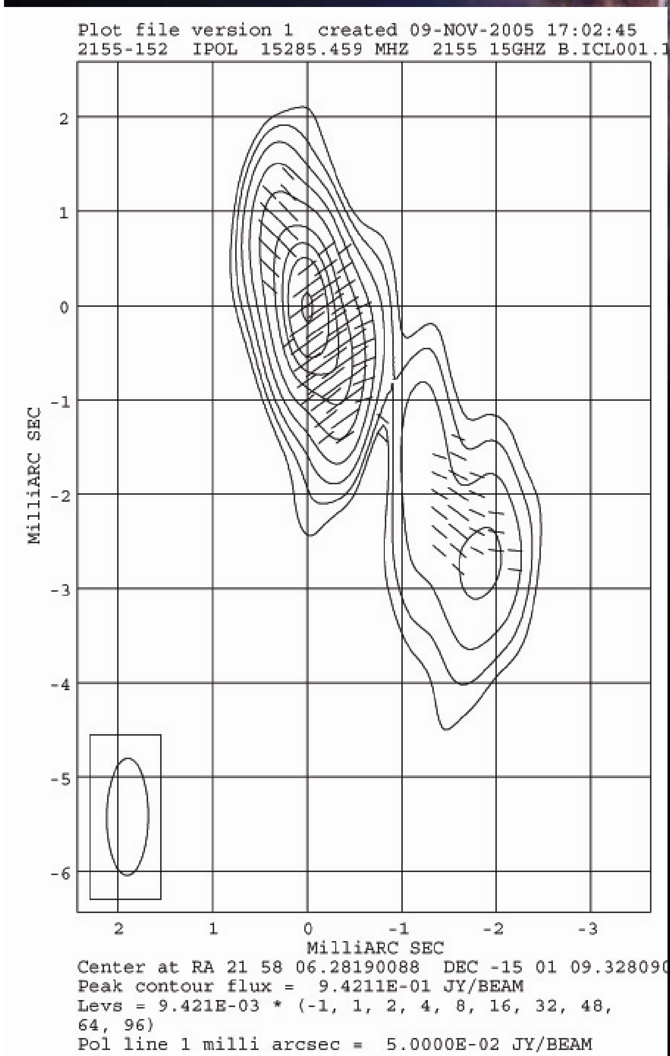

15285.459 MHZ
map cut off at 0.002 Jy

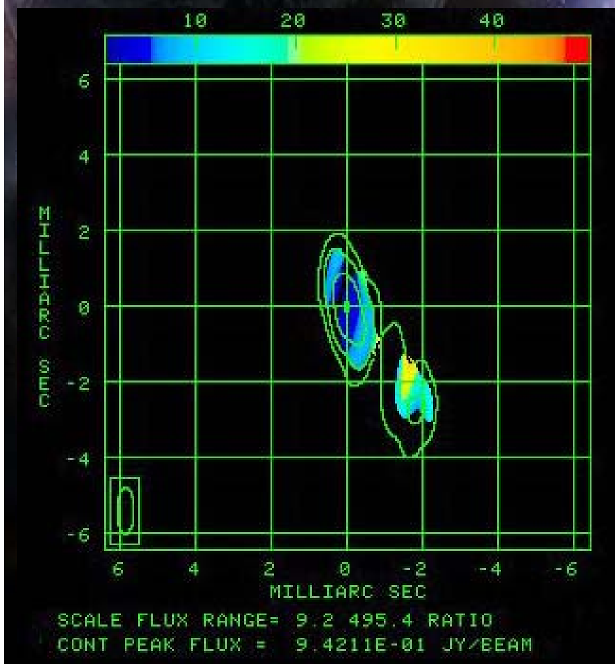

22235.459 MHZ
map cut off at 0.0025 Jy

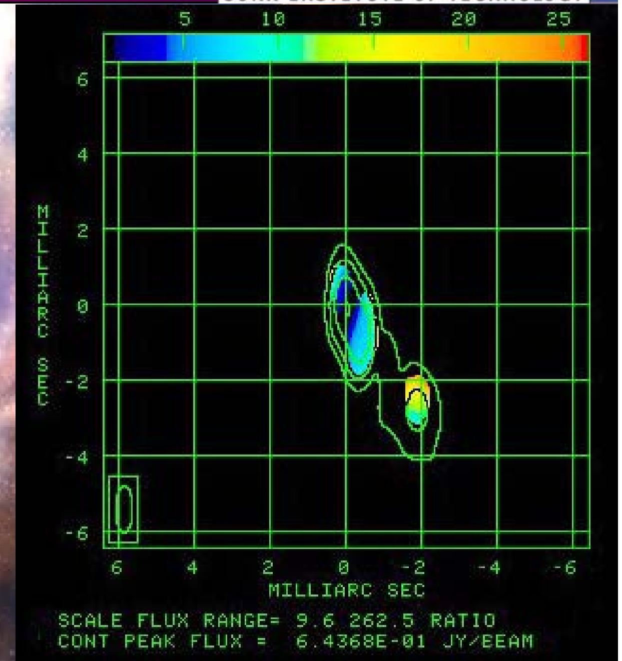

43135.459 MHZ
map cut off at 0.002 Jy

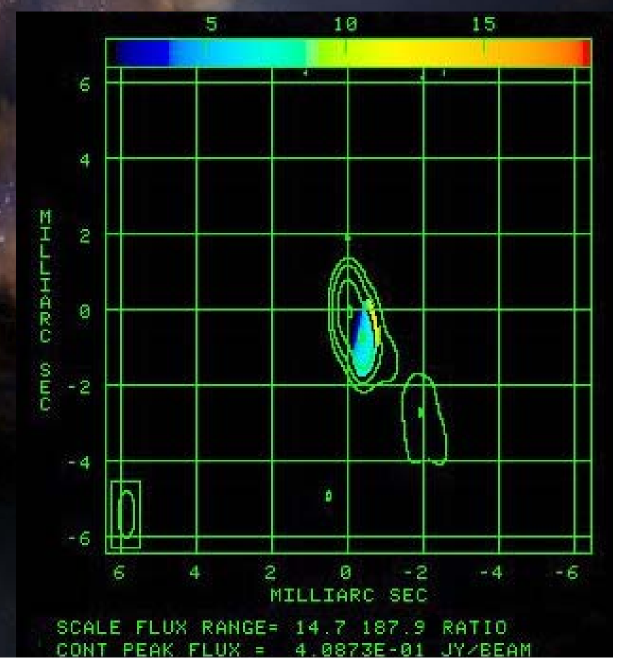

2155-152 (November 2004)

Spectral index maps

Combined from
15Ghz and 22Ghz
intensity maps

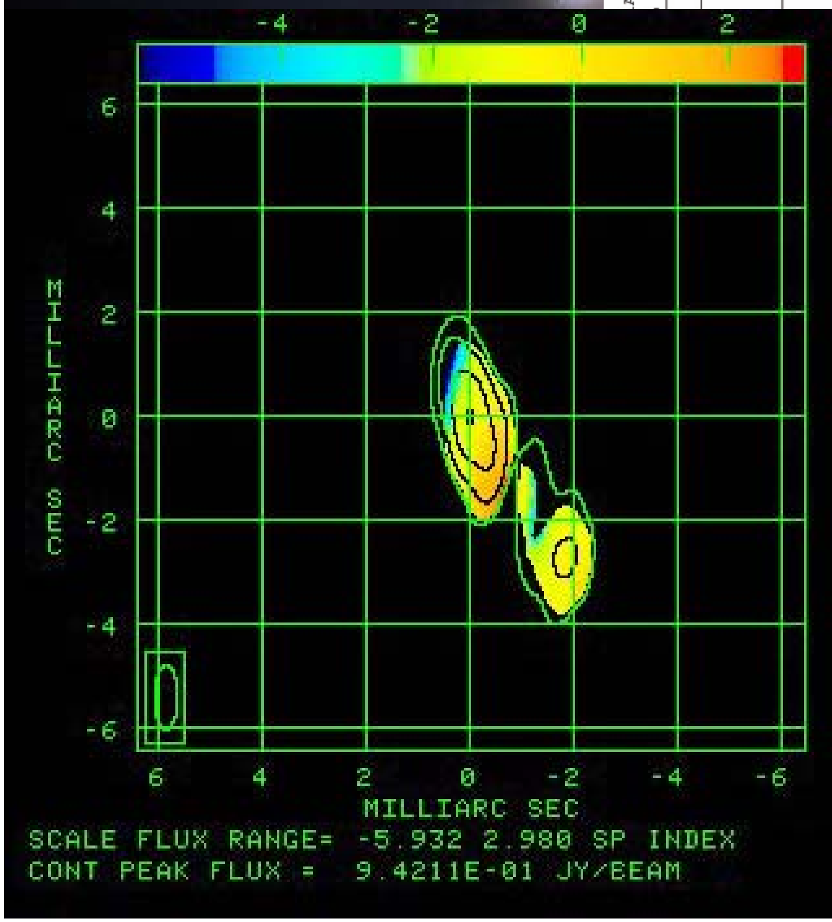

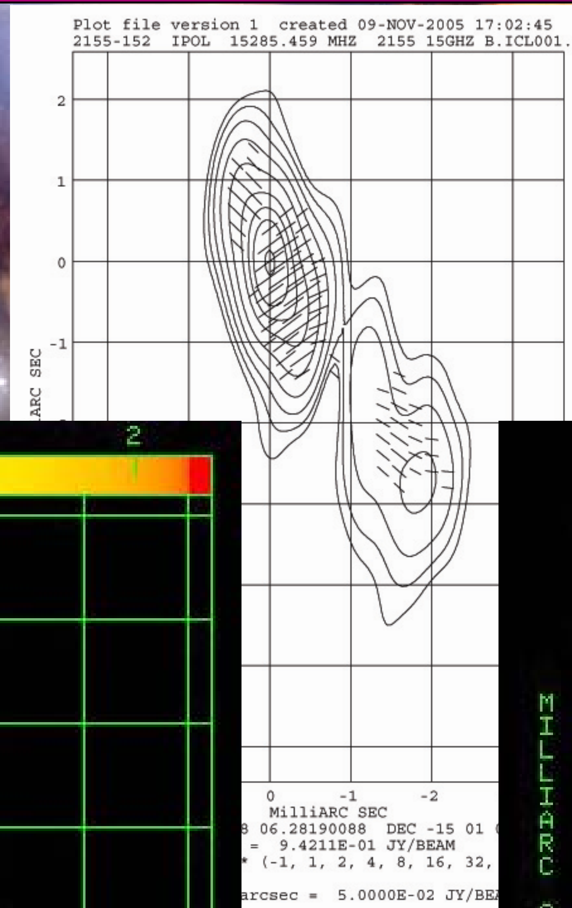

Combined from
22Ghz and 43Ghz
intensity maps

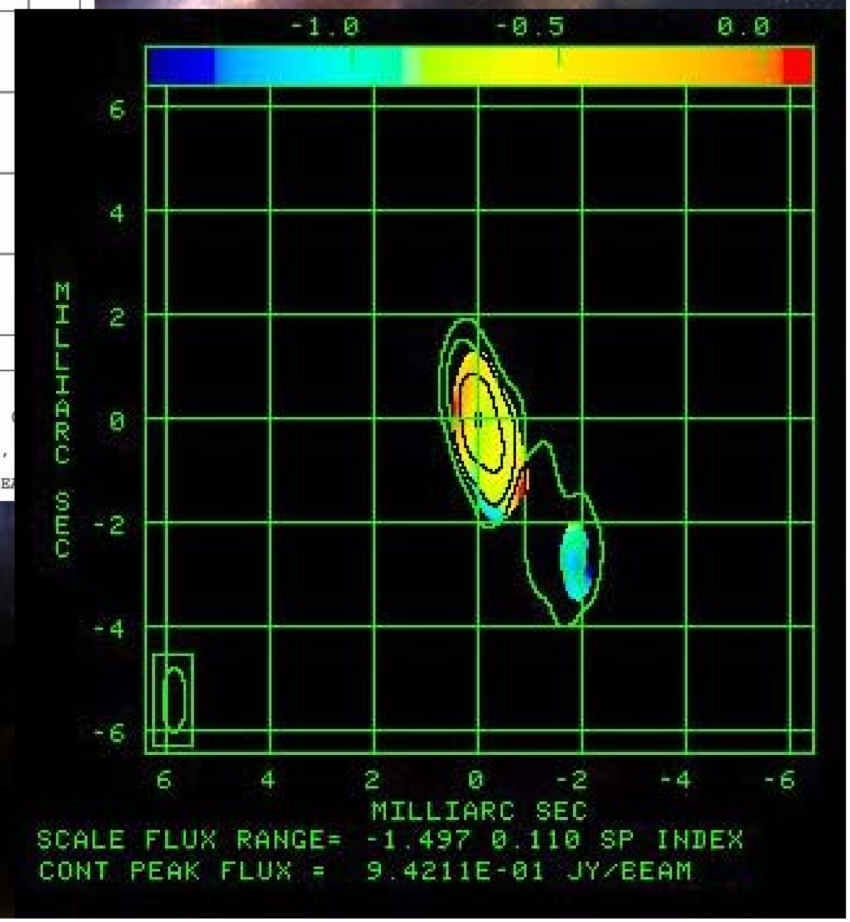

2155-152 (November 2004)

Rotation measure map

Made from
15Ghz, 22Ghz and 43Ghz

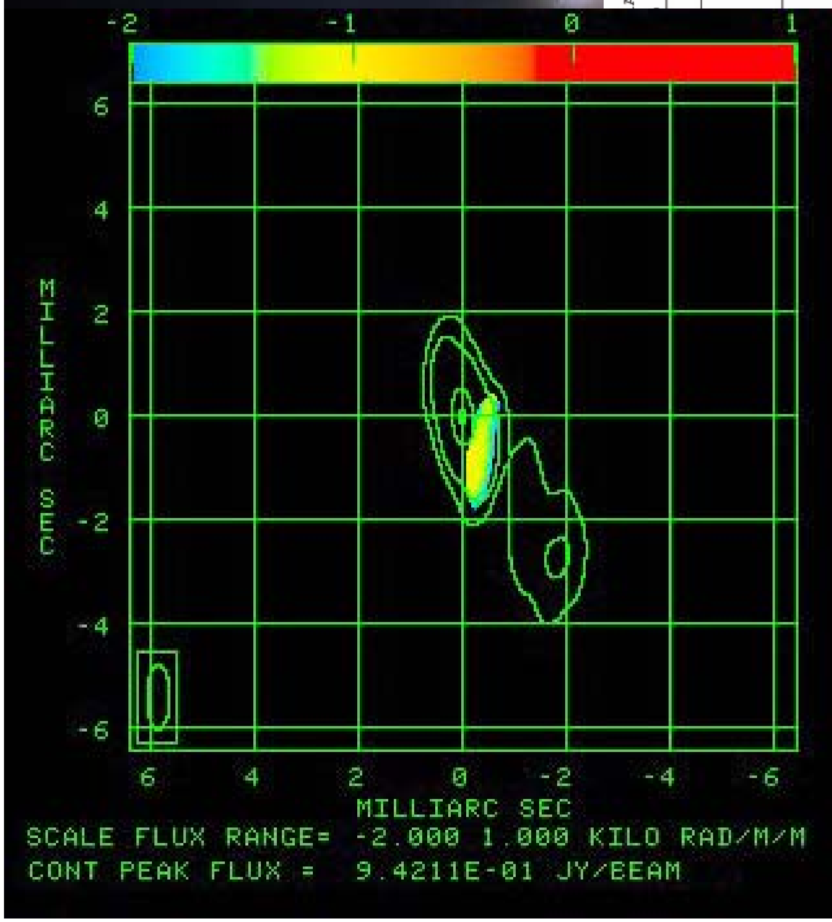

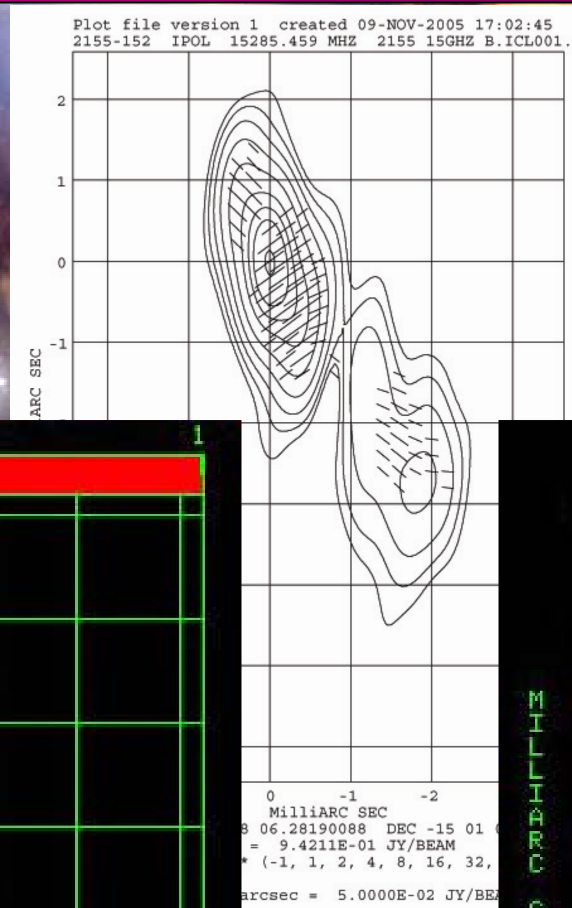

Made from
15Ghz and 22Ghz

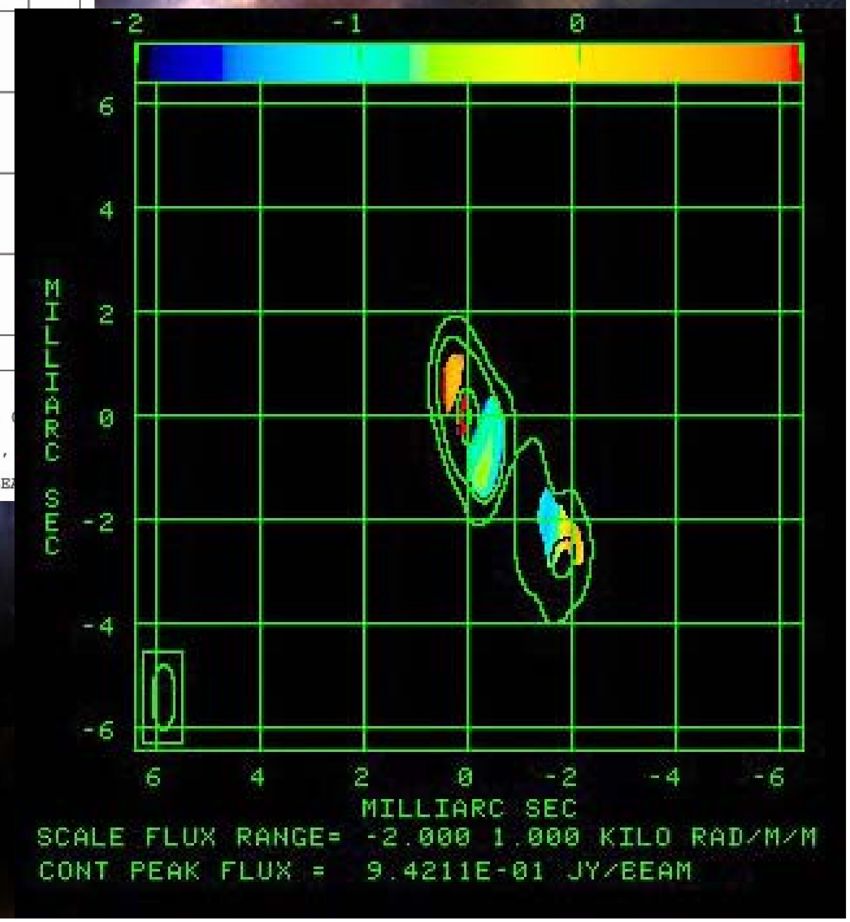

Summary

- All sources are weakly polarized in the core in all frequencies
- All sources have typical behavior in spectral index (optically thick core, optically thin jets)
- All sources reveal high RM in their cores with typical values of ~ 1000 rad/m^2

Sources		Fractional polarization		Spectral Index		Rotation measure
		Core	Jet	Core	Jet	
0745+241	15 Ghz	< 3%	< 18%	~ 0.5	~ -0.8	-1000 – 1000 Rad/m^2
	22 Ghz	< 3%	< 20%			
	43 Ghz	< 3 %	< 15%	~ - 0.3	~ -1.0	
0851+202 (OJ287)	15 Ghz	< 8%	< 22%	~0.5 – 0.8	-1 – -.08	< 1000 Rad/m^2
	22 Ghz	< 5%	< 12%			
	43 Ghz	< 4%	–	~ 0.5	~ -1	
2155-152	15 Ghz	< 5%	< 20%	~ 0.7	~ -1	< 1500 Rad/m^2
	22 Ghz	< 4%	8 – 18 %			
	43 Ghz	< 4%	< 8 %	~ 0.5	~ -1.1	

Introduction

Project background

Current status

0745+241

2155-152

OJ287

Summary

Future work

1) Finish remaining images and model fit;

2) Joint Analysis of intensity and polarization images at three frequencies.

VSOP Polarization observation of 3C380

Andreas Papageorgiou
Cork Institute of Technology

6th ENIGMA Meeting

Kinsale, Nov 2005

Introduction

- Initial experiment: 1.6 GHz Space VLBI (VSOP) polarization observation of 3C380
  - Study the extended jet structure in 3C380 in total and polarized intensity at the highest resolution at that frequency so far.
  - “Exercise” in VSOP Polarimetry (VSOP polarimetry performed before but majority of sources were compact. 3C380 on the other hand has a continuous, smooth pc-scale jet)

Introduction

- Initial scope of the experiment extended by the inclusion of a 5 GHz observation of 3C380 (kindly provided by Antonios Polatidis).
- Observation of 3C380 turned multi-frequency
  - Spectral Index
  - Faraday Rotation
  - Magnetic Field
- One little problem. 5GHz was not a polarization observation. No Polarization Calibrators!

VSOP - HALCA

- Halca Antenna:
  - 8m diameter
  - Records only left Circular polarization → polarization mapping needs to be done on the complex plane (visibility plane)
  - Faulty gyros → unable to slew fast enough →Little problem: No polarization calibrators observed, No D-term calibrators observed.
- Halca has small sensitivity → Careful baseline weighting, even more so for polarization.

3C380

- Redshift: z=0.692
- FR Class: Compact Steep-Spectrum (CSS)
- Scale: 6.1kpc $arcsec^{-1}$ (H_o=75 km s^{-1} q_o=0.1)
- On kpc scales: One sided jet with two bright knots (radio and optical) (O'Dea et al. 1999) embedded in a diffuse halo (Wilkinson et al. 1991)
- On pc scales: Twisted one-sided radio jet and superluminal components (Polatidis & Wilkinson 1998).

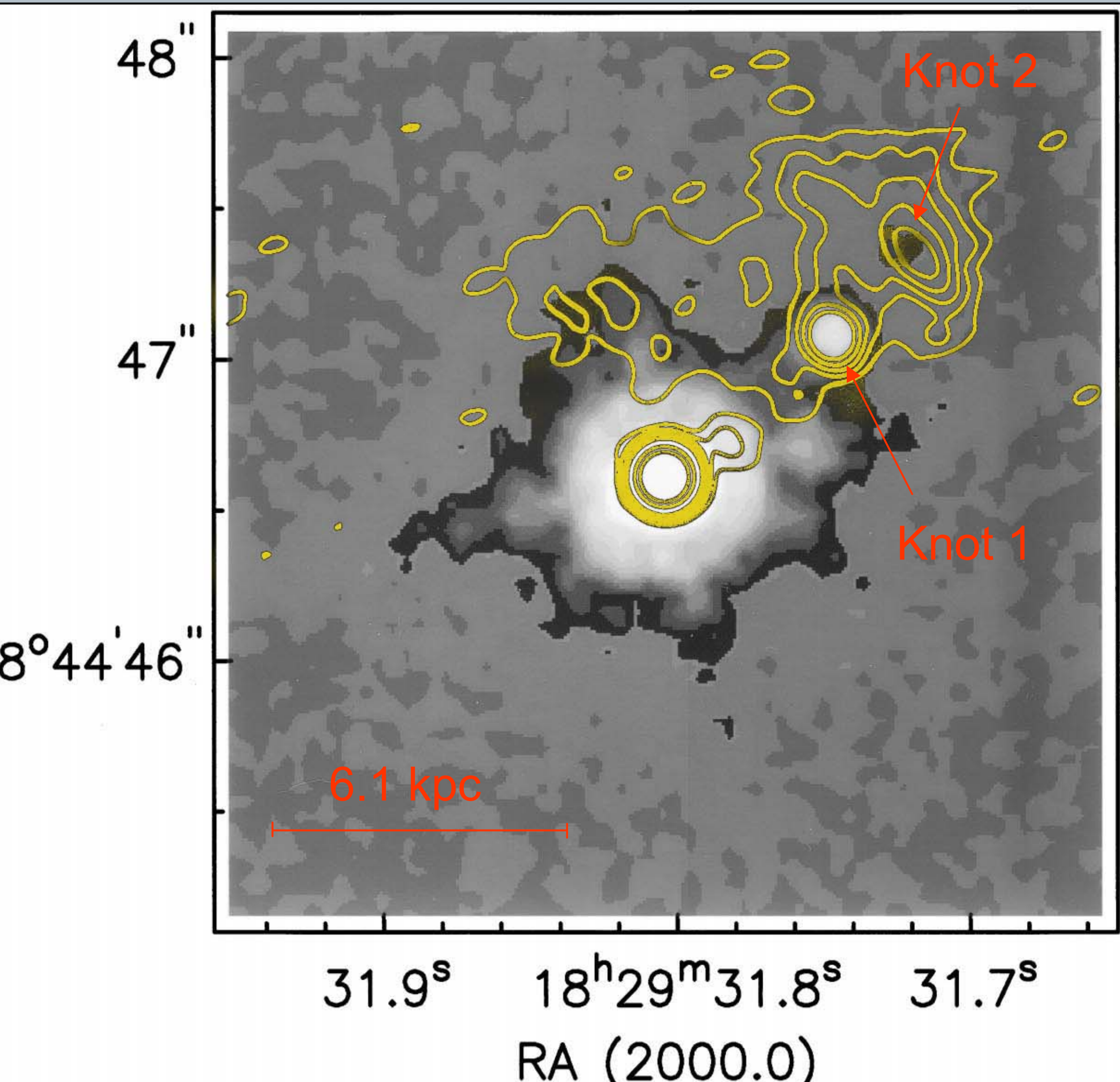

- The two knots are dominated by continuum light instead of emission lines.
- Cannot distinguish between mechanisms for optical continuum (Due to absence of optical polarization).
- Because of one-to-one radio-optical morphological correspondence and continuum emission, assume optical is due to synchrotron.

O’Dea et al, 1999AJ, 117, 1143

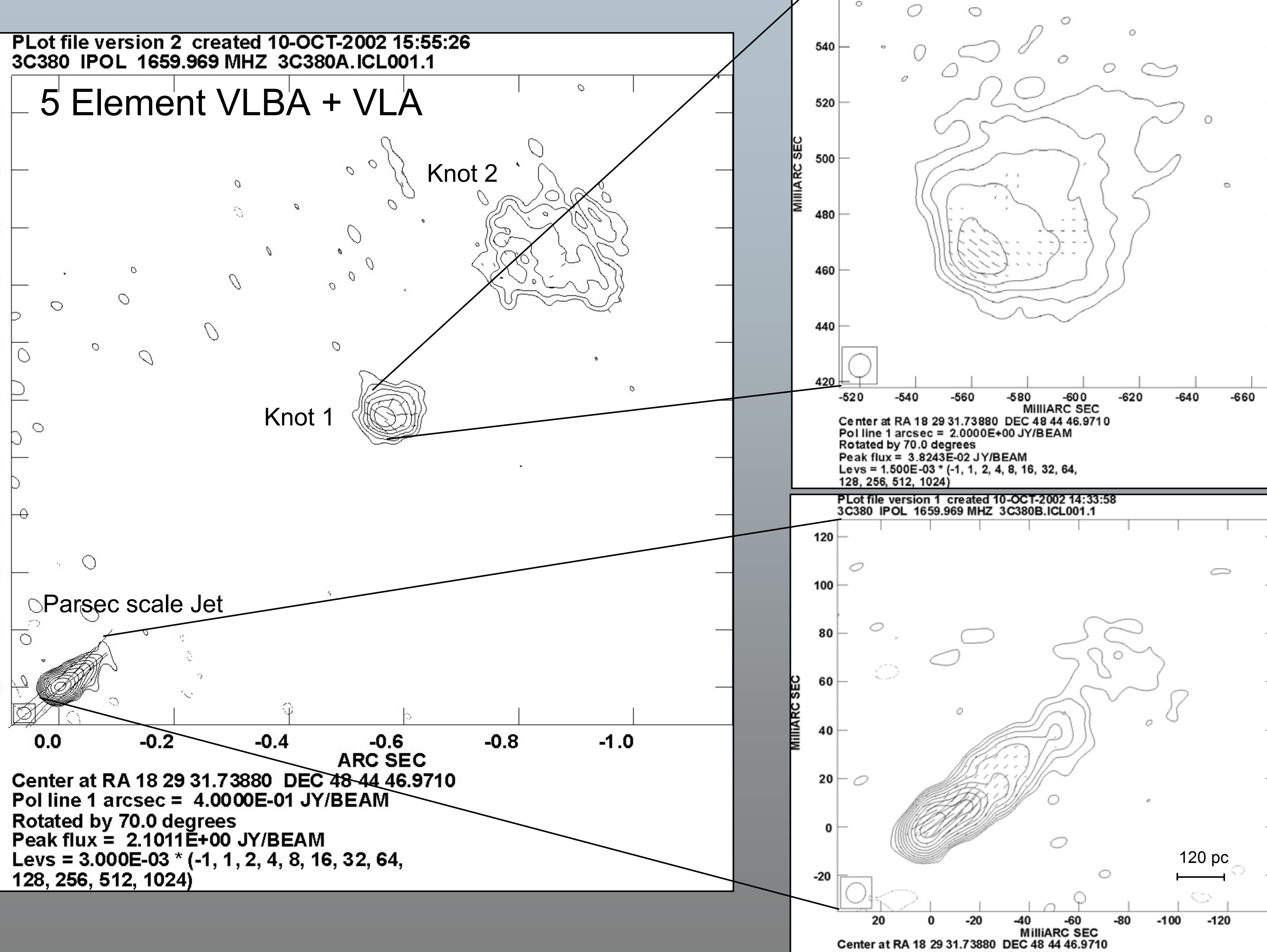

PLot file version 2 created 10-OCT-2002 15:55:26
3C380 IPOL 1659.969 MHZ 3C380A.ICL001.1
5 Element VLBA + VLA
Knot 2
Knot 1
Parsec scale Jet
0.0
-0.2
-0.4
-0.6
-0.8
-1.0
ARC SEC
Center at RA 18 29 31.73880 DEC 48 44 46.9710
Pol line 1 arcsec = 4.0000E-01 JY/BEAM
Rotated by 70.0 degrees
Peak flux = 2.1011E+00 JY/BEAM
Levs = 3.000E-03 * (-1, 1, 2, 4, 8, 16, 32, 64, 128, 256, 512, 1024)
MilliARC SEC
540
520
500
480
460
440
420
-520
-540
-560
-580
-600
-620
-640
-660
MilliARC SEC
Center at RA 18 29 31.73880 DEC 48 44 46.9710
Pol line 1 arcsec = 2.0000E+00 JY/BEAM
Rotated by 70.0 degrees
Peak flux = 3.8243E-02 JY/BEAM
Levs = 1.500E-03 * (-1, 1, 2, 4, 8, 16, 32, 64, 128, 256, 512, 1024)
PLot file version 1 created 10-OCT-2002 14:33:58
3C380 IPOL 1659.969 MHZ 3C380B.ICL001.1
MilliARC SEC
120
100
80
60
40
20
0
-20
120 pc
20
0
-20
-40
-60
-80
-100
-120
MilliARC SEC
Center at RA 18 29 31.73880 DEC 48 44 46.9710

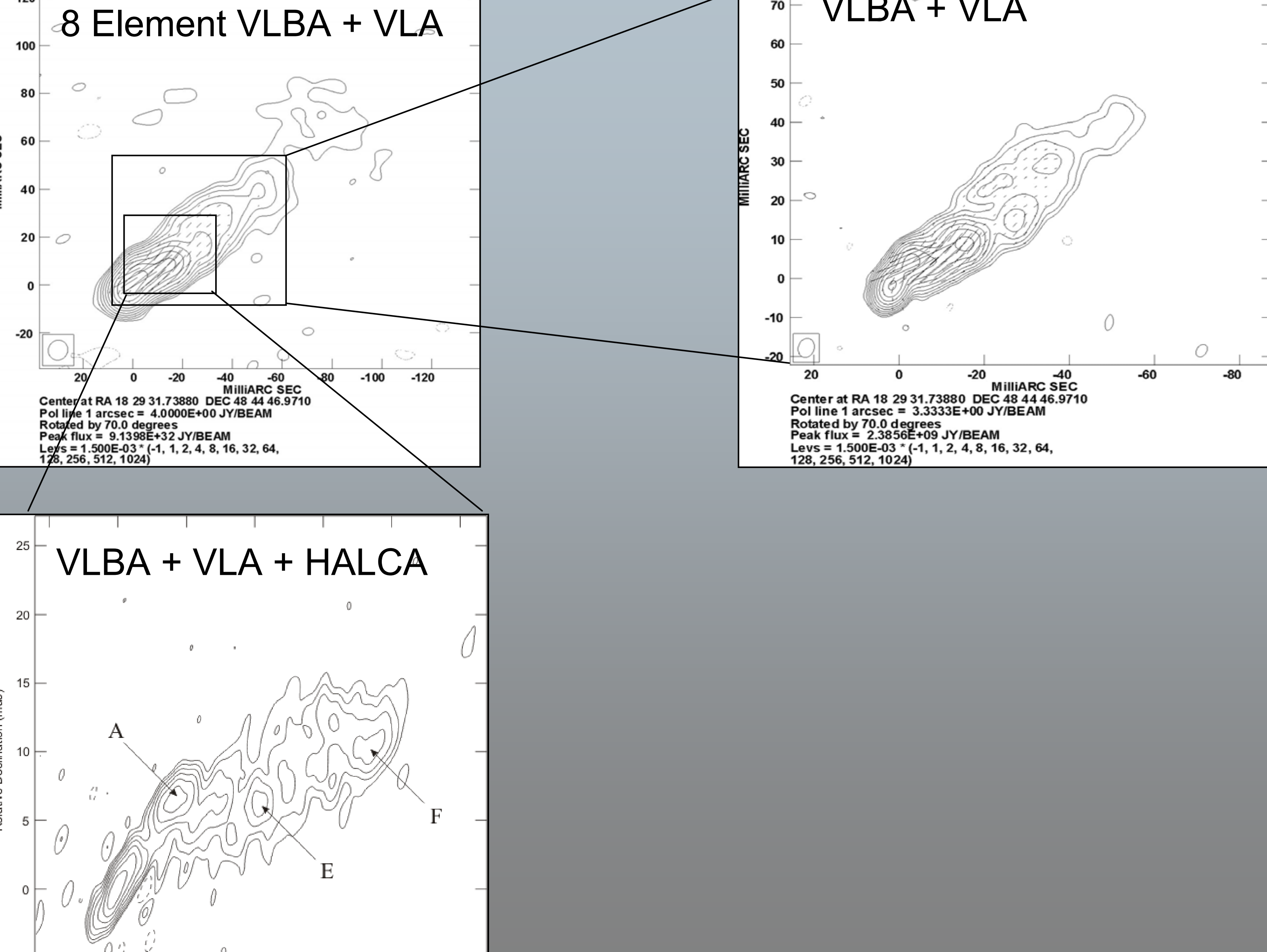
8 Element VLBA + VLA
VLBA + VLA
VLBA + VLA + HALCA
MilliARC SEC
Center at RA 18 29 31.73880 DEC 48 44 46.9710
Pol line 1 arcsec = 4.0000E+00 JY/BEAM
Rotated by 70.0 degrees
Peak flux = 9.1398E+32 JY/BEAM
Levs = 1.500E-03 * (-1, 1, 2, 4, 8, 16, 32, 64, 128, 256, 512, 1024)
MilliARC SEC
Center at RA 18 29 31.73880 DEC 48 44 46.9710
Pol line 1 arcsec = 3.3333E+00 JY/BEAM
Rotated by 70.0 degrees
Peak flux = 2.3856E+09 JY/BEAM
Levs = 1.500E-03 * (-1, 1, 2, 4, 8, 16, 32, 64, 128, 256, 512, 1024)
A
E
F

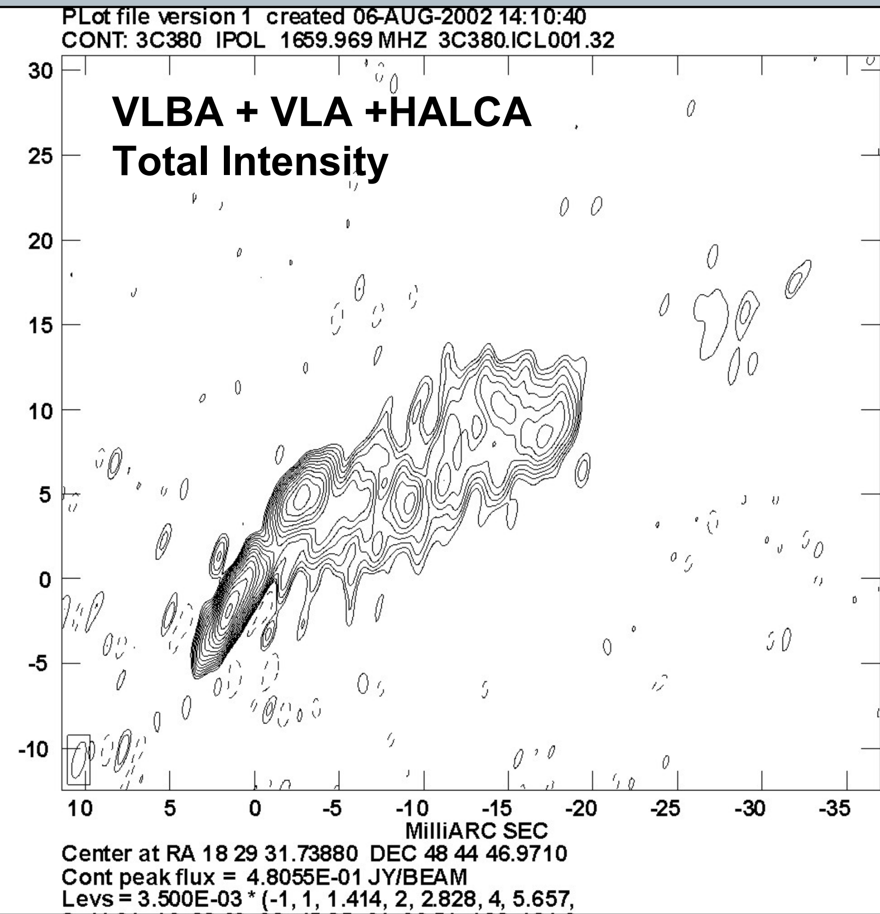

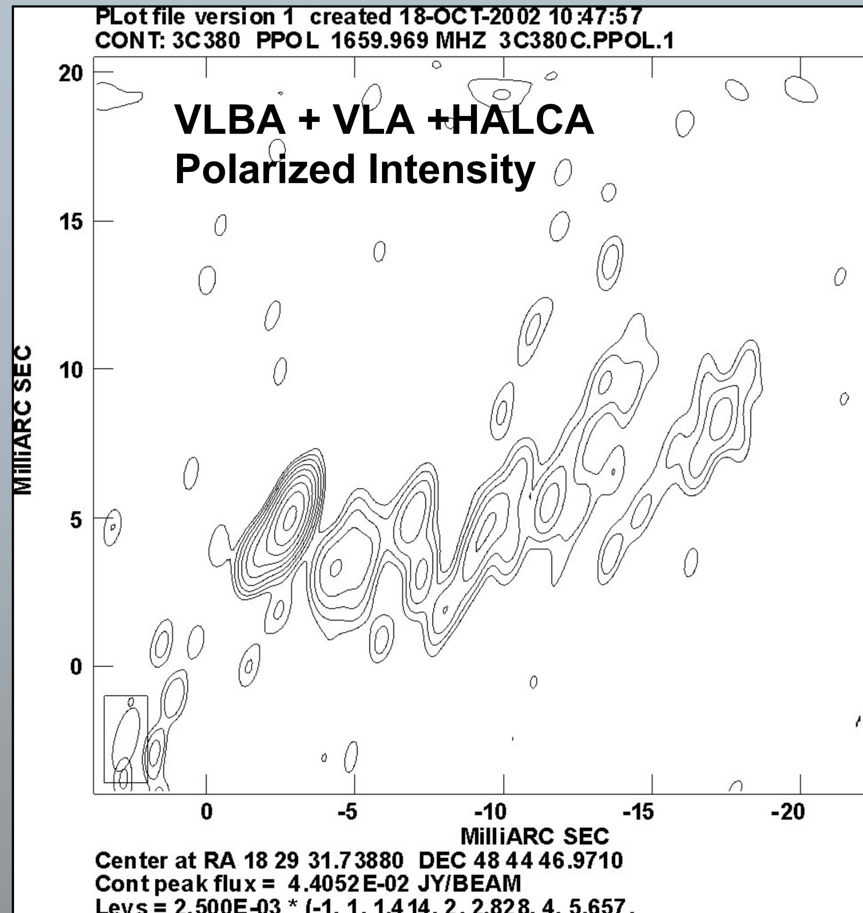

	Beam Size (mas)
VLBA+VLA 1.6 GHZ	4.97 x 3.72
VLBA 5 GHZ	2.14 x 1.37
VLBA+VLA+HALACA 1.6 GHz	2.13 x .074

5GHz EVPA Calibration

This project included observation of 3C279 (seen as a two component object in this frequency)

EVPA Calibration using the UMRAO data for 3C279 produced a systematic offset in the EVPAs (~15^{o}) → this was due to different RM values in the 2 components in 3C279 and 0.19 GHz difference in our observation and the UMRAO

Instead, component C4 was used, by comparing with extrapolated EVPA value in Taylor (1998) – Taylor reports 15GHz EVPA and RM values for C4. Taylor's observations were made 2 months after this work's observations.

Using values uncertainties from Taylor, EVPA calibration was performed with an uncertainty of ~11^{o}

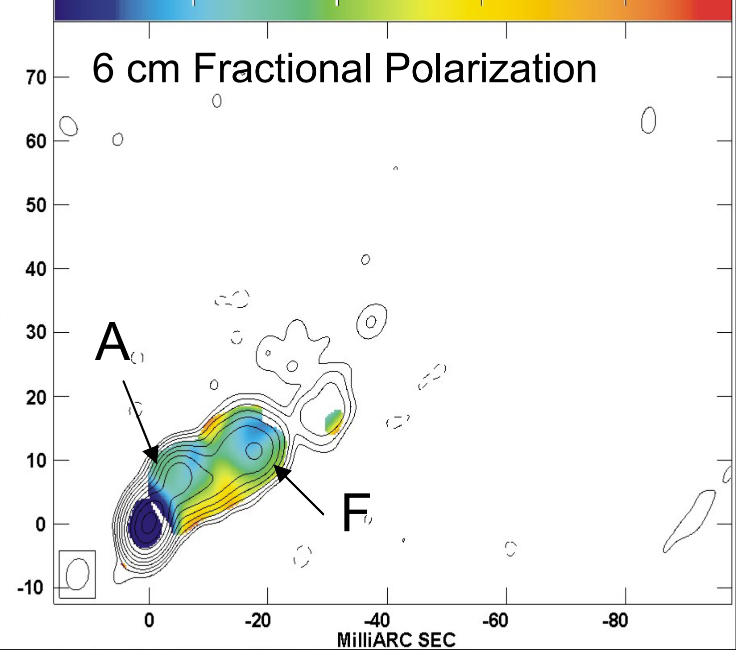
6 cm Fractional Polarization
A
F
MilliARC SEC
70
60
50
40
30
20
10
0
-10
0
-20
-40
-60
-80

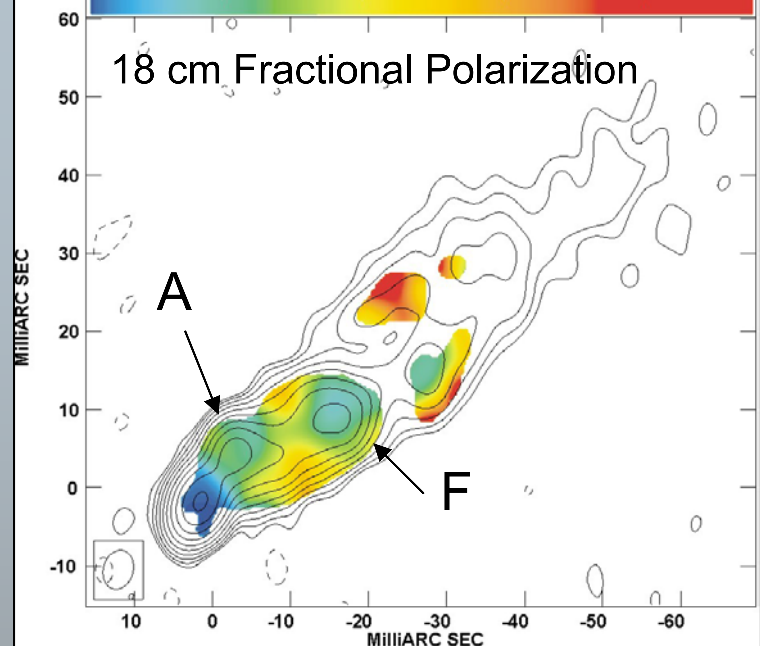
18 cm Fractional Polarization
A
F
MilliARC SEC
MilliARC SEC
60
50
40
30
20
10
0
-10
10
0
-10
-20
-30
-40
-50
-60

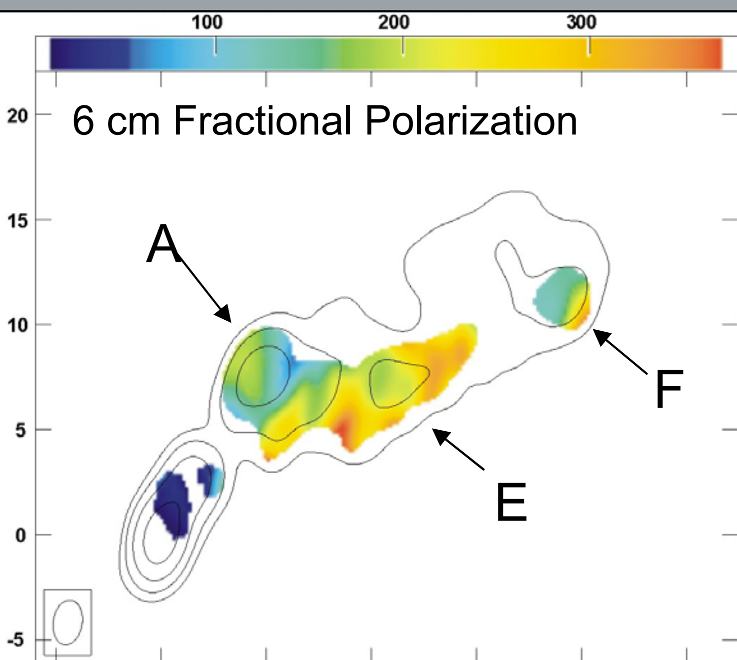
100
200
300
6 cm Fractional Polarization
A
E
F
20
15
10
5
0
-5

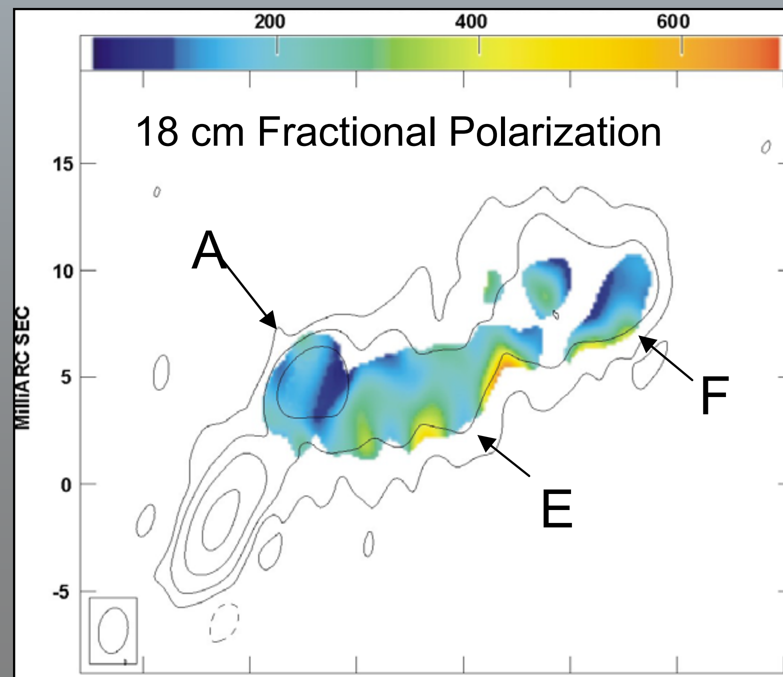
200
400
600
18 cm Fractional Polarization
A
E
F
MilliARC SEC
15
10
5
0
-5

Spectral Index

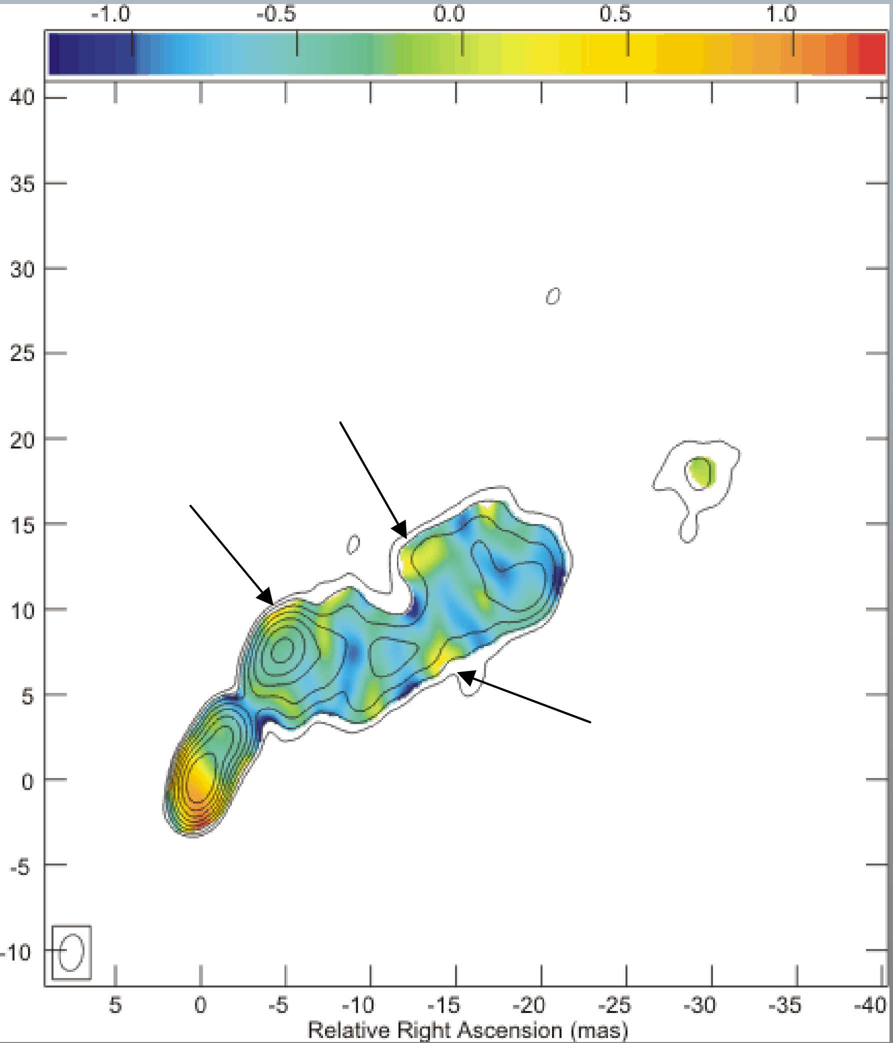

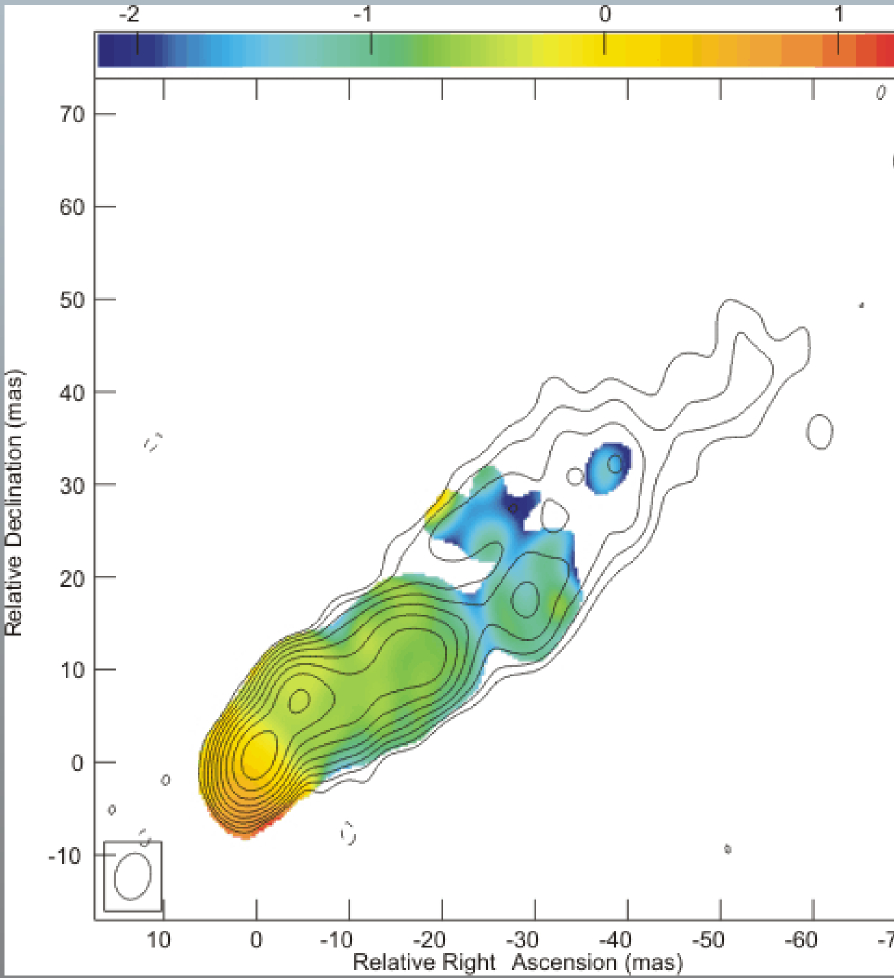

Faraday Rotation

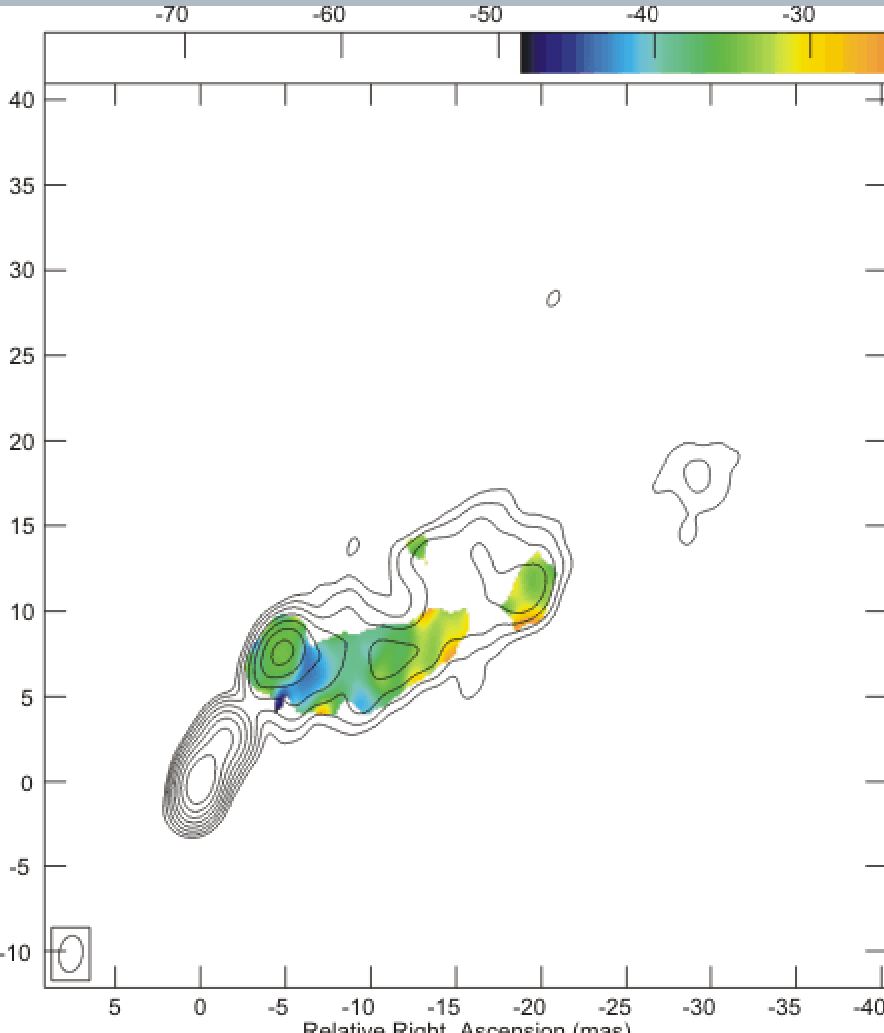

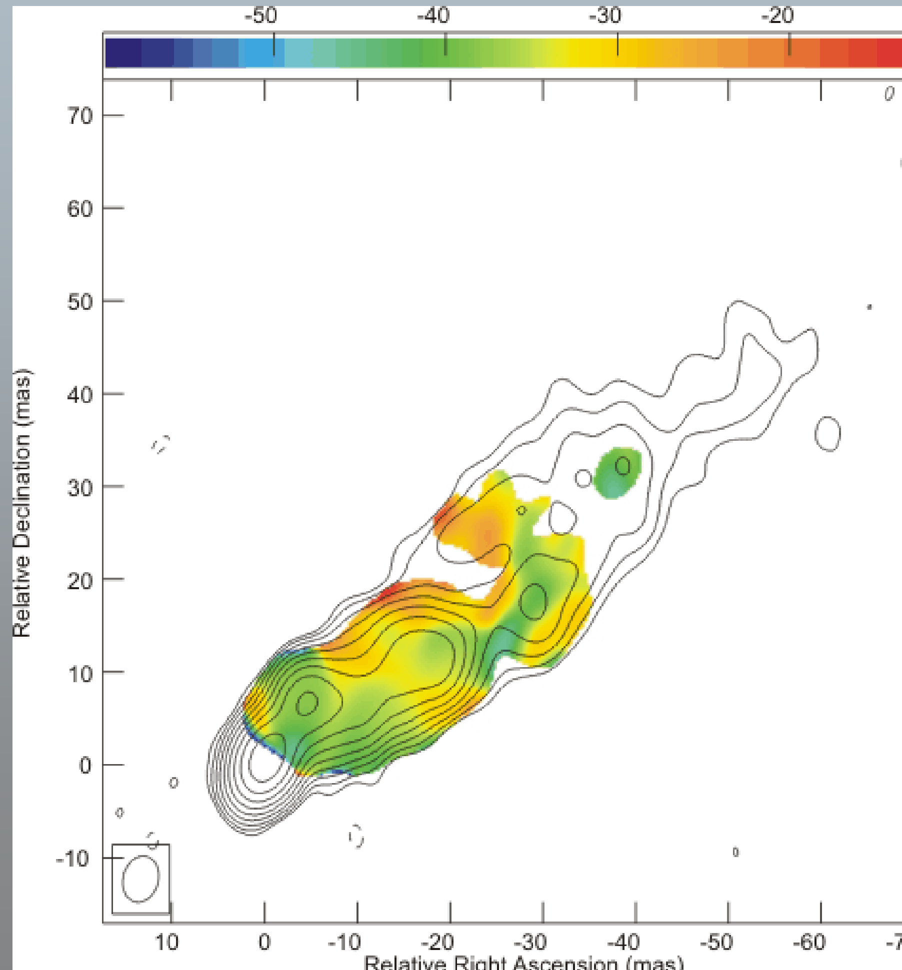

Magnetic Field

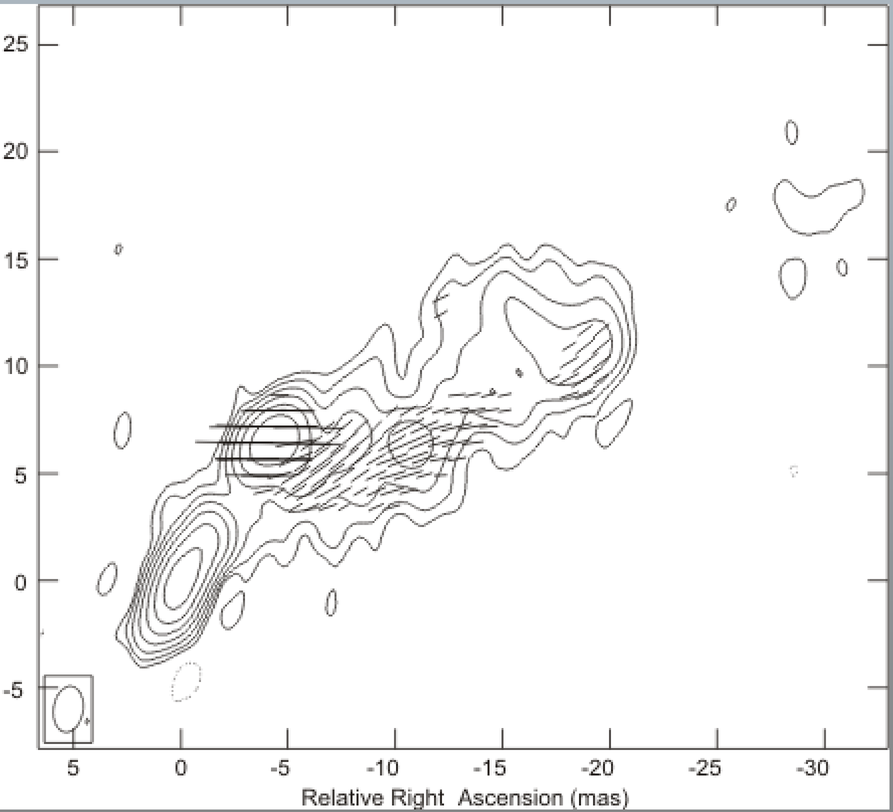

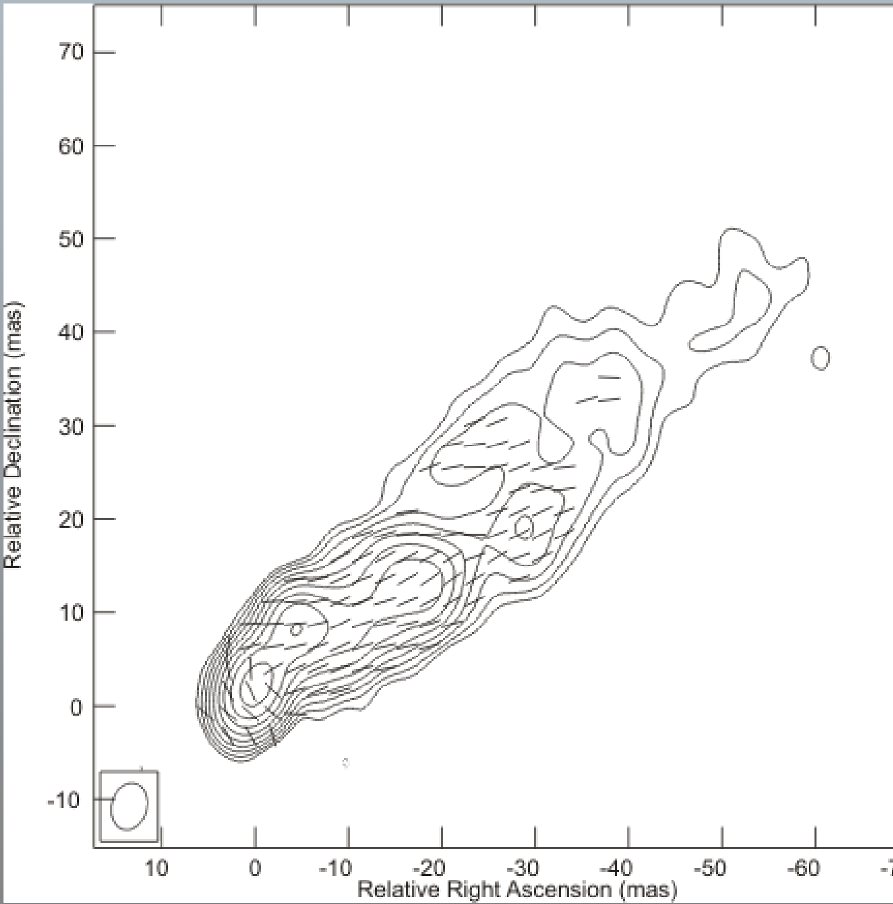

Evolution of component A

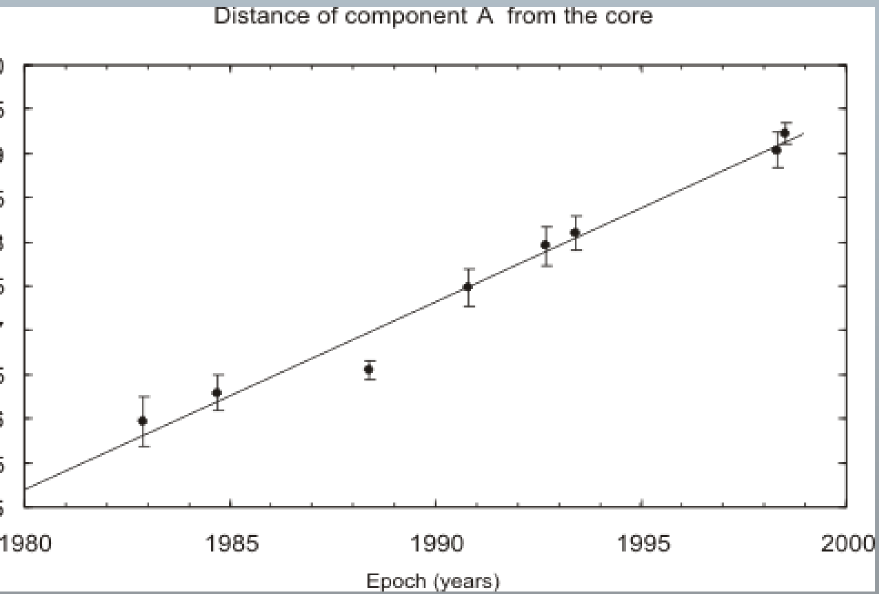

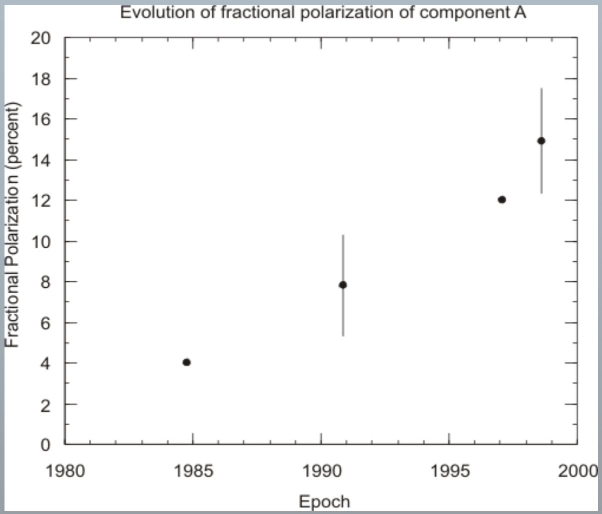

5GHz fractional polarization, rotation measure and projected magnetic field of component A at different epochs.

Epoch	m	σ_m	RM	σ_{RM}	θ_B	$\sigma_{\theta B}$	Reference
1984.8	4	-	-	-	-	-	1
1990.9	7.8	2.5	-	-	-	-	2
1997.1	12	-	4	50	-84	4.3	3
1998.3	14.9	2.6	-35	7	-91	12	4

References: (1) Cawthorne et al. 1993, (2) Cawthorne, unpublished, (3) Taylor 1998, (4) This work

Knot K1

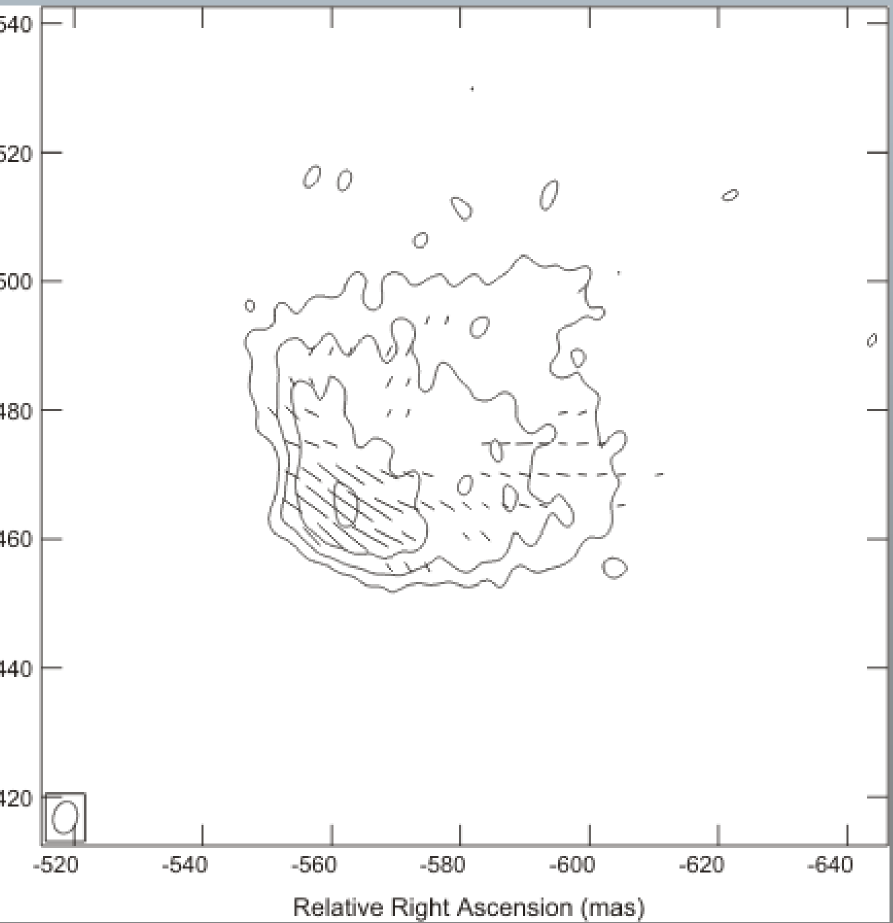

540
520
500
480
460
440
420
-520
-540
-560
-580
-600
-620
-640
Relative Right Ascension (mas)

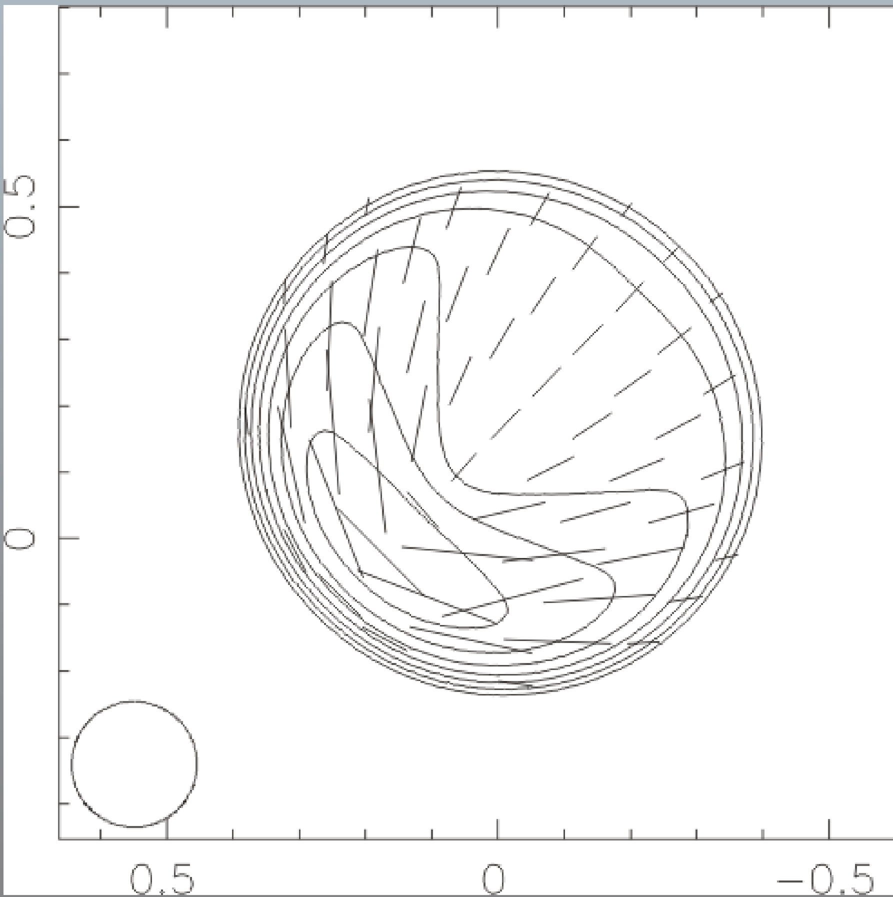

0.5
0
0.5
0
−0.5

Summary

- 3C380 mapped in I and P in 3 scales
- Spectral index map shows regions of inverted spectrum, as also reported by Kameno et al. Error analysis in this work finds them insignificant, although this does not include systematic errors due to different uv sampling (And I wouldn't now how to include them even if I wanted to!)
- Low uncertainty mapping of RM distribution at high frequency → Although structure can be seen it has little significance (1σ)
- Magnetic field structure shows tentative evidence of following jet ridge line
- Possibility of component A interacting with external cloud
  - Magnetic Field at an oblique angle to local jet direction
  - Fractional polarization edge-brightened
  - Fractional polarization on the rise
  - Inverted spectrum at the edge?
  - Absence of RM increase (to within 7 rad m^{-2})
- Knot A shows qualitative similarities to predictions from Conical shock models
- Space VLBI, excellent tool for multifrequency study of extended jet structure

Future Work

- VLBA proposal has been submitted to further study extended knots K1 and K2
- Experiment designed to include smaller baselines these used in this work in order to pick up more polarization at 5GHz (due to source extent, observation is not thermal noise limited)
- Will add further polarization data on the evolution of component A (only 2 published so far)

The OJ 287 polarization monitoring programme at Calar Alto

Jochen Heidt (LSW), Kari Nilsson (Turku)
& the ENIGMA-team

in support of
the OJ2005-2008 campaign

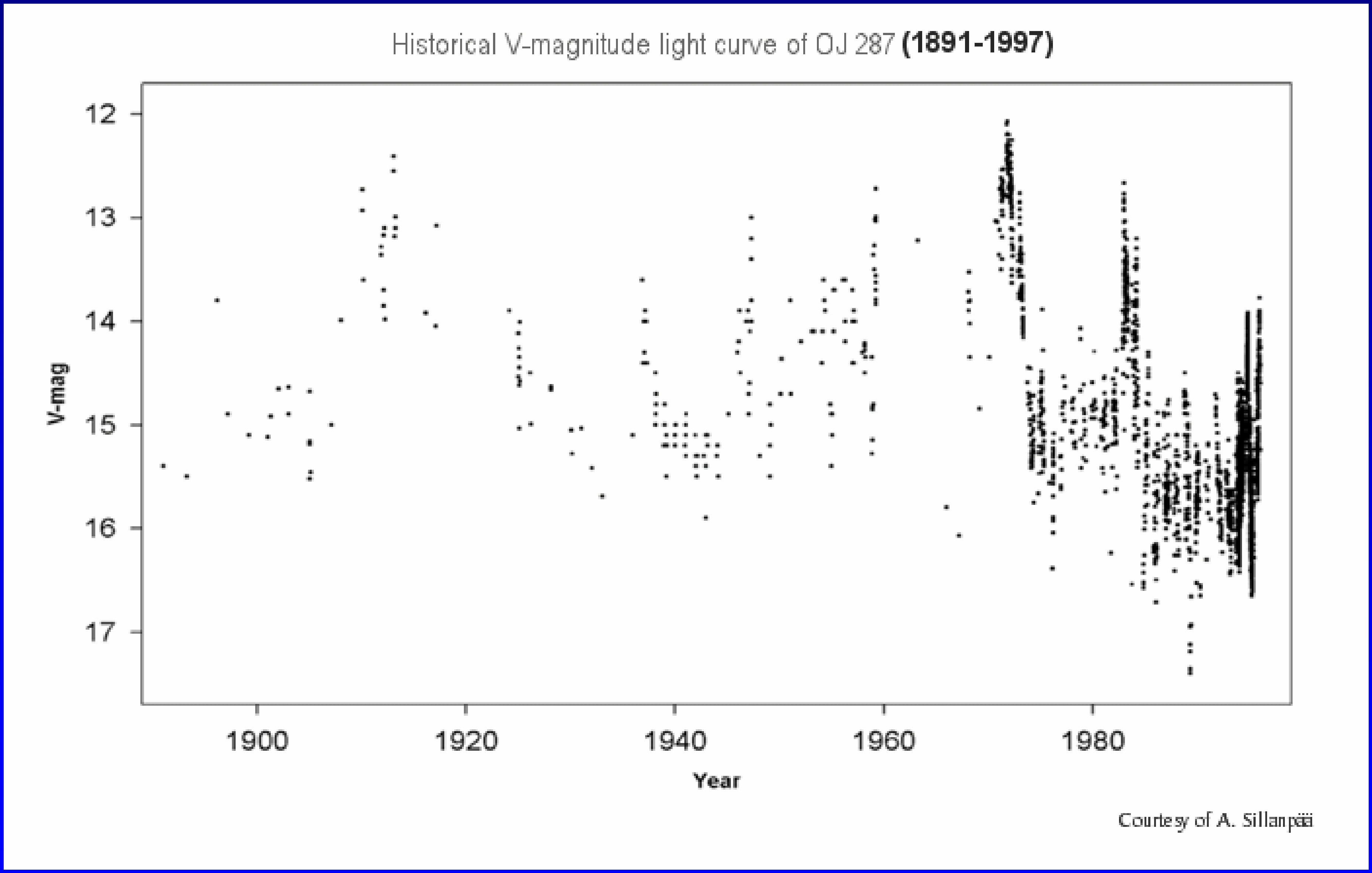
Historical V-magnitude light curve of OJ 287 (1891-1997)
12
13
14
15
16
17
V-mag
1900
1920
1940
1960
1980
Year
Courtesy of A. Sillanpää

Models to be tested

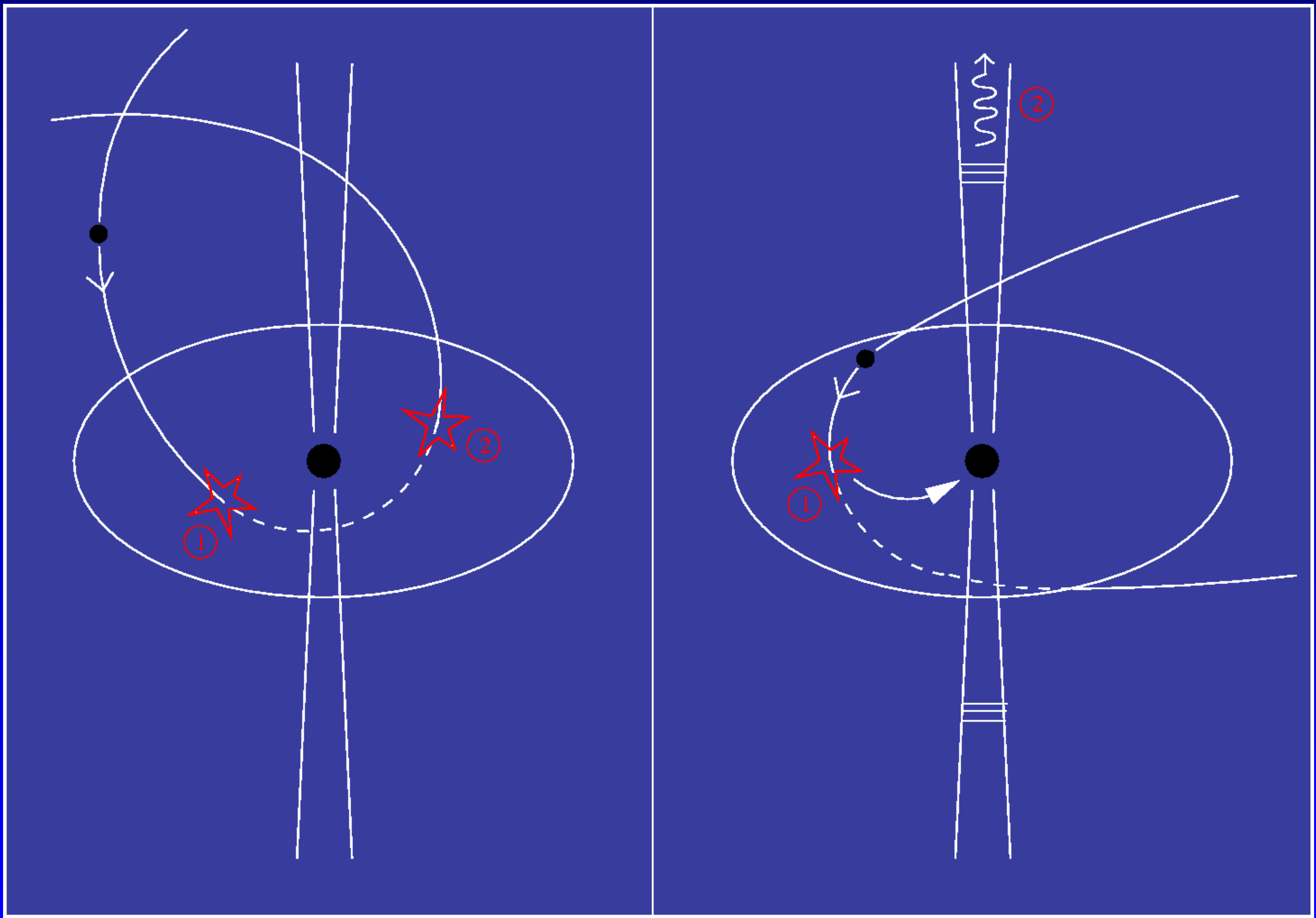

LV (Lehto & Valtonen 1998)   SV (Sillanpää, Valtaoja 1988, 2000)

LV model

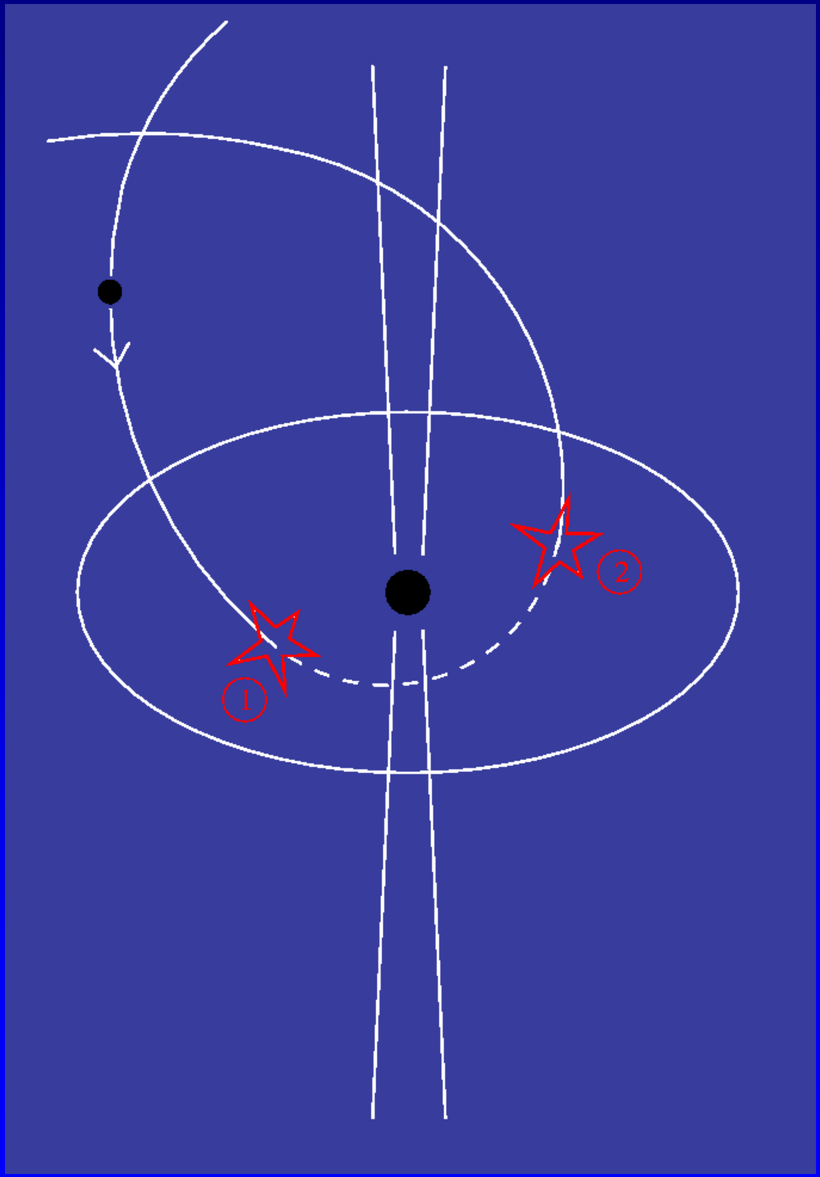

High primary mass ($1.7 \bullet 10^{10} M_{\odot}$)

$P_{orb} = 12.07$ y

Strong precession of the orbit

SV model

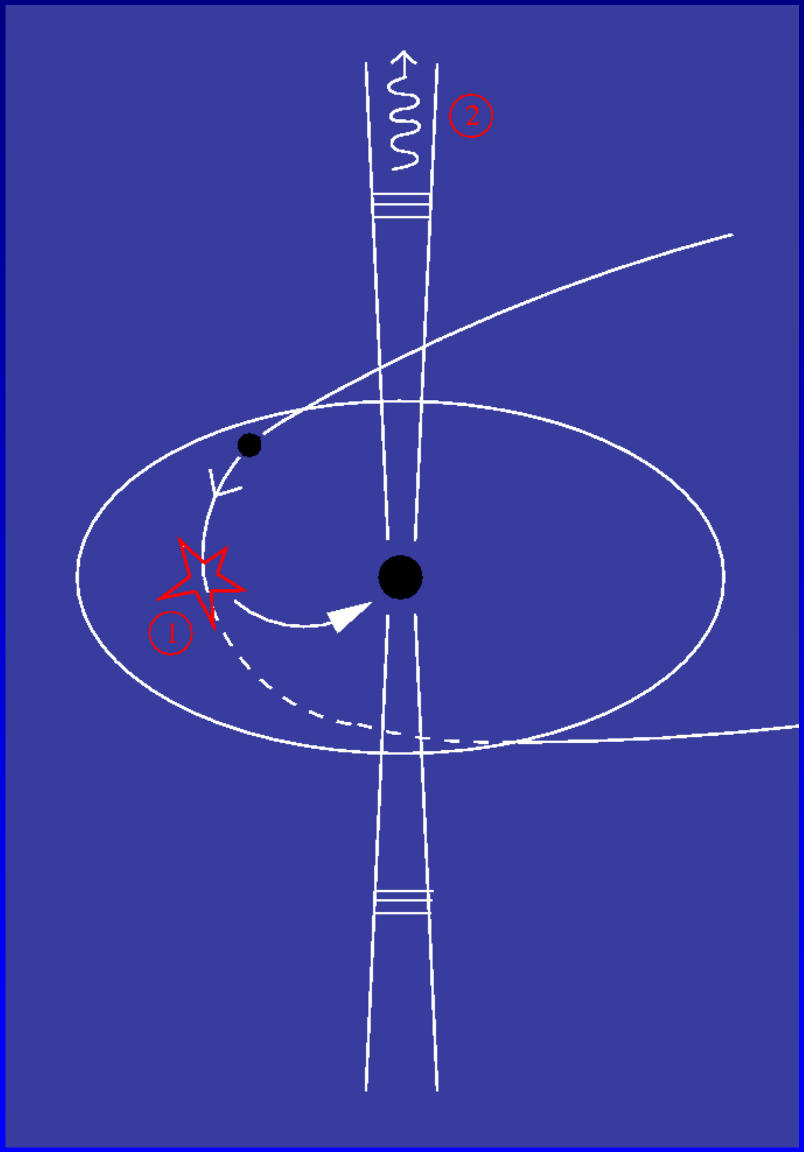

No constraint on BH masses

P_{orb}= 11.86 y

No precession

Different predictions

LV-model		SV-model
Outburst 1:	March 2006	September 2006
	not polarized	not polarized
	P decreases, PA no change (both models)	
Outburst2:	April 2007	October 2007
	not polarized	polarized
	P decreases, PA no change	P changes, PA changes

➔➔ Polarization measurements may help to distinguish between models!!!

The long-term polarization monitoring programme at Calar Alto

Calar Alto, 2.2m telescope + CAFOS equipped with Savart plate

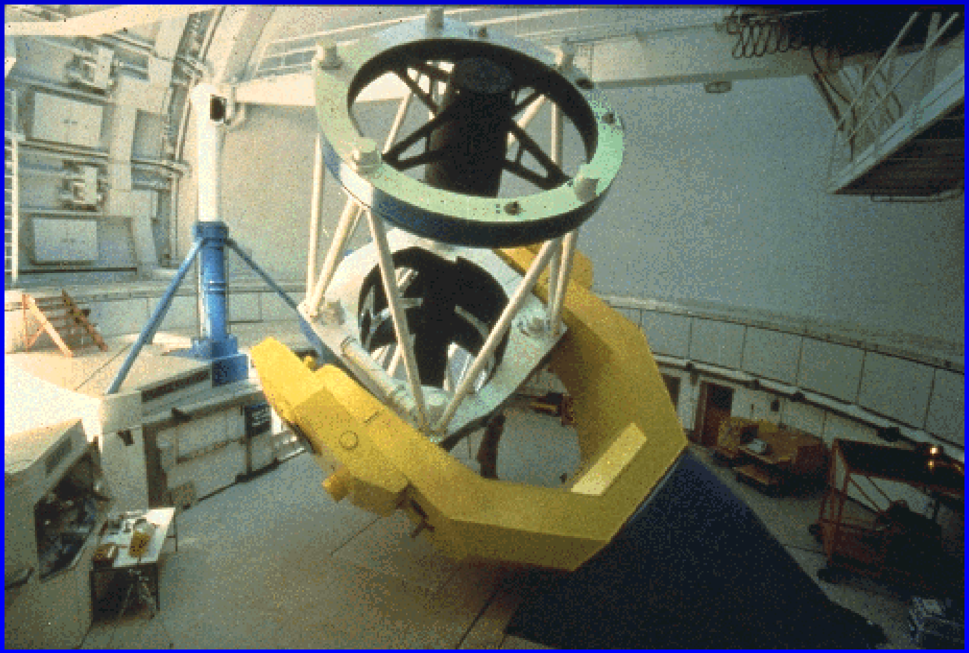

Observing strategy

Running time: Jan 2006 – May 2008

1 measurement every 3rd night in R-filter
(AM < 2, beginning of October until end of May)

~30min per measurement, 4 angles (0, 22.5, 45, 67.5) to derive full set of Stokes parameters ➔ 13n in total

➔ Test observations on Nov, 4th ➔ only 15-20min required

➔➔ consider to refine to B and R (λ-dependent poli)

Logistics (expo-times depending on brightness etc.) via JH,
"online" data reduction/archiving, feeding the WEB by KN

Provide "backbone" of polarization monitoring in combination with KVA

Test observations on Nov, 4

Instrumental parameters:

Polarization: 30%

Pol. ∠ : 15°

R-mag: ~13.5

0° 22.5°

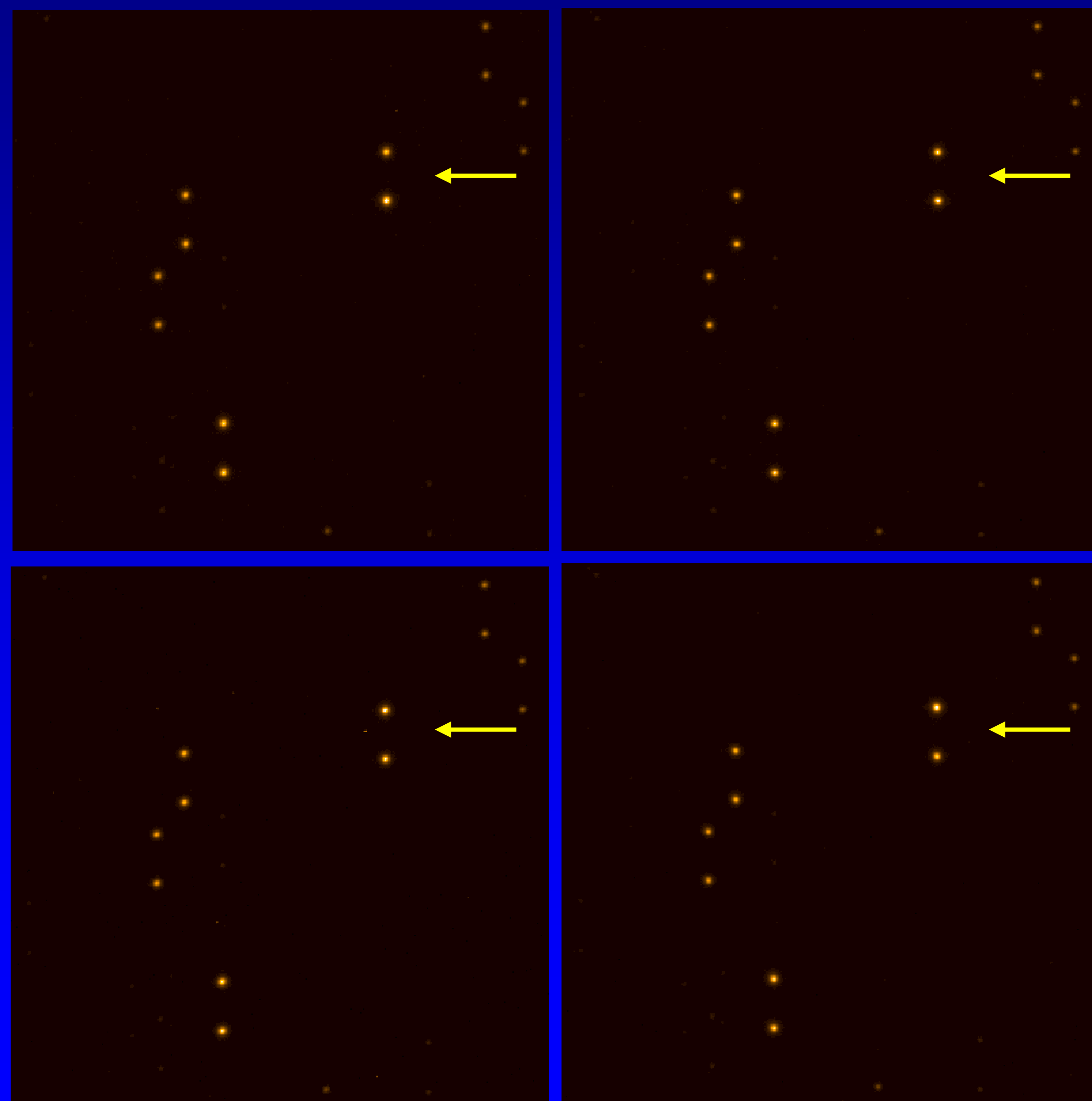

67.5° 45°

NRAO 150: A powerful quasar hidden by the Milky Way

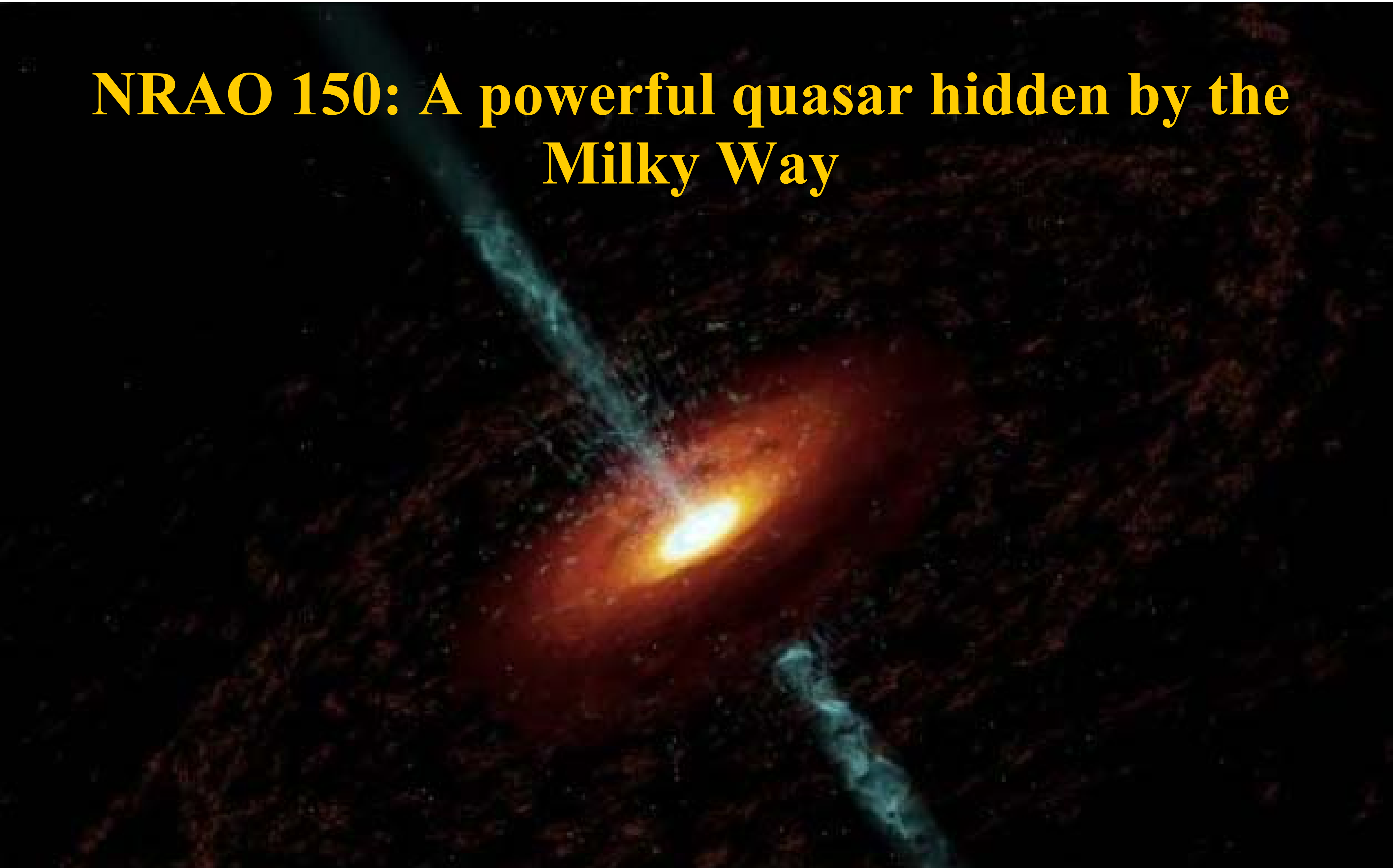

Iván Agudo

in collaboration with

T.P. Krichbaum, U. Bach, D. Graham, W. Alef, A. Pagels, A. Witzel, J.A. Zensus, M. Bremer, M. Grewing, J. A. Acosta, P. Rodríguez-Gil, H. Ungerechts, M. Tornikoski, M. Aller

Max-Planck-Institut für Radioastronomie

MAX-PLANCK-GESELLSCHAFT

Overview of the Talk:

Introduction

- A powerful AGN hidden by the Milky Way

Distance and classification of NRAO150

VLBI results on NRAO 150

- ~120º of inner to outer jet misalignment
- Global mm-VLBI Array
- Fast jet structural position angle rotation
- Is the jet in NRAO 150 rotating periodically?

Some thoughts about fast periodic behaviour

Summary

Introduction: A powerful AGN hidden by the Milky Way

- Intense radio-mm source
- First catalogued by Pauliny-Toth et al. (1966) at 1.4 GHz
- Monitored at radio-mm λ since beginning of the eighties
- Slowly quasi-sinusoidal variability
- Typical variability time scale of ~ 25yr
- ~12 Jy at 1.3cm and ~7 Jy at 3mm

Metsahövi 1 and 1.3 cm

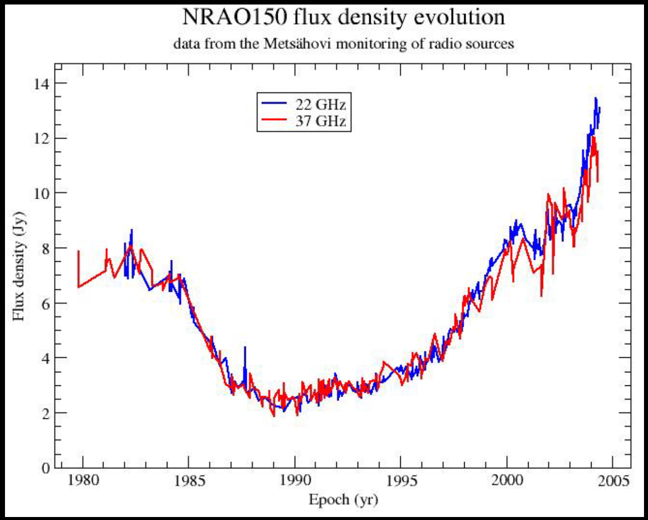

Tornikoski et al.

UMRAO 6, 4 and 2 cm

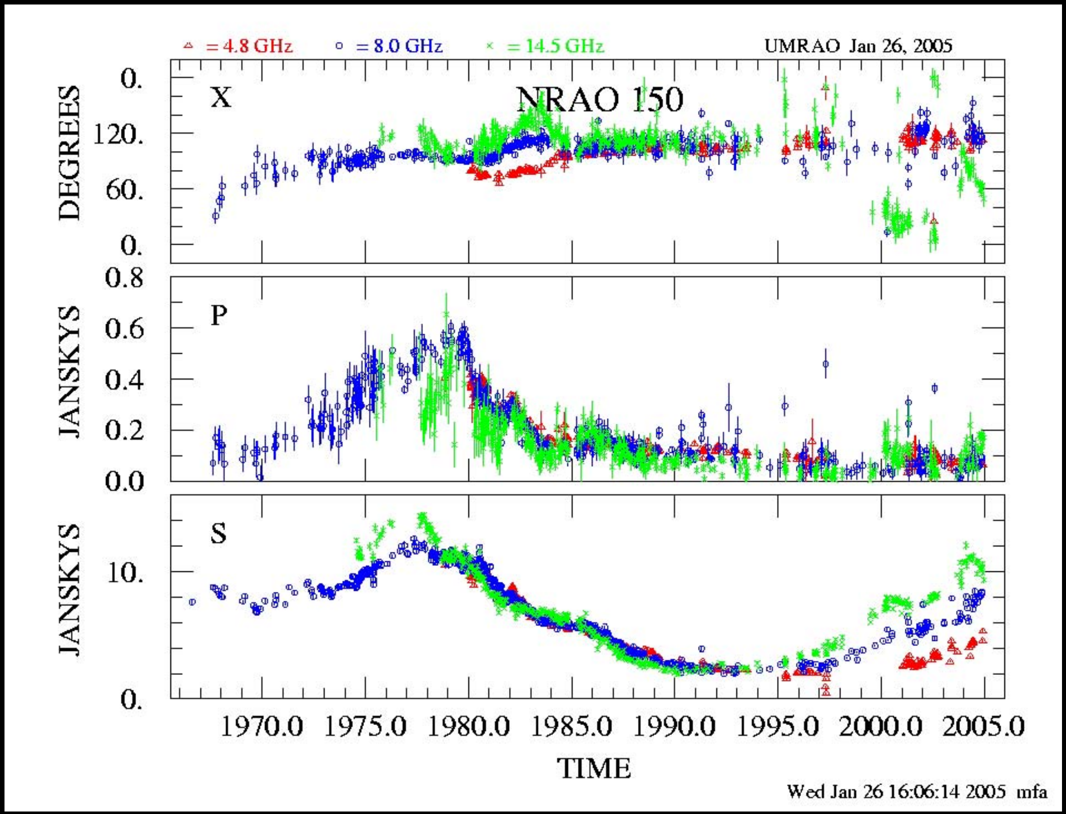

Aller et al.

Pico Veleta 1, 2 and 3 mm

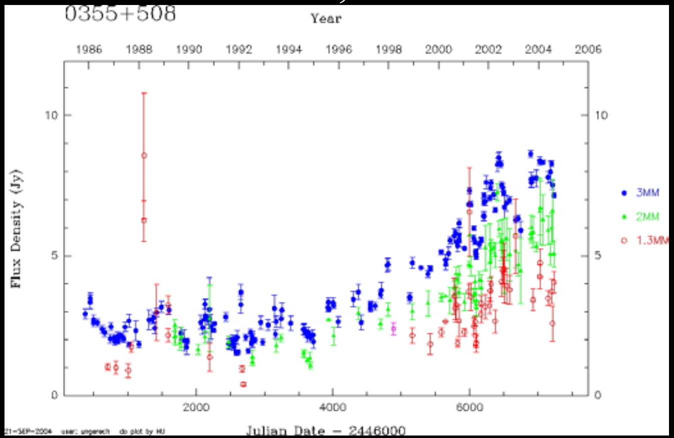

Ungerechts et al.

Introduction: A powerful AGN hidden by the Milky Way

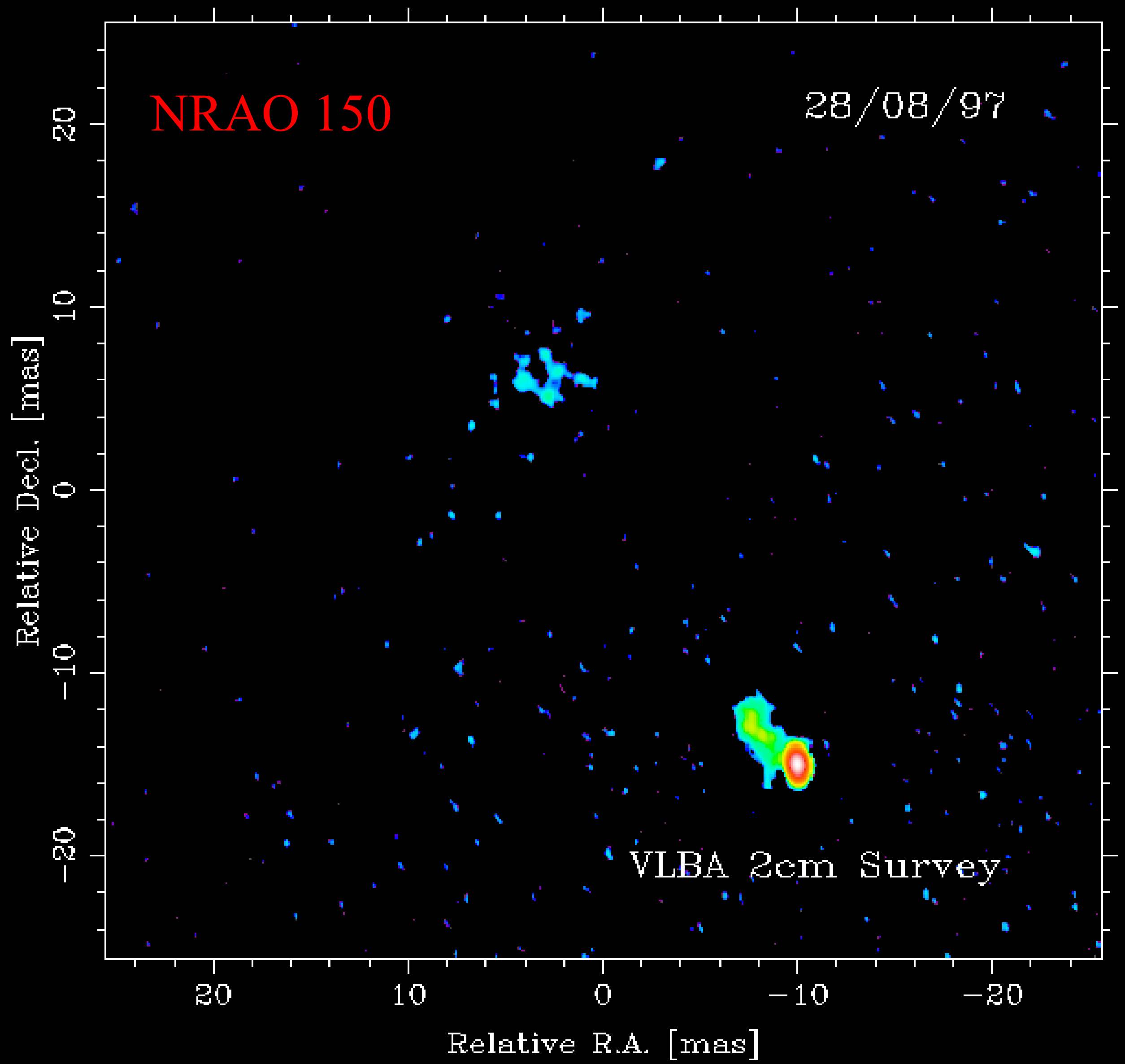

Kellermann et al. (1998)

- cm-VLBI scales shows a core dominated structure
- Jet extended up to ~30 mas to the North-East
- Detected in X-rays by ROSAT (0.1-2.4 keV) Flux $\approx 4.3 \times 10^{-13}$ erg/(cm^{2}s)

Introduction: A powerful AGN hidden by the Milky Way

NRAO 150

R band

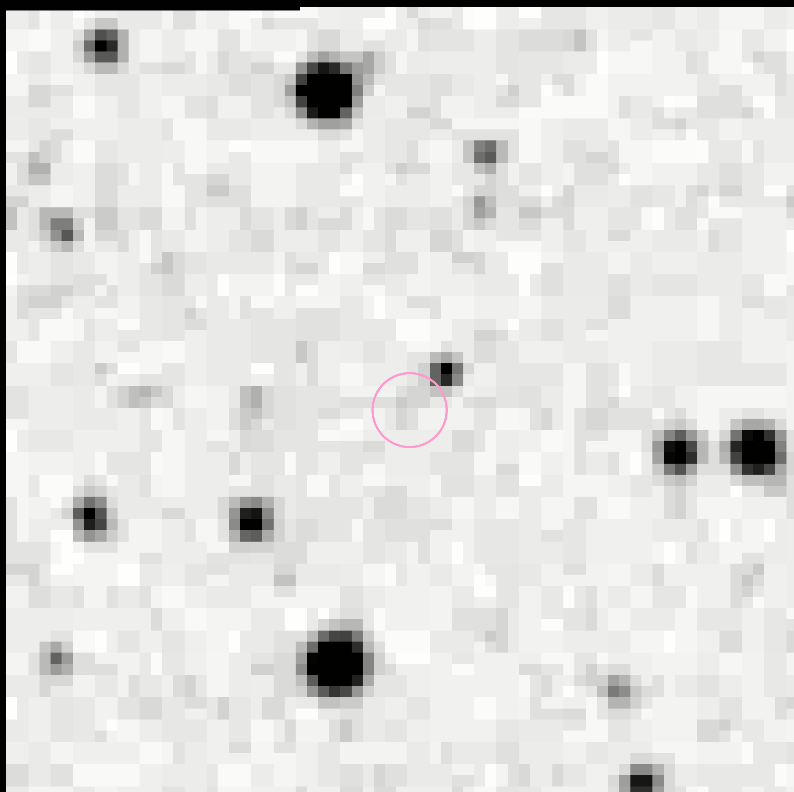

Palomar group (1994)

≈14 mag. in Ks band

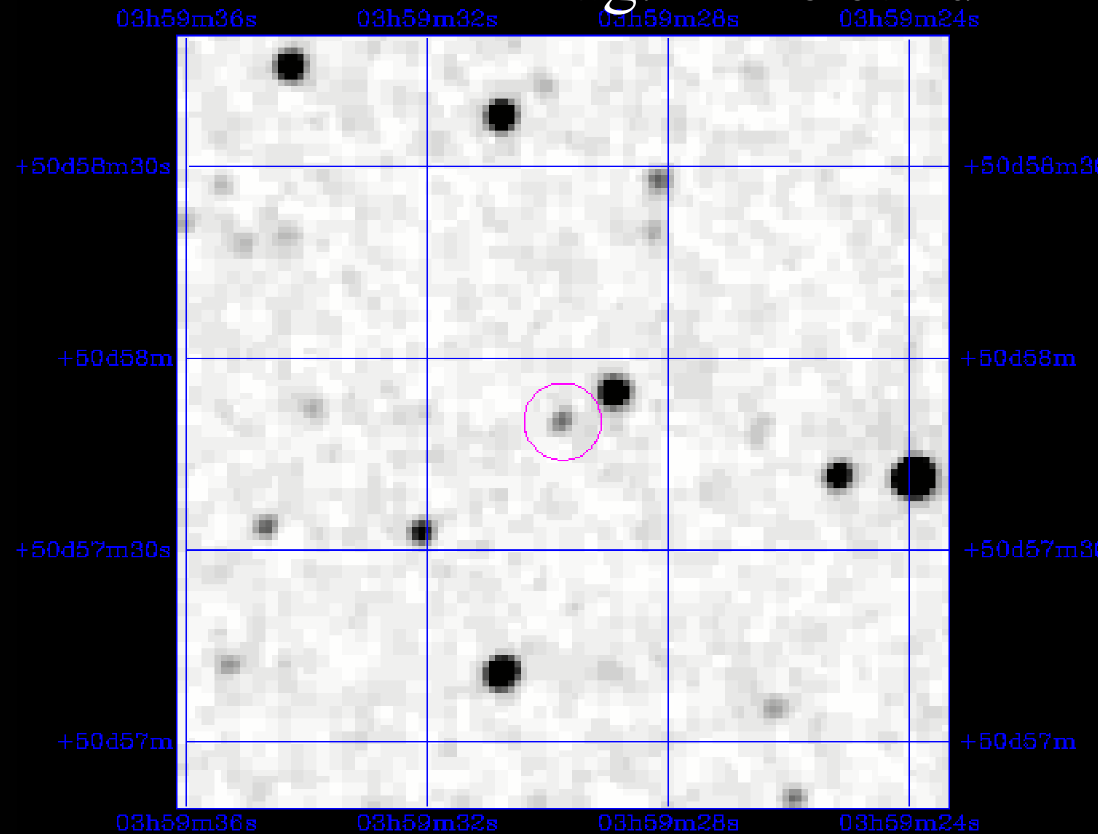

2MASS archive

- Empty field in the Palomar survey
- Source extinction by the Milky Way (Galactic Latitude -1.6º)
- Distance unknown

- Not completely absorbed in the n-IR
- And quite bright. ~14 mag. in Ks band
- Measure its spectrum in the IR in order to determine its *z*?

Distance and classification of NRAO 150

4.2 m William Herschel Telescope
(La Palma, Spain)

LIRIS (Long-slit Intermediate Resolution Infrared Spectrograph)

NRAO 150 LIRIS on the 4.2m WHT 26th March 2005

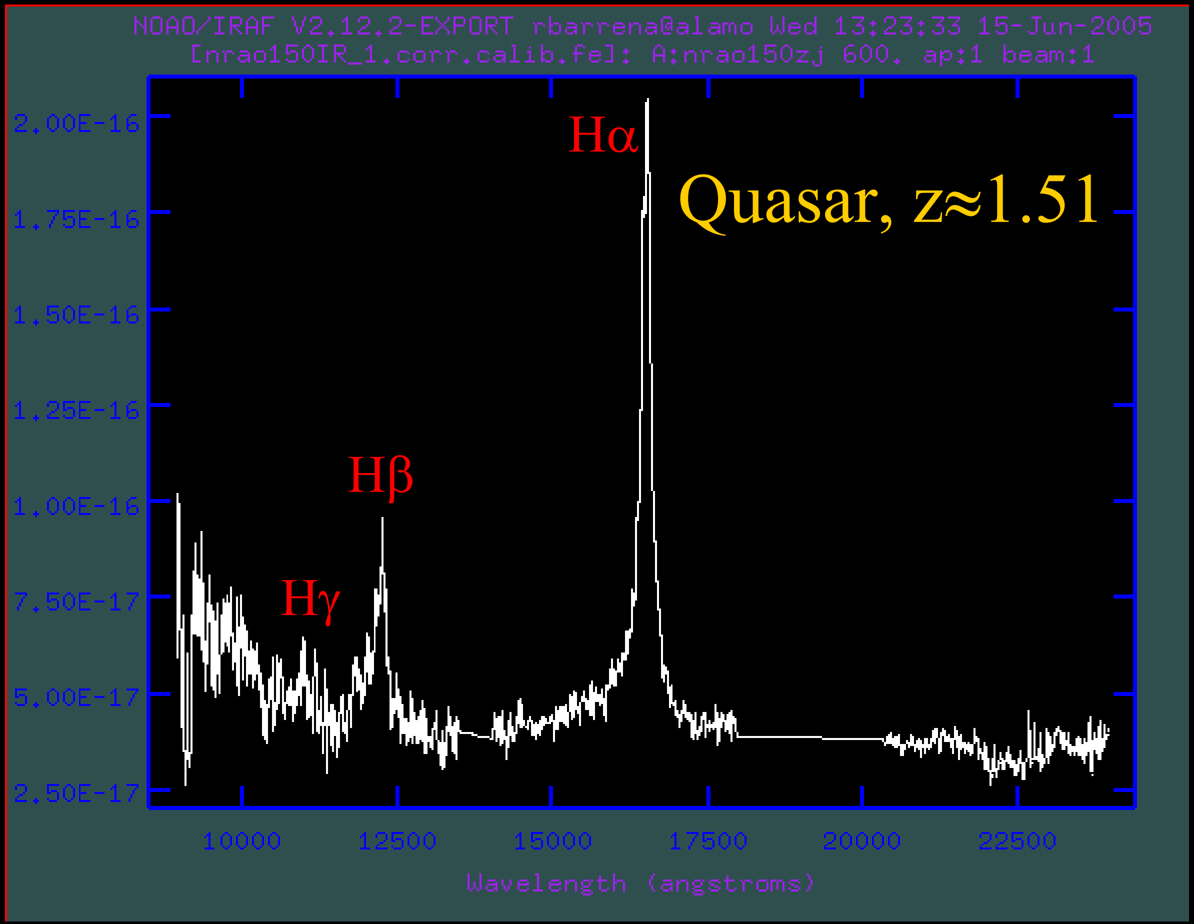

J.A. Acosta, I. Agudo, R. Barrena, P. Rodríguez-Gil, in preparation

- Typical line fluxes for intermediate z quasars (Netzer et al. 2004)

Hα-Luminosity $\approx 3.17\times10^{11}$ $L_{\odot}$

Hβ-Luminosity $\approx 6.85\times10^{10}$ $L_{\odot}$

Distance and classification of NRAO 150

4.2 m William Herschel Telescope
(La Palma, Spain)

LIRIS (Long-slit Intermediate Resolution Infrared Spectrograph)

NRAO 150 LIRIS on the 4.2m WHT 26th March 2005

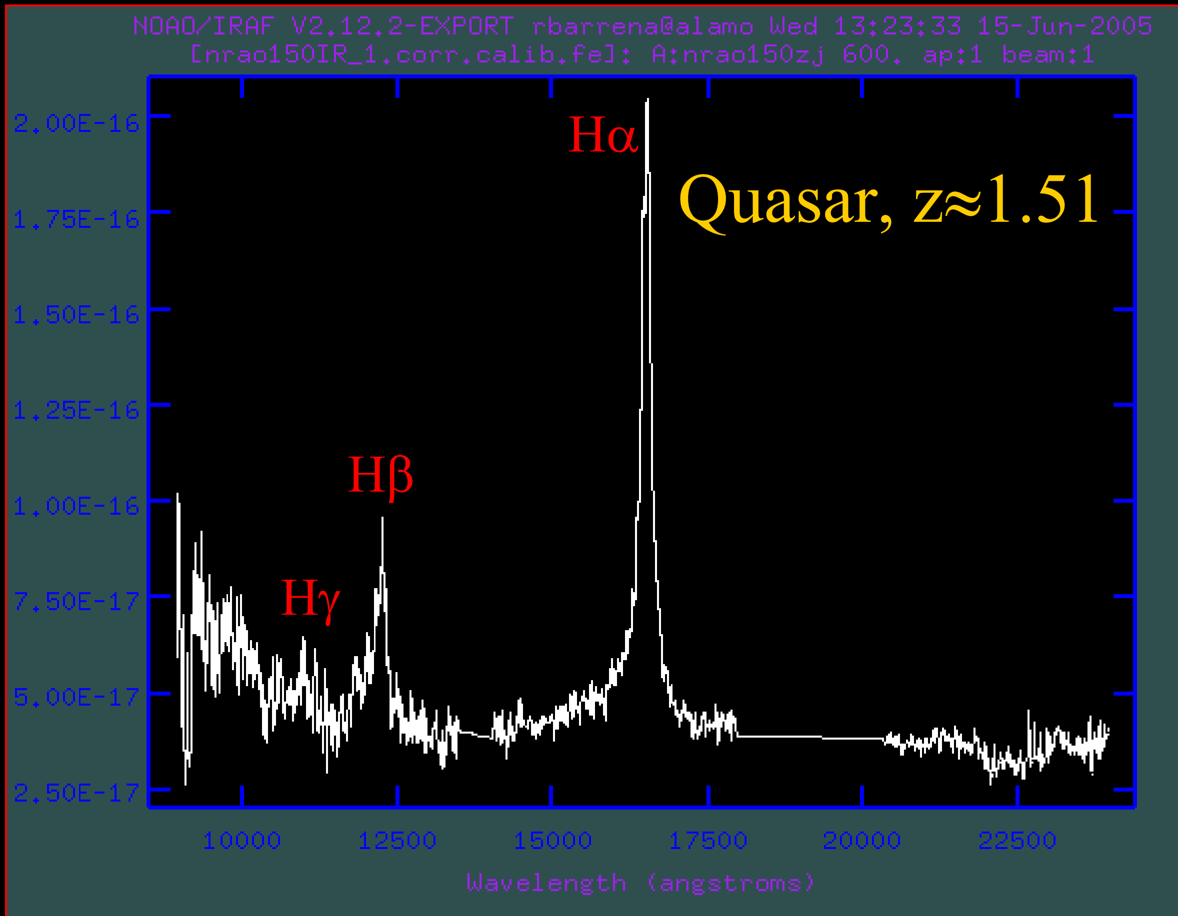

J.A. Acosta, I. Agudo, R. Barrena, P. Rodríguez-Gil, in preparation

- Optical and IR photometry not corrected for Galactic absorption (mag):

V≈ 18.27 R≈18.03 I≈16.67 J≈16.48 H≈15.15 Ks≈14.37

VLBI results: ~120º of inner to outer jet misalignment

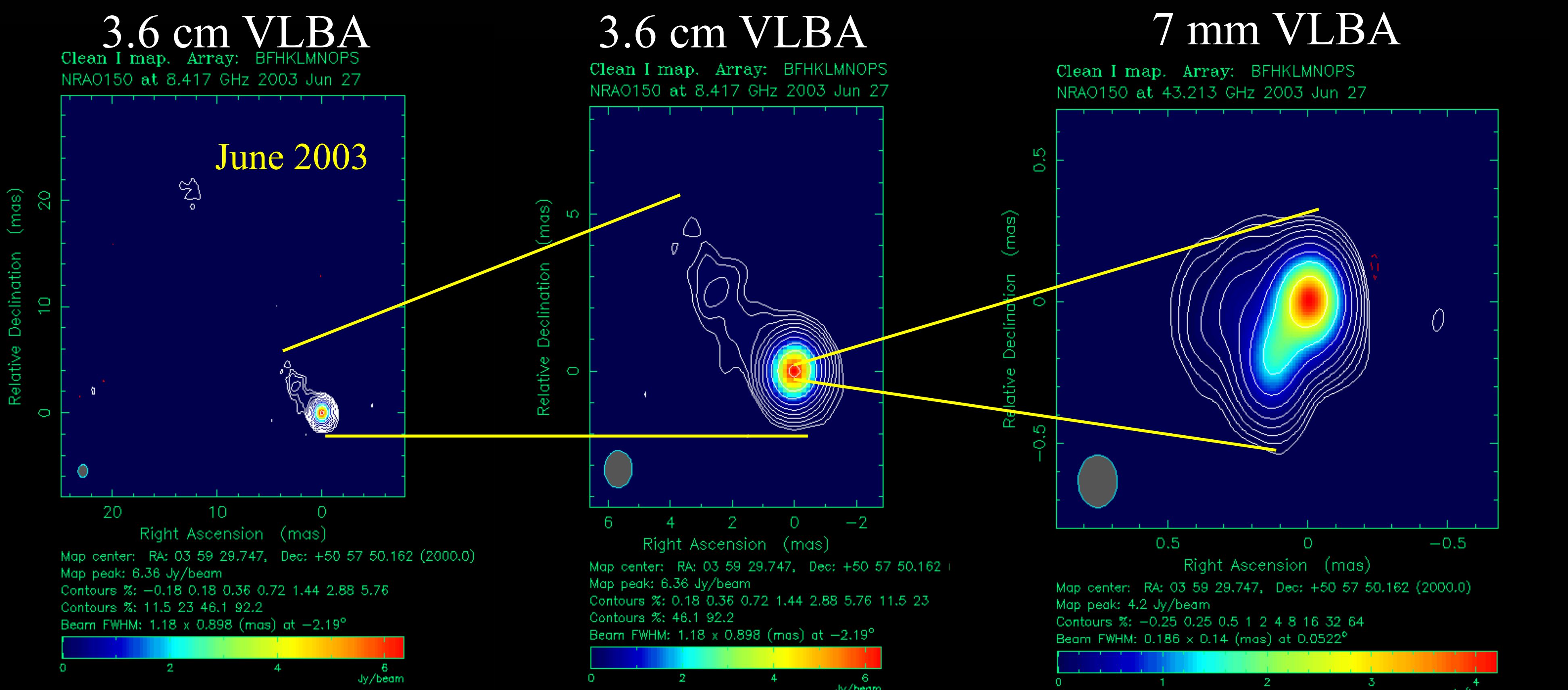

Agudo et al., in preparation

- New 7 mm and 3.6 cm-VLBA observations reveal a strong misalignment (of ~120º) within the first 0.5 mas

- Question: What produces this strong misalignment?
- Answer: Jet bend, alignment of the jet with line of sight and projection effects

- Another question: What produces the jet bend? Answer: 7-3 mm VLBI monitoring

VLBI results: Global mm-VLBI Array (GMVA)

The most sensitive 3mm interferometer

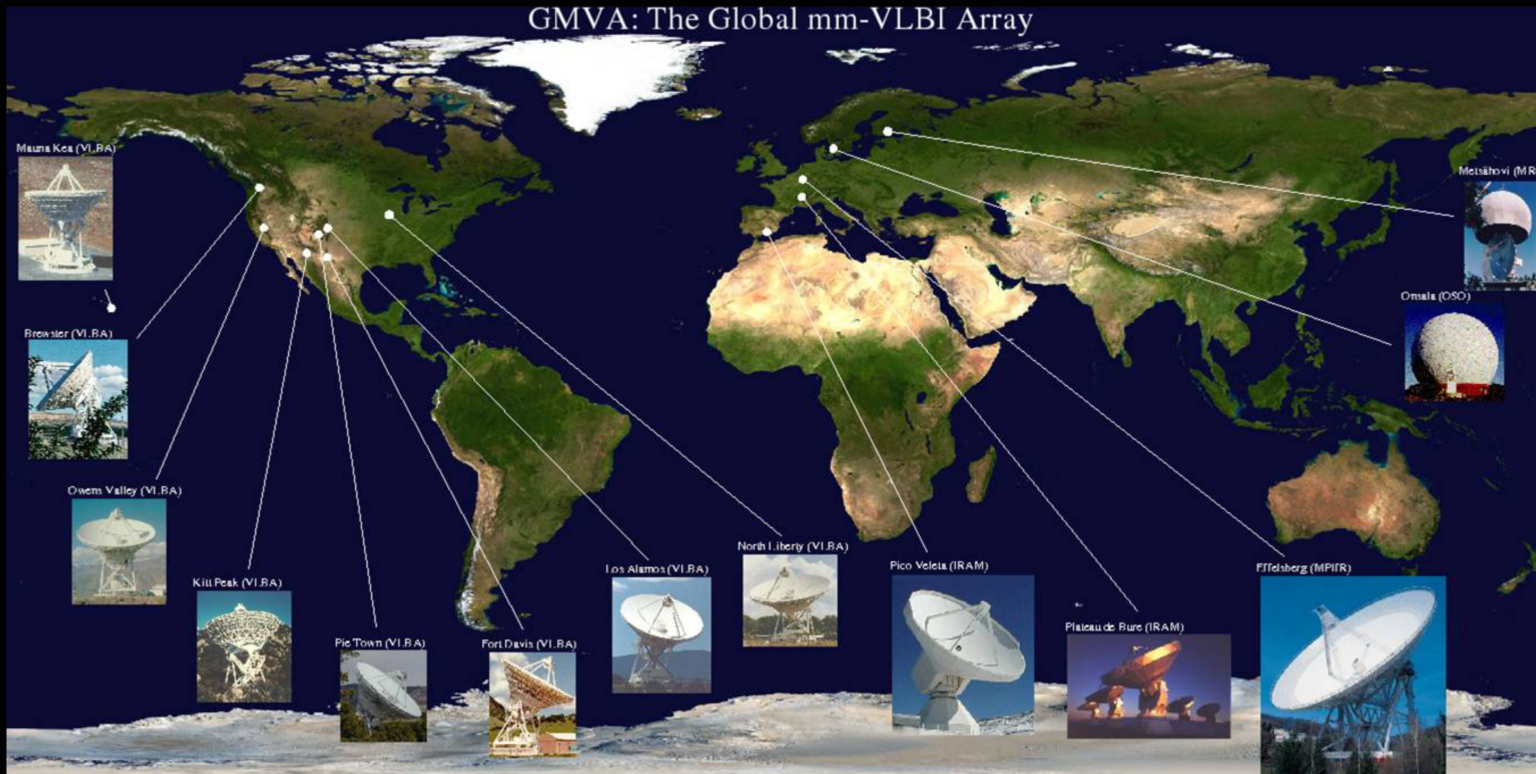

http://www.mpifr-bonn.mpg.de/div/vlbi/globalmm

Observes a 3 mm (86 GHz)

Angular resolution of 40 μas

Polarization being tested for sensitive stations

Baseline sensitivities of 80-100 mJy

Image sensitivities of 1-2 mJy

512 Mbps standard recording mode

VLBI results: Fast jet structural position angle rotation

Apr. 1999

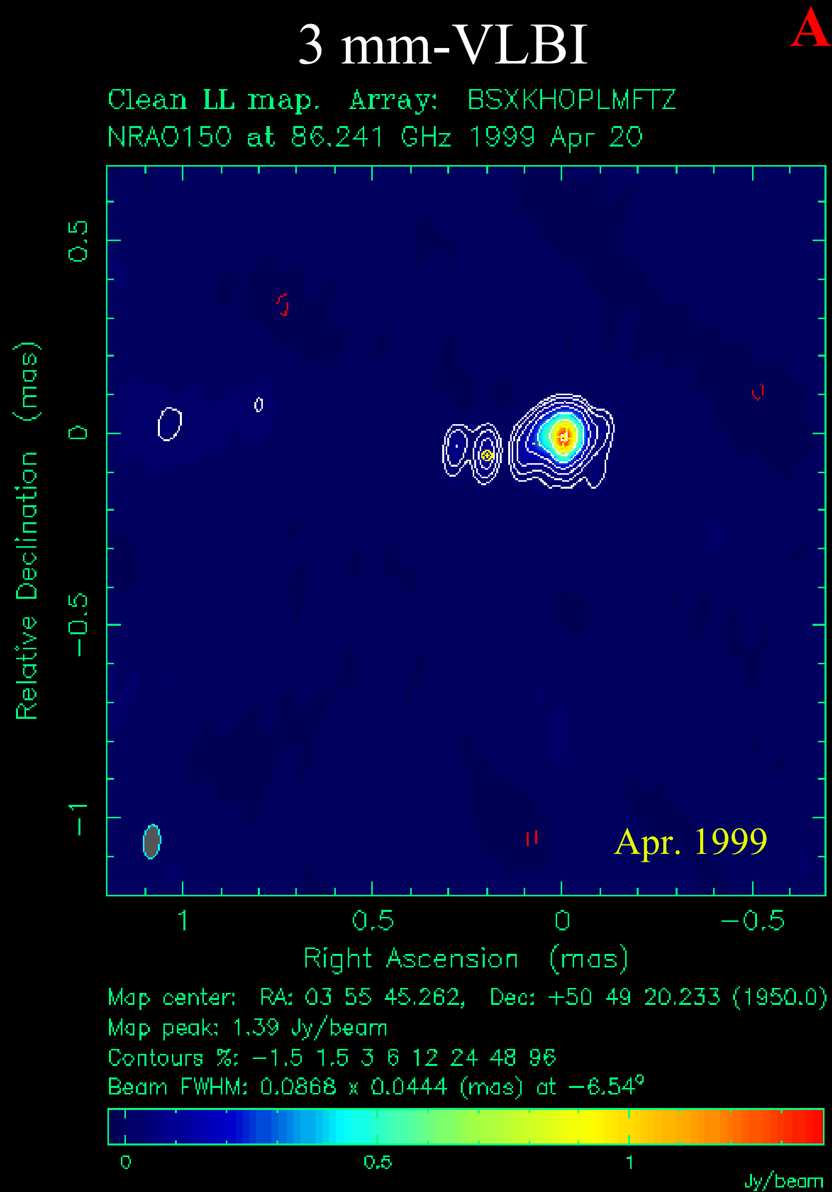

Jet features position respect to the core

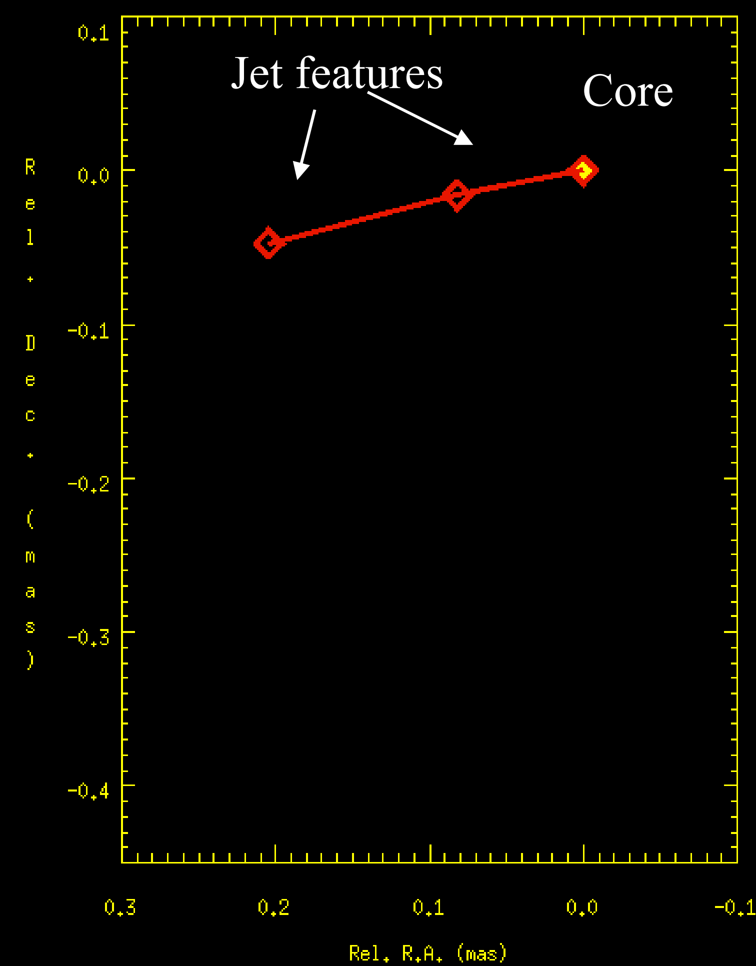

VLBI results: Fast jet structural position angle rotation

Oct. 2001

3 mm-VLBI

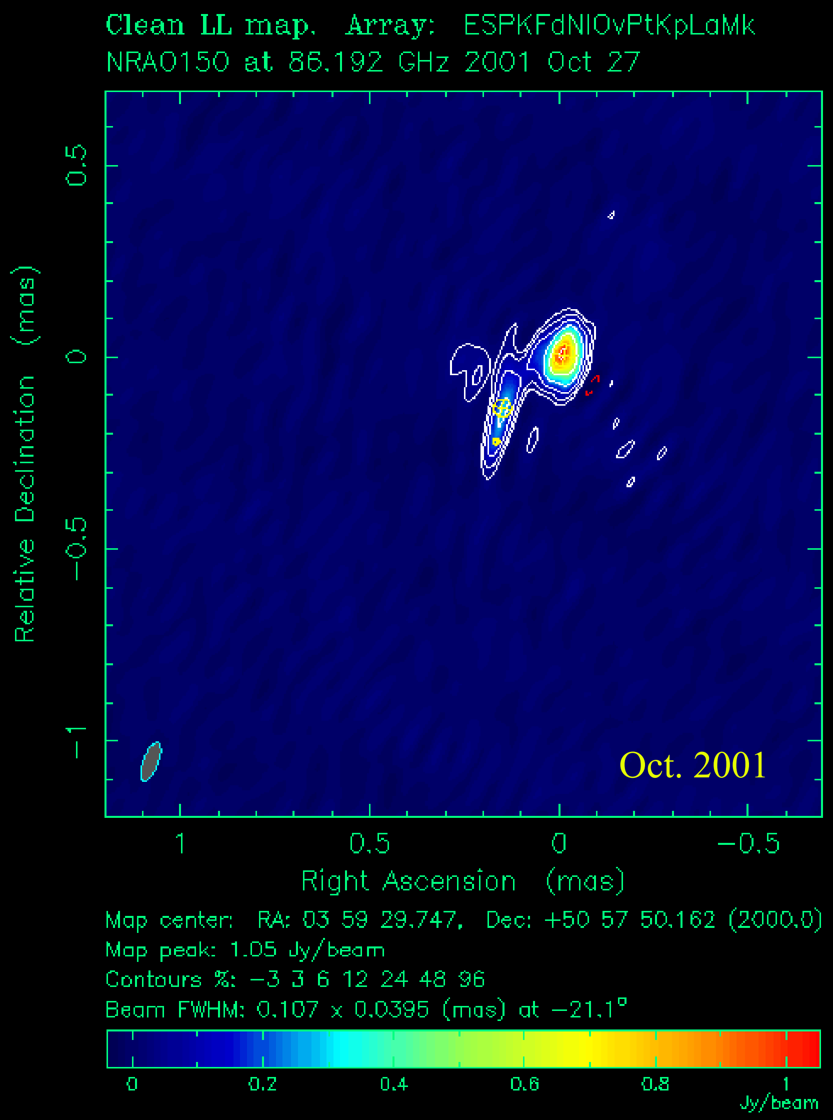

Jet features position respect to the core

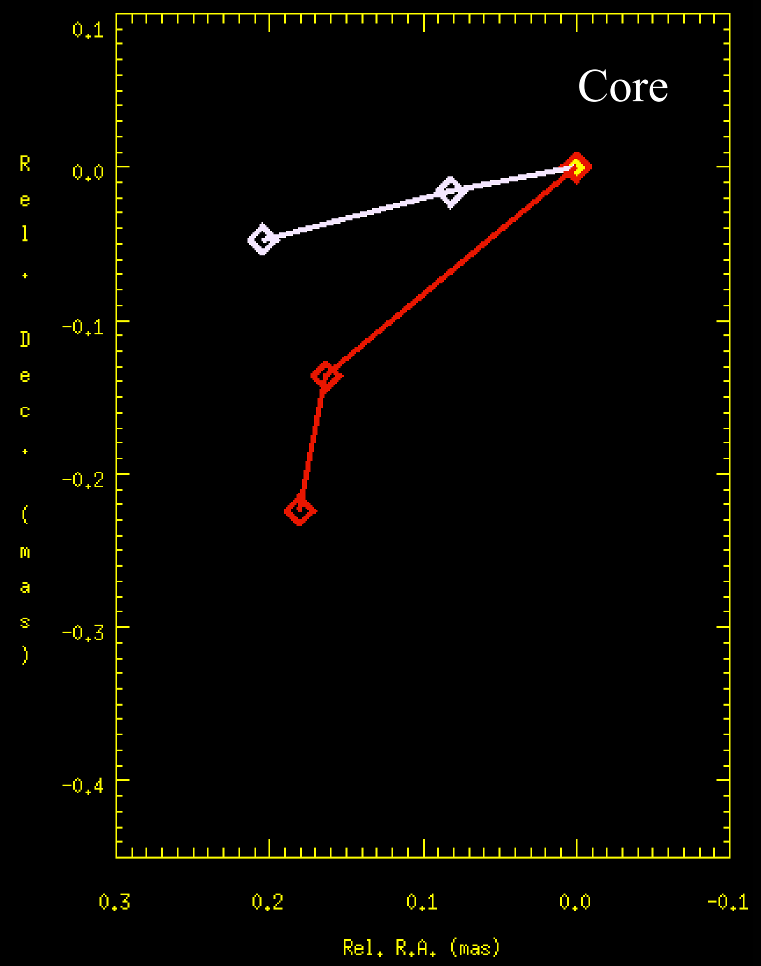

VLBI results: Fast jet structural position angle rotation

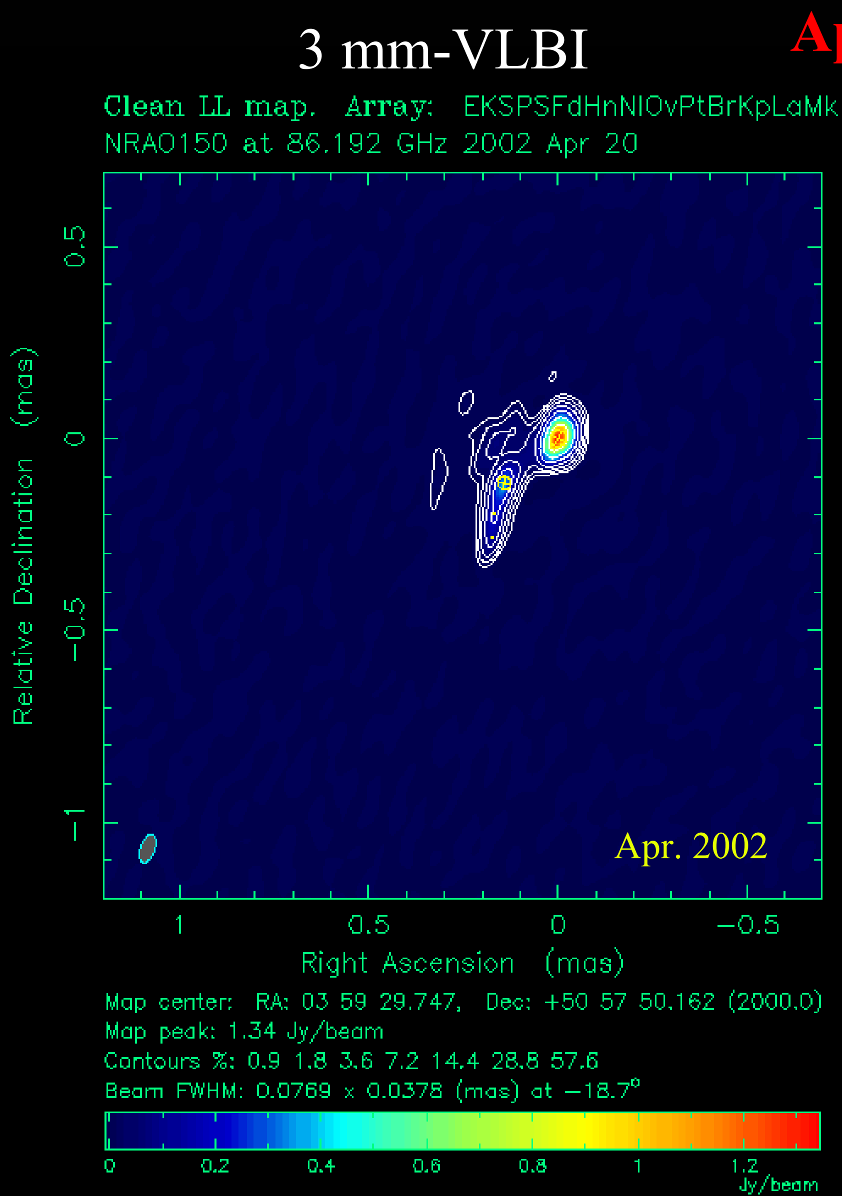

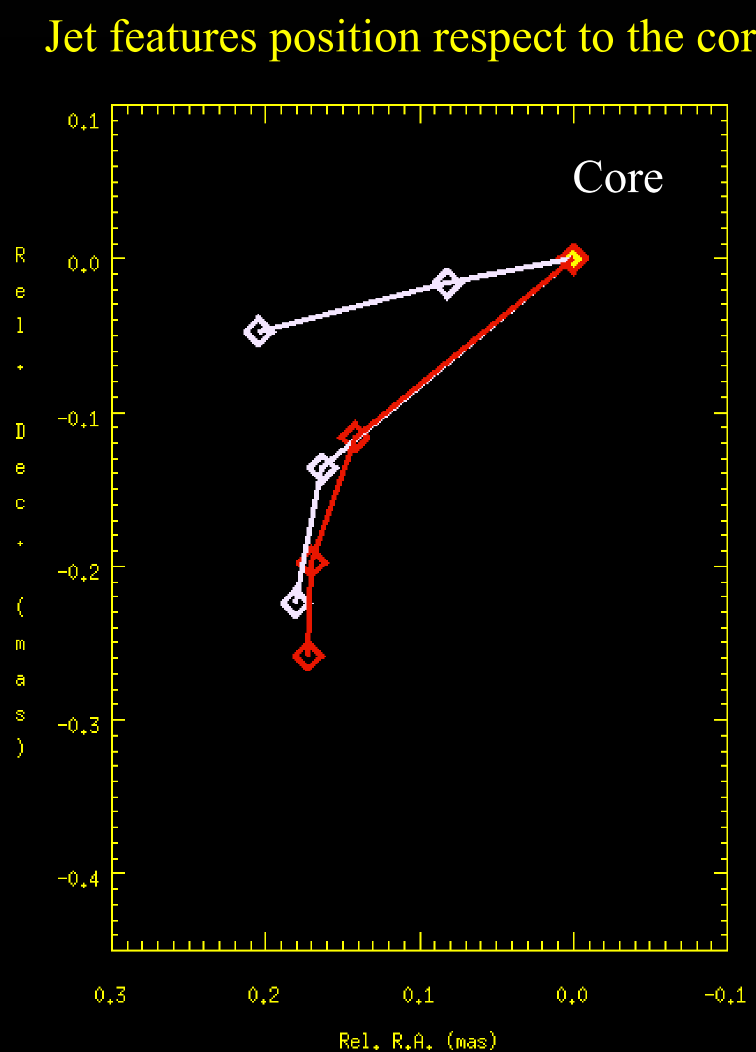

VLBI results: Fast jet structural position angle rotation

Jun. 2002

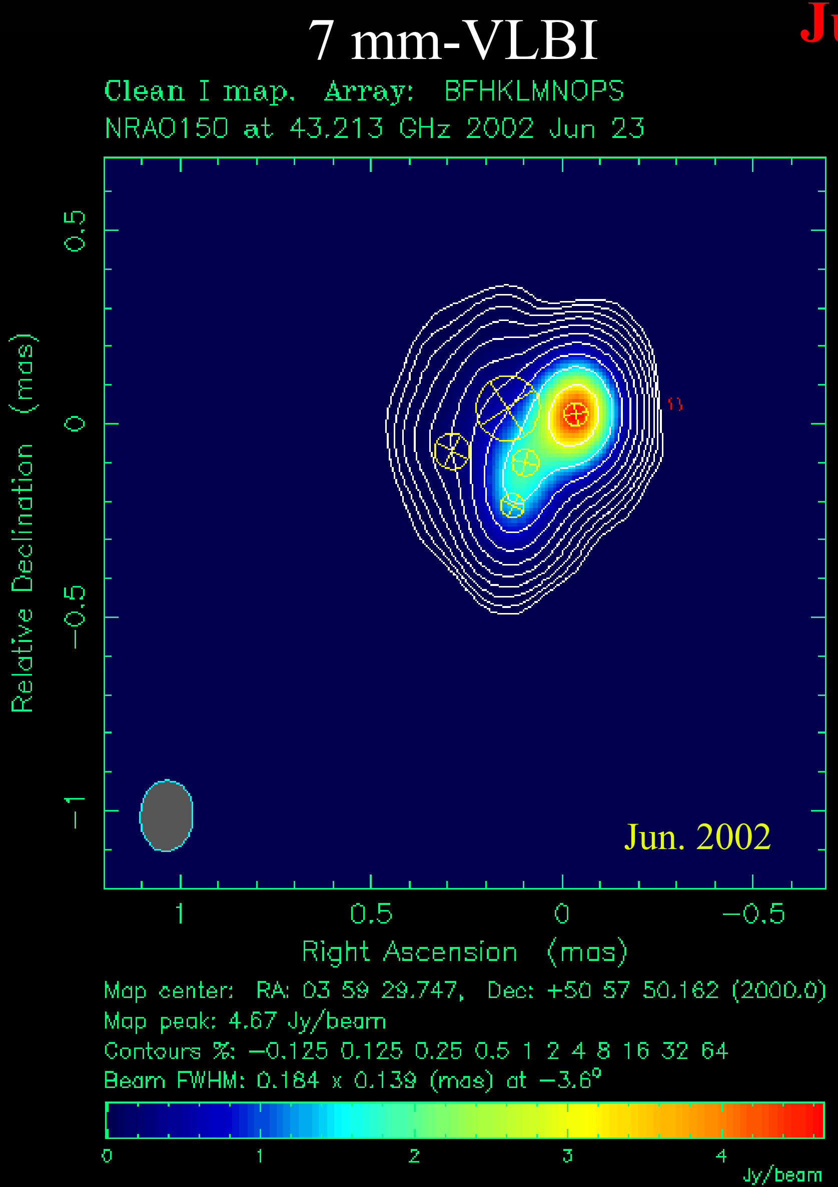

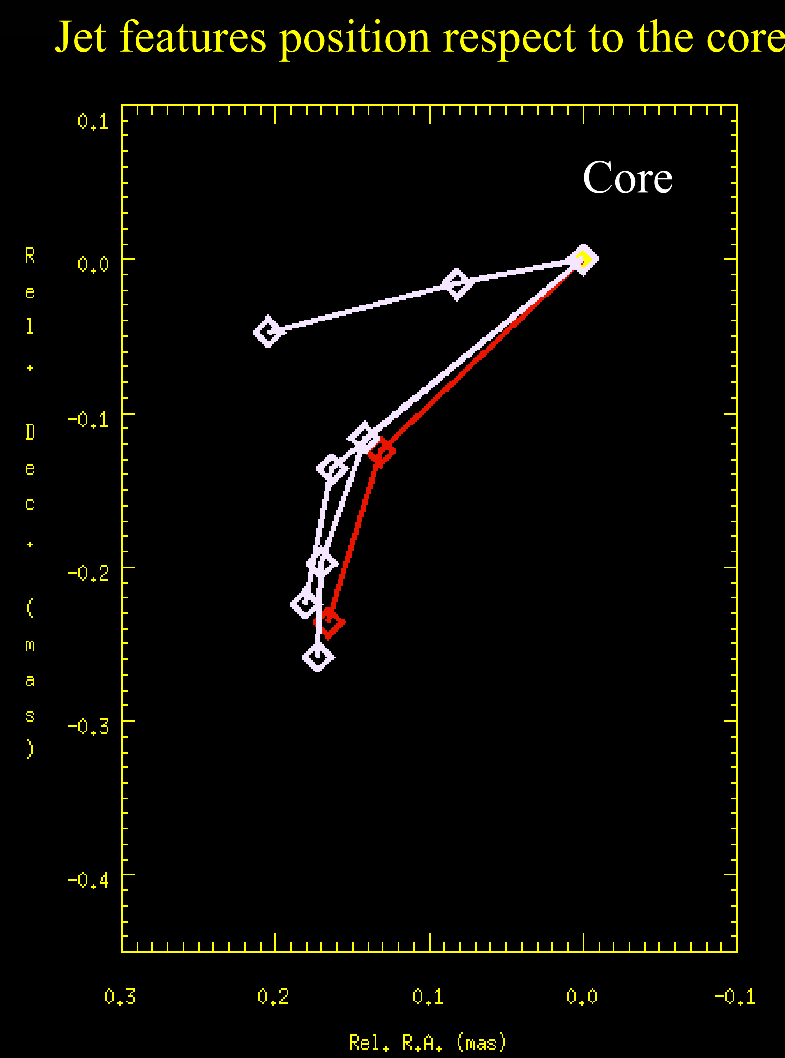

VLBI results: Fast jet structural position angle rotation

3 mm-VLBI

Oct. 2002

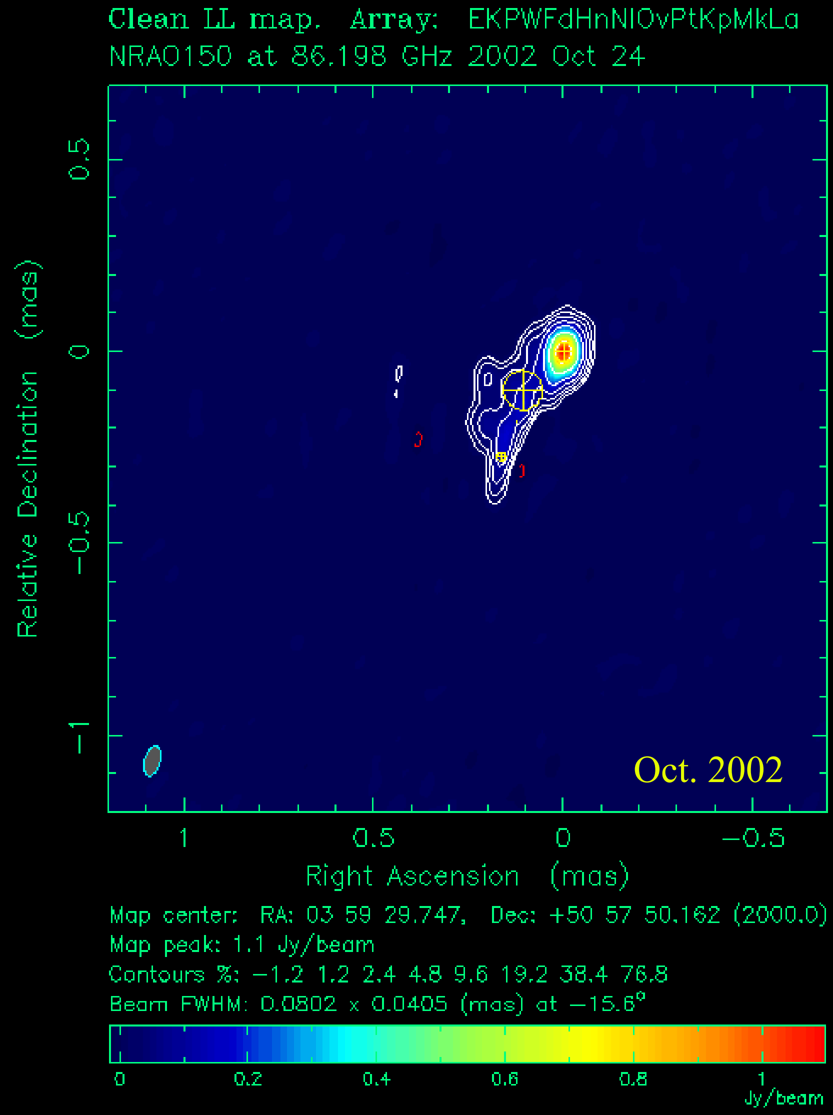

Jet features position respect to the core

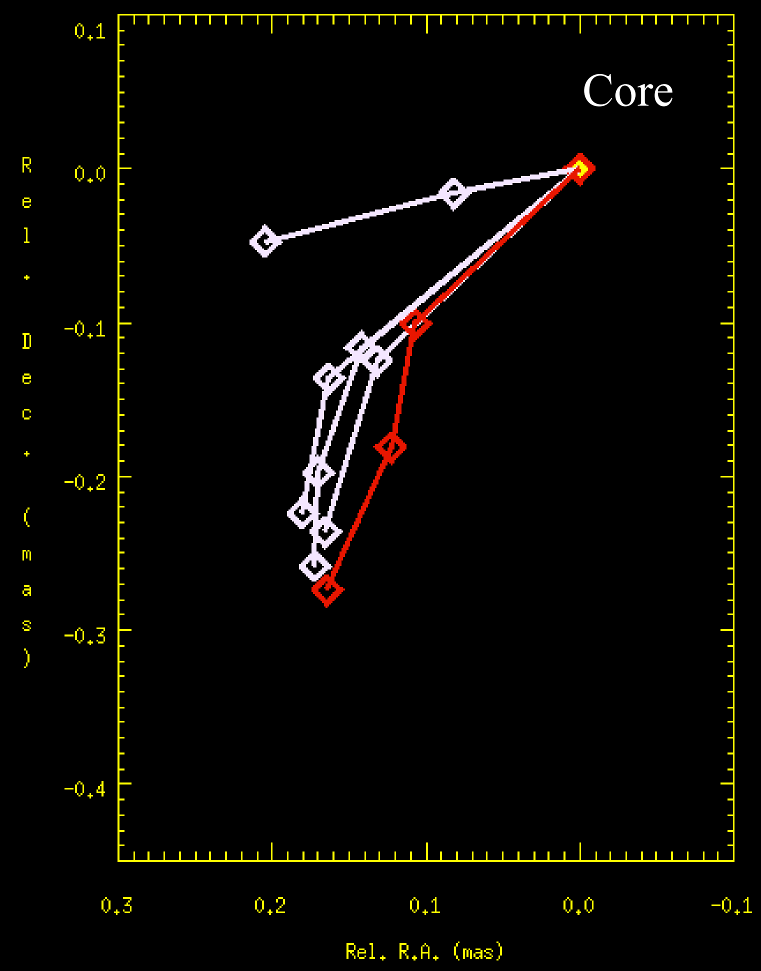

VLBI results: Fast jet structural position angle rotation

Mar. 2003

7 mm-VLBI

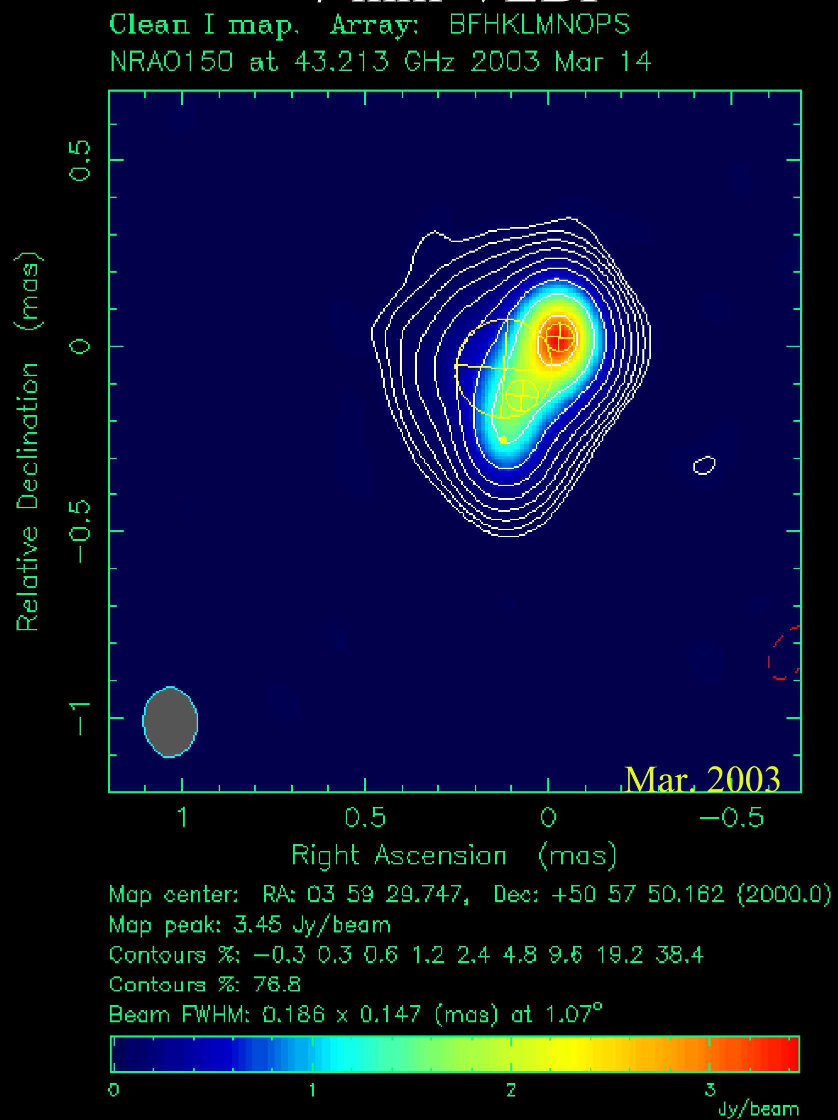

Jet features position respect to the core

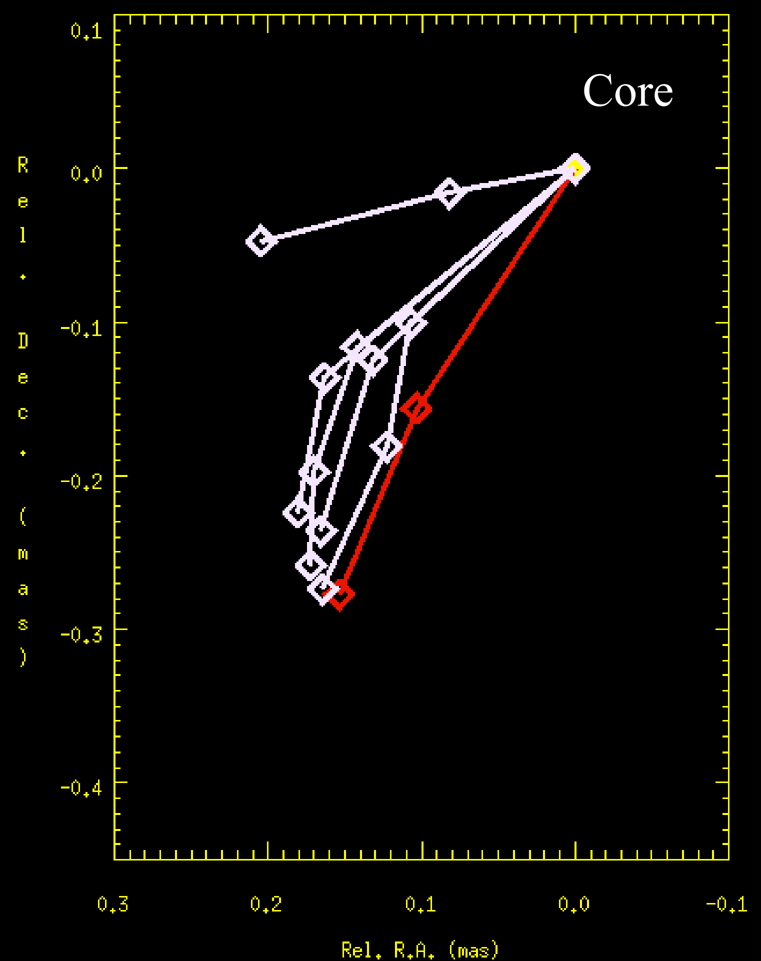

VLBI results: Fast jet structural position angle rotation

3 mm-VLBI

Apr. 2003

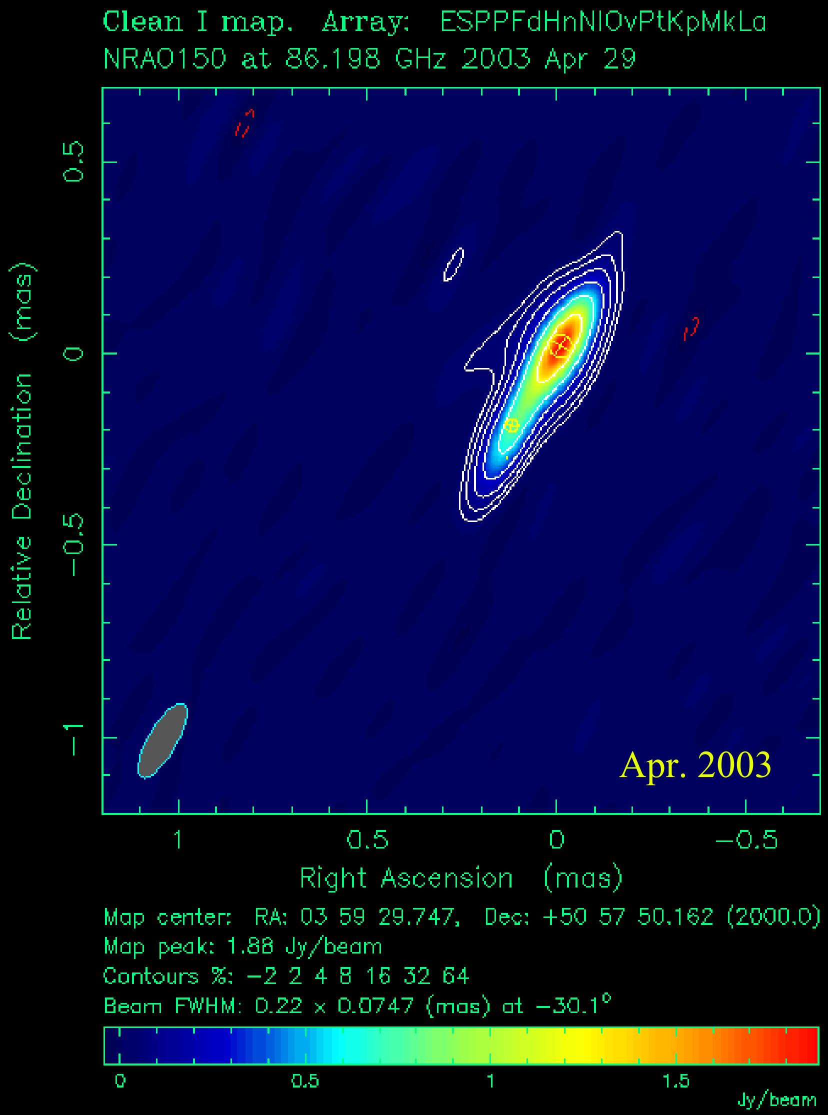

Jet features position respect to the core

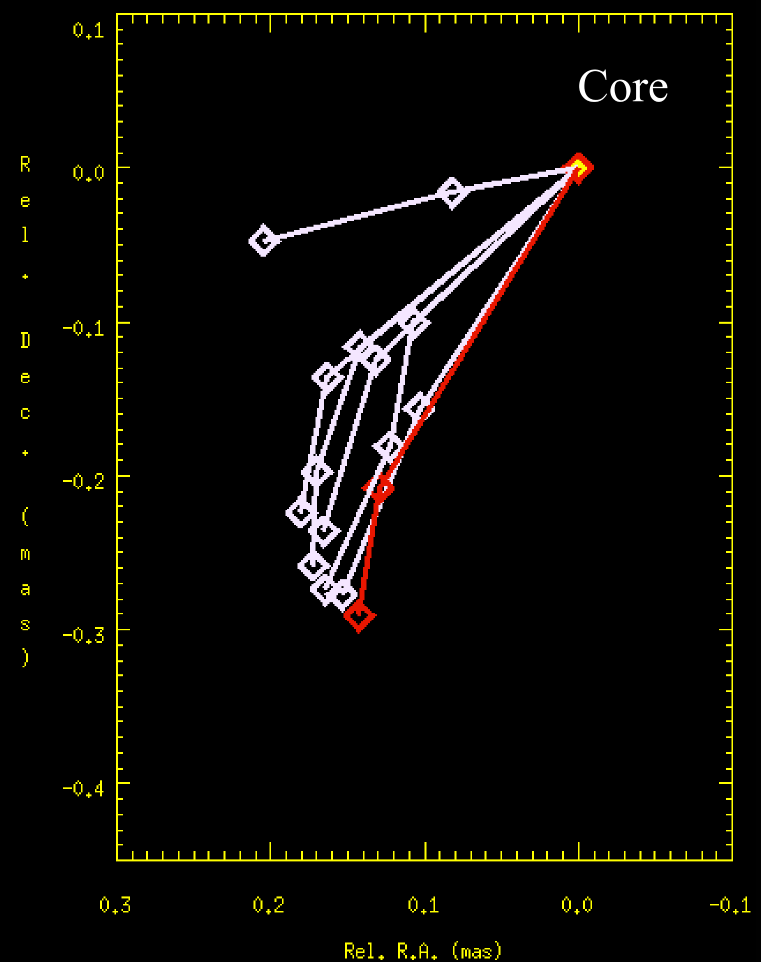

VLBI results: Fast jet structural position angle rotation

7 mm-VLBI

Jun. 2003

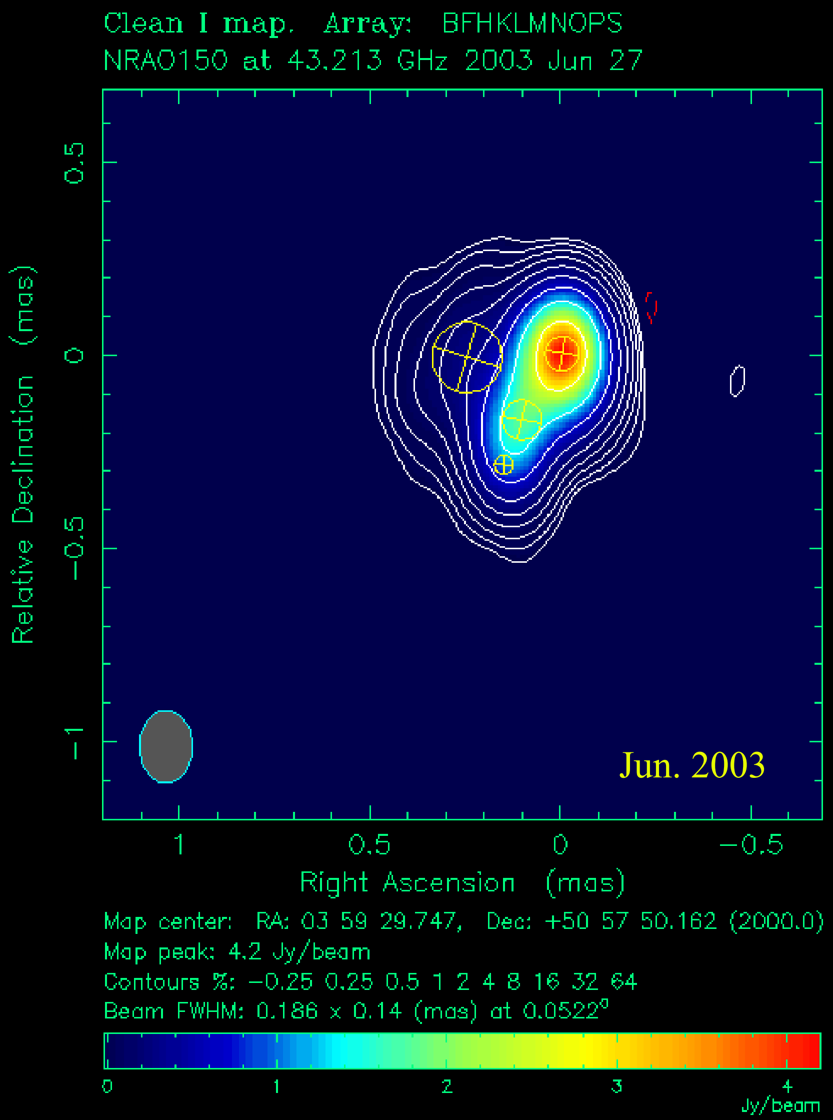

Jet features position respect to the core

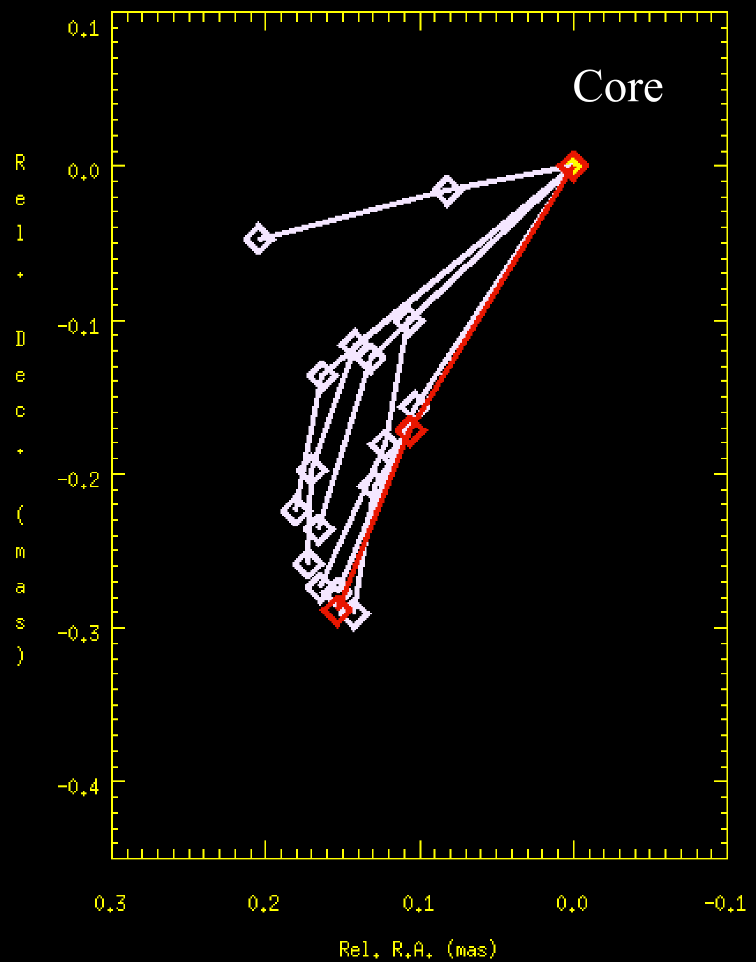

VLBI results: Fast jet structural position angle rotation

3 mm-VLBI

Apr. 2004

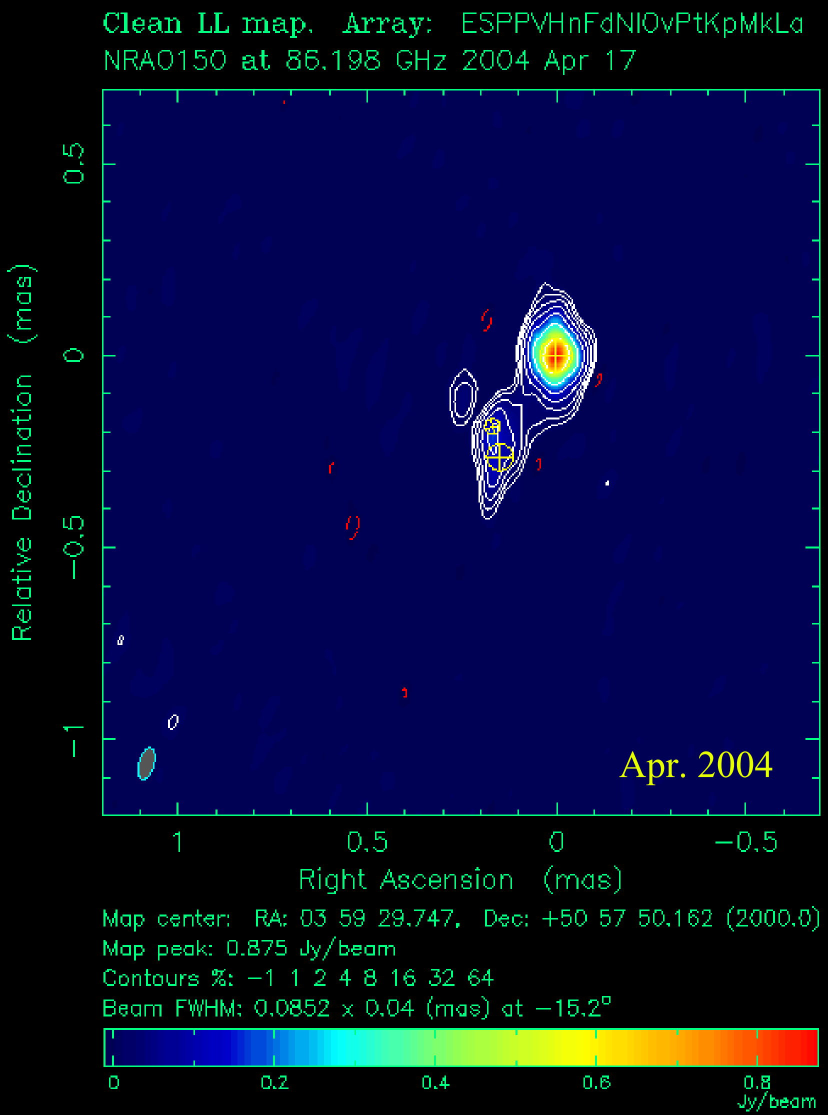

Jet features position respect to the core

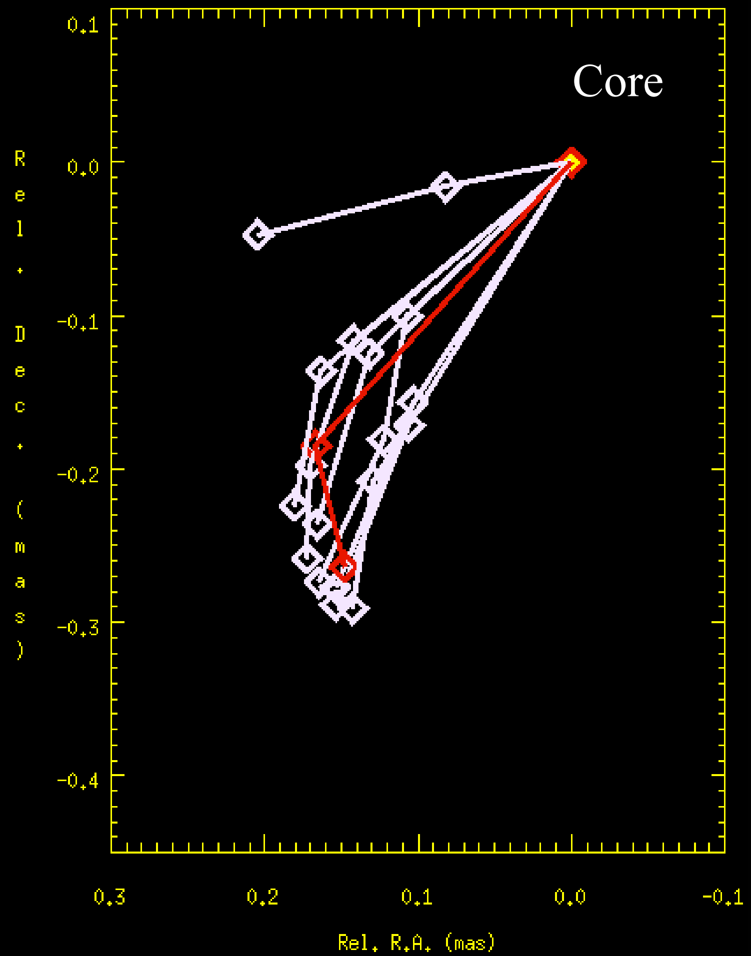

VLBI results: Fast jet structural position angle rotation

3 mm-VLBI images

GMVA and CMVA

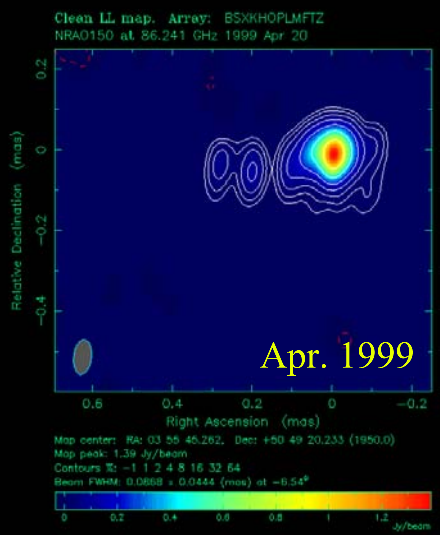

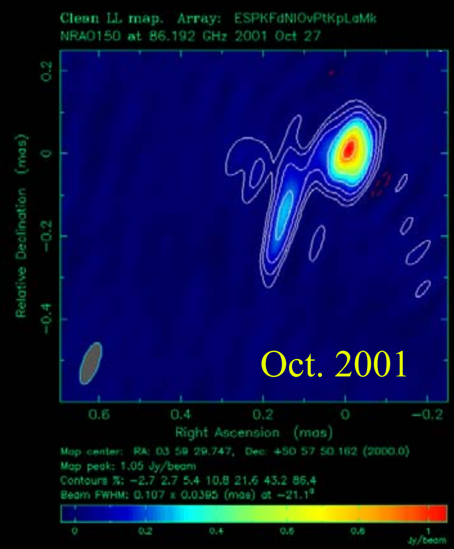

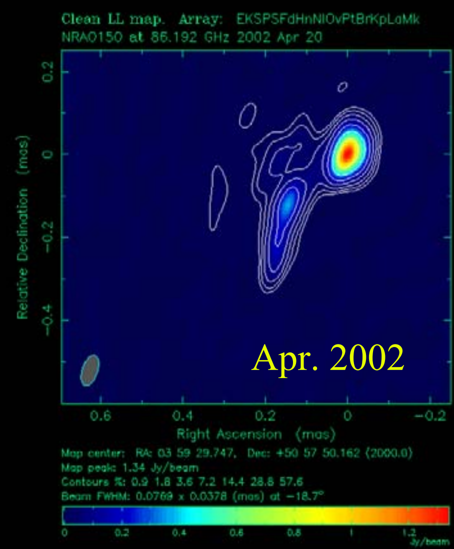

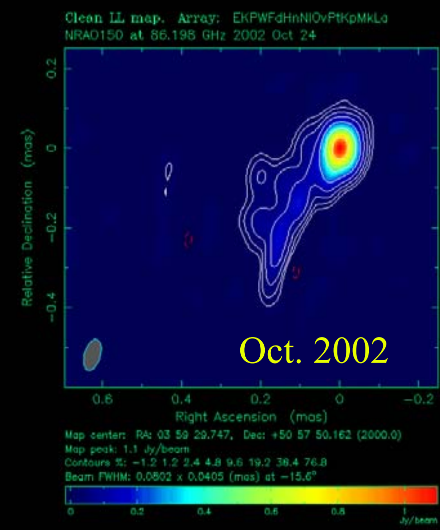

Agudo et al., in preparation

- Jet misalignment is likely produced by the rotation of the innermost jet.

- Rotation at an angular speed of ~10º/yr

- Change in the rotation direction of the jet before April 2004, which allows for the estimation of possible periodicity

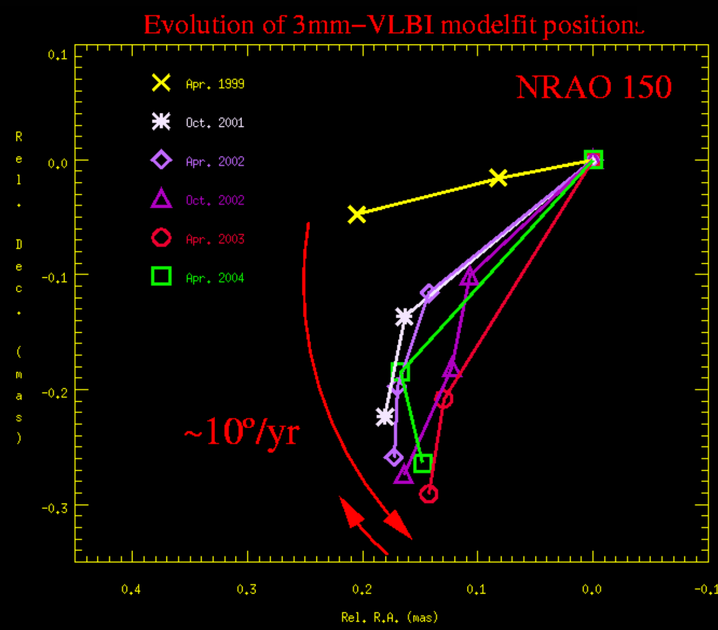

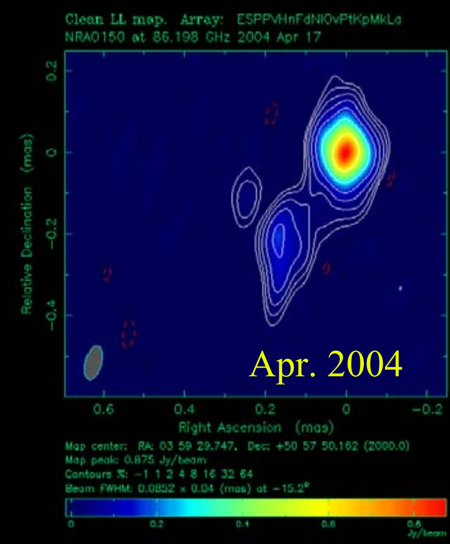

VLBI results: Fast jet structural position angle rotation

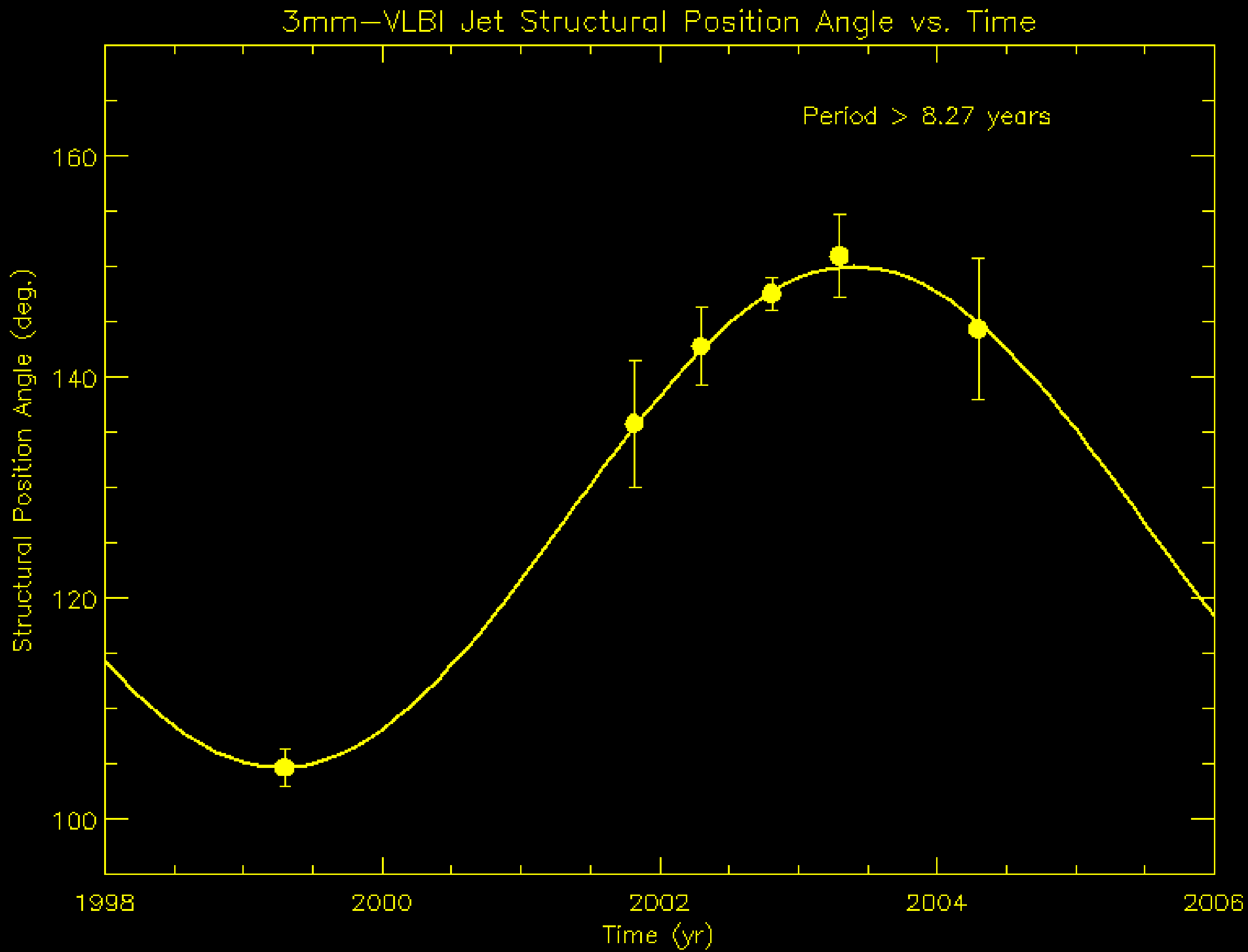

P = 8.3 yr.
Amp = 50º

- P has been fitted to be 8.3 years (in the observer's frame)
- Amplitude 50º (projected on the plane of the sky)

VLBI results: Fast jet structural position angle rotation

7 mm-VLBI

Aug. 2004

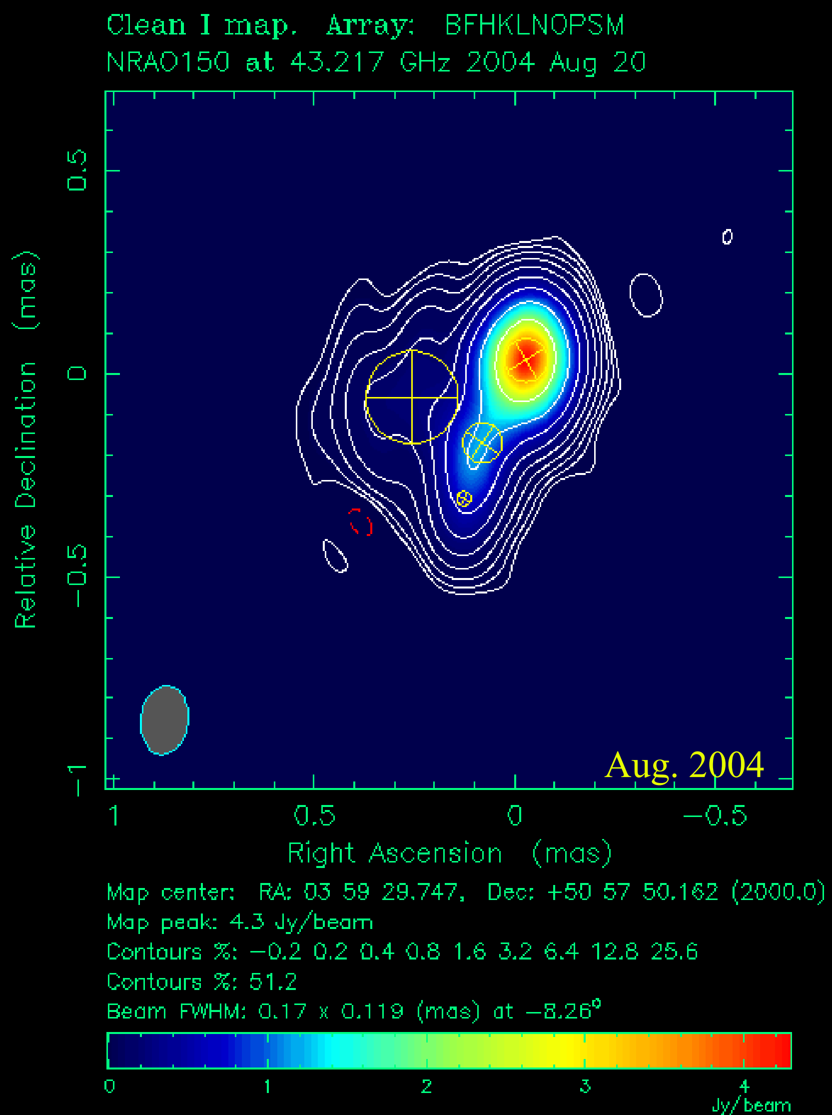

Jet features position respect to the core

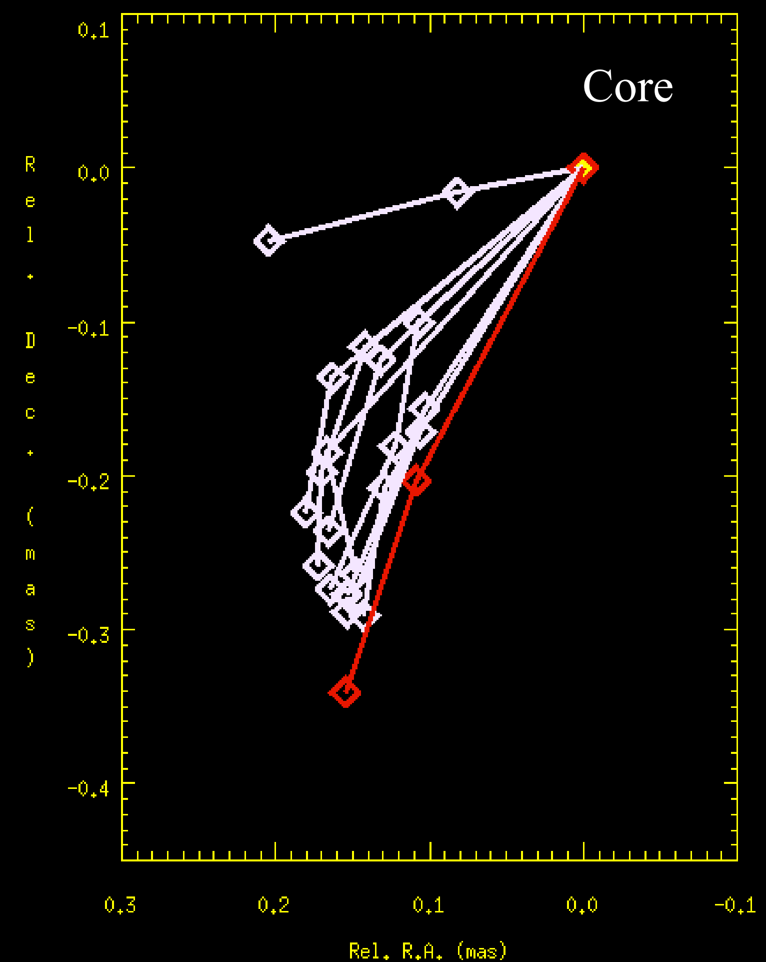

VLBI results: Fast jet structural position angle rotation

7 mm-VLBI

Dec. 2004

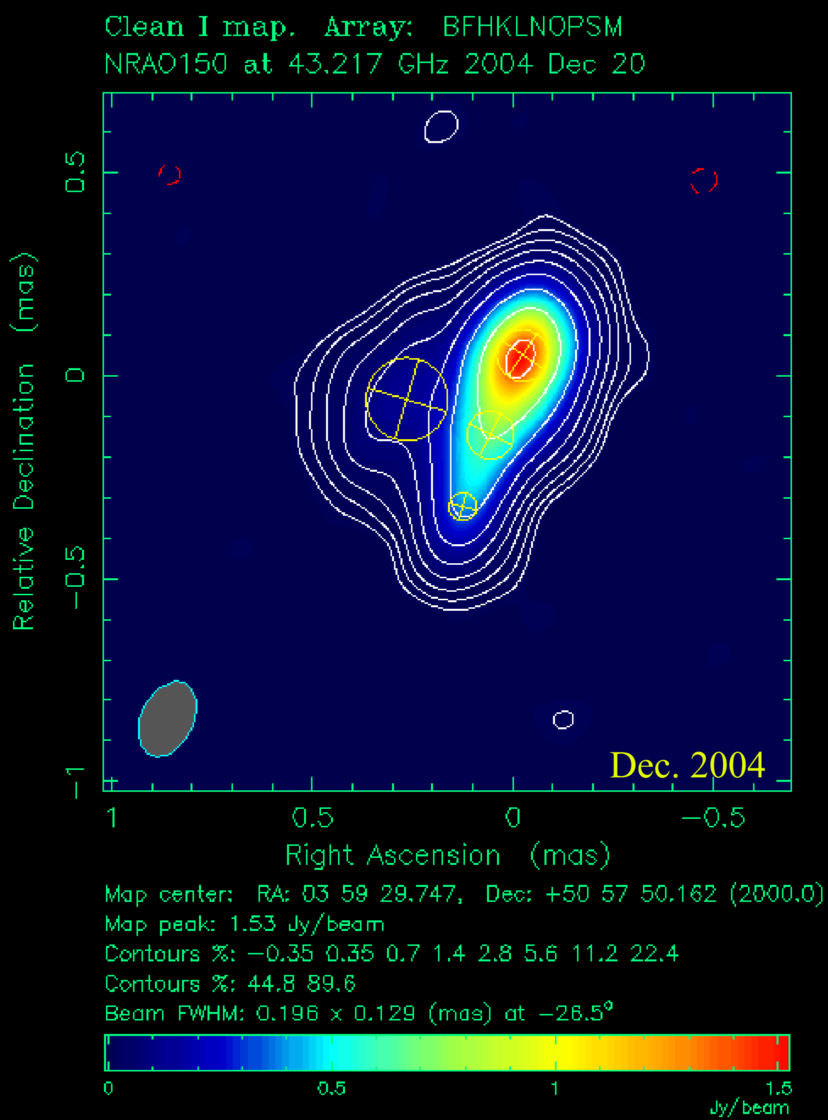

Jet features position respect to the core

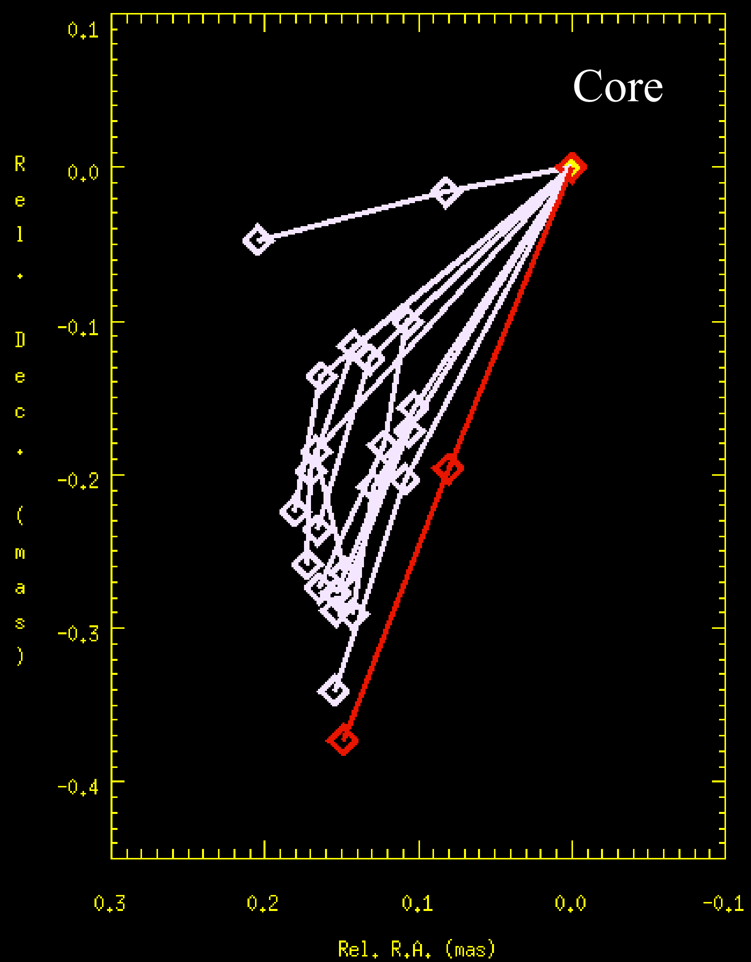

VLBI results: Fast jet structural position angle rotation

7 mm-VLBI

Apr. 2005

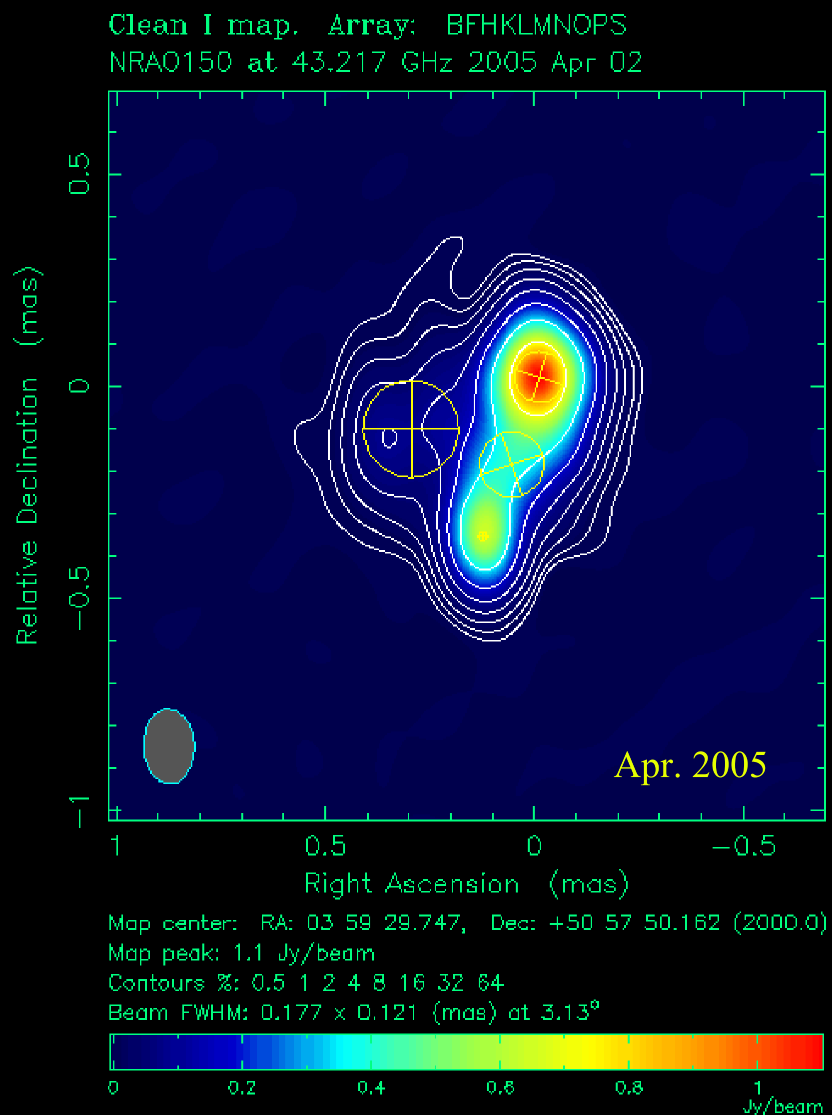

Jet features position respect to the core

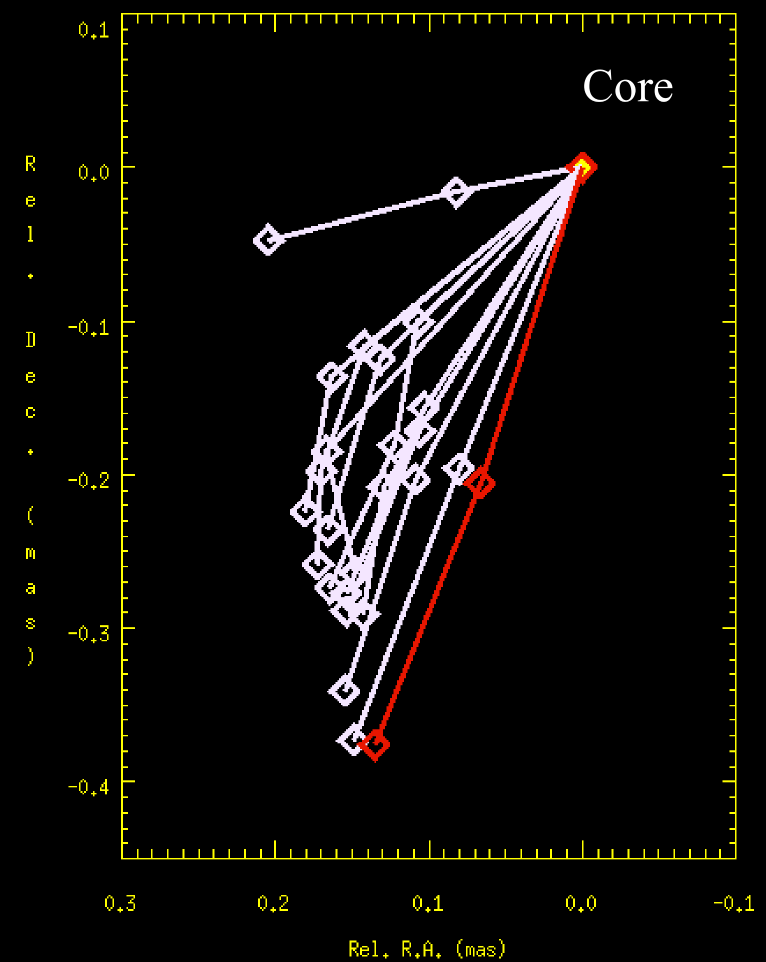

VLBI results: Is NRAO 150 rotating periodically?

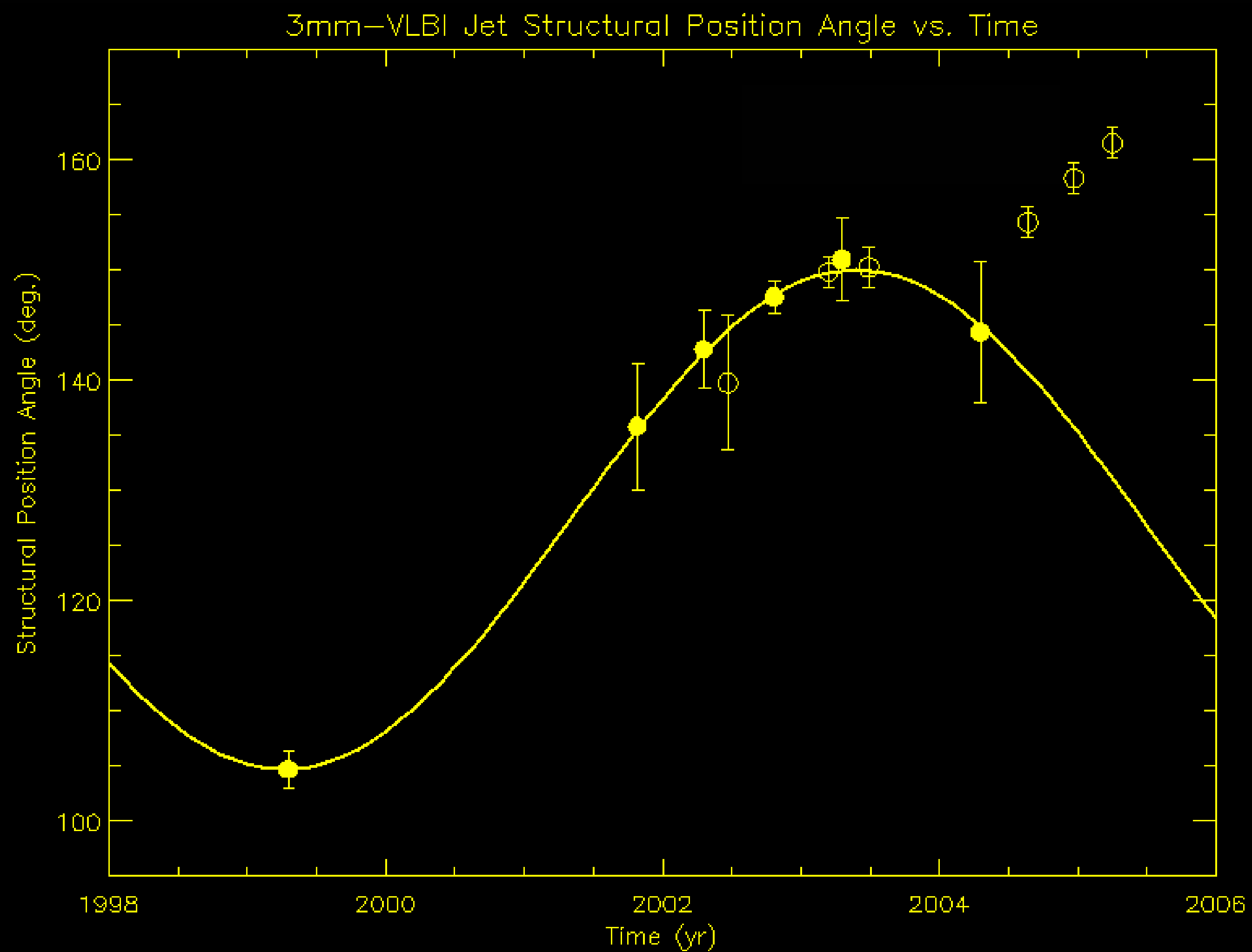

- The jet continued rotating in the plane of the sky in the original sense (counterclockwise)
- The new three points are completely off.

VLBI results: Is NRAO 150 rotating periodically?

Metsahövi 1 and 1.3 cm

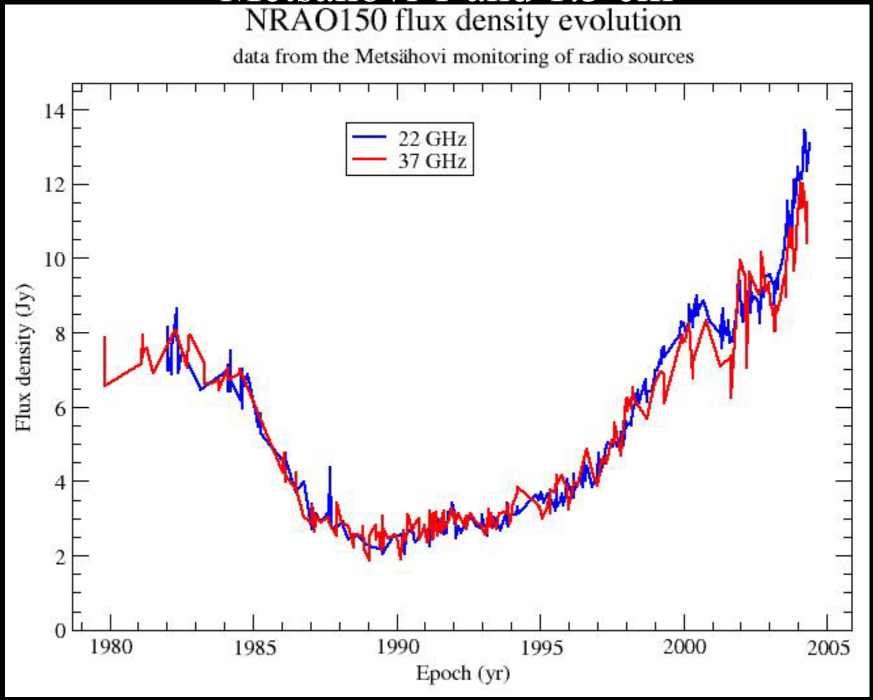

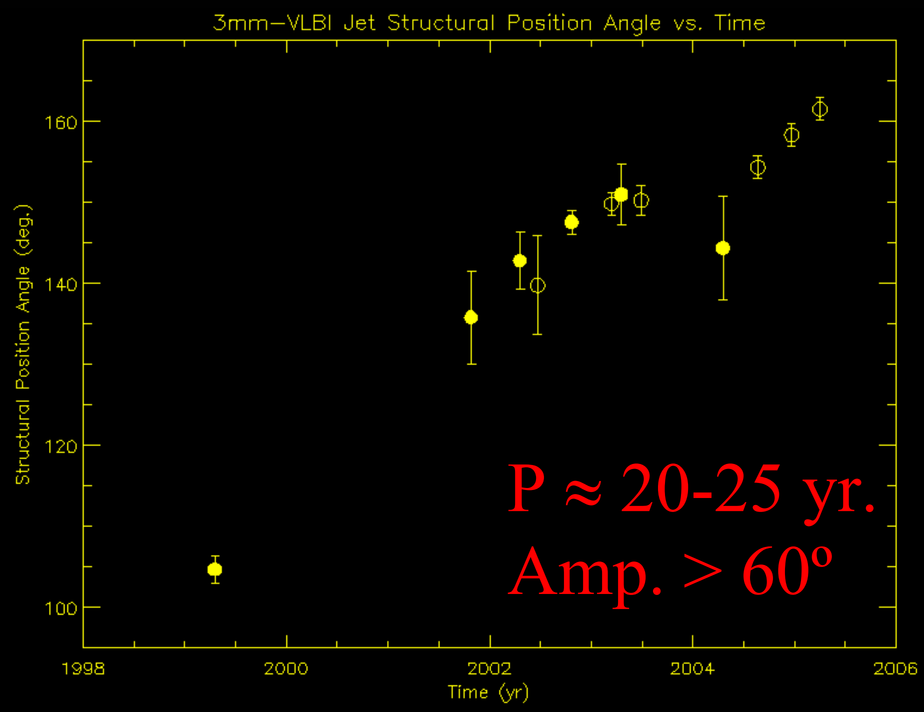

Tornikoski et al.

- If the jet rotation is correlated with the single-dish light curves of the source:
  - Possible periodic behaviour
  - P ≈ 20-25 yr
- It needs to be confirmed and constrained

Some thoughts about fast periodic behaviour

7mm-VLBA

BL Lac

Innermost jet position angle vs. time

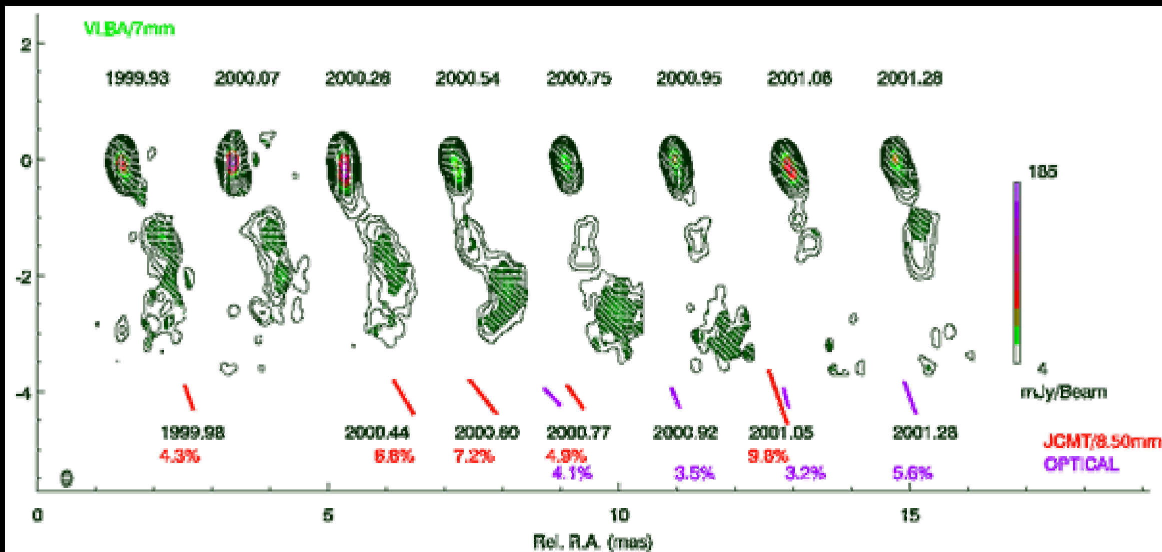

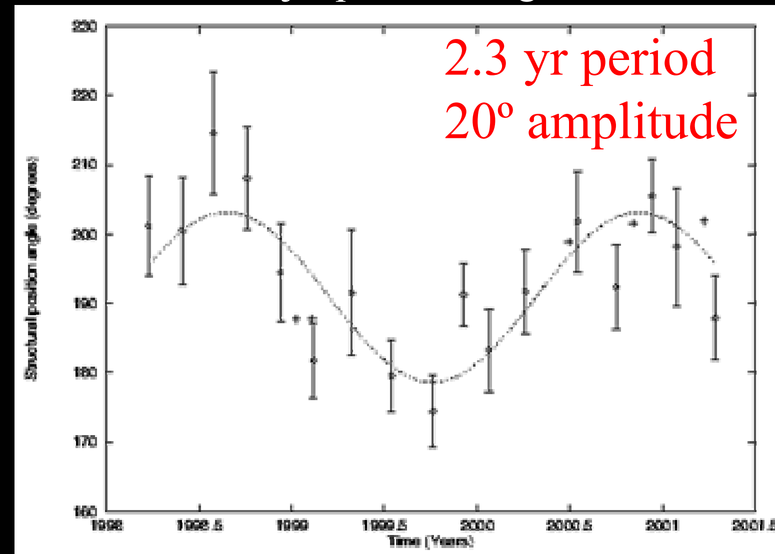

Stirling et al. (2003)

- Fast periodicities have also been reported in SgrA* and other AGN through different methods
- Produced in the innermost regions of the AGN (accretion disk or base of the jet)
- Their triggering perturbations should related to fundamental parameters of the accretion system (a, disk ang. mom., density…)
- Study of the phenomenon can enhance our knowledge of SMBHs and their environments (Liu & Melia 2002, Caproni et al. 2004, Lobanov & Roland 2005)

Summary: NRAO 150

IR identification and spectral classification

- Quasar
- $z \approx 1.51$
- Quantitative studies are now possible

Misalignment between the cm and the mm VLBI jet of $\sim 120^{o}$

Fast jet rotation (in the plane of the sky)

- $\sim 10^{o}$/yr
- Possible periodicity with $P \approx 20$-25 yr (needs to be constrained)

Surprising Correlations Between the Optical and Radio Emission of Active Galactic Nuclei

Denise C. Gabuzda
University College Cork

Paul Smith (Steward Obs.)
Liza Rastorgueva (Tuorla Obs.)
Shane O'Sullivan (UCC)

VLBI Polarisation Observations

Measurements of the properties of the "core" and "jet" magnetic fields on scales of parsecs (light years).

For optically thin regions (e.g., the jets),

$$B \perp \chi$$

$$m \leq 75\%$$

For optically thick regions (e.g., the cores),

$$B \parallel \chi$$

$$m \leq 10\text{–}15\%$$

Where χ is the polarisation angle and m is the degree of polarisation.

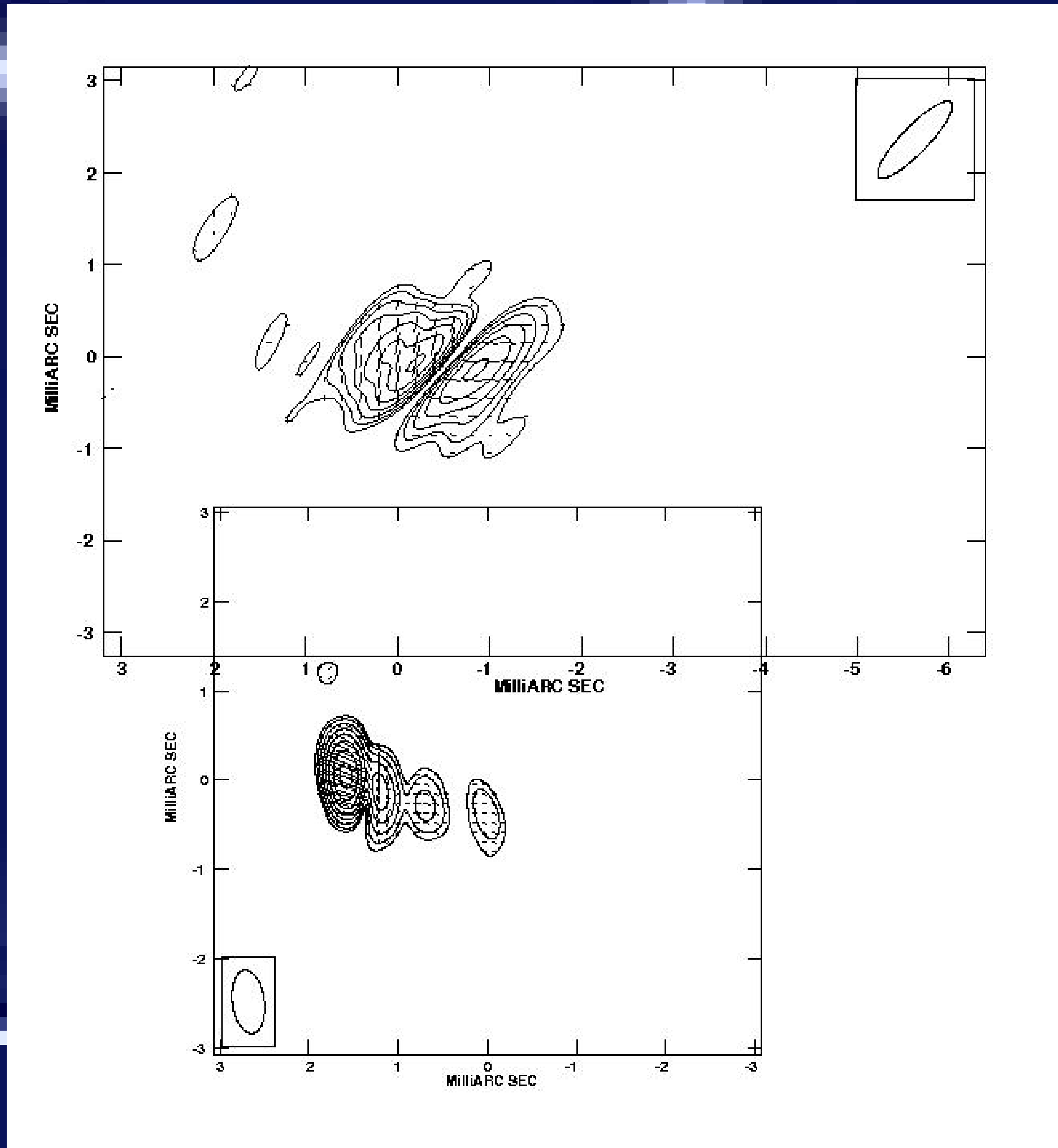
MilliARC SEC
MilliARC SEC
MilliARC SEC
MilliARC SEC

Observed polarisation angles can be affected by Faraday rotation – rotation of plane of polarisation due to different velocities of RCP and LCP components of EM wave when propagating through a magnetised plasma.

Depends on integral of electron density multiplied by line-of-sight component of B field.

Can be identified by the "lambda-squared" dependence of the polarisation angle on wavelength:

$$\chi = \chi_o + RM\, \lambda^2$$

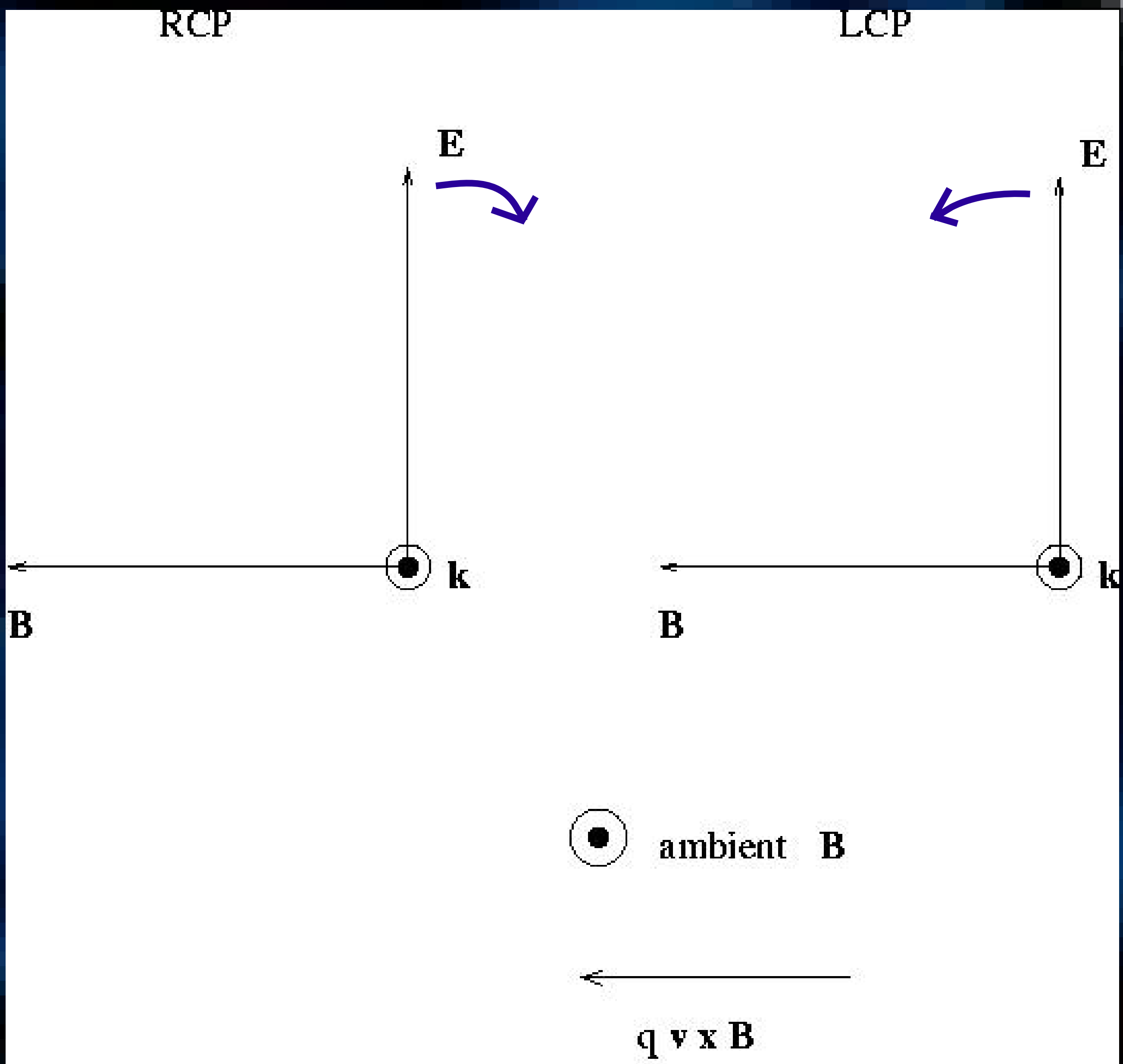

q v x B force is aligned with the rotation of the EM wave in one case and opposed to it in the other.

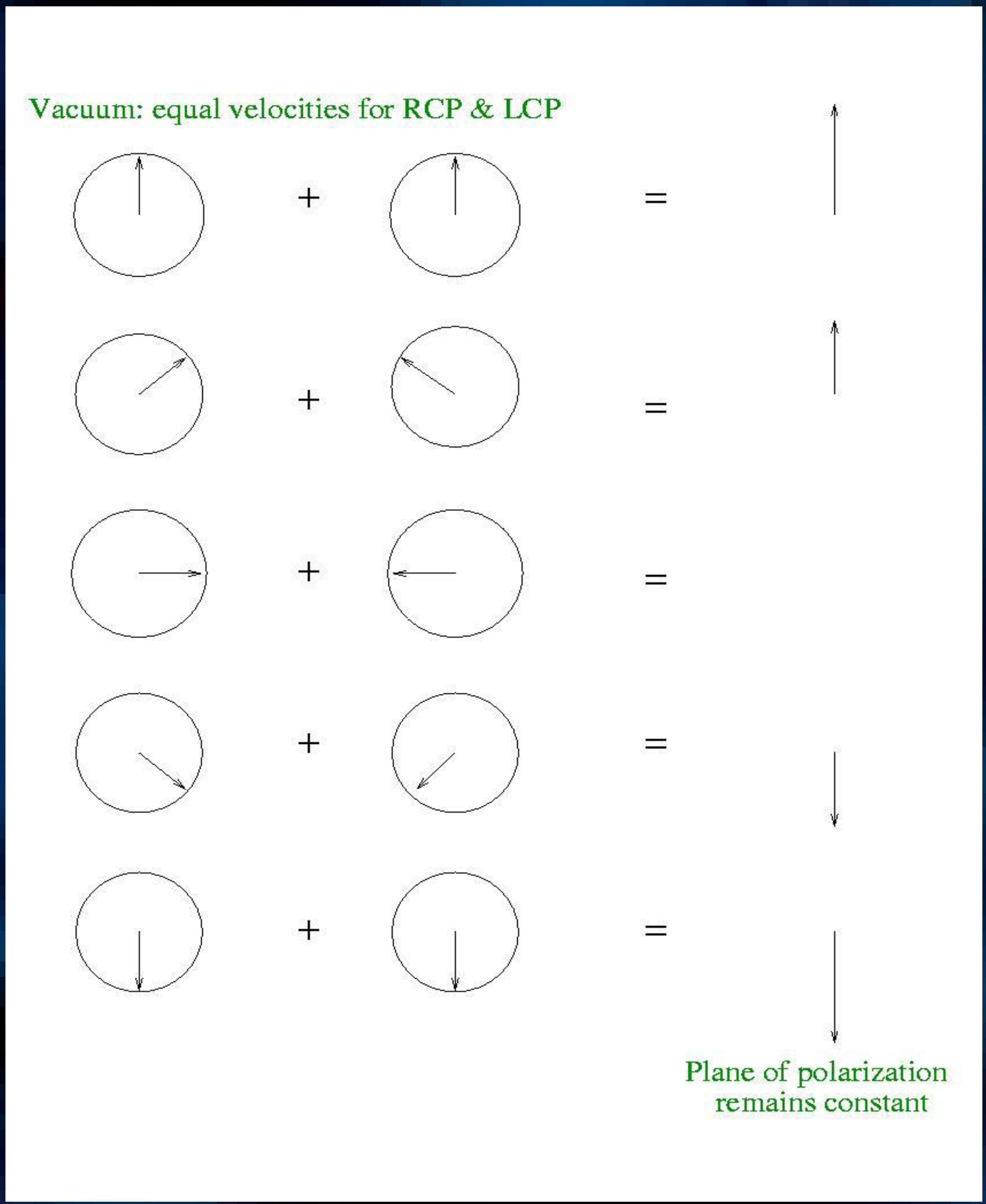
Vacuum: equal velocities for RCP & LCP
+
=
Plane of polarization
remains constant

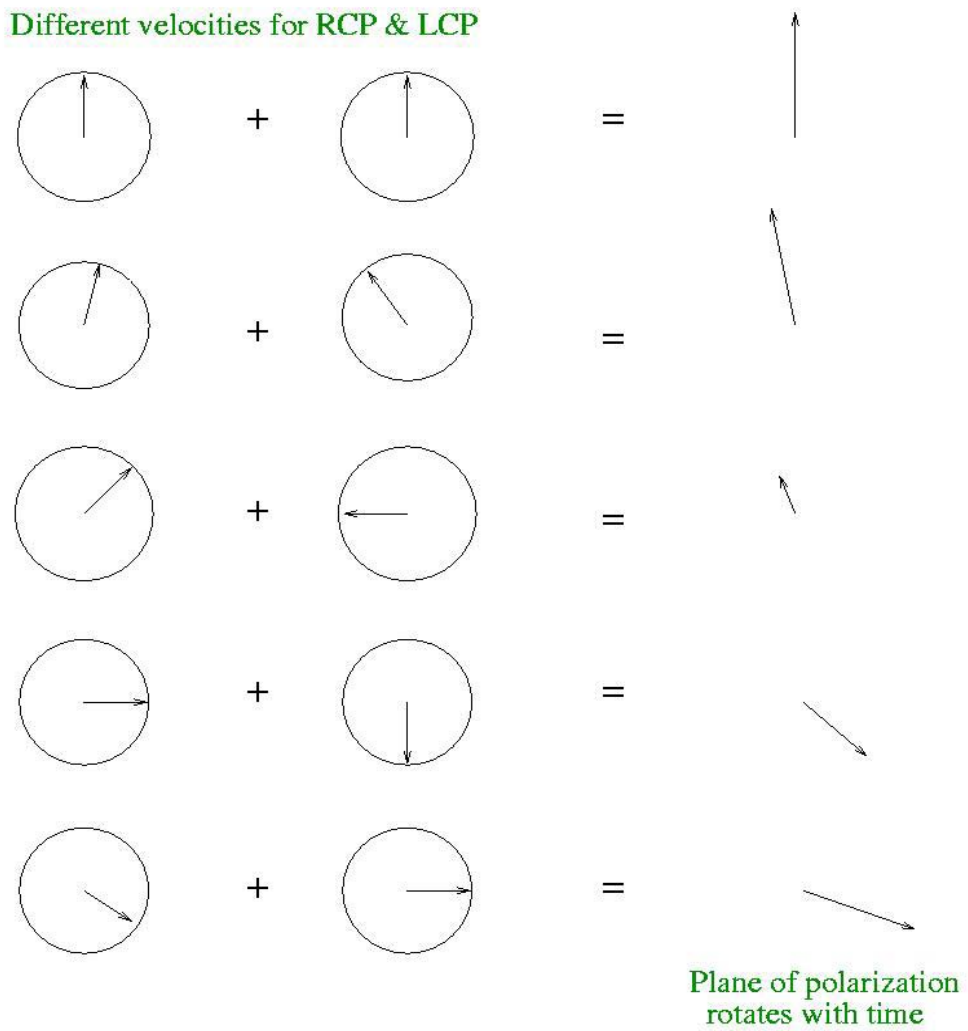
Different velocities for RCP & LCP
+
=
Plane of polarization
rotates with time

Observed radio polarisation angles are affected by three factors:

1) B field in emission region

2) optical depth of emission region

3) possible Faraday rotation

Standard picture of emission structure along the jet

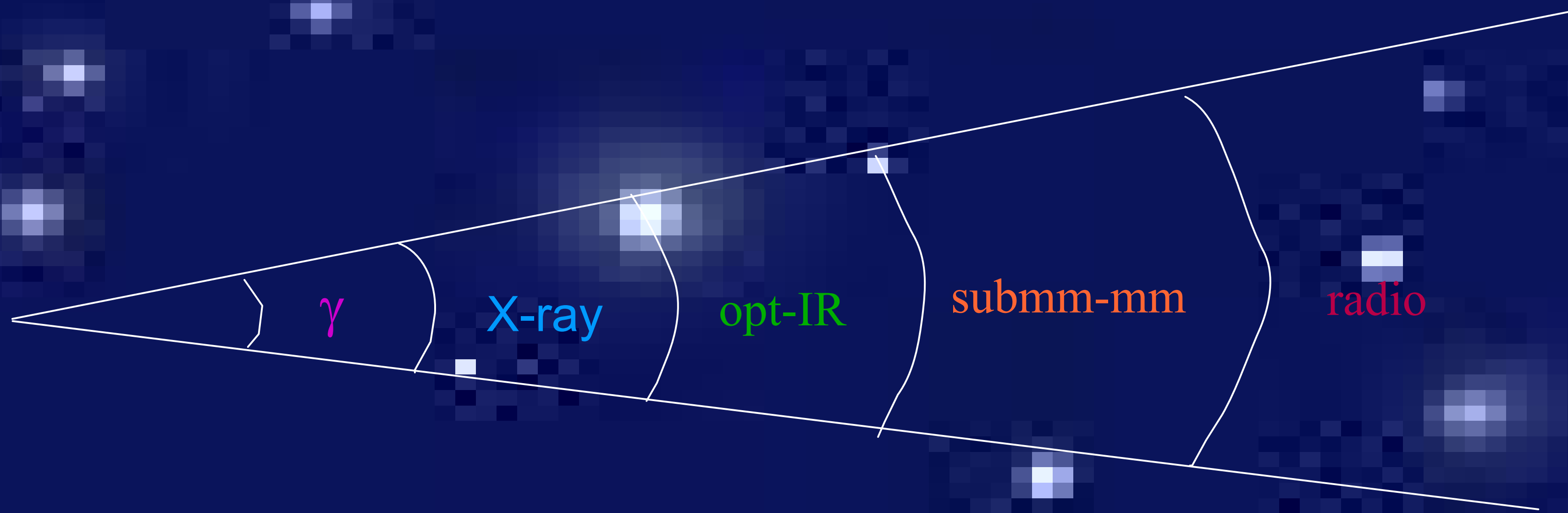

→Expect no obvious correlation between emission in very different wavebands

By and large, early searches for correlations between optical and radio variations of AGN yielded negative results...

Kinman et al. (1974) – coordinated observations at optical, mm, radio wavelengths

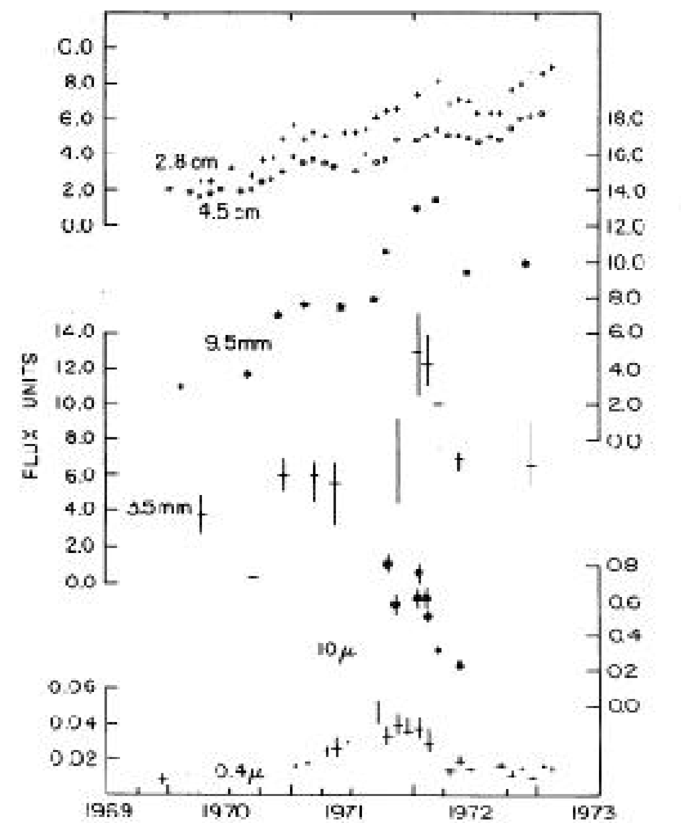

FIG. 1. Monthly means of fluxes of OJ 287 at different wavelengths. References: 0.44 μ—this paper and Visvanathan and Elliott (1973); 10 μ—Rieke (1972); 3.5 mm—this paper and E. E. Epstein (unpublished); 9.5 mm—this paper and Dent and Hobbs (1973); 4.5 and 2.8 cm—this paper and Medd, Andrew, Harvey, and Locke (1973). Vertical bars for 0.44-μ observations show the monthly range, while for 10-μ and 3.5-mm observations they are rms errors. The ordinate marked at the top left refers to both 2.8- and 4.5-cm observations; the other ordinates refer in sequence to each of the other wavelengths.

Pomphrey et al. (1976) – search for correlations between optical and radio variations – evidence for correlations found only in OJ287

Examples of optical & radio light curves...

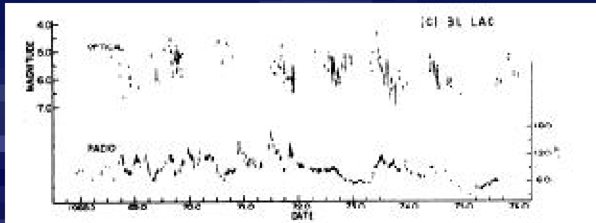

FIG. 1(c). BL Lac. Optical and Algonquin 2.8-cm observations. The optical record consists of Royal Greenwich data from 1968.5 to 1970.8 and Rosemary Hill data from 1971.5 to 1976.0. Most of the optical data were reduced using the sequence of Bertaud *et al.* (1969). However, Royal Greenwich data after 1970.0 used a revised sequence and an offset of $-0^m.08$ has been applied. The Royal Greenwich data following 1970.8 have not been plotted due to the density of the combined data sets.

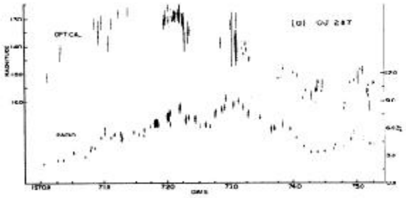

FIG. 1(a). OJ 287. Rosemary Hill and Algonquin 2.8-cm observations. Rosemary Hill points after mid-1971 are *B* magnitudes; earlier points are photographic (m_{pg}) magnitudes corrected to *B* magnitudes.

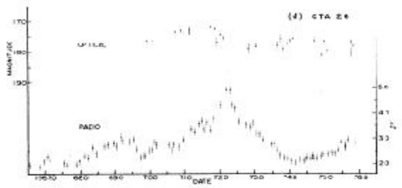

FIG. 1(d). CTA 26 (PKS 0336-01). Rosemary Hill photographic magnitudes and Algonquin 2.8-cm observations.

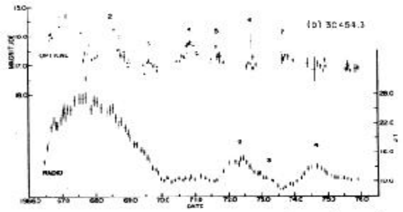

FIG. 1(b). 3C 454.3. Optical and Algonquin 2.8-cm observations. The optical record consists of Royal Greenwich *B* magnitudes (with a $-0^m.47$ offset) from 1966 to 1972.75; Rosemary Hill photographic (m_{pg}) magnitudes from 1968.9 to 1971.5, and Rosemary Hill *B* magnitudes from 1971.6 to 1975.9. Yale *B* magnitudes (with a $+0^m.125$ offset) from 1967.6 to 1971.0 reinforce the illustrated optical activity but are not included due to the high density of points. The numbering of events does not imply a one-to-one correlation between corresponding numbers (see text).

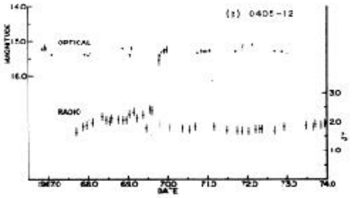

FIG. 1(e). PKS 0405-12. Royal Greenwich *B* magnitudes and Algonquin 2.8-cm observations.

...and correlation coefficients

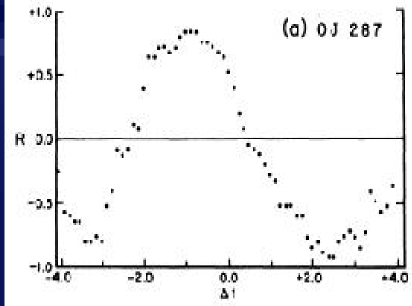

FIG. 2(a). Normalized cross-correlation coefficient (R) versus time shift (Δt) for the OJ 287 data presented in Fig. 1(a). (No interpolation has been used.)

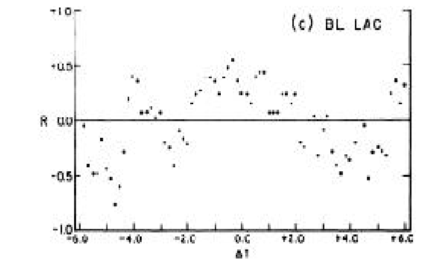

FIG. 2(c). Normalized cross-correlation coefficient (R) versus time shift (Δt) for the BL Lac data presented in Fig. 1(c).

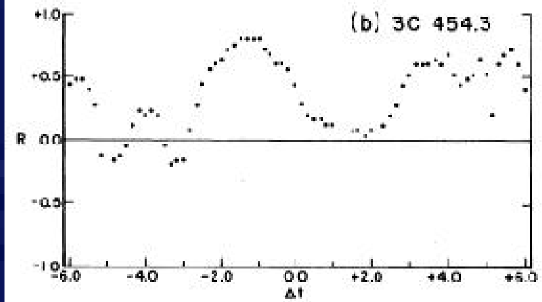

FIG. 2(b). Normalized cross-correlation coefficient (R) versus time shift (Δt) for the 3C 454.3 data presented in Fig. 1 and including the Yale Observatory data. (No interpolation has been used.)

Gabuzda, Sitko & Smith (1996): simultaneously measured optical and 6cm VLBI core polarisation angles nearly always aligned or perpendicular

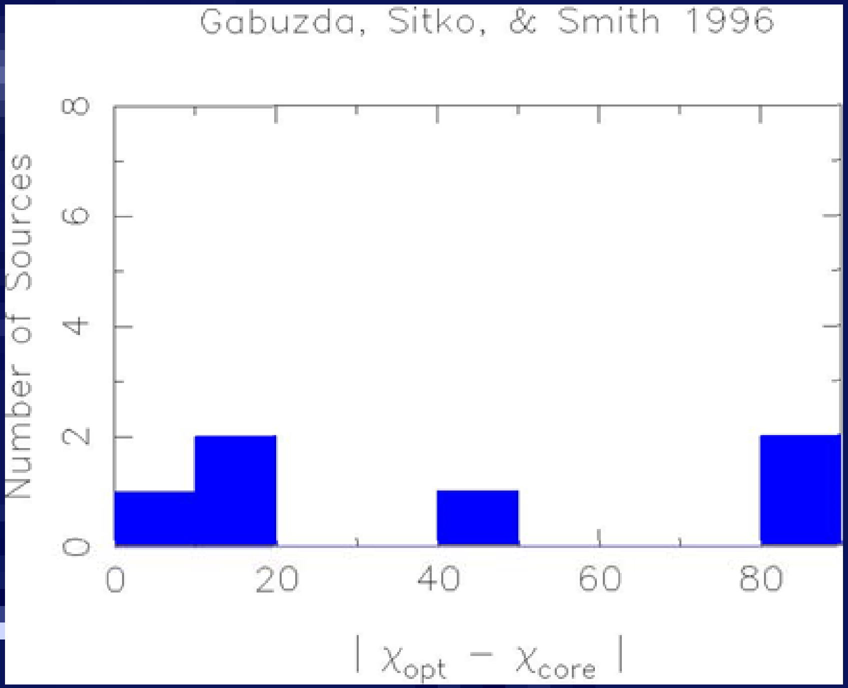

No correlation for jet pol. angles.

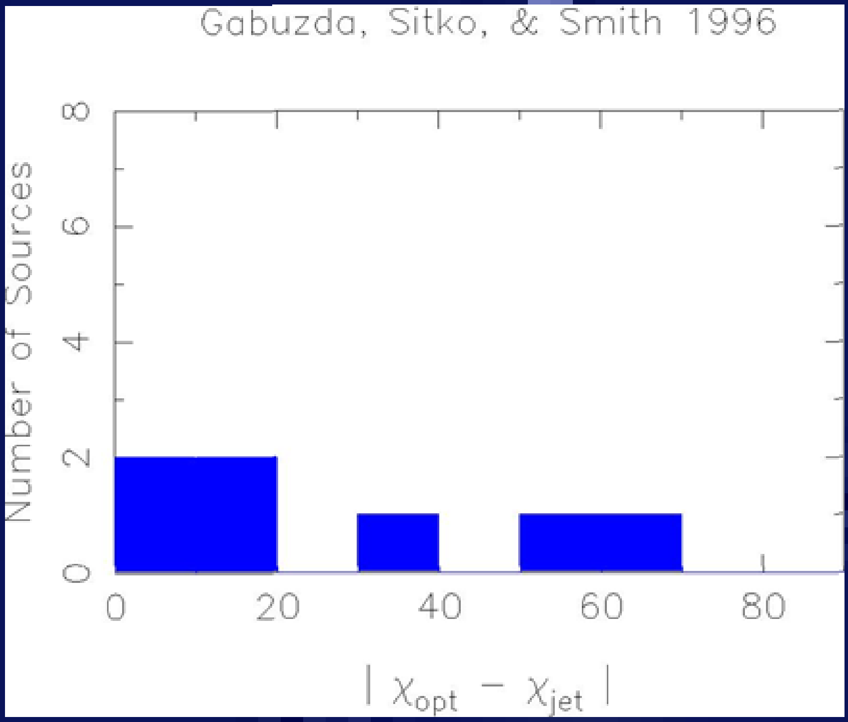

Binomial probability distribution for two outcomes A and B with unequal probabilities:

$$P_{chance} = (P_A)^{n_A} * (P_B)^{n_B} * \frac{n_{total}!}{n_A! n_B!}$$

Taking the two outcomes to be $\chi_{opt} - \chi_{VLBI}$ either (i) near the edges or (ii) in the centre of the histogram:

$$P_{chance} = (P_{edge})^{n_{edge}} * (P_{centre})^{n_{centre}} * \frac{n_{total}!}{n_{edge}! n_{centre}!}$$

$$P_{chance} = \left(\frac{4}{9}\right)^{n_{edge}} * \left(\frac{5}{9}\right)^{n_{centre}} * \frac{n_{total}!}{n_{edge}! n_{centre}!}$$

Probabilities for optical+VLBI measurements of Gabuzda, Sitko & Smith (1996):

Optical vs. Core: $n_{total} = 6,\ n_{edge} = 5,\ n_{centre} = 1 \longrightarrow P_{chance} = 6\%$

Optical vs. Jet: $n_{total} = 7,\ n_{edge} = 4,\ n_{centre} = 3 \longrightarrow P_{chance} = 29\%$

Trend confirmed after addition of new data:

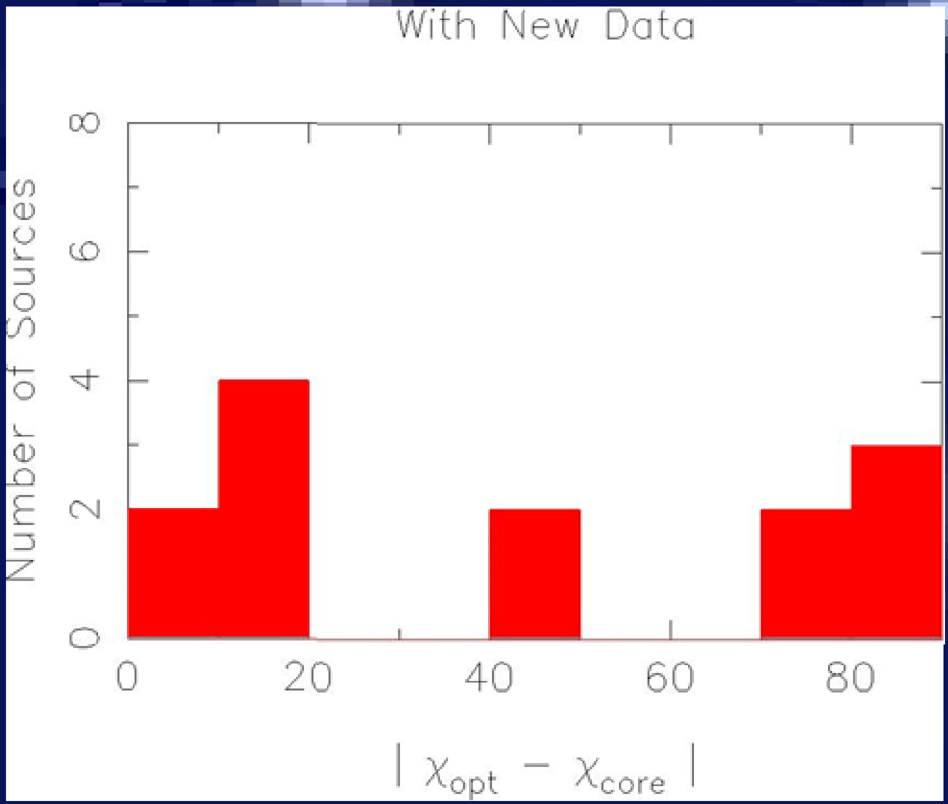

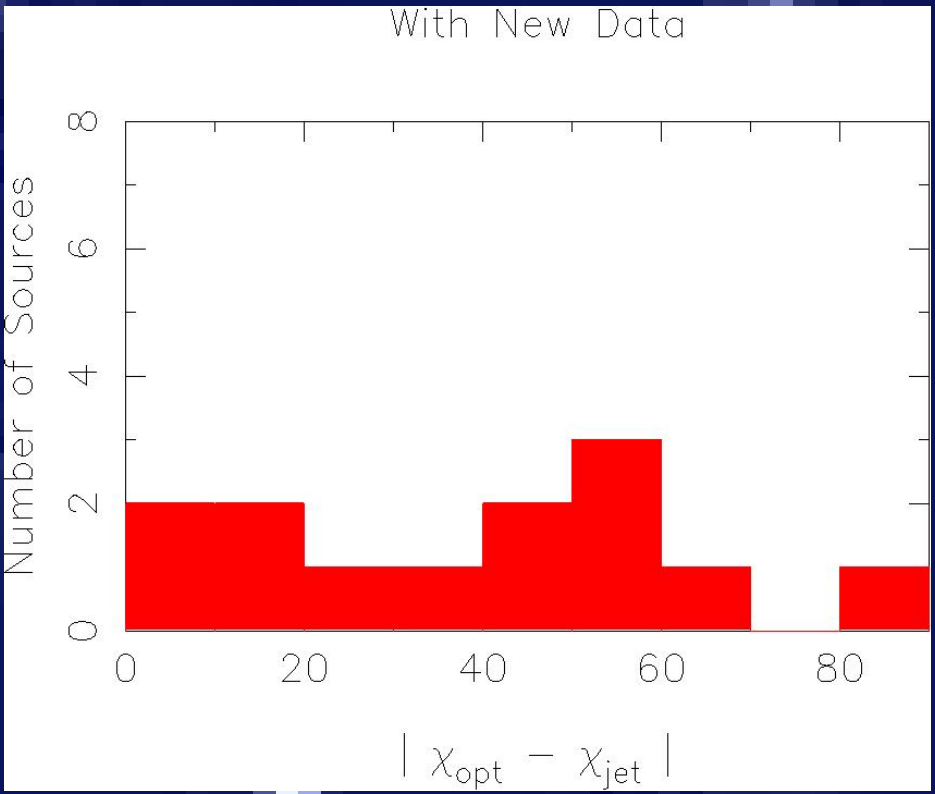

Probabilities with addition of new data:

Optical vs. Core: $n_{total} = 13,\ n_{edge} = 11,\ n_{centre} = 2 \longrightarrow P_{chance} = 0.3\%$

Optical vs. Jet: $n_{total} = 13,\ n_{edge} = 5,\ n_{centre} = 8 \longrightarrow P_{chance} = 20\%$

Bimodal distribution can be understood if

1) optical and VLBI-core polarisation angles are intrinsically aligned

2) VLBI cores with aligned/perpendicular polarisation angles are optically thin/thick
(emission in optical is always optically thin)

Simple prediction:

More and more cores with aligned optical and radio polarisation angles should be observed as move toward higher radio frequencies, where observed cores are more dominated by optically thin regions

New simultaneous optical and 2cm+1cm+7mm VLBA polarisation data obtained to test this hypothesis:

August 2002 – 6 BL Lac objects

March 2003 – 8 BL Lac objects + blazar 3C279

Optical observations obtained on 60” (August 2002, white light) or 90” (March 2003, R) telescopes at Kitt Peak, simultaneous with VLBA observations to within one day

Comparison of VLBI core and optical polarisation angles

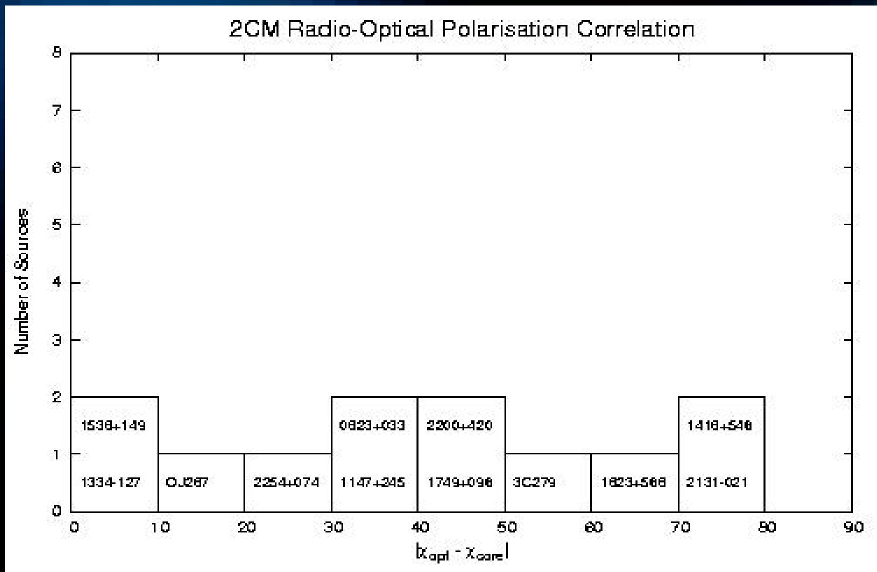

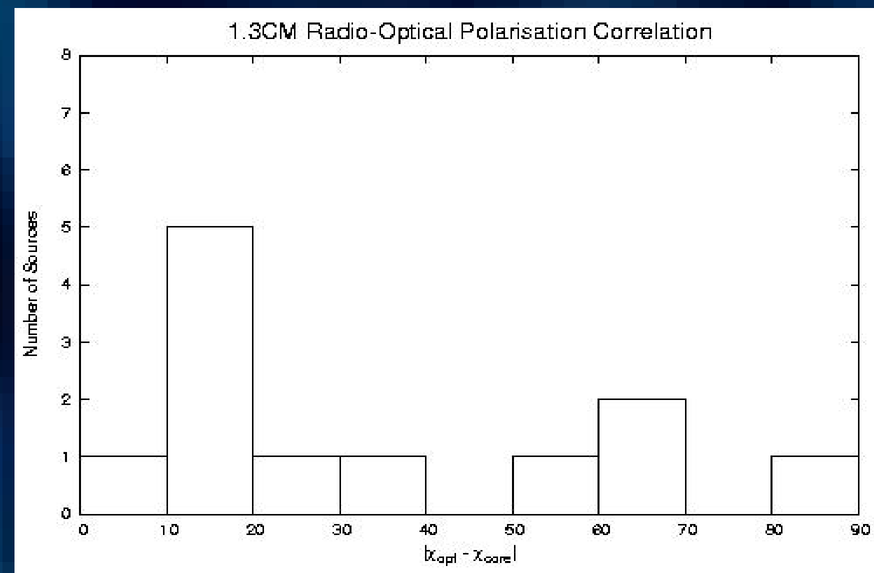

Clear correlation appears at high radio frequencies!

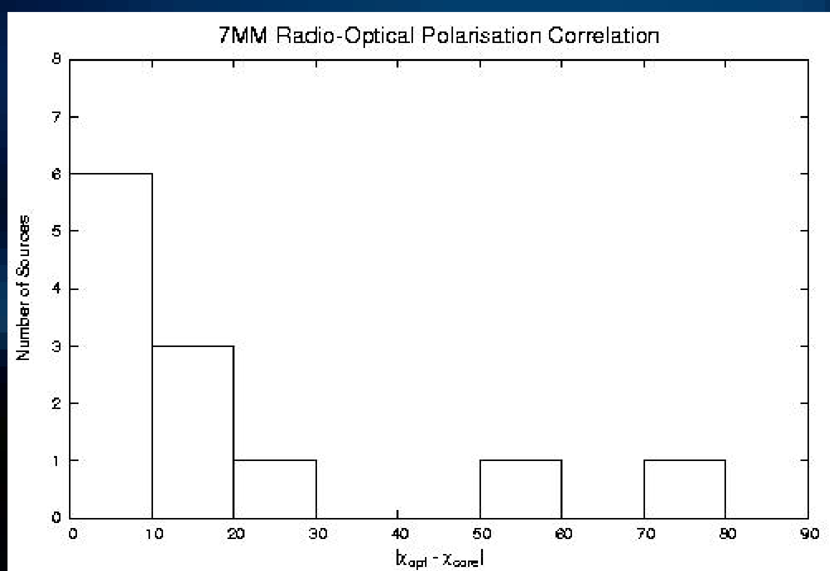

Examples of optical and VLBI polarisation angle correlations

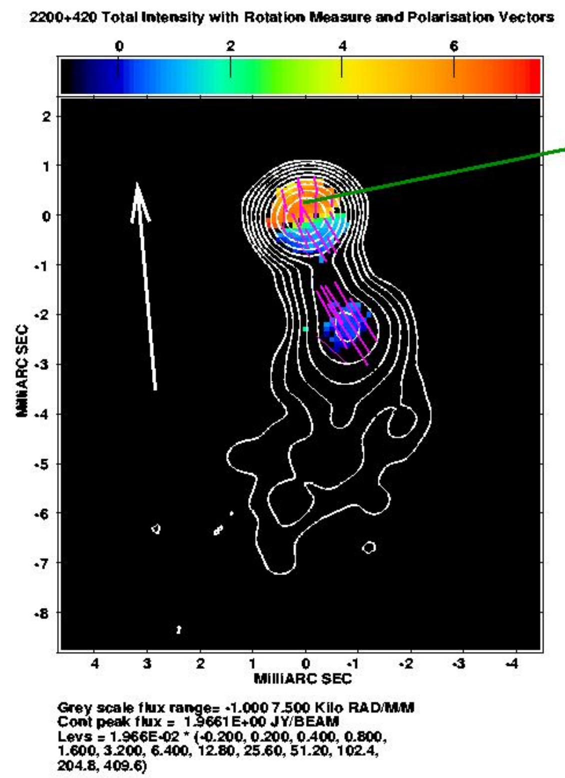

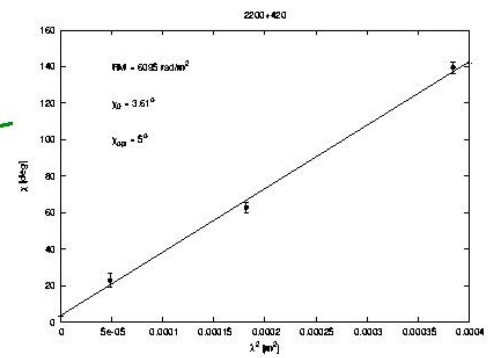

Correcting for Faraday rotation

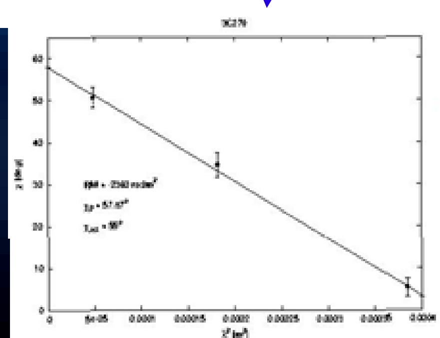

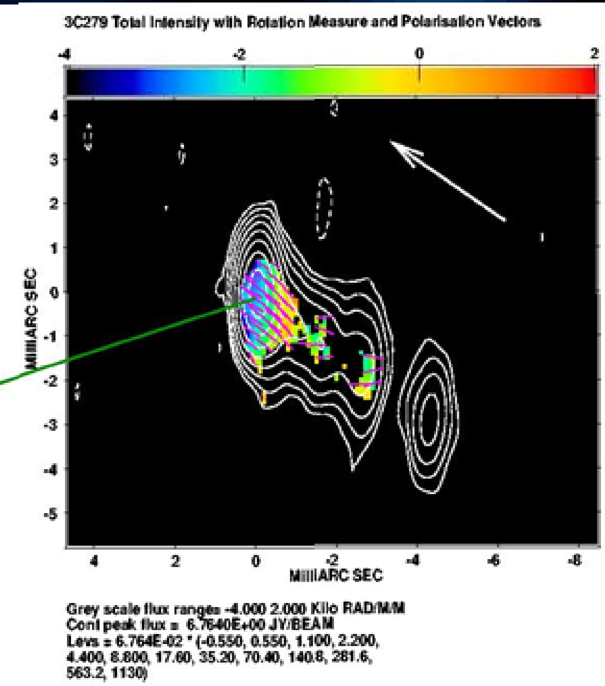

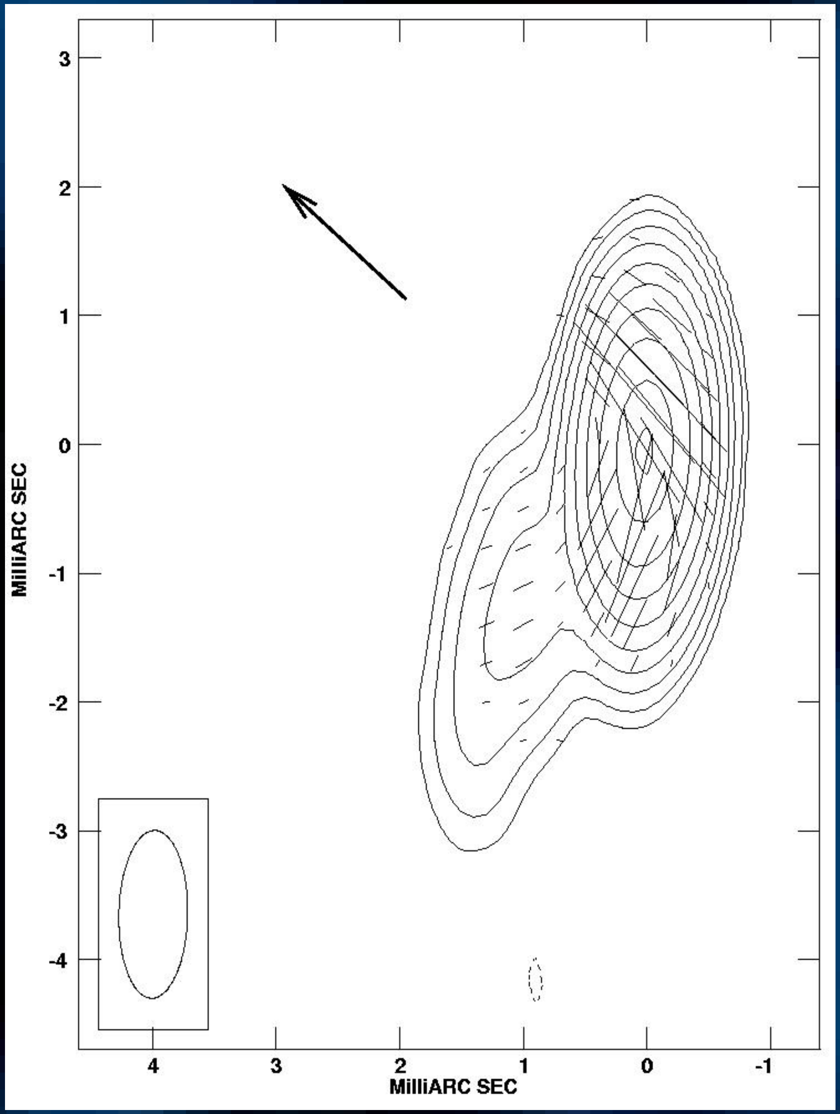

Optical polarisation better aligned with polarisation in inner jet than core?

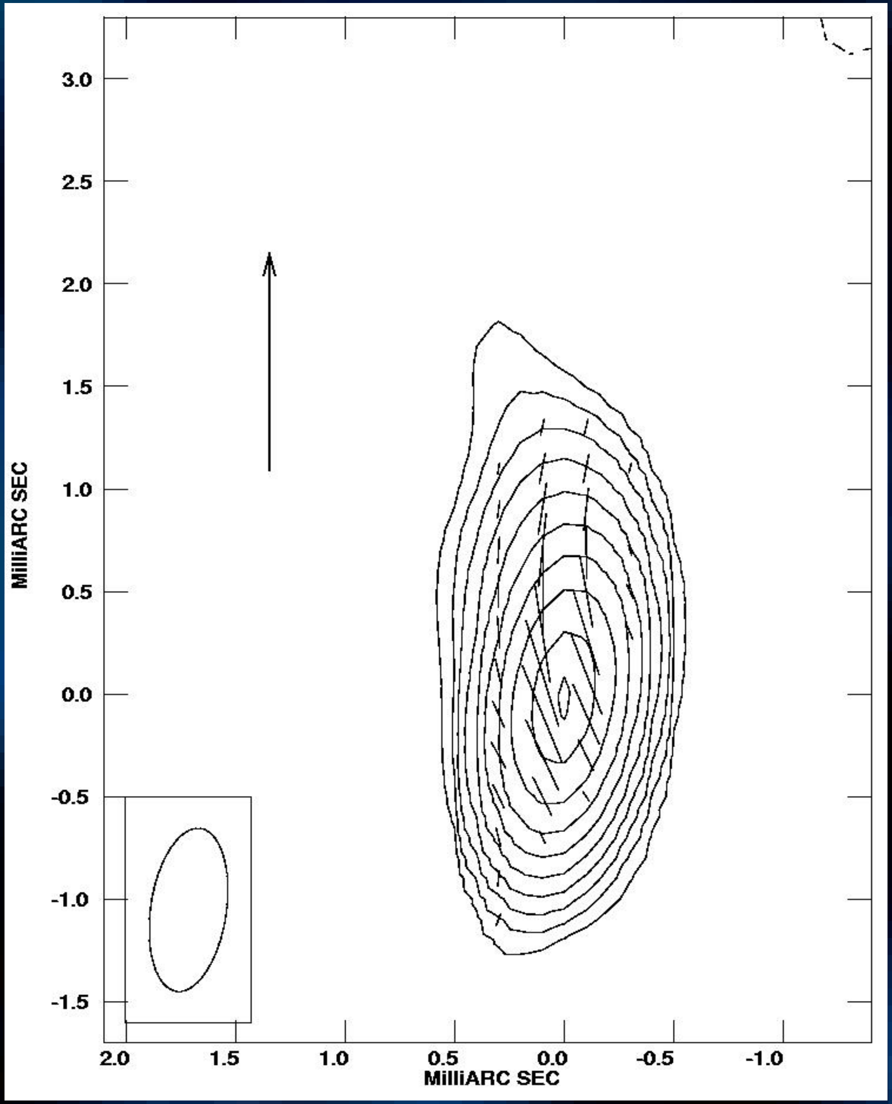

B field in core region is not always perpendicular to jet direction

Summary

-- Comparison of polarisation angles for high-frequency VLBI core and in optical show surprisingly strong tendency for the two angles to be aligned

-- Correlation becomes noticeably stronger as we move toward higher radio frequencies:

1) more radio cores are optically thin
2) lower influence of potentially strong core Faraday rotation on radio polarisation angles

-- The B fields in the regions giving rise to the optical and VLBI-core polarisation have the same geometry – either:

1) the optical and radio emission are co-spatial OR
2) they arise in different regions of the jet, but the jets are quite straight

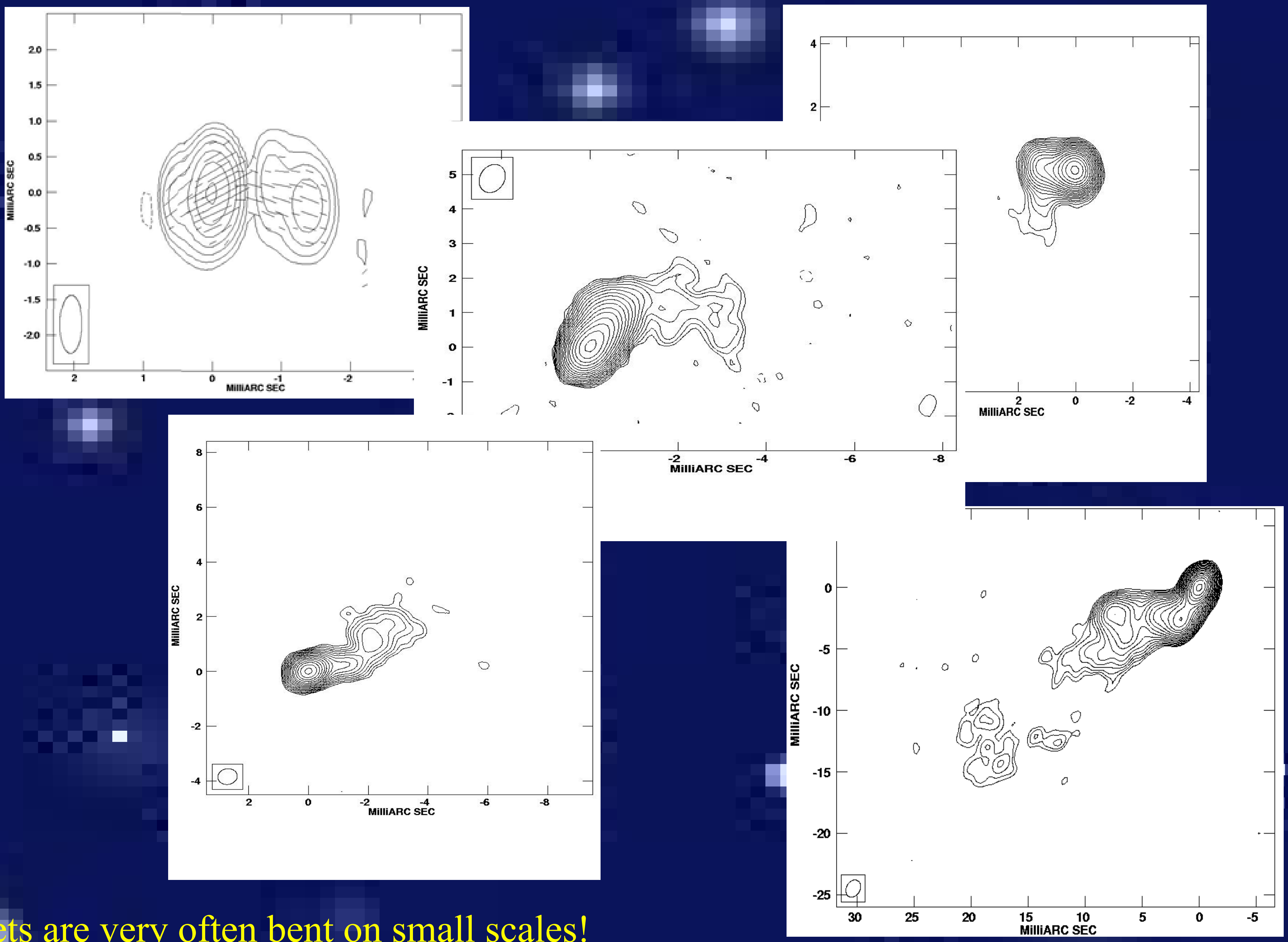

But jets are very often bent on small scales!

Future Work

-- Search for correlations between degree of polarisation in optical and properties of VLBI core (degree of polarisation, radio spectral index)

-- New simultaneous optical and 2cm+1cm+7mm VLBA polarisation observations obtained for an additional 26 AGN – 6 BL Lac objects, 12 HPQs, 8 LPQs

→how common are optical—VLBI correlations for various classes of AGN?

→ is the presence of optical—VLBI correlations associated with any particular activity state or B-field structure?

Analysis of 22GHz and 37GHz observations

6th ENIGMA meeting
18-25 November 2005
Kinsale, Ireland

Mirko Tröller
Metsähovi Radio Observatory

Outline

- The Sample
- Motivation
- Methods
- Examples
- Outlook

Observations – Metsähovi monitor programme

- 14 m dish
- AGN Flux density monitoring at 22GHz and 37GHz

Mirko Tröller
Metsähovi Radio Observatory

The sample

Selection of best observed objects::

- 25 BL Lac objects
- 23 Low polarized quasars
- 20 High polarized quasars
- 5 Quasars
- 5 Galaxies

Motivation

- determine and characterize the variability
- find characteristic timescales
- test angle orientated models
- study the spectral evolution of flares
- determine shape of flares (if possible)
- determine rise and decay times (t_{heat} & t_{cool})

Method I

Structure function analysis:

- constrain of mechanism
- compare t_{max} & source-sample to test angle dependent models
- determine amplitudes to characterize variability
- determine noise

Method II & III

Discrete cross correlation (Edelson&Krolik '88) of 22GHz and 37GHz (and higher)

- determine time lag
- determine noise

Fitting of the flares to

- calculate rise and decay time
- determine amplitude

Example HPQ - 0234+285

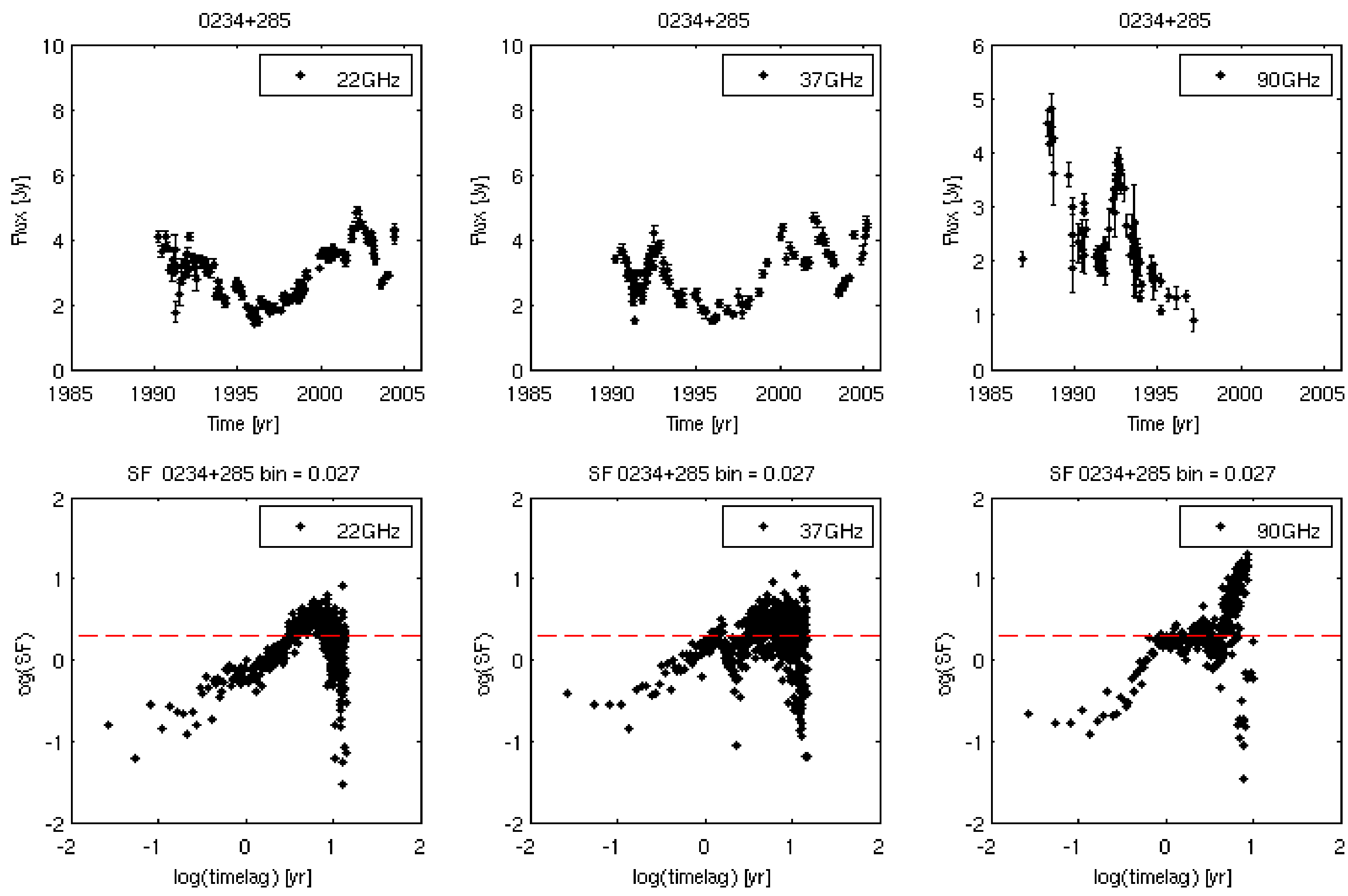

Mirko Tröller
Metsähovi Radio Observatory

Example LPQ - 0552+398

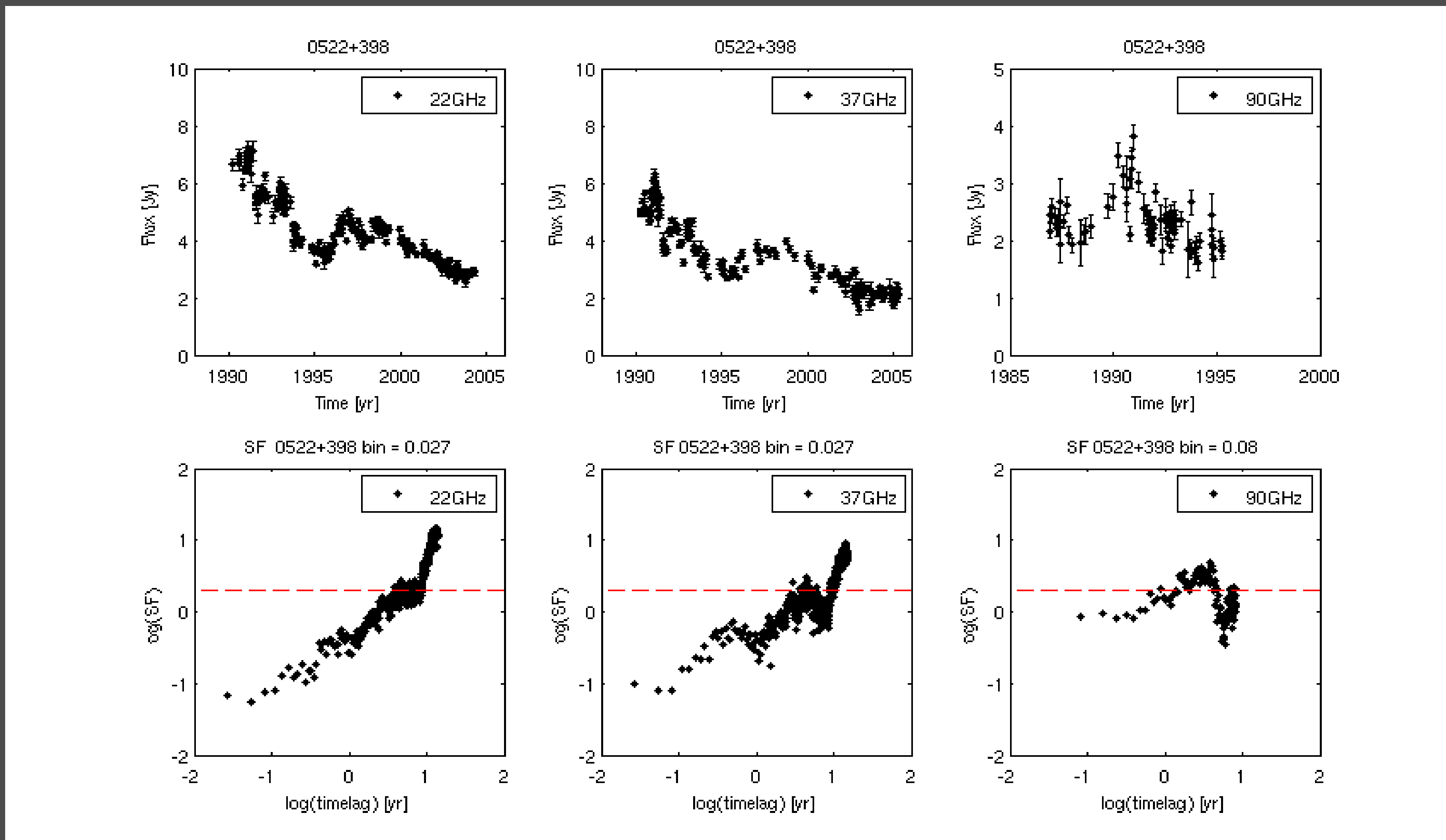

Mirko Tröller
Metsähovi Radio Observatory

Example BL Lac - 1413+135

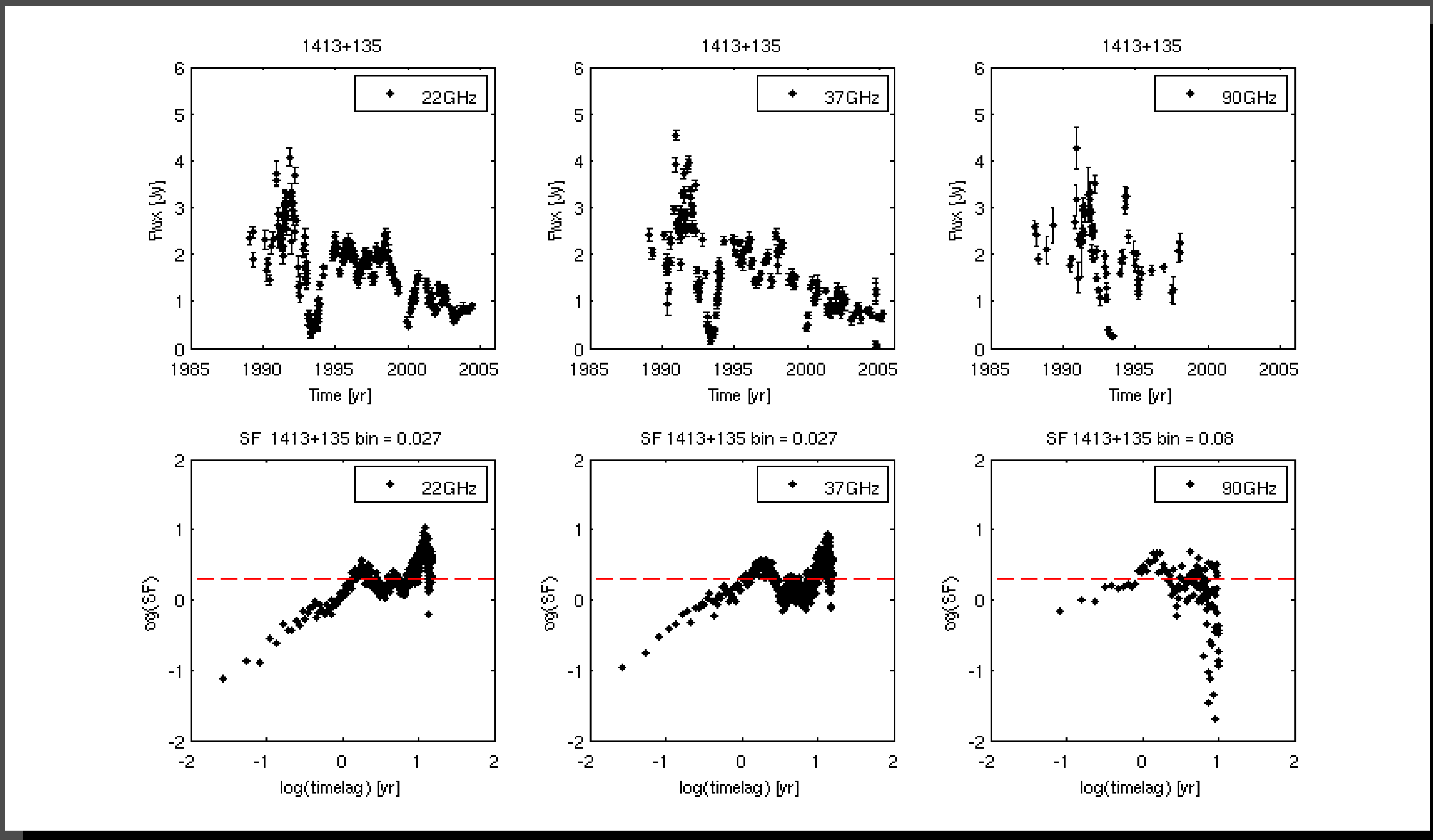

"Results"

	0234+285			0552+134			1413+135		
GHz	22	37	90	22	37	90	22	37	90
# obs	144	105	79	216	170	72	240	186	70
S_min	1.4	1.5	0.9	2.3	1.5	1.6	0.3	0.3	0.3
S_max	4.9	4.7	4.8	7.2	6.3	3.8	4.1	4.6	4.3
S_mean	2.8	2.9	2.5	4.3	3.5	3.3	1.7	1.6	2.1
sigma	0.8	0.8	0.9	1.1	1.2	0.4	0.8	0.8	0.8
var	0.7	0.6	0.8	1.2	1.5	0.2	0.6	0.6	0.6
fra_var	2.5	2.1	4.3	1.9	3.1	1.4	11	49	18
alpha	0.81	0.65	1.08	0.8	0.96	0.53	0.85	0.73	0.6

Correlations

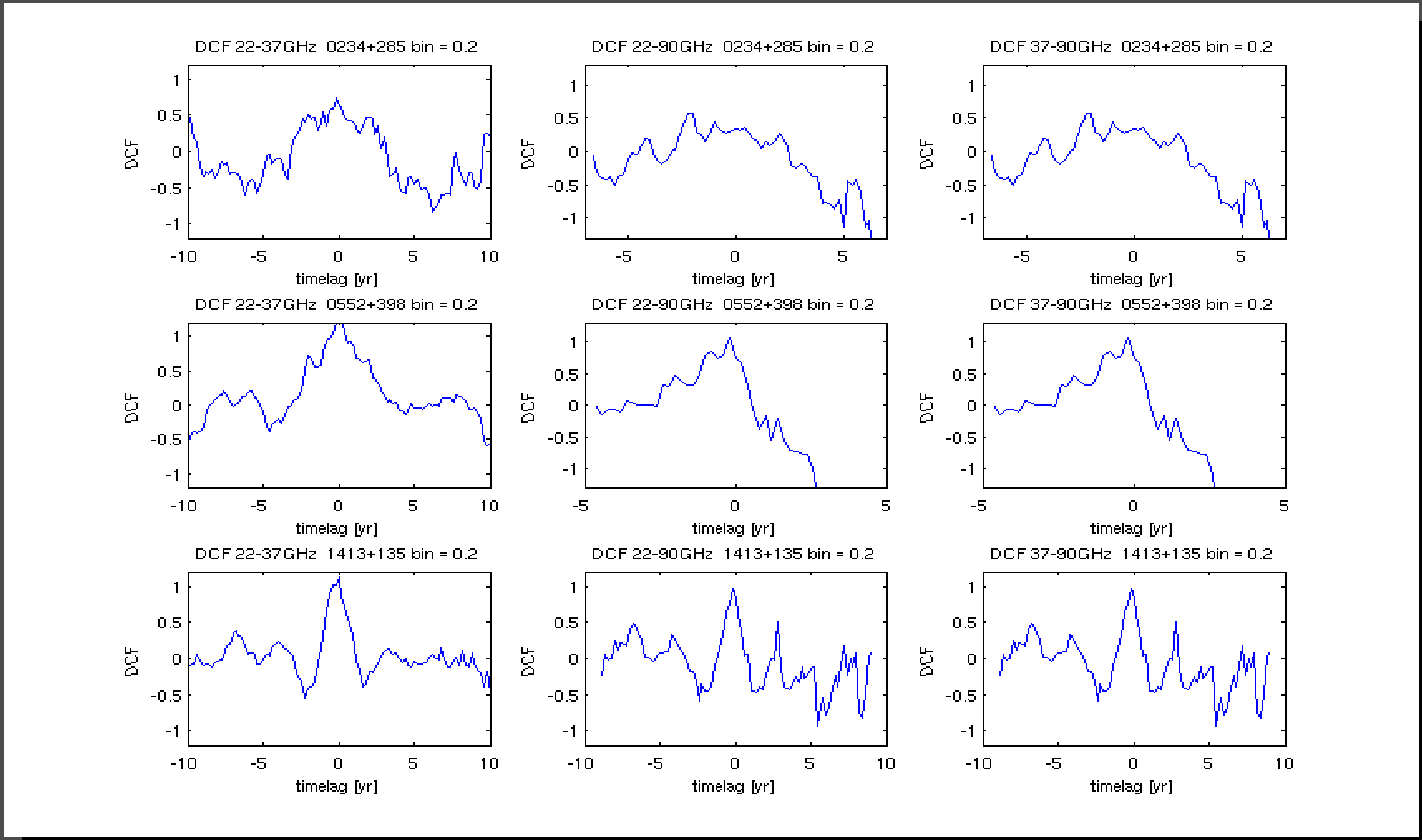

Mirko Tröller
Metsähovi Radio Observatory

Outlook - future method

Wavelet analysis of 22GHz and 37GHz data

compare this with SF, FT(PDS) and cross correlation

Thanks for your attention

The cyclo–synchrotron process and particle heating through absorption of photons

Krzysztof Katarzyński

Osservatorio Astronomico di Brera (OAB, Italy)

Outline

- from cyclotron to synchrotron emission
- correction for the synchrotron emissivity
- approximation of the cyclo-synchrotron emissivity
- particle heating through absorption of photons
- self-absorbed part of the synchrotron spectrum

Three emission regimes

We may distinguish three emission regimes:

- cyclotron emission $\longrightarrow$ $\boxed{\beta \ll 1}$
- cyclo-synchrotron emission $\longrightarrow$ $\boxed{0.1 \lesssim \beta \lesssim 0.9}$
- synchrotron emission $\longrightarrow$ $\boxed{\beta \lesssim 1}$

where β is the particle velocity in units of c.

Note that $p = \beta\gamma$ is the particle momentum, γ is the particle Lorentz factor related to the total energy by $E = \gamma m_e c^2$.

Cyclotron emission

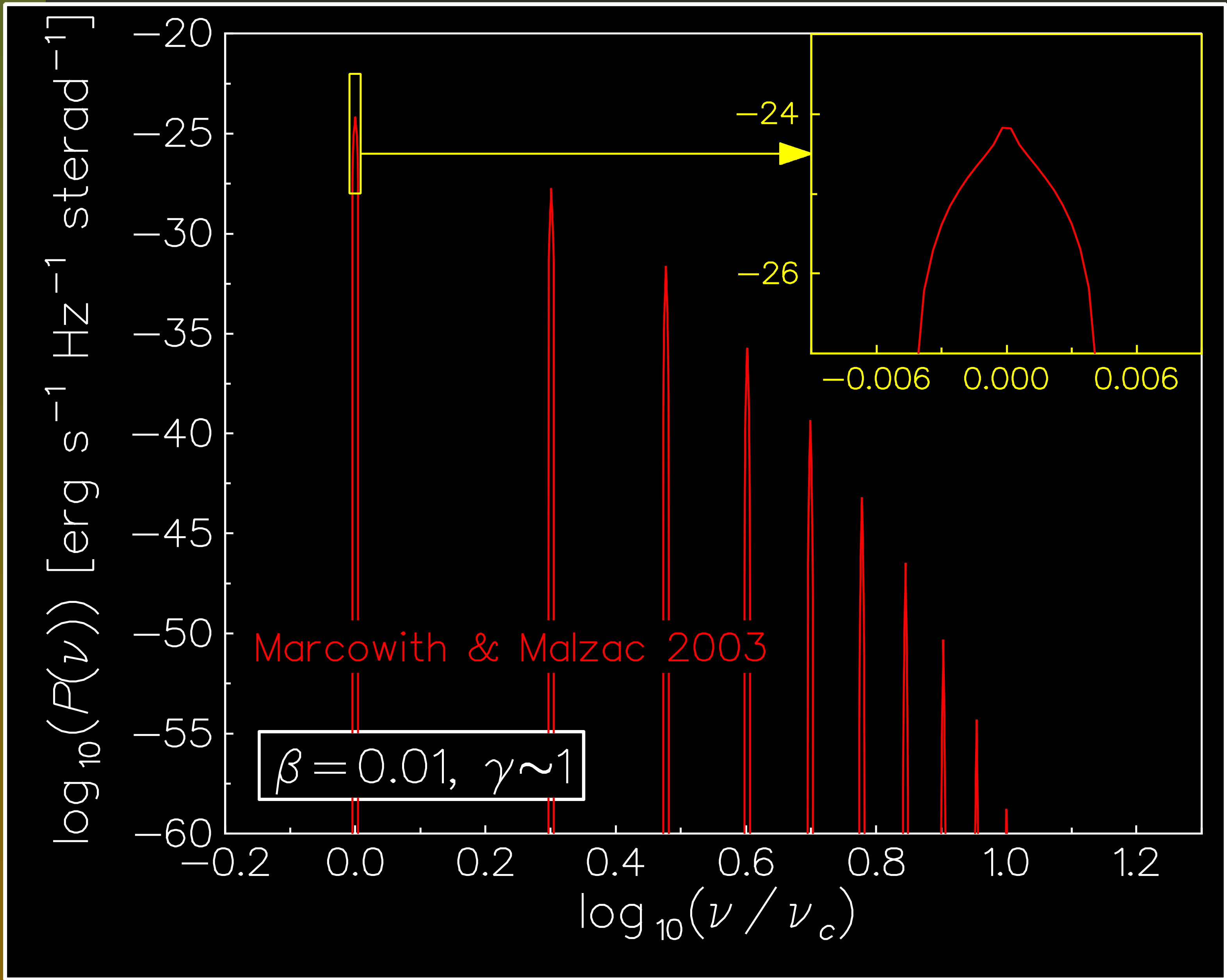

OAB-Italy

Cyclo-synchrotron emission

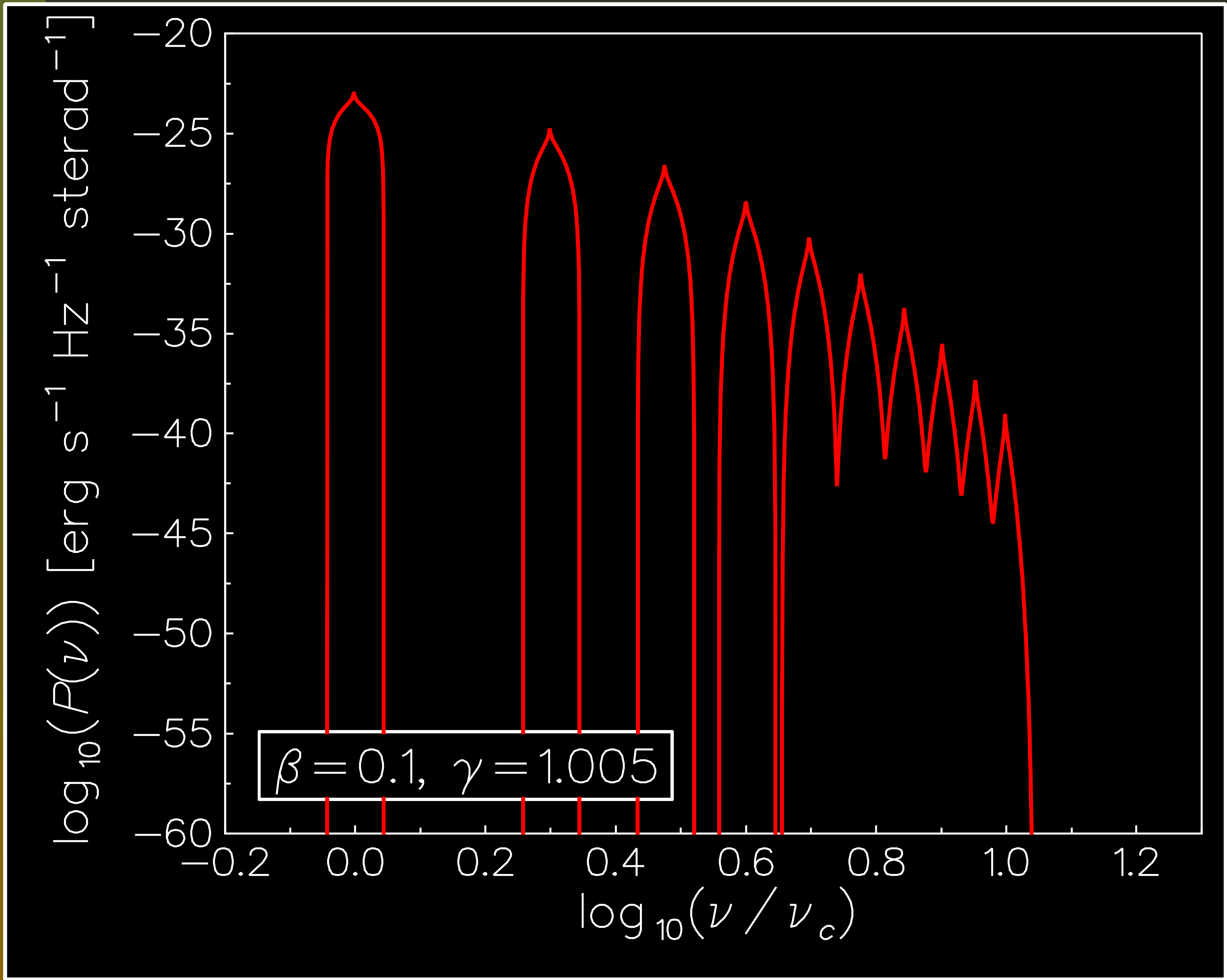

Cyclo-synchrotron emission

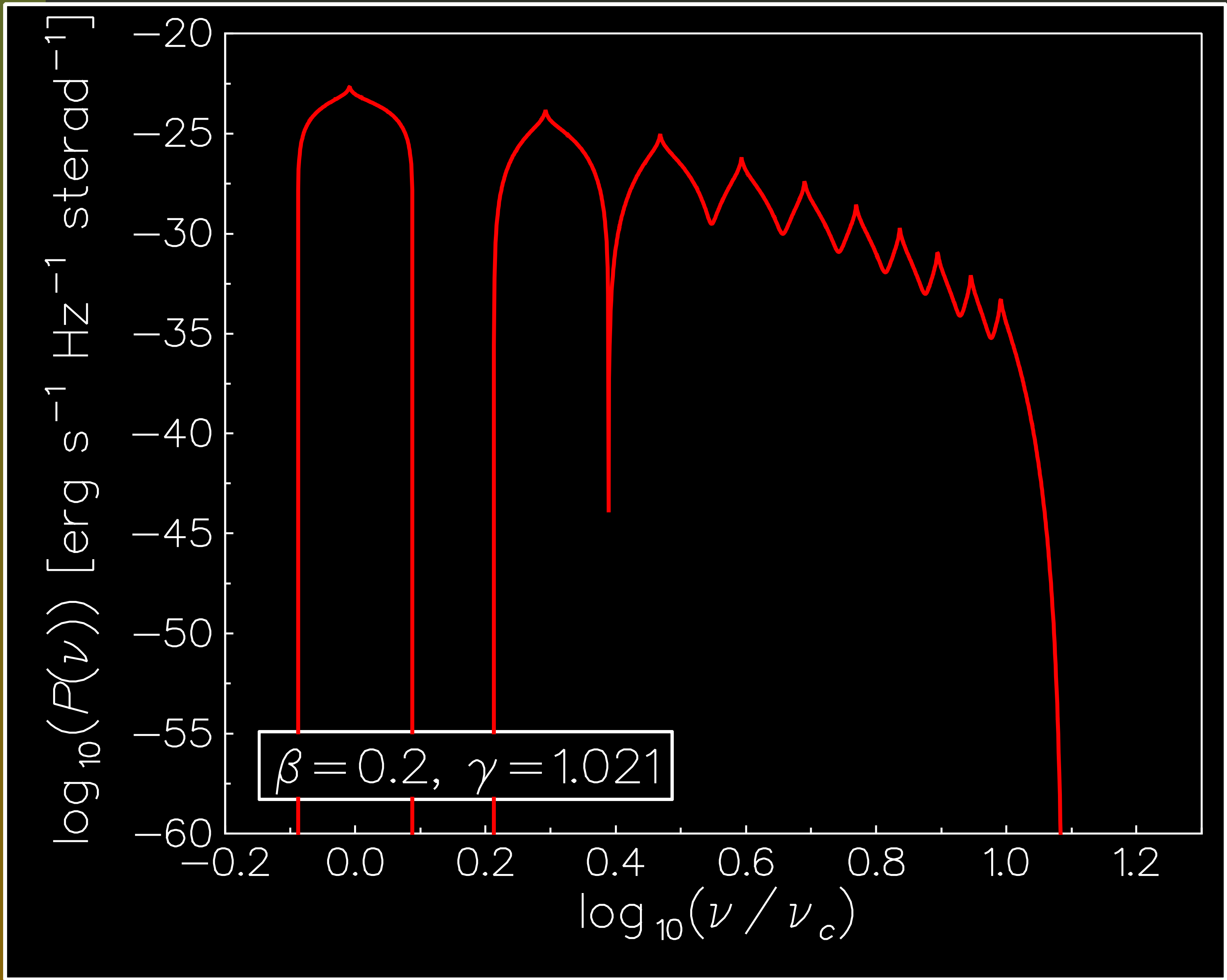

OAB-Italy

Cyclo-synchrotron emission

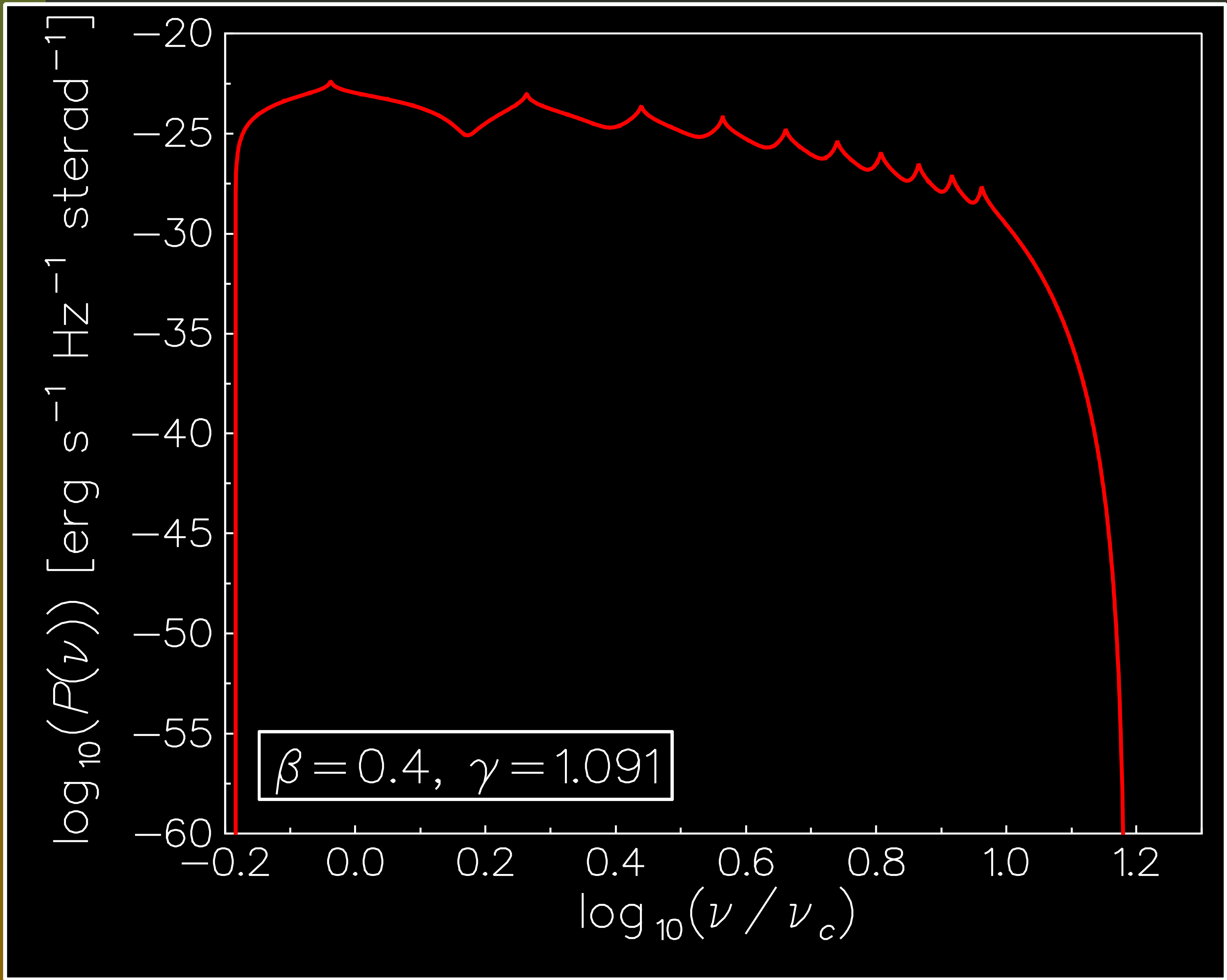

Cyclo-synchrotron → synchrotron

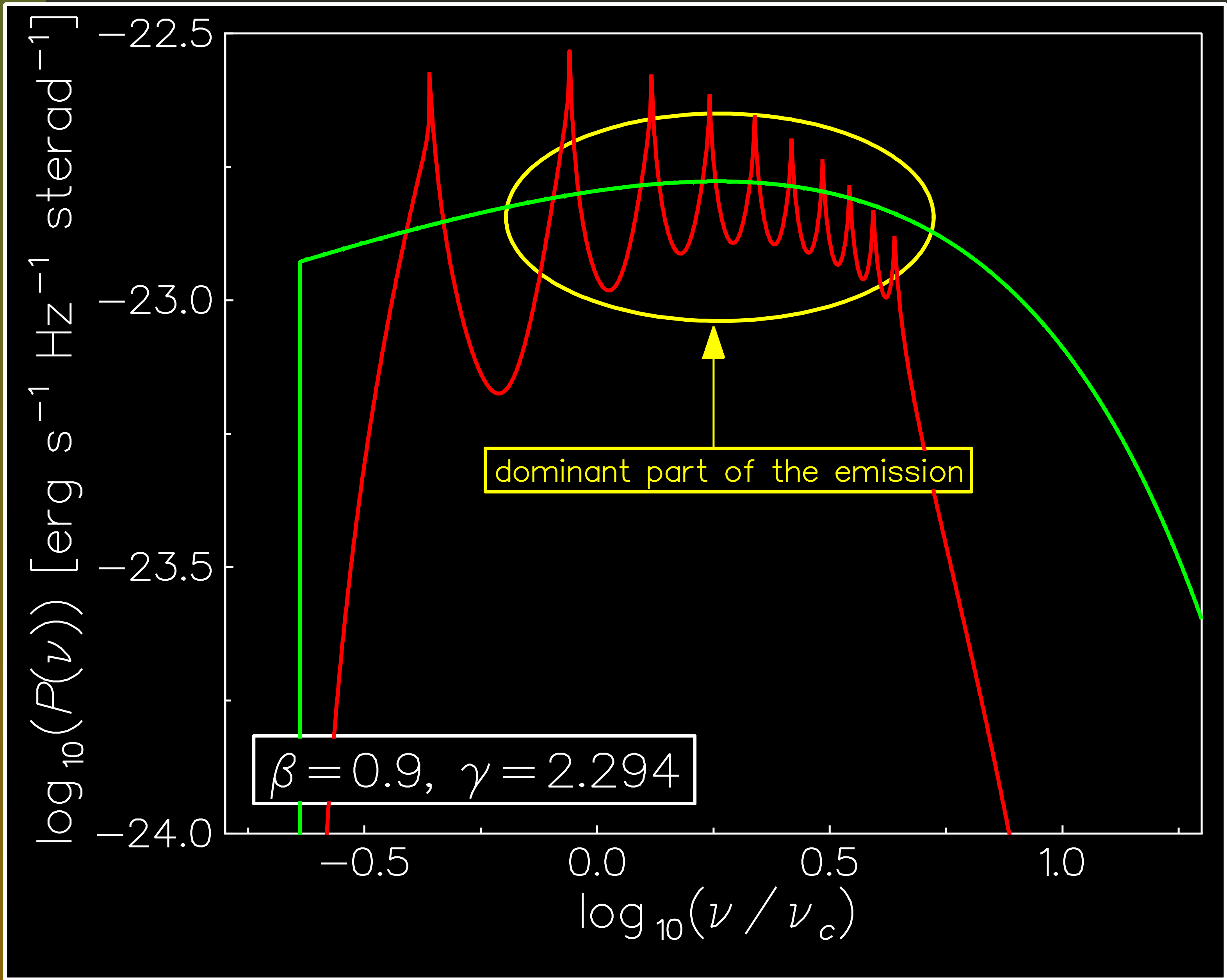

Correction of the synch. emission

The synchrotron power spectrum of a single particle in random magnetic field, integrated over an isotropic distribution of pitch angles

$$P_s(\nu,\gamma) = \frac{3\sqrt{3}}{\pi}\frac{\sigma_{\rm T} c U_B}{\nu_c}\, x^2 \left\{ K_{4/3}(x)K_{1/3}(x) - \frac{3}{5}x\left[K^2_{4/3}(x) - K^2_{1/3}(x)\right]\right\}$$

where $x = \nu/(3\gamma^2\nu_c)$ and $K_y(x)$ is the modified Bessel function of order y (Crusius & Schlickeiser 1986, Ghisellini, Guilbert, & Svensson 1988), integrated over the frequency range does not provide the correct cooling ratio

$$\dot{\gamma}_c = \frac{4}{3}\frac{1}{m_e c^2}\sigma_{\rm T}\, c\, U_B\, p^2, \quad U_B = \frac{B^2}{8\pi}$$

for $\boxed{\gamma \lesssim 15}$.

The correction term

In order to correct the synchrotron emissivity we multiply the standard formula by

$$s(\gamma) = \frac{\dot{\gamma}_c(\gamma)}{\int_{\nu_{\rm min}}^{\infty} P_s(\nu,\gamma) d\nu},$$

where $\nu_{\rm min}(\gamma) = \frac{\nu_c}{\gamma(1+\beta)}$. Note that for $\gamma \gg 15$ this correction term becomes negligible. The correction provides self-consistently correct value of the total emitted power for any particle energy.

Corrected synchrotron emission

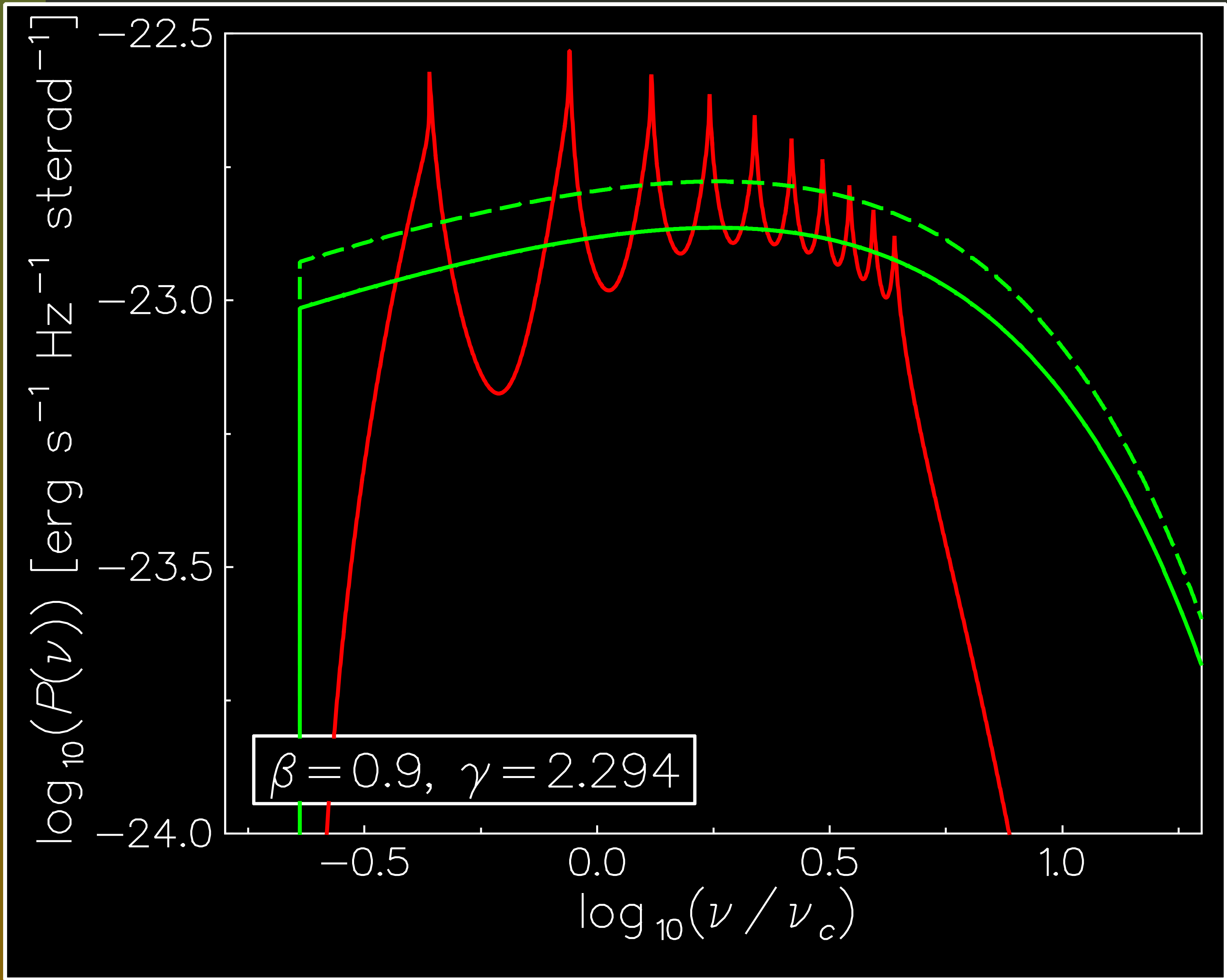

Synchrotron emission

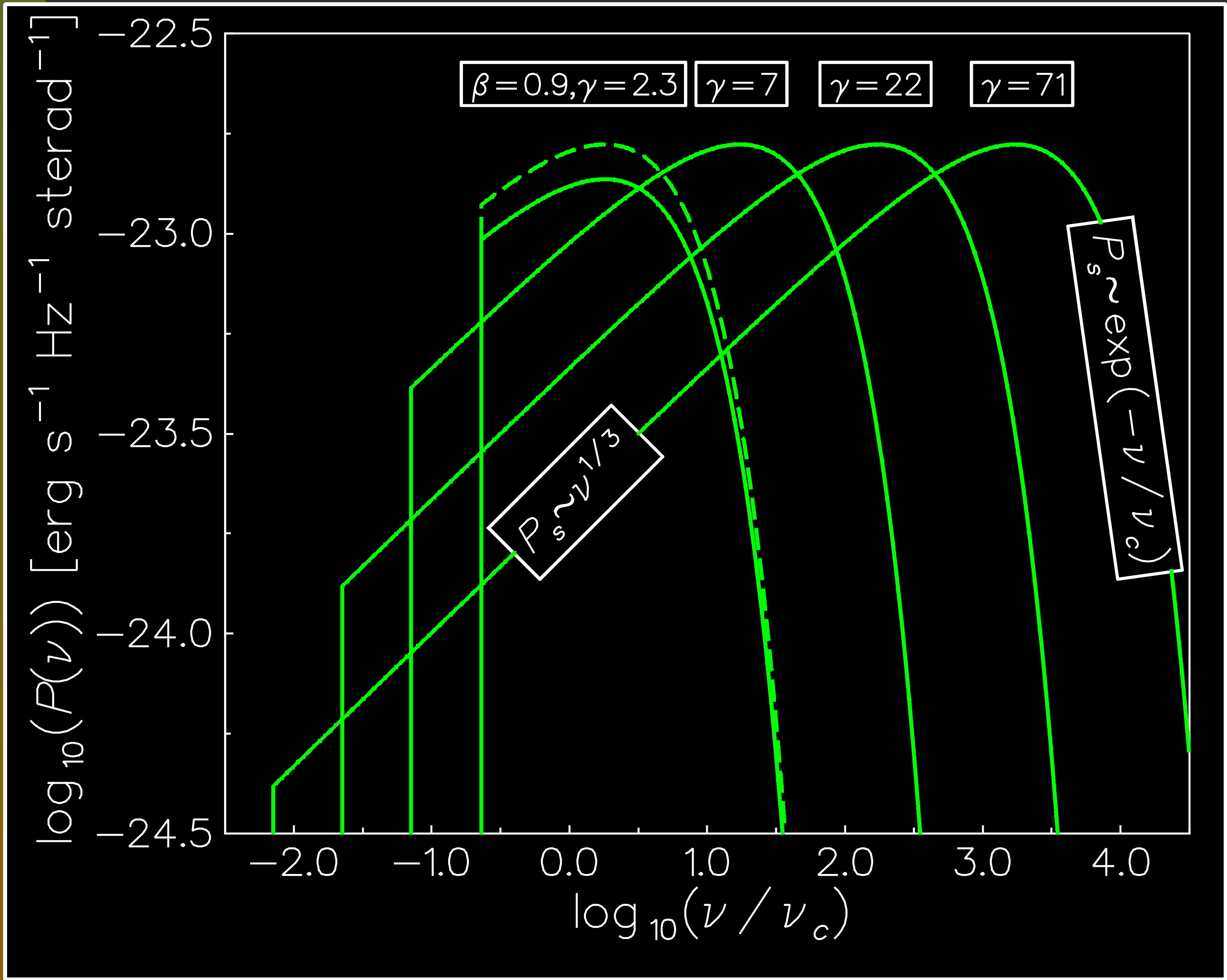

Approximation for cyclo-synch. emission

Approximation for the cyclo-synchrotron emission proposed by Ghisellini, Haardt & Svensson (1998)

$$P_{cs}(\nu, p) = \frac{4}{3}\frac{\sigma_{\mathrm{T}} c U_B}{\nu_c} p^2 f(p) \exp\left[f(p)\left(1 - \frac{\nu}{\nu_c}\right)\right],$$

$$f(p) = \frac{2}{1 + ap^2}$$

where $a = 3$, $\nu_{\mathrm{c}} = eB/(2\pi m_{\mathrm{e}} c)$ is the Larmor frequency, $U_B = B^2/(8\pi)$ is the magnetic field energy density and B is the magnetic field intensity.

Approximation of cyclo-synch. emission

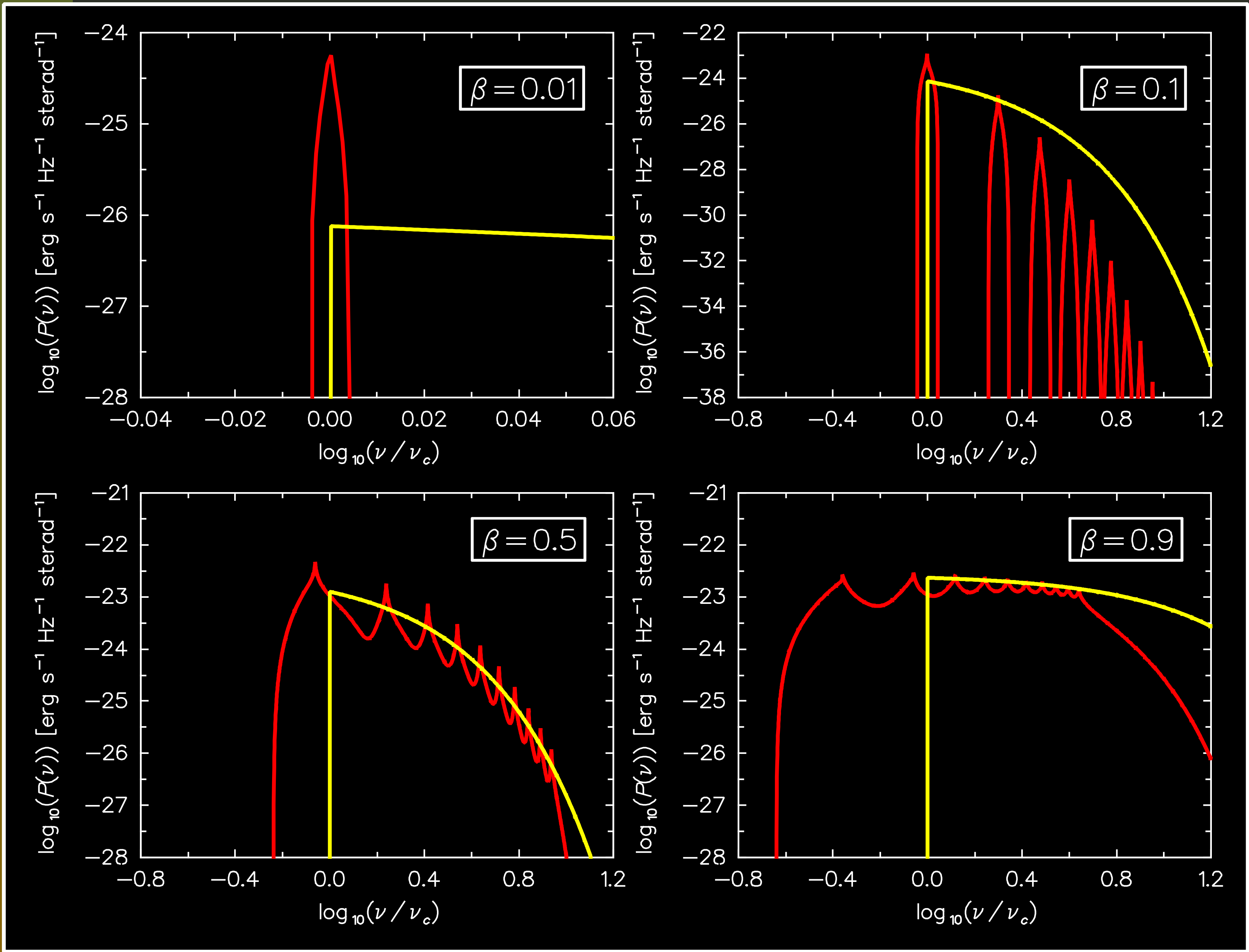

Approximation of cyclo-synch. emission

Improved approximation for the cyclo-synch. emission

$$
\begin{aligned}
P_{cs} &= \frac{4}{3}\frac{\sigma_{\mathrm{T}} c U_B}{\nu_c} p^2 c(p) g(\nu,p) f'(p) \exp\left[f'(p)\left(1-\frac{\nu}{\nu_c}\right)\right] \\
f'(p) &= \frac{2}{1+ap^2}\frac{p^2+b}{p^2}, \qquad g(p,\nu) = \frac{\nu-\nu_{\min}(p)}{\nu} \\
c(p) &= \left\{\exp\left[f'(p)\left(1-\frac{\nu_{\min}}{\nu_c}\right)\right]\right. \\
&- \left. f'(p)\frac{\nu_{\min}}{\nu_c}\exp[f'(p)]\mathrm{Ei}_1\left[f'(p)\frac{\nu_{\min}}{\nu_c}\right]\right\}^{-1},
\end{aligned}
$$

where $a = 3.65$, $b = 0.02$ and Ei is the exponential integral.

Approximation of cyclo-synch. emission

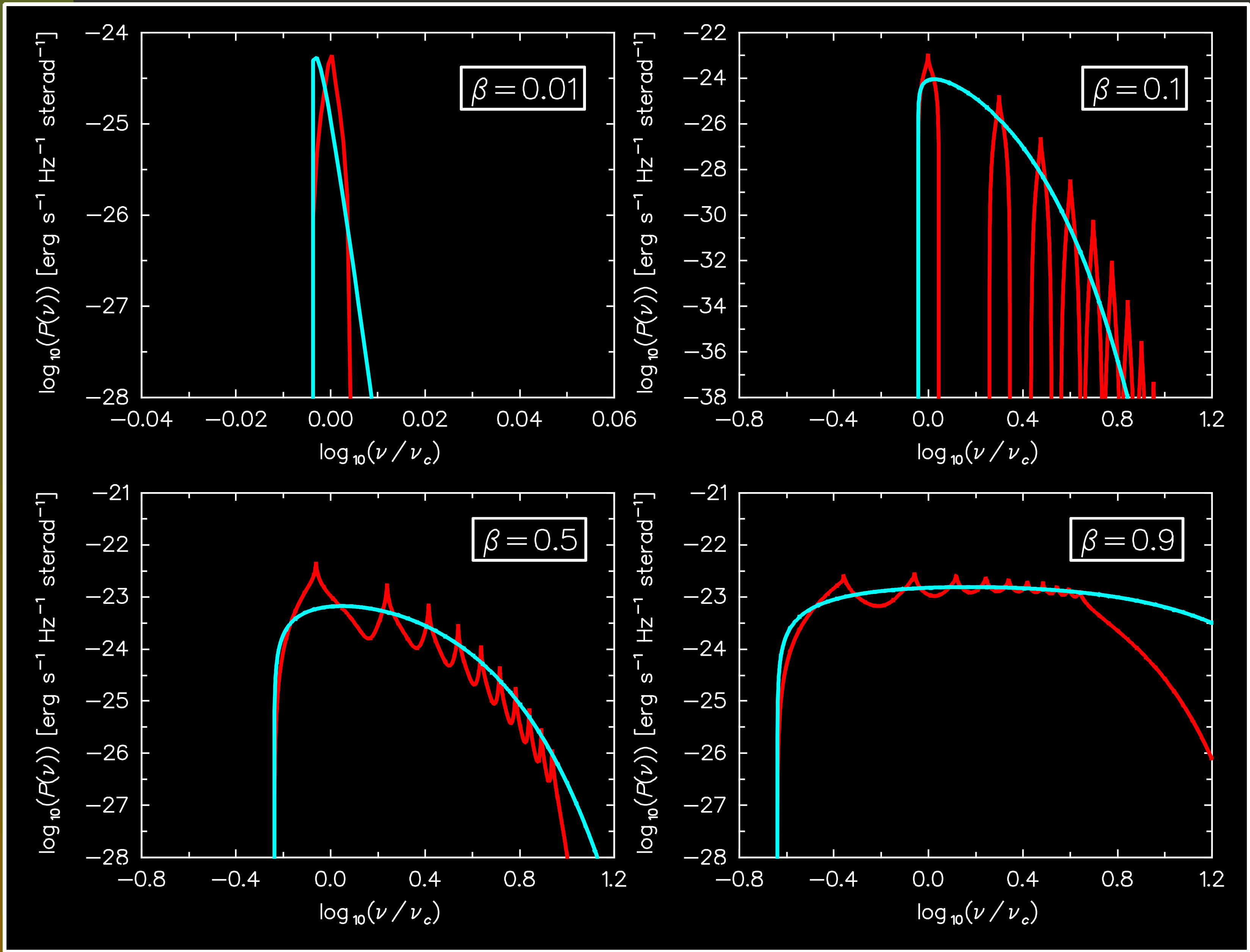

Cyclotron → Synchrotron

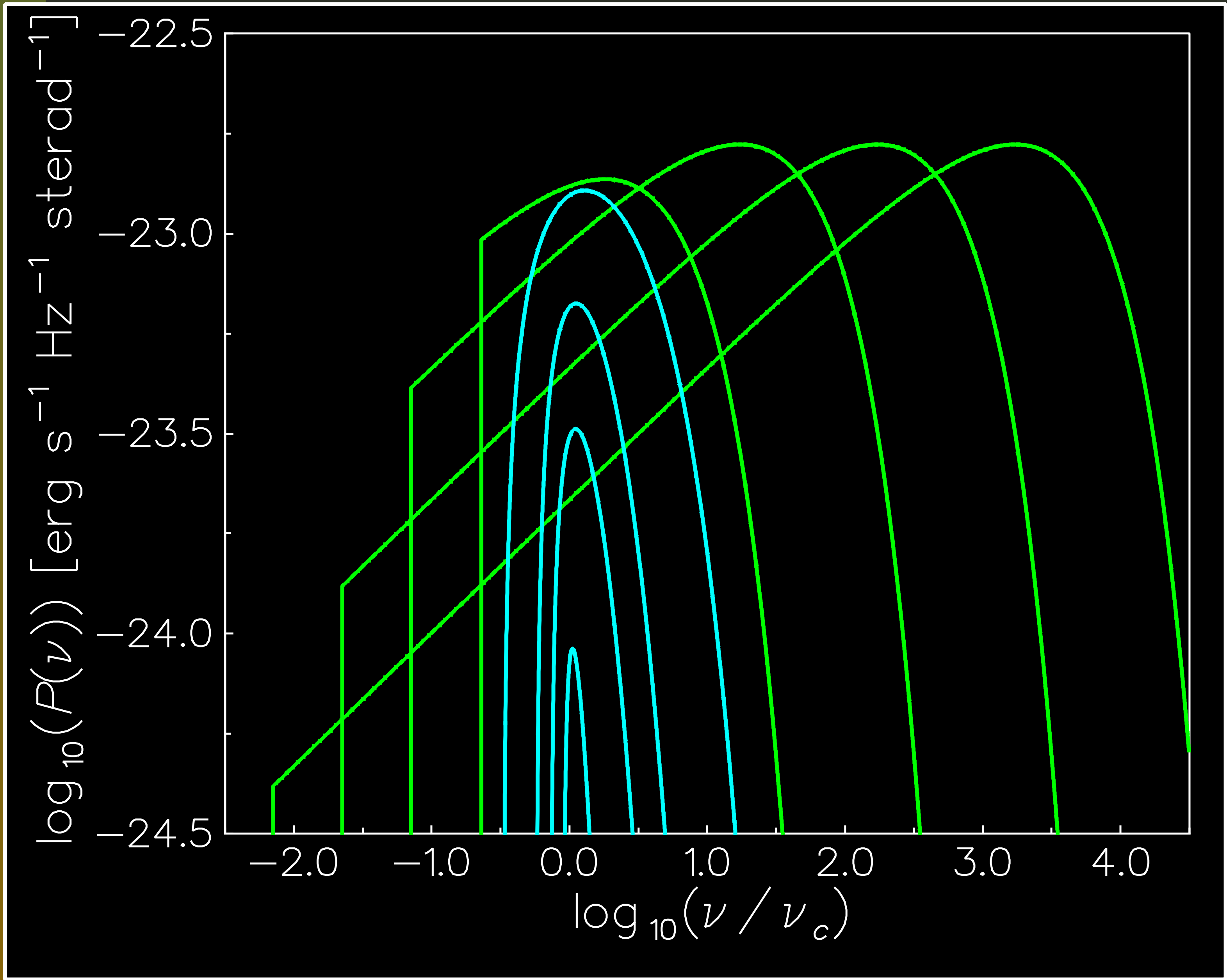

Heating through absorption of photons

- Part of the synchrotron emission can be absorbed by the electrons. This is well known synchrotron self-absorbtion process.
- The absorption process is changing the particle energy that leads to the modification of the particle energy spectrum.
- The continuous radiative cooling and simultaneous heating through the self-absorption (synchrotron boiler) may lead to an equilibrium stable distribution of the particle energy. This stable distribution must be thermal or quasi-termal (Ghisellini & Svennson 1988).

An alternate stationary solution?

- There is the theory so call Plasma Turbulent Reactor developed in the 1970s in a series of papers (Norman 1977, Norman & ter Haar 1975, Kaplan & Tsytovich 1973) that postulates the existence of the stable equilibrium solution for the power law particle energy distribution

$$N(\gamma) \sim \gamma^{-3}$$

- However, the stability of this solution was already questioned in the 1960s, before this theory was developed (Rees 1967, McCray 1969).
- We demonstrate explicitly that the γ^{-3} distribution not only is unstable, but is not even an equilibrium solution.

Heating vs Cooling

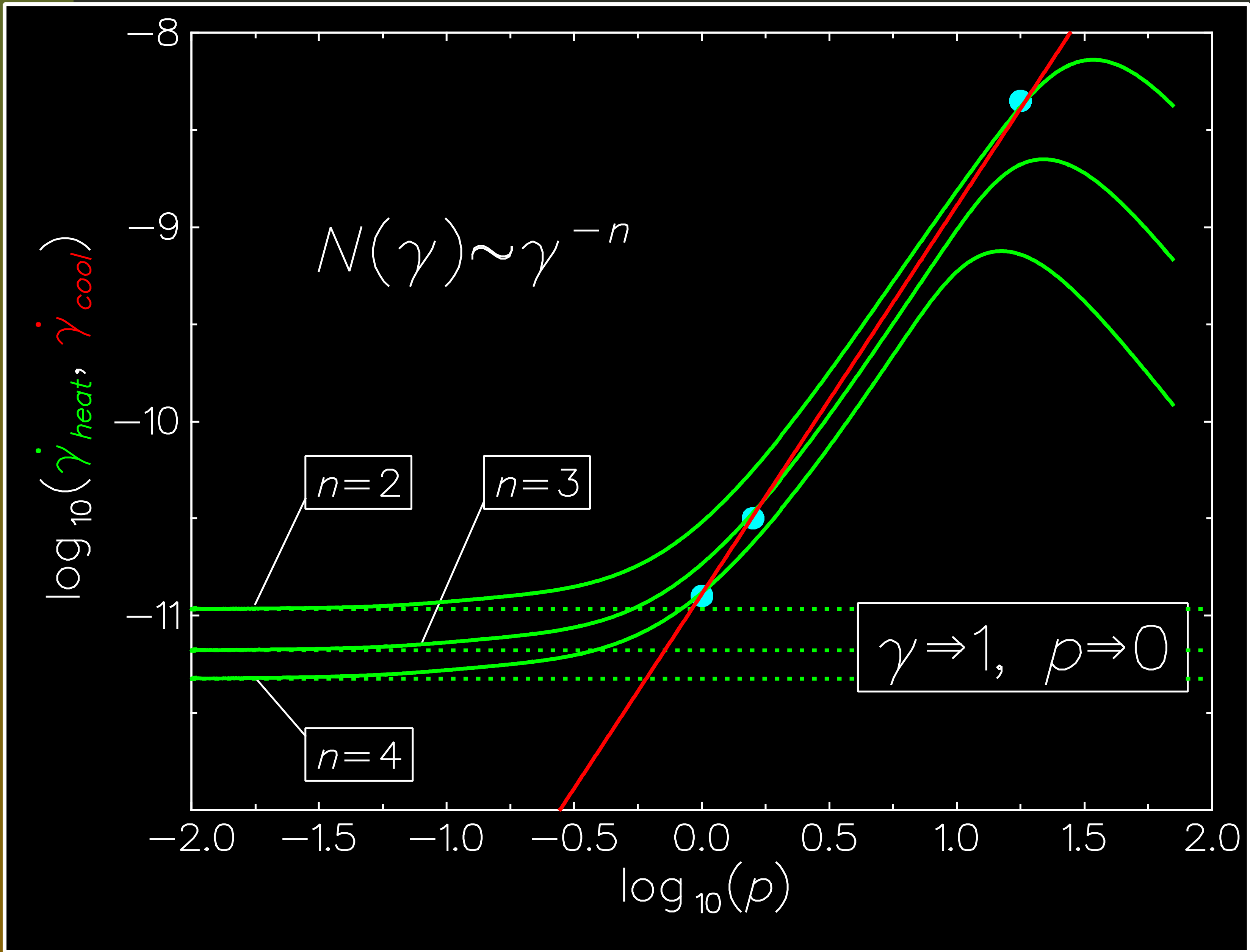

Self-absorbed part of the spectrum

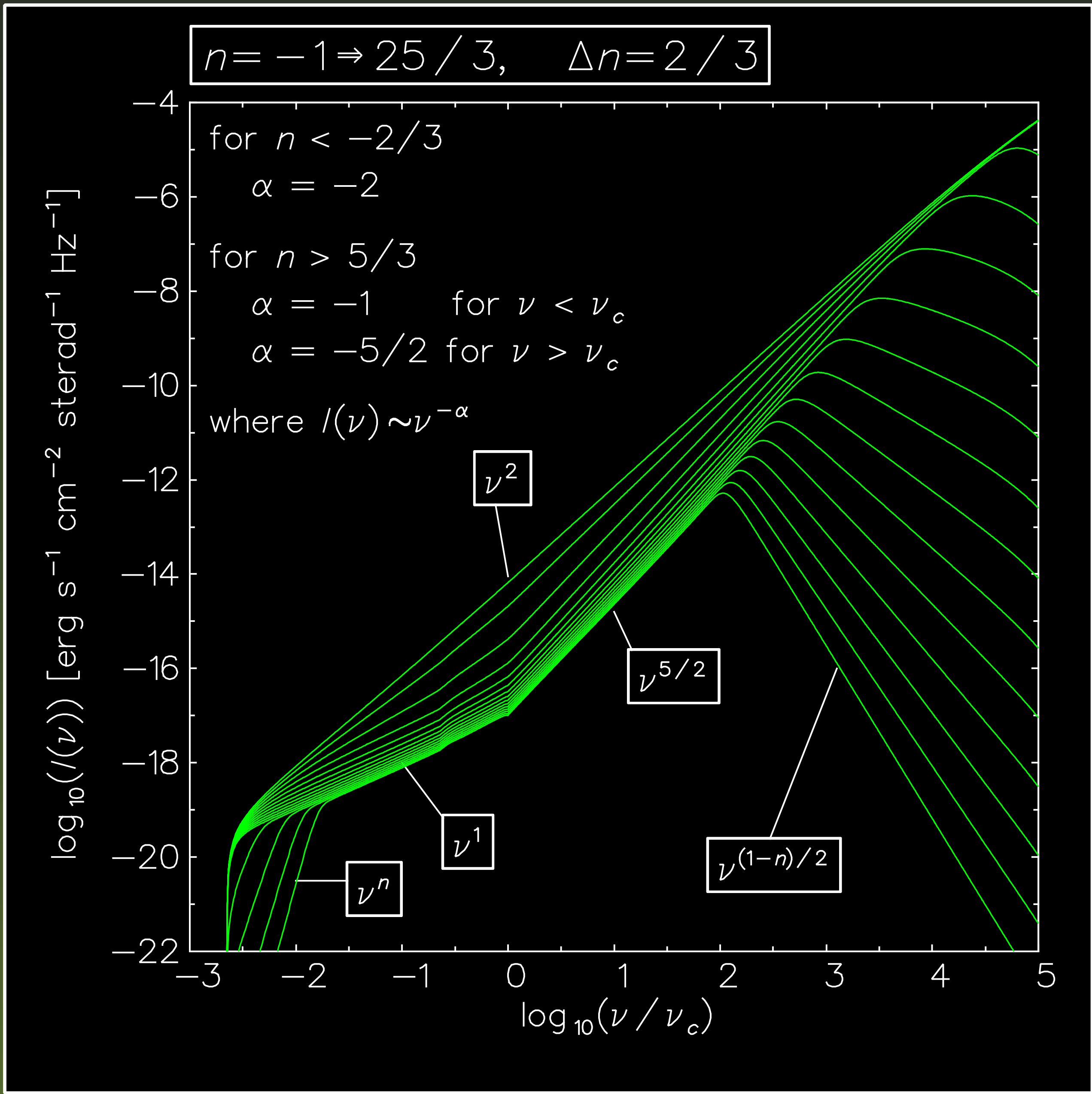

Conclusions – 1

- The approximation of the cyclo-synchrotron spectrum by harmonics requires precise description of more that ten first harmonic. Moreover, it is quite difficult to integrate numerically such spectrum and very difficult to obtain correct numerical derivative.
- We propose the approximation that well describes the spectrum for the wide range of the particle energy ($0.01 \leq \beta \leq 0.9$). Moreover, our formula provides self-consistently correct value of the total emitted energy. Since we use the continuous function there are no problems with the numerical integration or derivative.

Conclusions – 2

- Using our approximation of the cyclo-synchrotron emissivity we show that the stationary equilibrium solution ($N(\gamma) \sim \gamma^{-3}$) postulated by the Plasma Turbulent Reactor theory not only is unstable, but is not even an equilibrium solution.
- Analyzing the self-absorbed part of the spectrum produced by a homogeneous spherical source we show that above the limiting value of n = 5/3 the spectral index have three different values $\alpha = \boxed{-n} \quad \rightarrow \quad \boxed{\text{-1}} \quad \rightarrow \quad \boxed{\text{-5/2}}$.

References

Crusius, A. & Schlickeiser. R. 1986, A&A, 164, L16

Ghisellini, G., Guilbert, P., & Svensson, R., 1988, ApJ, 334, L5

Ghisellini, G., & Svensson, R., 1991, MNRAS, 252, 313

Ghisellini, G., Haardt, F., & Svensson, R., 1998, MNRAS, 297, 348

Kaplan, S.A., & Tsytovich, V.N., 1973, *Plasma Astrophysics* (Elmsford, N.Y.: Pergamon).

McCray, R., 1969, ApJ, 156, 329.

Marcowith, A., & Malzac, J., 2003, A&A, 409, 9

Norman, C.A., 1977, *Journal of Physics*, 106, 26.

Norman, C.A., & ter Haar, D., 1975, *Physics Reports*, **6**, 307.

Rees, M.J., 1967, MNRAS, 136, 279.

Magnetic Driving of AGN Jets: Observational Implications

Nektarios Vlahakis

University of Athens

in collaboration with Arieh Königl, Felipe Marin (Univ. of Chicago)

Outline

- observations
- MHD modeling of the pc-scale acceleration
- implications: collimation, jet kinematics, polarization

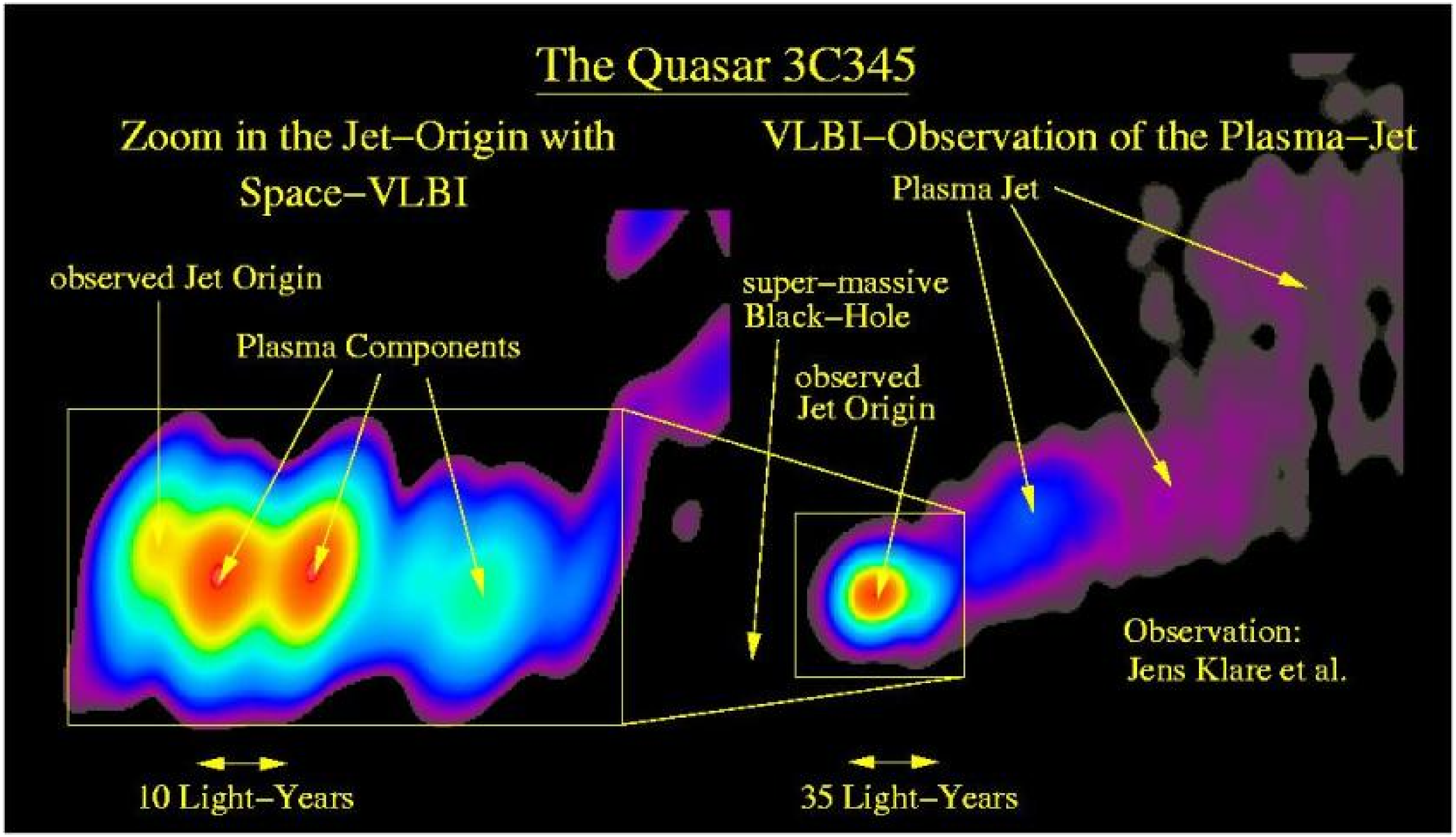

(credit: Klare et al)

The plasma components move with superluminal apparent speeds

They travel on curved trajectories

The trajectories differ from one component to the other

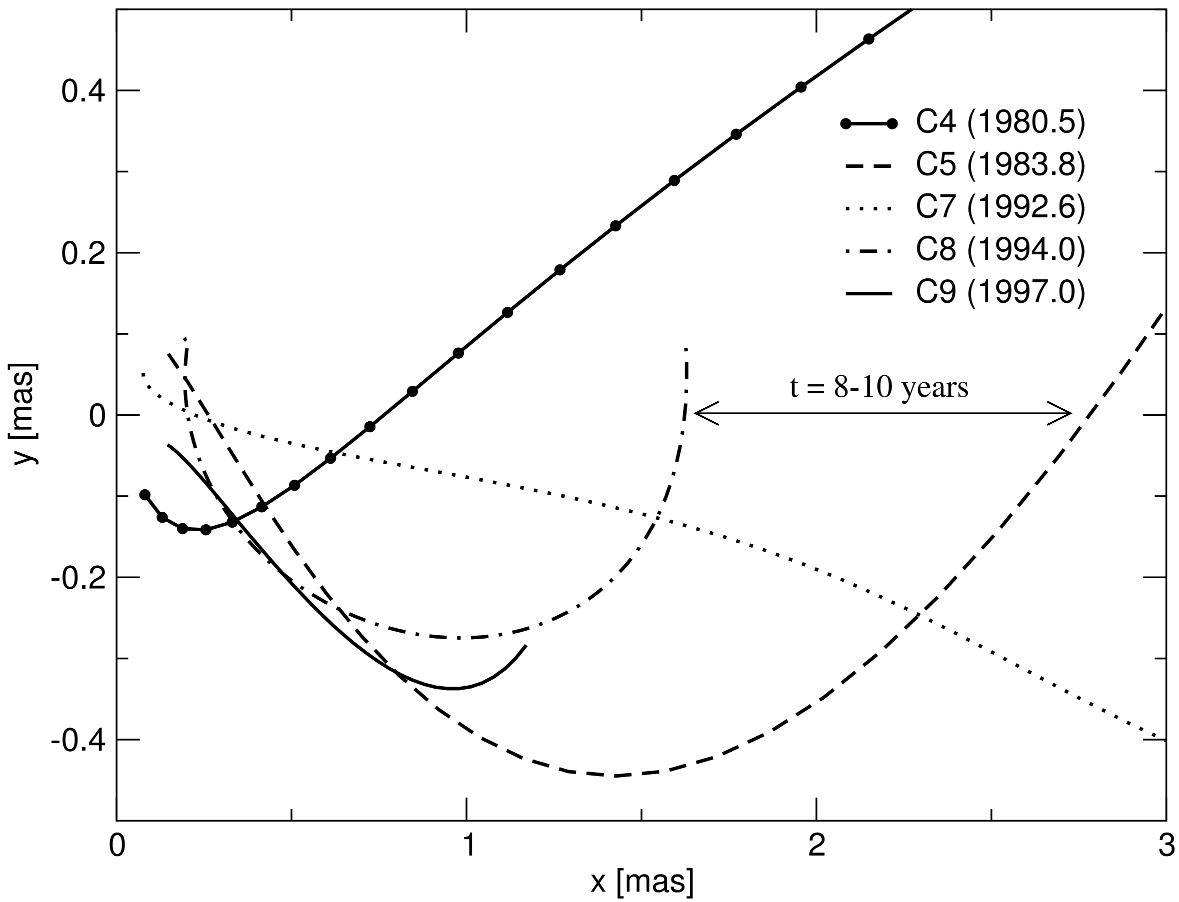

(credit Klare et al)

Implications on the dynamics

- Superluminal apparent motion $\Rightarrow \beta_{\rm app}(t_{\rm obs}) = \dfrac{\beta \sin\theta_V}{1-\beta\cos\theta_V}$
  (small θ_V, β close to 1)

- **If** we know $\delta(t_{\rm obs}) \equiv \dfrac{1}{\gamma\,(1-\beta\cos\theta_V)}$
  we find $\beta(t_{\rm obs})$, $\gamma(t_{\rm obs})$, $\theta_V(t_{\rm obs})$

- Compare radio- and high energy emission (SSC) $\Rightarrow \delta$ (e.g., Unwin et al 1997)

- For the C7 component of 3C 345 Unwin et al (1997) inferred that the Doppler factor changes from ≈ 12 to ≈ 4 ($t_{\rm obs} =$ 1992 – 1993) $\Longrightarrow$ acceleration from $\gamma \sim 5$ to $\gamma \sim 10$ over $\sim 3-20$ pc from the core
  (θ_V changes from ≈ 2 to $\approx 10^o$)

- Piner et al (2003) inferred an acceleration from $\gamma = 8$ at $r < 5.8$pc to $\gamma = 13$ at $r \approx 17.4$pc in 3C 279 using a similar approach

- A more general argument (Sikora et al 2005):
  - ⋆ lack of bulk-Compton features $\rightarrow$ small ($\gamma < 5$) bulk Lorentz factor at $\lesssim 10^3 r_g$
  - ⋆ the γ saturates at values $\sim$ a few 10 around the blazar zone ($10^3 - 10^4 r_g$)

So, relativistic AGN jets undergo the bulk of their acceleration on parsec scales ($\gg$ size of the central black hole)

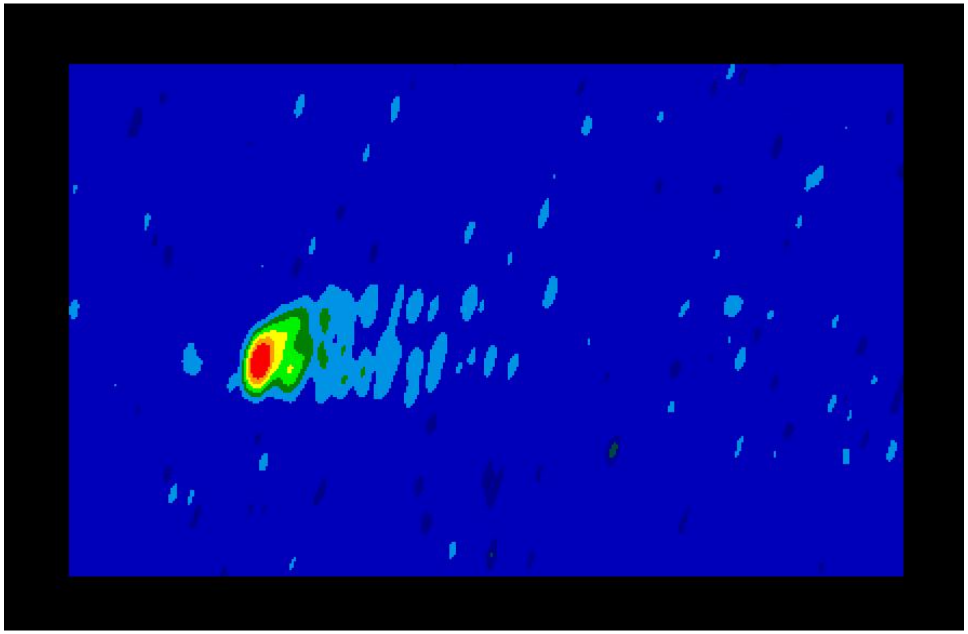 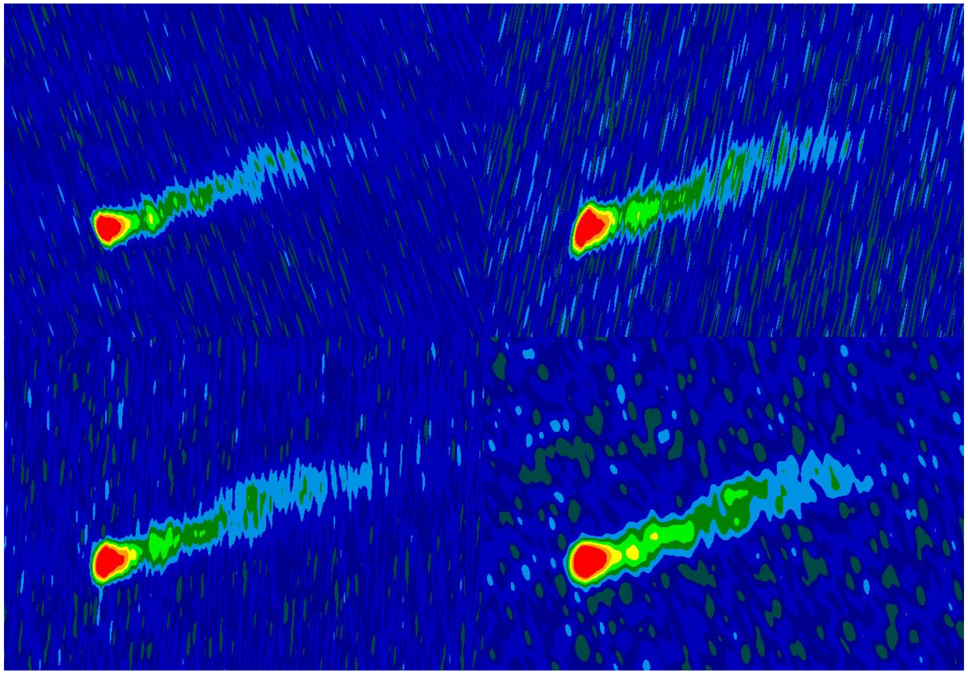

(left Global VLBI + VSOP, right Global VLBI)

Collimation in action (at approximately $100 r_g$) in M87. In the formation region, the jet is seen opening widely, at an angle of about 60 degrees, nearest the black hole, but is squeezed down to only 6 degrees a few light-years away.

(from Junor, Biretta, & Livio 1999)

Hydro-Dynamics

- In case $n_e \sim n_p$, $\gamma_{\rm max} \sim kT_i/m_pc^2 \sim 1$ even with $T_i \sim 10^{12}K$
- If $n_e \neq n_p$, $\gamma_{\rm max} \sim (n_e/n_p) \times (kT_i/m_pc^2)$ could be $\gg 1$
- With some heating source, $\gamma_{\rm max} \gg 1$ is in principle possible

However, even in the last two cases, HD is unlikely to work because the HD acceleration saturates at distances comparable to the sonic surface where gravity is still important, i.e., very close to the disk surface (certainly at $\ll 10^3 r_g$)

Collimation is another problem for HD

Relativistic Magneto-Hydro-Dynamics

- Outflowing matter
- large scale electromagnetic field
- thermal pressure

We need to solve:

- Maxwell + Ohm equations
- mass + entropy conservation
- momentum equation

Self-similar, relativistic, disk-wind models

- axisymmetry
- steady-state
- ideal MHD (no resistivity)
- special relativity

The problem reduces to the two components of the momentum equation: one along the flow (gives γ) and one in the transfield direction (gives the field- and stream-line shape).

- boundary conditions of the form $r^x \times f(\theta)$ lead to separation of variables (radial self-similarity)
  - similar to the nonrelativistic model of Blandford & Payne 1982
  - cold versions of the model: Li et al 1992, Contopoulos 1994

Vlahakis & Königl – application to 3C345

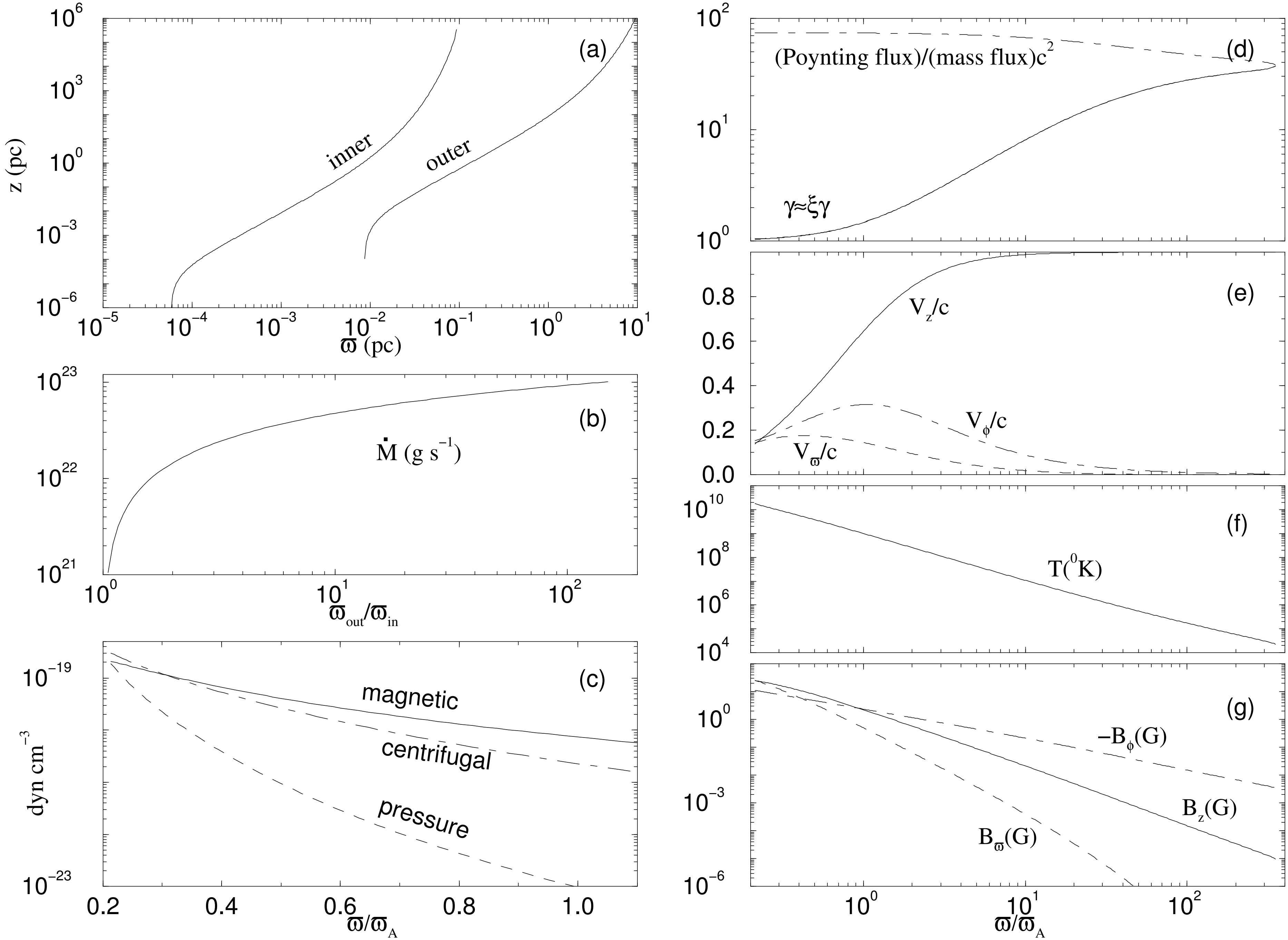

Jet kinematics

- due to precession? (e.g., Lobanov & Roland)
- instabilities? (e.g., Hardee, Meier)

bulk jet flow may play at least a partial role

to explore this possibility, we used the relativistic self-similar model (Vlahakis & Königl 2004)

since the model gives the velocity (3D) field, we can follow the motion of a part of the flow

Vlahakis, Marin, & Königl, in preparation

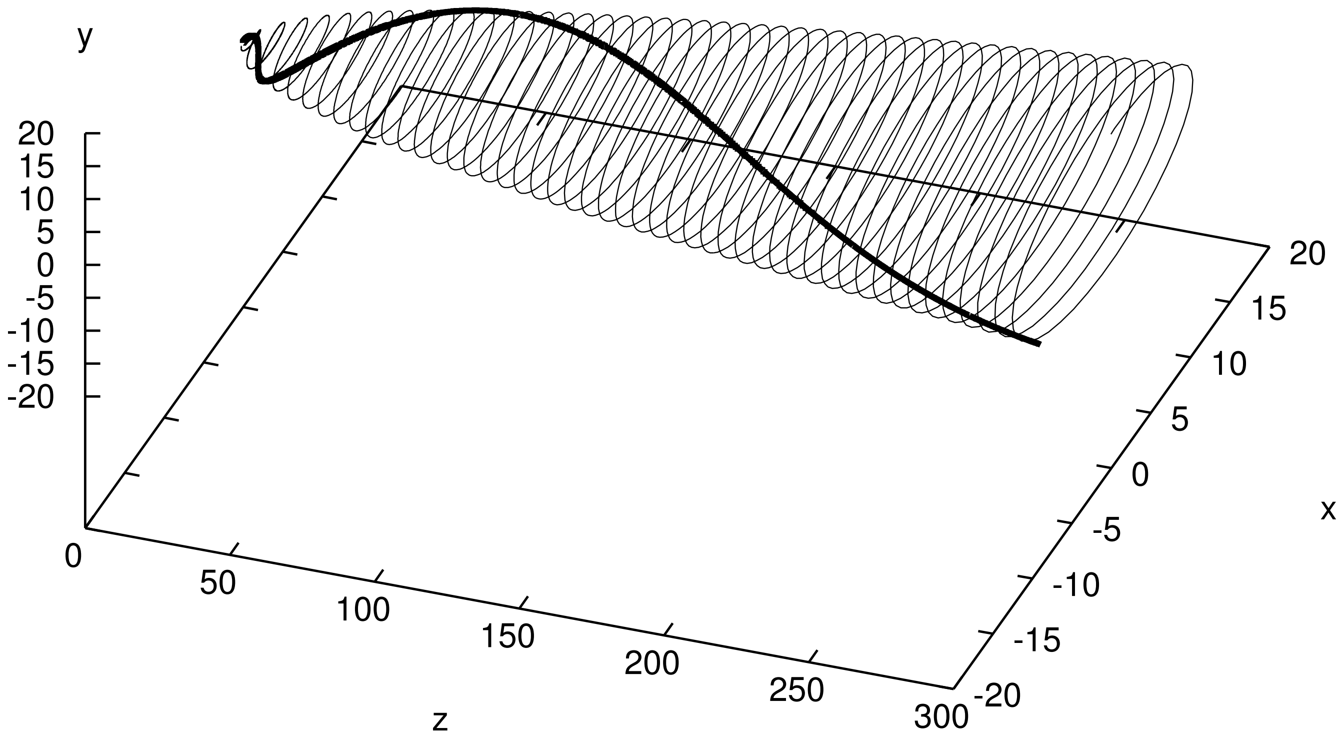

For given $\theta_{\rm obs}$ (angle between jet axis and line of sight) and ejection area on the disk (r_o, ϕ_o), we project the trajectory on the plane of sky and compare with observations. Find the best-fit parameters r_o, $\theta_{\rm obs}$, ϕ_o.

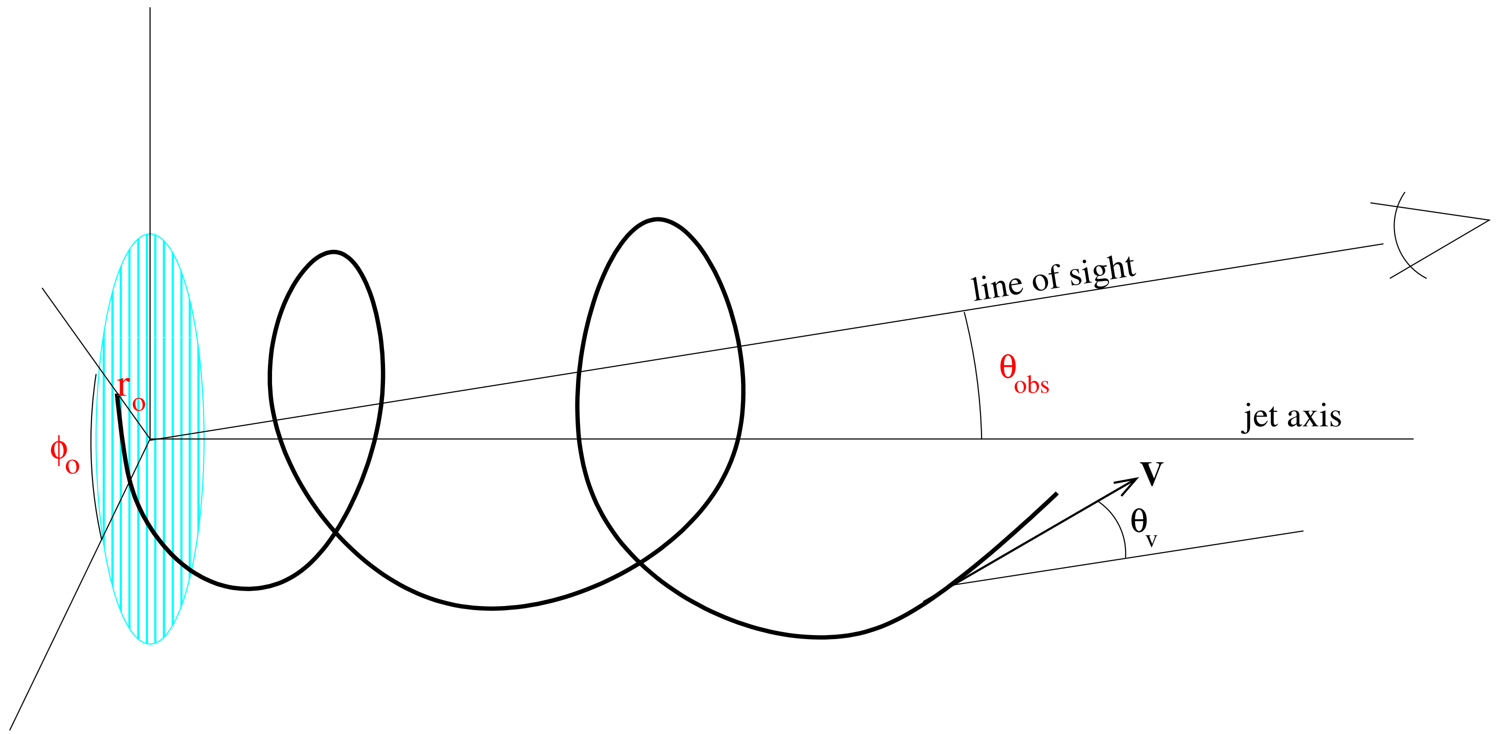

For $\theta_{\rm obs} = 1^{\rm o}$ and $\phi_o = 0^{\rm o}$, $60^{\rm o}$, $120^{\rm o}$, $180^{\rm o}$, $240^{\rm o}$, $300^{\rm o}$ (from top to bottom):

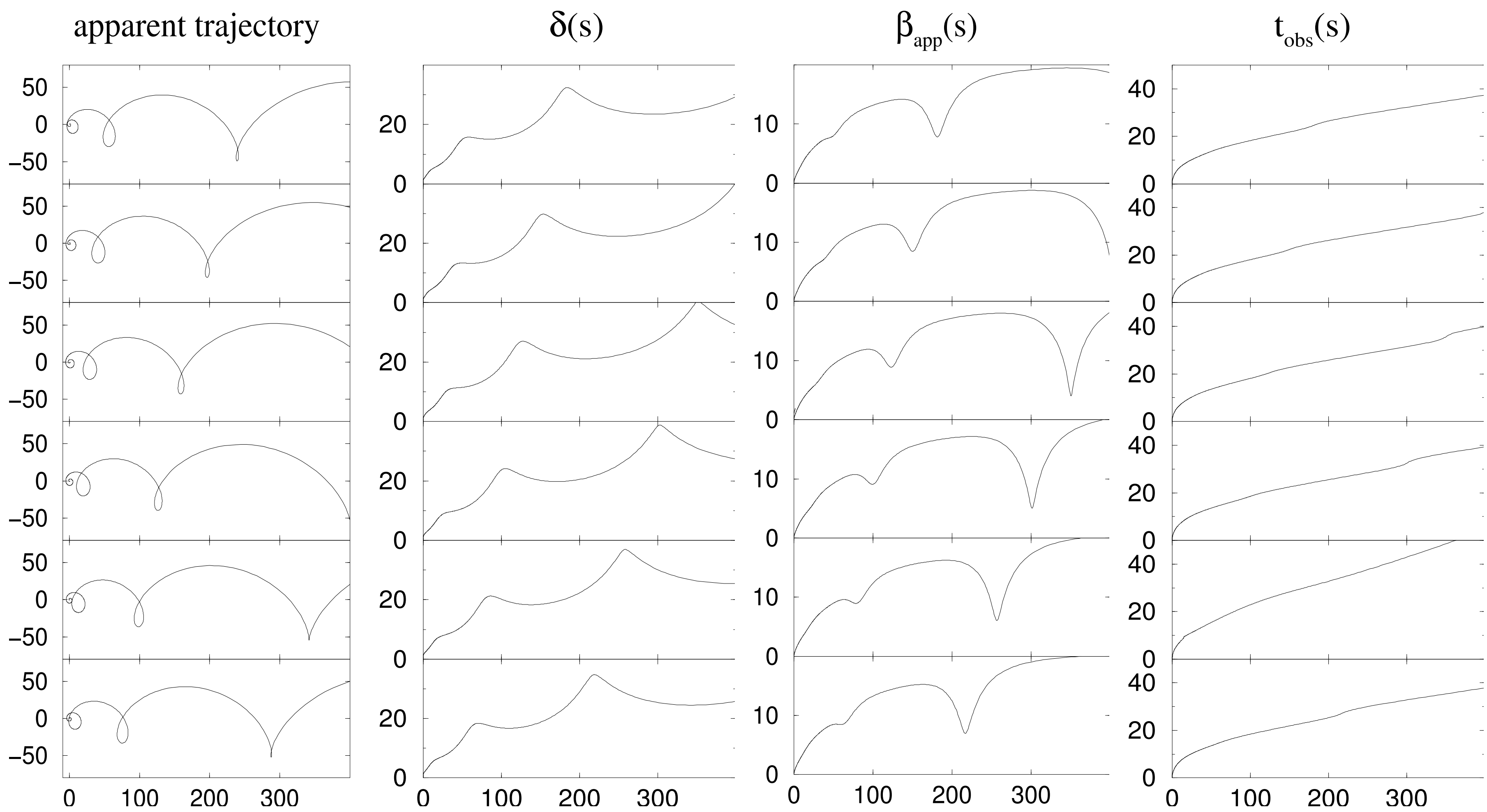

best-fit to Unwin et al results: $r_o \approx 2 \times 10^{16}$cm, ϕ_o=180^o, $\theta_{\rm obs}$=9^o

apparent trajectory

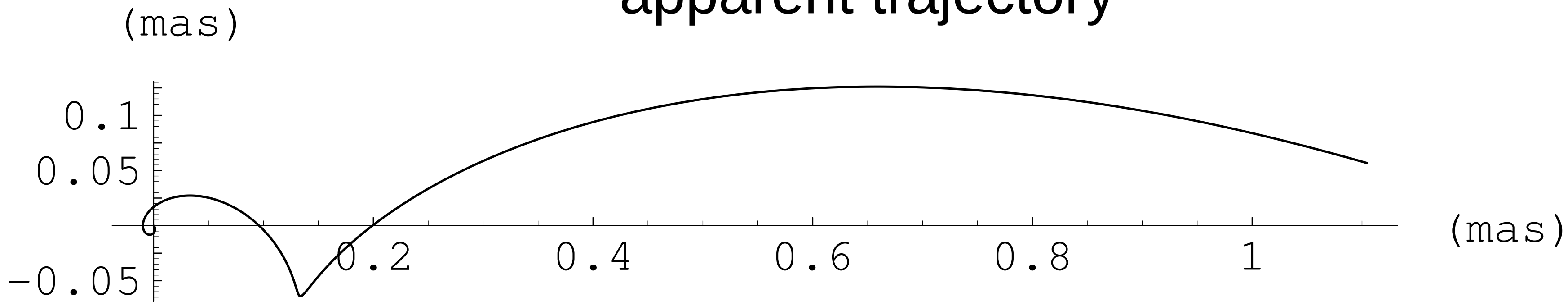

Trajectory of C7

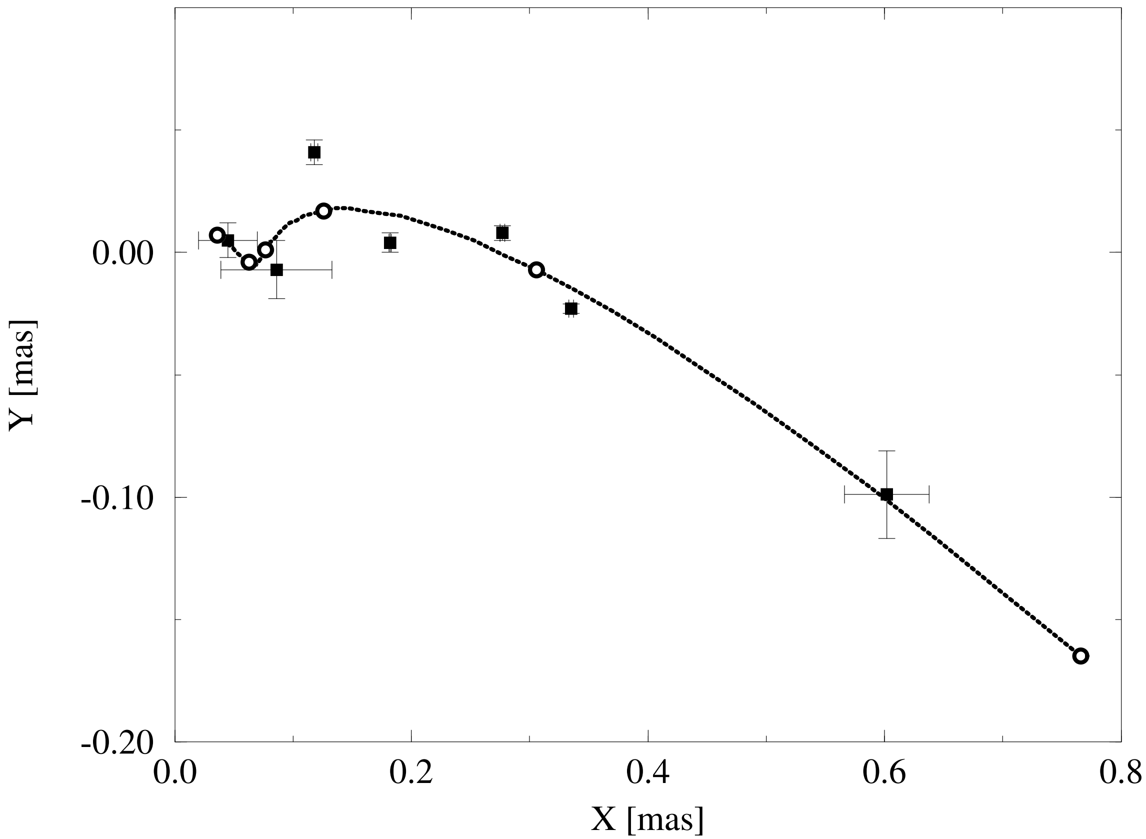

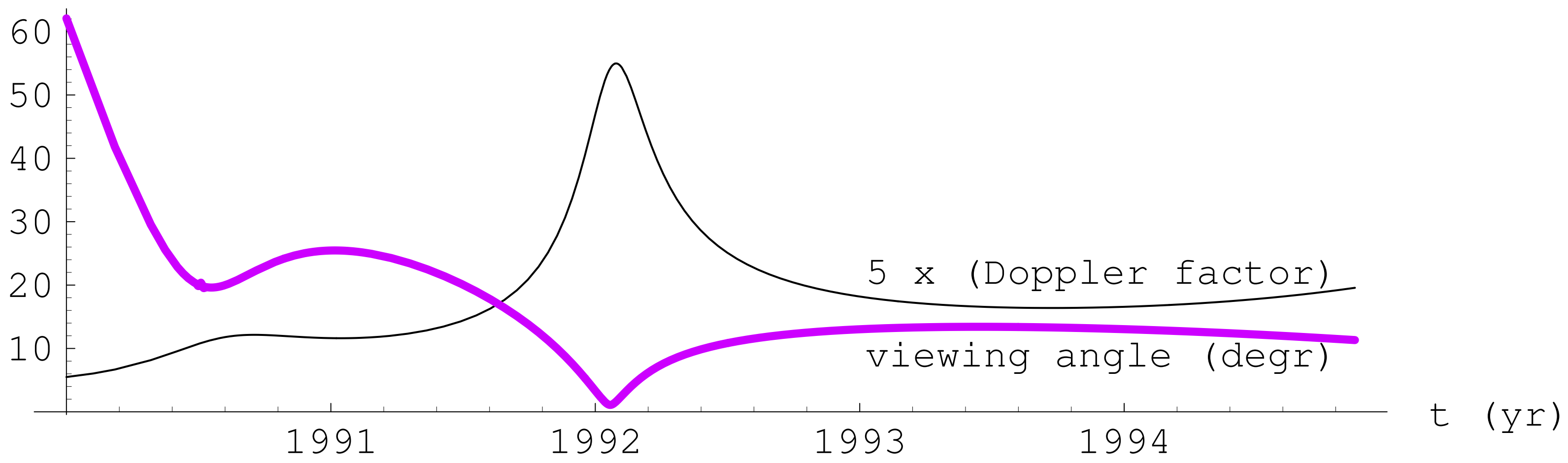
60
50
40
30
20
10
5 x (Doppler factor)
viewing angle (degr)
t (yr)
1991
1992
1993
1994

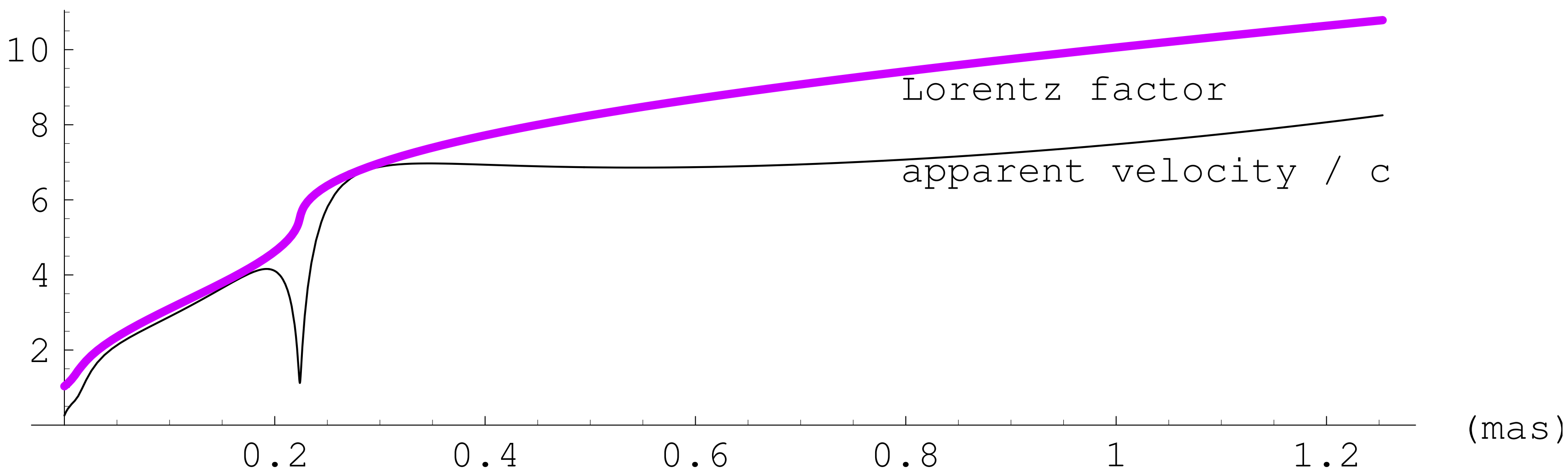
10
8
6
4
2
Lorentz factor
apparent velocity / c
(mas)
0.2
0.4
0.6
0.8
1
1.2

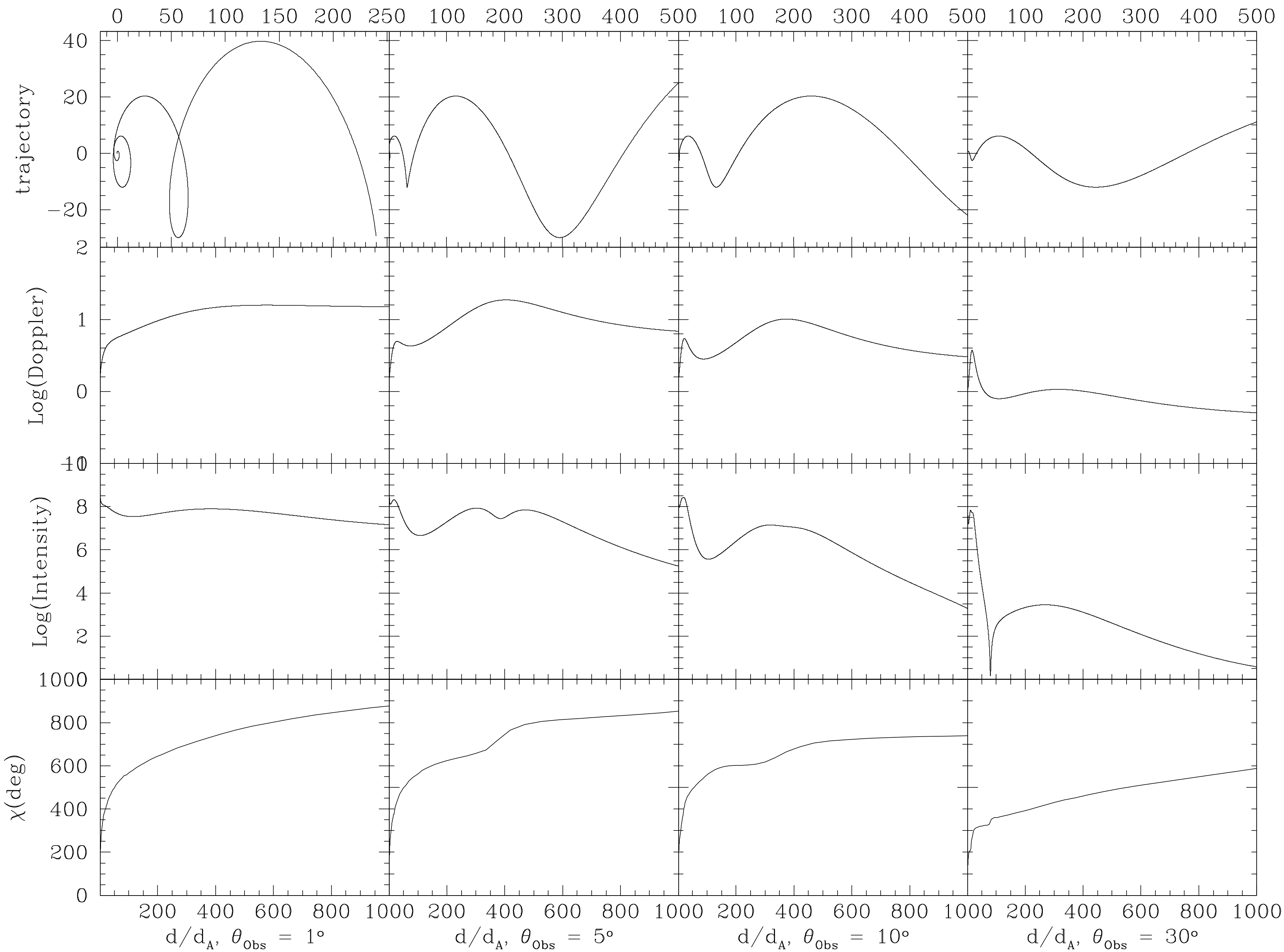

trajectory
Log(Doppler)
Log(Intensity)
χ(deg)
d/d_A, θ_Obs = 1°
d/d_A, θ_Obs = 5°
d/d_A, θ_Obs = 10°
d/d_A, θ_Obs = 30°

Summary

- ⋆ Blazar jets are likely accelerated at relatively large distances from the disk ($\gg r_g$)
- ⋆ Magnetic driving provides a viable explanation of the jet bulk acceleration (with efficiencies $\sim 50\%$)
- ⋆ Collimated flows are naturally produced
- ⋆ The intrinsic rotation of the jets could explain the observed kinematics

– next steps: comparison with polarization maps

The ideal MHD equations

Maxwell:

$$\nabla \cdot \mathbf{B} = 0\,, \nabla \times \mathbf{E} = -\frac{\partial \mathbf{B}}{c\partial t}\,, \nabla \times \mathbf{B} = \frac{4\pi}{c}\mathbf{J} + \frac{\partial \mathbf{E}}{c\partial t}\,, \nabla \cdot \mathbf{E} = \frac{4\pi}{c}J^0$$

Ohm: $\mathbf{E} + \frac{\mathbf{V}}{c} \times \mathbf{B} = 0$

mass conservation: $\left(\frac{\partial}{\partial t} + \mathbf{V} \cdot \nabla\right)(\gamma\rho_0) + \gamma\rho_0 \nabla \cdot \mathbf{V} = 0\,,$

energy $U_\mu T^{\mu\nu}_{,\nu} = 0$: $\left(\frac{\partial}{\partial t} + \mathbf{V} \cdot \nabla\right)\left(\frac{P}{\rho_0^\Gamma}\right)dt = 0$

momentum $T^{\nu i}_{,\nu} = 0$:

$$\gamma\rho_0 \left(\frac{\partial}{\partial t} + \mathbf{V} \cdot \nabla\right)(\xi\gamma\mathbf{V}) = -\nabla P + \frac{J^0\mathbf{E} + \mathbf{J} \times \mathbf{B}}{c}$$

Hard TeV spectra of blazars and the constraints to the IR intergalactic background

K. Katarzyński
G. Ghisellini
F. Tavecchio
J. Gracia

6th Enigma Meeting, 22-25 November, Kinsale

Outline

Introduction
- Synchrotron self-Compton
- Absorption by the IR background

TeV absorption for distant blazar

Conclusions

The synchrotron self-Compton paradigm

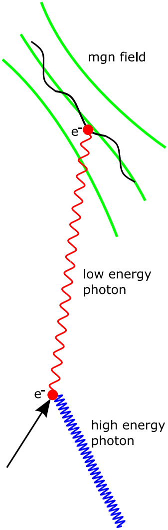

- population of electrons in a magnetized medium produces synchrotron radiation $I_{\rm S}$
- $I_{\rm S}$ photons collide with electrons of the *same* population
- and gain energy through inverse-Compton scattering $I_{\rm IC}$

two distinct components:

- $I_{\rm S}$ at X-ray energies (keV)
- $I_{\rm IC}$ at TeV energies

SSC – from electrons to TeV photons

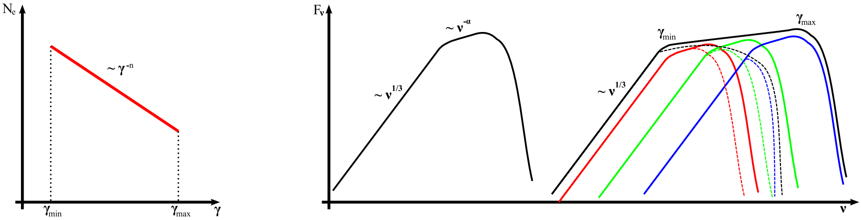

- inverse-Compton scattering off mono-energetic electrons produces "image" of I_{S} peak at higher energies
- total Compton spectrum, I_{C}, as superposition of all "images" over the electron distribution
- I_S, I_{IC}: similar shape (α), but shift in frequency
- modifications due to Klein-Nishina cross-section, $\sigma_{\mathrm{KN}} \neq \sigma_{\mathrm{T}}$

SSC in a nutshell

- power-law electron distribution $\gamma_{\min} < \gamma < \gamma_{\max}$: $N_e(\gamma) \sim \gamma^{-n}$
- usually $\gamma_{\min} = 1$
- from shock-acceleration models $n > 2$
- synchrotron component $F_\nu \sim \nu^{-\alpha}$, $\alpha = (n-1)/2 > 1/2$ & low-energy tail $\alpha = -1/3$
- slope of inverse-Compton component $\alpha_{TeV} \approx \alpha > 1/2$ **or** low-energy tail $\alpha_{\mathrm{TeV}} = -1/3$ if $\gamma_{\min} \gg 1$

Attenuation by pair-production ...

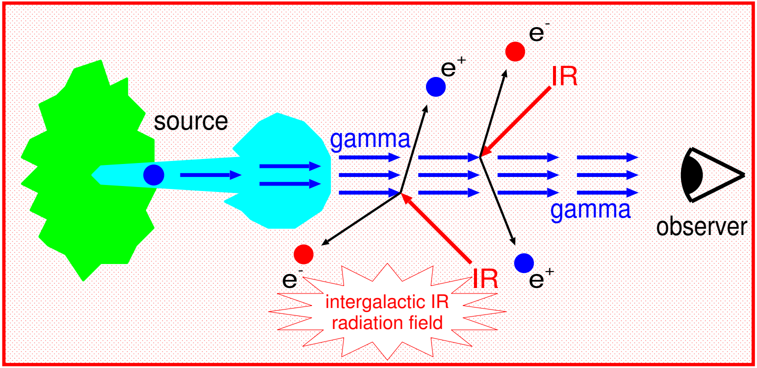

TeV photons scattering off low-energy photons may produce pairs
$\gamma + \mathrm{IR} \rightarrow e^+ \, e^-$

… from the infrared background

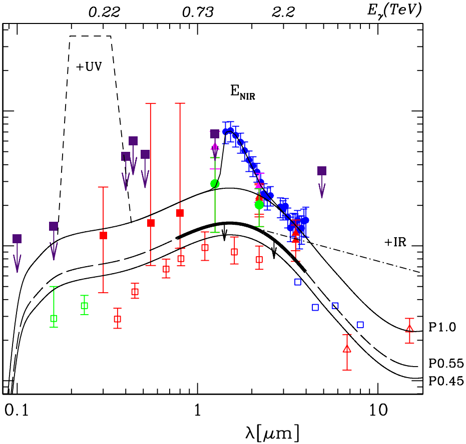

Aharonian et al 2005

intergalactic (IR) background not well known

lower limit given by integration over resolved galaxies/AGN

Intrinsic vs absorpted spectrum – or spectral inversion

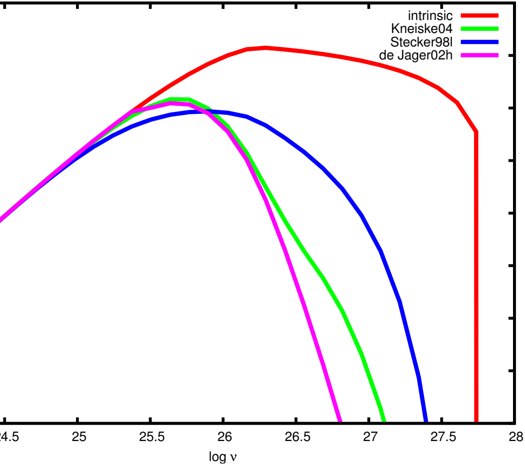

total absorption depends on:

- distance travelled along the line of sight and on the local IR background density, ie. redshift z
- strongly on the incident energy, ie. strong absorption at high energies

Disentangling blazars and IR background

- observed spectra from distant blazars contain information on both, the IR background radiation field history, and the intrinsic properties of the source
- for blazar studies, this must be corrected for
- for IR studies, this allows meassurement if IR level
- these two independent processes need to be disentangle

assuming the intrinsic blazar spectrum is known (or at least well understood), one can constrain the IR background level from TeV observations of blazars at high redshift

The case of 1E1101-232

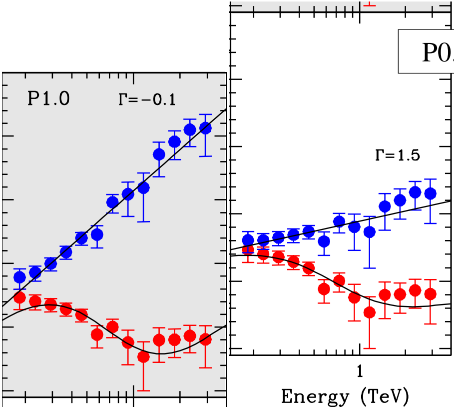

Aharonian et al, astro-ph/0508073

- $z = 0.186 \rightarrow$ strong absorption
- Aharonian et al. assume intrinsic SSC slope $\alpha \geq 0.5$ ($\Gamma \geq 1.5$)
- then, IR background absorption must be low
- claim upper limit close to minimum value from resolved galaxies

Is 1E1101-232 a "crazy" source?

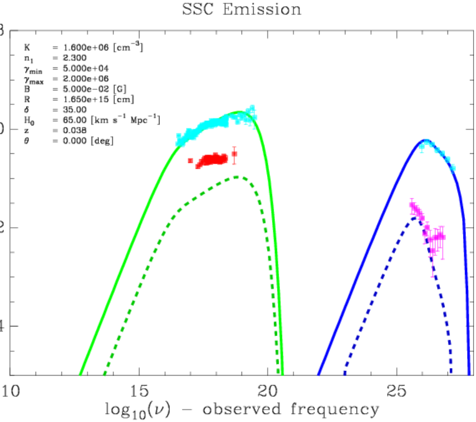

why is TeV spectrum so hard?

not brighter than others, eg Mrk 501

Fitting blazars with high $\gamma_{\min}$

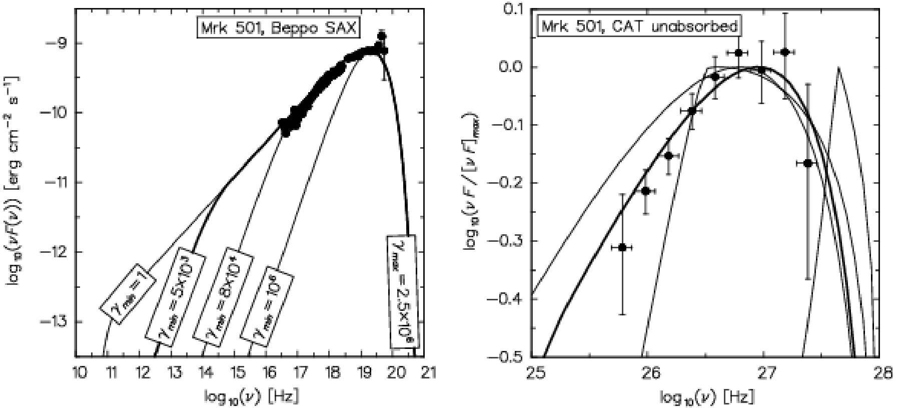

very steep spectra in TeV possible ($\alpha_{\text{TeV}} = -1/3$), even for standard values of $n = 2.3$

Fitting 1E1101-232 with high absorption

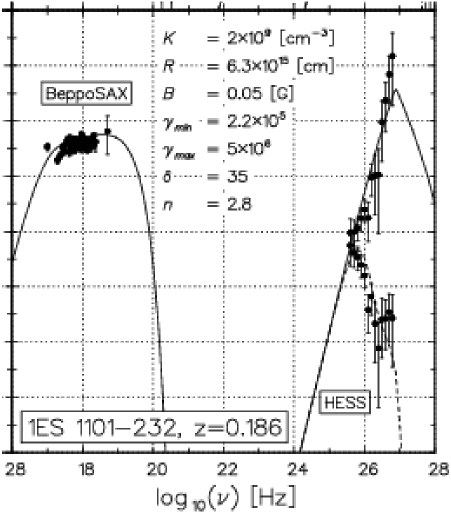

- with high $\gamma_{\min} = 2.2 \times 10^5$, we can match the low energy-tail ($\alpha_{\mathrm{TeV}} = -1/3$) to the TeV data, instead of the usual $\alpha_{\mathrm{TeV}} = (n-1)/2$
- due to the steeper intrinsic spectrum, we can accomodate much higher absorption levels than Aharonian et al. (eg. Kneiske et al 2004)

Application to other sources – Mrk 501 & Mrk 421

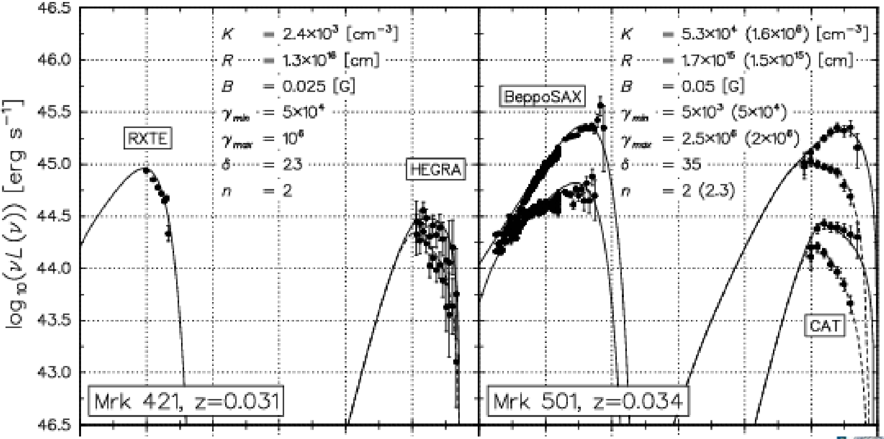

Application to other sources – PKS 2155-304

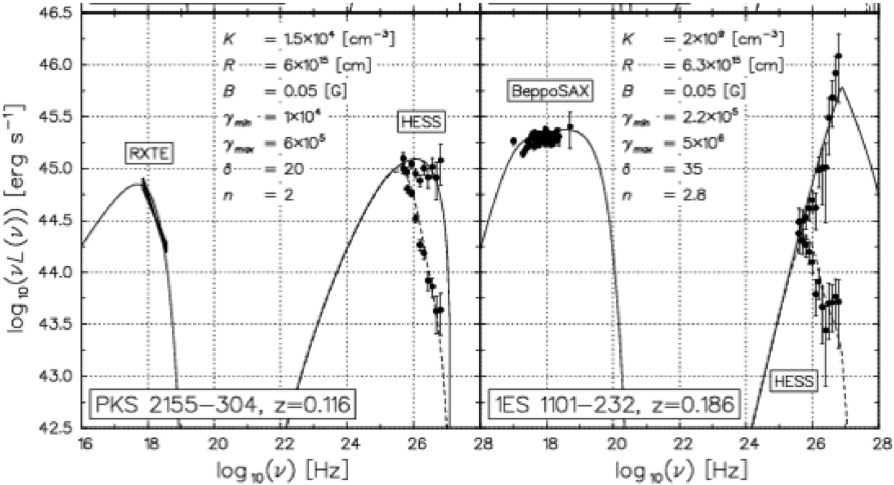

Summary and conclusions

- a small modification to the SSC scenario can fit the steep spectrum of 1E1101-232
- similar scenario can be applied to a number of sources
- even relatively high IR background levels can be accommodated
- we show by example, that the Aharonian et al *upper limit* is strongly model-dependent
- the *observed* spectral index can take almost any value, due to IR background absorption (even spectral inversion)
- the hardest possible *intrinsic* spectral index from one-zone SSC models is $\alpha = -1/3$ (due to a deficit of soft electrons)
- *if* SSC is the correct scenario *and* observations constrain all parameters (not available so far), then this could lead to an *upper limit* on the IR background

Outlook

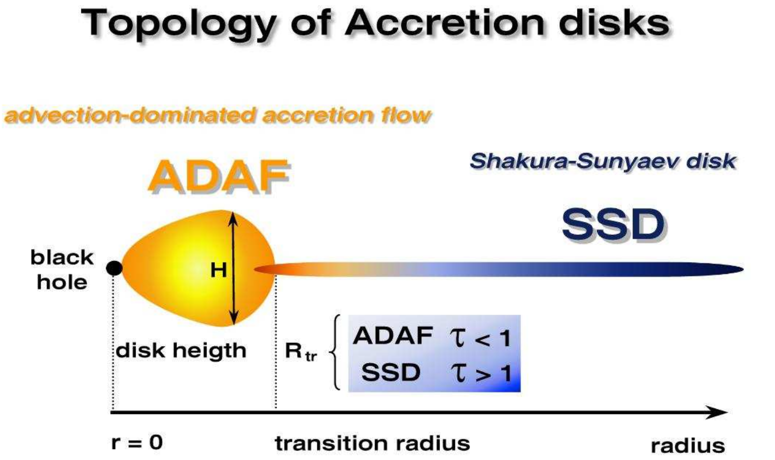
Topology of Accretion disks
advection-dominated accretion flow
ADAF
Shakura-Sunyaev disk
SSD
black hole
H
disk heigth
R tr
ADAF τ < 1
SSD τ > 1
r = 0
transition radius
radius

more material ...

SSC – electron distribution

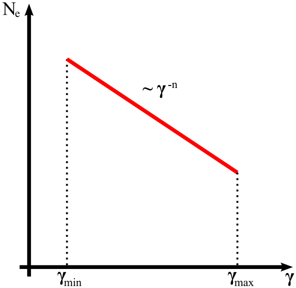

Non-thermal electron distribution:
Number density of electrons $N_{\rm e}(\gamma)$ as a function of energy γ ($E_{\rm tot} = \gamma mc^2$)

- powerlaw of slope n, ie. $N_e(\gamma) \sim \gamma^{-n}$
- lower cut-off at γ_{min}, usually $\gamma_{min} = 1$
- upper cut-off at γ_{max}

SSC – synchrotron emision

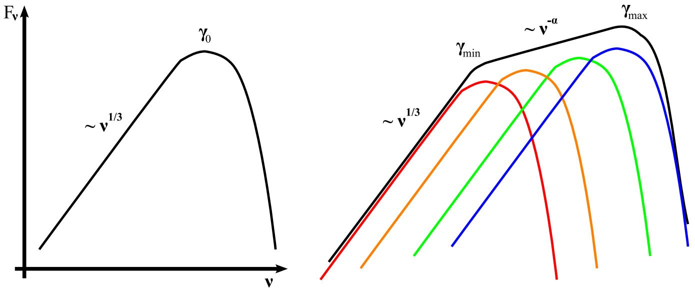

total spectrum is the super-position of the radiation produced by mono-energetic electrons and consists of 3 branches,

- exponential cut-off at high energy above $\gamma_{\max}$
- intermediate branch with slope $\alpha = (n-1)/2$ ($F_\nu \sim \nu^{-\alpha}$)
- low-energy tail below $\gamma_{\min}$ with slope $\alpha = -1/3$

Max-Planck-Institut für Radioastronomie

Emmanouil (Manolis) Angelakis
Under the supervision of A. Kraus

ENIGMA RTN

The 6000-source survey

In collaboration with:
MPIfR: A. Zensus, A. Witzel, T. Krichbaum
CALTECH: A. Readhead, T. Pearson, R. Bustos

Abstract

5998 NVSS sources (Condon et al. 1998) detected at 1.4 GHz have been being observed at 2 additional frequencies 4.85 and 10.45 GHz with the 100-m telescope in order to study their spectral behavior

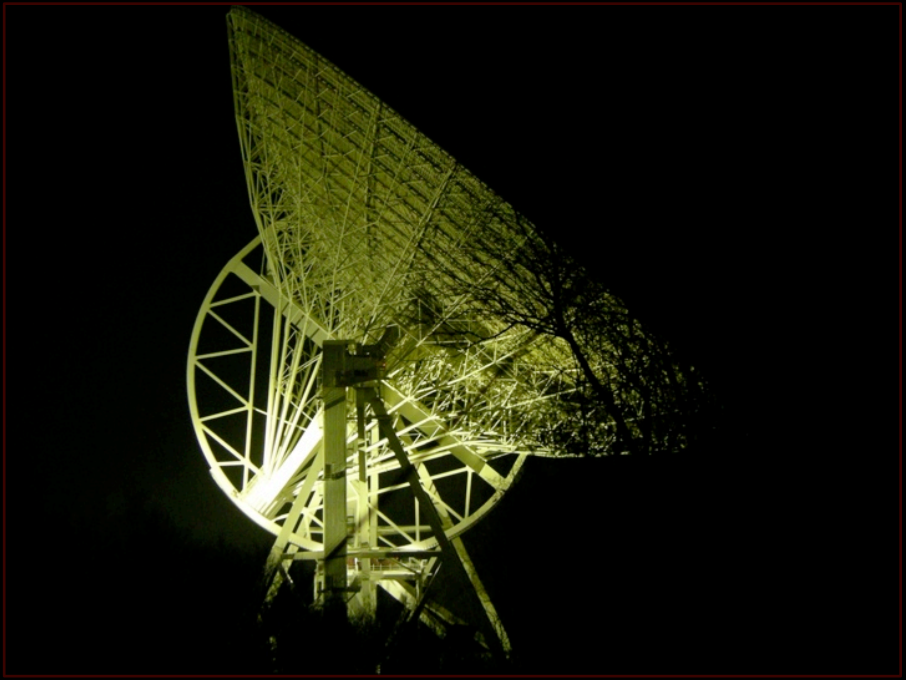

Motivation: the Cosmic Background Imager

CBI is an 13-element interferometer operating between 26-36 GHz observing the anisotropies in the Cosmic Microwave Background Radiation

courtesy of R. Bustos

Motivation: the problem

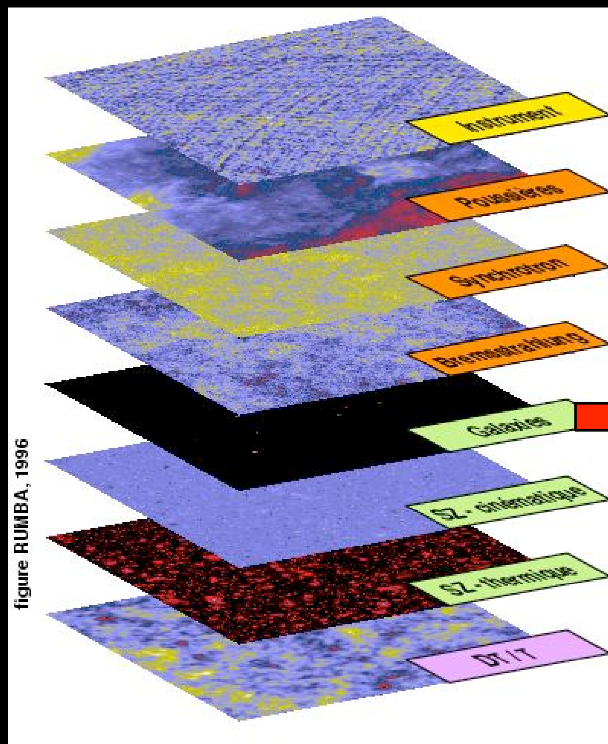

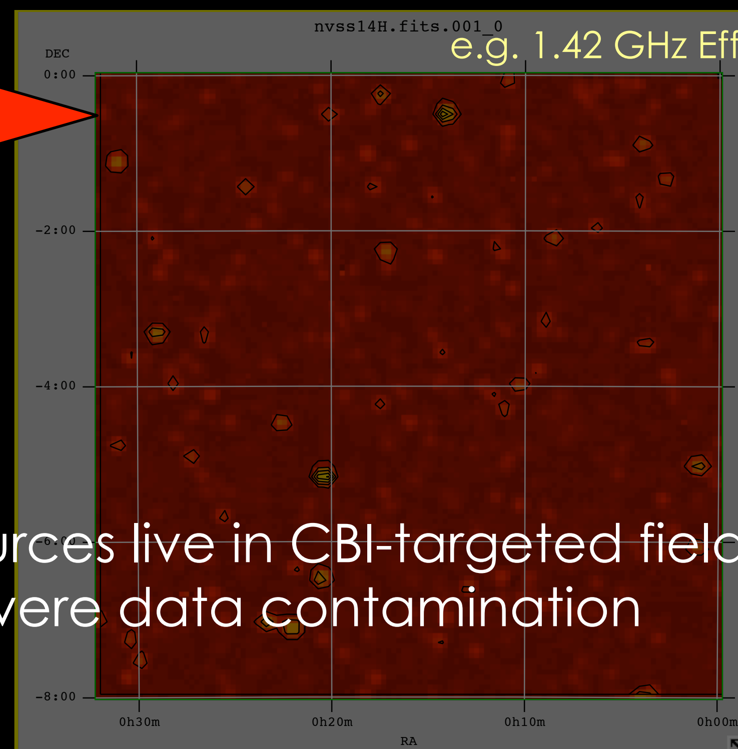

e.g. 1.42 GHz Effelsberg map

5998 extragalactic radio-sources live in CBI-targeted fields
the possibly causing severe data contamination

Motivation: the problem

unnecessary loss of data!

02h CBI field with NO point sources

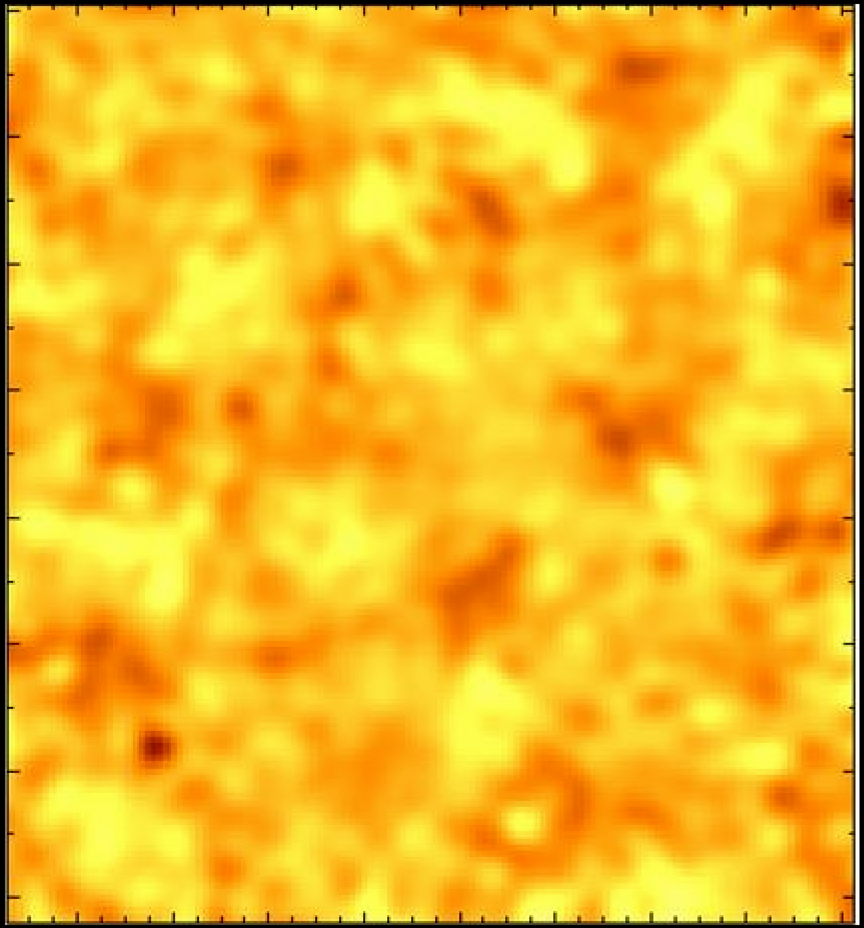

Motivation: the "solution"

target the sources at the CBI frequency band (26-36 GHz) and hope that there will be no sources "emerging" at high frequencies!

Motivation: the real solution

Identify the spectral behavior of the sources as worked out from the 1.4, 4.85 and 10.45 GHz observations

A Step Spectrum Source

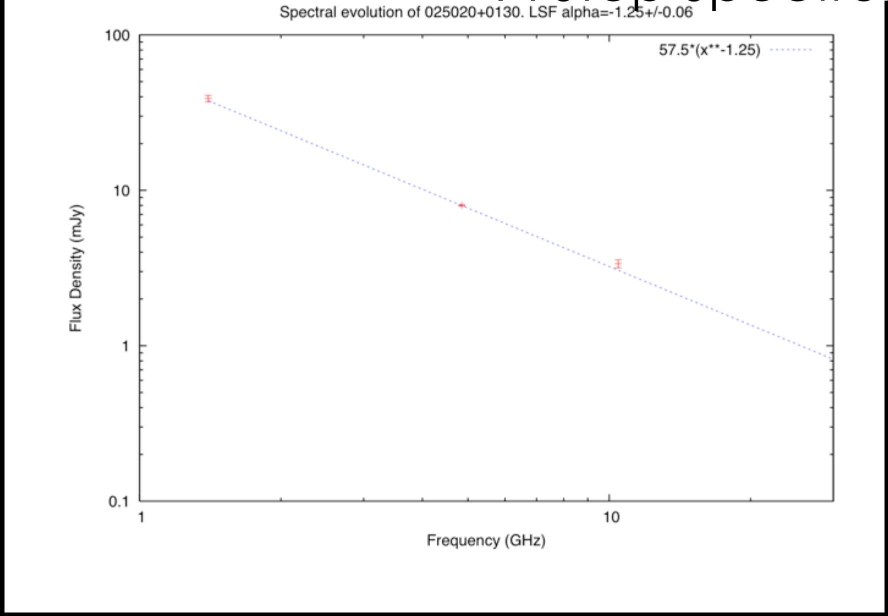

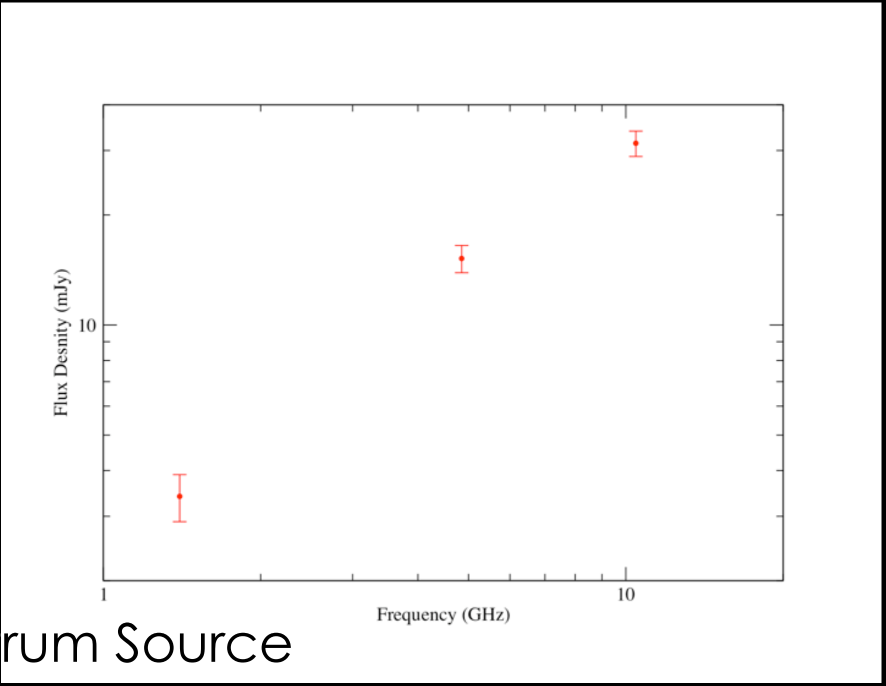

An Inverted Spectrum Source

Completion

02-Hr field

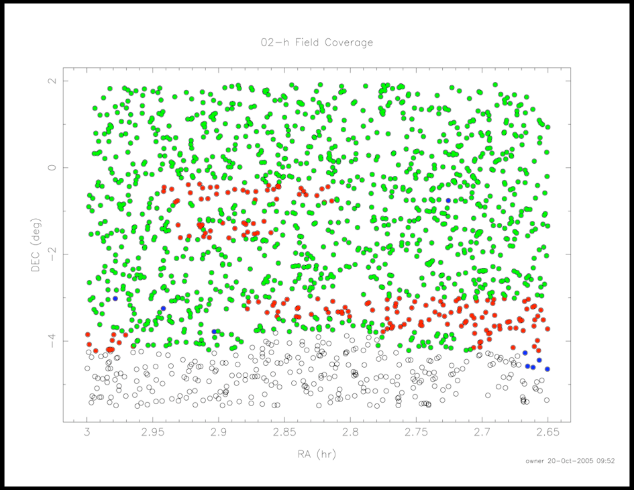

20-Hr field

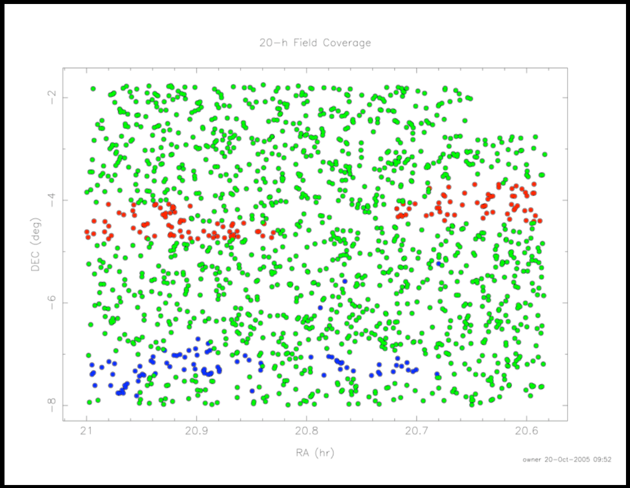

08-Hr field

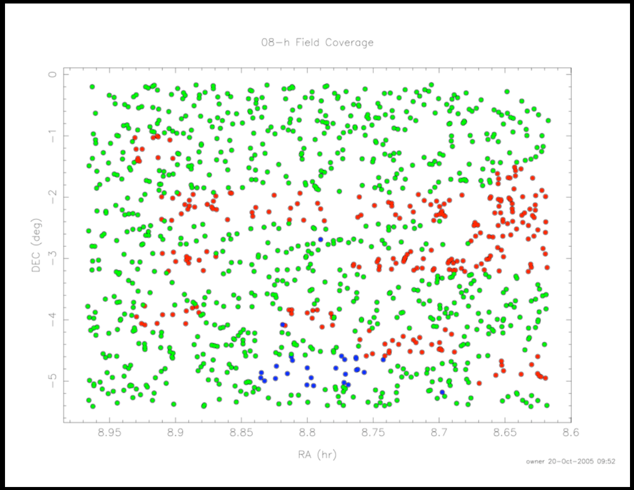

14-Hr field

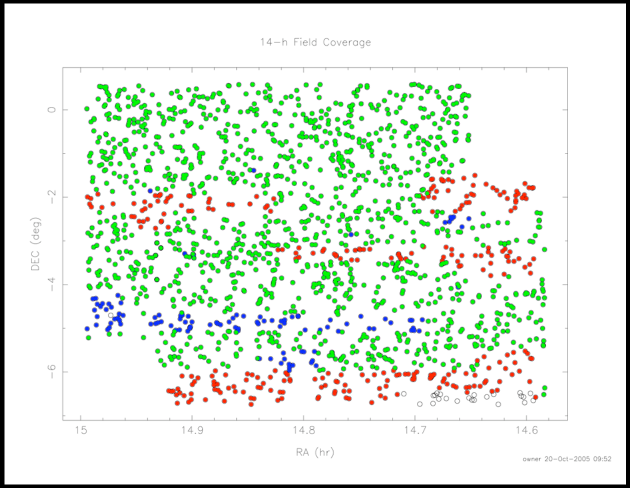

Results: CBI-wise

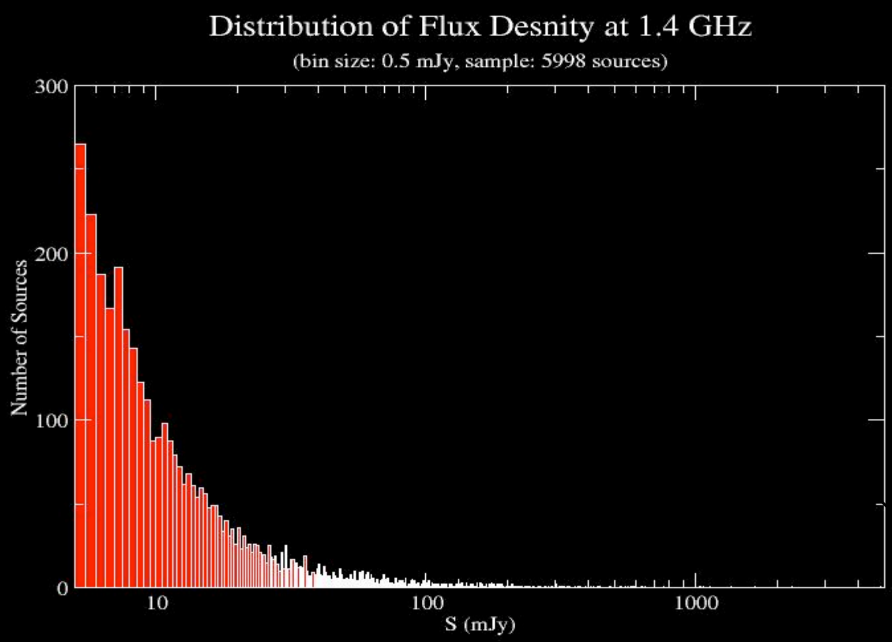

assume <alpha>=-0.5

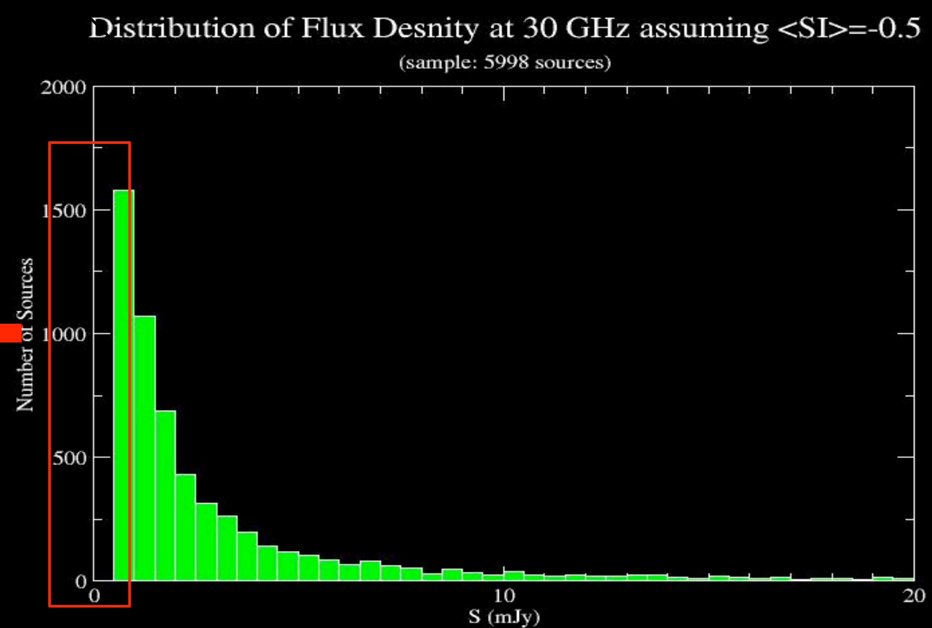

27% of the sources are in the safe zone of <1 mJy

Results: CBI-wise

out of 4612 trusted observations:

- 2118 (46%) sources have NOT been detected at any of the 2 frequencies

- 1594 (35%) sources have ONLY been detected at 4.85 GHz

- 657 (14%) have been detected at BOTH frequencies

- 243 (5%) have been detected ONLY at 10.45 GHz

Results

Spectral Index distribution

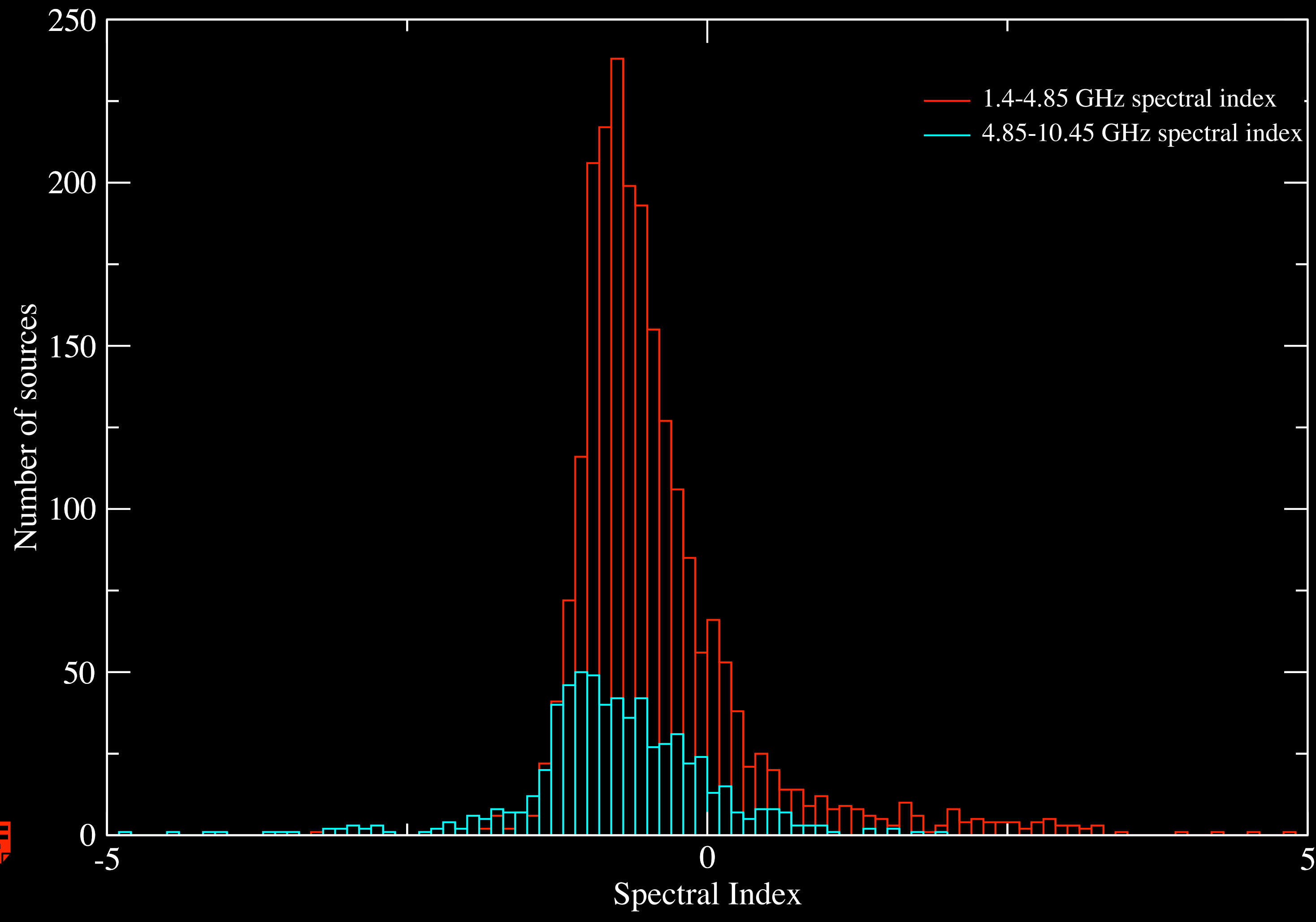

Results: the "repeatability" plots

6 cm repeatability plot

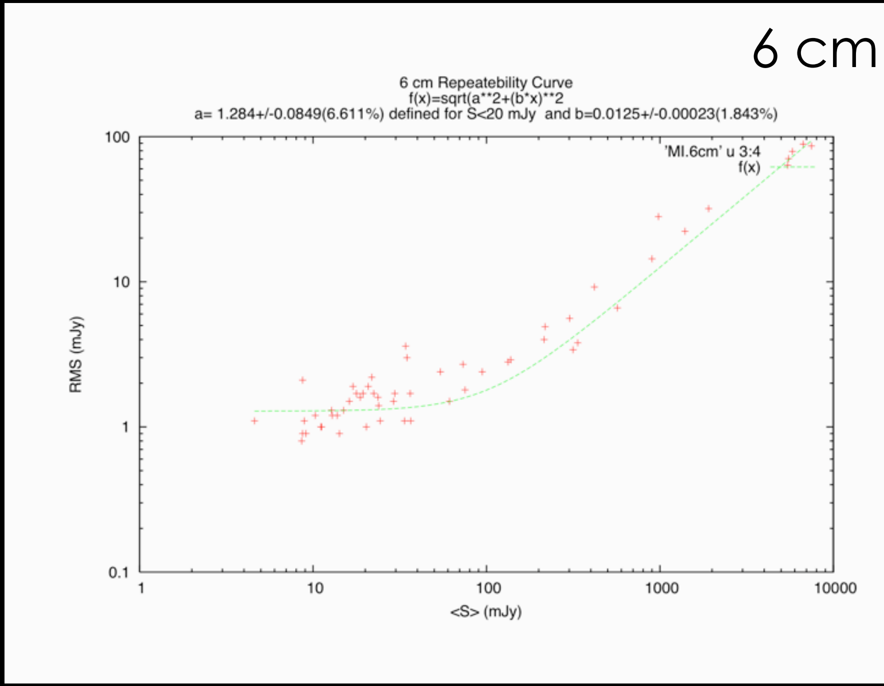

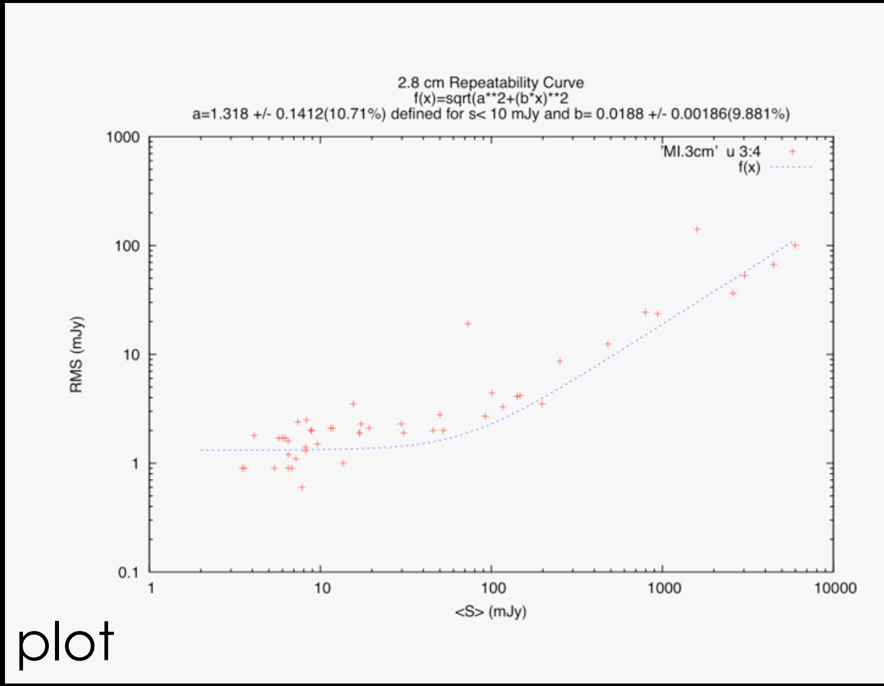

6 cm repeatability plot

Results: the "repeatability" plots

6 cm repeatability plot

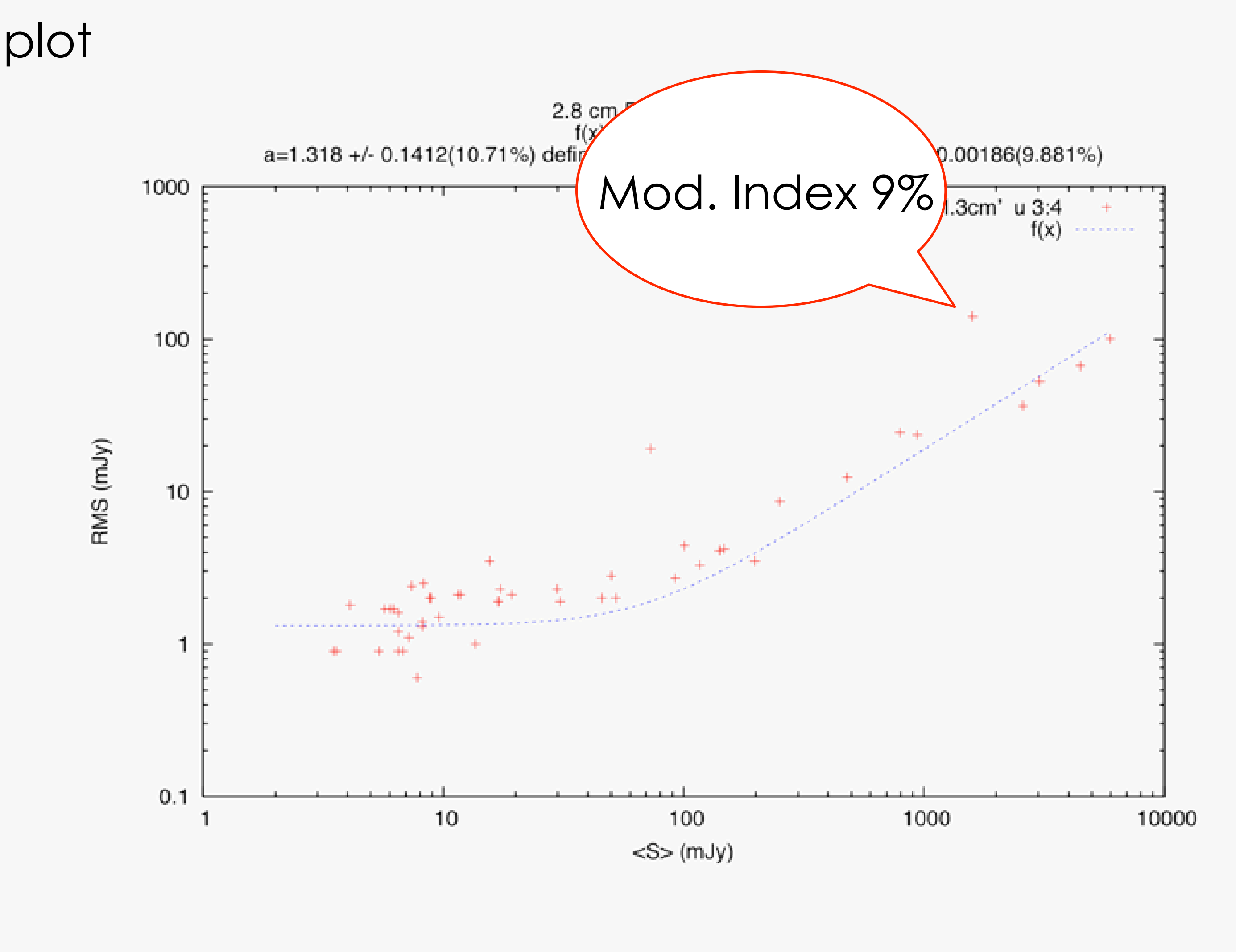

Results: NGC1052

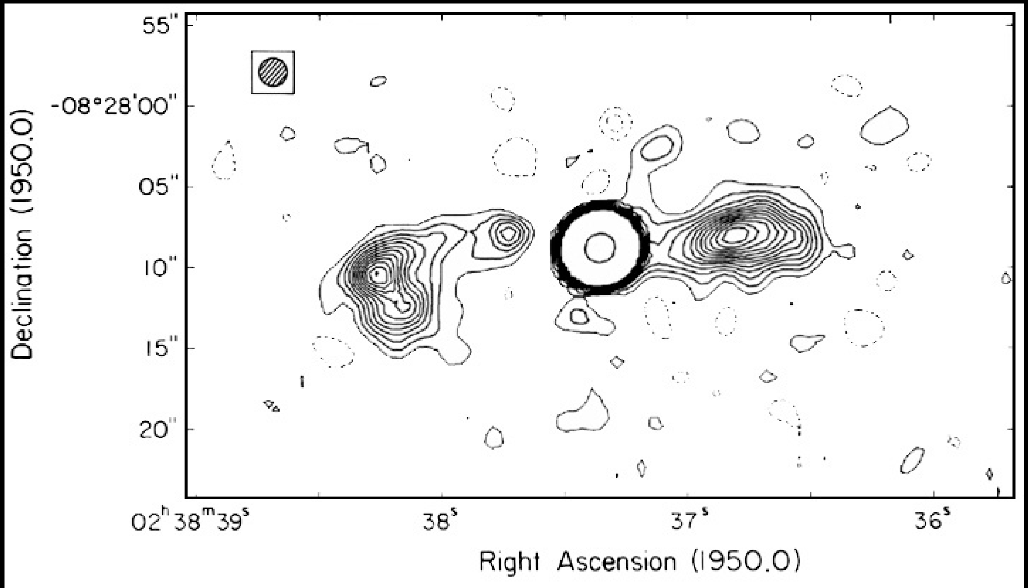

FIG. 1b

1984ApJ...284..531W

Taken from NED facility

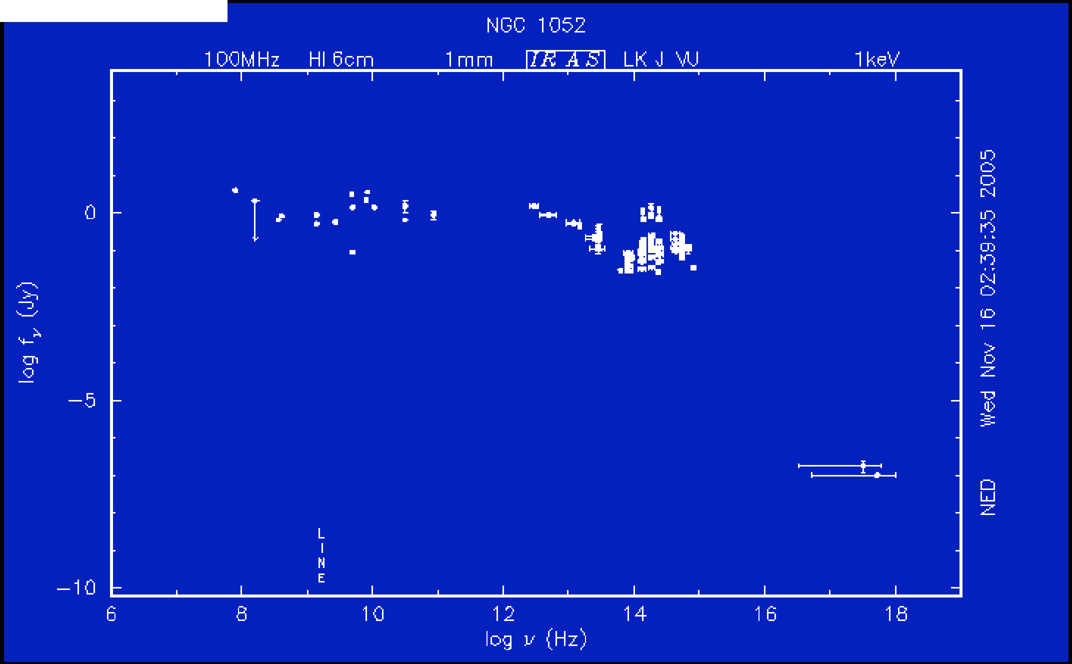

Results: NGC1052

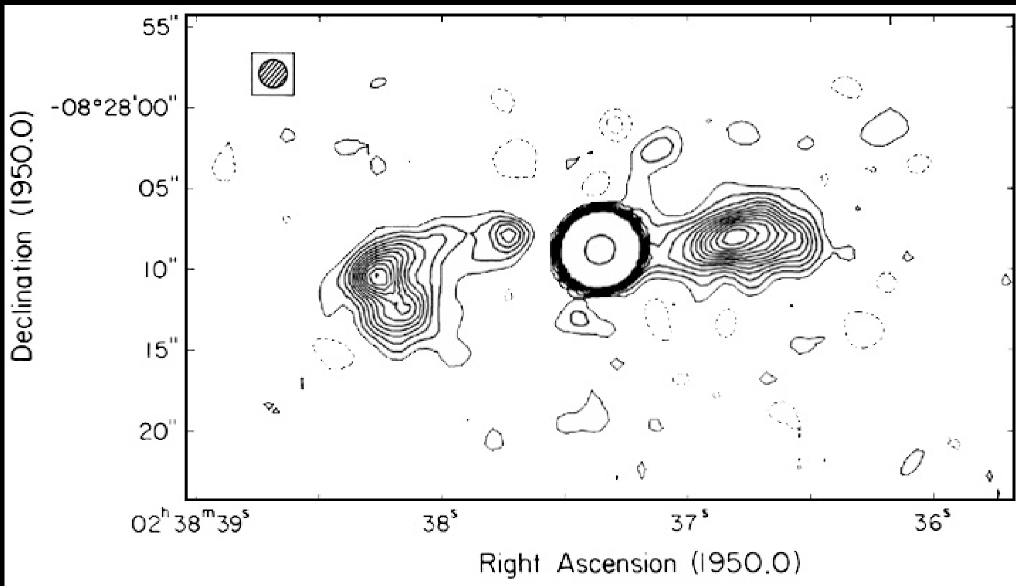

Fig. 1b

1984ApJ...284..531W

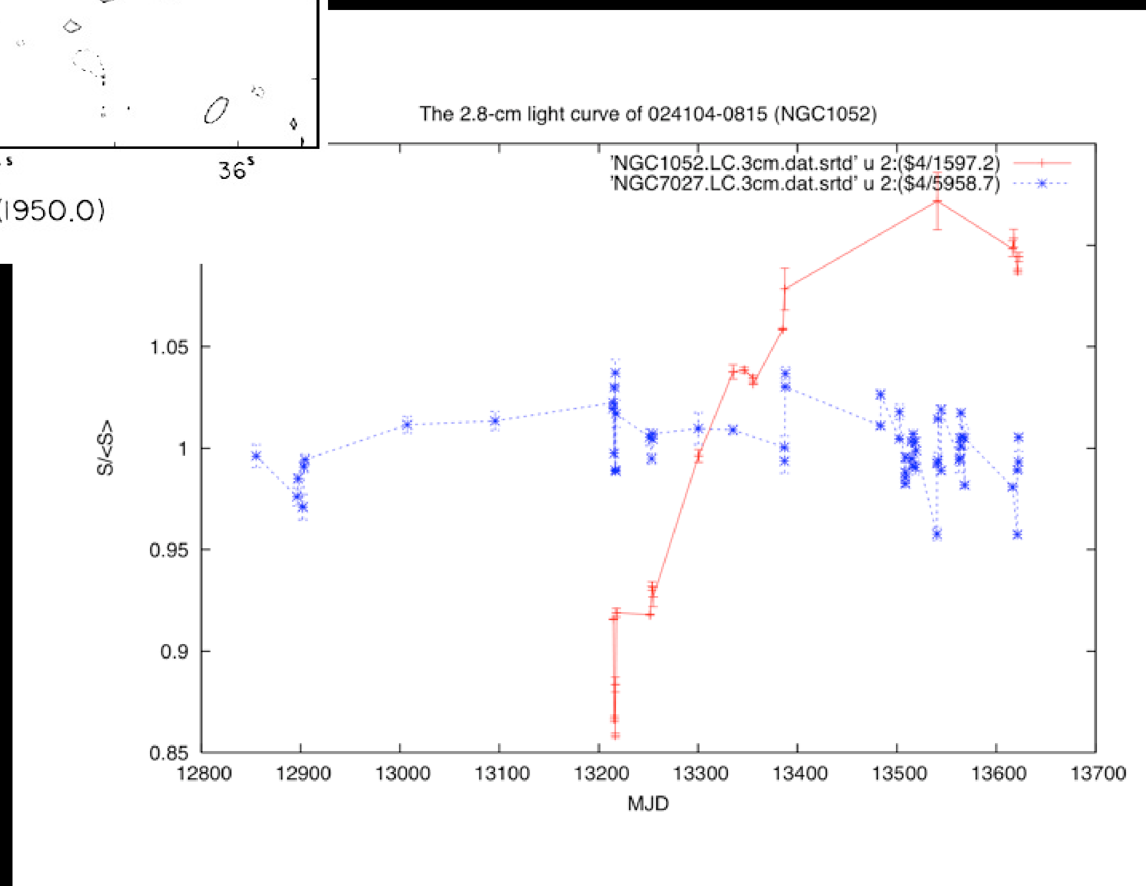

Results: NGC1052

1984ApJ...284..531W

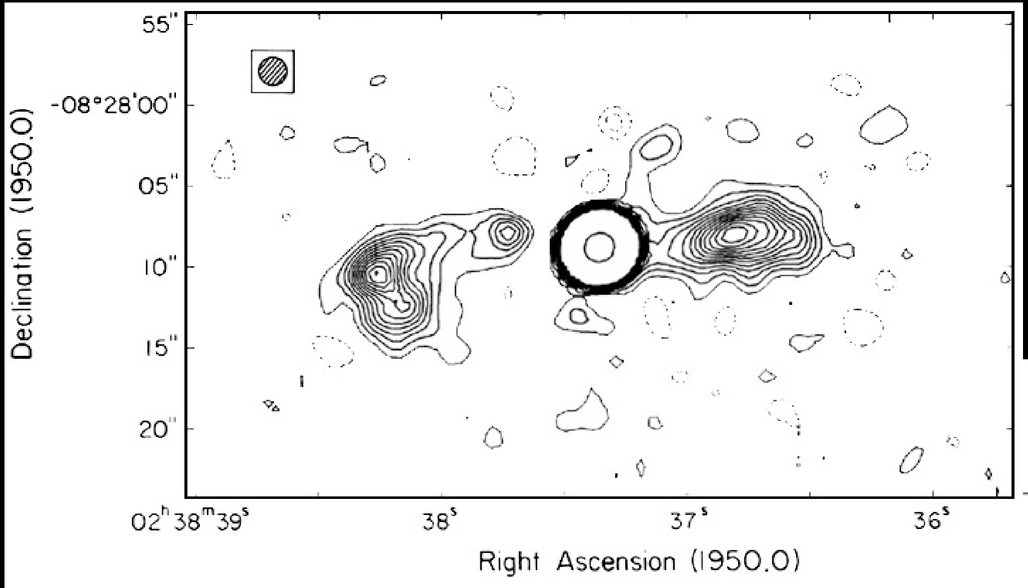

FIG. 1b

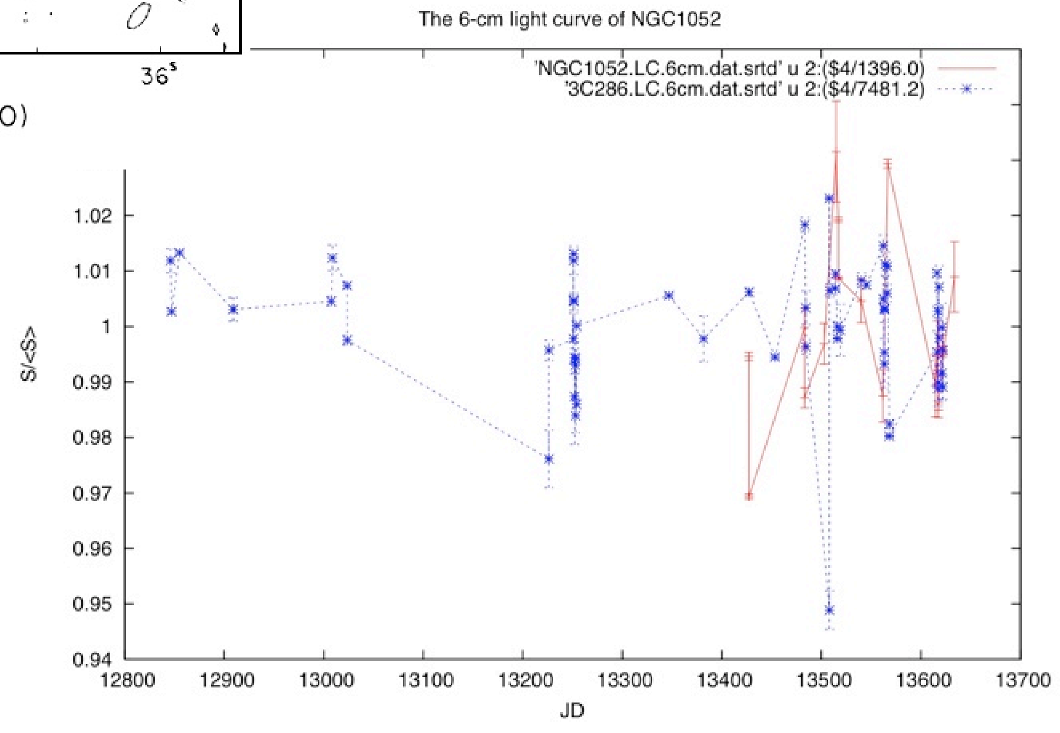

Results: 025515+0037

6 cm repeatability plot

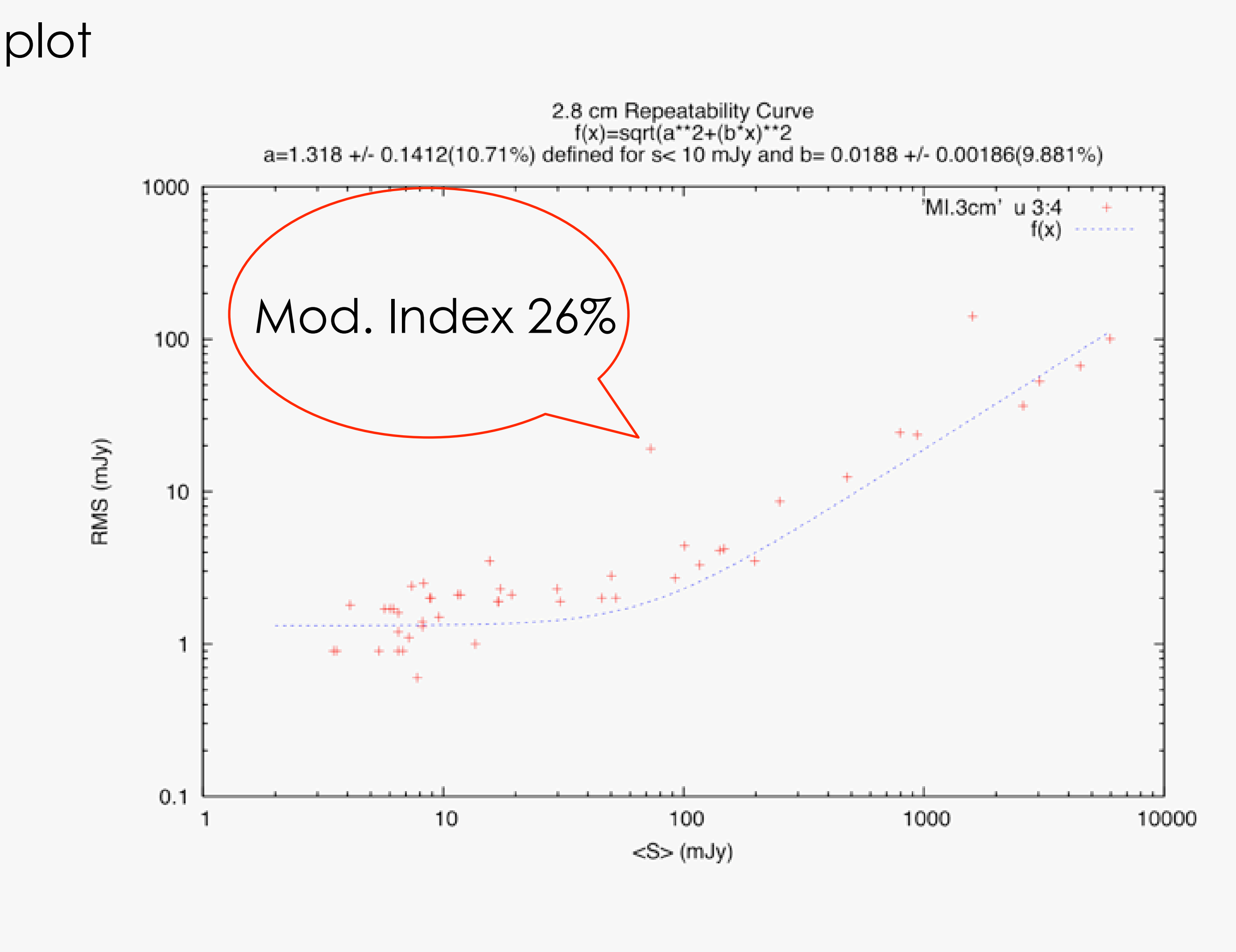

Results: 025515+0037

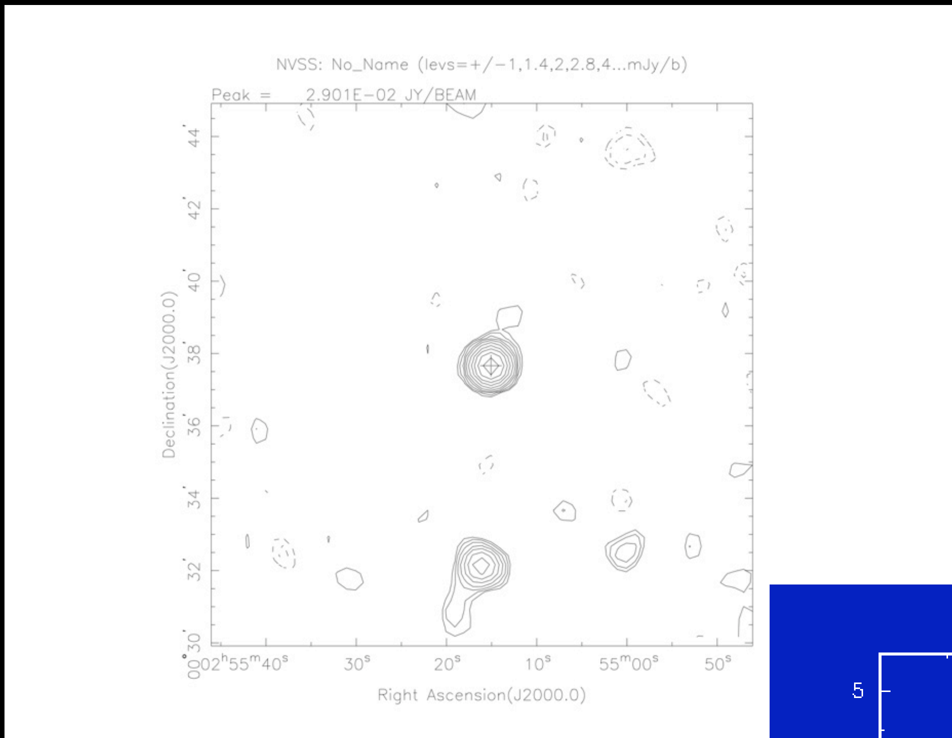

Condon et al. 1998

Taken from NED facility

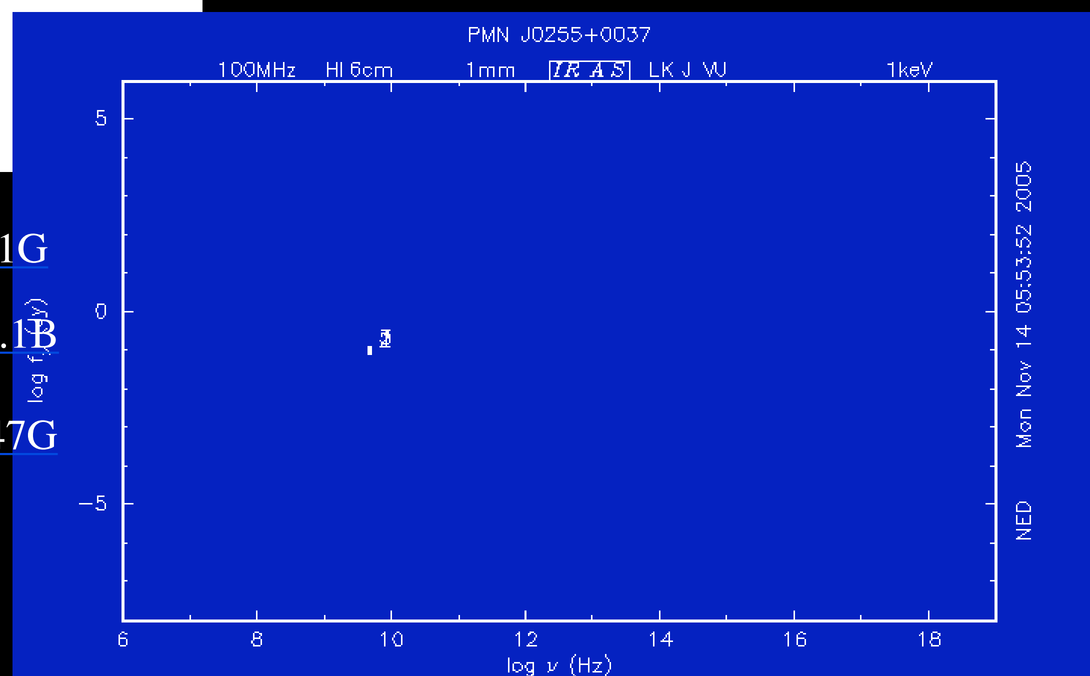

1 4.85 GHz 95+/- 15mJy 1991ApJS...75.1011G

2 4.85 GHz 90+/- 15 %mJy 1991ApJS...75....1B

3 4.85 GHz 104+/- 12mJy 1995ApJS...97..347G

Results: 025515+0037

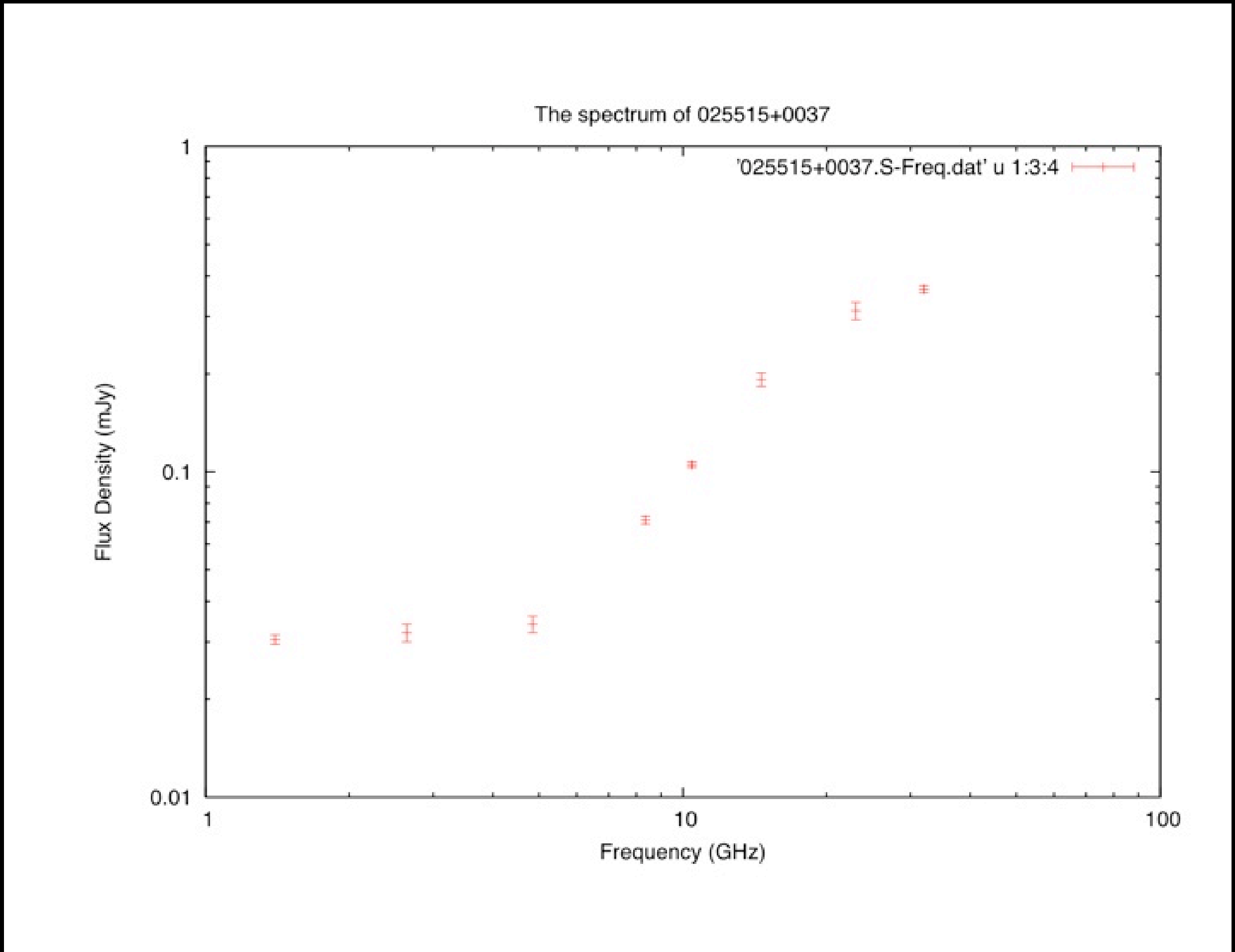

Results: 025515+0037

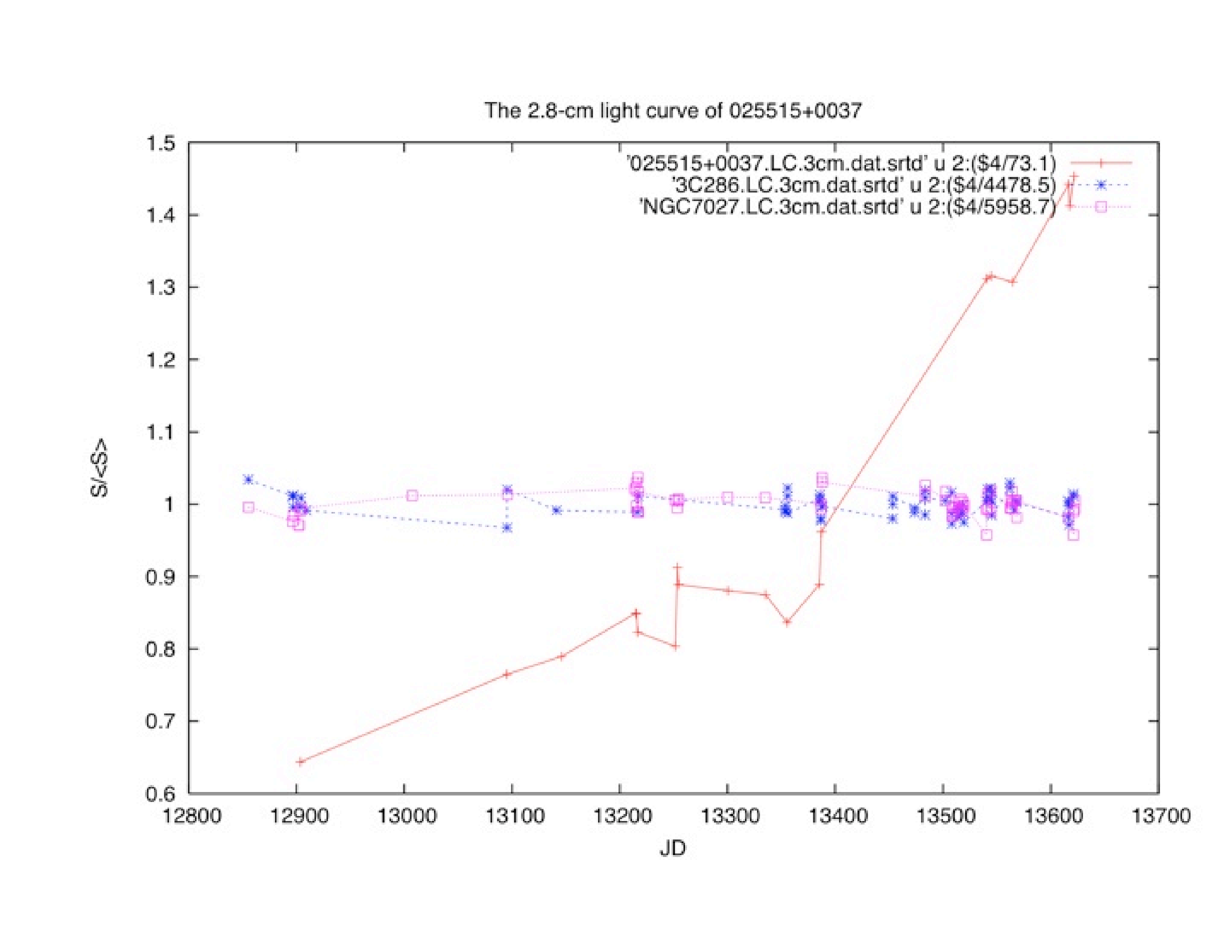

Results: 025515+0037

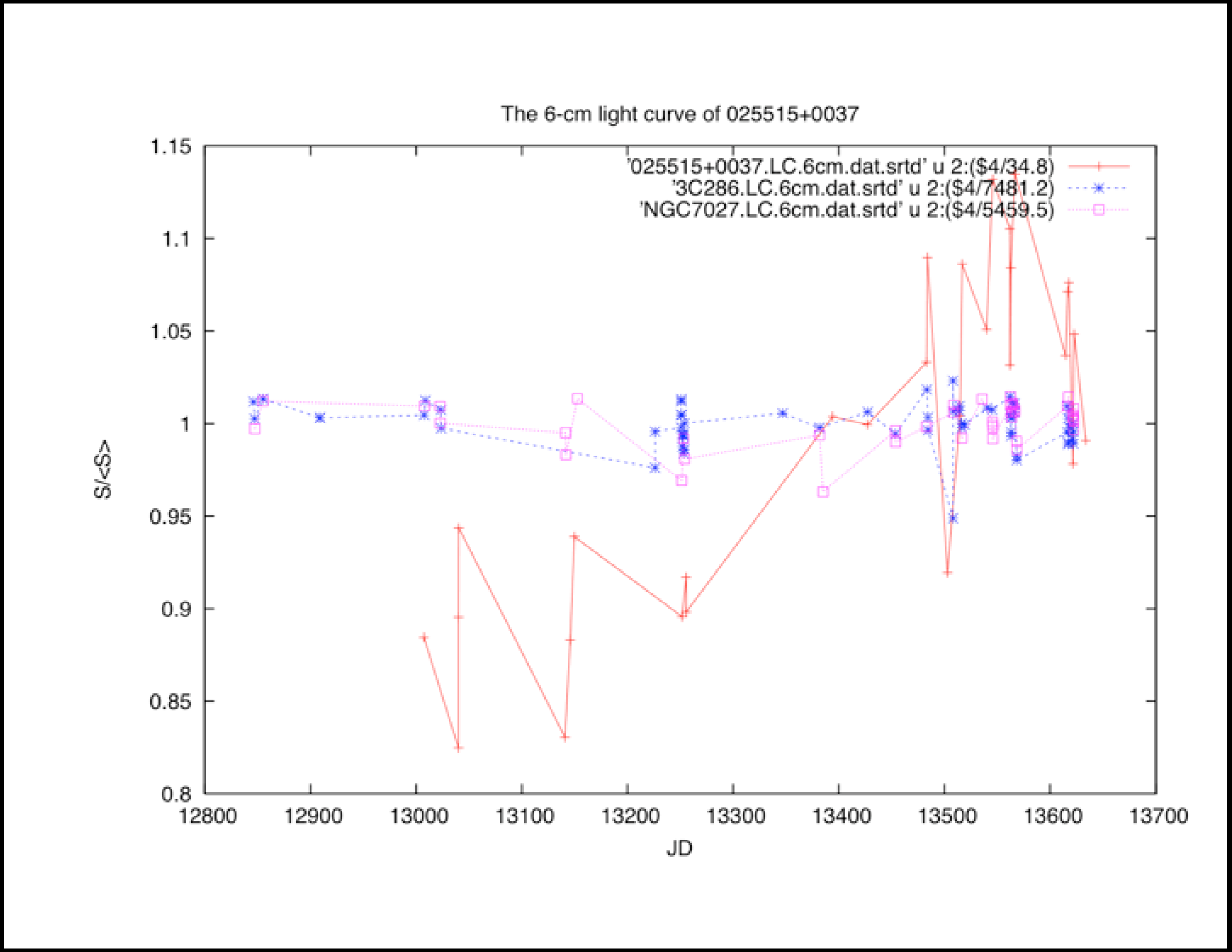

Results: 025515+0037

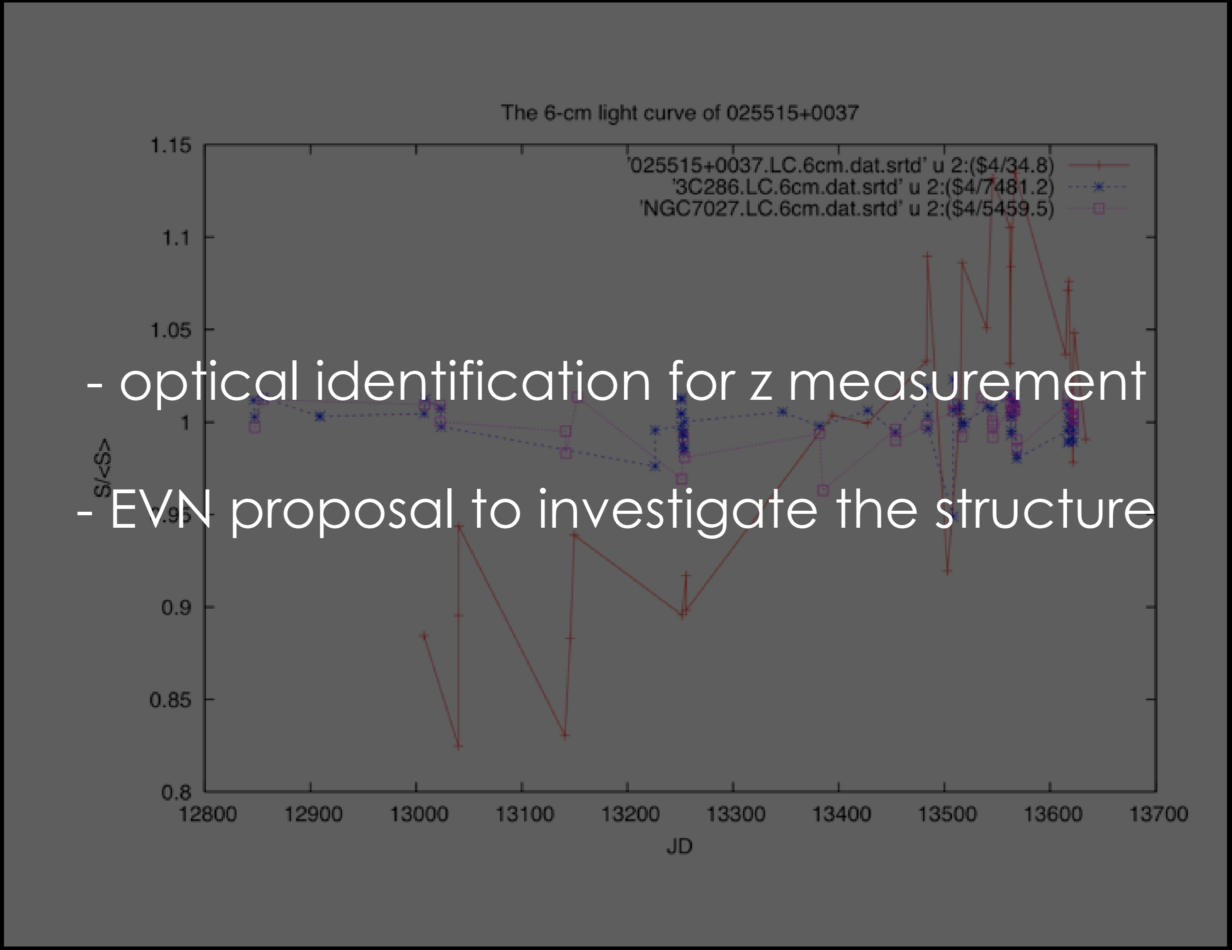

- optical identification for z measurement

- EVN proposal to investigate the structure

Immediate future plans

- resolve the confusion problem

- publish the spectral index results

- discover new inverted spectrum sources
(attempt optical identifications)

- conduct thorough studies of the source counts

- initiate luminosity function studies etc.

Thank you for your attention

Thank you for your attention

Was: Variations of the high energy cutoff in Blazars

Is: Comments on the discussion following Jose's talk yesterday

Stefan J. Wagner
LSW Heidelberg

Blazars and the CIB

Blazar models in general not well constrained.
Concensus: Nonthermal emission.
Constraints on spectral index.

Strategy: Determine spectra of Blazars,
assume minimum SED, and multiply/add
until constraints on Blazar SED are violated.

Best sources: high redshift, flat spectra:
New HESS sources: 1101-232, 2356-36

Constraints on diffuse EBL

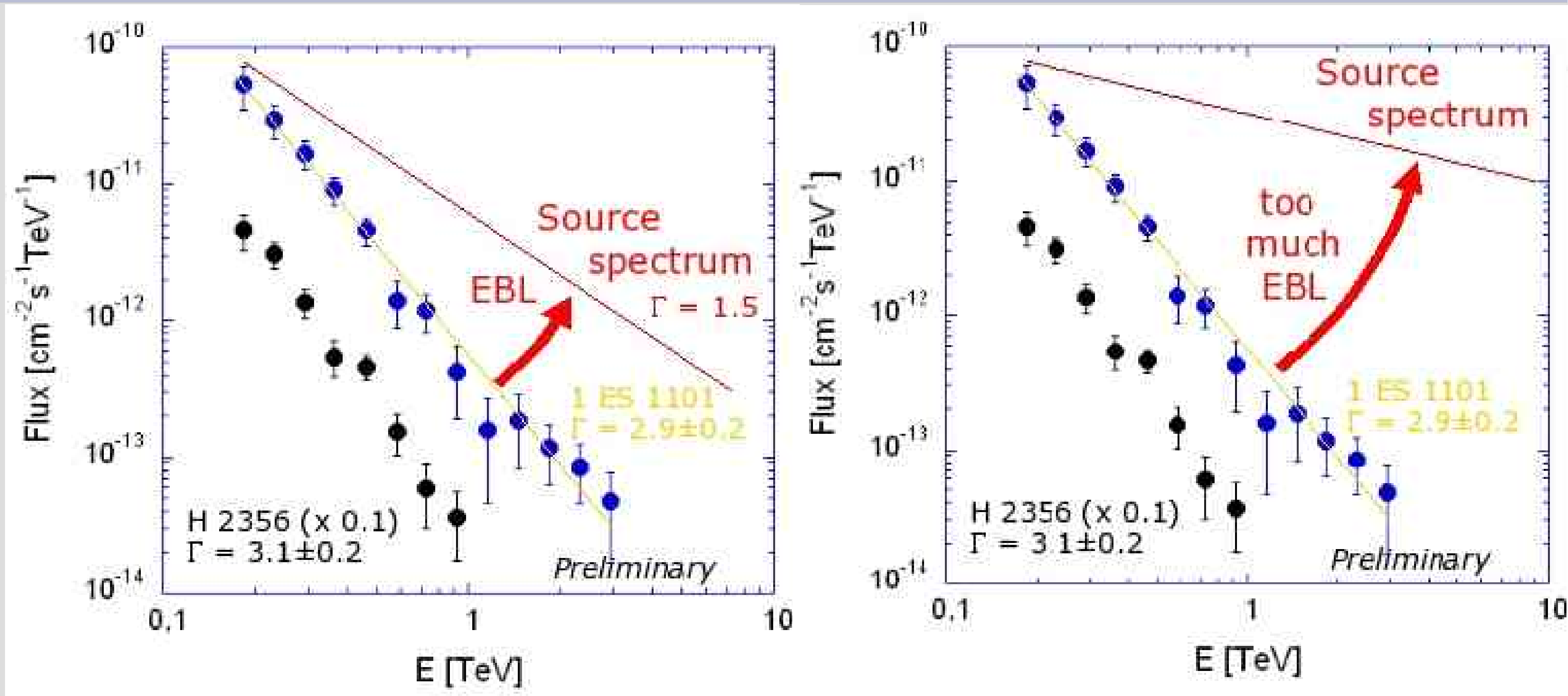

shock acceleration: s=1.5 Protons: Gamma=1.5

IC: Gamma > 1.5 unless no radiative cooling **and** IC fully in Thomson limit [Gamma = (s+1)/2 =1.25]

Constraints on diffuse EBL

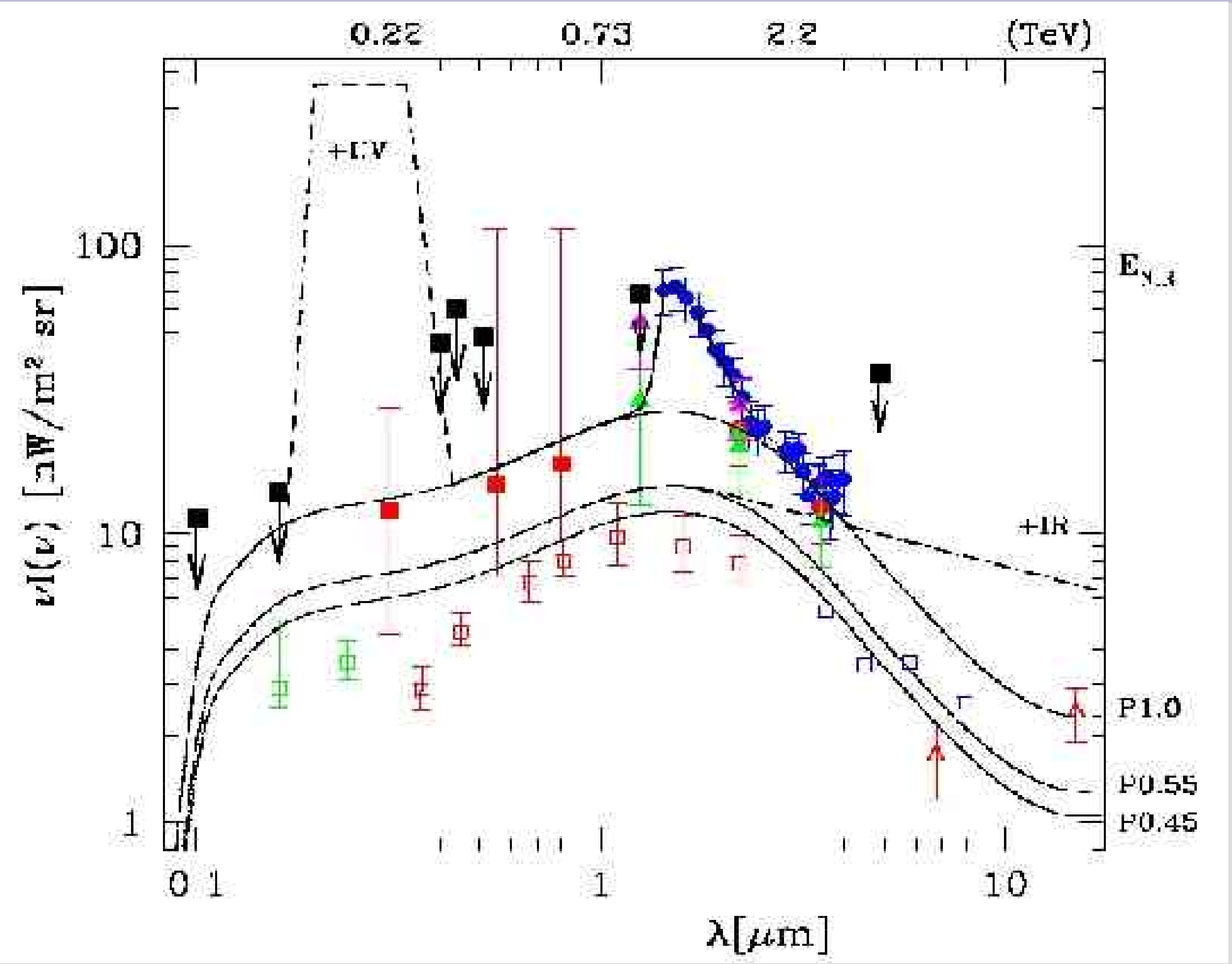

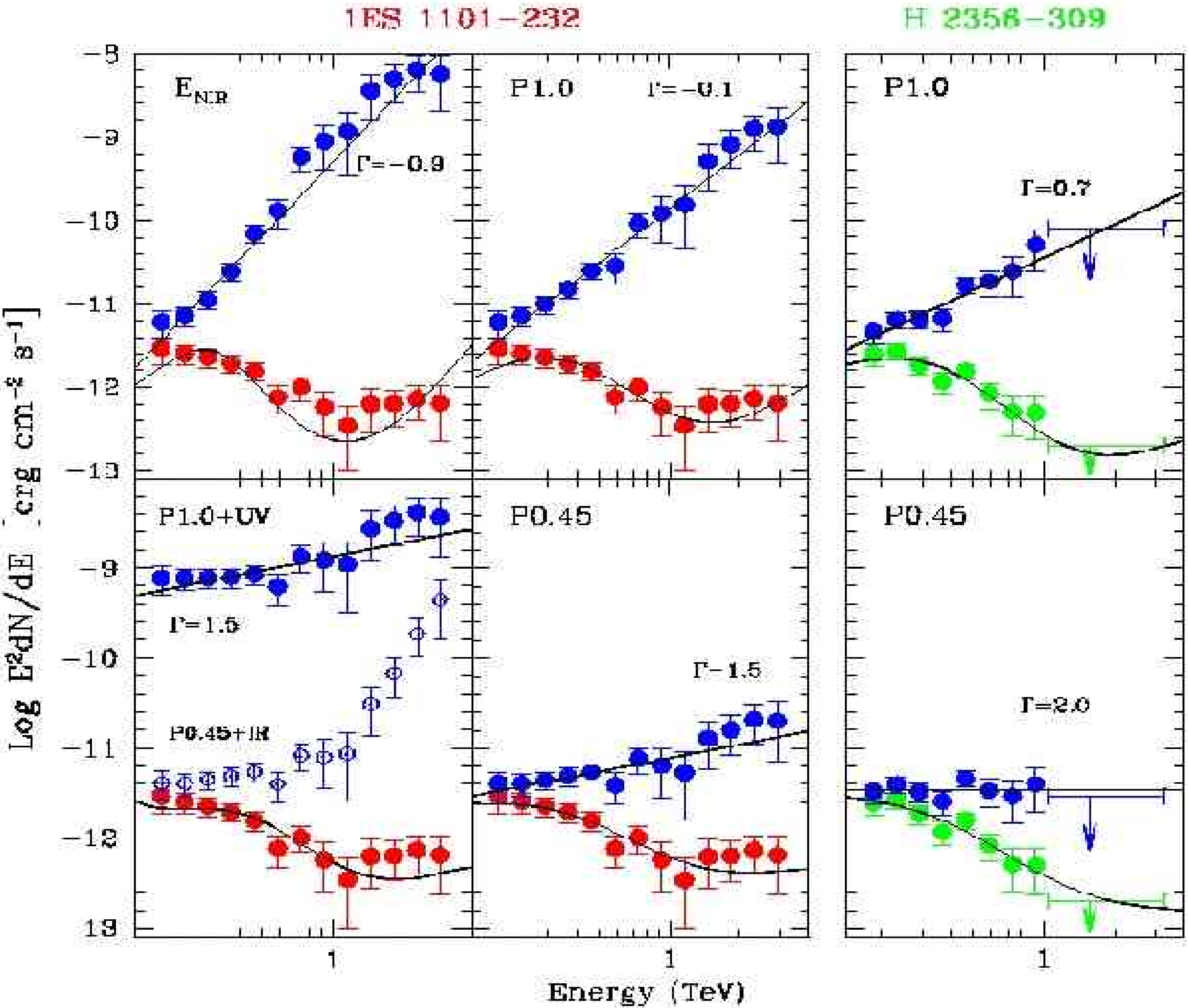

1ES 1101-232
H 2356-309
E_NIR
Γ=-0.9
P1.0
Γ=-0.1
P1.0
Γ=0.7
P1.0+UV
Γ=1.5
P0.45+IR
P0.45
Γ=1.5
P0.45
Γ=2.0
Log E²dN/dE (erg cm⁻² s⁻¹)
Energy (TeV)

1990s: CGRO

EGRET (70 MeV up to a few GeV):

Blazars dominated
by Gamma-Emission

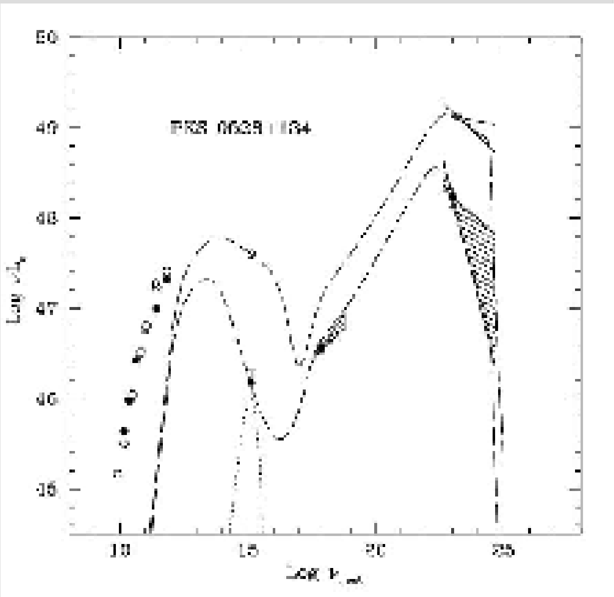

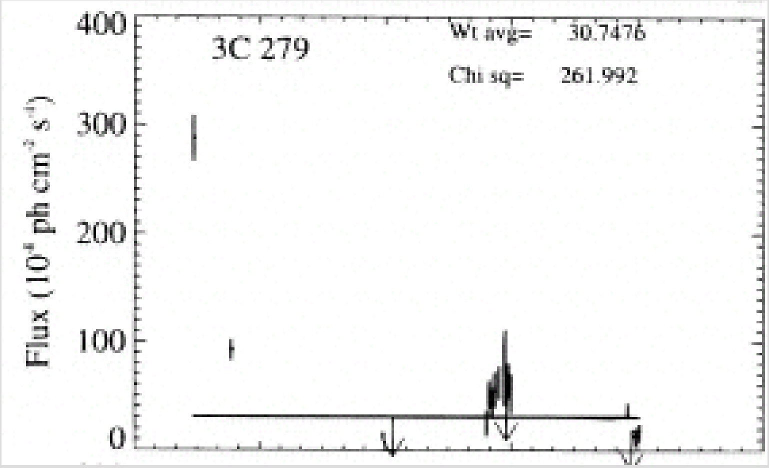

Significant
variability

challenge: simultaneous SED required
Many sources observed simultaneously

TeV opacity of the universe

Empirical Measurements of CIB:

taken from Hauser & Dwek, ARAA, 2001 updated (Costamante et al., in 2004)

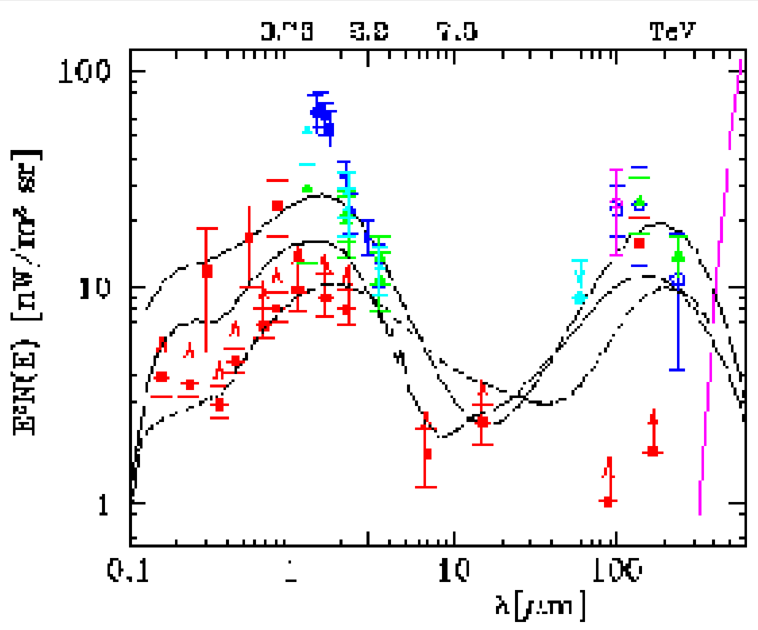

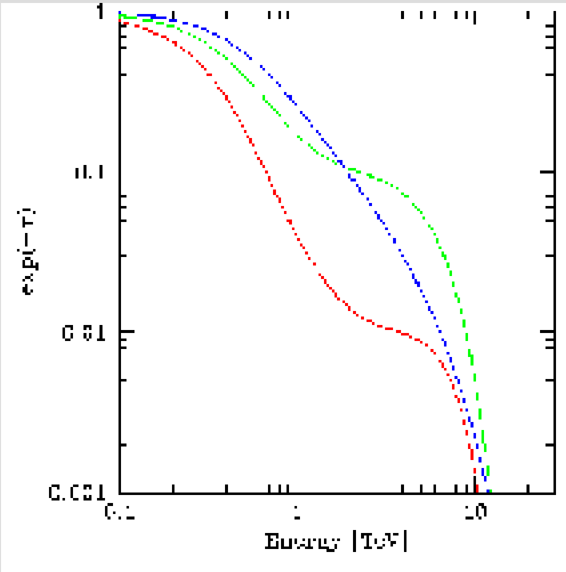

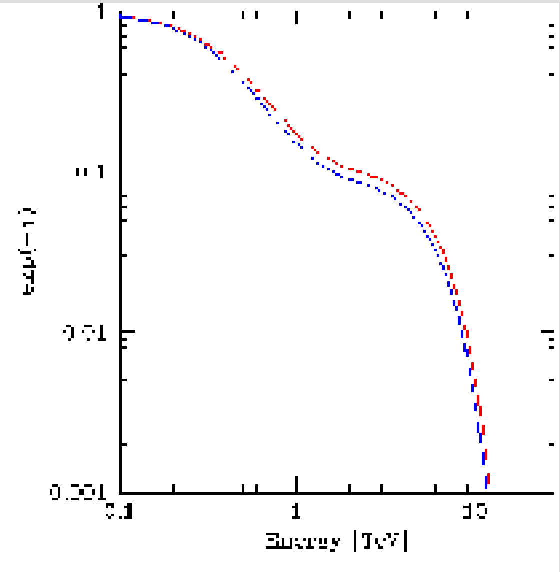

Effect of absorption: Extinction (E, z, SFH)

(Costamante et al., 2004)

PKS 2155-304

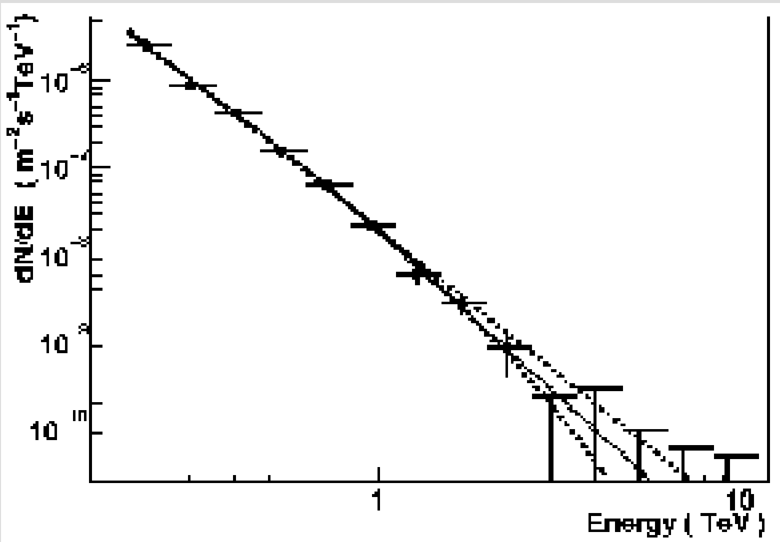

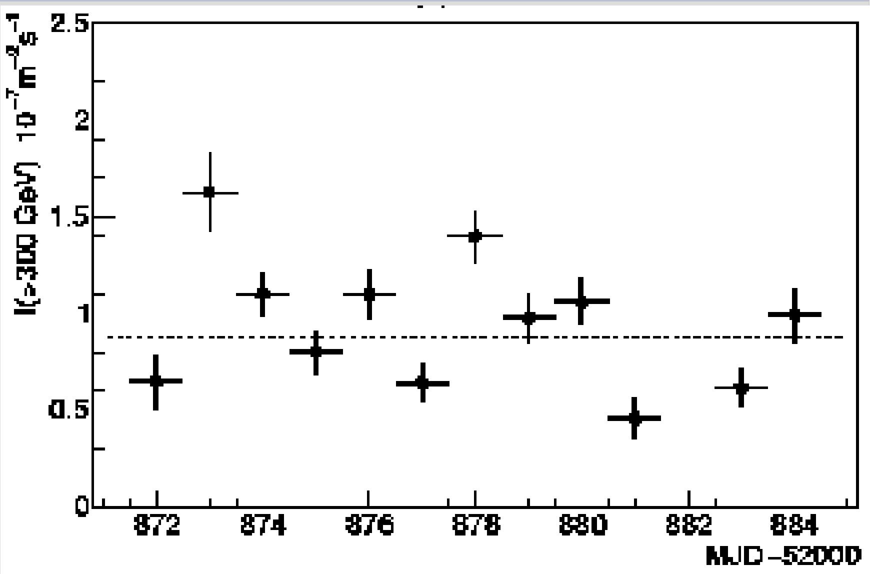

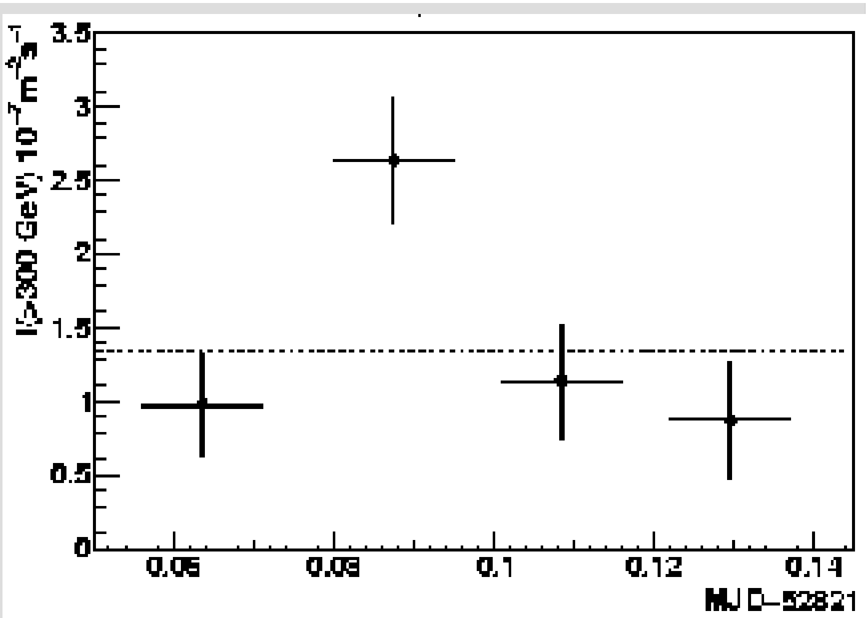

Detection in 2002, 2003 with single telescope already: astro-ph/0411582

Powerlaw spectrum, Index: -2.9
variability: years – minutes

Suggests Doppler factor $\mathcal{D}$ ~ 50

PKS 2155-304

2003 campaign

H.E.S.S.

XTE/PCA

Optical

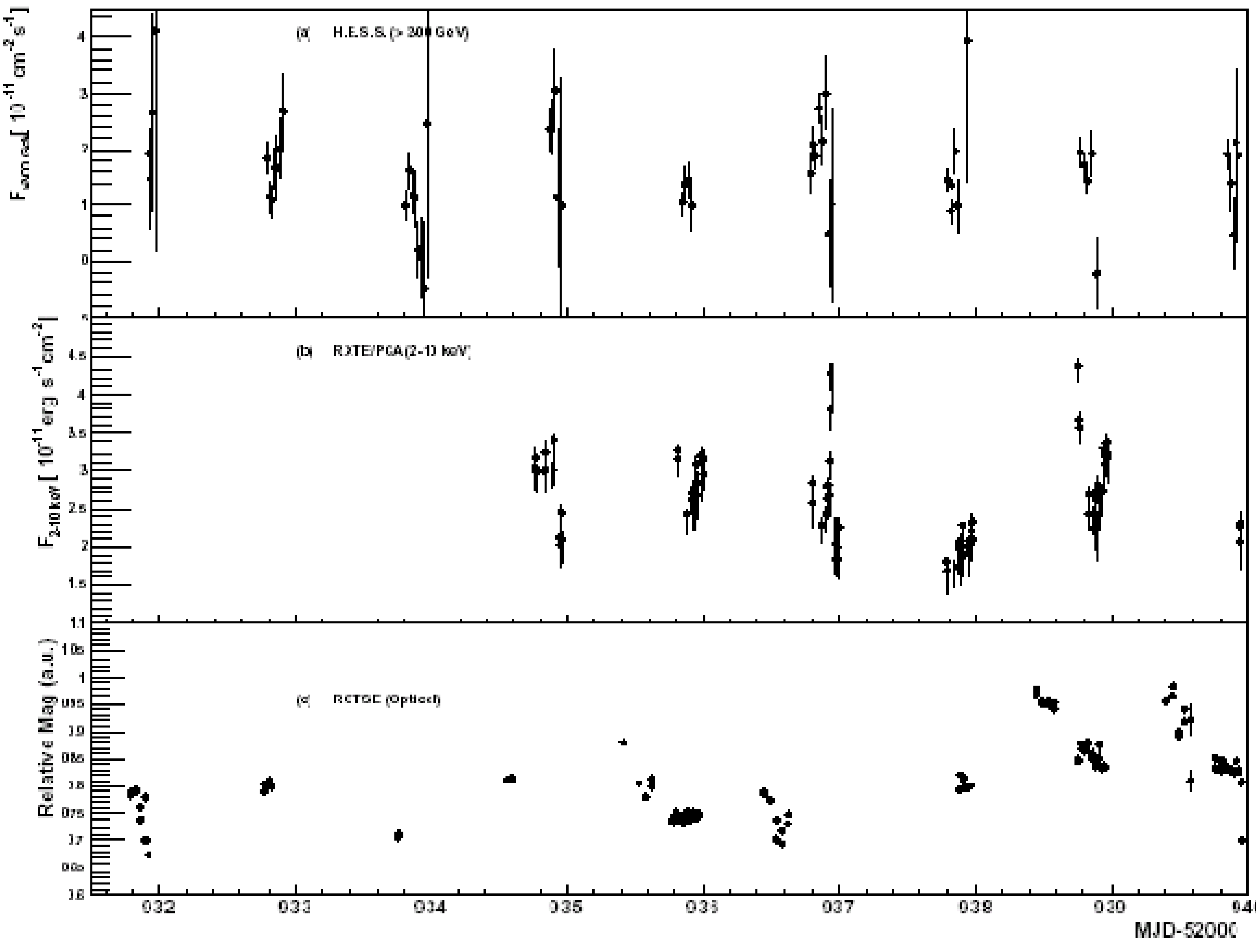

PKS 2155-304

TOO campaign triggered by a high state

Trigger activation delayed by 8 days,
PKS 2155-304 had faded

run-by-run detections
X-ray variability
weak VHE variability
no correlation run-by-run

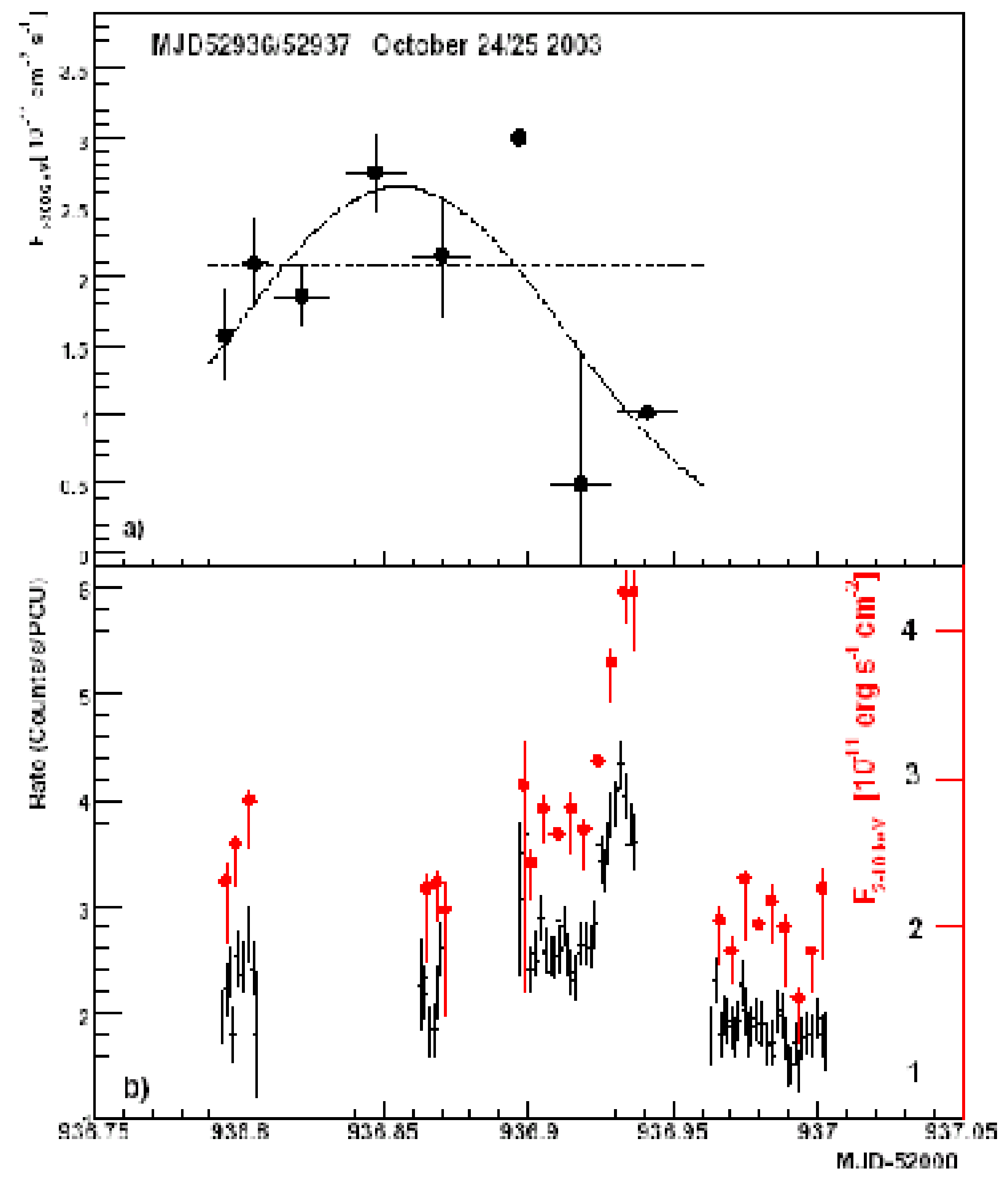

Modelling PKS 2155-304

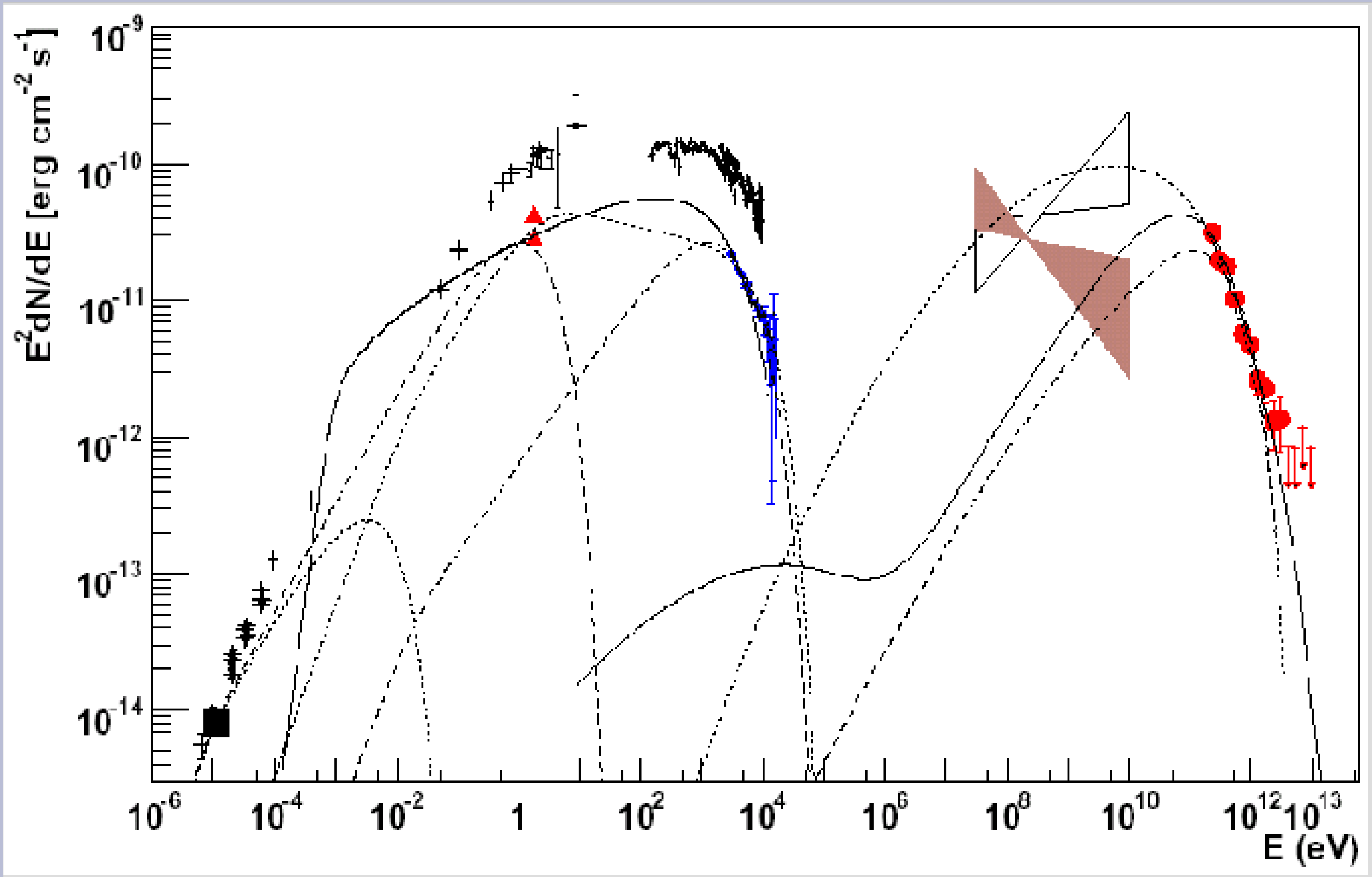

Conclusions on EBL

Any plausible AGN emission model suggests that EBL in optical-NIR range ~ deep counts

NIR excess (Pop III signature) ruled out
Strong UV bump ruled out

No room left for significant distributions from LSBG, intergalactic/-cluster stars, subluminous CF stars, .. (WYSIWYG star formation history)

TeV universe is big (studies of EBL evolution)
applications: redshift upper limits in extreme Blazars

Challenges: Cosmology, Fundamental physics

Correlations

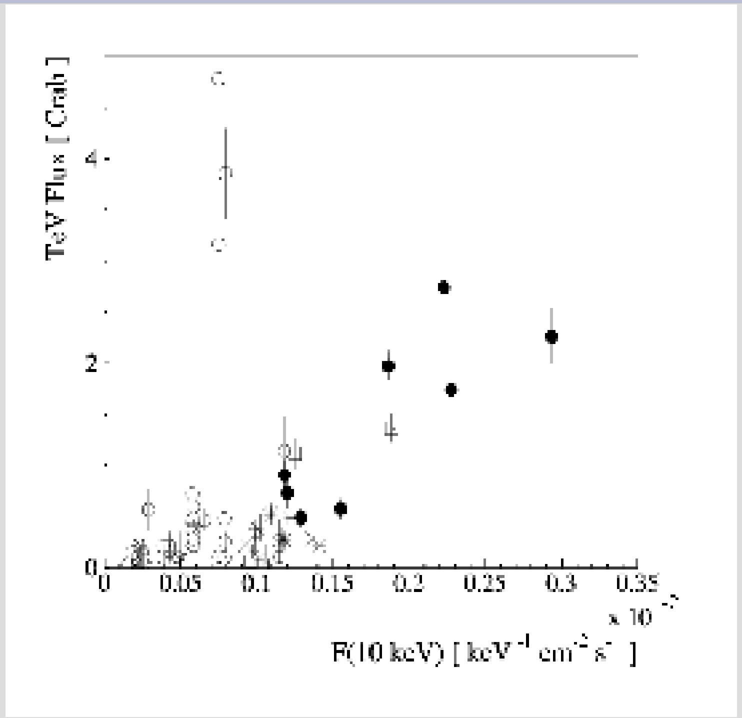

"Orphan flares"

Krawczynski et al., ApJ 601, 151

Single-zone models rarely provide good fits to temporal evolution.

Bicknell & Wagner, 2003

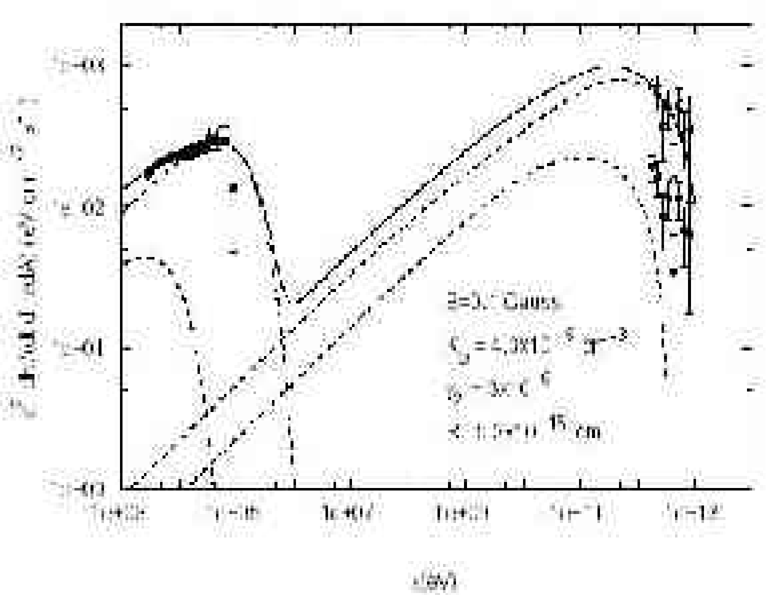

VHE emission from Blazars

spectral lags within
one passband
e.g. Mrk 501:

(Wagner & Lamer, 1999, 2001)

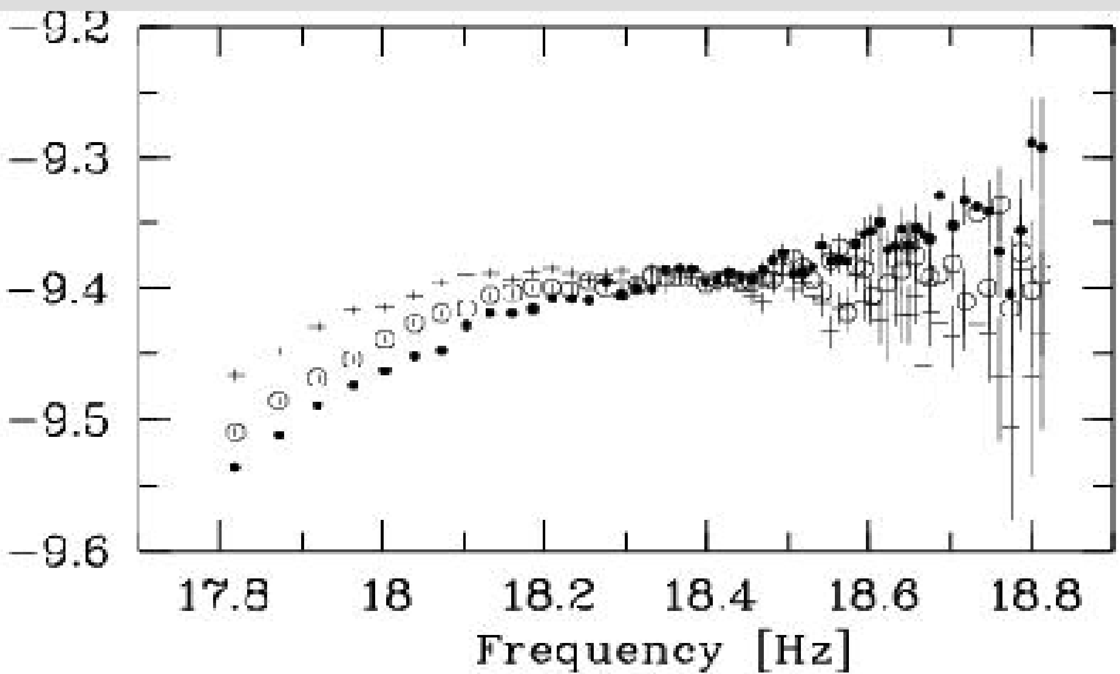

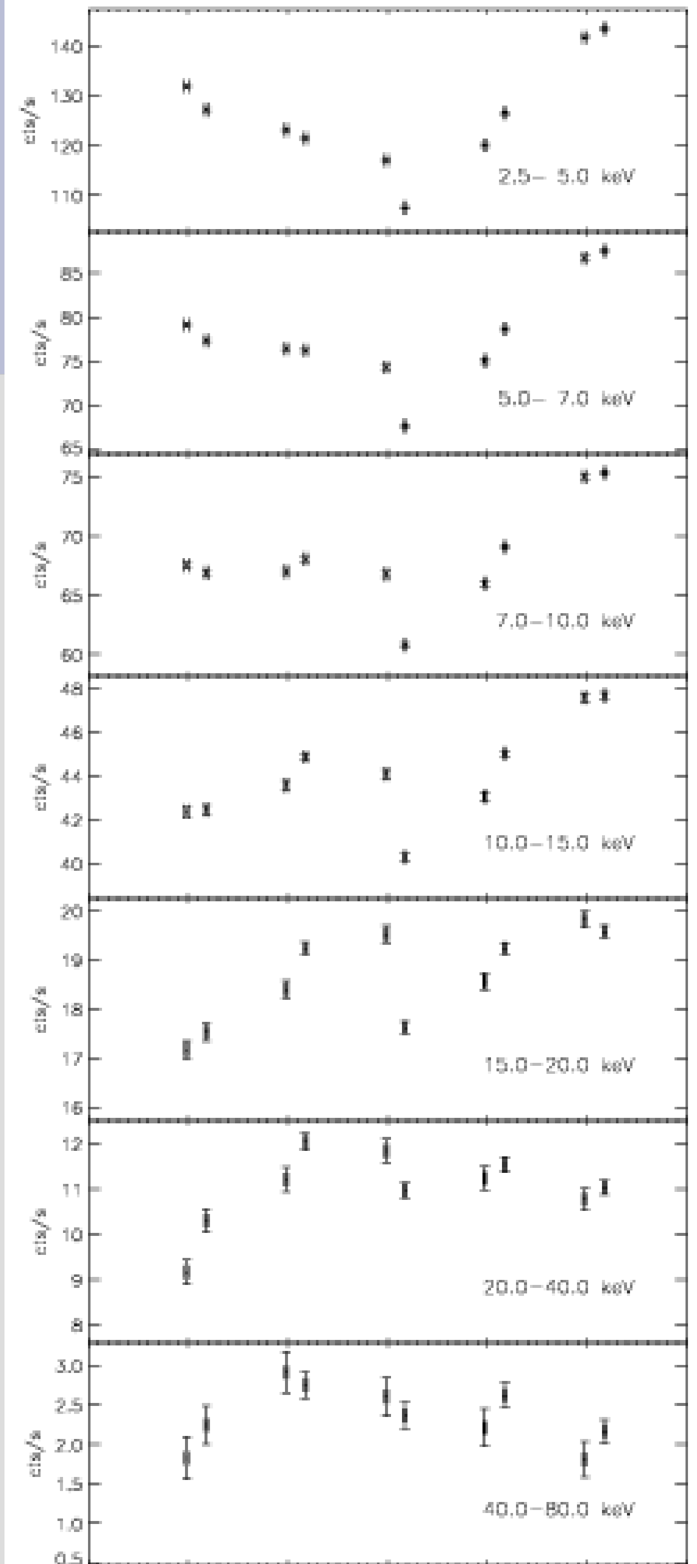

MKN421 ”Final Chapter”

Dimitrios Emmanoulopoulos

6th ENIGMA meeting, Kinsale 22-25 November 2005

Landessternwarte Heidelberg

ENIGMA

Overview

- The complete light curve
- Time Series analysis
- A new method
- Application

MKN421 1996-2005

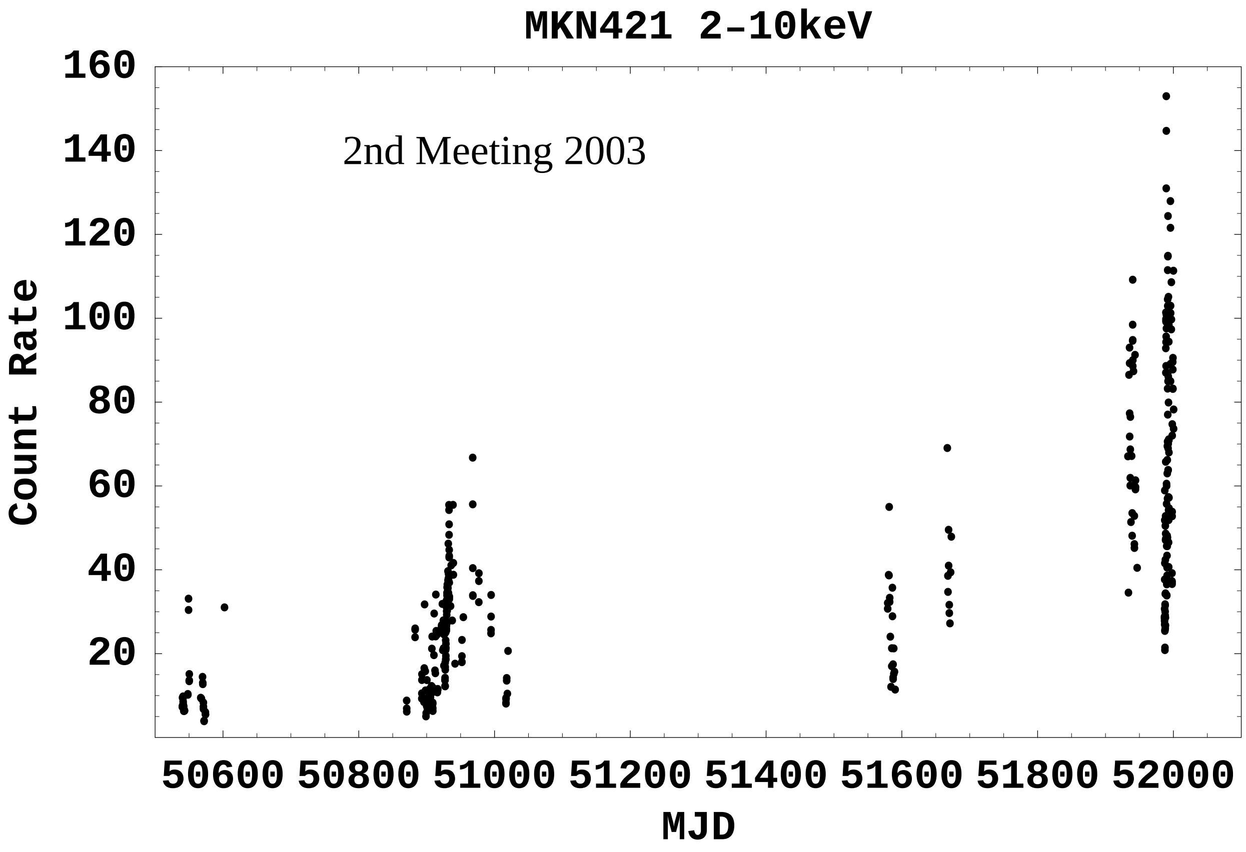

MKN421 1996-2005

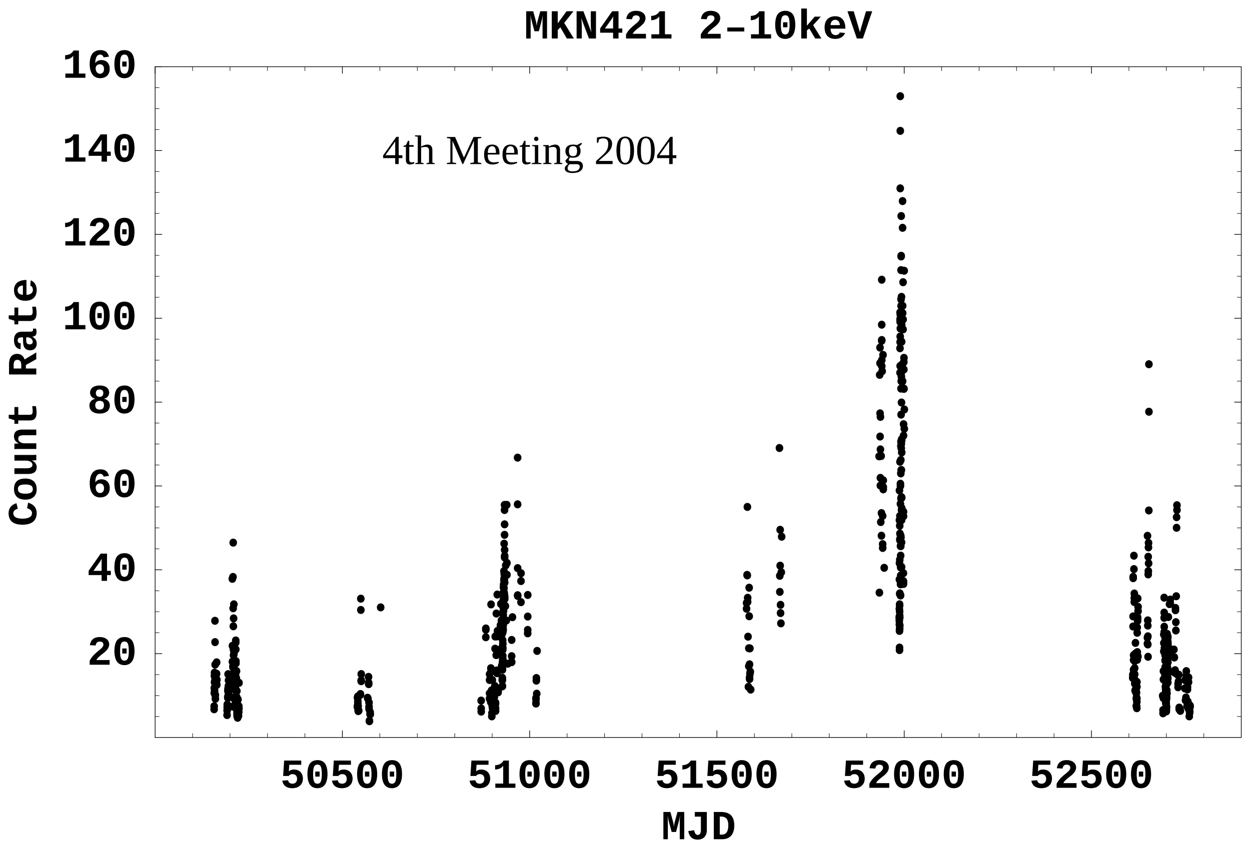

MKN421 1996-2005

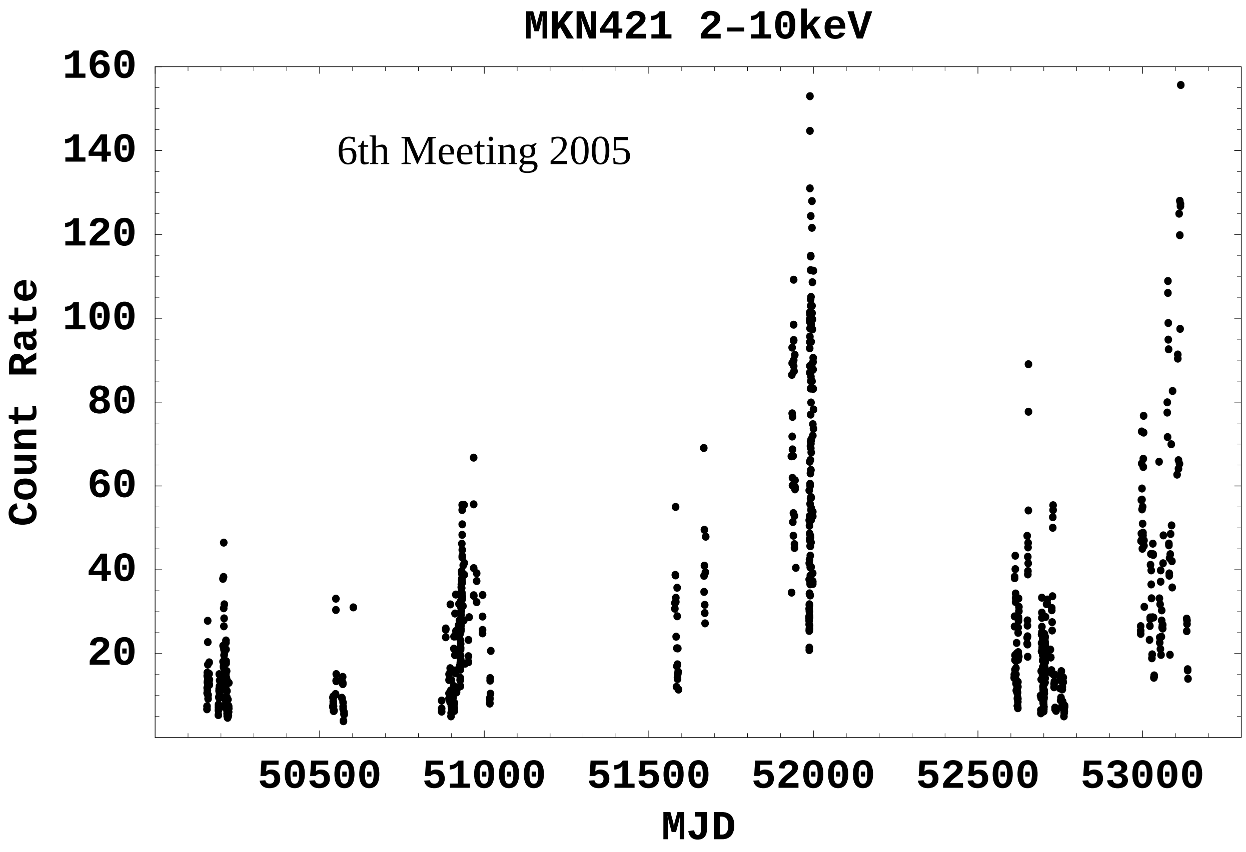

Total observation time: ~1.4Msec

A Short Reminder

Periodogram

$$P(f_j) = \underbrace{\frac{2\Delta t}{N}}_{C} \left| \sum_{i=1}^{N} x_i e^{2\pi f_j t_i} \right|^2 = C \left[\left| \sum_{i=1}^{N} x_i \cos 2\pi f_j t_i \right|^2 + \left| \sum_{i=1}^{N} x_i \sin 2\pi f_j t_i \right|^2 \right]$$

where

$f_j = \frac{j}{N\Delta t}$ and $j = 1, 2, ..., N/2$ ($f_{N/2} \equiv f_{Nyq}$).

The total variance of the observed process

$S^2 = \sum_{j=1}^{N/2} P(f_j) \Delta f$

but also

$S^2 = \frac{1}{N-1} \sum_{j=1}^{N} (x_i - \overline{x})^2$

Artificial Red-Noise LC

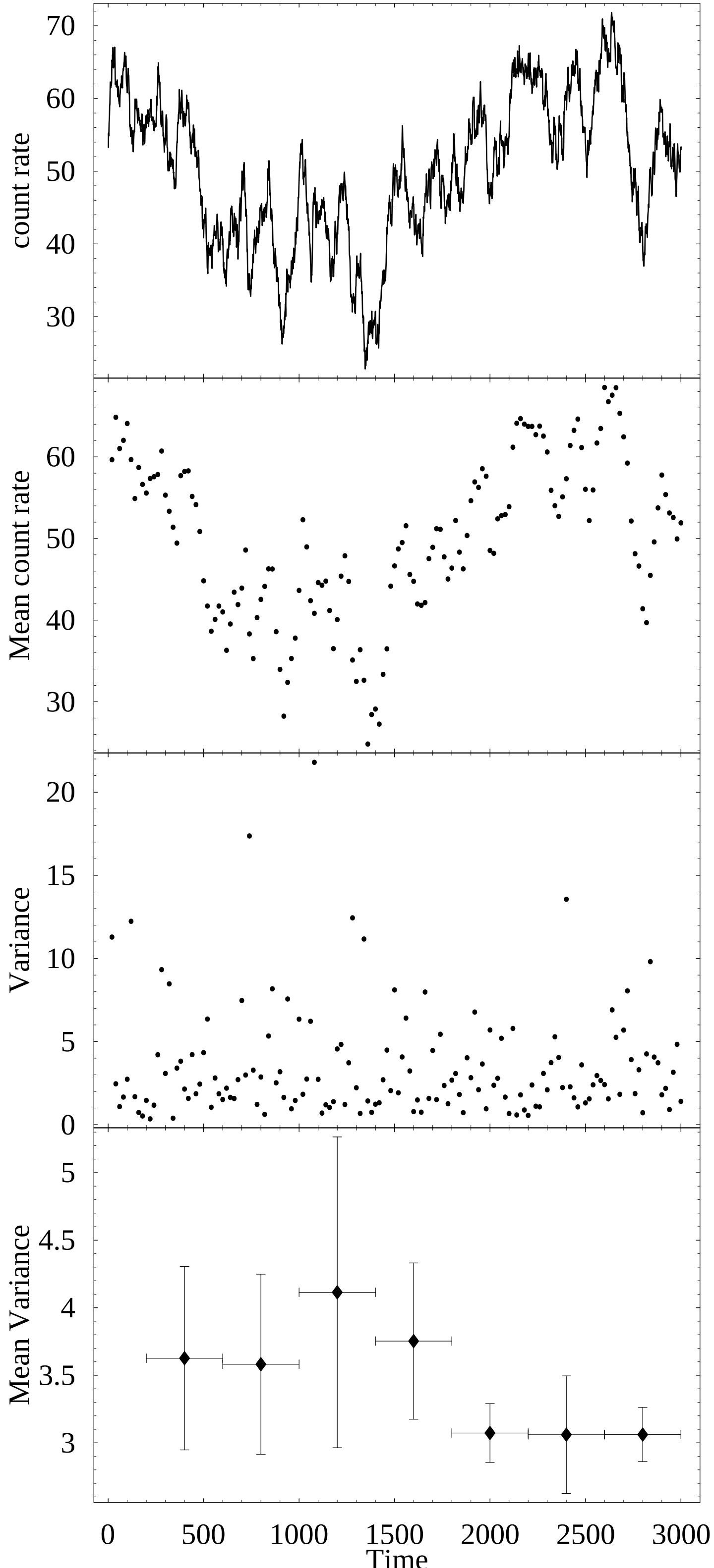

PDS doesn't vary →
Variance doesn't vary →
Stationary process

Mean and Variance change with time, What's wrong?

Fluctuations in the statistical moments are intrinsic in the Red-Noise processes

Timmer&Koenig 1995
Vaughan 2003
Bendat&Pierstol 1986

Excess Variance

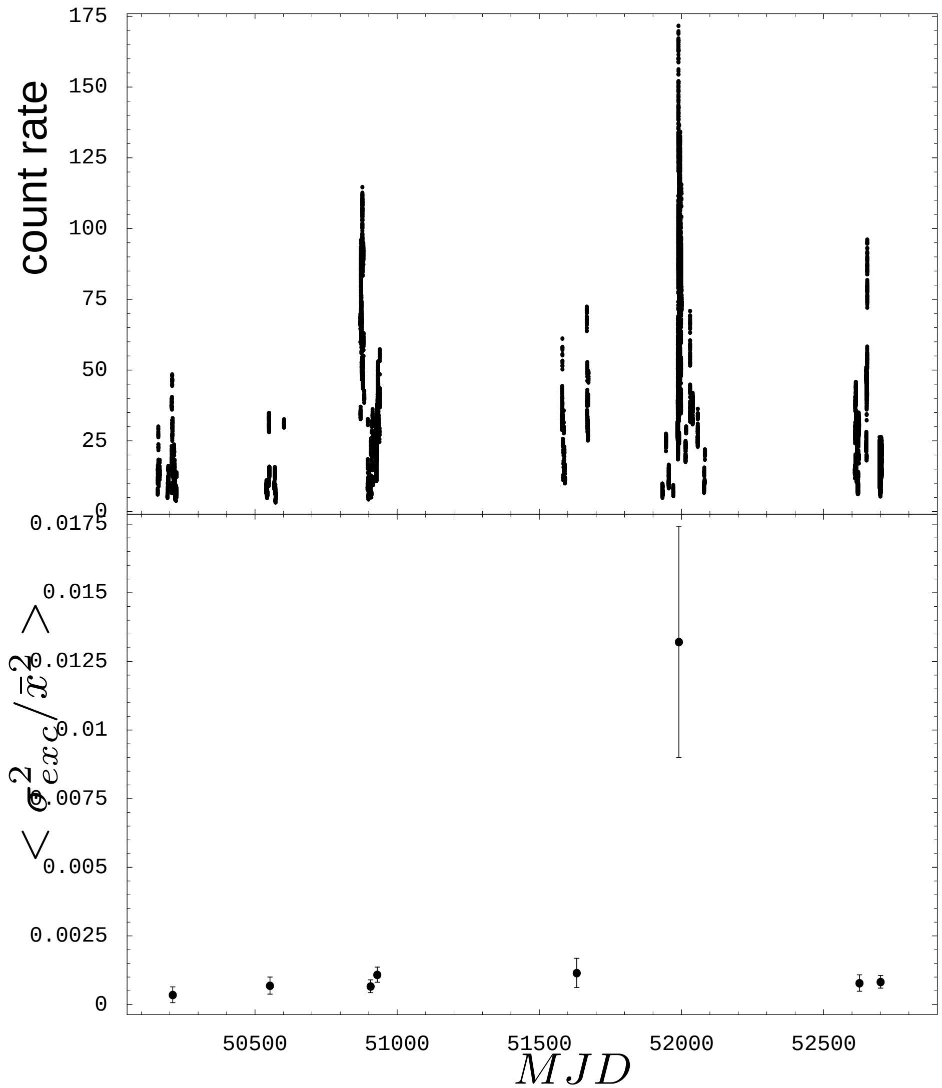

- The source can be characterized by two energetic levels.
- Genuine non-stationarity.
- The lower state occurs more often than the higher one (Higher probability).

Excess Variance

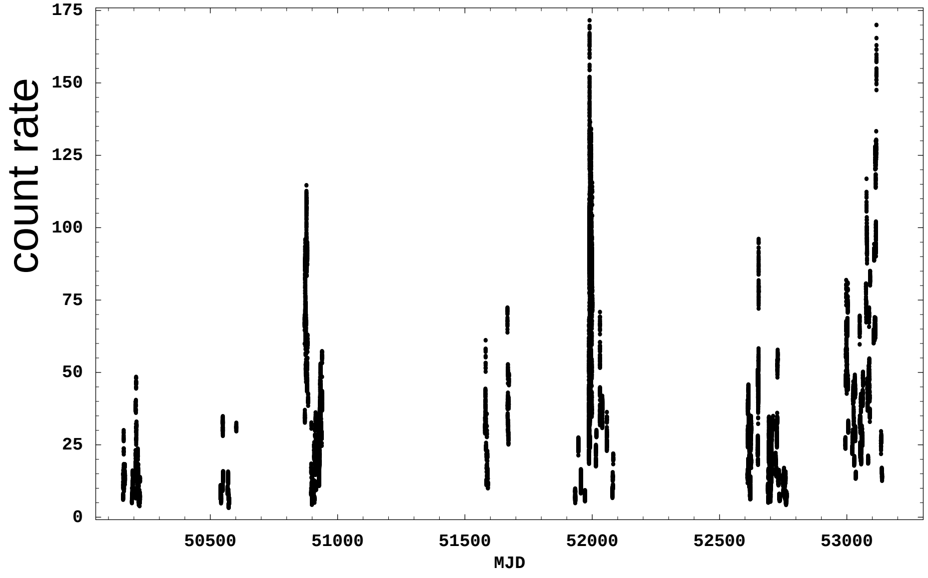

- The source can be characterized by two energetic levels.
- Genuine non-stationarity.
- The lower state occurs more often than the higher one (Higher probability).

Excess Variance

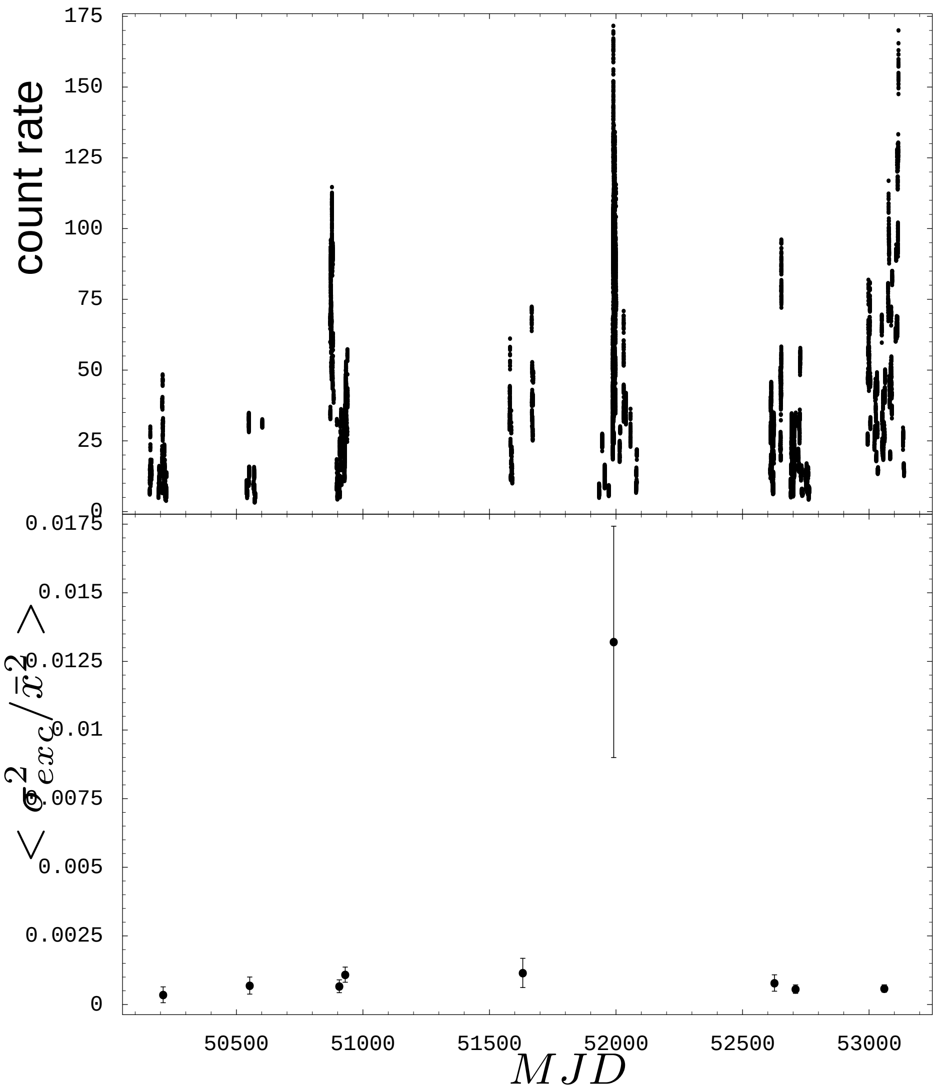

- The source can be characterized by two energetic levels.
- Genuine non-stationarity.
- The lower state occurs more often than the higher one (Higher probability).

Excess Variance

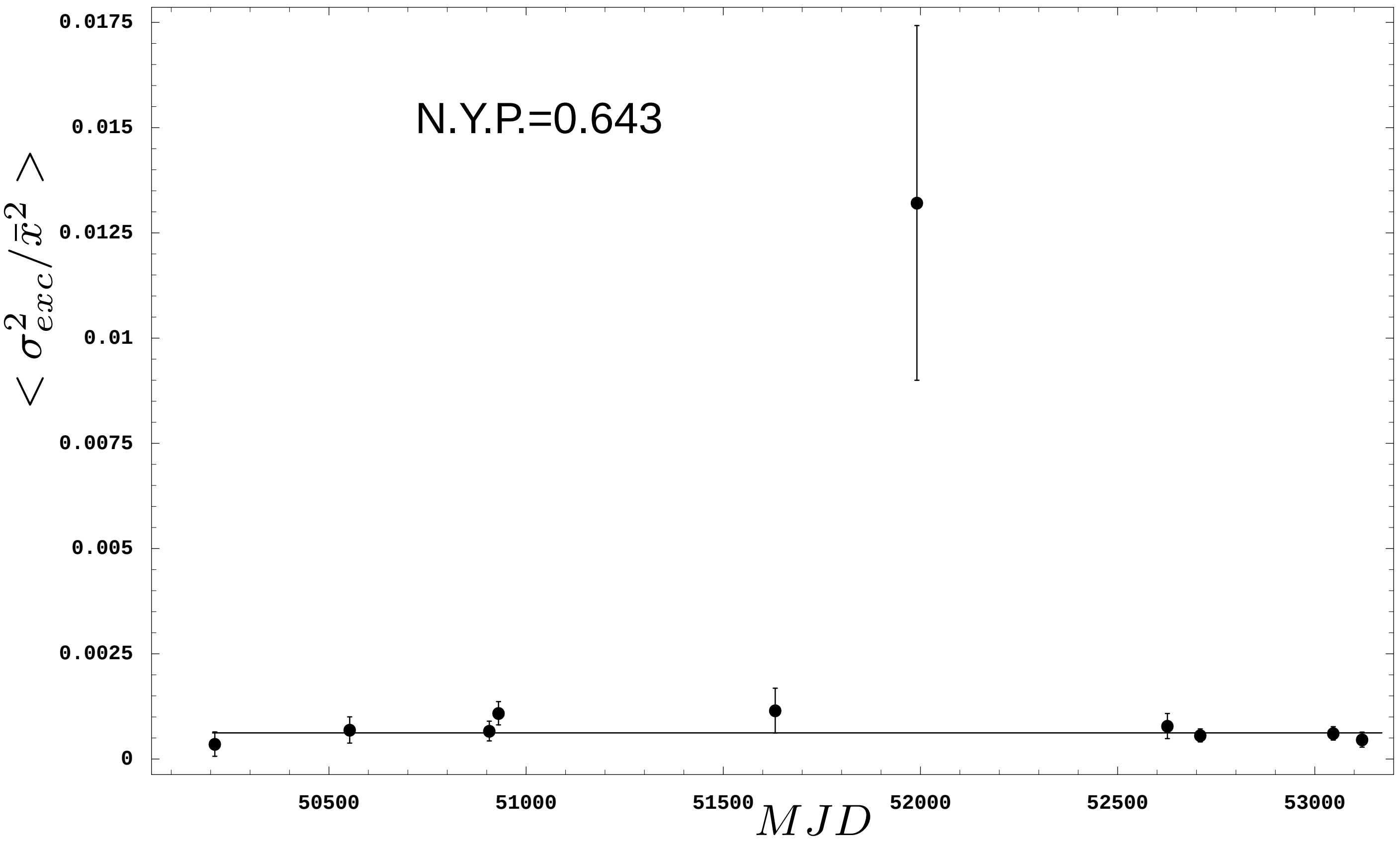

Structure Functions

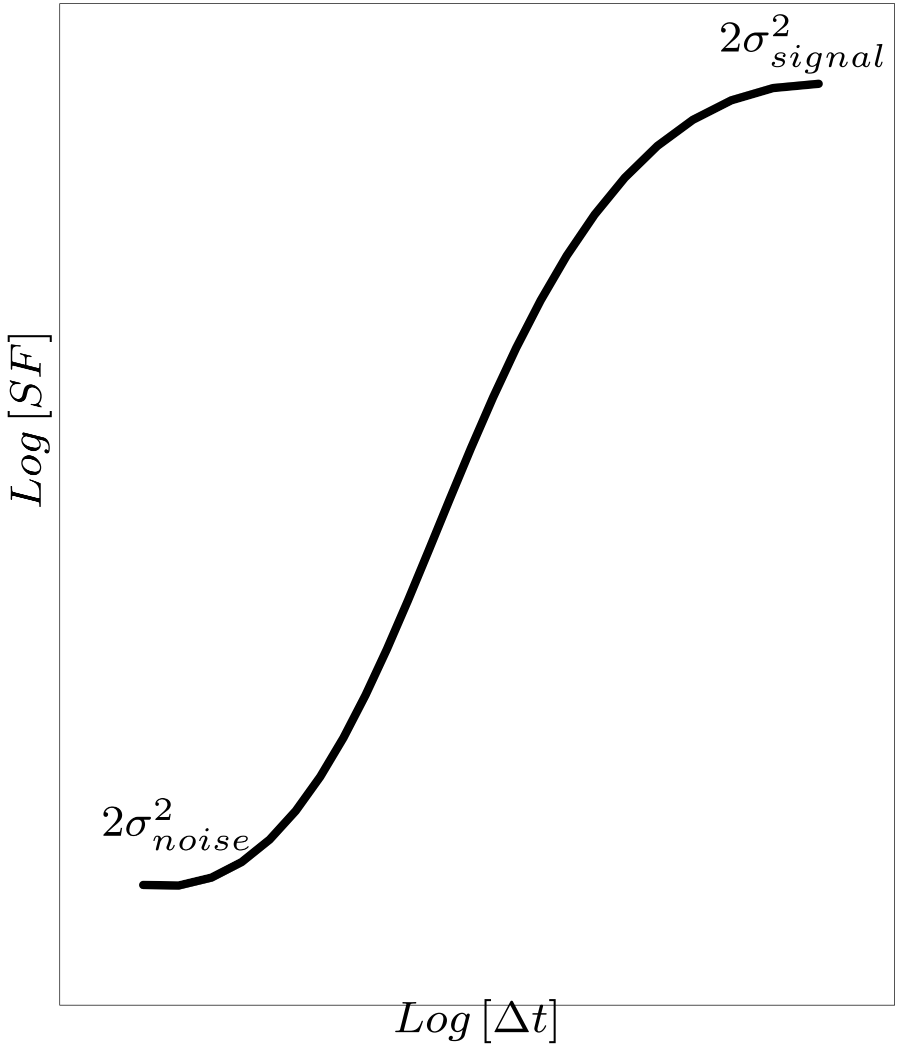

$$S_x(\tau) = \frac{1}{N(\tau)} \sum \left[x(t+\tau) - x(t) \right]^2$$

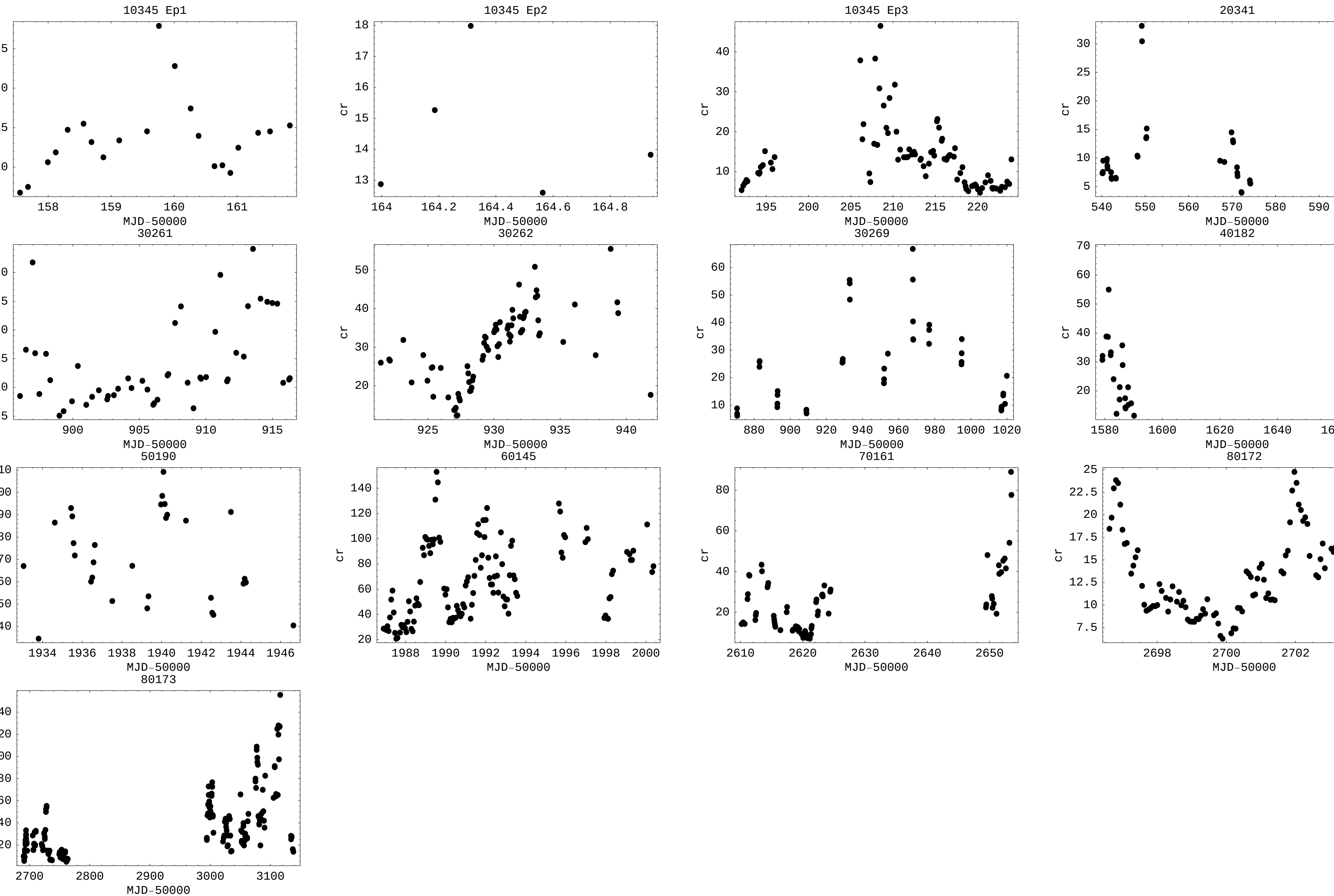
10345 Ep1
10345 Ep2
10345 Ep3
20341
30261
30262
30269
40182
50190
60145
70161
80172
80173
cr
MJD-50000

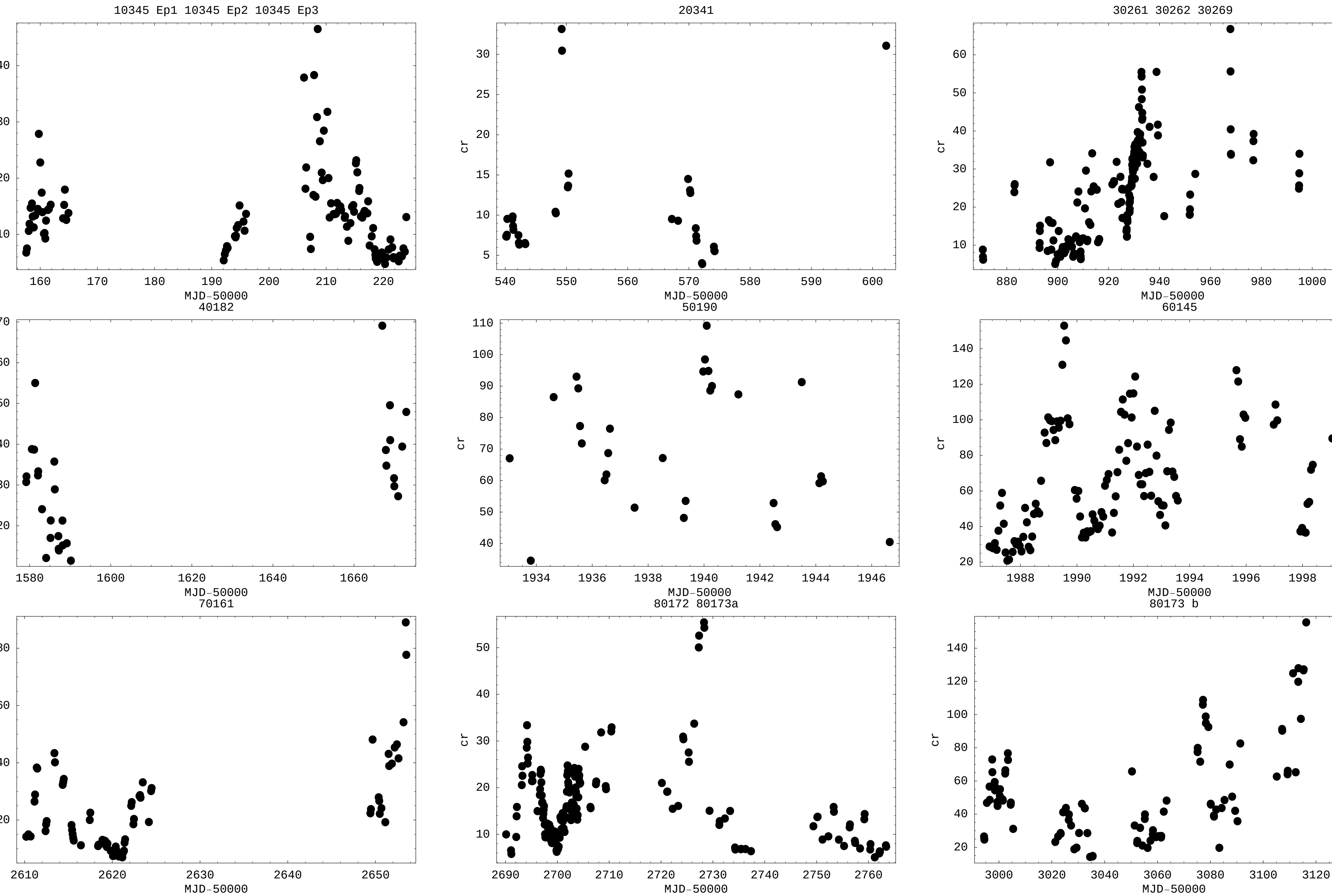
10345 Ep1 10345 Ep2 10345 Ep3
20341
30261 30262 30269
40182
50190
60145
70161
80172 80173a
80173 b
cr
MJD-50000

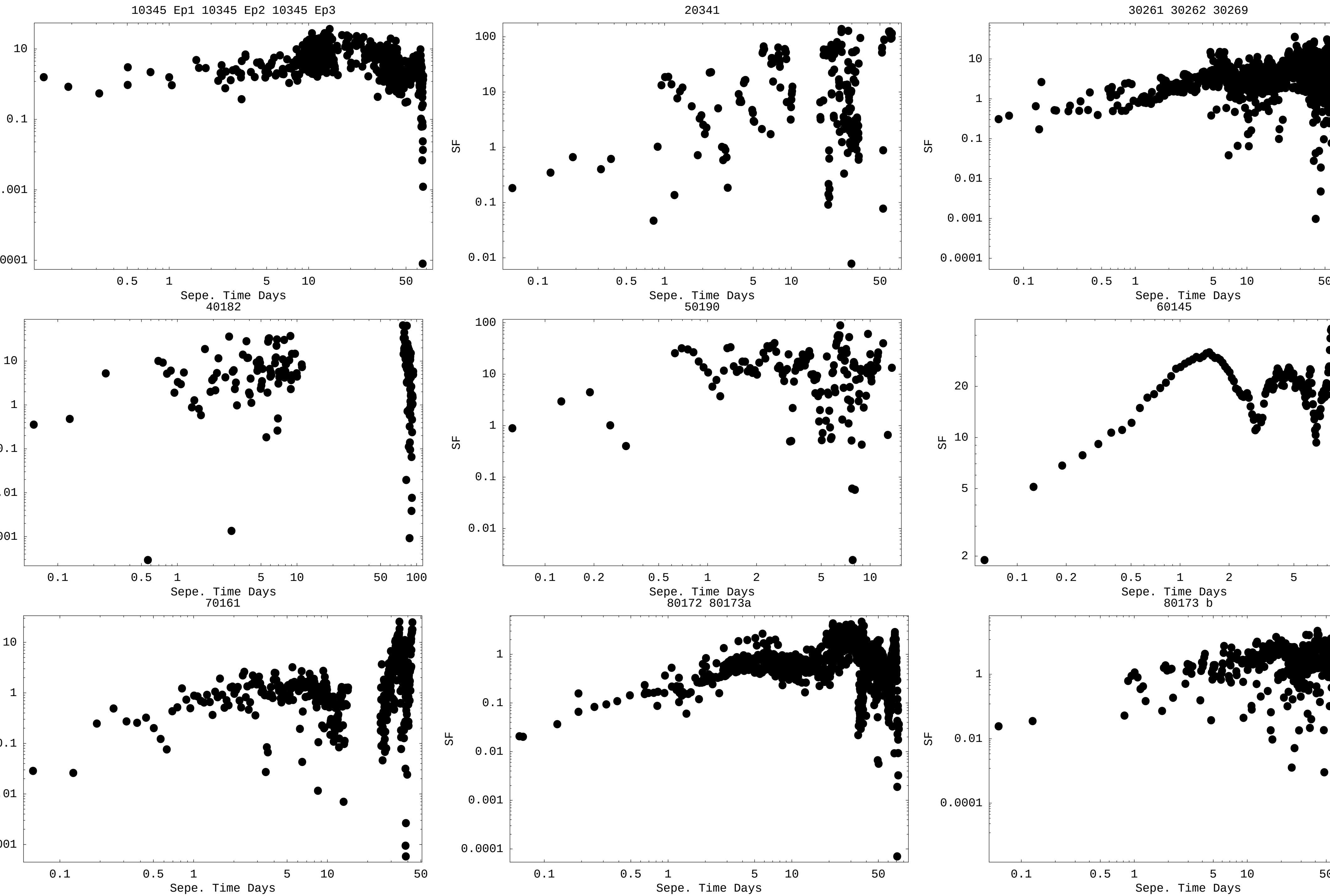
10345 Ep1 10345 Ep2 10345 Ep3
20341
30261 30262 30269
40182
50190
60145
70161
80172 80173a
80173 b
SF
Sepe. Time Days

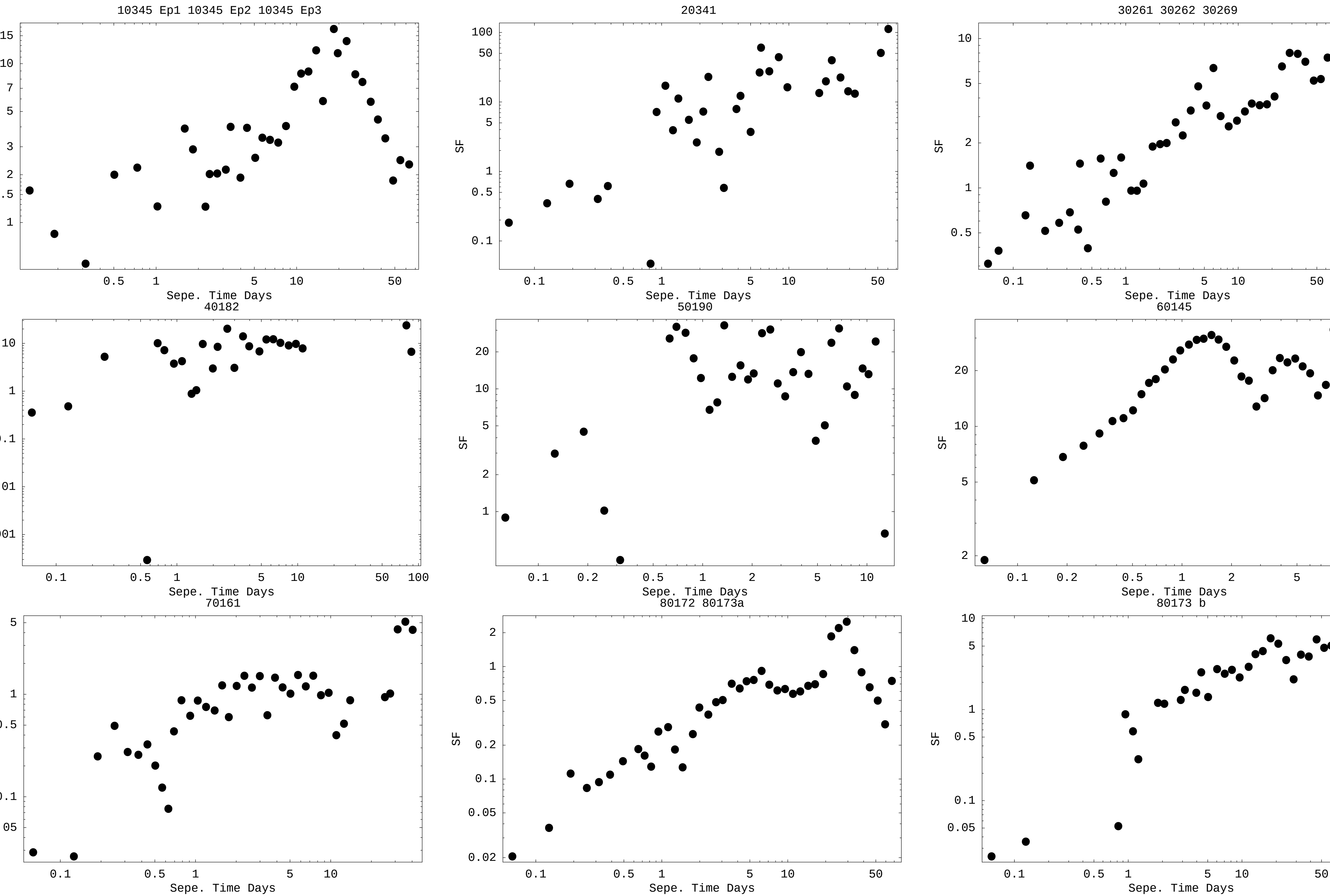
10345 Ep1 10345 Ep2 10345 Ep3
20341
30261 30262 30269
40182
50190
60145
70161
80172 80173a
80173 b
SF
Sepe. Time Days

Rescaled Range method R/S (Mandelbrot 1972)

Assume the time-series set:

$0.2, 0.5, 0.1, 0.7, 0.5, 0.3, 0.6$

Rescaled Range method R/S (Mandelbrot 1972)

Assume the time-series set:

$$\underbrace{0.2, 0.5, 0.1, 0.7, 0.5, 0.3}_{1\times 6}$$

$$\underbrace{0.2, 0.5, 0.1, 0.7, 0.5}_{1\times 5}$$

$$\underbrace{0.2, 0.5, 0.1, 0.7}_{1\times 4}$$

$$\underbrace{0.2, 0.5, 0.1}_{1\times 3}, \underbrace{0.7, 0.5, 0.3}_{1\times 3}$$

$$\underbrace{0.2, 0.5}_{1\times 2}, \underbrace{0.1, 0.7}_{1\times 2}, \underbrace{0.5, 0.3}_{1\times 2}$$

Rescaled Range method R/S (Mandelbrot 1972)

Assume the time-series set:

$$\underbrace{0.2, 0.5, 0.1, 0.7, 0.5, 0.3}_{1\times 6}$$

$$\overline{x_A} = \frac{\sum_{n=1}^{N_A} x_{n,A}}{N_A}$$

$$\underbrace{0.2, 0.5, 0.1, 0.7, 0.5}_{1\times 5}$$

$$d_{N_A,A} = \sum_{n=1}^{N_A} \left(x_{n,A} - \overline{x_A}\right.$$

$$\underbrace{0.2, 0.5, 0.1, 0.7}_{1\times 4}$$

$$R_A = Max\left[d_{N_A,A}\right] - Min\left[d_{N_A,A}\right]$$

$$\underbrace{0.2, 0.5, 0.1}_{1\times 3}, \underbrace{0.7, 0.5, 0.3}_{1\times 3}$$

$$S_A = \sqrt{\frac{\sum_{n=1}^{N_A}\left(x_{n,A} - \overline{x_A}\right)^2}{N-1}}$$

$$\underbrace{0.2, 0.5}_{1\times 2}, \underbrace{0.1, 0.7}_{1\times 2}, \underbrace{0.5, 0.3}_{1\times 2}$$

$$\left(\frac{R}{S}\right)_N = \frac{\sum_{A=1}^{\lfloor 6/N \rfloor}\left(\frac{R_A}{S_A}\right)}{\lfloor 6/N \rfloor}$$

Rescaled Range method R/S

$$\frac{R}{S} = cN^{H}$$

We want to specify the "Hurst Exponent" H

The probability of our data set to continue the same "course" as time goes on.

Rescaled Range method R/S

$$\frac{R}{S} = cN^{H}$$

We want to specify the "Hurst Exponent" H

The probability of our data set to continue the same "course" as time goes on.

- $0.5 < H < 1$: long-term memory (persistent time-series)
- $H = 0.5$: independant process
- $0 < H < 0.5$: anti-persistent time-series

R/S

Red Noise

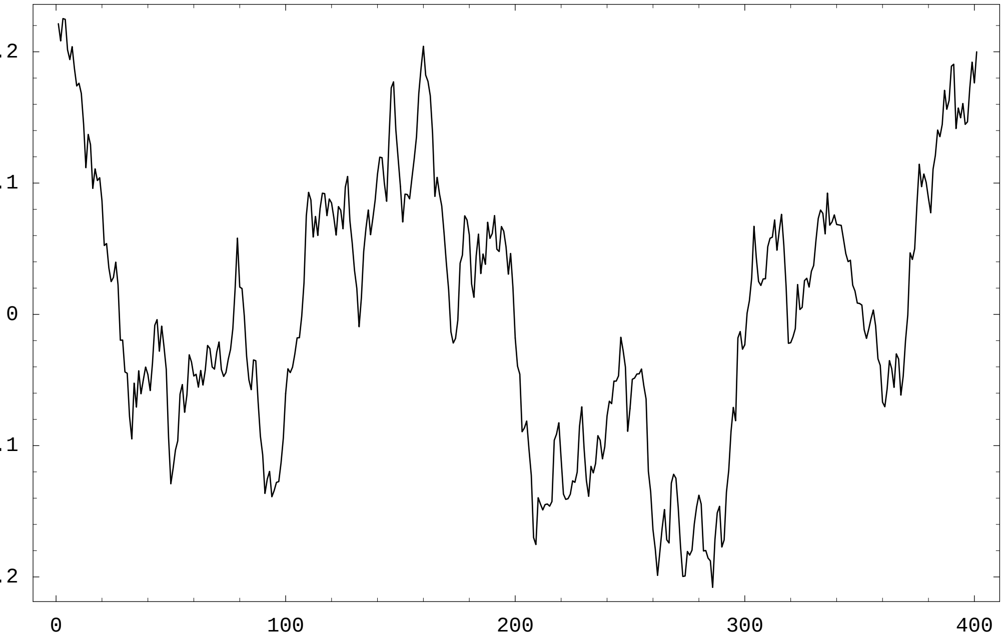

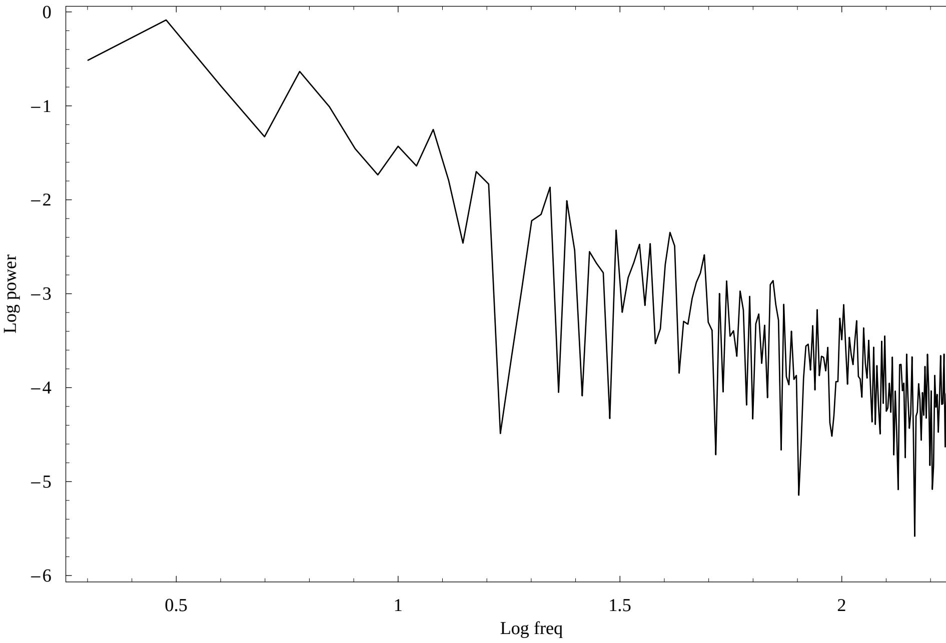

R/S

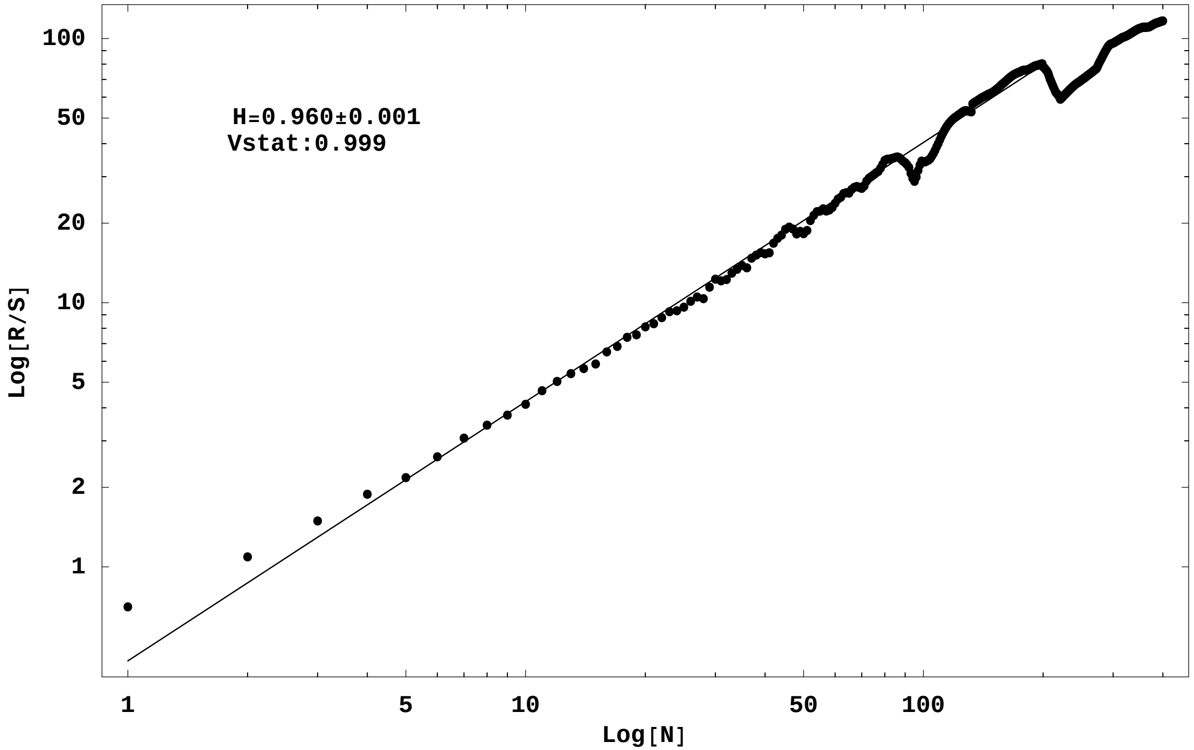

V statistics

$V_N = \frac{(R/S)_N}{\sqrt{N}}$ and $u = \langle V_N \rangle$

$F(u) = 1 + 2\sum_{k=1}^{\infty}(1 - 4k^2u^2)e^{-2(ku)^2}$

R/S

The SF

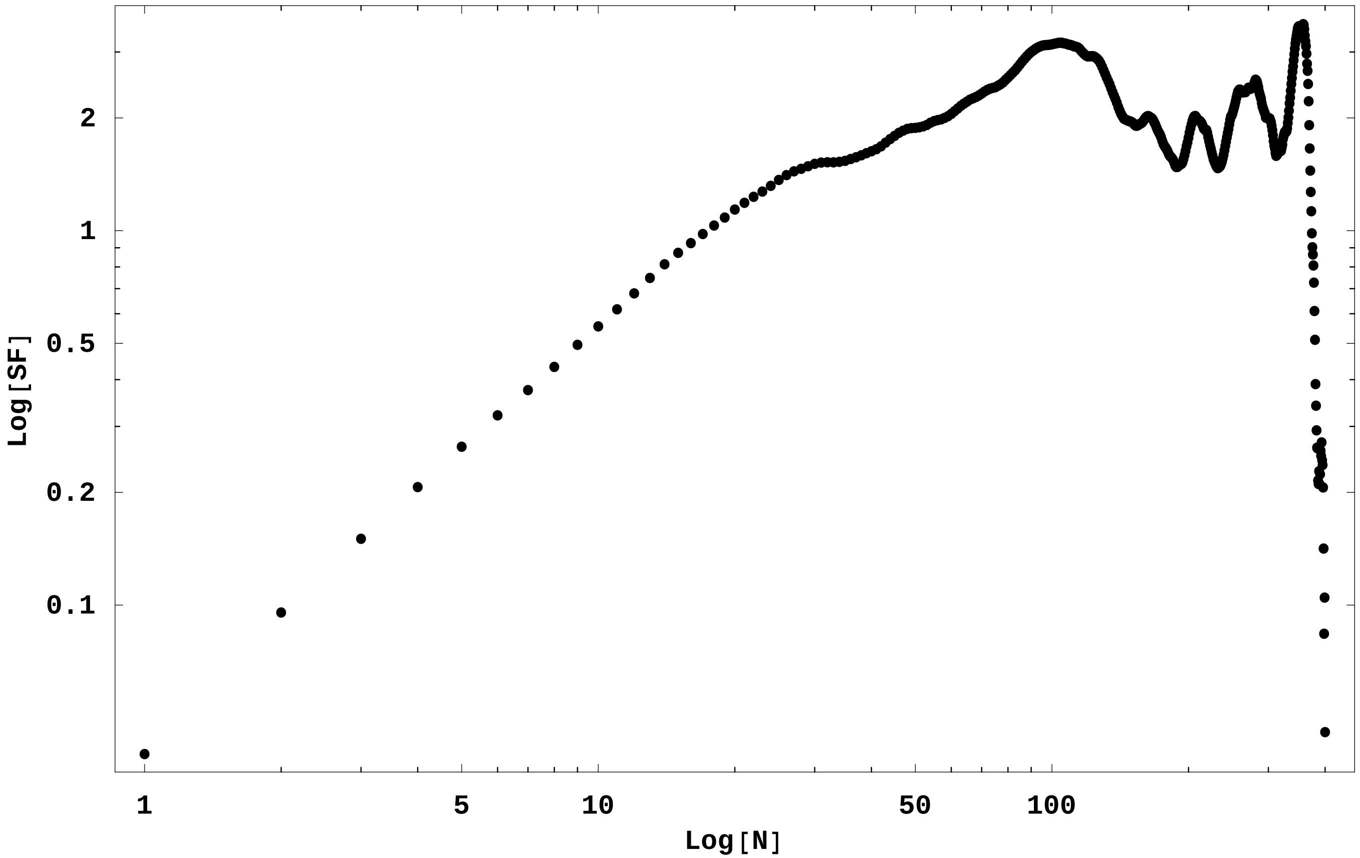

R/S for MKN421

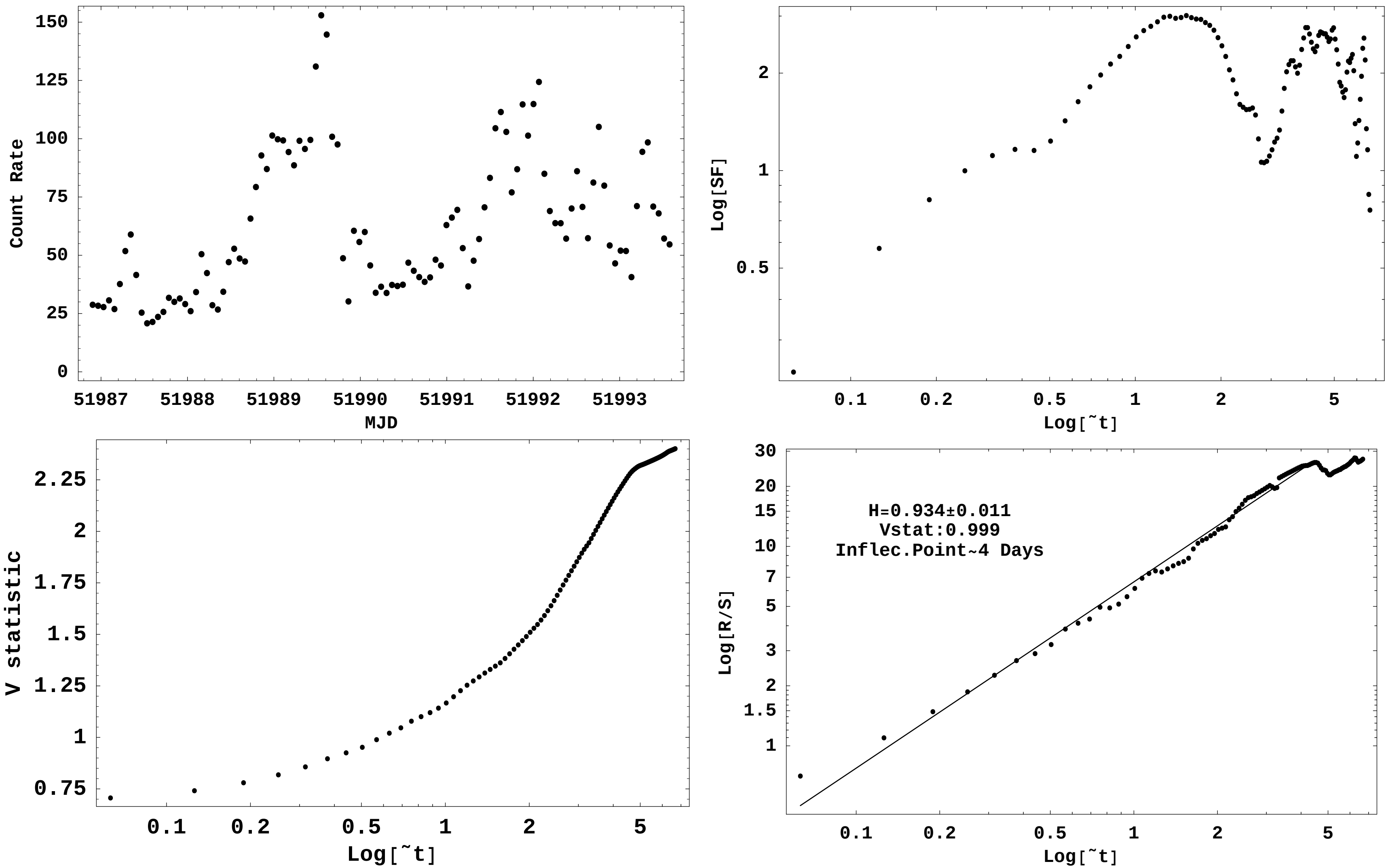

R/S for MKN421

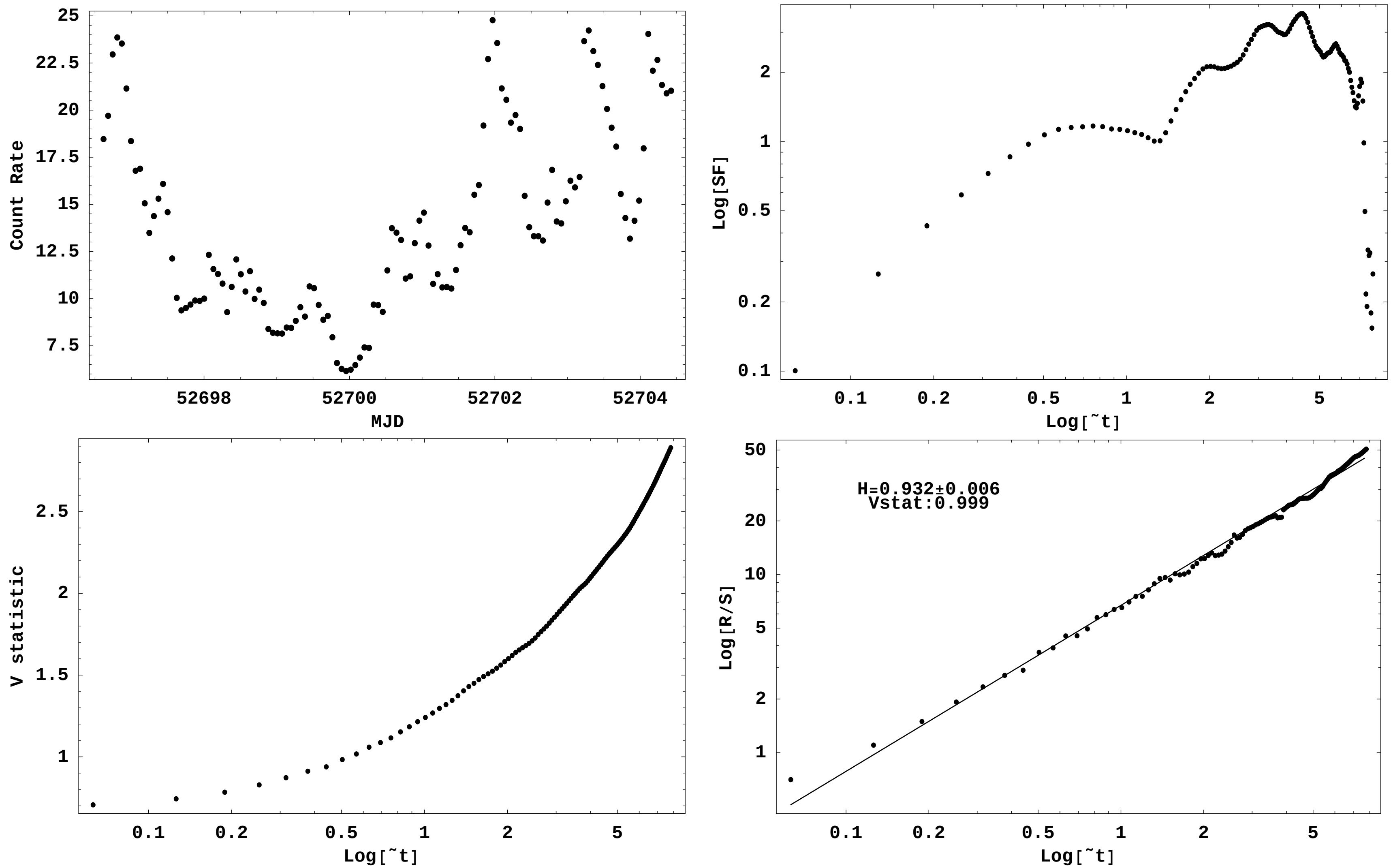

Conclusions for the R/S

- The measurements in the bins are normally distributed $\rightarrow$ we can apply Linear regression to specify H.
- Based on V-statistics we can have a robust estimate about the nature of the variations.
- We don't have "wiggling" patterns and "fake" breaks that can indicate a FALSE time scale.
- We have to use higher statistical moments to extract the complete information for our system (i.e. Principal Component Analysis, Generalized Dimensions)

Conclusions for the R/S

- The measurements in the bins are normally distributed $\rightarrow$ we can apply Linear regression to specify H.
- Based on V-statistics we can have a robust estimate about the nature of the variations.
- We don't have "wiggling" patterns and "fake" breaks that can indicate a FALSE time scale.
- We have to use higher statistical moments to extract the complete information for our system (i.e. Principal Component Analysis, Generalized Dimensions)

Conclusions for the R/S

- The measurements in the bins are normally distributed $\rightarrow$ we can apply Linear regression to specify H.
- Based on V-statistics we can have a robust estimate about the nature of the variations.
- We don't have "wiggling" patterns and "fake" breaks that can indicate a FALSE time scale.
- We have to use higher statistical moments to extract the complete information for our system (i.e. Principal Component Analysis, Generalized Dimensions)

Stefano Ciprini

Tuorla Astronomical Observatory

University of Turku - Piikkiö, FINLAND

(EC Young Researcher Training Network ENIGMA)

OJ 287, PKS 2155-304, PKS 0735+178: Multifrequency Campaigns and Variability Monitoring

(Tasks: 1-2-3-4)

6th ENIGMA Meeting

November 22-25, 2005 – Kinsale, Cork, IRELAND

Talk Outline

- OJ 287: first results on the XMM multifrequency campaign of spring 2005
- *Interlude 1*
- PKS 2155-304: optical monitoring during the HESS multifrequency campaign of summer-autumn 2004
- *Interlude 2*
- PKS 0735+178: final issues by the long-term optical monitoring
- *Interlude 3*

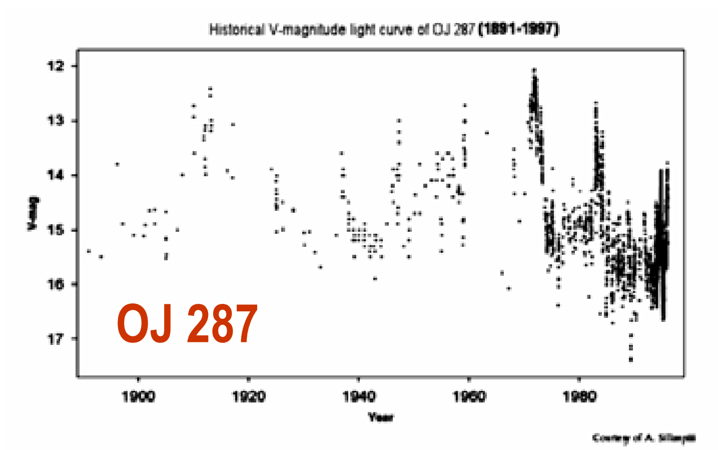

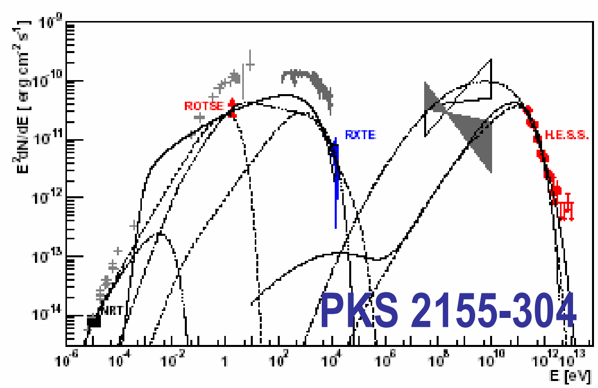

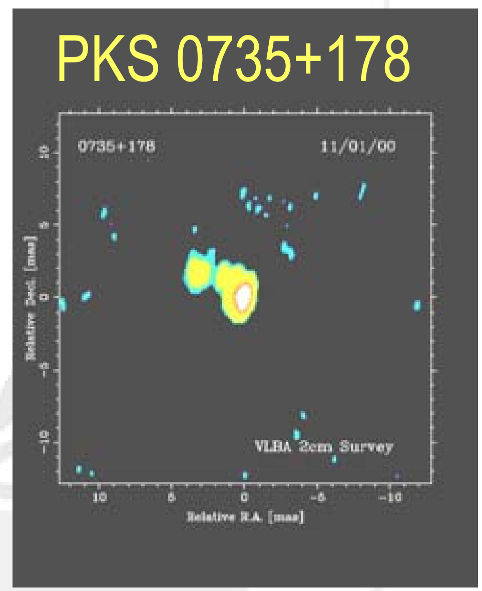

Part 1:
OJ 287

First Results on the XMM-Newton Multifrequency Campaign of Spring 2005

OJ 287 Long-term Campaign

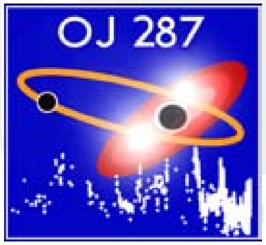

OJ 287: 2005-2008 long-term project (ENIGMA Campaign)

Motivation: OJ 287 is the only extragalactic source showing a convincing evidence of a major periodical component in the historical optical light curve, with outbursts occurring every 11-12 years (the last was monitored by the OJ94 project, period 1993-1997). The next outburst is expected to occur in the period 2005-2007. The origin of periodicity is unknown but likely is to hold important clues to blazar variability in general.

OJ 287 2005-2008 Project and Enigma Campaign web-page:

http://www.astro.utu.fi/OJ287MMVI/ *

OJ 287 is declared as a key object and one of the main research topic of the Network (see Task 4 of the Enigma science-rationale). This blazar was also chosen as target of the collaborative activities by Young Researchers (YRs).

OJ 287 Enigma-YRs Wiki web-page:

http://www.lsw.uni-heidelberg.de/projects/enigma_young/wiki/

* MMVI = 2006

OJ 287: ENIGMA Observations

- **Long-term monitoring** (OJ 287 2005-2008 Project and ENIGMA Campaign) begun in late 2004 (PM/CM: L. Takalo, A. Sillanpää).
- **VLBA** radio structure/polarization observations in 5 bands: 6 times, 8h for the period 2005-2006 (more obs. planned in 2007-08) (PI: T. Savolainen).
- **VLBA** and **Global 3mm-VLBI** radio-mm structure/polarization observations (as a calibrator, April 4 and 17, 2005, PI: I. Agudo).
- **ESO VLT** spectroscopic optical observations (4 epochs, PI: K. Nilsson).
- **XMM-Newton** X-ray observations: 2 pointings of about 40 ksec each in cycle AO-4 (April 12, and November 3-4, 2005, PI: S. Ciprini).
- **WEBT-ENIGMA** intensive campaign around the 2 XMM pointing dates (CM: S. Ciprini)
- ToO **Effelsberg 100m** radiotelescope flux/polarization observations on April 12 and Nov. 8-9-10 (ToO PI: L. Fuhrmann)
- 4 sessions of **Global 3mm-VLBI** observations in period Oct.2005-Apr.2007 (PI: E. Rastorgueva, K. Wiik).
- **MAGIC** Cherenkov telescope observations in January (10h) and November 2005 (>5h, this last in ToO mode, PI: E .Lindfors)
- Optical polarization monitoring at **NOT** (PI: K.Nilsson) and **CalarAlto** (2006-2008, PI: J. Heidt)
- *Other (non-Enigma teams) obs.: RXTE; SWIFT? (Giommi et al.); INTEGRAL? (Pian et al.); SPITZER? (Marscher et al.), …*

OJ 287: XMM-Newton Obs. & Coordinated Campaigns

OJ 287 observed by XMM-Newton twice (April 12, and November 3-4, 2005).

WEBT consortium radio-optical and coordinated campaign in April 2005 and October-November 2005 (part 1-2).

ENIGMA long-term monitoring and participation also to the intensive and short-term campaign.

Goals of the XMM-Newton Obs. & Coord. Campaign

- ❑ Spectral-temporal behaviour of OJ 287 on both short-long time scales and in different brightness states (before and during the outburst).
- ❑ X-ray data likely provide information on the high-energy (IC) spectral component, while radio-to-optical observations map the behaviour of the synchrotron component.
- ❑ Possibly clarify underlying physics, relevance of geometrical and energetic models.
- ❑ Search for multifrequency correlations.

Visibility of OJ 287 by XMM in 2005:

Source name	Other names	Redshift	EGRET detection	X-rays past observations	X-rays integral flux [erg cm^{-2} s^{-1}]	XMM AO-4 source visibility periods	Optical visibility window†
OJ 287	PKS 0851+202 PG 0851+202	$z = 0.306$	YES	Einstein,EXOSAT,ROSAT ASCA,*BeppoSAX*	$1.35\text{-}5.0 \times 10^{-12}$ (2-10 keV) (ASCA, SAX)	2005.Apr.12 - 2005.May.05 2005.Oct.16 - 2005.Nov.18	Oct-May

† Calculated for the mean latitude of the WEBT and ENIGMA collaboration telescopes.

The 2 XMM pointings performed in 2005:

April 12, 2005

Target_Name	RA	Dec	Position_Angle	
OJ 287	08:54:48.87	+20:06:30.6	285:05:17.8	
XMM Obs_Duration	XMM Obs: **Start Time**	XMM Obs: **End Time**	Satellite Revolution	IB
40000 sec	2005-04-12 at 12:55 UT	2005-04-13 at 00:03 UT	0978	E3

November 3-4, 2005

Target - PI	RA	Dec	Position_Angle	
OJ 287 - S. Ciprini	08:54:48.87	+20:06:30.6	104:13:22.6	
XMM Obs_Duration	XMM Obs: **Start Time**	XMM Obs: **End Time**	Satellite Revolution	IB
51000 sec	2005-11-03 at 20:59 UT	2005-11-04 at 11:09 UT	1081	E3

XMM-Newton Space Observatory

XMM-Newton has three mirror modules:

- Instruments behind:
  1) RGS-1 and MOS-1
  2) RGS-2 and MOS-2
  3) pn

- EPIC:
  MOS1, MOS2 and pn
- RGS:
  RGS-1, RGS2
- OM: Optical Monitor

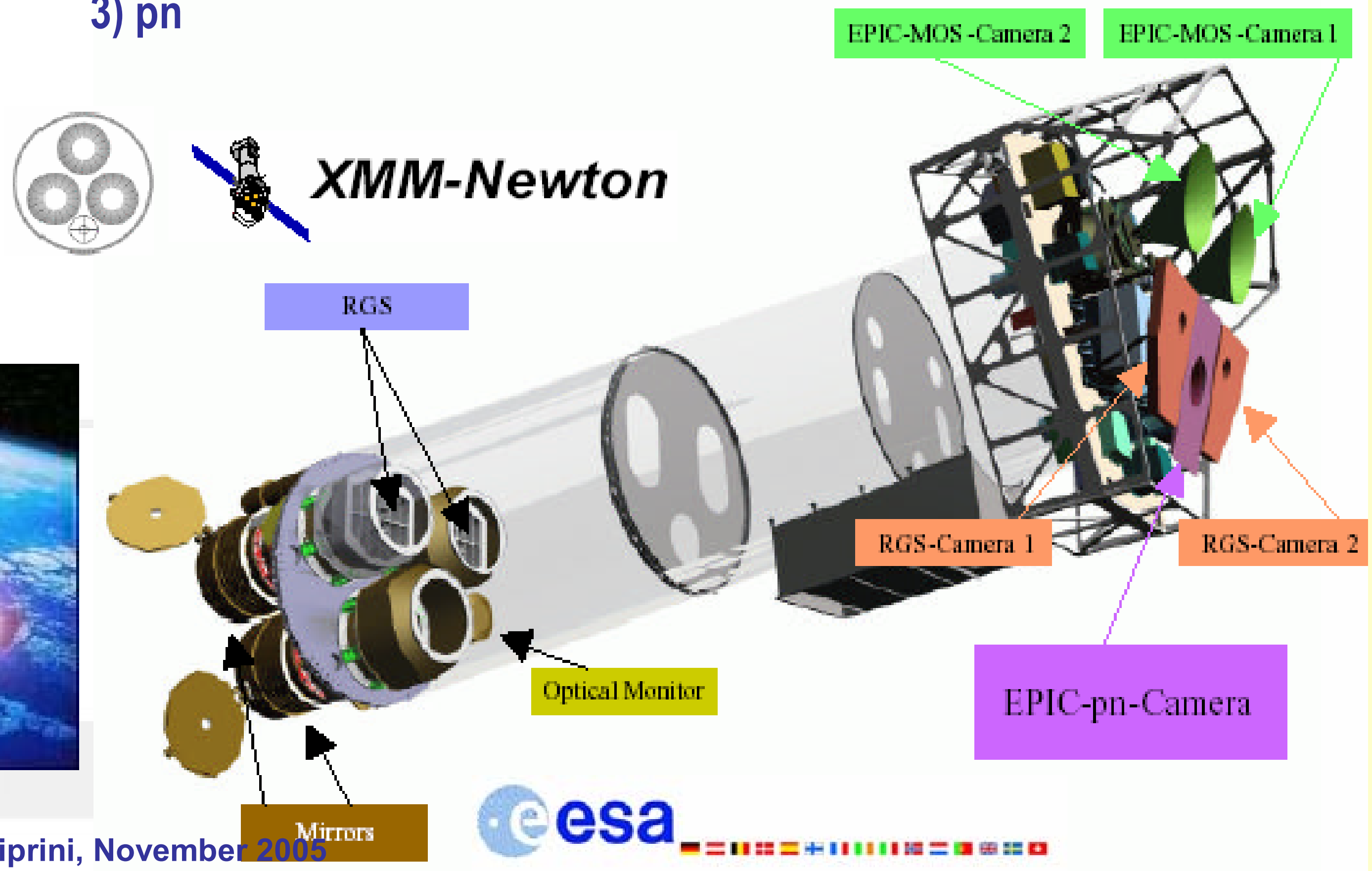

XMM-Newton: OJ 287 First Observation of April 12, 2005

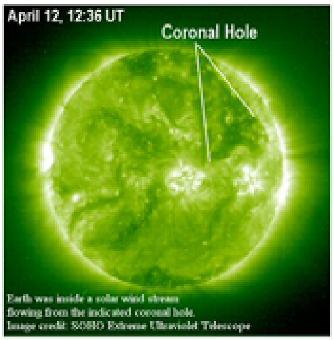

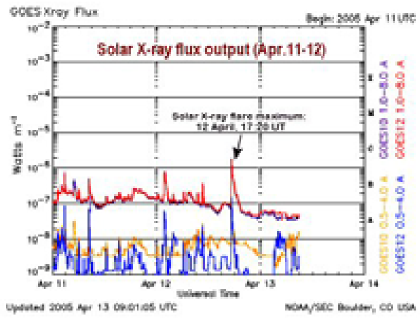

Observation heavily affected by high background radiation (caused by solar wind and earth proton belt) and stopped. Original 40 ksec granted (with overheads) only about 11 ksec performed and only about 5 ksec useful for science analysis.

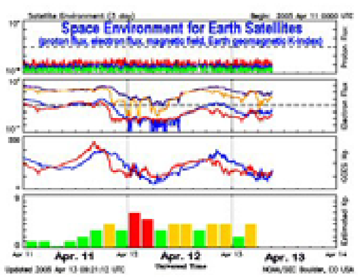

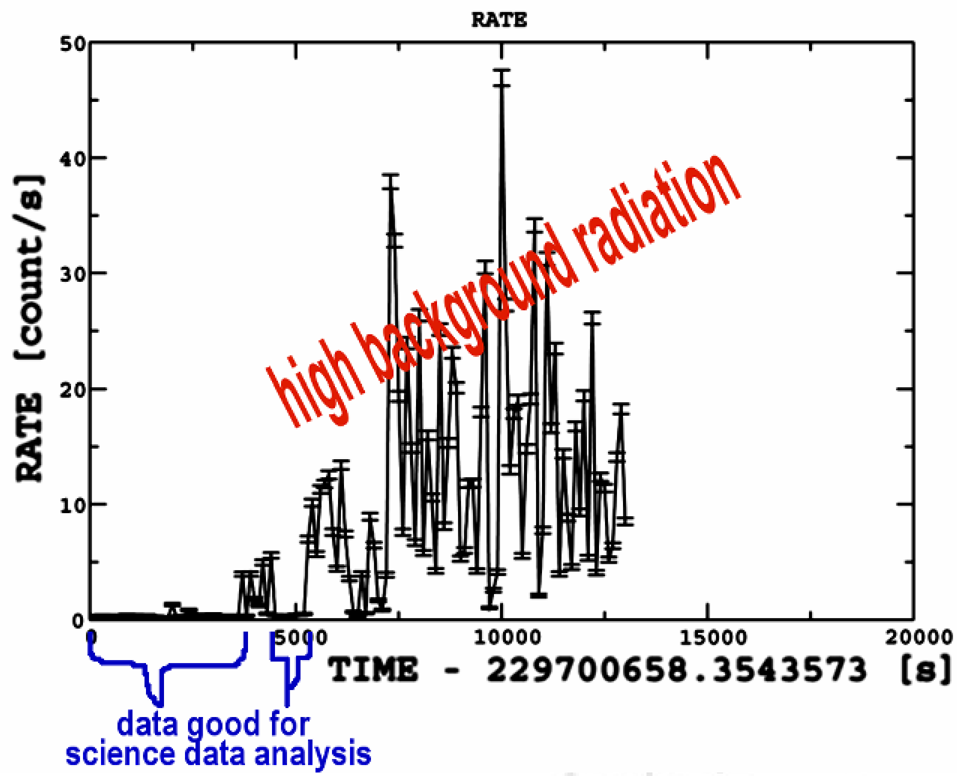

Data screening: screen out bad data; only time windows no affected by high background radiation are useful to science analysis (images and spectra extractions, time series, etc.) (unfortunately < 5 ksec).

No RGS detection, EPIC & OM ok.

A Preliminary EPIC pn Spectrum

Date: April 12, 2005

OJ 287, z=0.306, about 4 ksec data - Preliminary XMM-Newton *EPIC pn* spectrum

Model: single power law + absorption (galactic) in the 0.3-10 KeV range

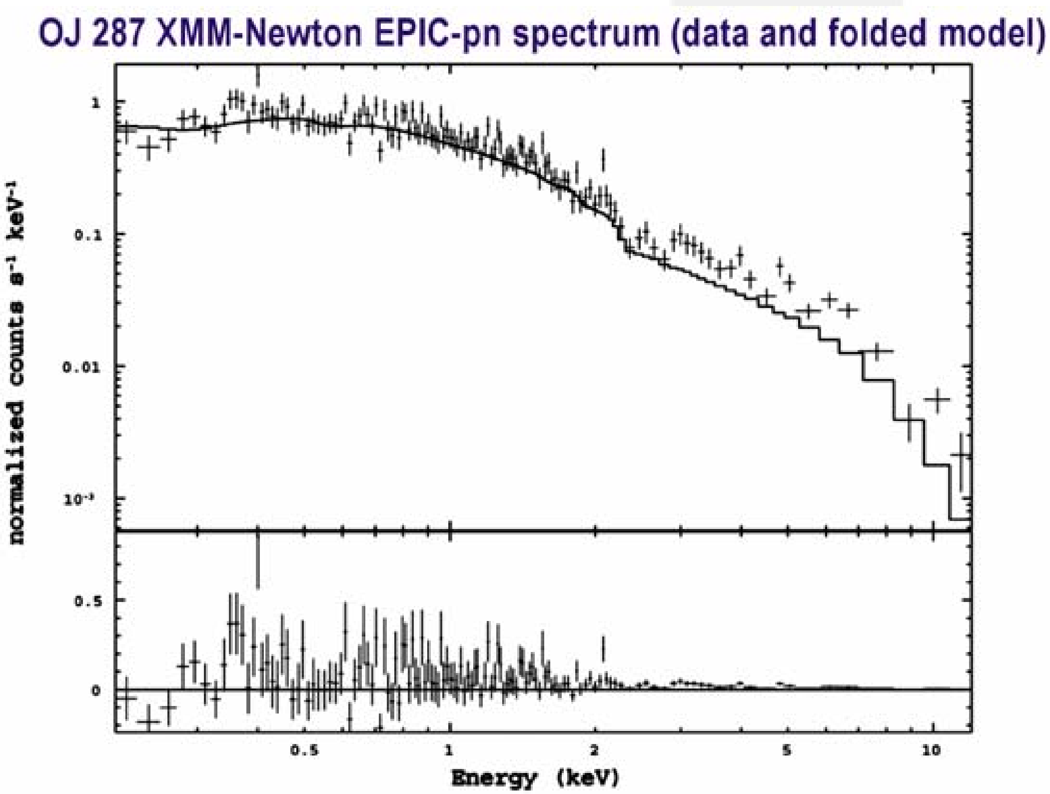

XSPEC fit:

$N_H = 2.53 \times 10^{20}\ cm^{-2}$

$\Gamma = 1.734 \pm 0.010$

$\chi_r^2 = 0.5$, d.o.f.=2359

Other X-ray Sources in the Field of OJ 287

Large frame (no full) used. Some other serendipitous sources detected by the EPIC-pn and EPIC-MOS detectors: identification and cross-check in progress. Anyway low count rates, hence no great science possible.

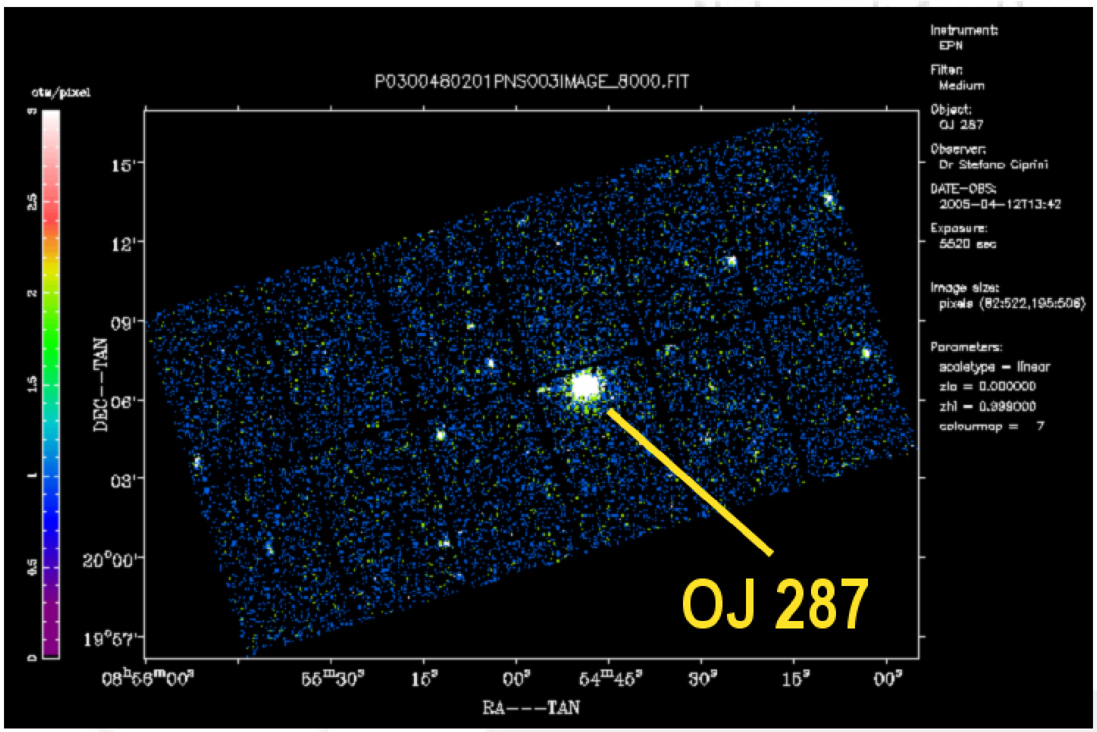

ra	dec	candidates
08h54m00.25s	+20d02'53.2"	
08h54m00.41s	+20d13'48.2"	SAO 80493 . 08 54 00.50 +20 13 49.4 star F5/6 V.
08h54m00.52s	+20d13'48.6"	
08h54m00.57s	+20d13'49.0"	
08h54m03.28s	+20d07'44.3"	2003ApJ. 582 1011S Luyten cat. P 426-29 - 08 54 01.96 +20 07 00.6, High proper-motion Star
08h54m03.30s	+20d07'45.8"	2MASX J08540282+2007500 – 08h54m02.8s +20d07m50s Galaxy
08h54m03.30s	+20d07'46.6"	
08h54m03.36s	+20d07'47.2"	
08h54m06.92s	+20d03'31.7"	
08h54m08.04s	+20d02'59.5"	
08h54m08.23s	+20d03'00.9"	1WGA J0854.1+2003 - 08h54m08.7s +20d03m13s XraySource
08h54m09.40s	+20d13'36.7"	
08h54m09.57s	+20d13'38.9"	
08h54m09.58s	+20d13'38.8"	
08h54m09.66s	+20d13'38.4"	
08h54m10.23s	+19d59'02.2"	
08h54m13.94s	+20d03'54.0"	2003MNRAS.346.1125G obj: 184 . 08h54m13.9s +20d03m48s galaxy (bulge, + tail?)
08h54m21.23s	+20d03'56.3"	MDS usp00-10 - 08h54m18.7s +20d03m51s Galaxy z=0.457300
08h54m24.88s	+20d11'20.1"	IC 2422 08h54m24.3s +20d13m29s G
08h54m24.90s	+20d11'19.0"	
08h54m24.93s	+20d11'19.6"	
08h54m24.93s	+20d11'20.0"	
08h54m25.47s	+20d05'46.3"	
08h54m28.46s	+20d06'30.7"	
08h54m28.89s	+20d04'29.4"	
08h54m29.26s	+20d04'31.9"	
08h54m29.26s	+20d04'31.9"	
08h54m29.98s	+20d10'44.5"	NVSS J085432+201256 08h54m32.6s +20d12m56s RadioS
08h54m35.06s	+20d03'06.8"	
08h54m35.19s	+20d07'58.9"	
08h54m35.25s	+20d14'26.0"	
08h54m35.25s	+20d14'28.6"	
08h54m35.29s	+20d08'01.0"	
08h54m35.52s	+20d14'26.2"	
08h54m37.95s	+20d16'48.5"	
08h54m39.53s	+20d18'15.8"	
08h54m46.62s	+20d10'36.7"	IC 2423 - 08h54m47.1s +20d13m13s Galaxy
08h54m48.74s	+20d02'44.3"	
08h54m48.90s	+20d06'30.2"	OJ 287
08h54m48.90s	+20d06'31.5"	OJ 287
08h54m48.90s	+20d06'31.5"	OJ 287
08h54m48.91s	+20d06'31.1"	OJ 287
08h54m48.91s	+20d06'31.9"	OJ 287
08h54m48.95s	+20d06'32.0"	OJ 287
08h54m48.96s	+20d06'31.5"	OJ 287 — IRAS counterpart 1987A&AS...70...95D
08h54m55.73s	+20d06'22.7"	OJ 287
08h54m55.92s	+20d06'17.2"	OJ 287
08h54m55.94s	+20d06'20.1"	OJ 287
08h54m58.85s	+20d12'47.0"	
08h55m03.84s	+19d56'22.5"	
08h55m03.95s	+20d07'22.2"	
08h55m04.00s	+19d55'24.8"	1WGA J0855.0+1955 08h55m04.0s +19d55m29s XrayS
08h55m04.10s	+20d07'23.7"	
08h55m08.98s	+19d59'19.3"	
08h55m09.25s	+19d59'18.5"	NVSS J085510+200050 . 08h55m10.5s +20d00m50s RadioS
08h55m11.20s	+20d00'33.7"	
08h55m11.30s	+20d00'31.5"	
08h55m11.34s	+20d00'30.7"	
08h55m12.13s	+20d04'39.1"	
08h55m12.20s	+20d04'38.0"	
08h55m12.20s	+20d04'38.0"	
08h55m12.25s	+20d04'35.0"	
08h55m30.63s	+20d07'07.5"	
08h55m30.63s	+20d07'07.5"	
08h55m39.71s	+20d00'16.3"	SAO 80512 . 08 55 39.679 +20 00 17.00 double star
08h55m39.75s	+20d00'21.0"	1WGA J0855.6+2000 - 08h55m39.5s +20d00m19s XrayS
08h55m39.87s	+20d00'21.7"	
08h55m39.88s	+20d00'21.4"	
08h55m51.50s	+20d03'37.2"	GSC 01400.00455 . 08 55 51.57 +20 03 38.2 coronal X-ray eclipsing binary (W Uma type)
08h55m51.50s	+20d03'41.1"	

Optical Photometric Sequence Adopted

Priority to R-band observations (recommended for small telescopes).
Data collected as "instrumental magnitudes" for target and comparison stars.
Data reduction and light curve assembling (absolute mag calculation, colour effects, offset, etc.) in progress.

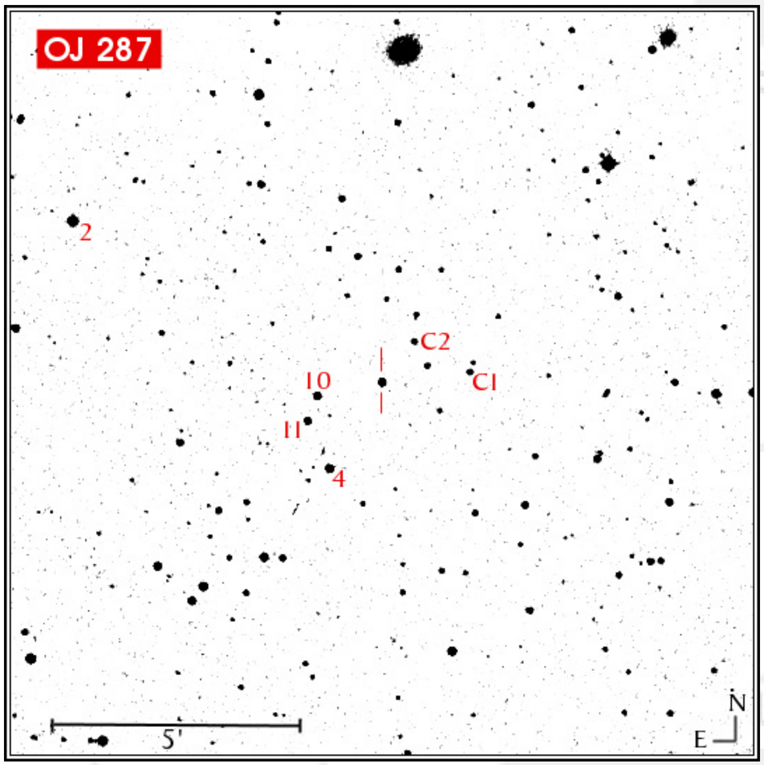

UBVRI and *JHK* Johnson-Cousins absolute photometry sequences for comparison stars. *VRI* calibration for stars 4, 10, 11, C1, C2 adopted by Fiorucci & Tosti (1996), because more reliable than that in Gonzalez-Perez et al. (2001).

Optical-near-IR photometry of comparison stars
(UBV: Johnson, RI: Cousins, JHK: ~Johnson)

Star/Band	U	B	V	R	I	J	H	K
4	15.49 ±0.07	15.01 ±0.06	14.18 ±0.04	13.74 ±0.04	13.28 ±0.04	12.647 ±0.001	12.206 ±0.001	12.114 ±0.003
10	15.00 ±0.05	15.01 ±0.05	14.60 ±0.05	14.34 ±0.05	14.03 ±0.05	13.612 ±0.003	13.325 ±0.003	13.256 ±0.008
11	15.39 ±0.07	15.47 ±0.07	14.94 ±0.04	14.65 ±0.05	14.32 ±0.05	13.889 ±0.004	13.568 ±0.005	13.521 ±0.011
C1	...	...	15.88 ±0.07	15.50 ±0.07	15.08 ±0.07	...	14.337 ±0.109	13.782 ±0.029
C2	...	...	16.12 ±0.08	15.66 ±0.08	15.21 ±0.08	14.474 ±0.006	14.045 ±0.011	14.023 ±0.022
2	13.49 ±0.04	13.45 ±0.04	12.80 ±0.04	12.46 ±0.05	12.06 ±0.07	...	...	...

- Data references:
  - stars 4, 10, 11, C1, C2 in VRI: Fiorucci M. & Tosti G. 1996, A&AS 116, 403
  - stars 4, 10, 11 in UB (and star 2 in UBVRI): Smith P. et al. 1985, AJ, 90, 1184
  - stars 4, 10, 11, C1, C2 in JHK: González-Pérez J.N., Kidger M.R., & Martín-Luis F. 2001, AJ, 122, 2055

Coord. Campaign: Preliminary Optical R-band Light-curve

Date: Oct. 2004 - May 2005 (last observing season)
ENIGMA monitoring observations + intensive WEBT campaign (part 1):

- Intermediate brightness level. Brightness increase of 2 mag in about 2.5 months.
- Mild flaring during the XMM-Newton pointing (April 12): increase of ~ 0.8 mag in 8 days, decrease of ~ 1.4 mag in 13 days.

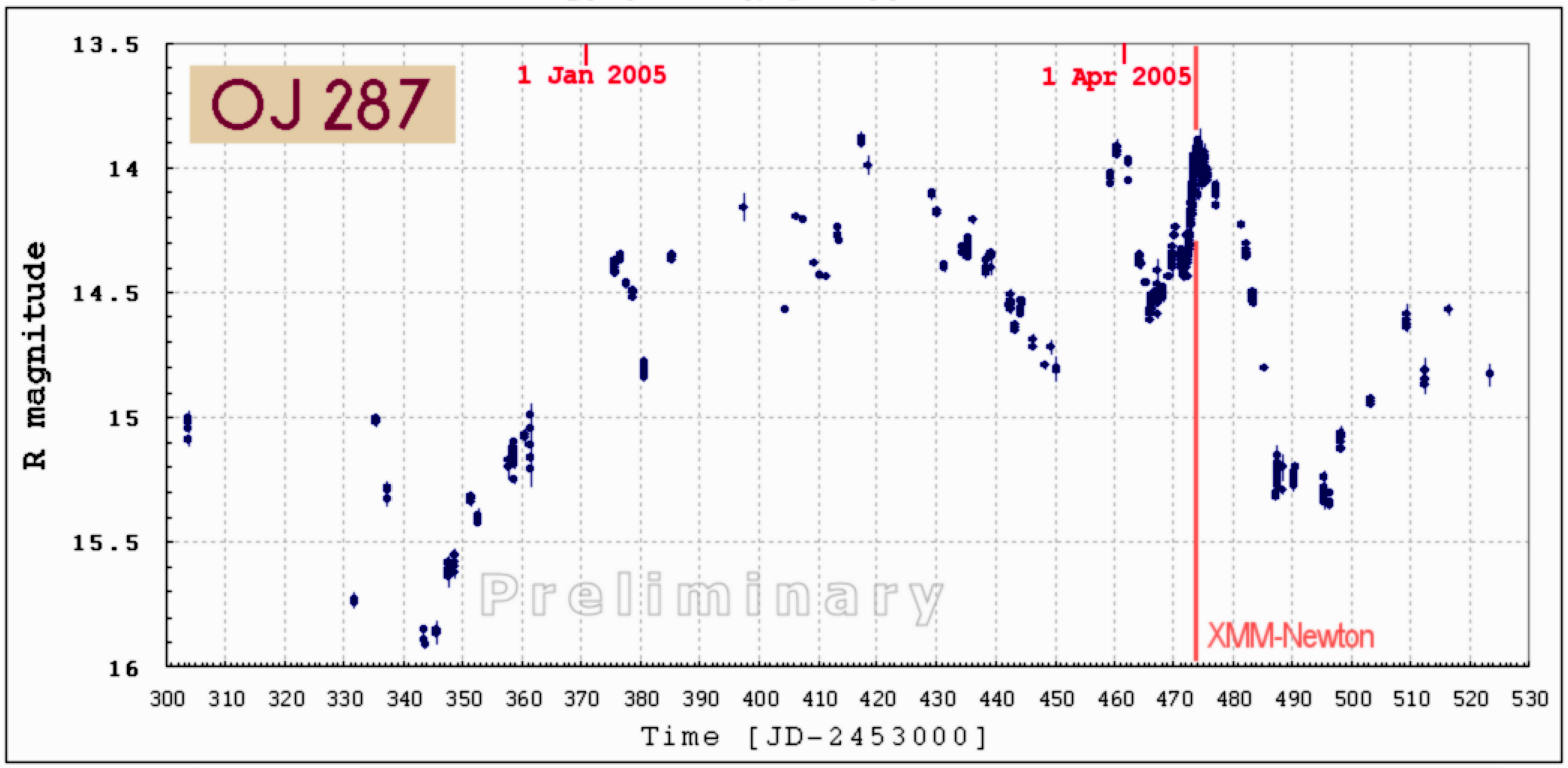

Coord. Campaign: Preliminary Optical Light-curves

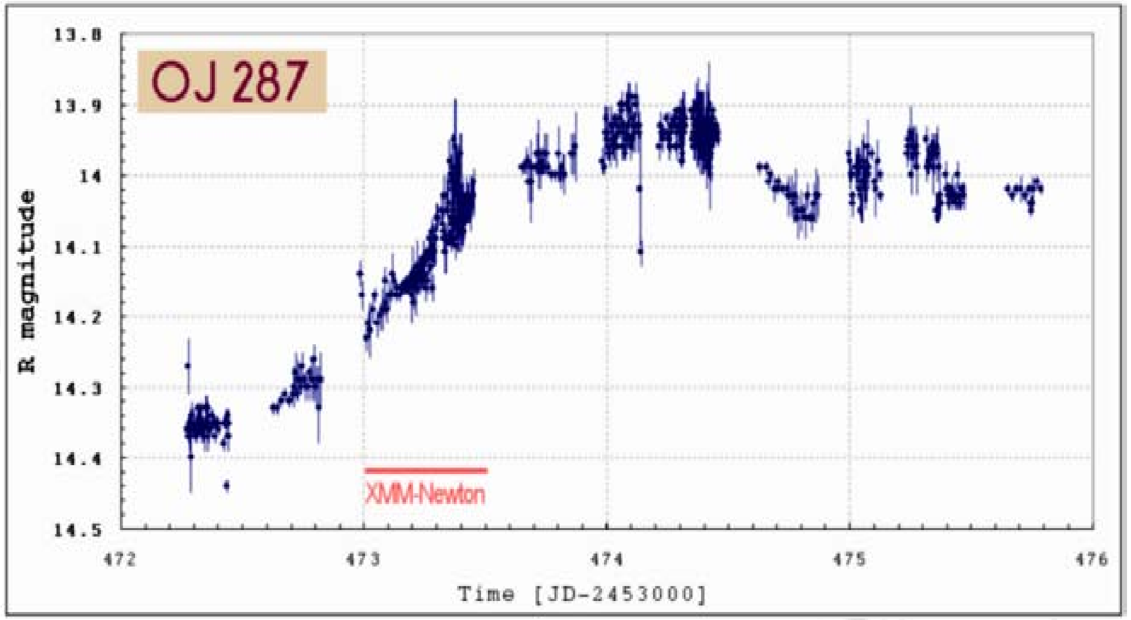

Date: April 12
(XMM-Newton 1st pointing)

- ❑ About 0.3 mag brightness increase in less than 9 hours

- ❑ Possible optivcal Intra-Day Variability

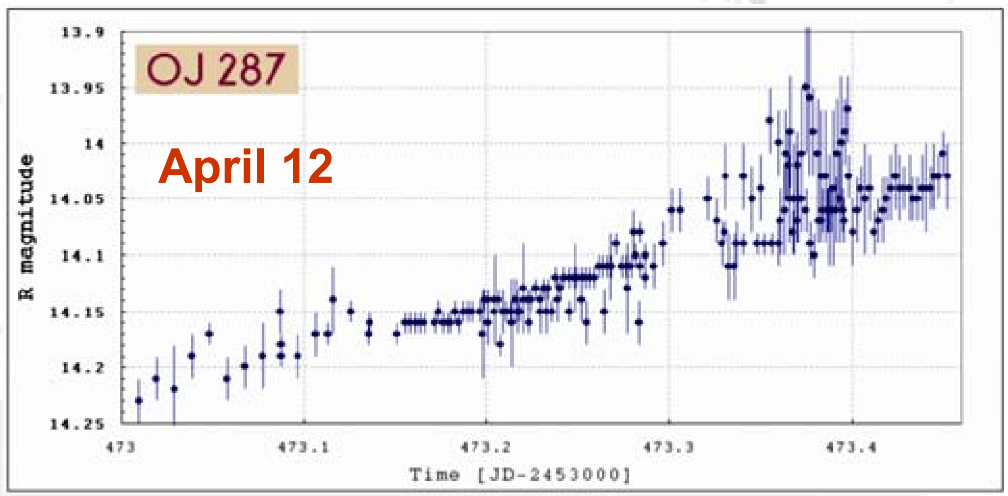

Coord. Campaign: Preliminary Radio Results

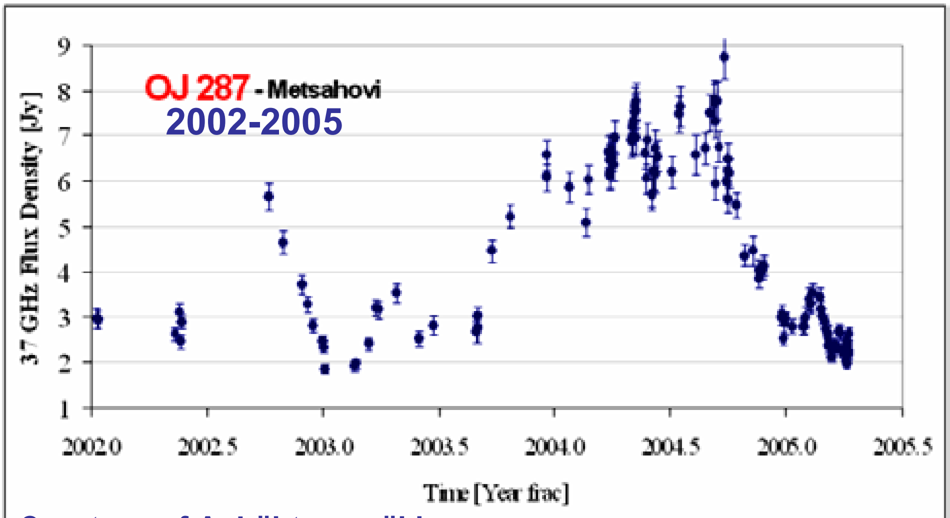

Courtesy of A. Lähteenmäki

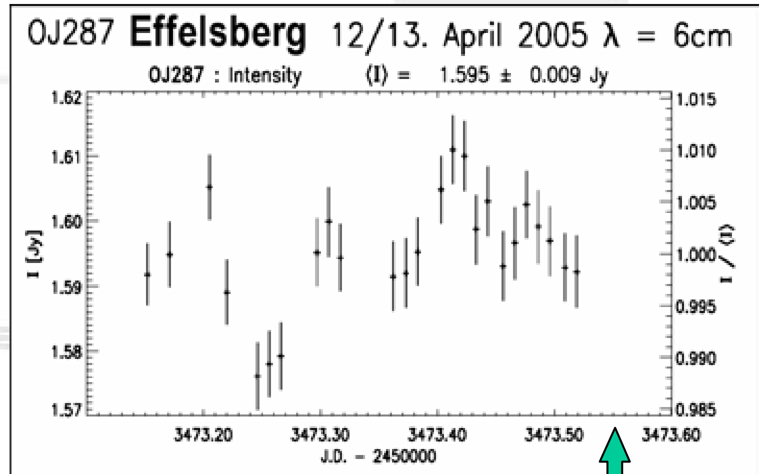

Courtesy of L. Fuhrmann

IDV ~ 3%

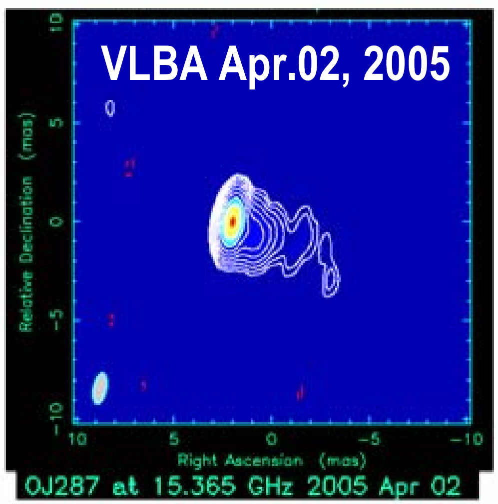

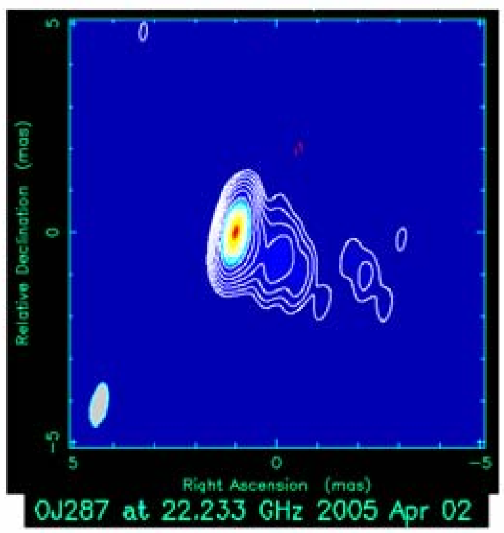

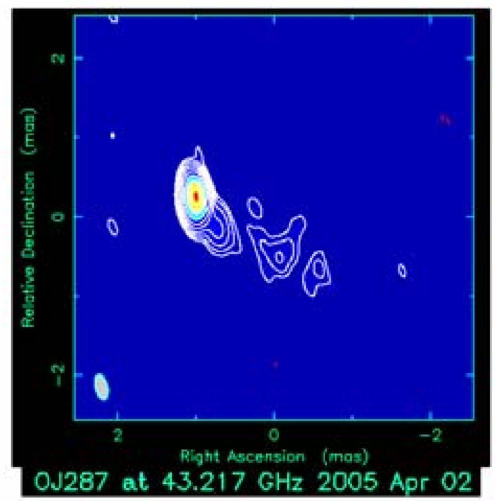

Courtesy of I. Agudo

Interlude (break) 1: Networks of Observatories

ENIGMA as a radio-optical telescope Network
www.lsw.uni-heidelberg.de/projects/enigma/

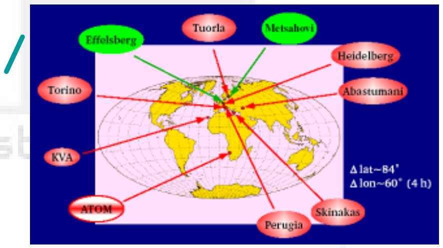

The Whole Earth Blazar Telescope (**WEBT**)
www.to.astro.it/blazars/webt/

The Global Telescope Network (**GTN**, formerly GLAST Telescope Net.)
gtn.sonoma.edu/public/

RoboNet (1.0 = Liverpool + Faulkes telescopes)
www.astro.livjm.ac.uk/RoboNet/

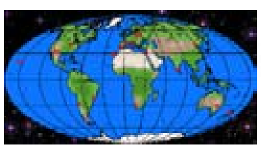

Whole Earth Telescope (**WET**, 1986 the older network of global telescopes?)
wet.physics.iastate.edu

American Association of Variable Star Observers (**AAVSO**, founded in 1911)
www.aavso.org

MOA Global Network
www.physics.auckland.ac.nz/moa/global_network.html

Interlude (break) 1: Networks of Observatories

The Whole Year Blazar Telescope (WYBT)
wybt.fisica.unipg.it

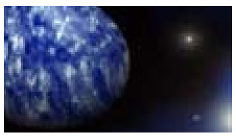

Global Network of Astronomical Telescopes (GNAT)
www.darksky.org/gnat/

Heterogeneous Telescope Networks Workshop (E-Star)
www.estar.org.uk

Monitoring Network of Telescopes (MONET)
monet.uni-goettingen.de

Tennessee State University Automated Astronomy Group
schwab.tsuniv.edu

Burst Observer and Optical Transient Exploring System (BOOTES)
laeff.esa.es/BOOTES/

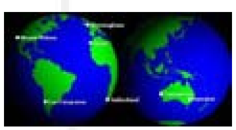

Birmingham Solar Oscillations Network (BISON)
bison.ph.bham.ac.uk

Interlude (break) 1:
Networks of Observatories

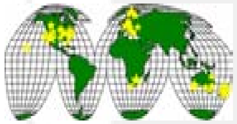

Center for Backyard Astrophysics (CBA)
`cba.phys.columbia.edu`

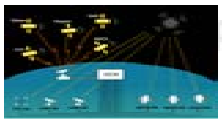

The Gamma ray bursts Coordinates Network (GCN)
`gcn.gsfc.nasa.gov`

The Optical Transient Center (OTC)
`otc.pereplet.ru`

… and other!

Radio: European-VLBI (`www.evlbi.org`), VLBA (`www.vlba.nrao.edu`), global mm-VLBI (`www.mpifr-bonn.mpg.de/div/vlbi/globalmm/`)...

- ❑Possible collaboration and partnership; exchange of know-how, contacts, philosophy, information, technical solutions, etc… Right mix of collaboration and competition.
- ❑ Rules to be followed, data sharing with the international scientific community, data-archives, really open-wide opportunities and decentralization of science results.
- ❑ Involvement for amateur observatories, for students, teachers, large public, sponsors, industries, national and international funding agencies, etc...
- ❑ The Future: intelligent robotic telescope networks, web services, high precision photometry, large amount of data, large interaction with amateur astronomers and public outreach…

Part 2: PKS 2155-304

Optical Monitoring During the HESS Multifrequency Campaign of Summer-autumn 2004

PKS 2155-304: Opt. Monitoring in the HESS Campaign of 2004

PKS 2155-304 (z=0.117): it is one of the brightest and most intensively studied (especially in X-rays band) prototypes of high-energy BL Lac.

- ❑ Observed repeatedly by HESS Cherenkov telescope (campaigns in 2002, 2003, 2004).
- ❑ Observations by MAGIC (large zenith angle) planned.
- ❑ PKS 2155-304 was monitored by the Tuorla team using the KVA optical telescope (R-band intranight photometry and unfiltered polarization observations in Aug.-Sept. 2004), in the frame of the 2004-HESS multifrequency campaign (HESS, opt., radio, RXTE, Spitzer…).

KVA observations invited by the ENIGMA Coordinator as a further YRs collaborative project).

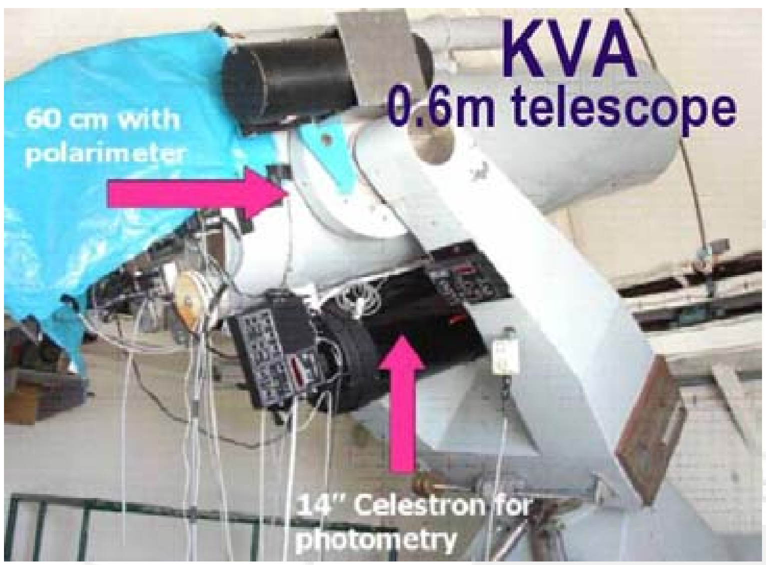

Remote and in-situ observations.

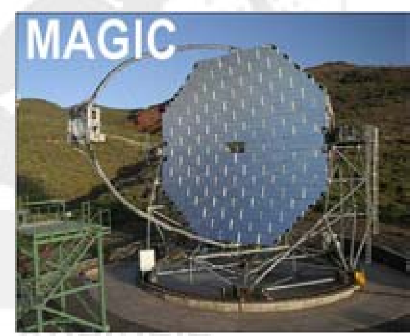

PKS 2155-304: Opt. Monitoring in the HESS Campaign of 2004

- A total of 440 R-band photometric data points obtained in 13 nights (observers: E. Lindfors (in-situ), S. Ciprini, L. Ostorero, data reduction: K. Nilsson).
- Average of 38 frames per night in the period August 3 – September 23, 2004.
- Simultaneous polarimetric obs. (white-light) in 4 nights (Sept. 8-9, 9-10, 12, 22-23).
- Optical brightening (up to R = 12.55±0.01 mag, i.e. flux about 31 mJy) observed in Sep. 8-10.

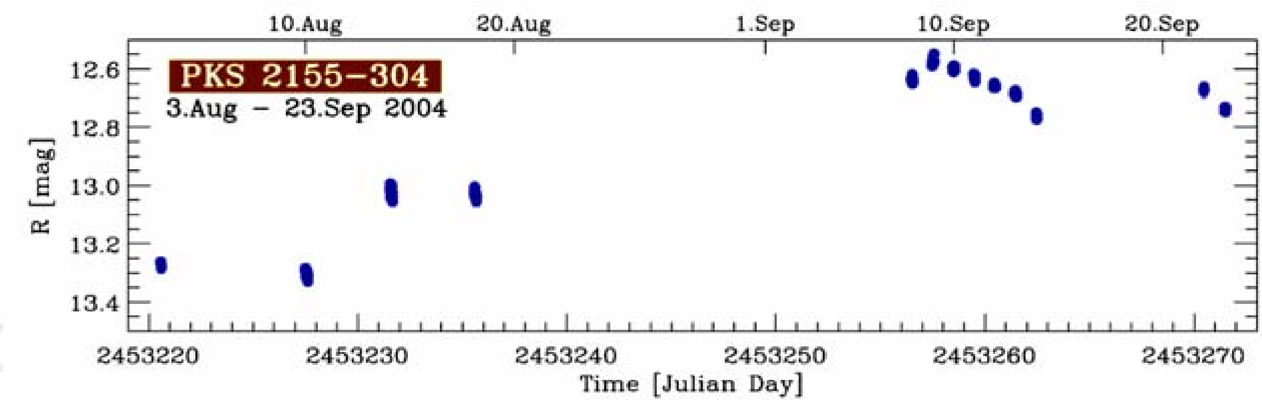

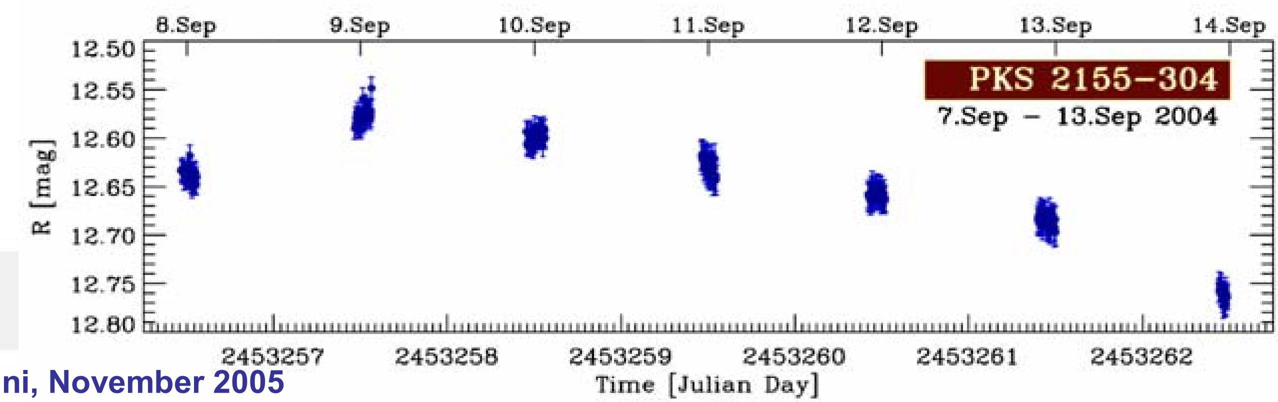

PKS 2155-304: Opt. Monitoring in the HESS Campaign of 2004

- ❑ Preliminary inspection on the 13 intra-night light curves does not show any relevant signature of IDV.
- ❑ The relatively high level of linear optical polarization (~12%) recorded during Sep. 9-10 might provide a signature of the synchrotron nature of this flare.
- ❑ Interesting to search for possible correlations and time lags with simultaneous X-ray and TeV data (RXTE, HESS).

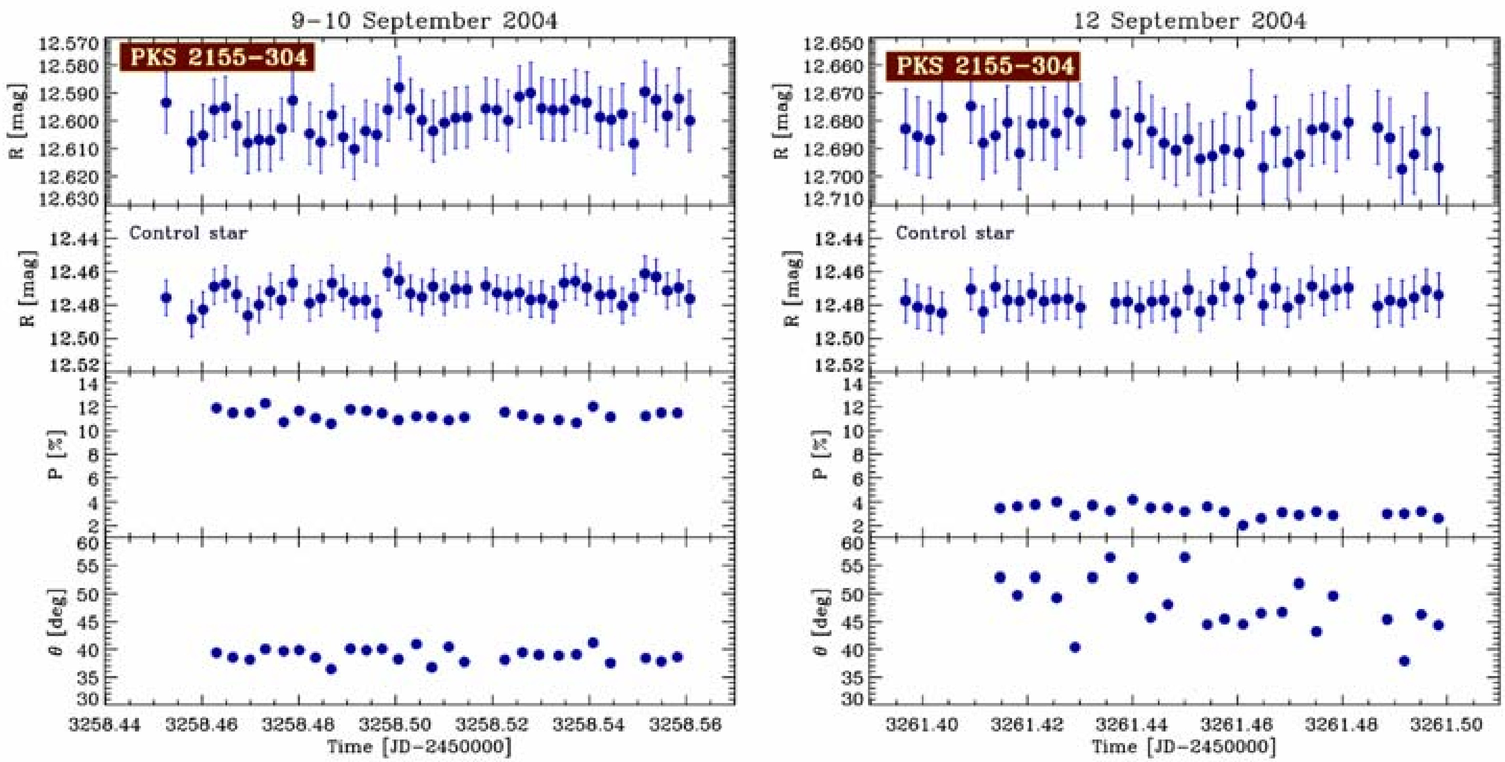

PKS 2155-304: Opt. Monitoring in the HESS Campaign of 2004

SED of PKS 2155-304. Compilation of data obtained around mid-90s. Solid lines are a Synchrotron Self Compton (single-zone), and time-dependent cooling modeling of observations performed during the famous EGRET flare of Nov.1997 (Mark 6, RXTE, opt. data).
Data from the HESS campaign of Oct.-Nov.2003 (Aharonian et al. 2005) added for comparison, showed that the simple SSC one-zone model with K-N cutoff is not sufficient here.
The qualitative nominal sensitivity energy ranges of MAGIC and HESS are superimposed (but MAGIC can observe PKS 2155-304 only at large zenith-angles (~47° at best), so its lower energy limit is similar to the HESS limit). KVA optical data of Aug.-Sept.2004 are reported for comparison.

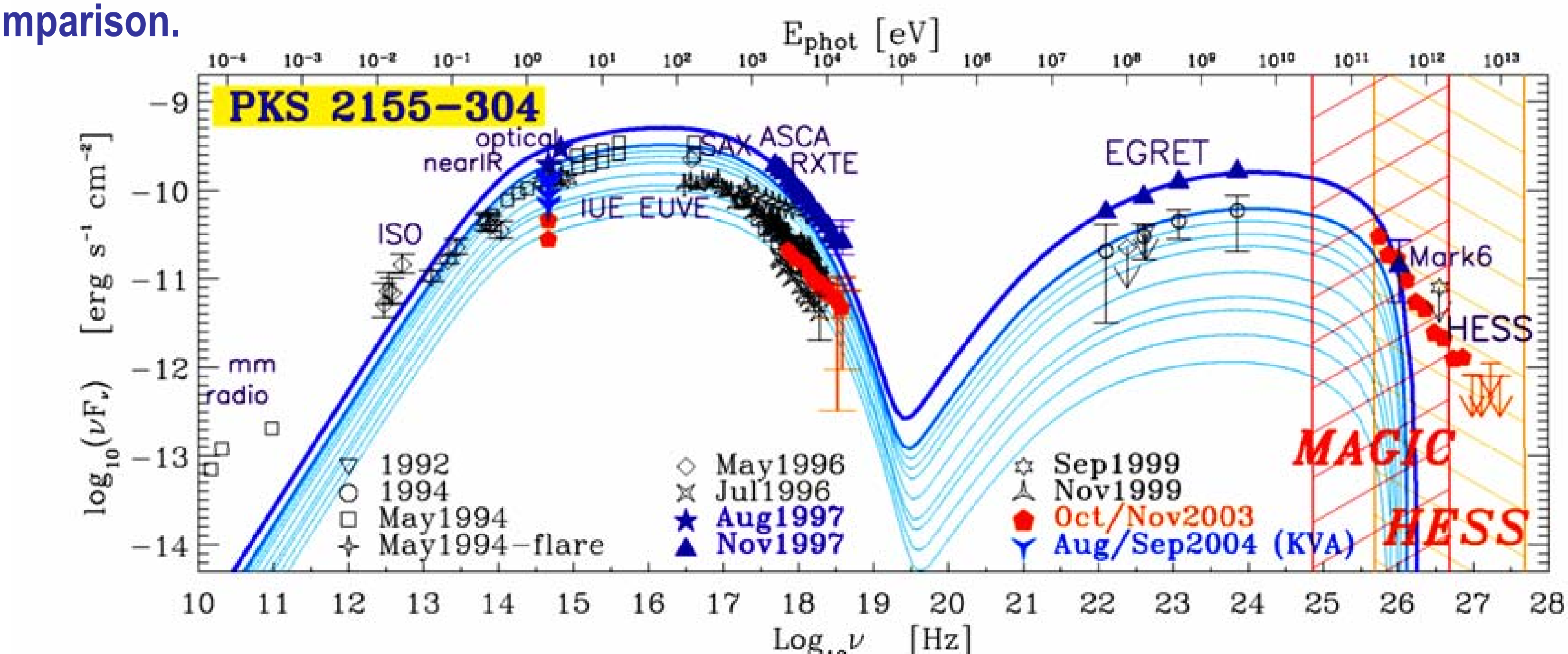

Interlude (break) 2:
Proposals Submitted

Recently 4 proposals (blazar topic) have been submitted to European facilities as PI in the last calls (response awaited):

- 2 proposals for ESA XMM-Newton (Cycle AO-5)

- 1 proposal for ESO Very Large Telescope (Period 77)

- 1 proposal for Nordic Optical Telescope (Period 33)

Much ado (and work/time) about nothing? YES! Acceptance probability is very low (the total number of proposal submitted is large especially in extragalactic astronomy, no "extremely important" hypotheses to be tested…).

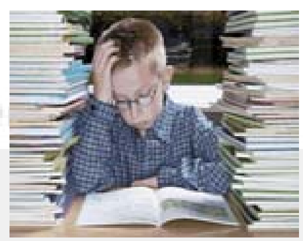

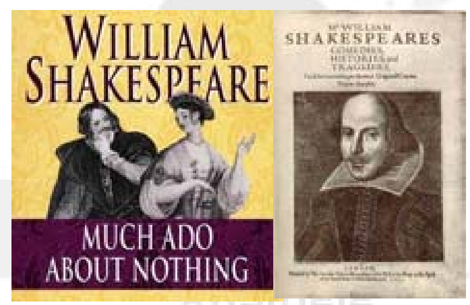

Part 3:
PKS 0735+178

Final Issues by the Long-term Optical Monitoring

10-years Optical Monitoring of PKS 0735+178

10 years of unpublished optical monitoring data (*BVRI* bands) on PKS 0735+178 (the "cosmic conspiracy" blazar).

Data from Perugia University Observatory (Italy), INAF-Torino Observatory (Italy), Tuorla Observatory (Finland), Sabadell Observatory. (Spain). Optical data from Shanghai Obs. (Qian & Tao 2004) also added to improve the sampling.

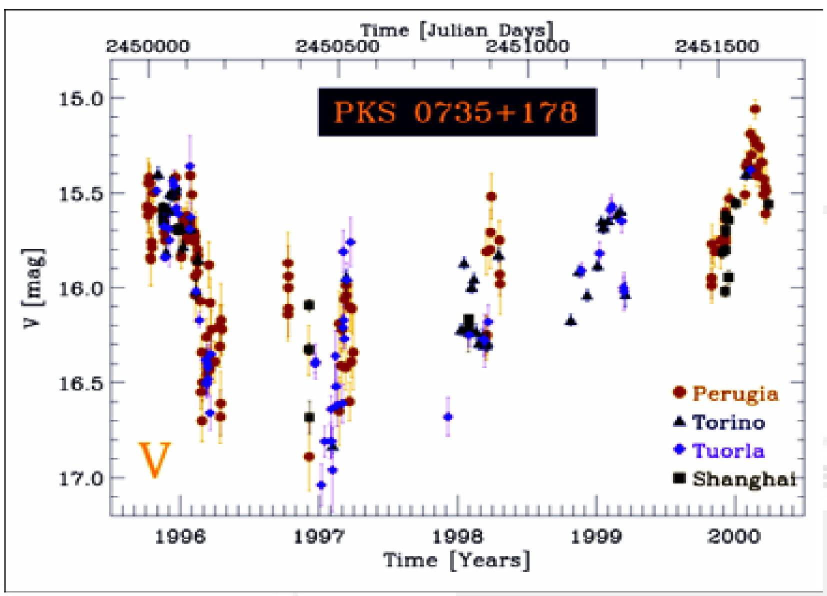

DATA POINTS PER OBSERVATORY

Obs.	B	V	R	I	Tot.	Period
Perugia	0	226	490	281	997	Feb1993-Feb2004
Torino	75	38	150	0	263	Dec1994-Apr2002
Tuorla	0	55	0	0	55	Oct1995-Feb2001
Sabadell	0	0	17	0	17	Dec2001-Feb2004
Shanghai	0	115	52	138	305	Jan1995-Dec2001
Total	75	434	709	419	1637	

STATISTICS

	B	V	R	I
Total data points	75	434	709	419
Start date [JD-2449000]	698	45	21	420
End date [JD-2449000]	3354	4053	4053	4053
Total period N_{tot} [days]	2657	4001	4032	3633
Nights with data N_{on}	52	297	459	259
N_{on}/N_{tot} fraction	0.019	0.074	0.171	0.071
Mean num. points × night	1.44	1.46	1.51	1.62
Total mean gap Δt [days]	35.9	9.3	5.8	8.7
Longest gap [days]	780	352	375	356
Average brightness [mag]	16.319	15.760	15.301	14.693
Max brightness [mag]	15.863	14.544	14.16	13.59
Min brightness [mag]	17.453	16.94	16.87	15.97
Variab. range Δm [mag]	1.59	2.39	2.71	2.38
Absorption coeff.† [mag]	0.152	0.117	0.094	0.068
Data standard deviation	0.256	0.368	0.515	0.453
Data skewness	1.23	0.386	0.329	0.155
Data kurtosis	3.791	1.087	0.019	0.400
Max flux [mJy]	2.21	6.1	7.3	9.9
Min flux [mJy]	0.51	0.67	0.60	1.1

10-years Optical Monitoring of PKS 0735+178

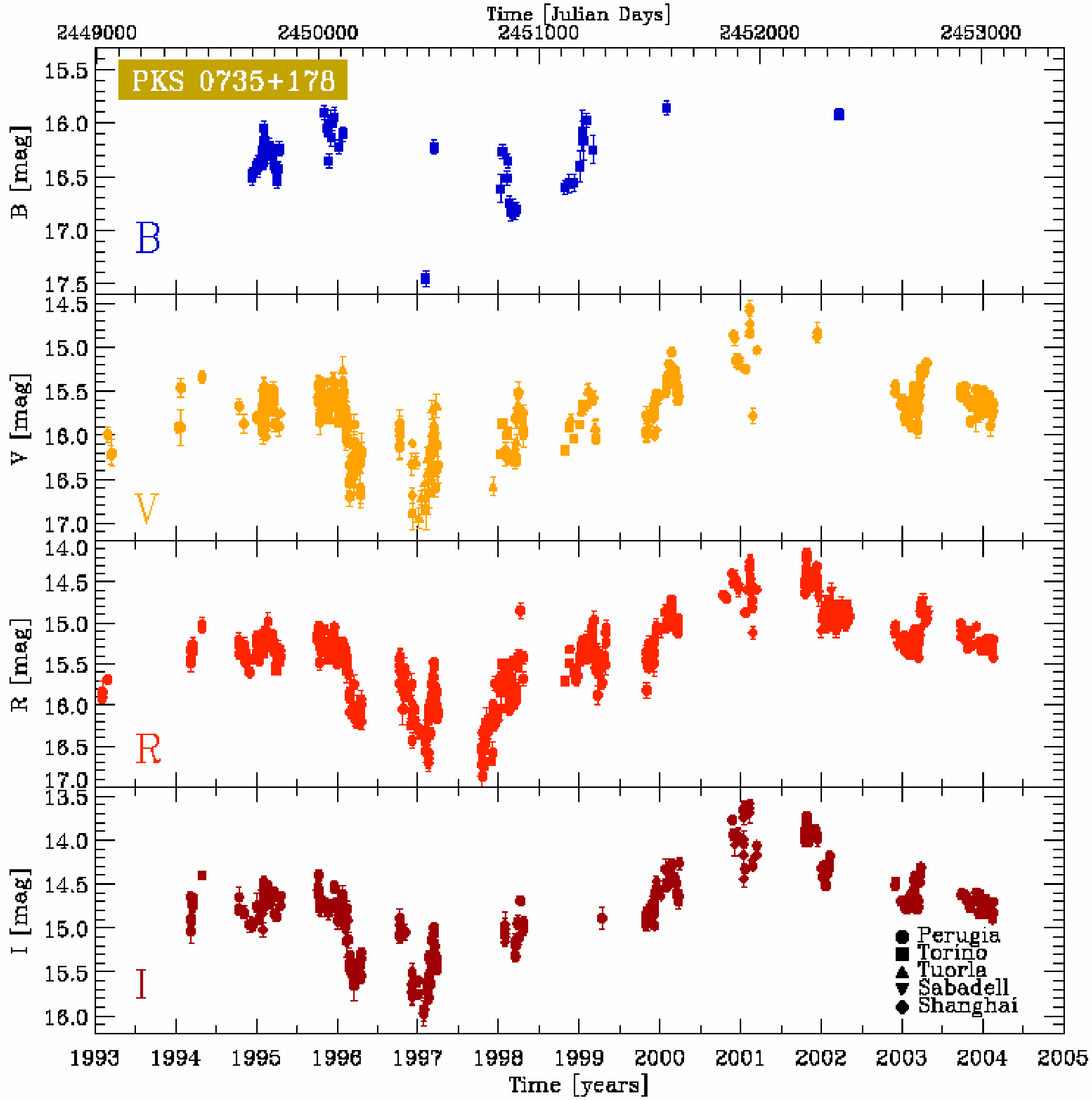

- Data from different observatories are in agreement within the uncertainties.
- PKS 0735+178 showed rapid optical variations connected to slower variations (as appear in the radio flux light curves). Light curve best sampled is in R-band.
- 11 observing seasons, 10 years light curves, 1637 photometric data points.
- Our improved data sampling recorded also fast optical flares.

PKS 0735+178: a Refined Comp. Stars Phot. Sequence

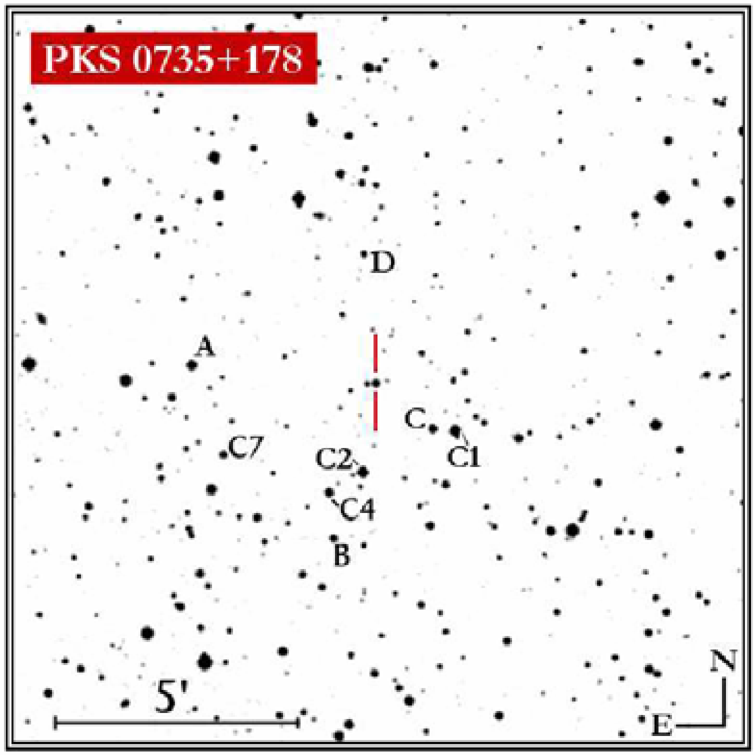

A new unpublished photometric *VRI* (Johnson-Cousins) calibration of comparison stars in the field of PKS 0735+178 (stars C1, C, D, C2, C4, C7, A) obtained at Perugia Observatory in few years.

PHOTOMETRIC SEQUENCES FOR PKS 0735+178 COMPARISON STARS (PERUGIA UNIVERSITY OBSERVATORY)

Star	R.A. (J2000.0)	Dec. (J2000.0)	V [mag]	R_c [mag]	I_c [mag]
C1..	07 38 00.5	+17 41 19.9	13.26 ± 0.04	12.89 ± 0.04	12.57 ± 0.04
C..	07 38 02.4	+17 41 22.2	14.45 ± 0.04	13.85 ± 0.04	13.32 ± 0.04
D..	07 38 08.3	+17 44 59.7	15.90 ± 0.05	15.49 ± 0.05	15.12 ± 0.06
C2..	07 38 08.5	+17 40 29.2	13.31 ± 0.04	12.79 ± 0.04	12.32 ± 0.04
C4..	07 38 11.6	+17 40 04.4	14.17 ± 0.05	13.80 ± 0.04	13.48 ± 0.04
C7..	07 38 20.7	+17 40 51.2	15.01 ± 0.06	14.70 ± 0.06	14.37 ± 0.05
A..	07 38 23.4	+17 42 43.0	13.40 ± 0.05	13.10 ± 0.05	12.82 ± 0.05

PREVIOUS LITERATURE PHOTOMETRIC SEQUENCES FOR PKS 0735+178 COMPARISON STARS

Star	U [mag] (a)	B [mag] (a)	V [mag] (a)	R [mag] (a)	I [mag] (a)	U [mag] (b)	B [mag] (b)	V [mag] (b)	B [mag] (c)	U [mag] (d)	B [mag] (d)	V [mag] (d)
A..........	13.87	13.87	13.40	13.14	12.85	13.92	13.88	13.42	13.89	...	...	...
C..........	16.26	15.48	14.40	13.87	13.33	16.39	15.50	14.48	...	...	...	...
D..........	16.65	16.48	15.80	15.45	15.16	16.94	16.62	15.91	16.62	...	...	...
B..........	...	...	...	...	...	15.54	15.49	14.94	...	...	...	...
C2........	...	...	...	...	...	...	...	...	...	15.04	14.35	13.33
C4........	...	...	...	...	...	...	...	...	...	14.95	14.81	14.21
C7........	...	...	...	...	...	...	...	...	...	15.76	15.64	15.04

[(a)] Values by Smith et al. (1985); [(b)] values by Wing (1973); [(c)] values by Veron & Veron (1975); [(d)] values by McGim et al. (1976) (C2 = star 3, C4 = star 1, C7 = star 2).

PKS 0735+178: Detailed Analysis of Single Seasons

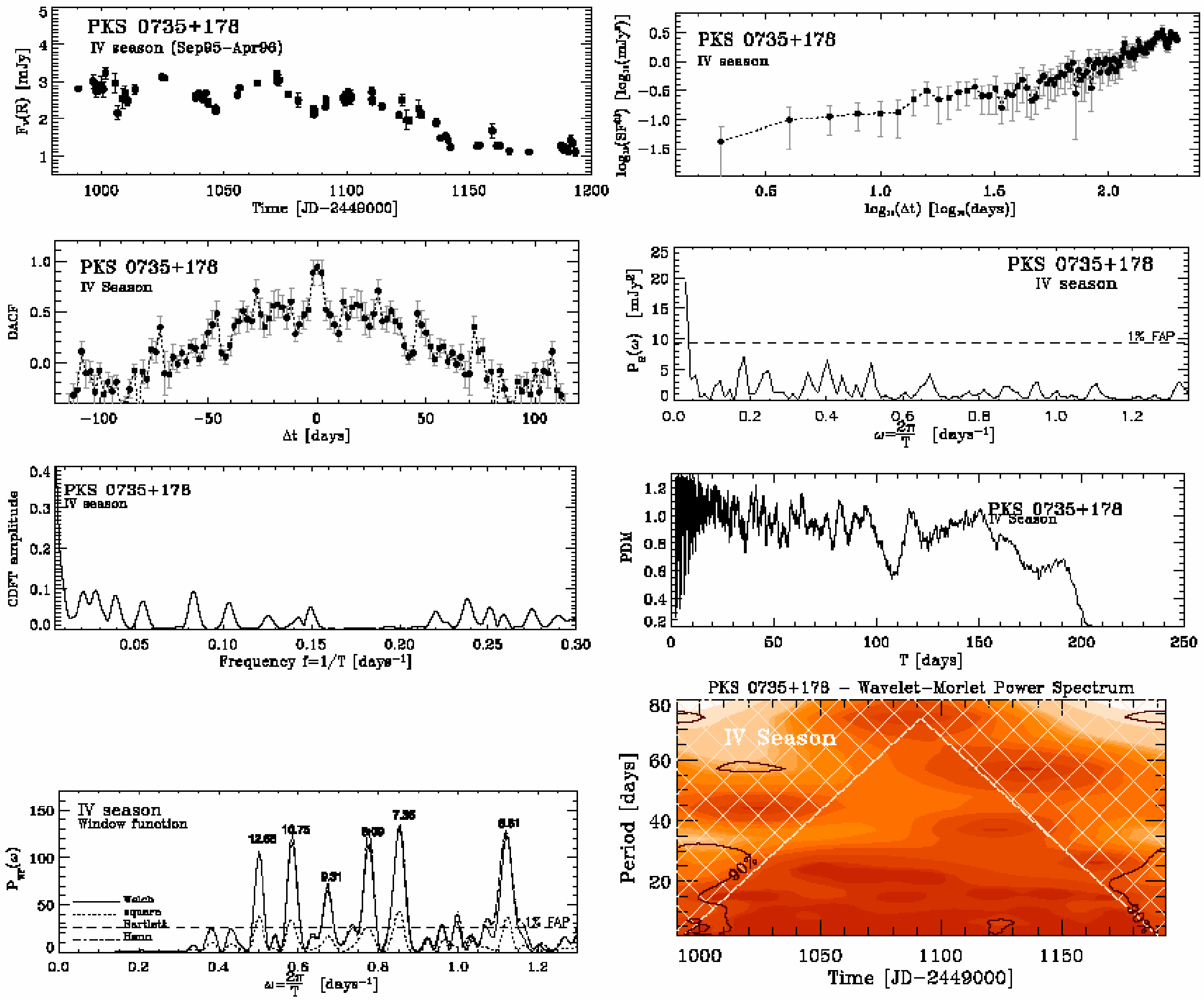

- Discrete Correlation Function (standard and Z-transform implementations), DACF, Z-DACF.
- Structure Function SF.
- Clean Fourier decomposition CDFT.
- Lomb-Scargle Periodogram LSP.
- Phase Dispersion Minimization PDM.
- Light Curve Folding.
- Discrete Wavelet Transform DWT.
- gaps Window Function periodogram GWFP.

IV observing season (Sept. 1995 - Apr. 1996)

PKS 0735+178: Detailed Analysis of Single Seasons

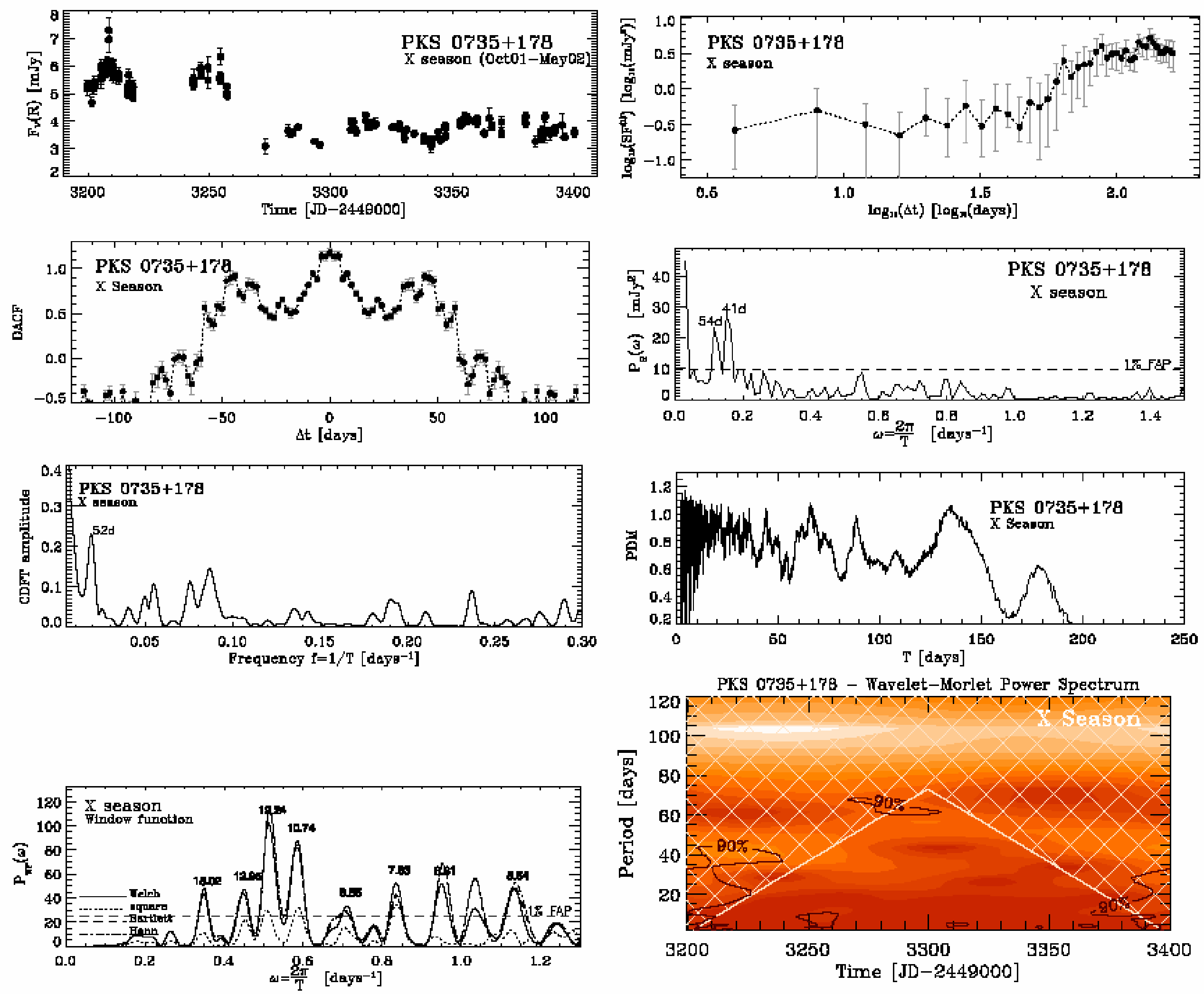

- Discrete Correlation Function (standard and Z-transform implementations), DACF, Z-DACF.
- Structure Function SF.
- Clean Fourier decomposition CDFT.
- Lomb-Scargle Periodogram LSP.
- Phase Dispersion Minimization PDM.
- Light Curve Folding.
- Discrete Wavelet Transform DWT.
- gaps Window Function periodogram GWFP.

X observing season (Oct. 2001 – May 2002)

PKS 0735+178: Historical Light-curve Analysis

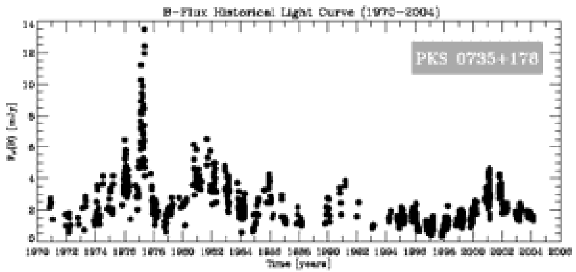

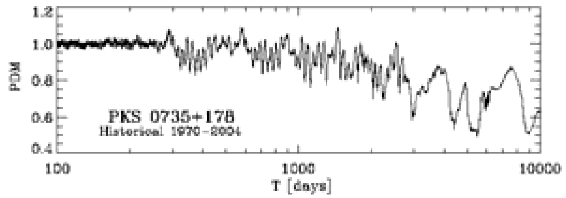

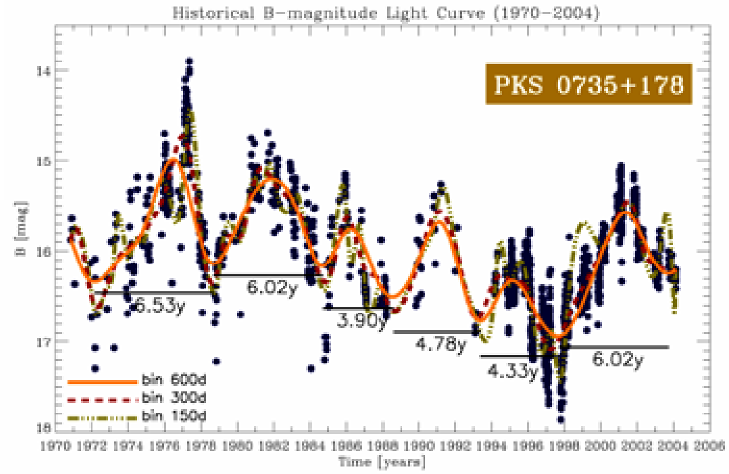

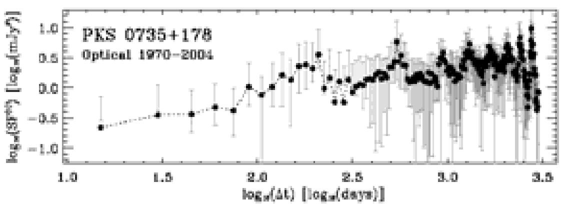

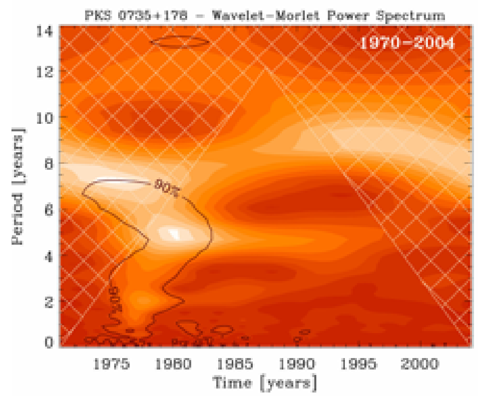

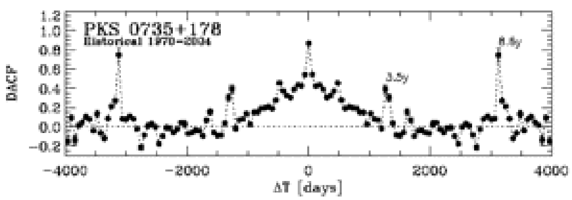

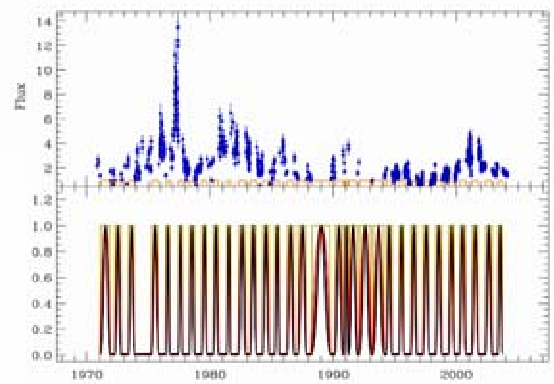

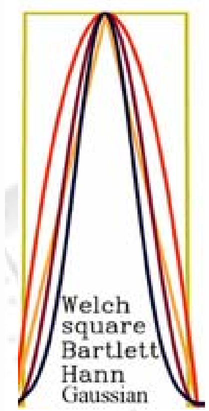

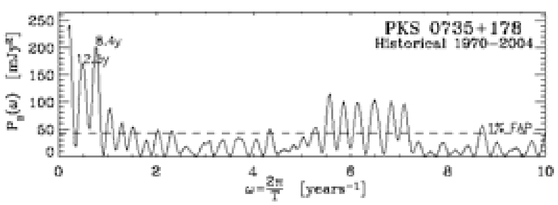

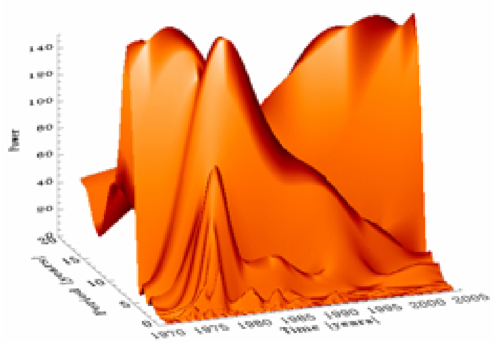

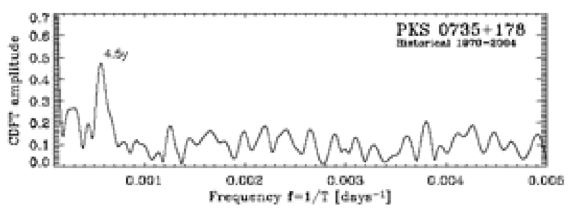

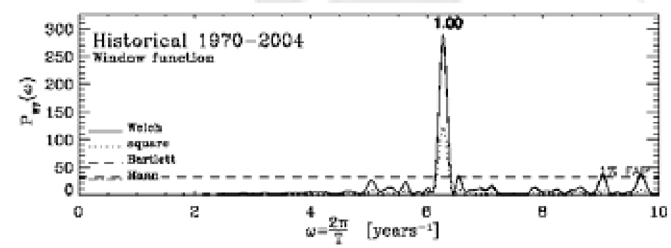

Sixth Enigma Meeting - Stefano Ciprini, November 2005

PKS 0735+178: Optical Timescales

Lotto, bingo or reliable timescales?

Characteristic timescales revealed by statistical analysis performed with SF, DACF, CDFT, LSP, PDM, DWT, GWFP (when the signature is well identifiable) .

The data sets investigated: historical B-flux light curves (complete 1906-2004 and best sampled 1970-2004 sets, also a separated analysis of the pre-1970 part; timescales investigates between 2 and 20 years) and single observing seasons in R-band (timescales investigated between few days to 100 days).

Criteria adopted to avoid fake/spurious recurrences given by gaps and irregular sampling: only the more relevant timescales, recurrent and appeared in more than one method, different from gaps window function features, and smaller than 1/2 or 1/3 of time-series extension were considered.

Observing season	Duration [days]	N_{on}	$< n >$	$< \Delta t >$ [days]	Δt_{max} [days]	$SF\ T_{dr}$ [days]	PSD slope α	$SF\ T_{to}$ [days]	$DACF\ T_{pe}$ [days]	$LSP\ T_{pe}$ [days]	$CDFT\ T_{pe}$ [days]	$PDM\ T_{dr}$ [days]	$DWT\ T_{pe}$ [days]
B 1906-2004†	96.2y	989	1.7	20.7	12.78y	11.6y,25y,	...	...	8.6y,24.7y	8.6y,13.2y,33.7y	34y	12.6y,15.2y	13.7y
B 1906-1958†	52y	122	1.4	114	8.95y	12.3y, 18.5	...	...	11.4y	5.7y,10.8y	...	11.6y	10.9y
B **1970-2004**†	33.3y	867	1.8	7.8	1.63y	4.2y,8.1y,11.8y	1.5,2.0	210,1.5y	3.5y,8.6y	8.4y,12.5y	4.5y	8.2y,12.6y,15y	4.1y,4.8y
R III Oct.94-Apr95	191	43	1.8	2.5	20.8	79	...	...	18	...	...	18,78	25
R IV Sep95-Apr96	203	62	1.4	2.3	12.9	39	1.97 ± 0.25	...	28	...	...	...	34
R V Oct96-Apr97	178	53	1.6	2.1	17.9	50,79	1.77 ± 0.2	36	...	50,77	...	77	...
R VI Oct97-Apr98	189	11	1.5	2.8	15.9	29,66	...	...	68	...	...	33,66	...
R VII Oct98-May99	189	51	1.2	3.0	21.0	96	1.64 ± 0.09	31	96	53,102	...	30,54	48
R VIII Nov99-Mar00	144	35	1.4	2.7	22.2	83	1.84 ± 0.12	78	...	...	...	25	...
R IX Oct00-Mar01	153	20	1.4	5.6	31.2	83	...	...	33	...	...	...	40
R X Oct01-May02	201	62	2.3	1.4	24.8	69	1.46 ± 0.17	65	41	41,54	52	55,81	42
R XI Nov02-Apr03	144	42	1.1	3.3	24.9	24,60	2.34 ± 0.12	...	28	...	27	55,97	...
R XII Sep03-Feb04	148	33	1.0	4.6	21.0	55	...	...	...	...	...	56	...

† Time scales followed by "y" are expressed in years.

Interlude (epilogue) 3:
A Blazar Light Curves Pamphlet

Recent rumours and criticisms about blazar monitoring
(heard sometimes by theoreticians, model-makers, high-energy people, the same monitoring people, people external to blazar researches, the EC delegate during the 3rd meeting, etc…) :
■ The marvellous Era of the expected periodicities in many blazars is finished. ■ Blazar light curves have only a boring irregular, self-similar and random shape, with little physical outcomes. ■ It is a big observing effort for long-times, providing modest scientific results. ■ It is only the umpteenth addition of other data “pointlets” in a time series. ■ Why to collect thousands of light-curve data-points? ■ At this time the monitoring is an antiquated way to study AGN… etc.

Blazar radio and optical flux monitoring might have a lower appeal now, with respect to recent capabilities and results achieved in the fields of X-ray, gamma-ray astronomy, radio-interferometry and VLBI, deep optical-IR imaging-spectroscopy, etc.
But good science is only the latest-“fashion” or is it the “sexiest” ?
No, of course, and as everyone is biased towards his work it is suitable to end this presentation promoting a cause through the following propagandistic:

blazar light-curves pamphlet !

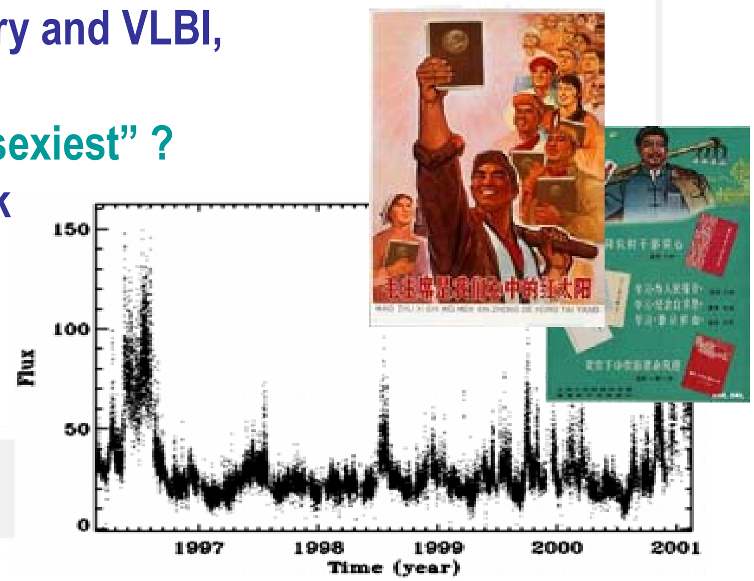

Interlude (epilogue) 3:
A Blazar Light Curves Pamphlet

- The radio-optical constant and long-term monitoring of blazar is necessary to characterize the variability of blazars. Any kind of theoretical or numerical model have to respect and explain the observed light curves.
- It is important from an historical point of view. In constructing an historical record of blazar variability on long scales we make an effort especially useful for the next generation of researchers and the future scientific community. This is an handsome, altruistic, precious and farsighted effort.
- The knowledge of the light curves on long and intermediate timescales is useful to be compared with the short-term behaviour observed during multifrequency campaigns.
- Time-series analysis is important in many research fields (physics, geology, chemistry, biology, climate, medicine, economy, finance, etc.), therefore we can expect that is still important also for blazar and AGN research topics.
- The temporal behaviour of blazar is irregular but no trivial (red noise, chaos, long-term memory, self similarity, intermittence… complexity).
- Periodical components are not ruled out still (for example OJ 287 and other few blazars, helical motion of VLBI component in several blazars, etc…)
- Triggers and alerts for astronomical satellites and large telescopes are always based on a regular and constant radio-optical monitoring. (No monitoring means No ToO, thus *No party*…)

Interlude (epilogue) 3:
A Blazar Light Curves Pamphlet

- The puzzling questions about blazars and AGN cannot be entirely resolved with short multiwavelenght snapshots (even if provided by complete and repeated multifrequency campaigns). We cannot ignore the behaviour in time of a blazar, time domain (=evolution) is an important window of the parameter-space of these sources, and it is important in astronomy, where it is not possible usually to verify physical hypotheses with the experiment.
Do not forget also serendipity.
- Also high-energy observatories are going to produce long time-series (eg. GLAST, a full sky-scanner gamma-ray telescope).
- Optical monitoring has direct links with technological aspects (CCD, automation-robotics, software, etc.), easy links with public outreach/education (amateur astronomers, cheap small telescopes means school/universities involvement, etc.)
and international cooperation (e.g. the cosmopolitan telescope networks…) .
- Finally we are monitoring the signal emitted by the heart of an AGN (this "may be" important…).

Final slogan: Blazar monitoring is alive! It is a big, long, patient, painstaking and farsighted useful observing effort, and time-series analysis is a very interdisciplinary work. Blazar monitoring, blazar light-curves, and time-series analysis are beautiful !

The End

Thank You for the attention

6th ENIGMA Meeting
November 22-25, 2005 – Kinsale, Cork, IRELAND

The colour of S5 0716+71 during the ENIGMA-WEBT core campaign

Luisa Ostorero

(Landessternwarte Heidelberg, Germany)

on behalf of the S5 0716+71 ENIGMA-WEBT collaboration

Outline

- Introduction
- *BVRI* core-campaign light curves
- Colour analysis
- Summary

Introduction

- S5 0716+71: z>0.3, BL Lac
- SED synchrotron peak expected in the IR-optical band

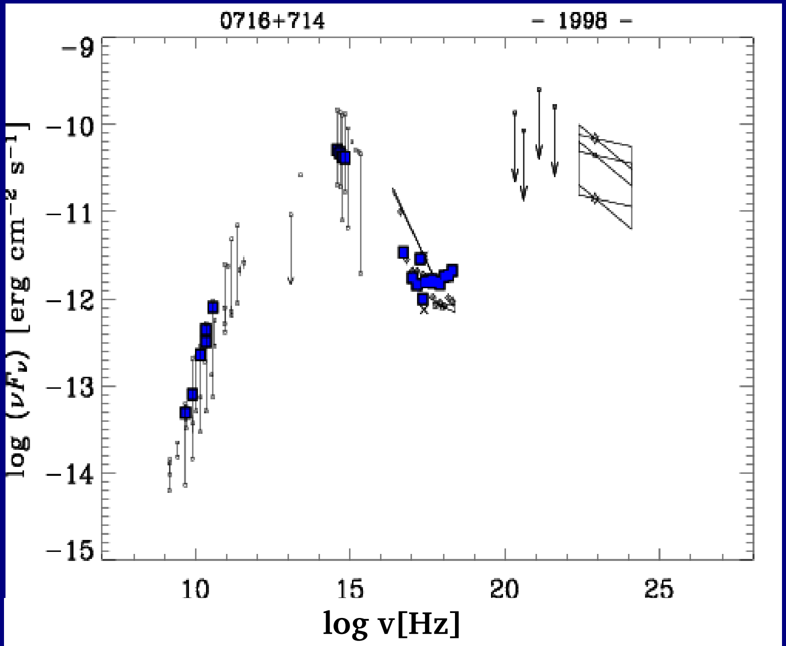

Introduction

- S5 0716+71: z>0.3, BL Lac, IDV
- SED synchrotron peak expected in the IR-optical band

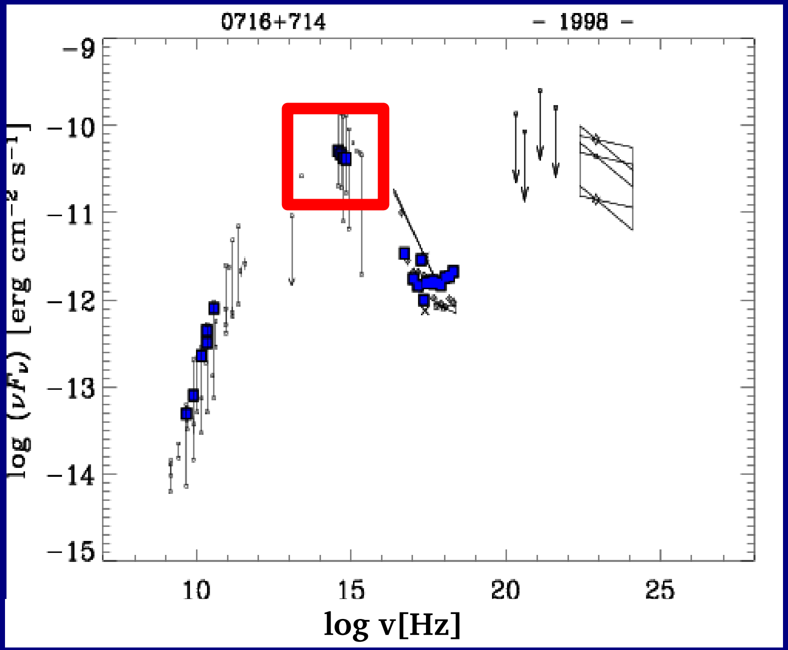

- Measurements of the optical spectrum ($F_\nu \sim \nu^{-\alpha}$) :

α_{BR} = [0.81 ; 1.01] (Feb-Mar 1994; Sagar et al. 1999)

α_{BR} = [0.81 ; 1.15] (Feb-Apr 1995; Ghisellini et al. 1997)

α_{BR} = [1.31 ; 1.57] (Feb 1999; Villata et al. 2000)

$<\alpha_{BR}>=1.26$ (1994 - 2002; Raiteri et al. 2003)

with $\alpha_{BR} = [(B-R)-(A_B-A_R)+2.5 \log(Fo_R/Fo_B)]/[2.5 \log(\nu_B/\nu_R)]$

Introduction

- Behaviour of optical spectrum and brightness:

  ★ **Years**: - different time evolution of colour and brightness (R03)
  - significant colour-brightness correlation: *"bluer-when-brighter"* (R03)

  $r=0.15$, $P(>r) = 2.3 \cdot 10^{-5}$

~ 8 years

Raiteri et al. 2003

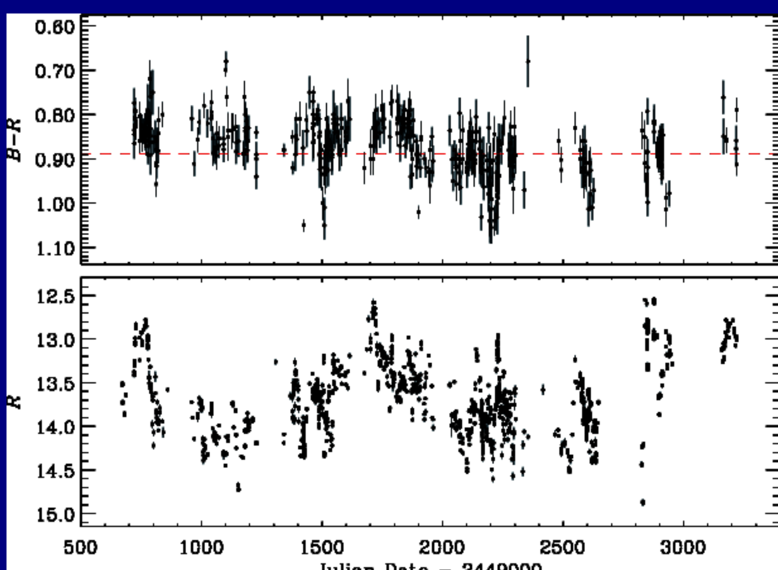

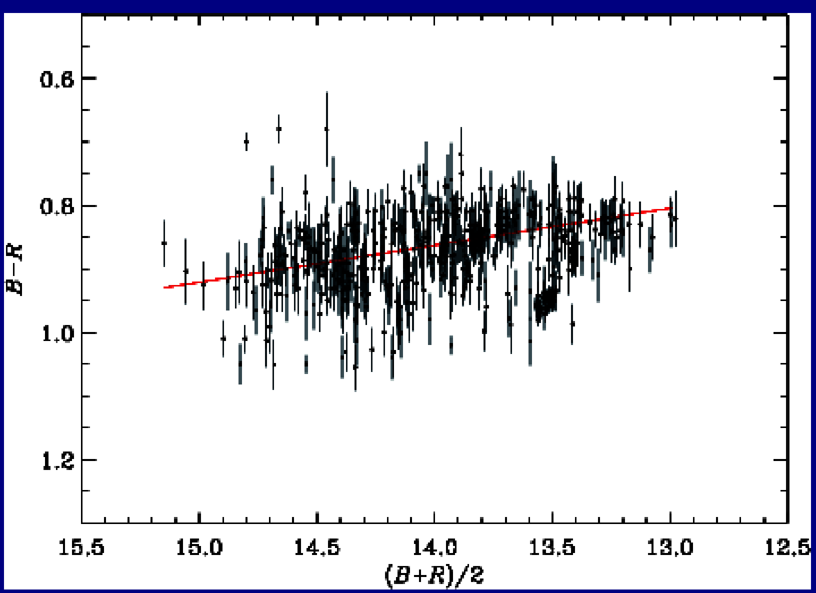

Introduction

- Behaviour of spectrum and brightness:

    ★ **Months, weeks**: - in general, no correlated time evolution of colour and brightness (G97)
    - "quiescent" state (R~14):
      "*flatter-when-brighter*" behaviour (G97);
      significant colour-brightness correlation: r=0.552, P(>r) =2.1· 10^{-2}
      (G97; see also Wagner et al. 1996)

~ 1 month

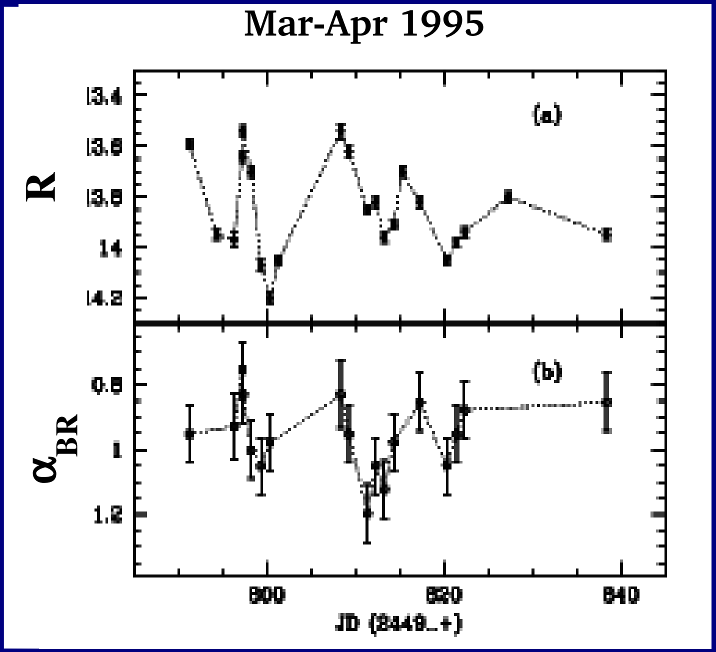

Ghisellini et al. 1997

Introduction

- Behaviour of spectrum and brightness:

  ★ **Days, hours**: chromatic *"bluer-when-brighter"* behaviour also recognized (V00, R03)

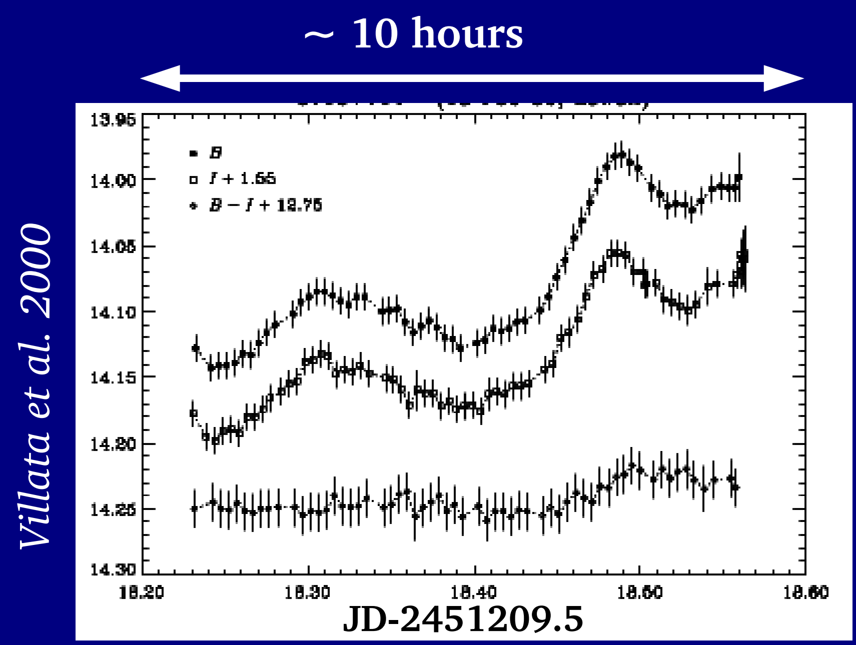

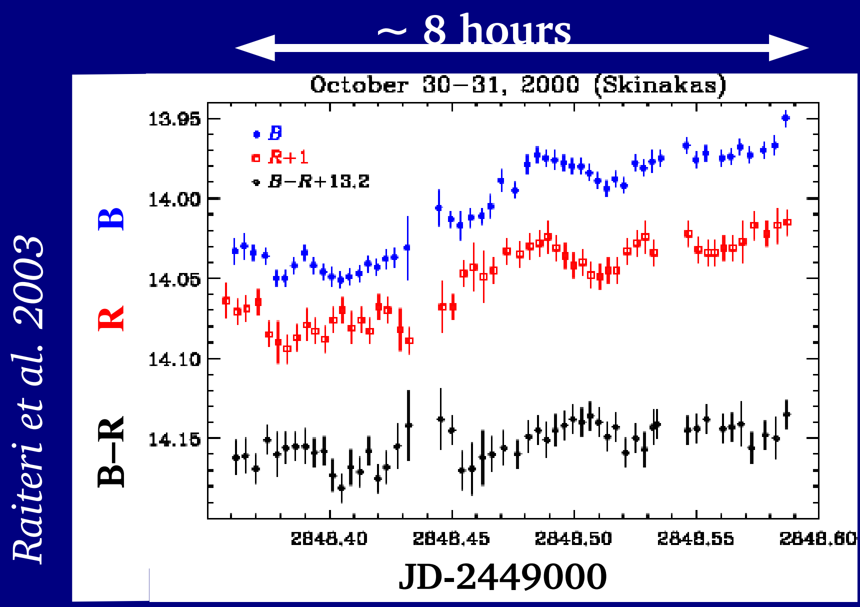

BVRI core-campaign light curves: sampling

- Observing strategy recommended for the core-campaign (Nov. 06-20, 2003)

  ★ *B-V-R-I* sequence: beginning/end of the night

  ★ *B-R-I* sequences: all nighttime hours (when possible)

- Unfavourable weather conditions, relative faintness of the source:

  ★ generally modest *B-V-R-I* data sampling from single observatories

  ★ unprecedented *B-V-R-I* global data sampling

BVRI core-campaign light curves: sampling

R–band light curve of the core campaign

- Lulin
- Mt. Maidanak
- Abastumani
- Crimean
- Tuorla
- MonteBoo
- Perugia
- Heidelberg
- Trebur
- Torino
- Hoher List
- Calar Alto
- KVA
- WHT
- Bell
- St. Louis
- WIYN
- Coyote Hill
- Univ. Victoria

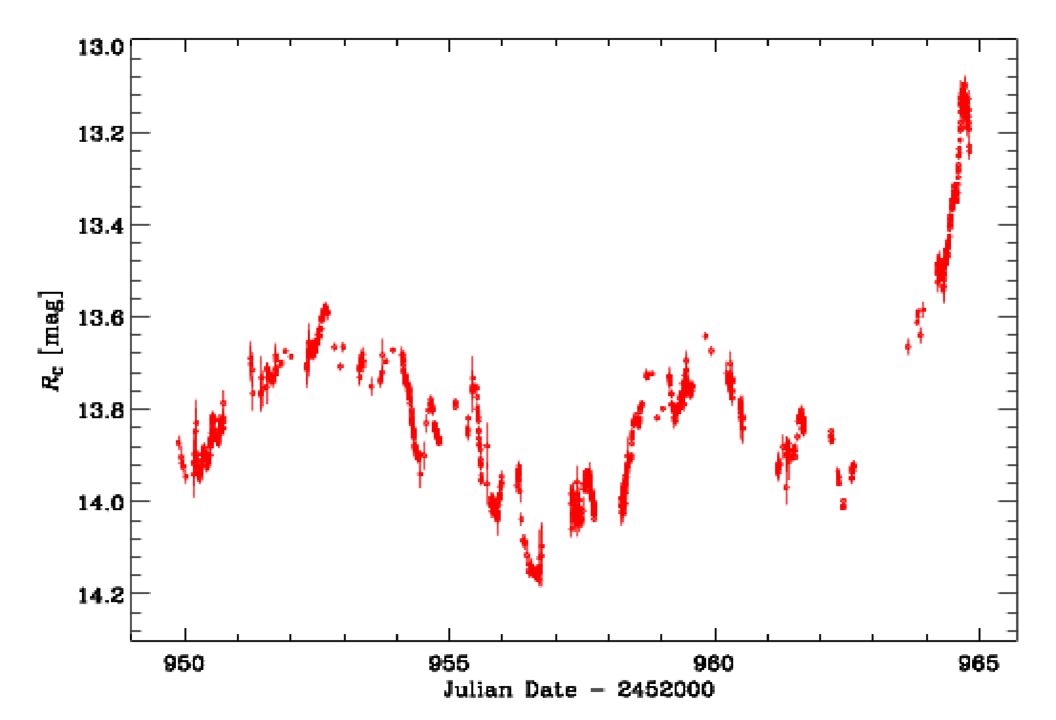

* 19 observatories
* 2849 data-points over ~15 days (~8 data/hour)
* inter-instrumental offsets: [- 0.03; + 0.07] mag

(Ostorero et al. 2005, subm.)

BVRI core-campaign light curves: sampling

R–band light curve from observatories which also took *B,V*, and/or *I* measurements

Lulin
Mt. Maidanak
Crimean
Tuorla
Perugia
Heidelberg
Torino
KVA
WIYN

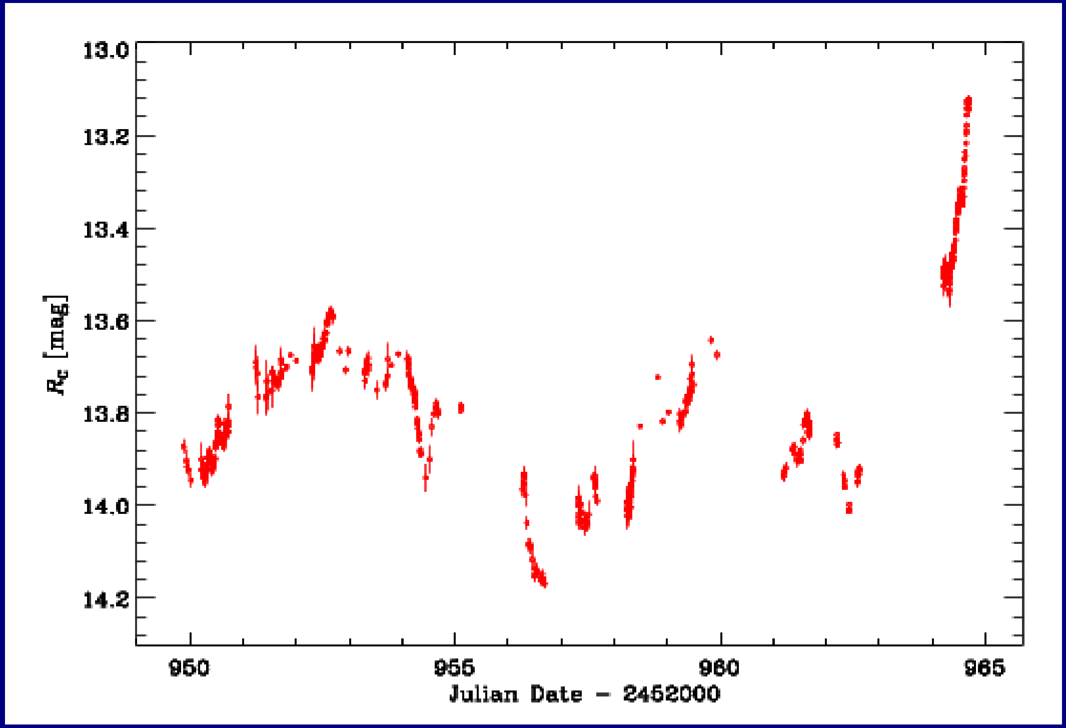

* 9 observatories
* 556 data-points over ~15 days (~1.6 data/hour)
* inter-instrumental offsets: [- 0.02; + 0.06] mag

BVRI core-campaign light curves: results

Scaled optical light curves (and data statistics) from the 9 observatories which took measurements in the in the *R* band and also in the *B*, *V*, and/or *I* bands

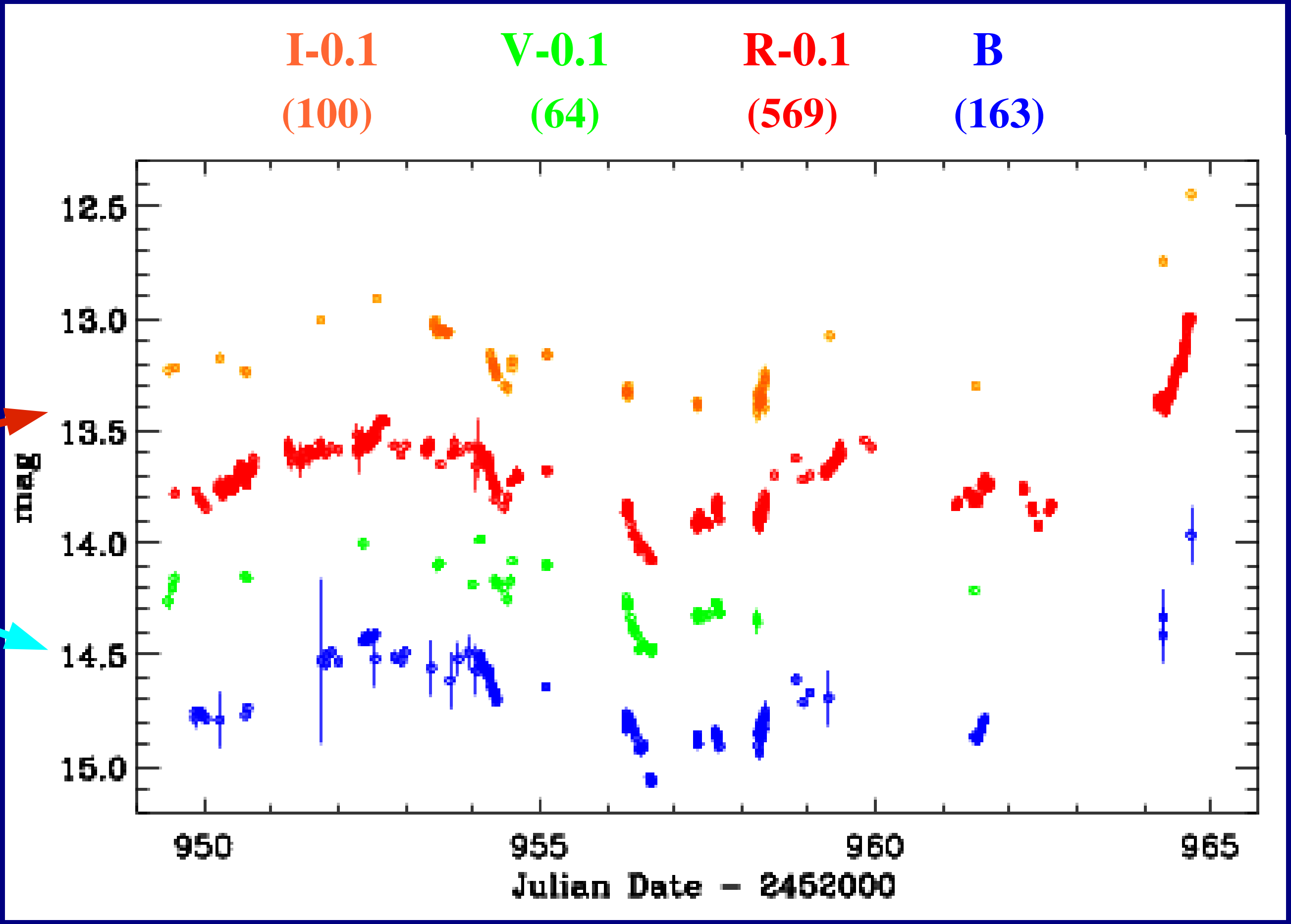

B and *R*: best-sampled light curves

(Calibration stars: 3 -5 -6; no inter-instrumental offsets applied)

Colour analysis: indices

Colour indices were computed by

- applying cuts on photometric accuracy: err_B<0.03 mag, err_VRI<0.02 mag
- coupling 2-filter (among B,V,R,I) data taken from the same observatory within a given Δt_{max} (no inter-instrumental offset applied)

in order to mimimize errors and spread.

Δt=30 min - Colour indices

Index	Mean	σ	N
B-V	0.435	0.040	195
B-R	0.844	0.044	717
B-I	1.355	0.021	134
V-R	0.414	0.017	233
V-I	0.931	0.016	49
R-I	0.527	0.021	154

B-R: best-sampled colour index

Colour analysis: *B-R* index

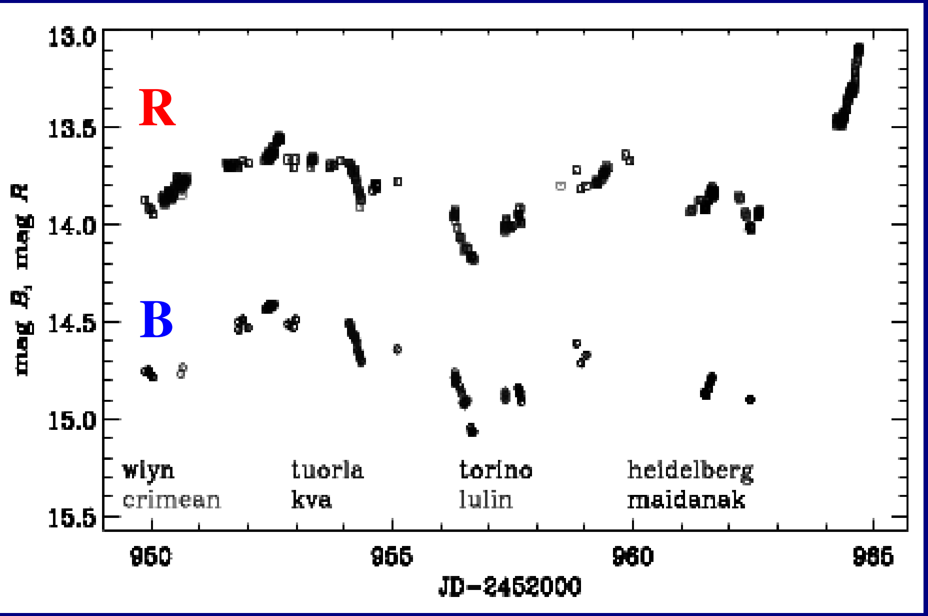

err_B<0.03 mag
err_R<0.02 mag

$\Delta t_{max,BR}$=30 min.

Colour analysis: *B-R* index

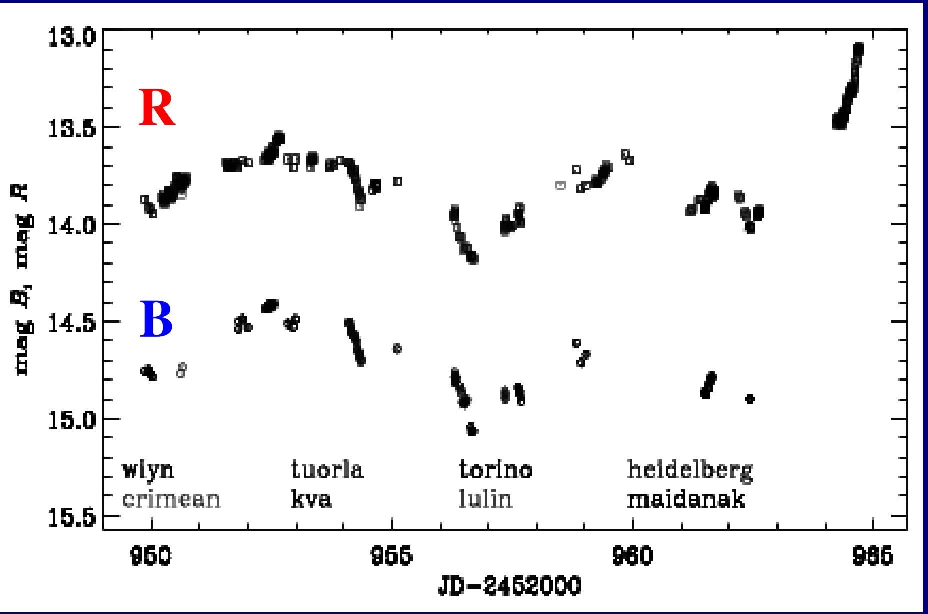

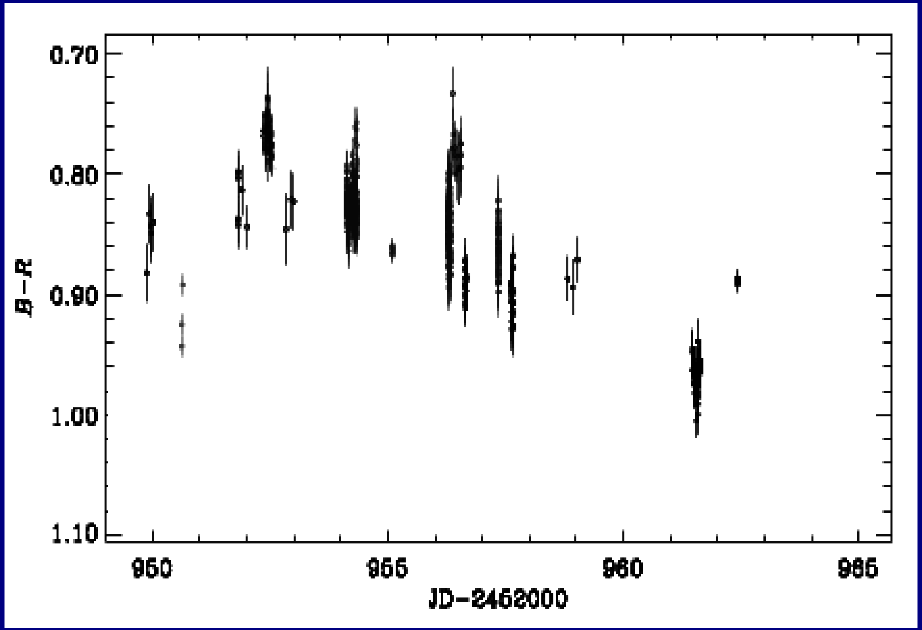

err_B<0.03 mag
err_R<0.02 mag

$\Delta t_{max,BR}$=30 min.

Colour analysis: *B-R* index

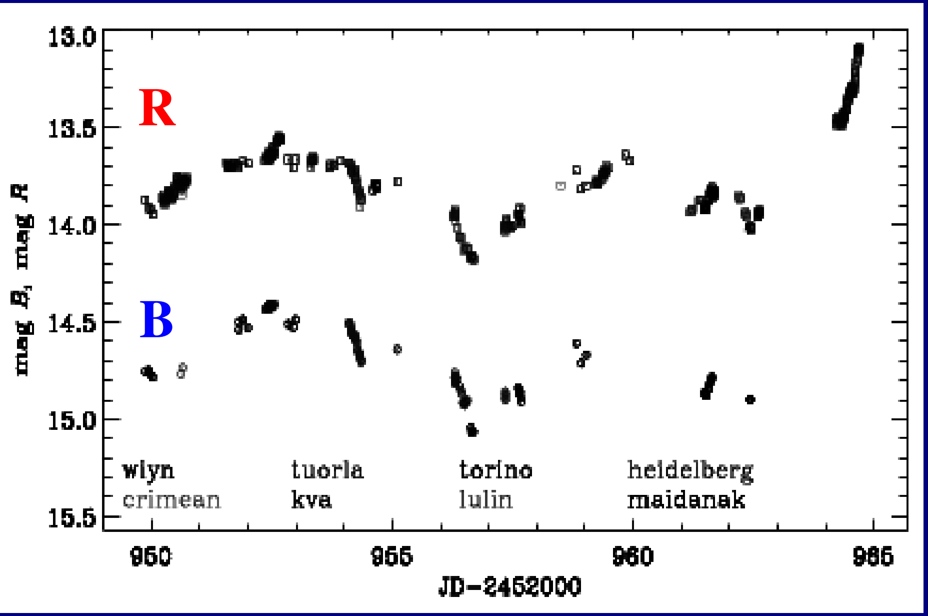

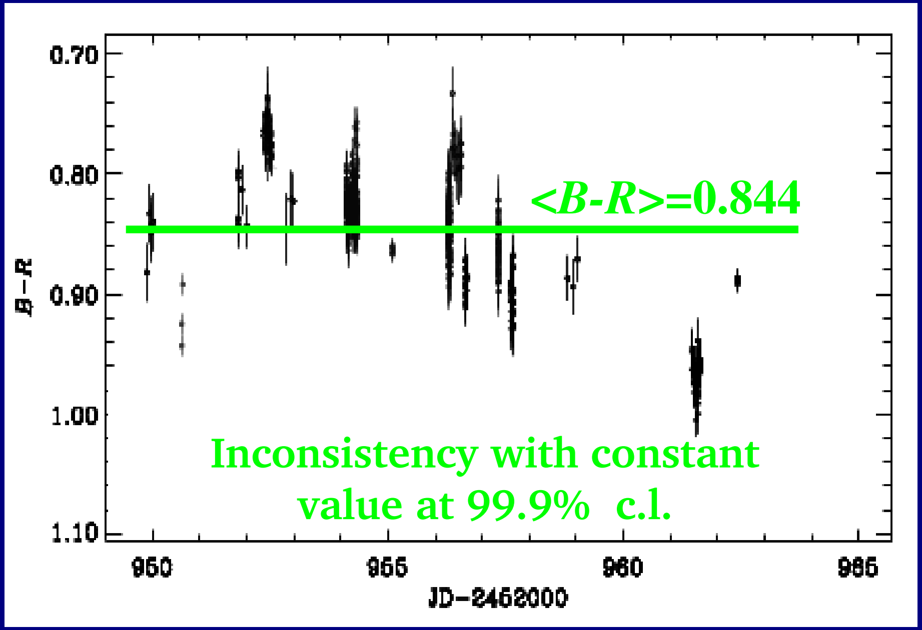

err_B<0.03 mag
err_R<0.02 mag

$\Delta t_{max,BR}$=30 min.

Colour analysis: *B-R* index

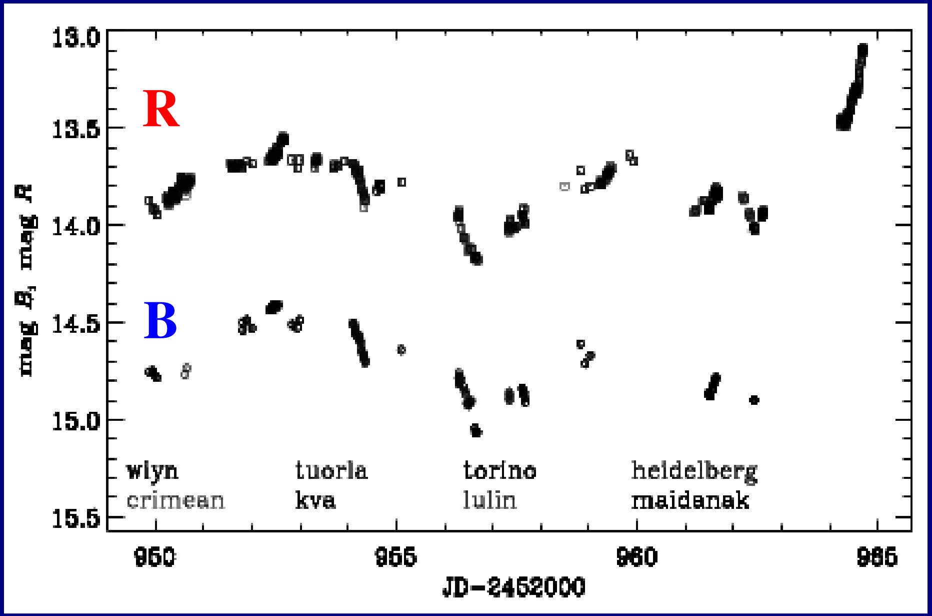

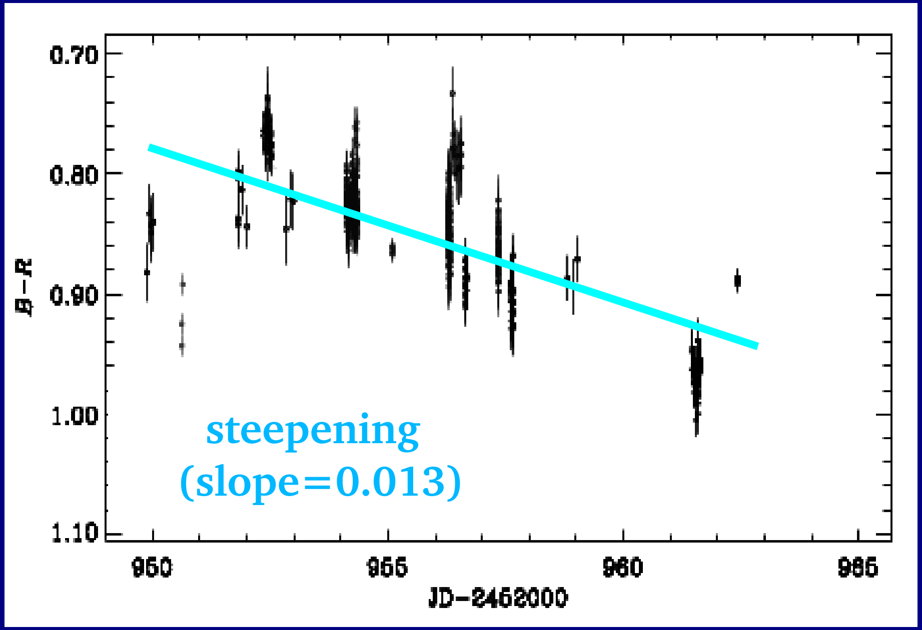

err_B<0.03 mag
err_R<0.02 mag

$\Delta t_{max,BR}$=30 min.

Colour analysis: *B-R* index

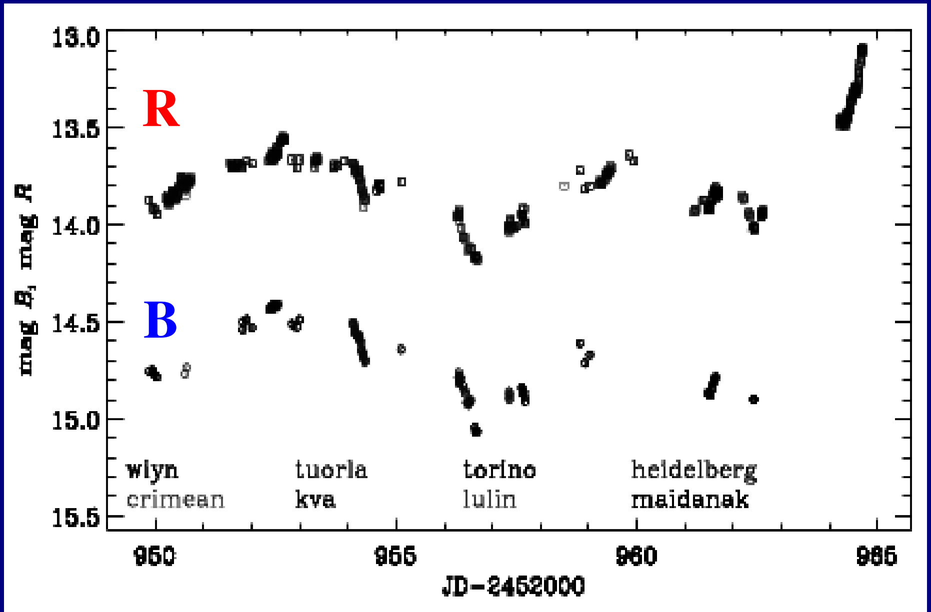

err_B<0.03 mag
err_R<0.02 mag

$\Delta t_{max,BR}$=30 min.

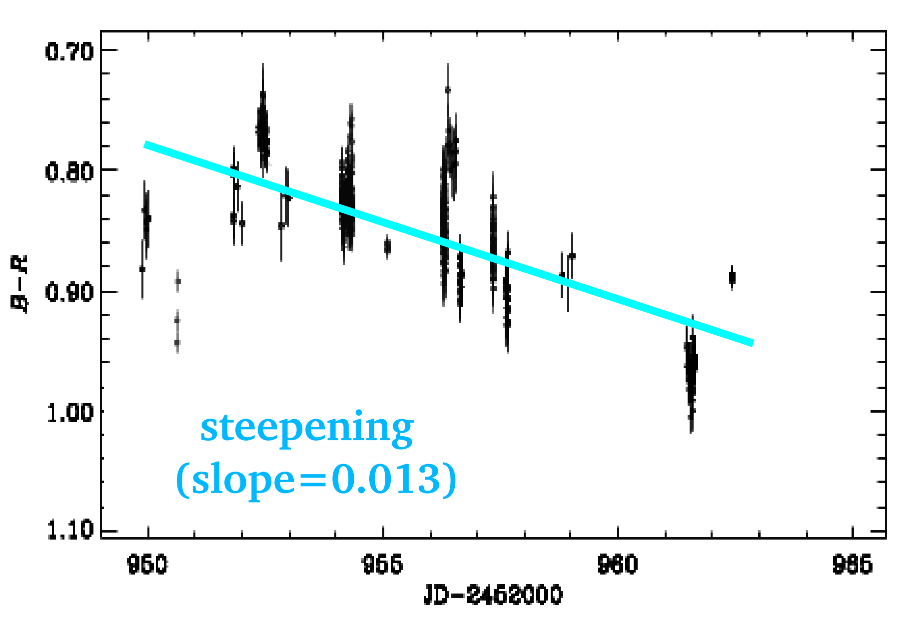

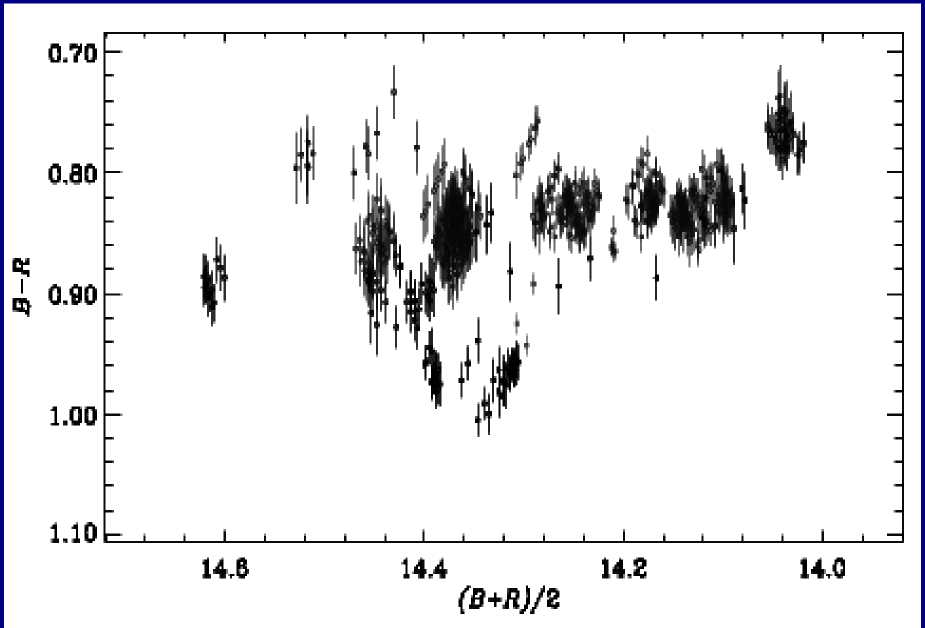

Colour analysis: *B-R* index

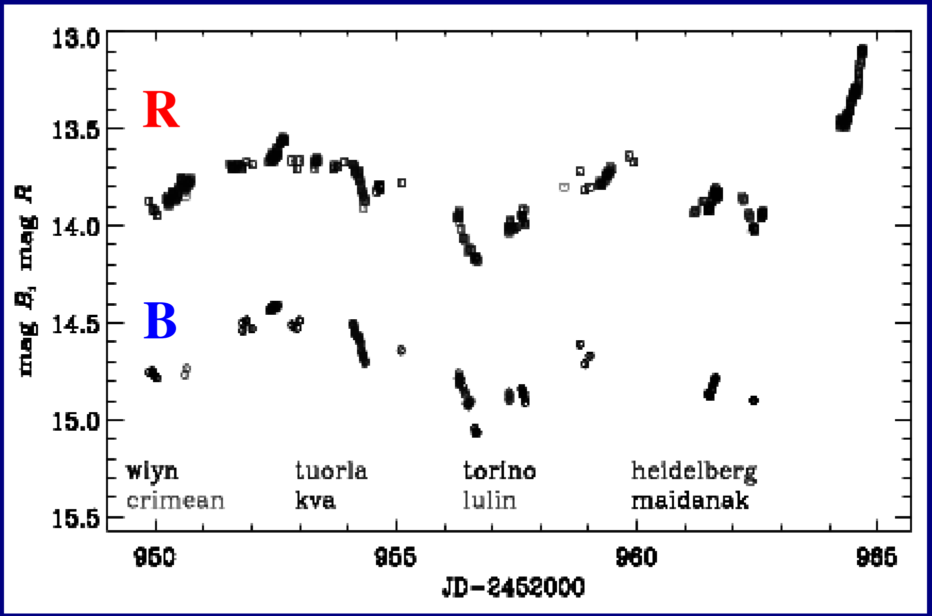

err_B<0.03 mag
err_R<0.02 mag

$\Delta t_{max,BR}$=30 min.

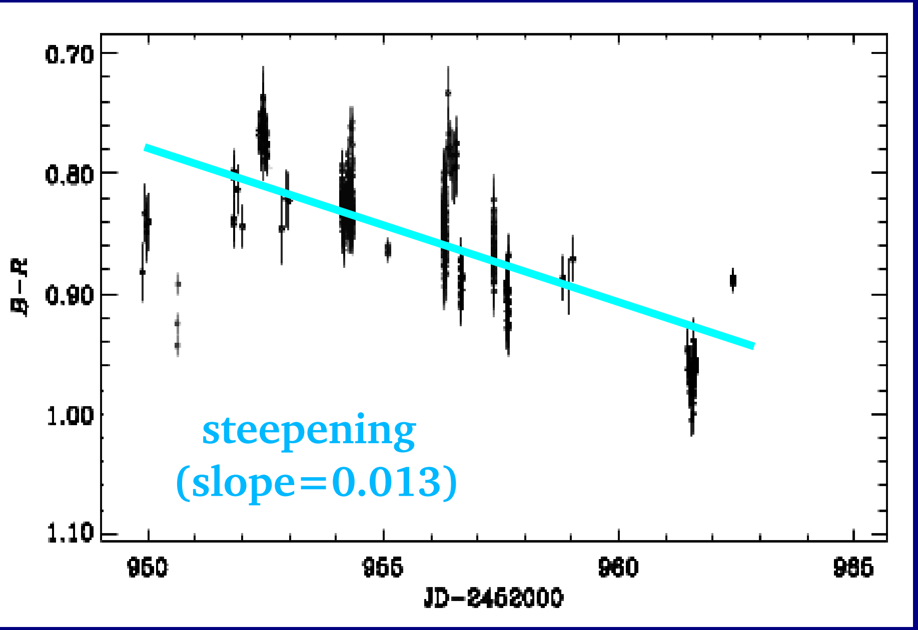

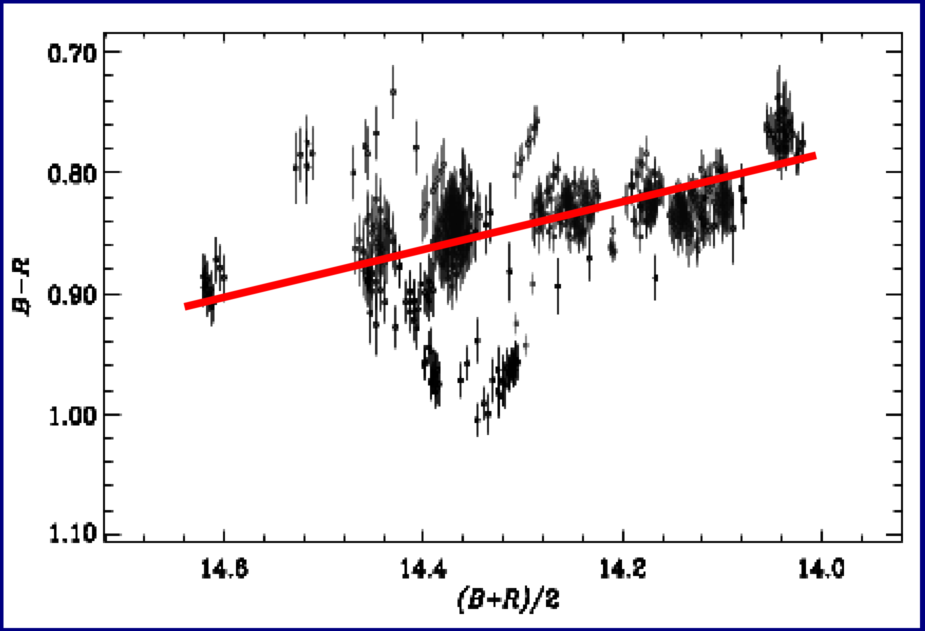

flatter-when-brighter (slope=-0.186)

$r_{Pearson}=0.477$; $P(>r)=5.151 \cdot 10^{-42}$

Colour analysis: *B-R* index

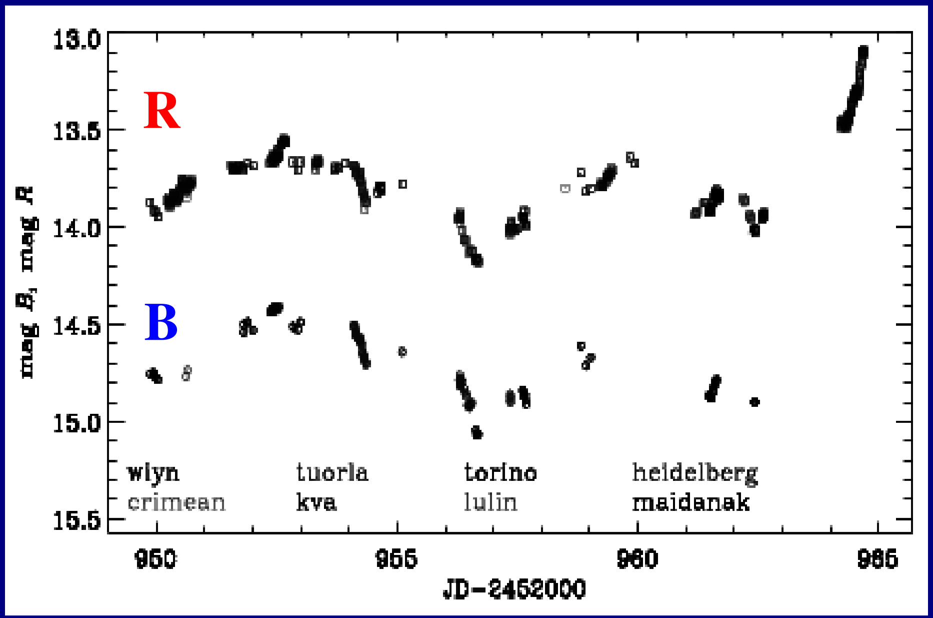

err_B<0.03 mag
err_R<0.02 mag

$\Delta t_{max,BR}$=30 min.

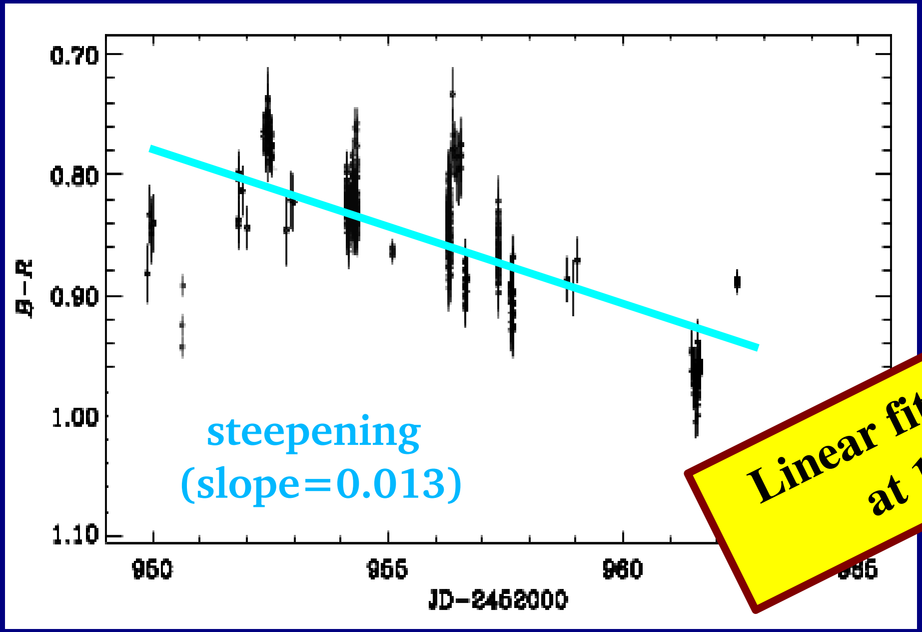

steepening
(slope=0.013)

Linear fit rejected at 1% s.l.

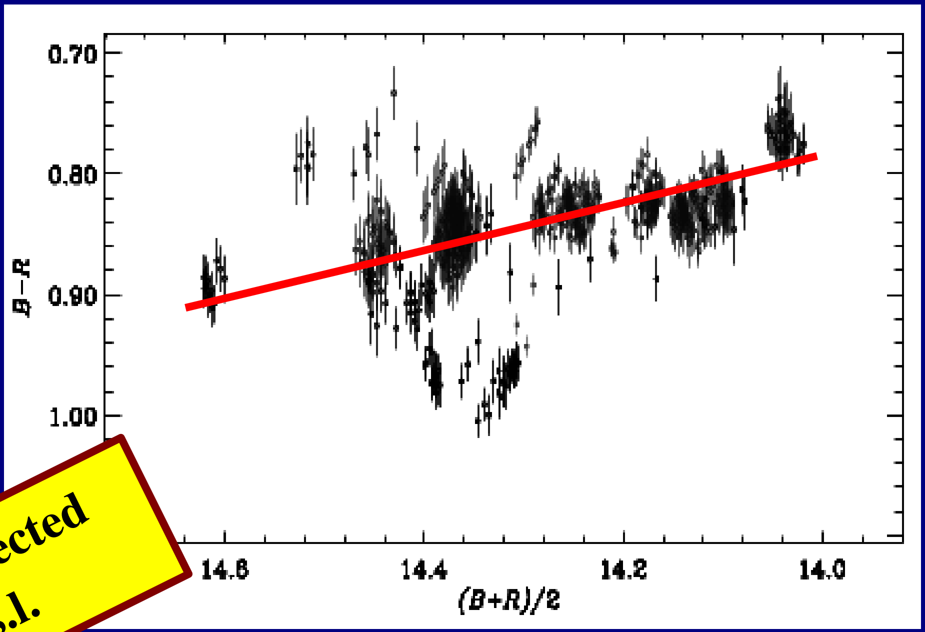

flatter-when-brighter (slope=-0.186)

$r_{Pearson}$=0.477 ; P(>r)=5.151 · 10^{-42}

Colour analysis: *B-R* index

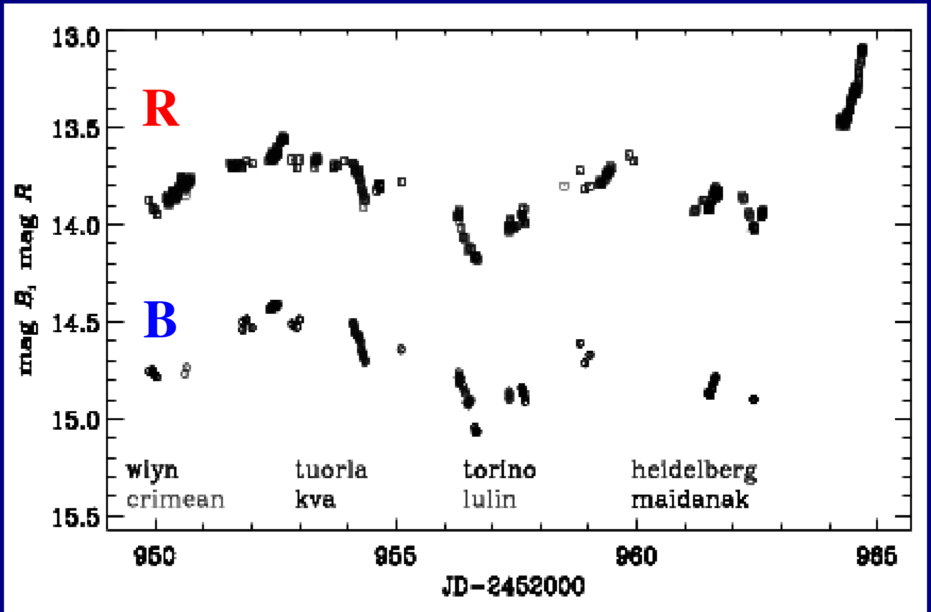

err_B<0.03 mag
err_R<0.02 mag

$\Delta t_{max,BR}$=30 min.

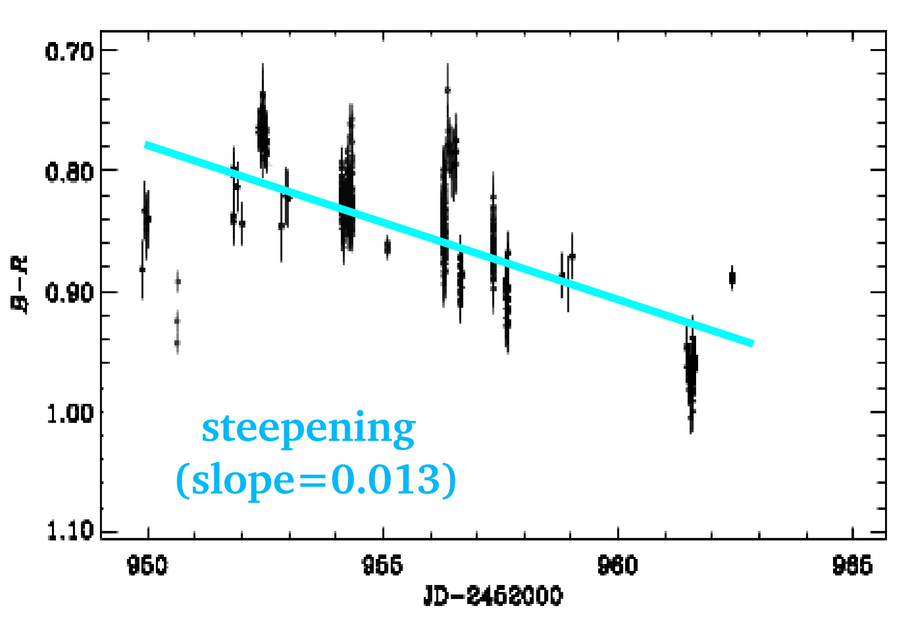

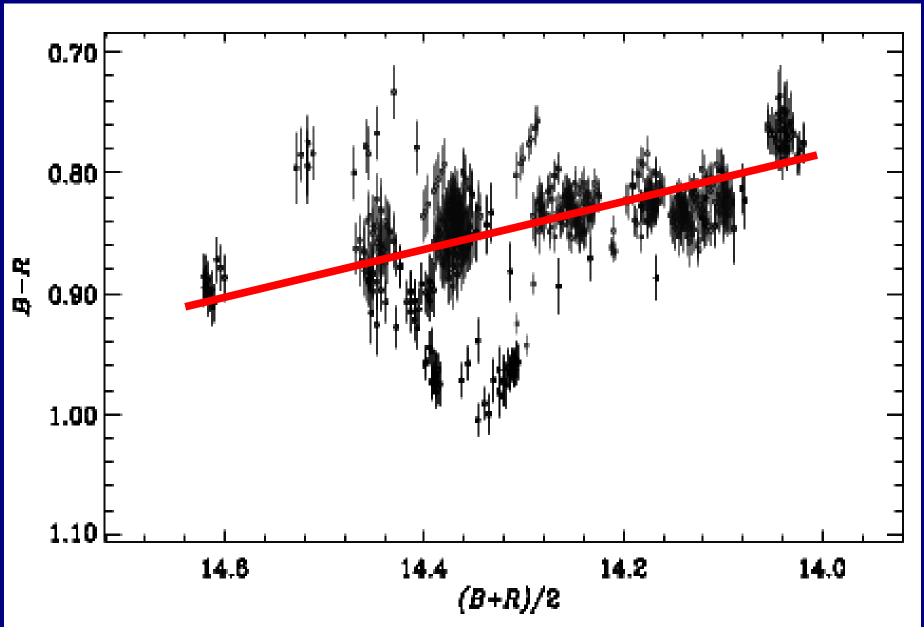

flatter-when-brighter (slope=-0.186)

$r_{Pearson}$=0.477 ; $P(>r)=5.151 \cdot 10^{-42}$

Colour analysis: *B-R* index

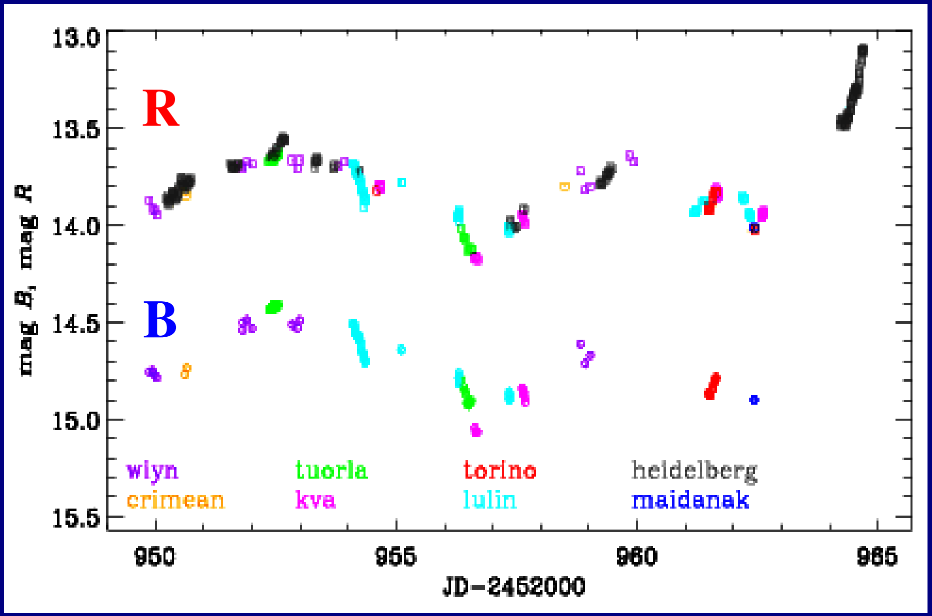

- Possible dependence of the *B-R* colour index on systematic inter-instrumental effects
- Lack of simultaneous *B-R* indices from different observatories prevents us to correct for instrumental offsets

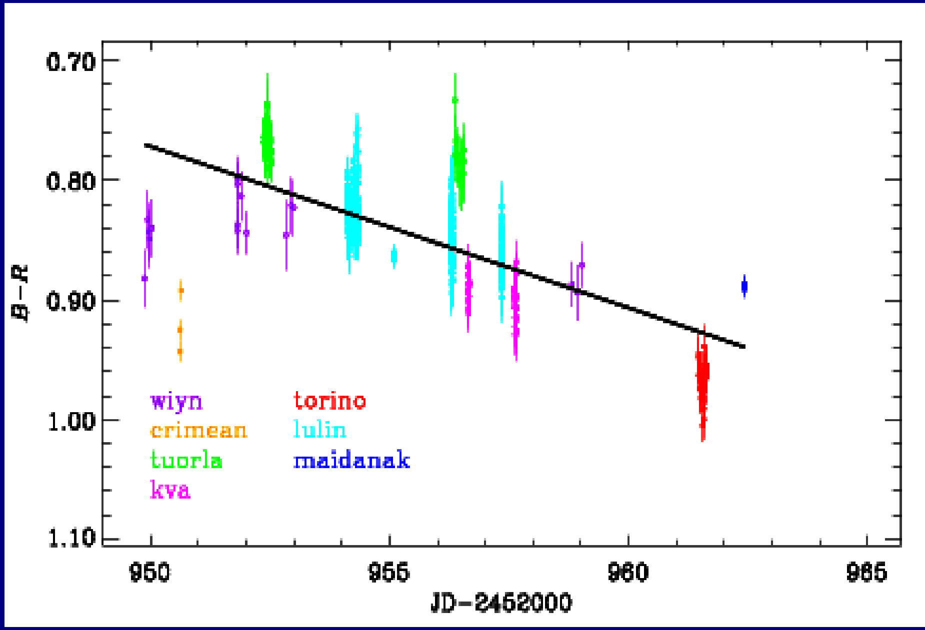

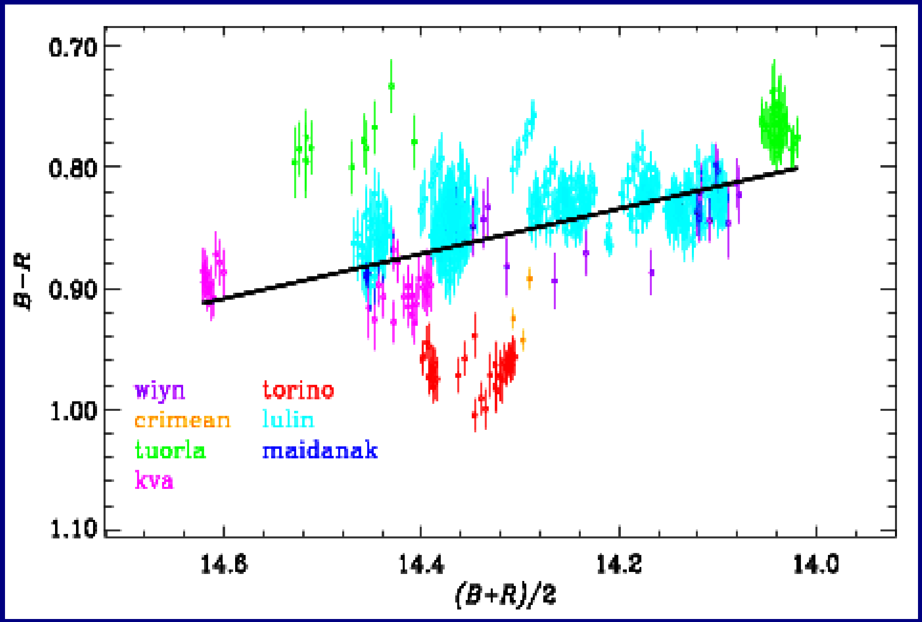

Colour analysis: intranight *B-R* index

Best single-telescope *BR* intranight observations: 1.0-m telescope at Lulin Observatory (Taiwan):

- **no well-defined trend in the colour variability**

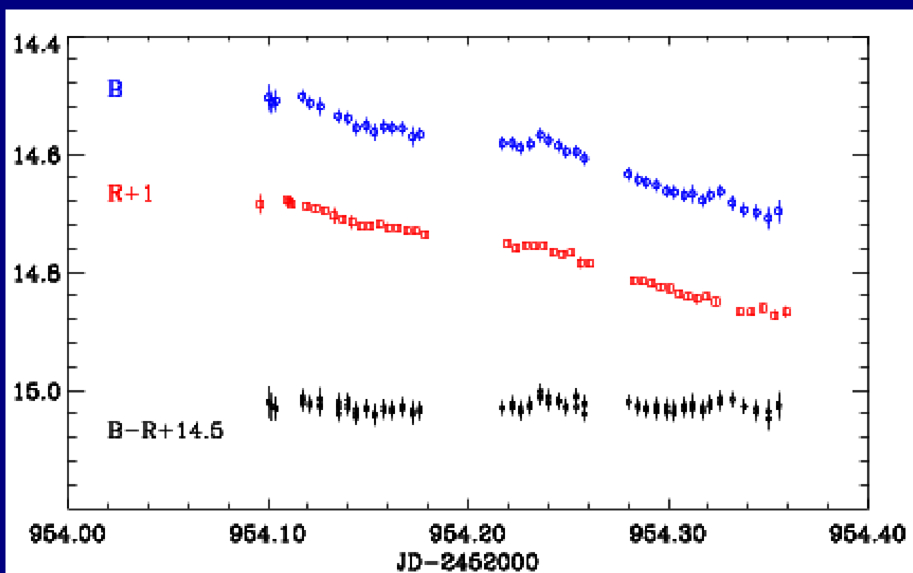

~ 7 hours

~ 1 hour

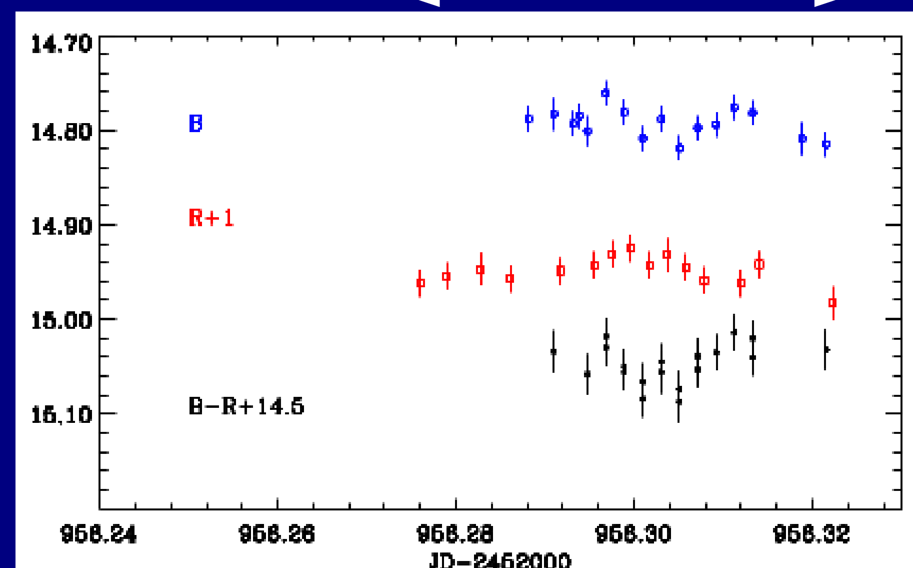

Summary

- The optical *BVRI* light curves of S5 0716+71 during the core campaign (Nov. 06-20, 2003) were assembled and the colour indices computed.
- Indication of steepening of the optical spectra during the 2-week campaign.
- Mean colour index: $<B\text{-}R> = 0.844$ ($<\alpha_{BR}> = 1.15$)

- No obvious correlation between the time evolution of the colour index and that of the brightness over the 2-week observing period.
- Significant correlation between colour indices and brightness: "*flatter-when-brighter*" chromatic behaviour.
- Possible systematic inter-instrumental effects might hide the colour time evolution, but would most likely weaken the colour-brightness correlation. Elimination of colour offsets difficult due to lack of simultaneous colour indices from different observatories.

- Single-telescope *BR* intranight measurements do not display any correlation between the time evolution of colour and brightness.

Structural variability in BL Lacertae

Uwe Bach, M. Villata, C.M. Raiteri
INAF-Osservatorio Astronomico di Torino

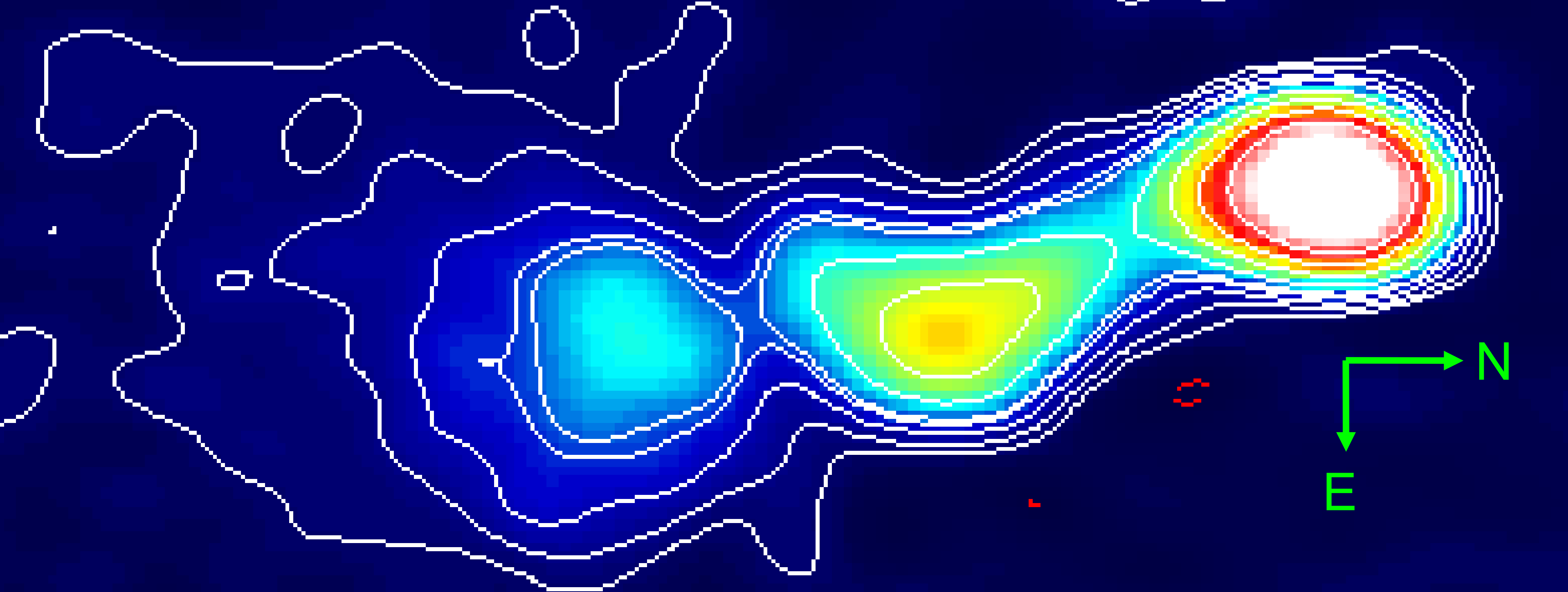

I. Agudo (MPIfR, Bonn), R.L. Mutel (U. Iowa), G. Denn (MSC, Denver), J.L. Gomez (IAA, Granda), et al.

6th ENIGMA Meeting, Kinsale, November 23, 2005

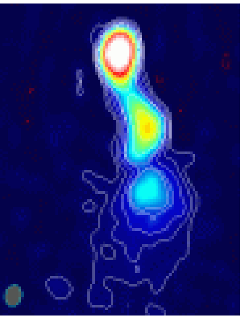

Contents

- Intro on BL Lacertae
- BL Lac on parsec-scales
  - VLBI images
  - light curve
  - spectral index
- Cross-Correlations
- Possible jet scenario
- Summary
- Outlook

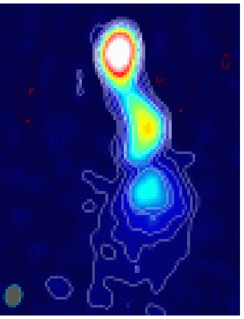

BL Lacertae

- Eponym of the BL Lac objects.
- redshift = 0.069 ~ 300 Mpc.
- Highly variable at all wavelengths.
- Correlated variability:
    - sub-mm and X-rays (Kawai et al 1991).
    - radio-spectrum and optical (Villata et al. 2004b).

VLBI observations show:

- Compact core and a bent parsec-scale jet.
- Nearly no kpc-scale structure.
- Regular ejections of superluminal jet components.

BL Lacertae

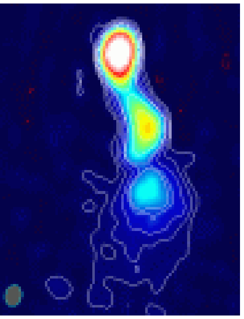

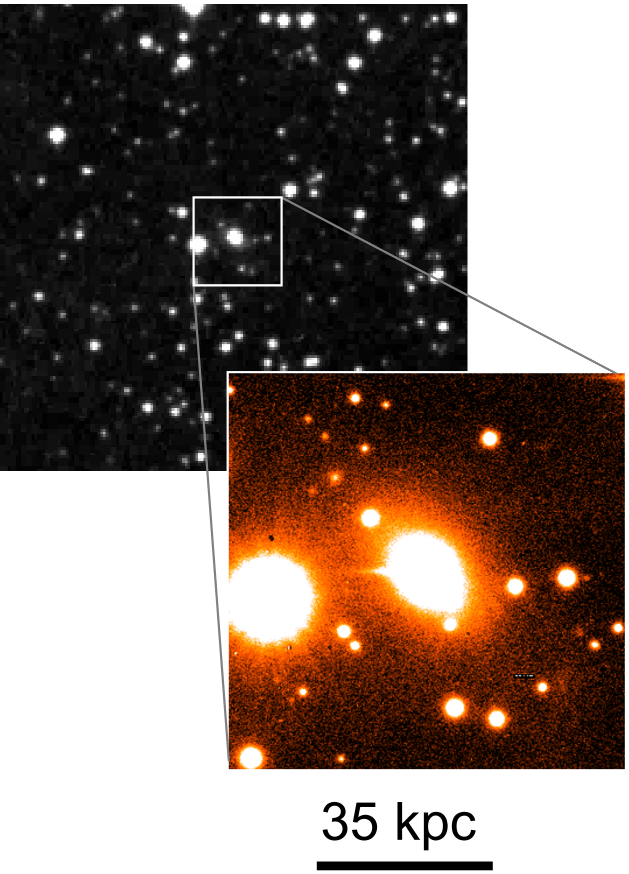

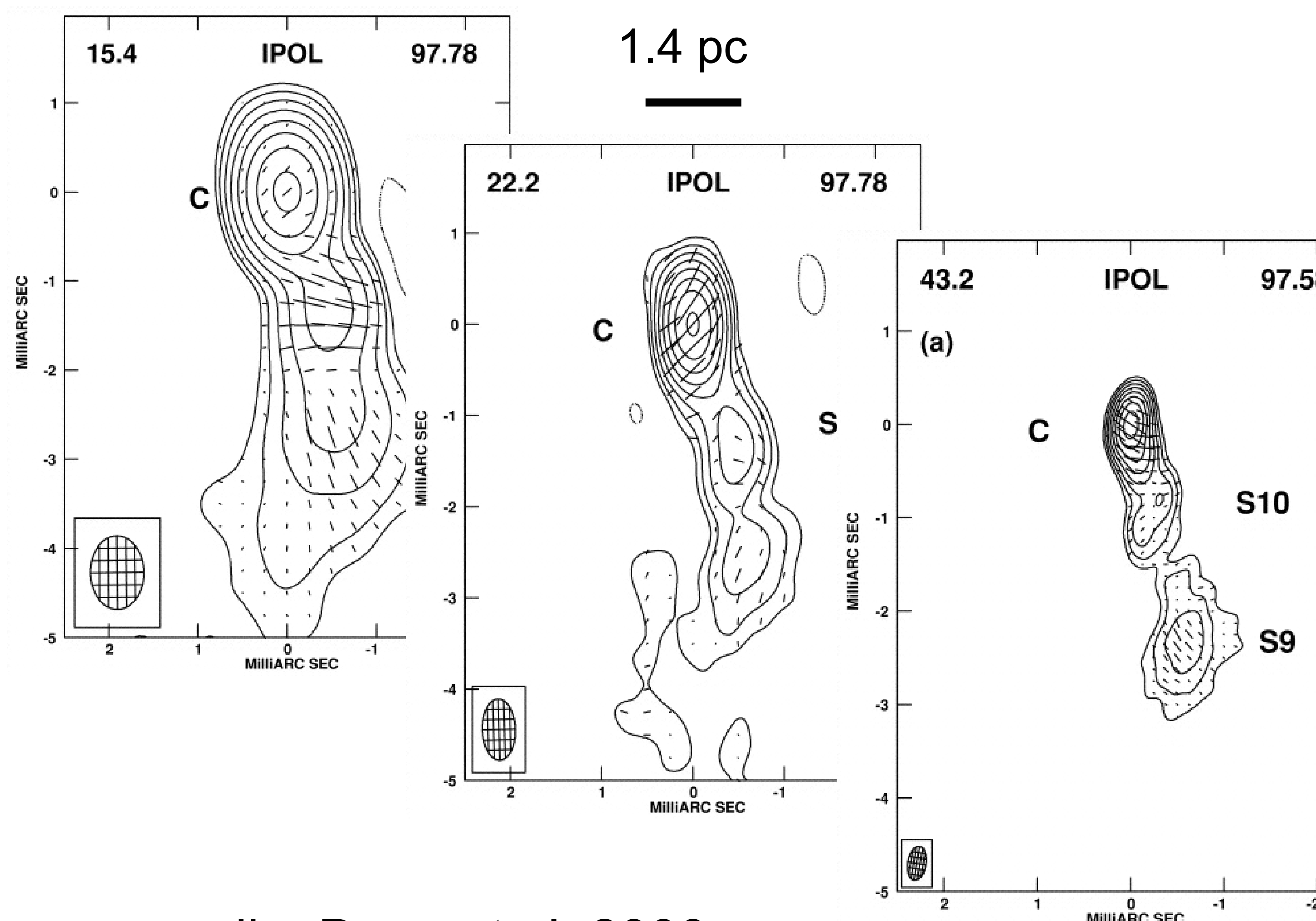

Optical: DSS and NOT images; radio: Denn et al. 2000

Correlated Variability

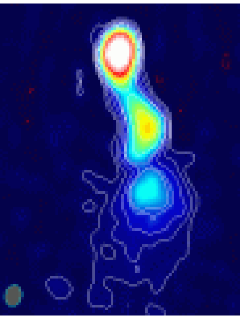

1994 2004

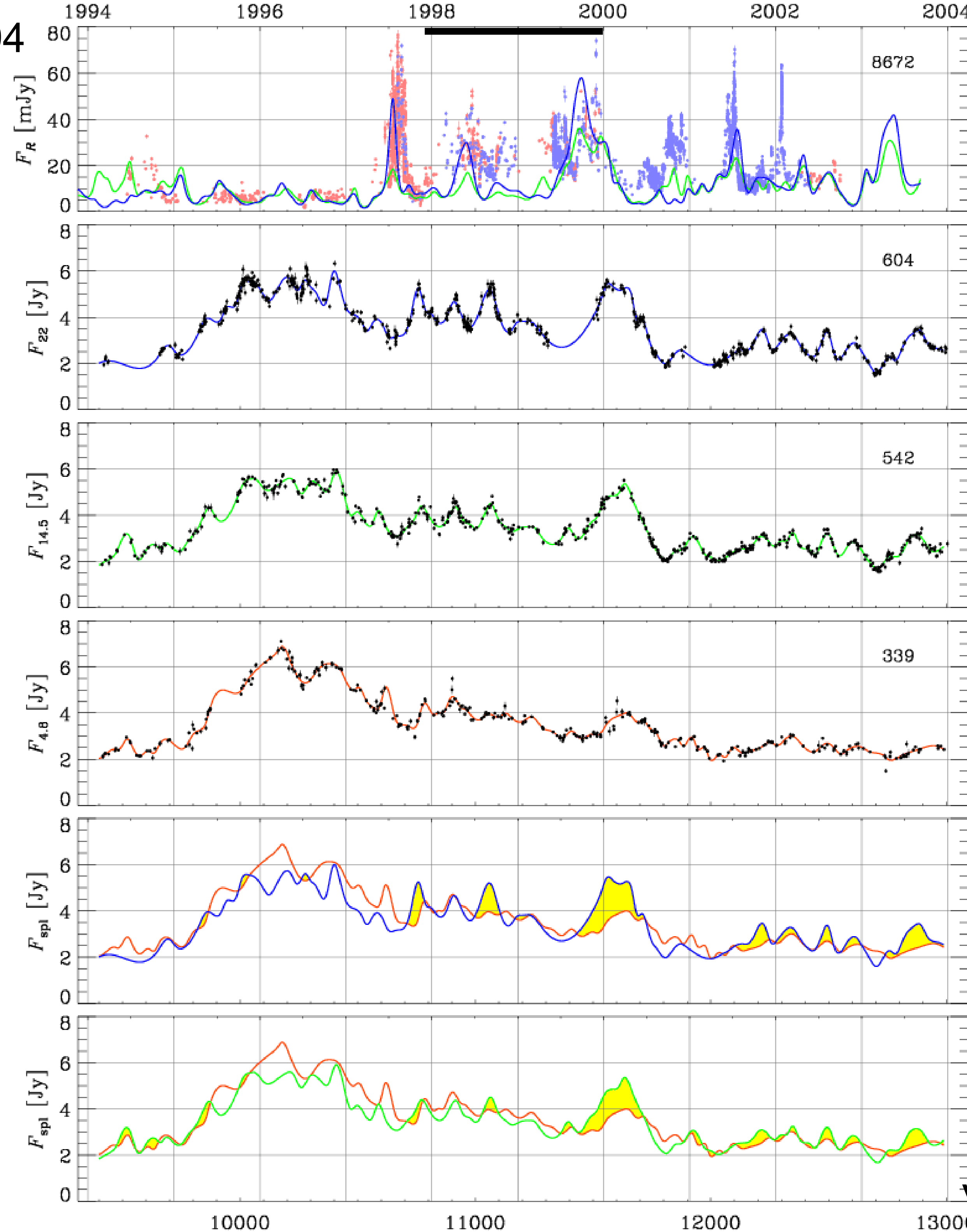

Villata et al. 2004b

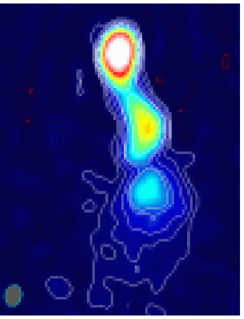

Radio Cross-Correlation

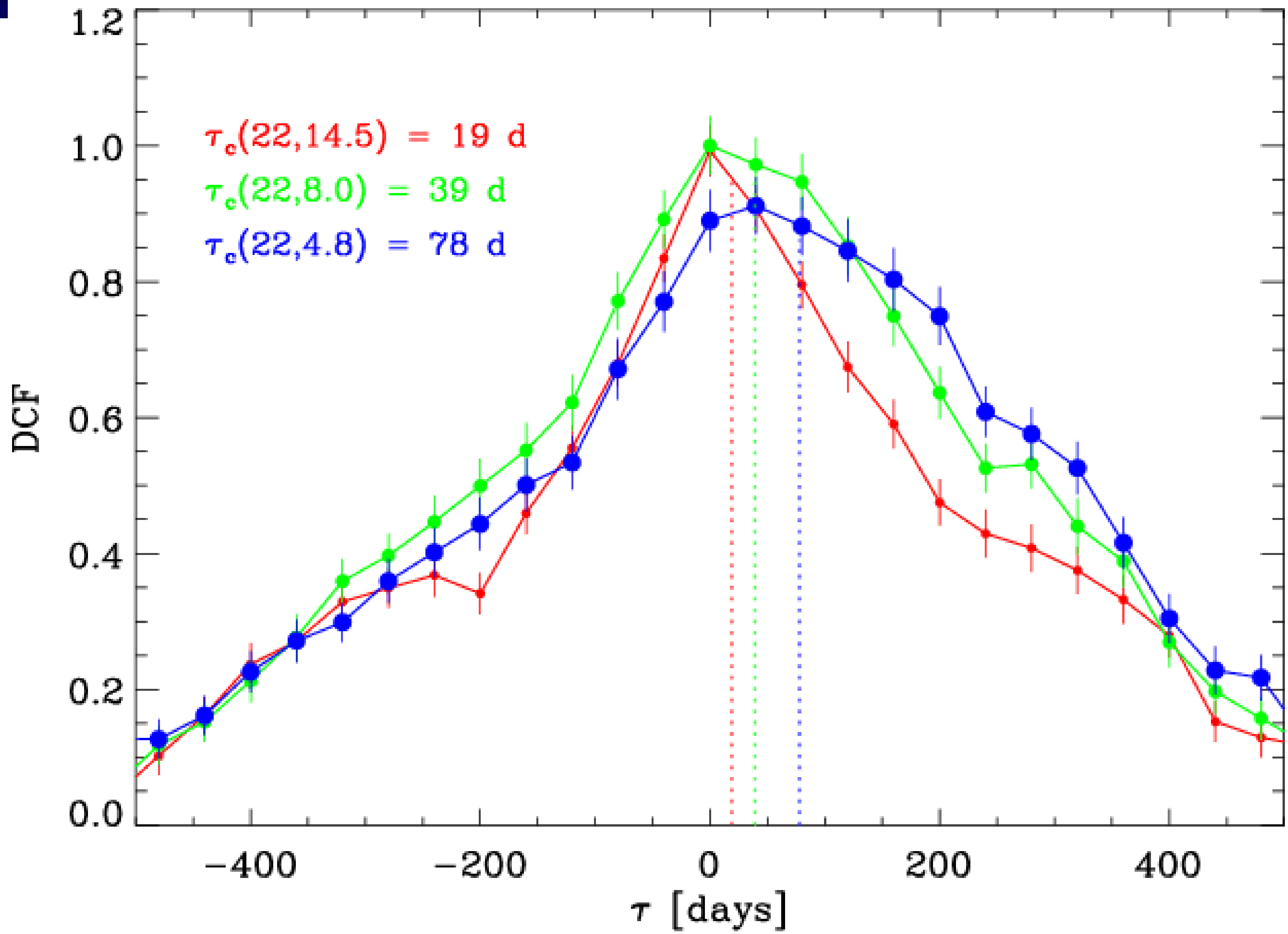

Villata et al. 2004b

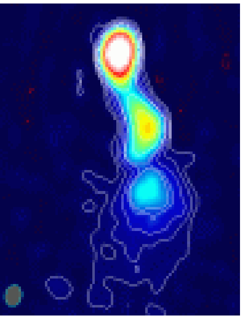

Cross-Correlations
R band-$h_{22/5}$

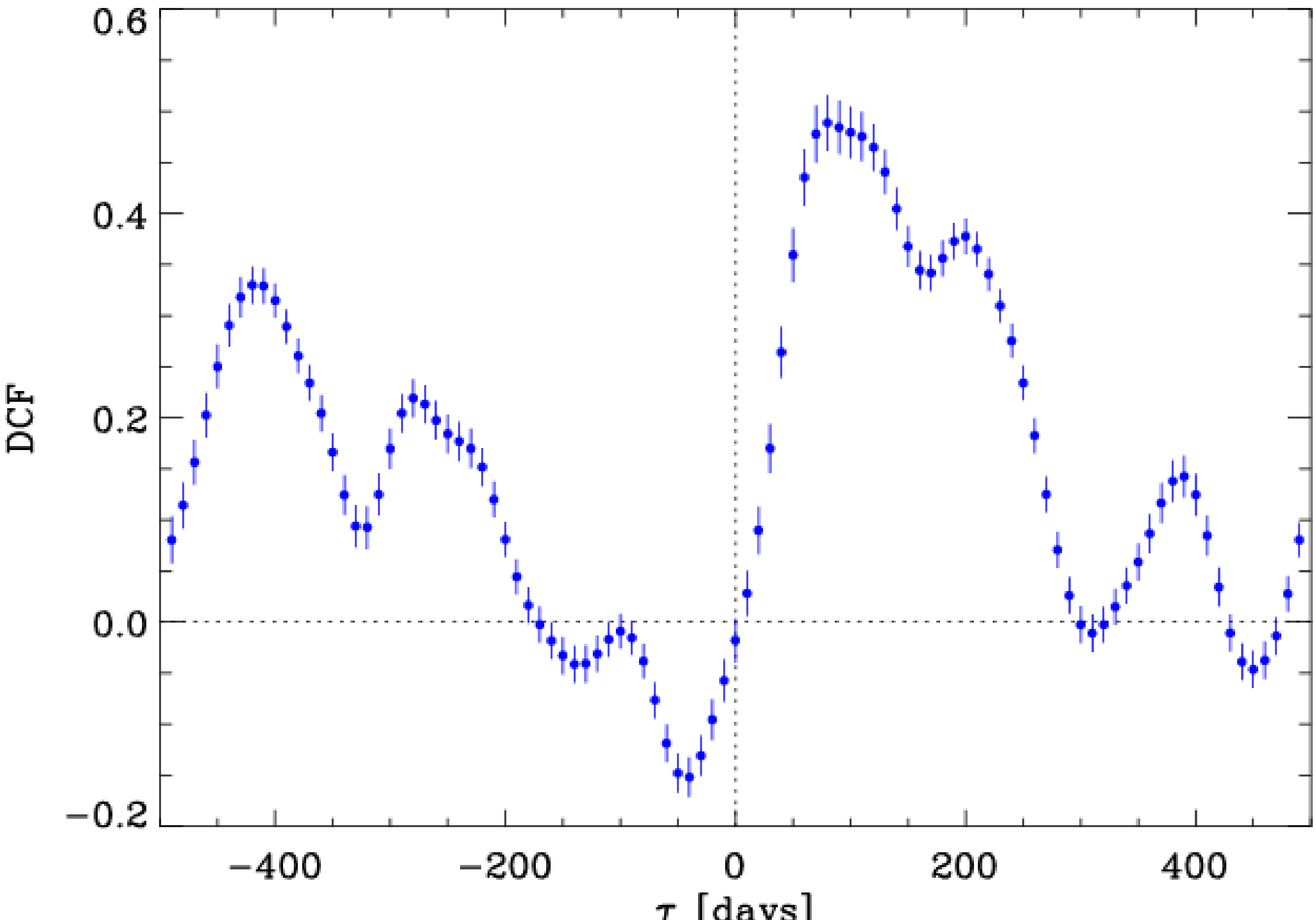

Villata et al. 2004b

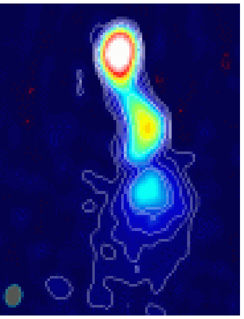

Very Long Baseline Interferometry (VLBI)

- Collected 108 epochs of VLBI data* (1995-2003):
  47 at 43 GHz, 29 at 22 GHz & 32 at 15 GHz.
- Spectral index maps (22/43 GHz) for all simultaneous epochs (#28)
- Separated light curves for the core and different parts of the jet

* VLBA 2cm Survey, MOJAVE, Mutel et al., Marscher et al., Gomez et al., own data

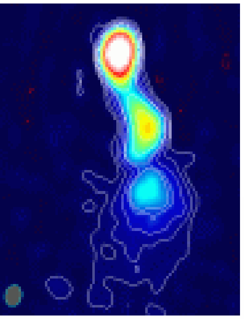

Series of 43 GHz Images

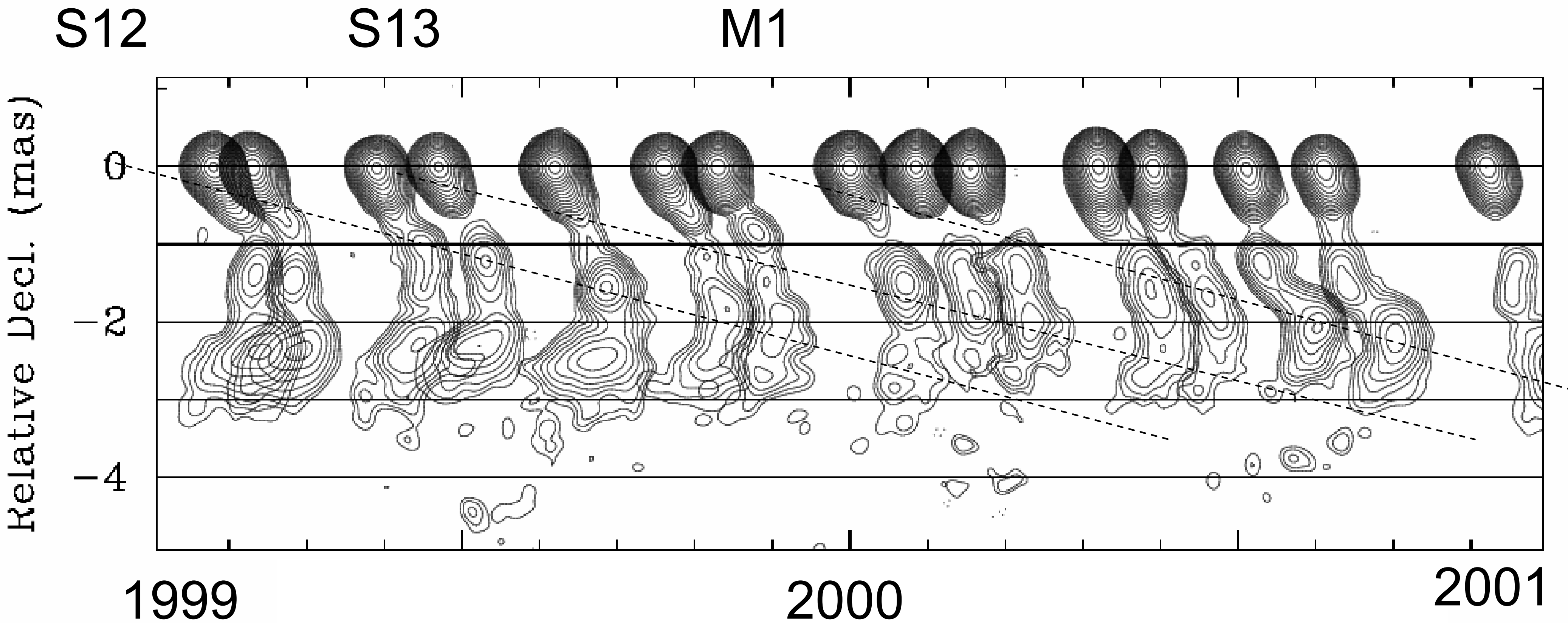

$\beta_{app} \approx 8\ c$

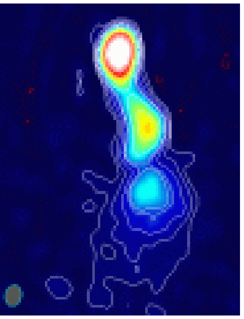

Core and Jet Regions

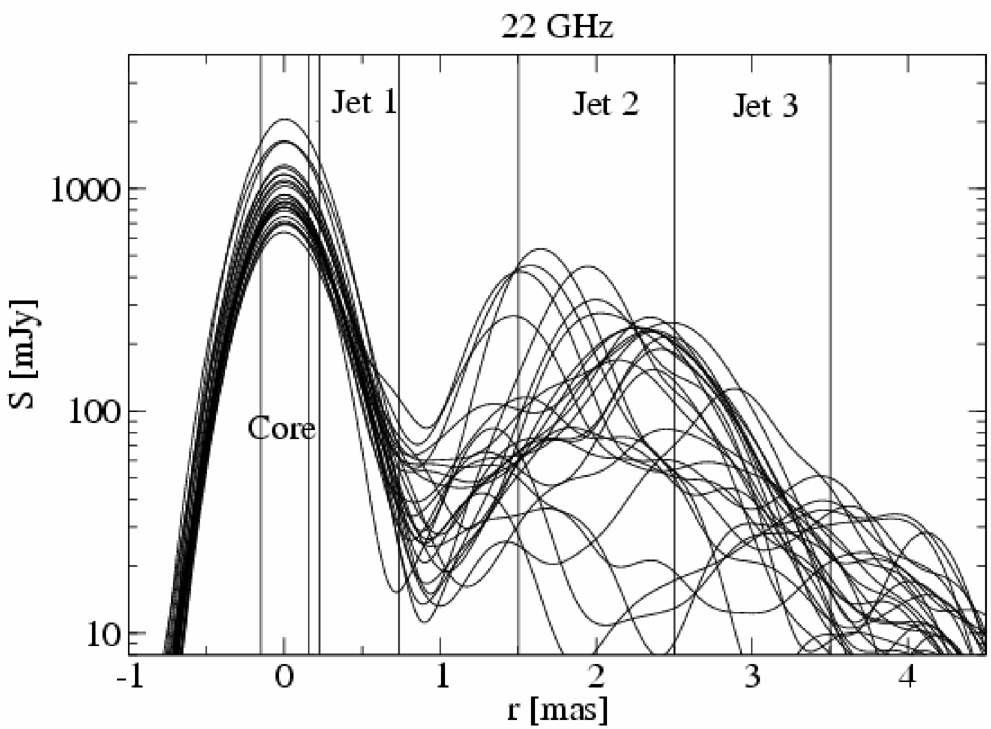

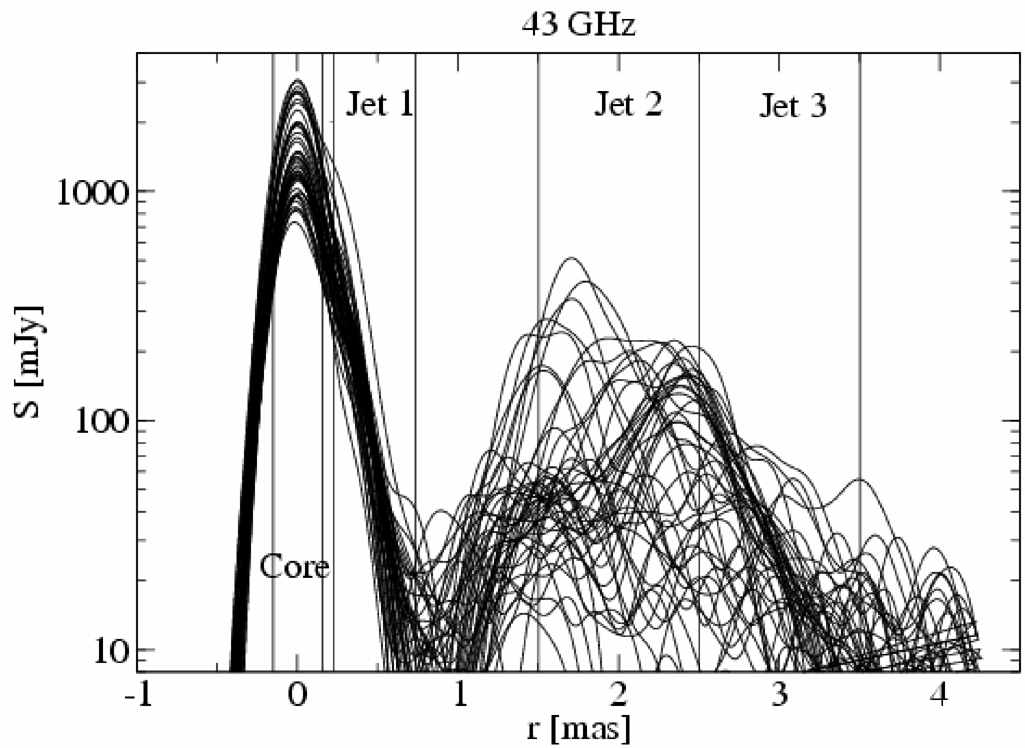

Light Curves

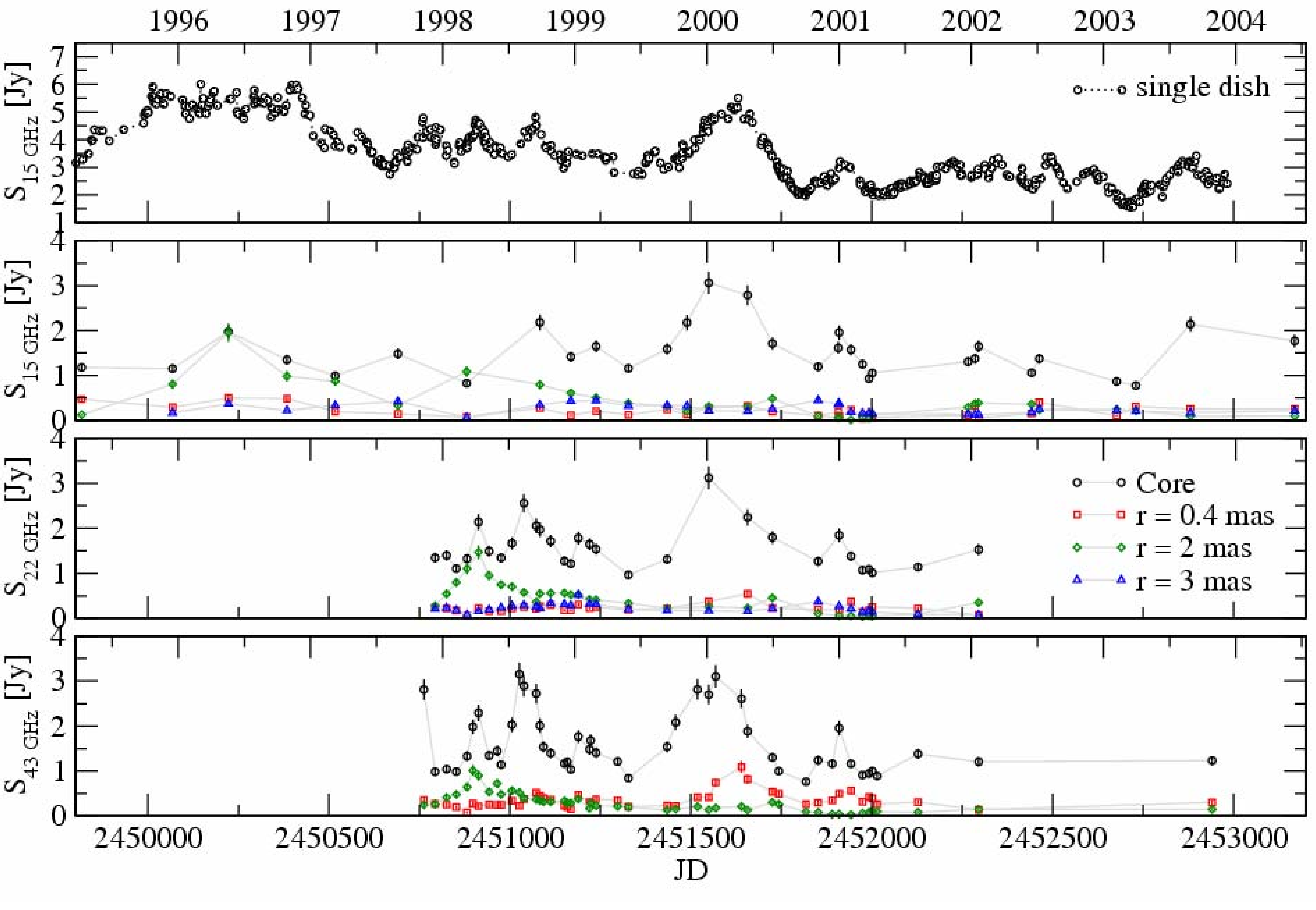

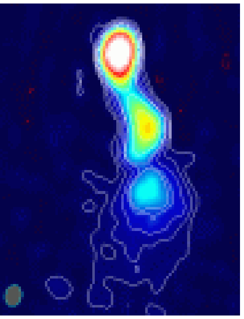

Spectral Index Images

1998.97 | 1999.16 | 1999.40

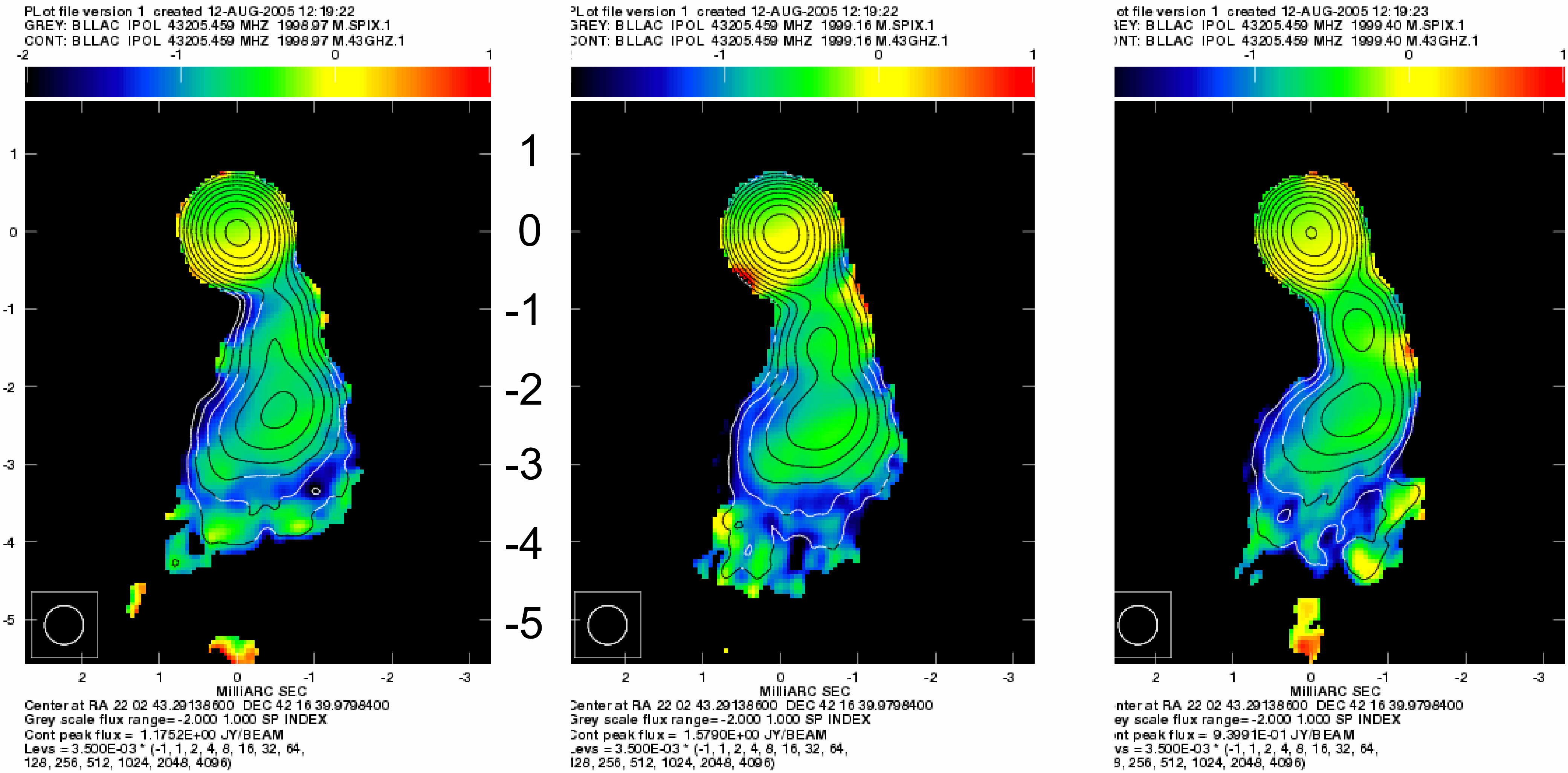

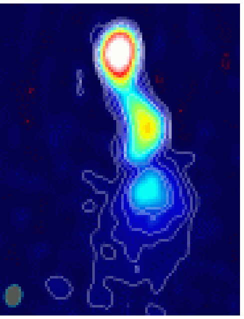

Evolution of α ($S \propto \nu^{\alpha}$)

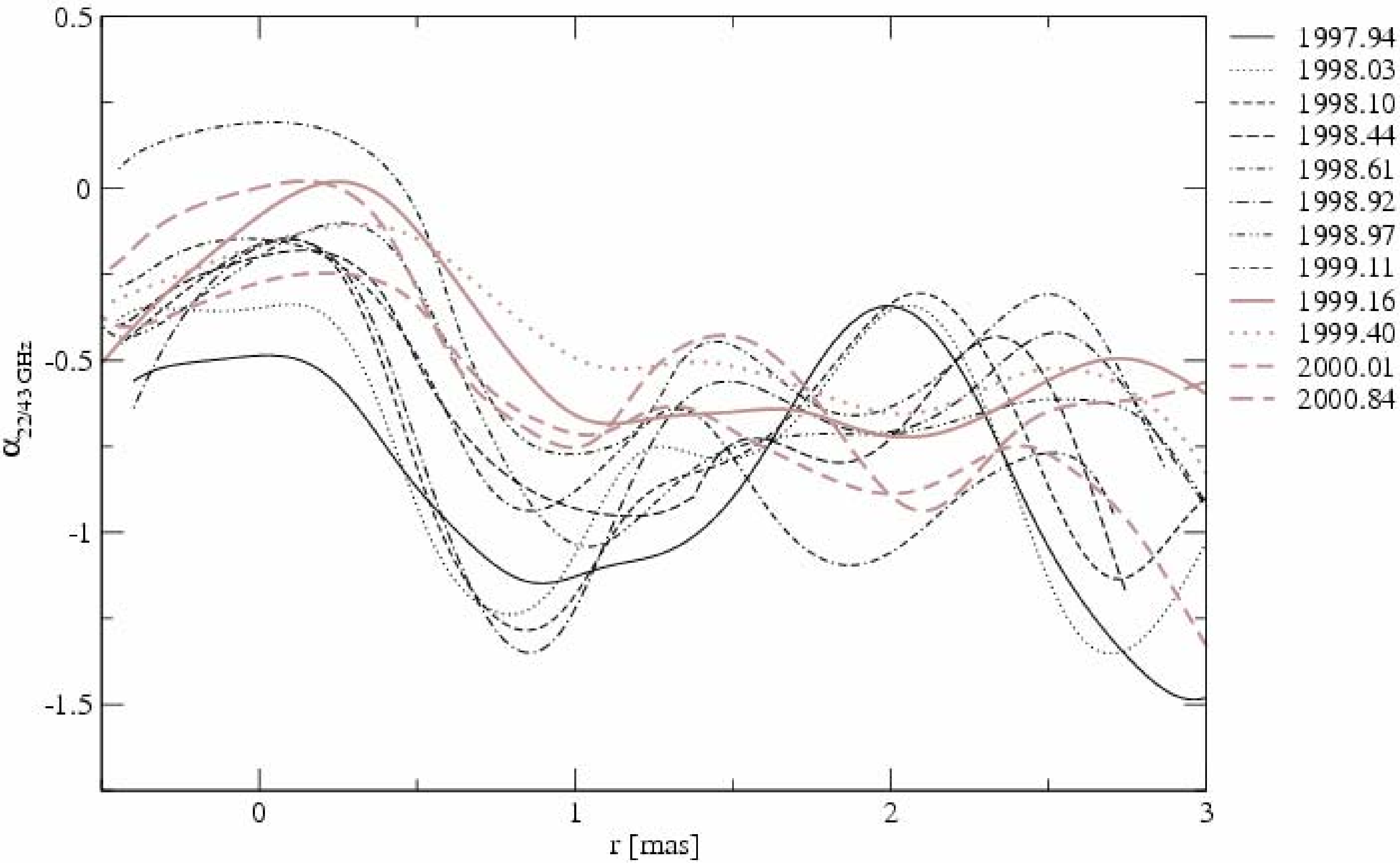

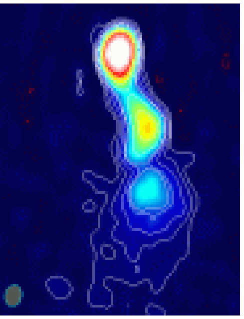

Single Dish Spectral Index

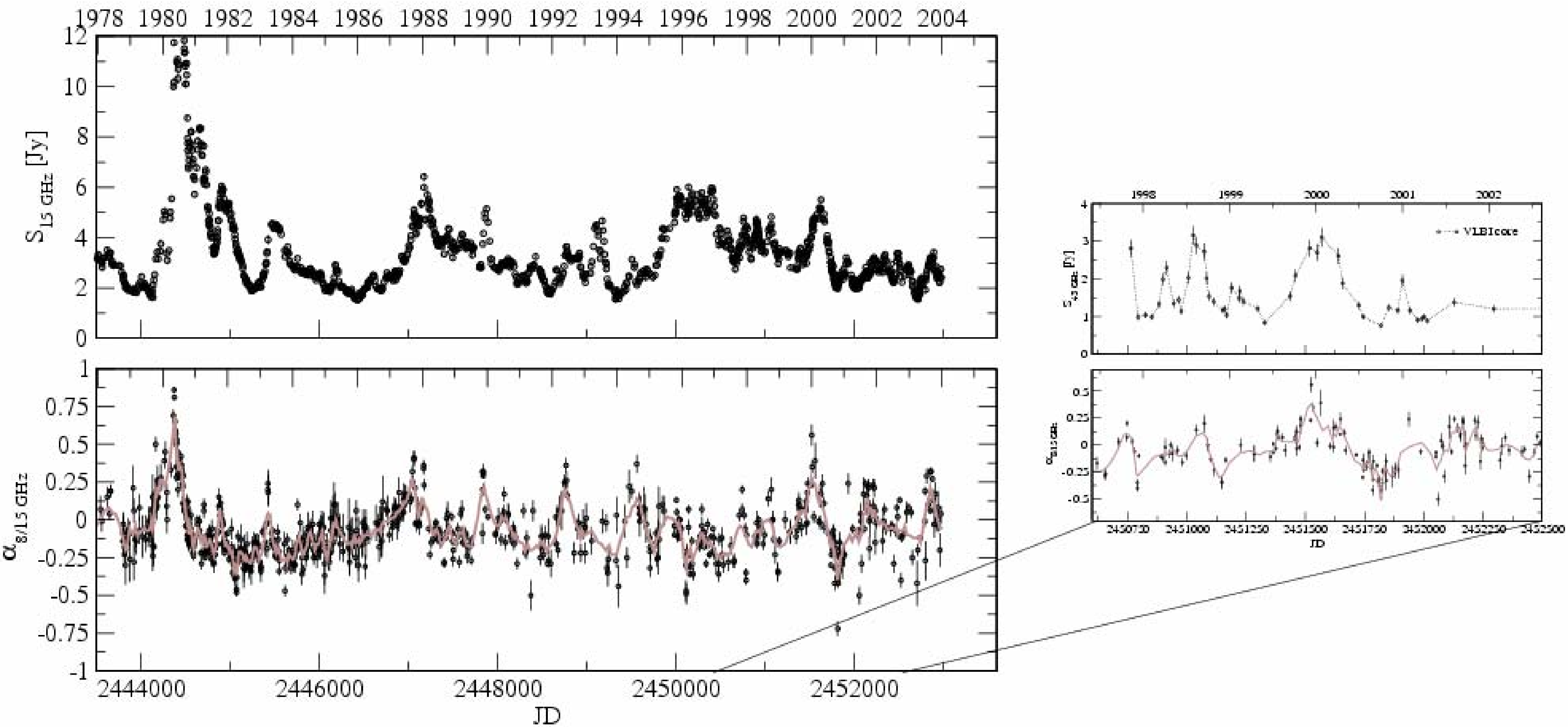

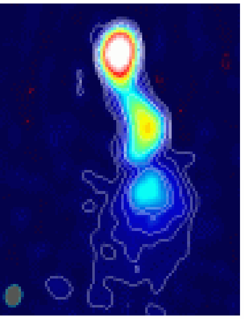

Single Dish Spectral Index

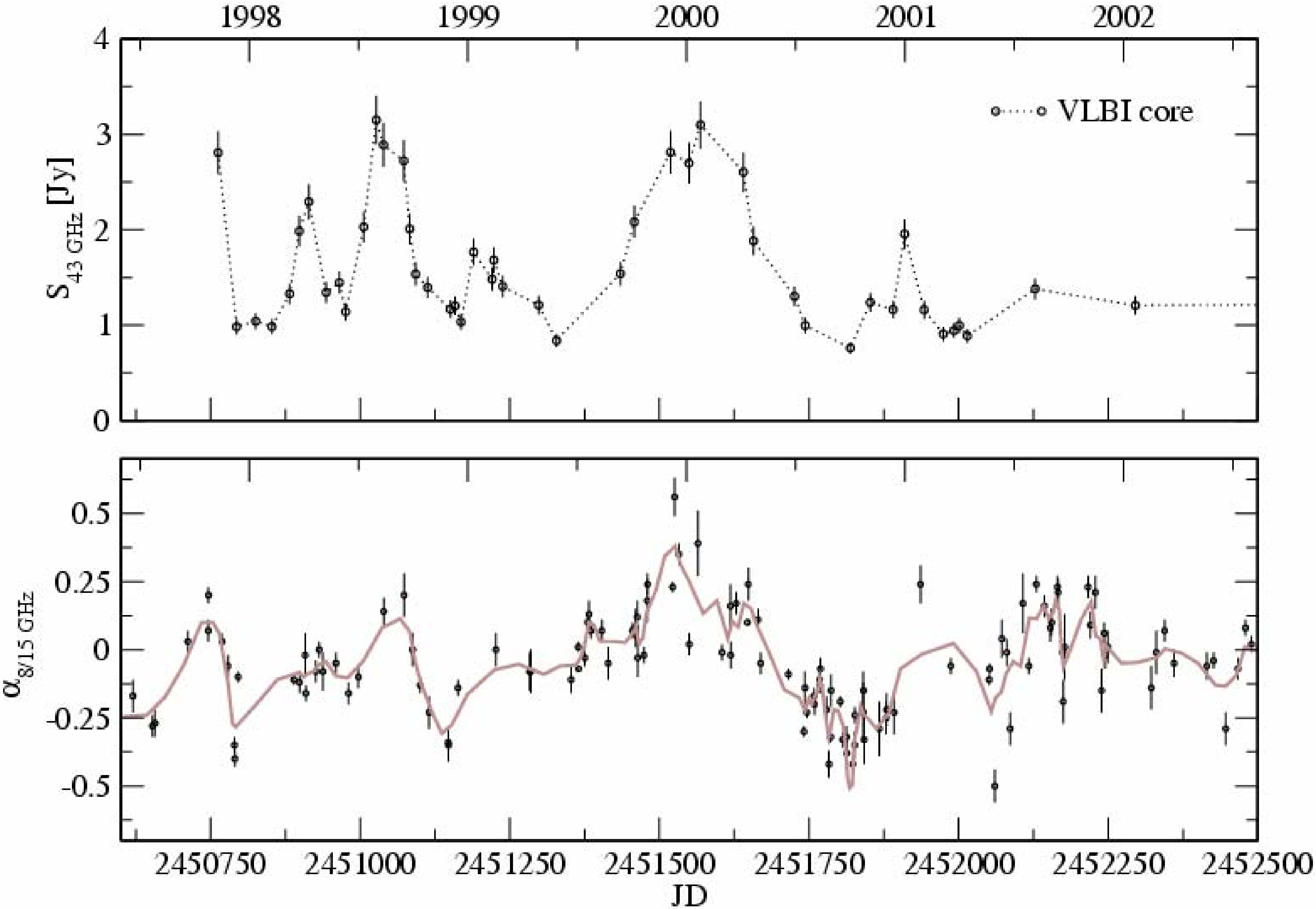

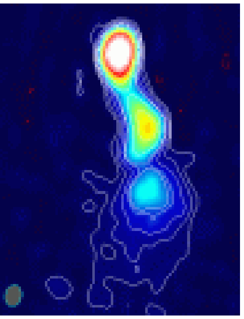

DCF: $\alpha_{8/15}$-VLBI Core

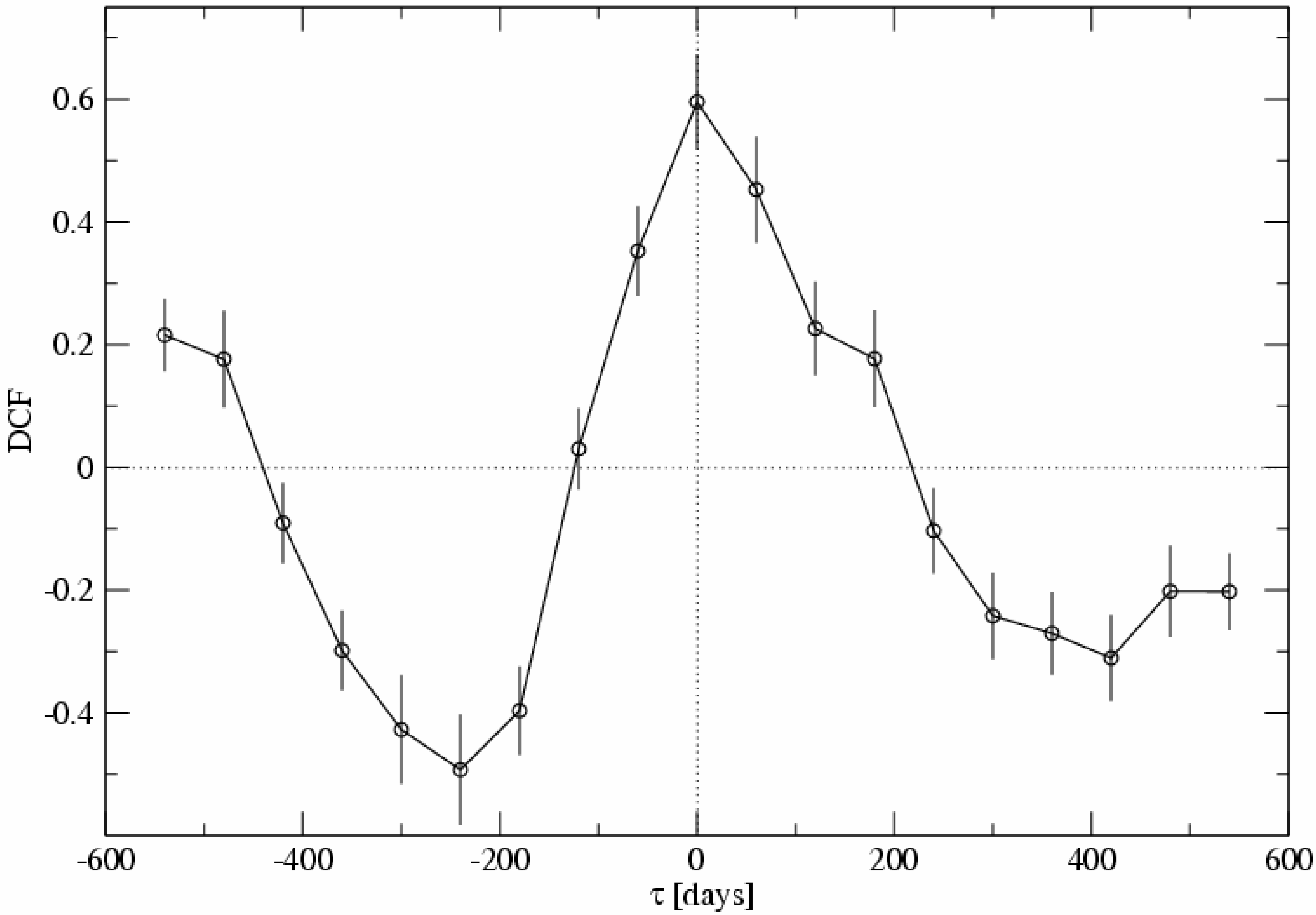

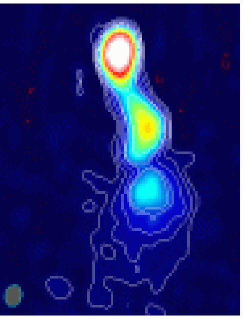

DCF: R-band-VLBI Core

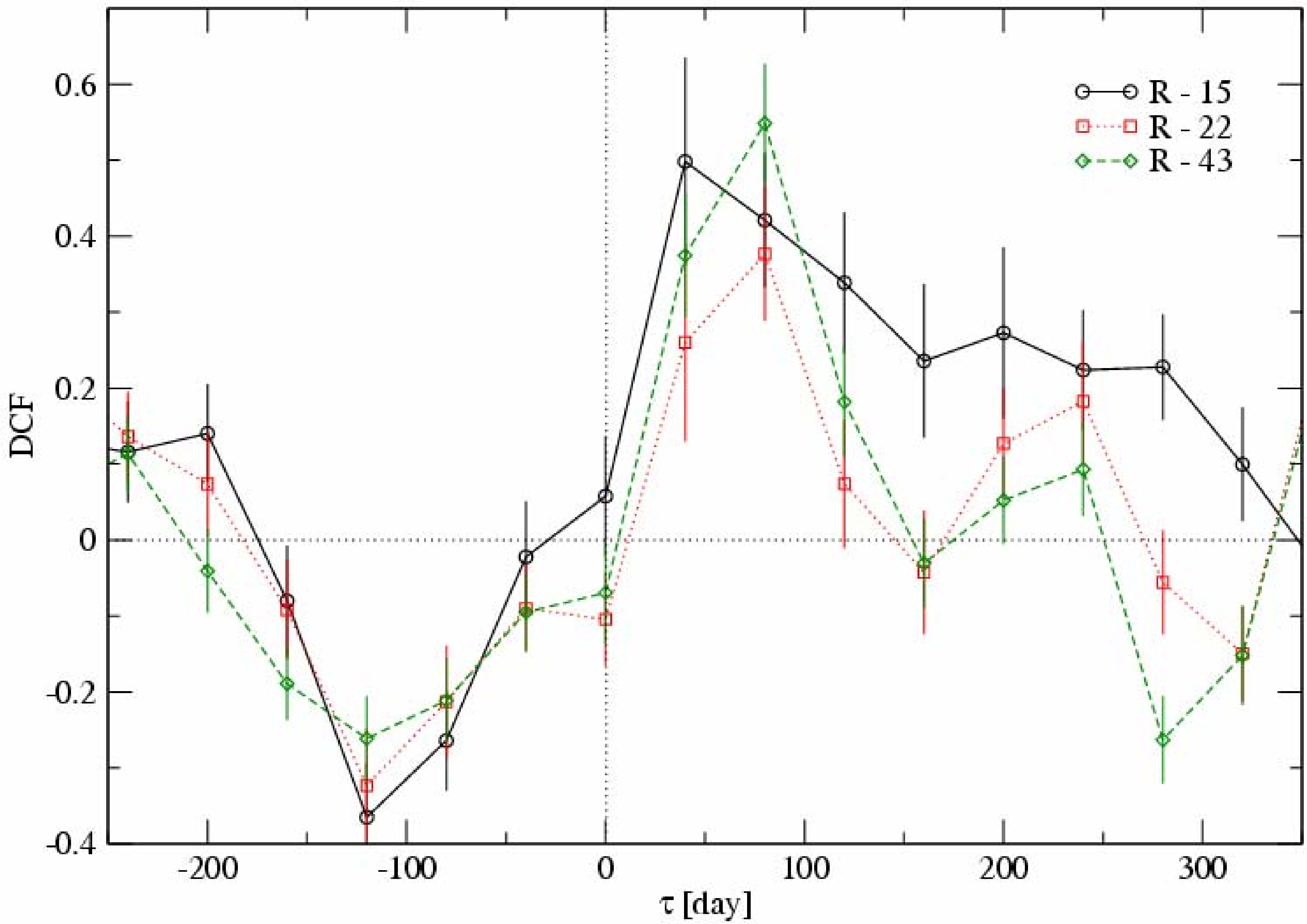

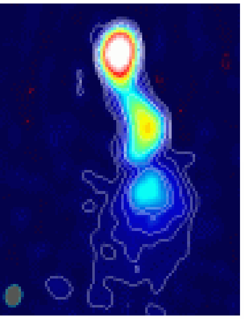

DCF: R band-Spectral Index

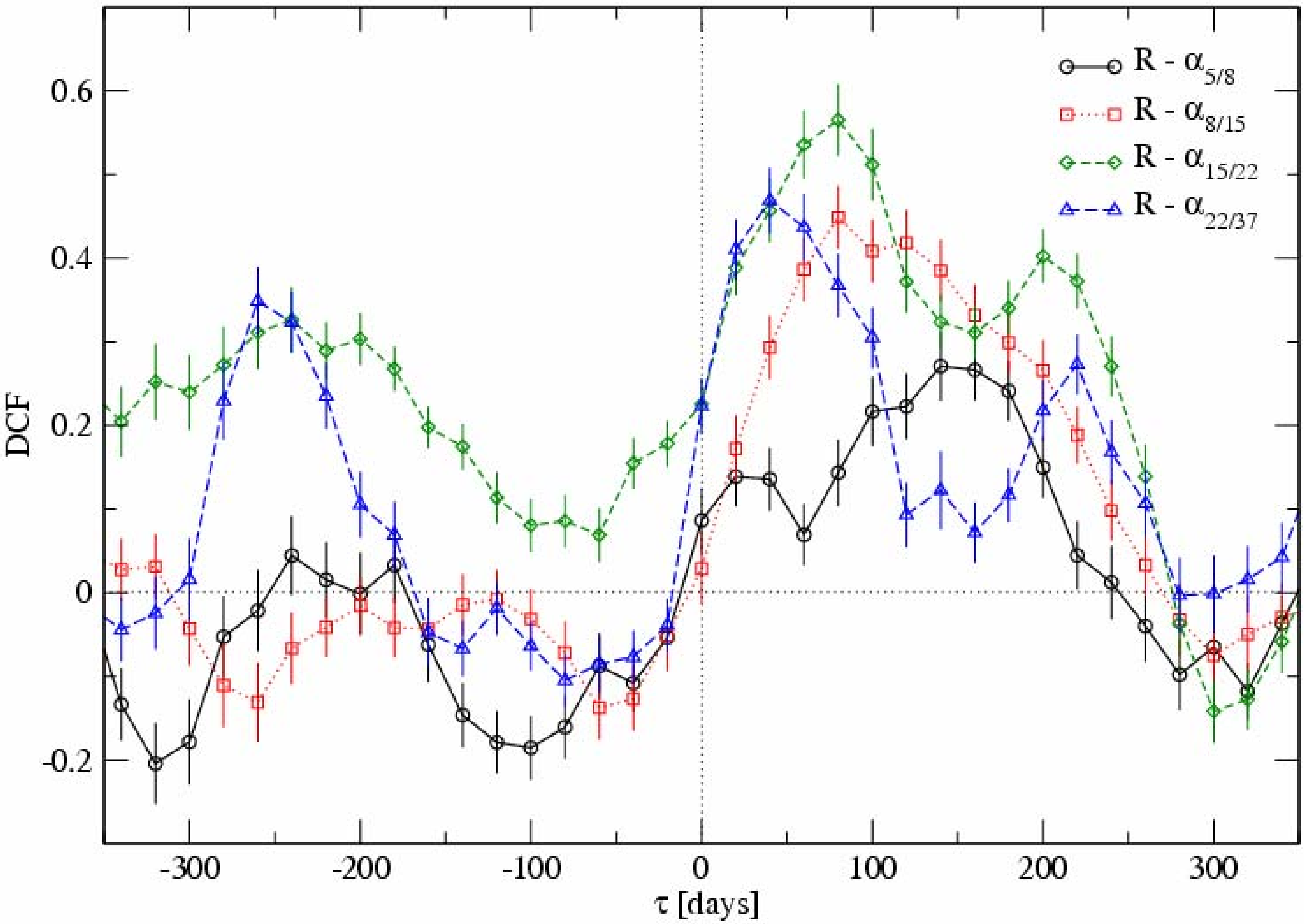

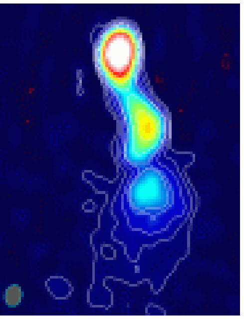

R band-Spectral Index DCF: 1000 Monte Carlo realizations

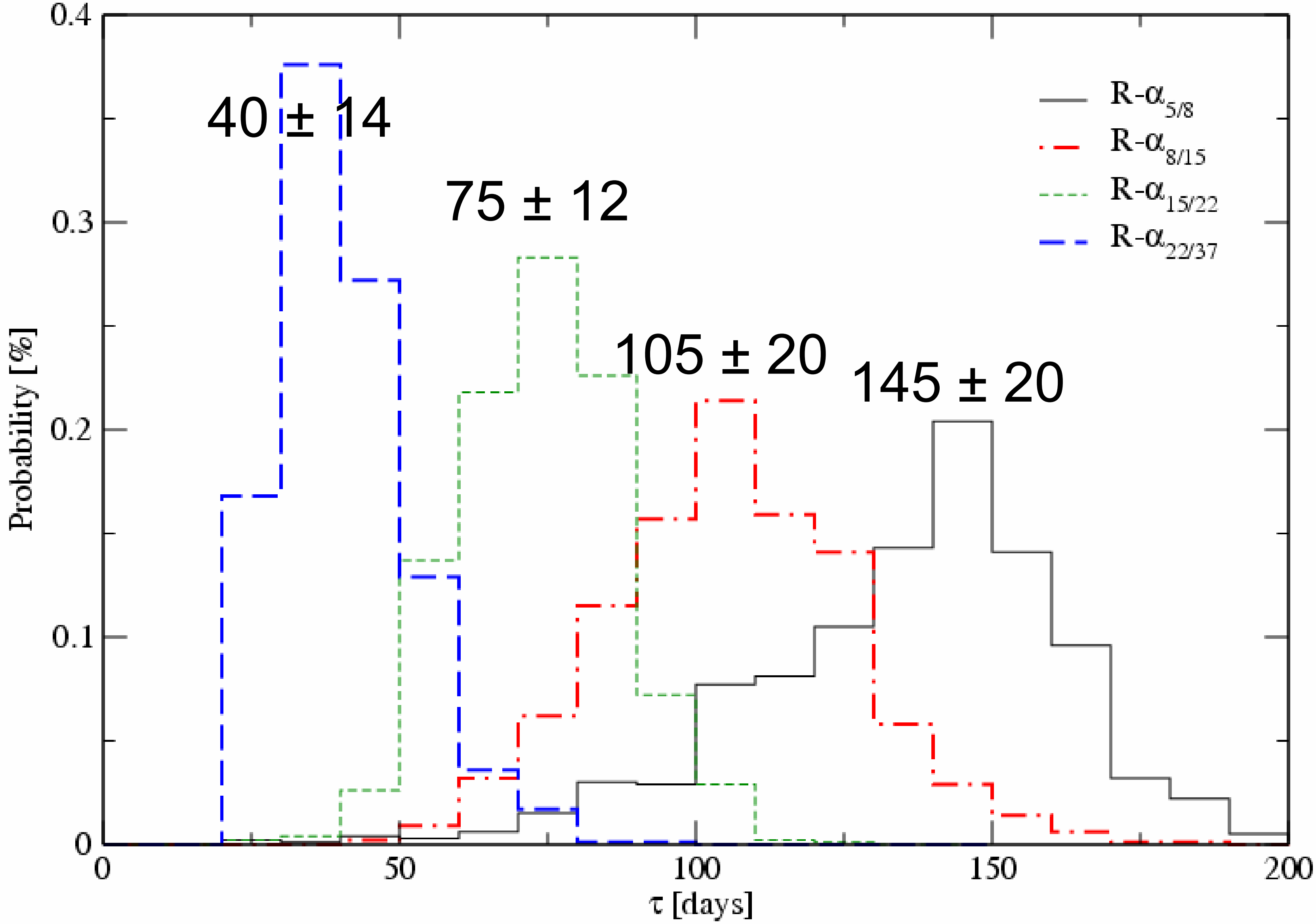

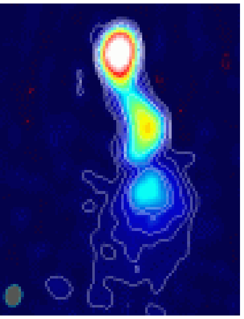

Optical Light Curve

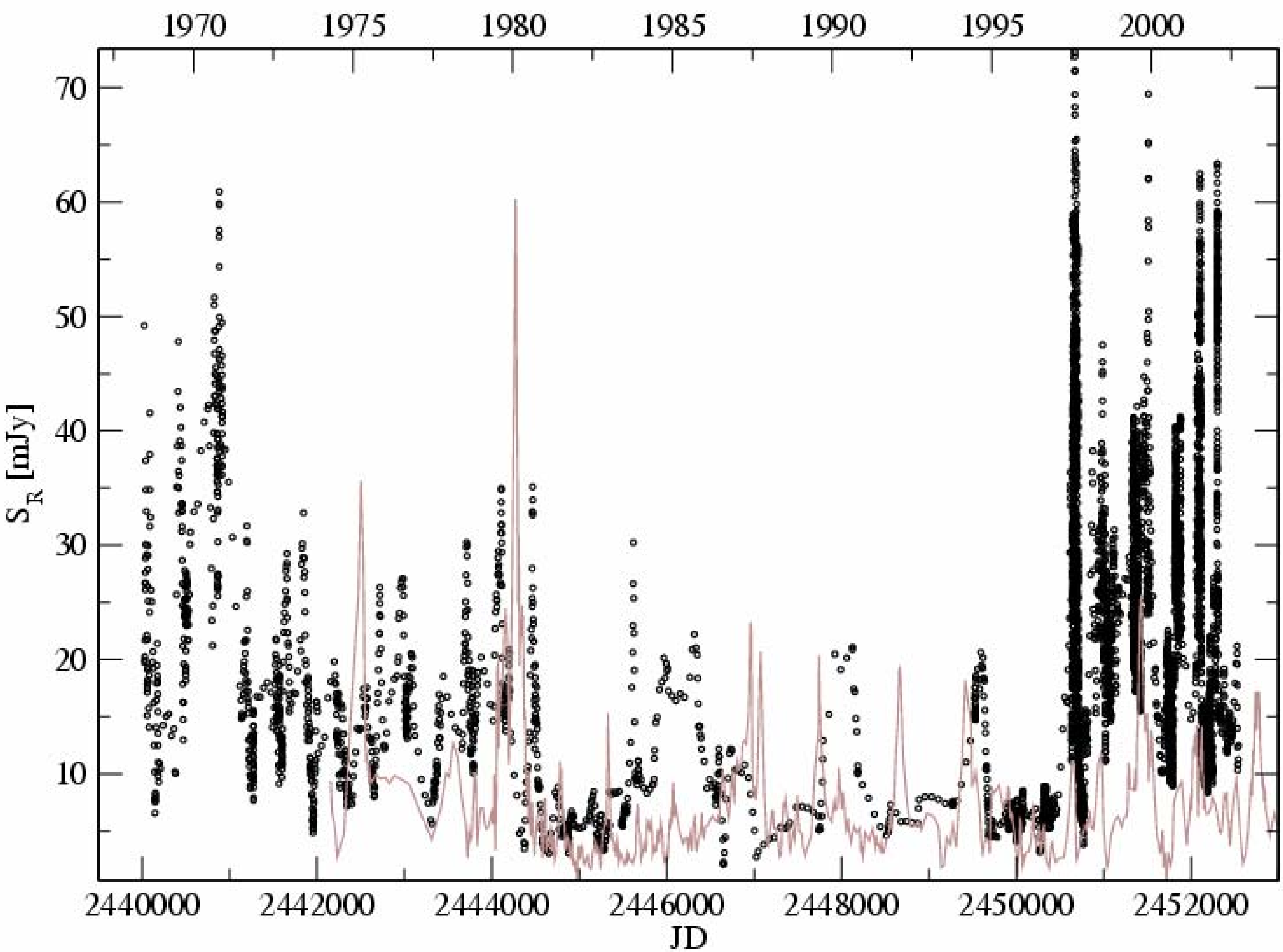

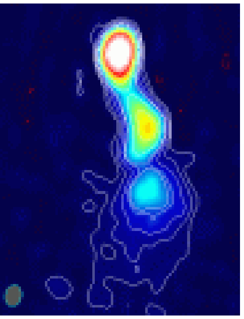

Variable Time Delay

DCF: R band-$\alpha_{8/15}$

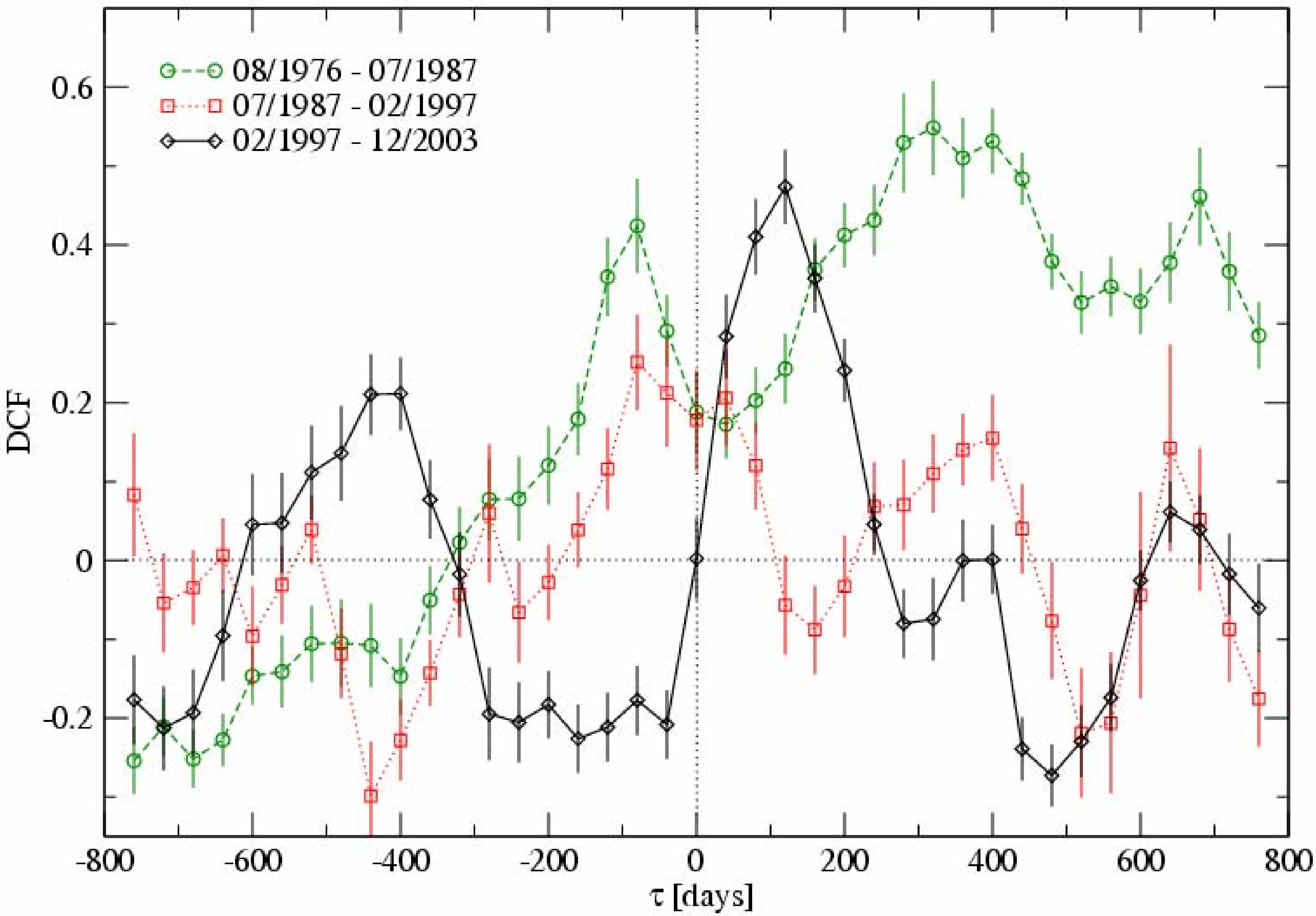

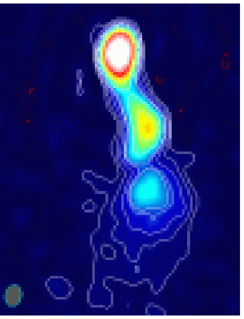

Time Delay vs. Frequency

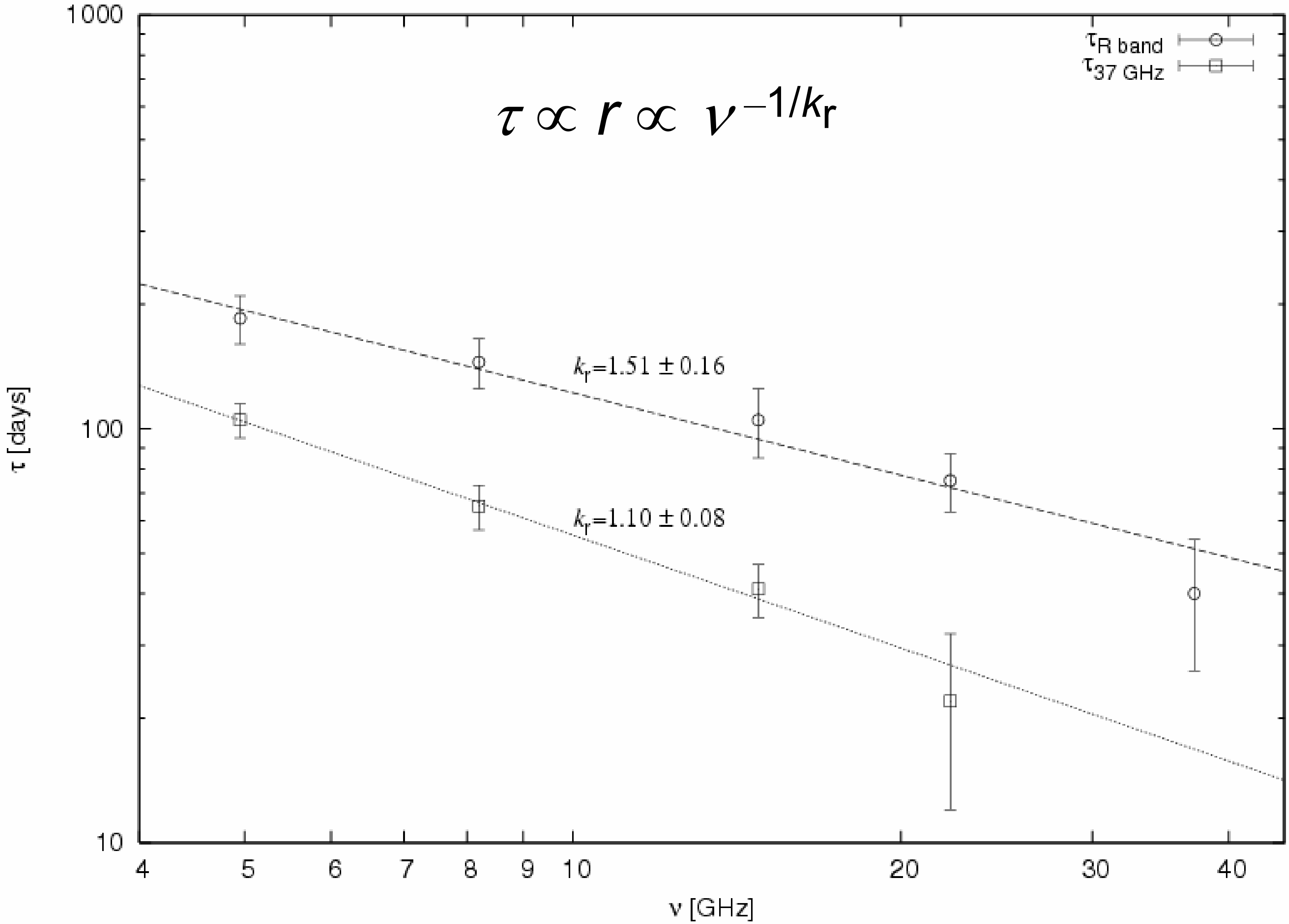

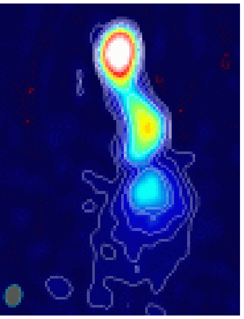

New Jet Components?

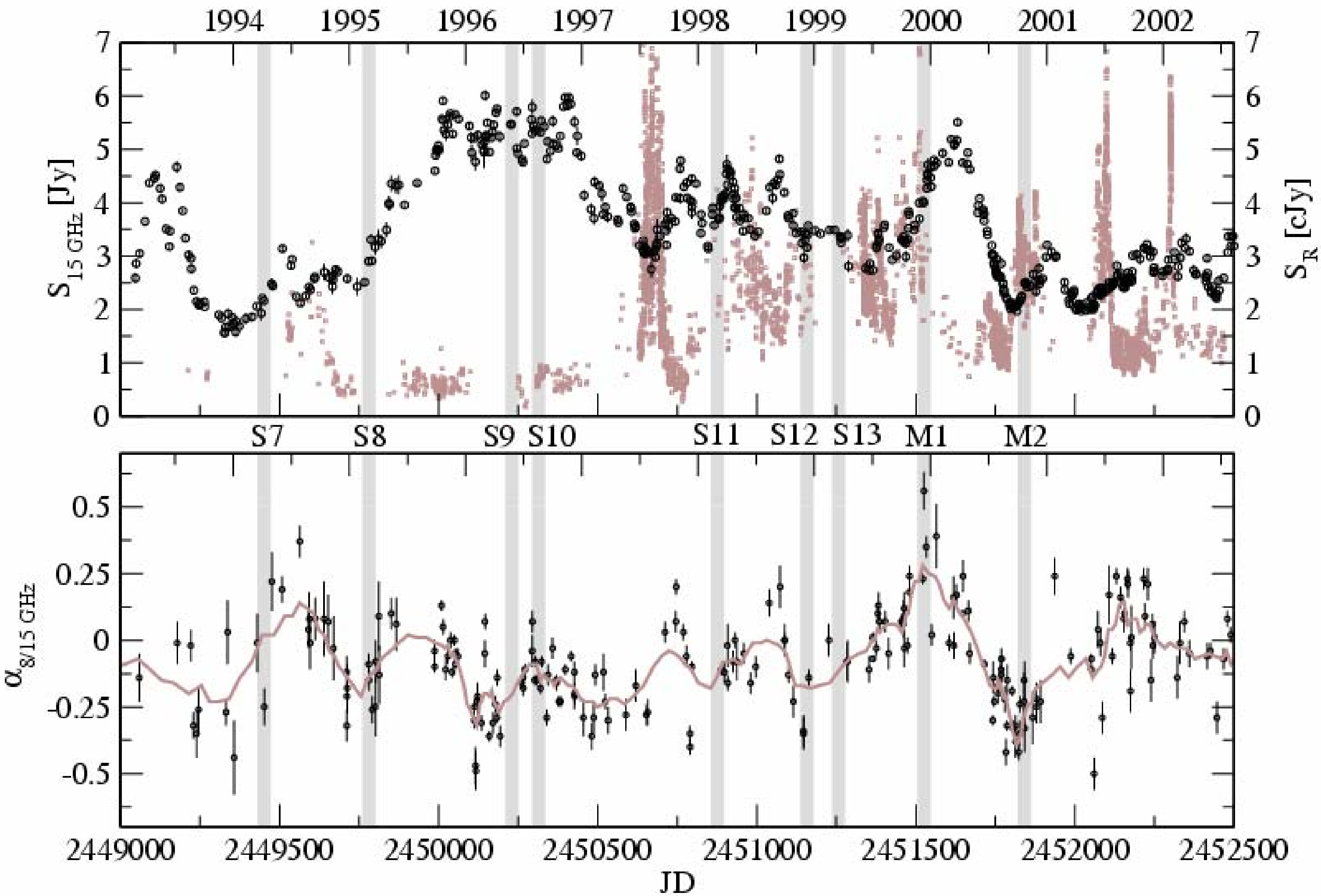

1999.5:

- X-ray variability + soft spectrum
- optical flare
- small radio flare
- no new jet comp.

1999.9:

- no X-ray monit. hard spectrum
- optical flare
- large radio flare
- new jet comp.

2000.8:

- X-ray variability + soft spectrum
- optical flare
- radio flare
- new jet comp.

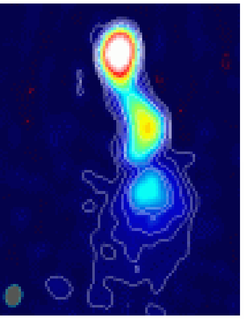

The 2000 Flare

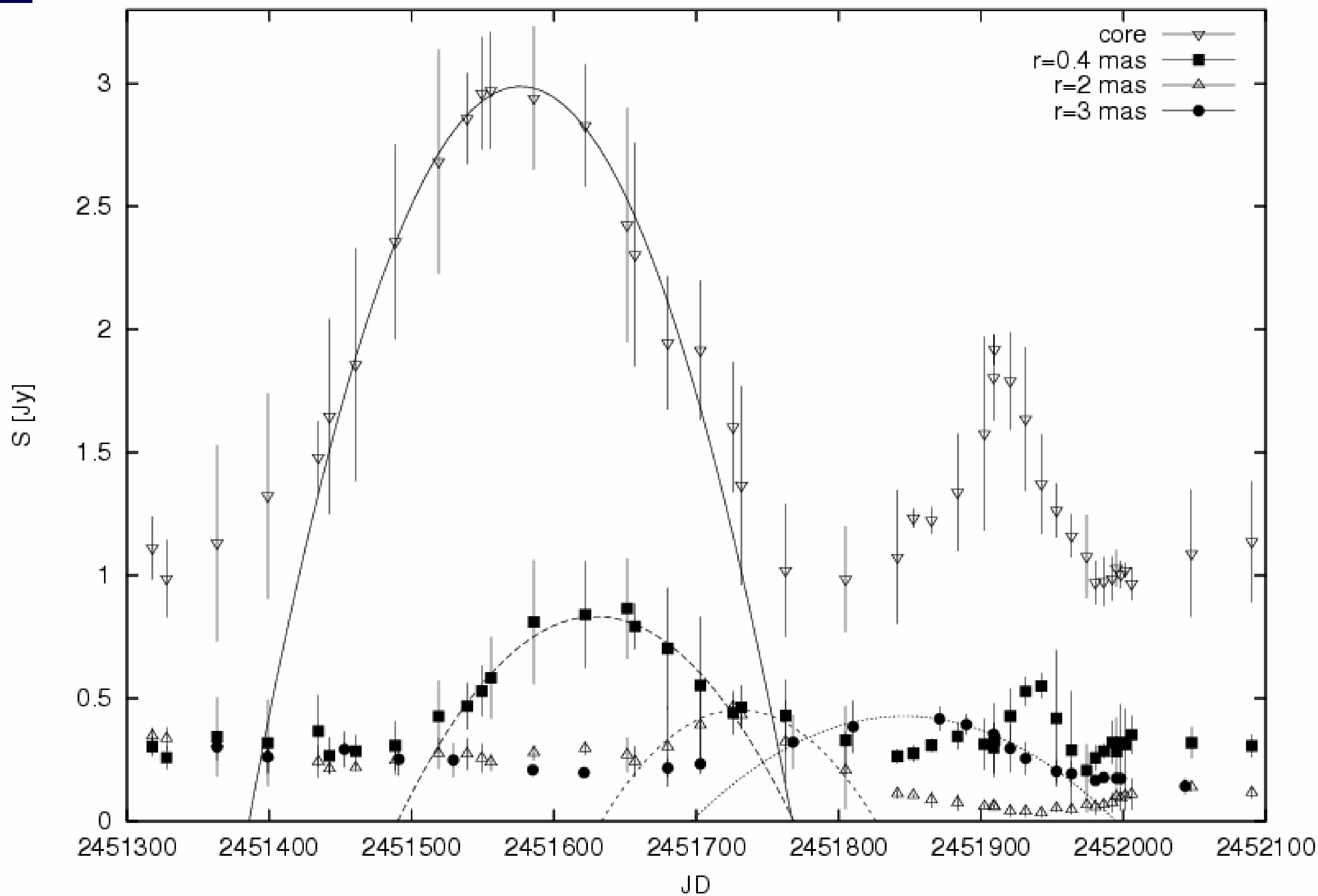

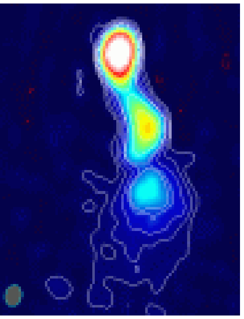

Precessing Jet?

- Sinusoidal variation at the base of the radio jet
- Same period was found in the EVPA at 7mm (VLBI) and at 1mm (single dish, HHT).
- A precessing jet model with β = 0.989 *c* and I = 9.2 ° can predict the component positions in the jet.

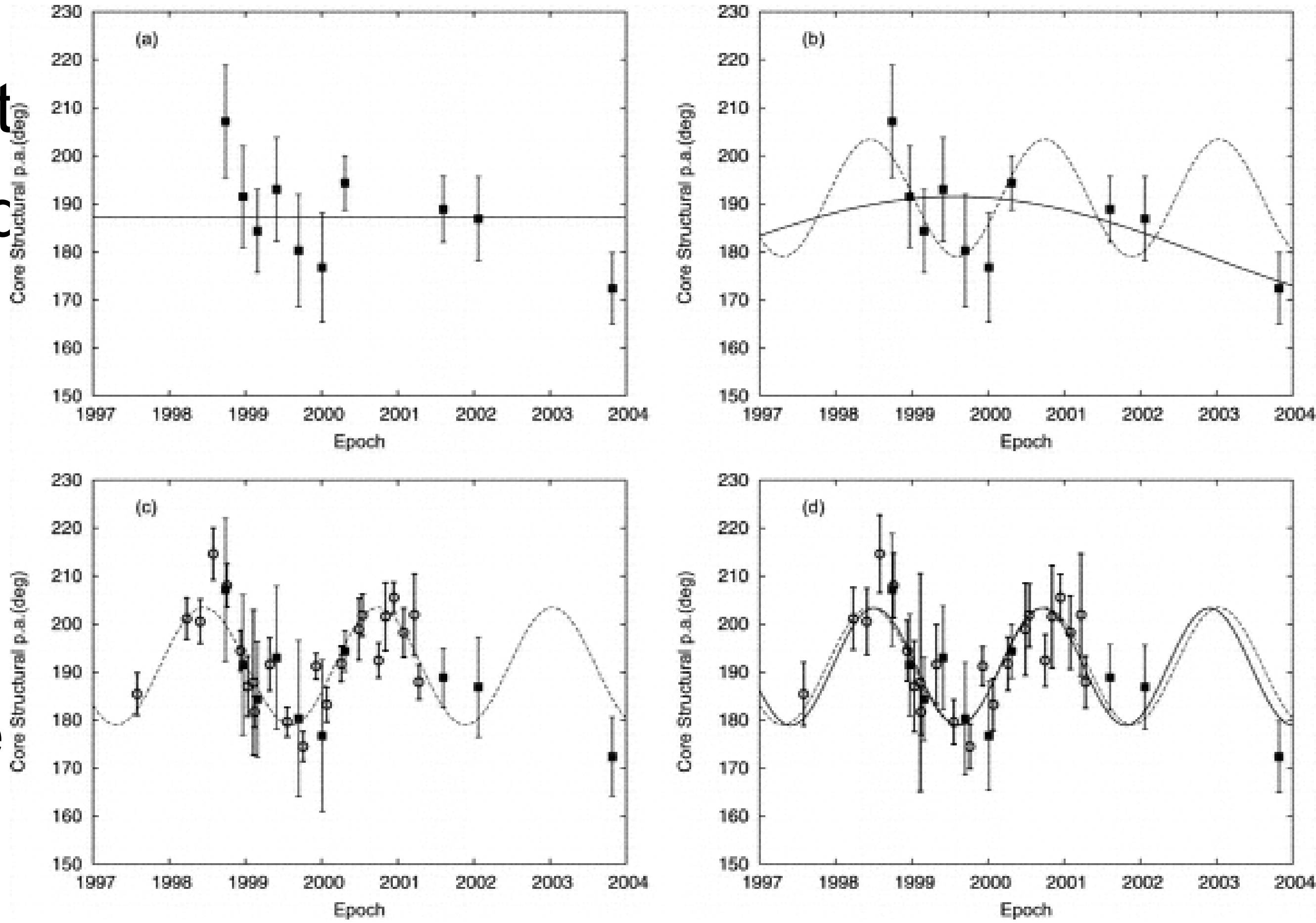

Stirling et al. 2003; Mutel & Denn 2005

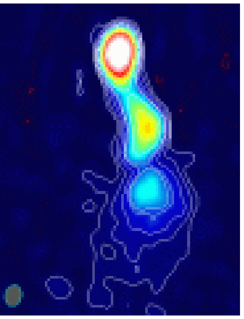

Summary

- Single dish light curves are "contaminated" by the appearance of prominent jet components.
- Using only the VLBI core variations yields better correlations with the optical variability.
- Single dish spectral index variations are manly due to the VLBI core variability.
- Optical variations lead the radio ones by 50 to 180 days.
- Power law dependence of τ suggests that the jet is not freely expanding.
- Different time lags and optical variability characteristics can be explained by a precessing helical jet structure.
- Some contemporaneous events from X-ray to radio suggest a common origin, but the sampling is too sparse to be sure.

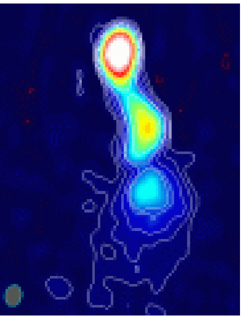

Outlook

Many blazars exhibit similar pc-scale jet structures like BL Lac (e.g., 3C 454.3, 3C 345, OJ287…) and a lot of VLBI data exists on them.

It might be worth to look at this!

The WEBT campaign on 3C 454.3

C. M. Raiteri, M. Villata

(INAF - Osservatorio Astronomico di Torino)

for the WEBT/ENIGMA collaboration

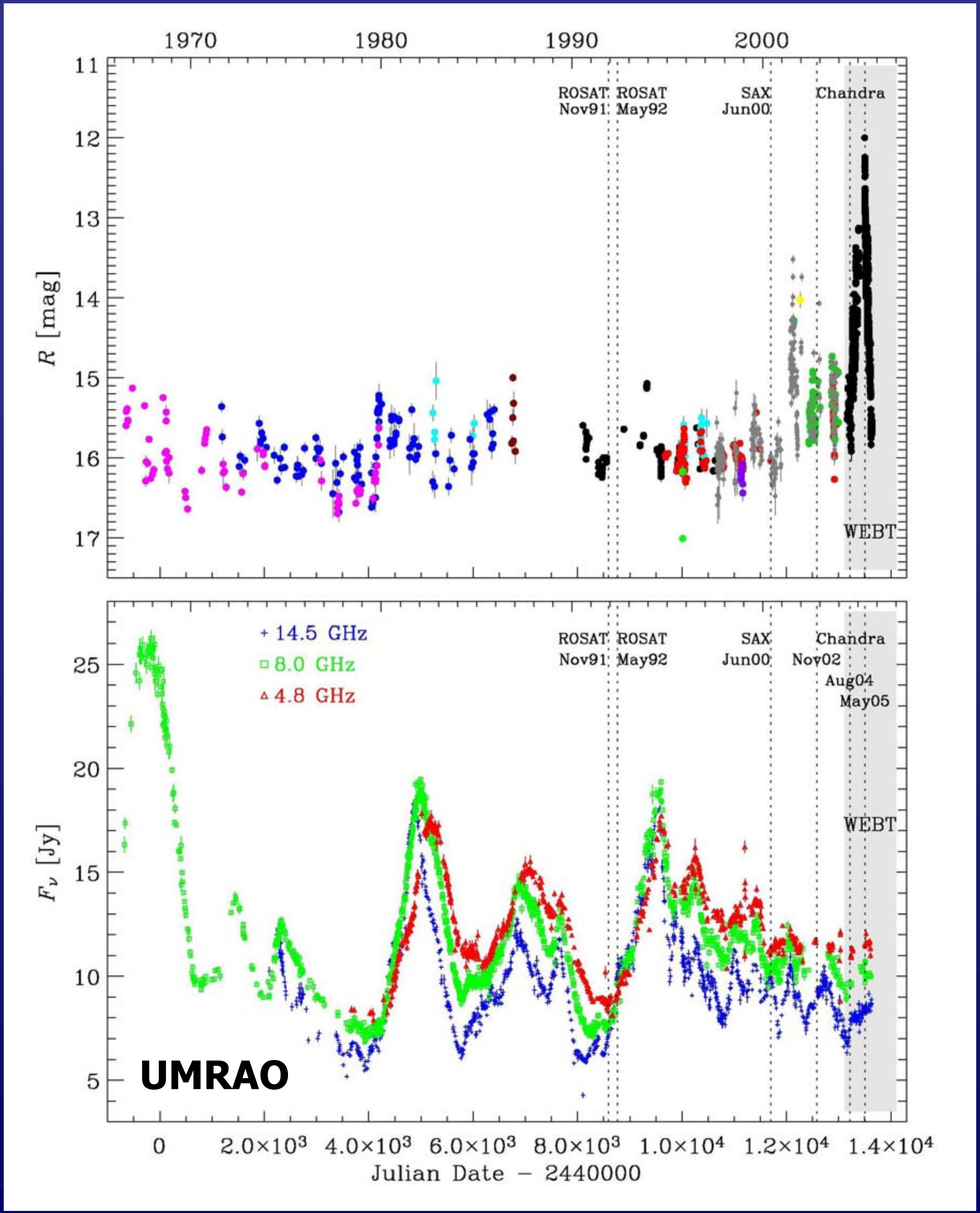

Motivation:

Exceptional optical outburst culminating in May 2005

Maximum brightness: ***R=12.0, ~ 4 mag brighter than the past average level***

In the last ~40 years, several big radio outbursts lasting ~2-3 years

But low state during the recent optical outburst

The WEBT campaign

(Villata et al. 2005, in preparation for A&A Letter)

Period: June 2004 to September 2005

5561 *UBVRI* observations from 18 telescopes + *JHK* + radio

R-band: 1492 points, 1139 in 143.6 days, between May 9.3 to September 30.0, 2005

Average time separation of 3.0 hours; only 4 gaps longer than 36 hours

BUT: some data are still missing…

Optical band: colour behaviour

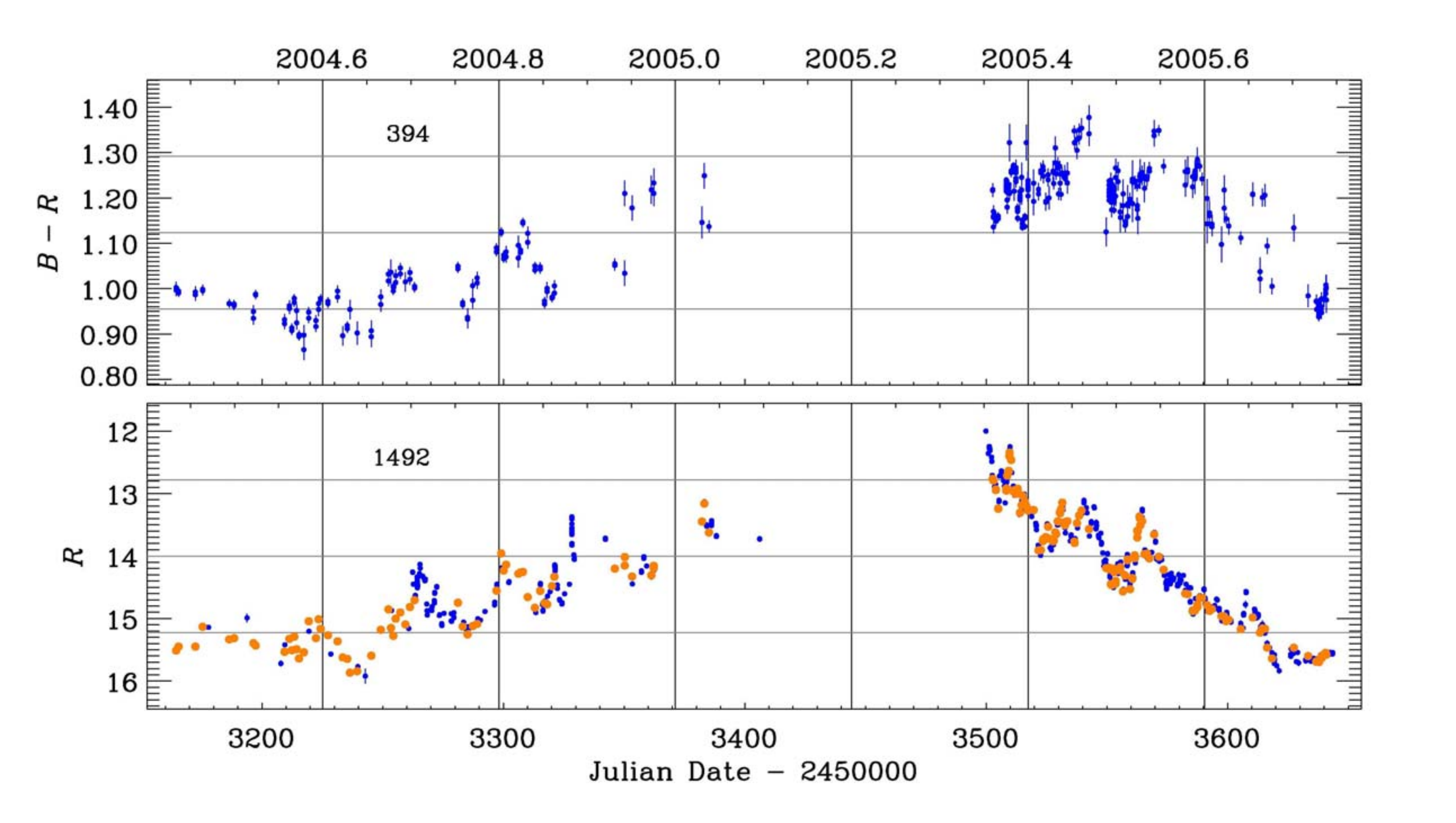

In fainter states: *redder when brighter* ⇒ accretion disc

In brighter states: saturation ⇒ jet dominance ⇒ *bluer when brighter* ?

The optical spectrum depends on the relative contribution of thermal and non-thermal radiation

Radio-near-IR-optical spectral variations

Pico Veleta mm data

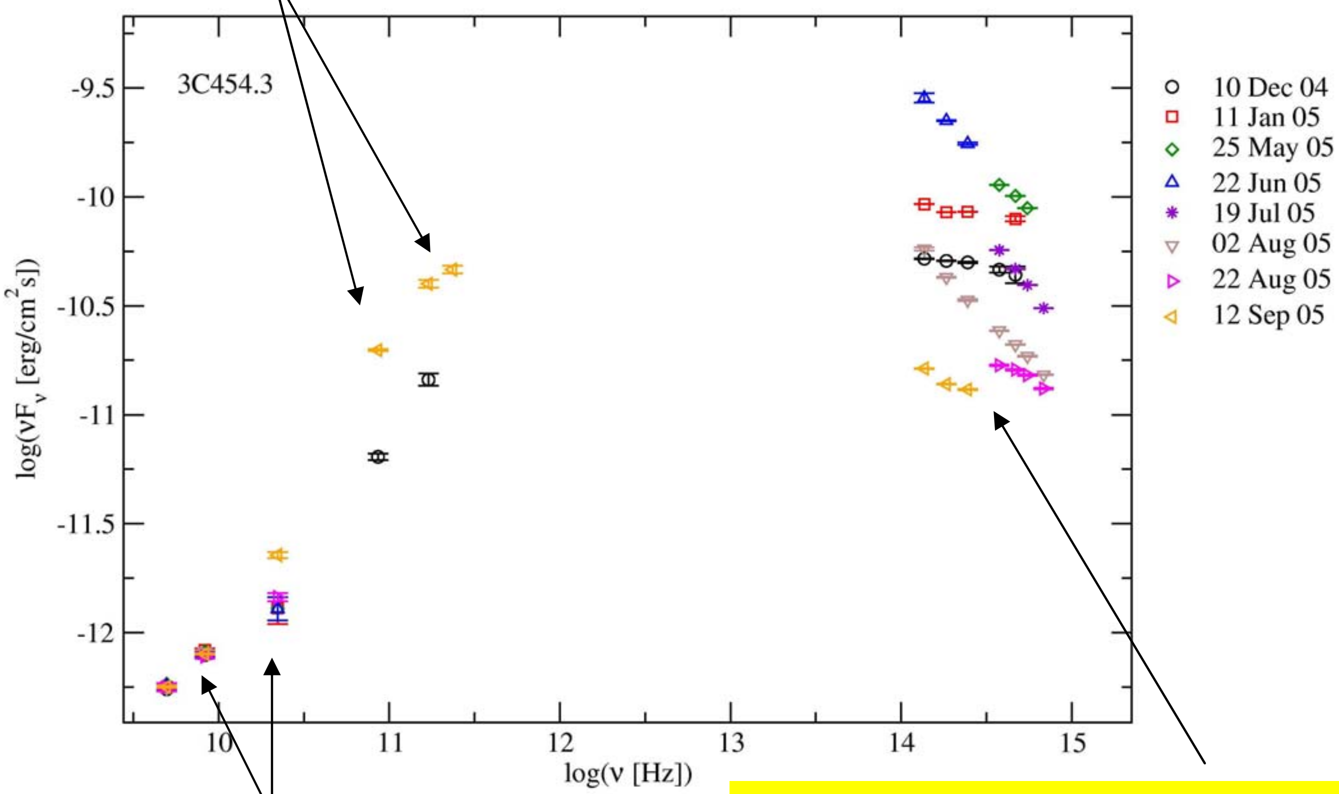

Medicina and Noto cm data (PI: Uwe Bach)

Campo Imperatore JHK data
Torino+Crimea BVRI data

1) Different slopes at similar bright.

2) In mid Sep. it was except. bright in the mm band and brighter than before at 22 GHz

36 GHz data from RT-22 in Crimea:

5.5 Jy in June 2004

8.5 Jy in May 2005

13.4 Jy in October 2005

It seems that the outburst has propagated from optical to mm and now is propagating to the cm band

Radio VLBA maps

I(tot)=10200 mJy

I(pol)=200 mJy

I(tot)=6290 mJy

I(pol)=103 mJy

I(tot)=6560 mJy

I(pol)=74 mJy

I(tot)=1710 mJy

I(pol)=15 mJy

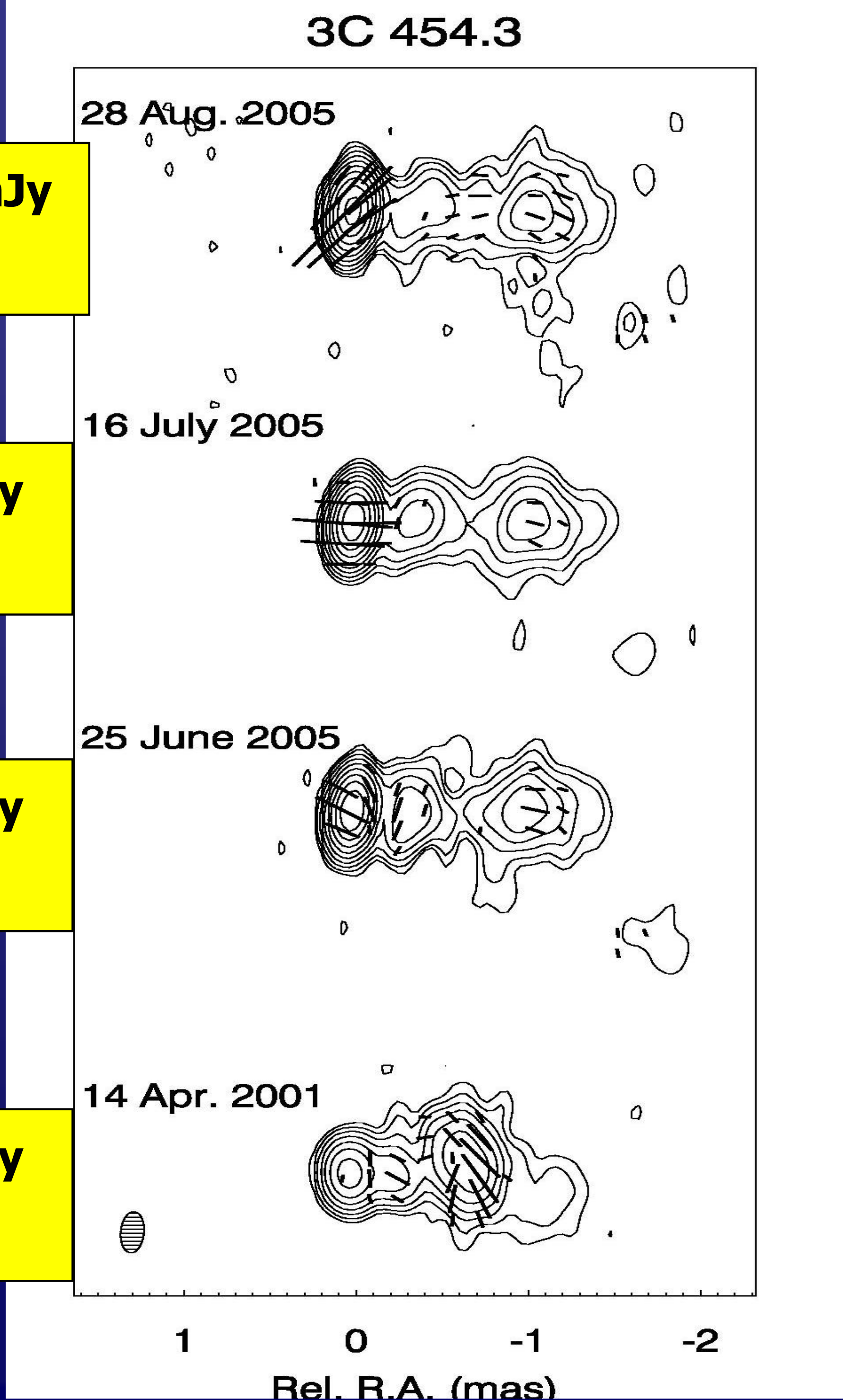

Global total and polarized intensity at 43 GHz

At this ν the brightening was already evident at the end of August.

A new component is emerging from the core?

High-energy observations in May 2005, during the optical outburst

RXTE : from an average over April 29 to May 10 data
$\Rightarrow$10.8 mCrab in the 2-12 keV range *(Remillard 2005, ATel 484)*

Swift: May 11-19 $\Rightarrow$ bright in optical and hard X-rays (Neil Gehrels, private comm.) see *Giommi et al. 2005, A&A, submitted*

INTEGRAL (PI: E. Pian): May 15-18 $\Rightarrow$ 1.6e-10 erg cm-2 s-1 in the 20-100 keV band *(Foschini et al. 2005, ATel 497)* see also *Pian et al. 2005, A&A, in preparation*

Chandra (PI: F. Nicastro): May 19-20 see *Villata et al. 2005, in preparation for A&A Letter*

The broad-band spectral energy distribution

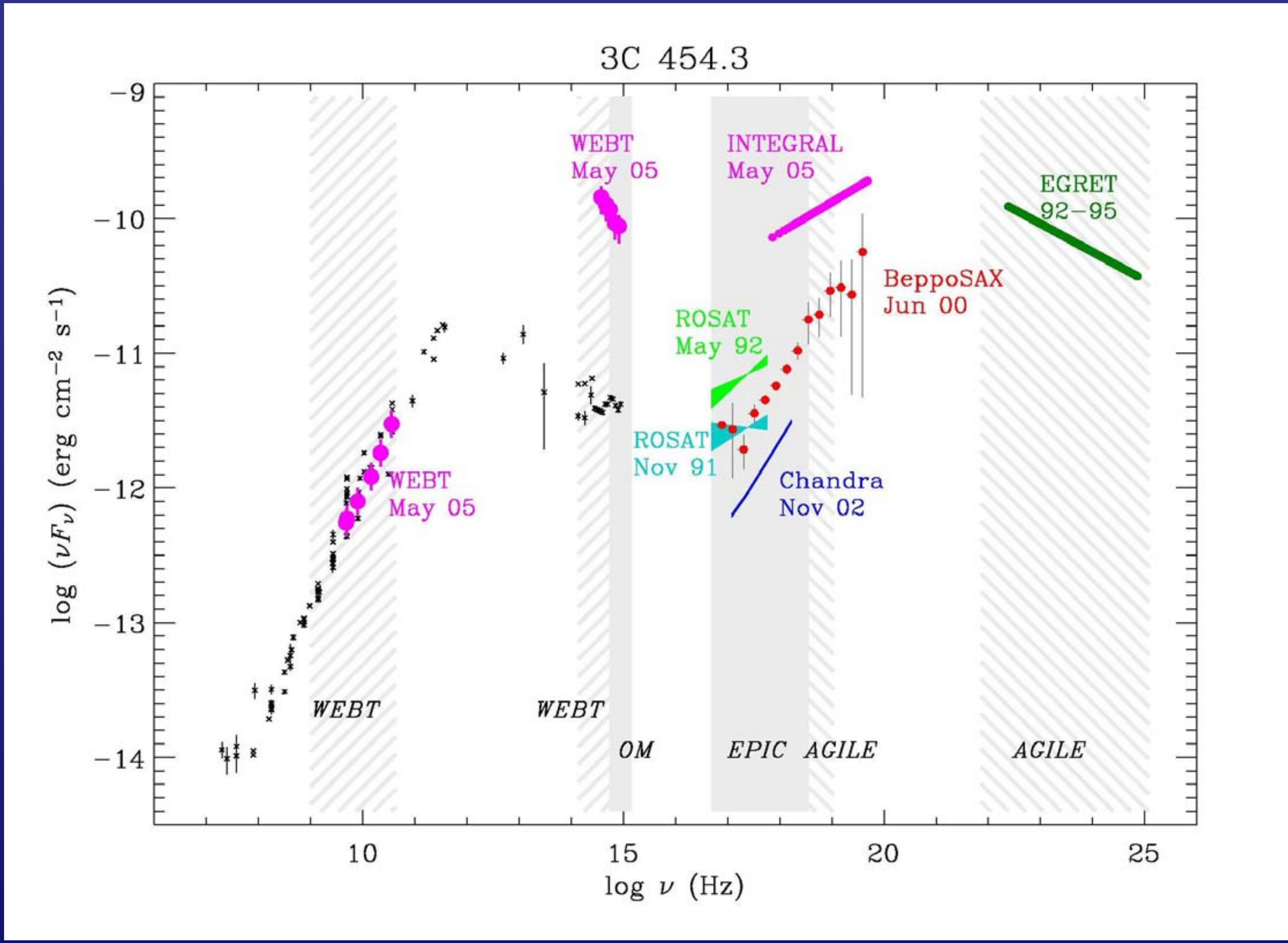

Past X-ray observations: faint radio and faint optical state

May 2005 X-ray observations: faint radio and bright optical state

The XMM-Newton proposal

(PI: C.M. Raiteri)

Three pointings requested in AO5, 10 ks each, to get X-ray (and UV) information during different phases of the expected radio outburst:

1. May 23 - July 2, 2006 ⇒ **ENIGMA PROJECT**
2. November 24, 2006 - January 1, 2007
3. May 23 - July 2, 2007

In these periods the source will likely be in the AGILE fov

$\Rightarrow$ gamma-ray information (30 MeV - 50 GeV)

A rapid and dramatic outburst in Blazar 3C 454.3 during May 2005

Lars Fuhrmann

G. Tosti, N. Marchili, A. Cucchiara,
G. Nucciarelli
Perugia/Torino Team

REM team

P. Giommi et al., ASI

S. Ciprini
Tuorla Team

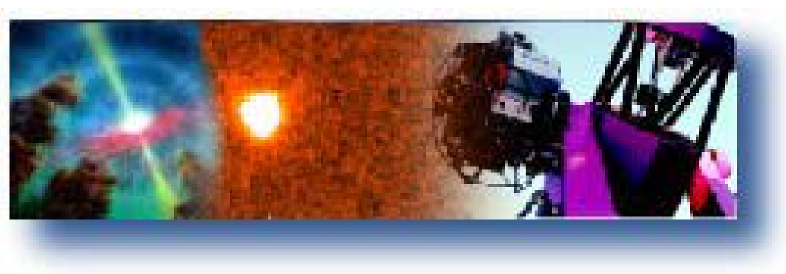

ENIGMA meeting, Nov. 2005

Overview

- blazar 3C 454.3: a few “facts“
- the outburst in spring 2005
- optical/IR monitoring with REM + AIT
- spectral evolution
- simultaneous SWIFT pointings in May
- Thomas: cm-mm observations

3C 454.3

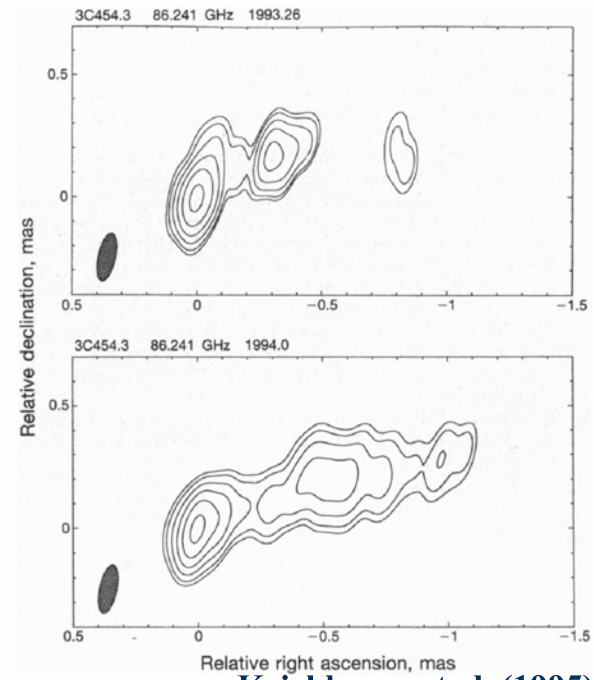

Krichbaum et al. (1995)

- highly variable quasar, z = 0.86
- compact, superluminal VLBI source
- radio: strong long-term variability over last decades
  - decimeter: interstellar scintillation (e. g. Altschuler et al. 1984)
  - cm - mm wavelengths: often correlated (e.g. Tornikoski et al. 1994)
    consistent periodicity of ~ 6 years (Ciaramella et al. 2004)
  - VLBI component ejections during radio outbursts and enhanced levels of gamma-ray flux (e.g. Pagels et al. 2004)
- optical: violently variable
  - B band data go back to 1900 (Angione 1968)
    → several outbursts

3C 454.3

- high optical polarisation and polarisation angle changes (Angel & Stockman 1980)

- radio-optical correlation? (e.g. Tornikoski et al. 1994, Balonek 1982)

  → time lag of ~ 1.2 yr

- intranight variability (e.g. Raiteri et al. 1998)

- higher energies:
  - strong and variable source detected by
    Einstein, ROSAT, COMPTEL, EGRET, OSSE
  - spectral maximum at MeV energies (e.g. Blom et al. 1995, Lin et al. 1996)

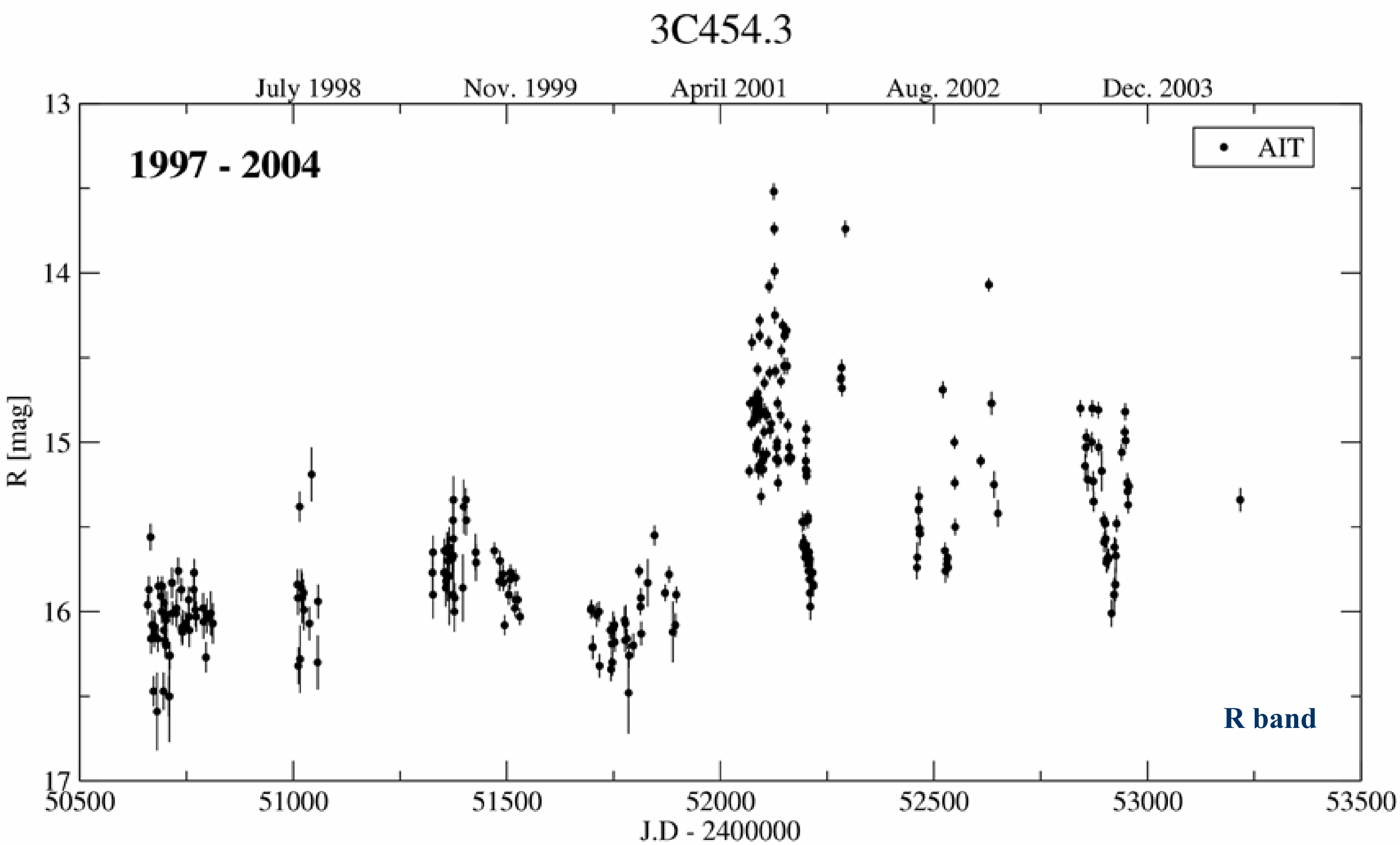
3C454.3
July 1998
Nov. 1999
April 2001
Aug. 2002
Dec. 2003
1997 - 2004
AIT
R [mag]
13
14
15
16
17
50500
51000
51500
52000
52500
53000
53500
J.D - 2400000
R band

Outburst in spring 2005

- **May: Balonek et al. reported a new, strong flare**

  → quasi-simult. broad band observations
  WEBT, X-ray/gamma-ray (e.g. Foschini et al. 2005, Pian et al. in prep.)

→ REM + AIT monitoring starting on May 11 until August 05 for 86 days (V,R,I,H bands)

1) Perugia: Automatic Imaging Telescope (AIT)

- 40cm fully robotic
- R, I bands
- 30 nights

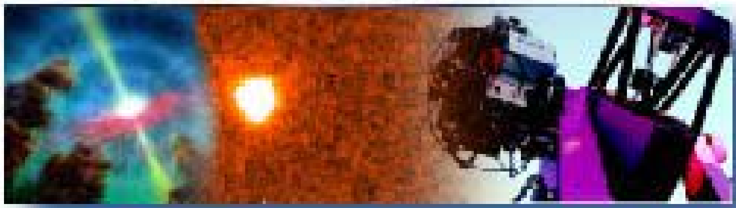

REM + AIT observations

2) REM: Rapid Eye Monitor at la Silla

- 60cm fully robotic
- REMIR: J, H, K bands
- ROSS: I, R, V
- 23 nights

- Reduction: standard aperture photometry
- diff. photometry using 5-8 standard reference stars

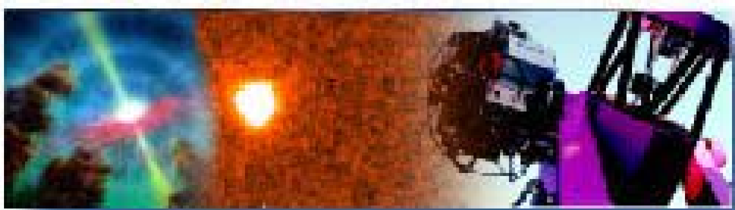

- **Maximum: 2 days before (R ~ 12 mag, Balonek 2005)**
- **long-term trend with faster flares**
- **first: V = 12.7, R = 12.2, I = 11.6, H = 9.4**
- **max. variations: ΔR = 2.6 over 75 days**

	T_{obs} [days]	N_{data}	$\langle mag \rangle$	Δ mag	$\langle F_\nu \rangle$ [mJy]	Δ F_ν [mJy]
V	60	48	14.16±0.73	2.37	13.7±9.7	36.6
R	86	85	13.57±0.63	2.61	17.5±10.0	47.6
I	86	72	12.90±0.65	2.46	25.4±15.4	64.6
H	42	167	10.18±0.36	1.60	92.6±30.7	142.6

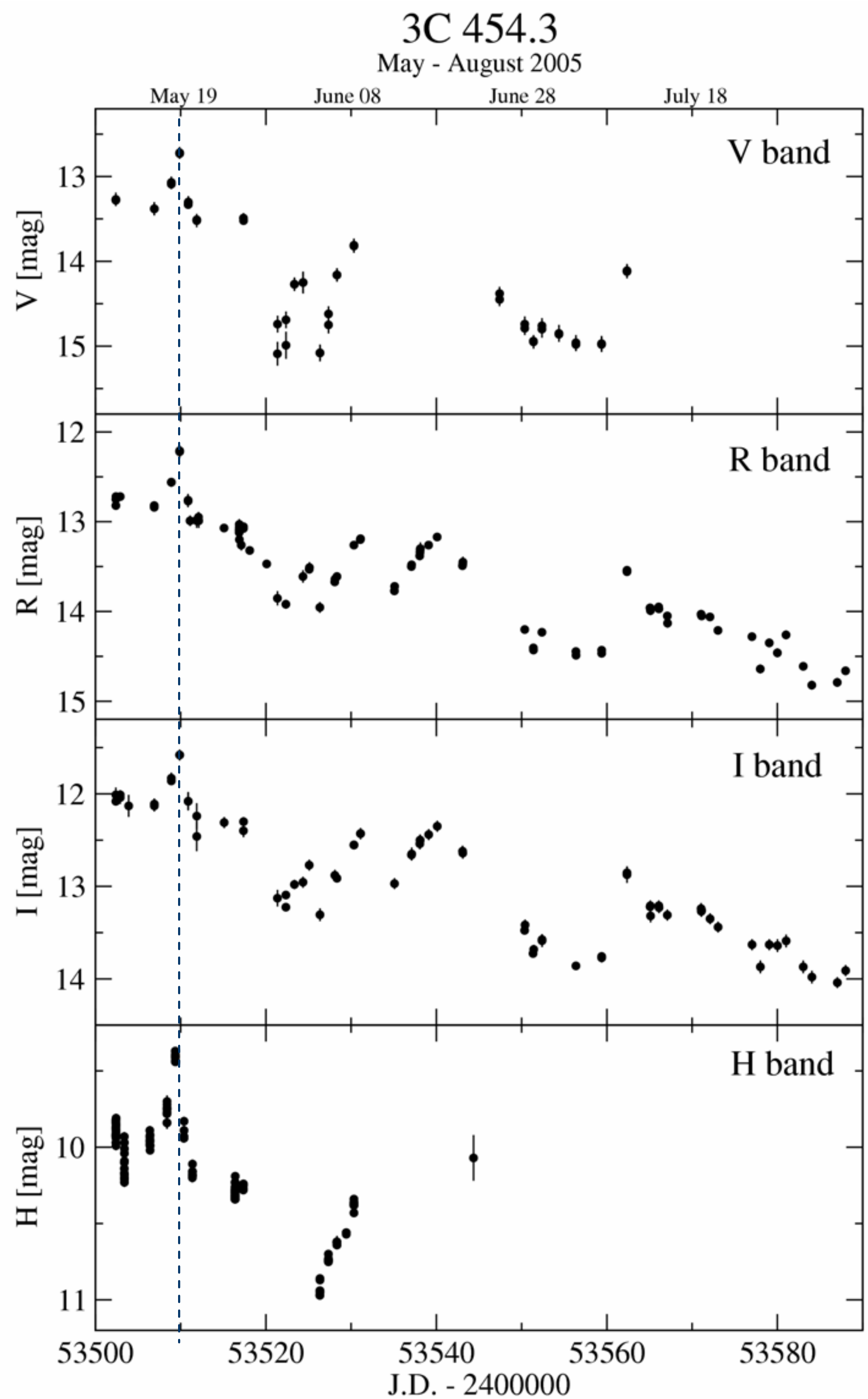

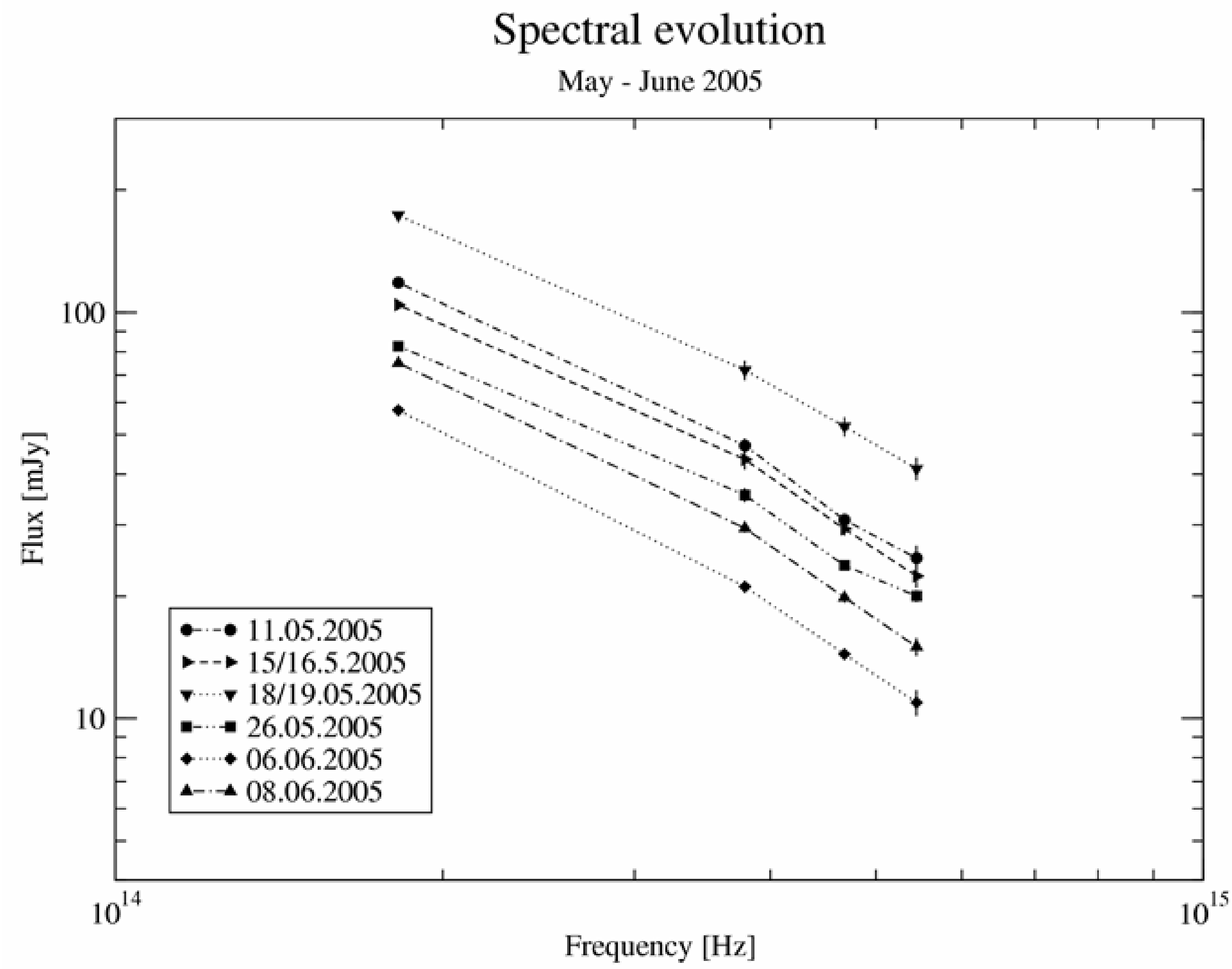

- **six epochs between May 11 and June 8**

→ **no strong, significant spectral changes**

→ **geometrical origin (helical/processing jet)**

- **$< \alpha >$ = 1.39 +/– 0.07 (F ~ $\nu^{-\alpha}$)**

→ **synchrotron peak below near-IR**

SWIFT observations

- 4 pointings: April 24 and May 11, 17, 19
- PI: P. Giommi

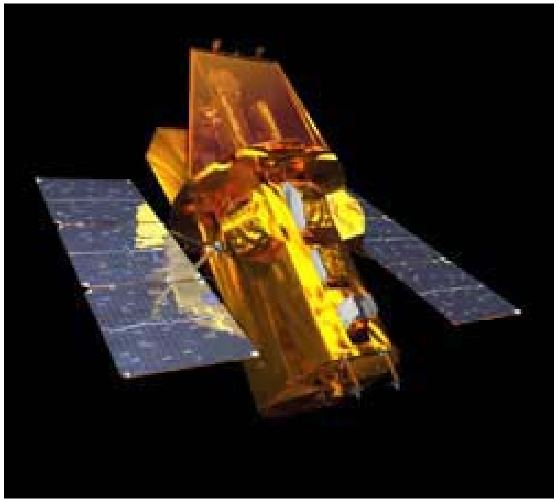

Burst Alert Telescope (BAT):

15 - 150 keV

X-ray Telescope (XRT):

0.3 - 10 keV

UV/Optical Telescope (UVOT):

170 - 650 nm

First results:

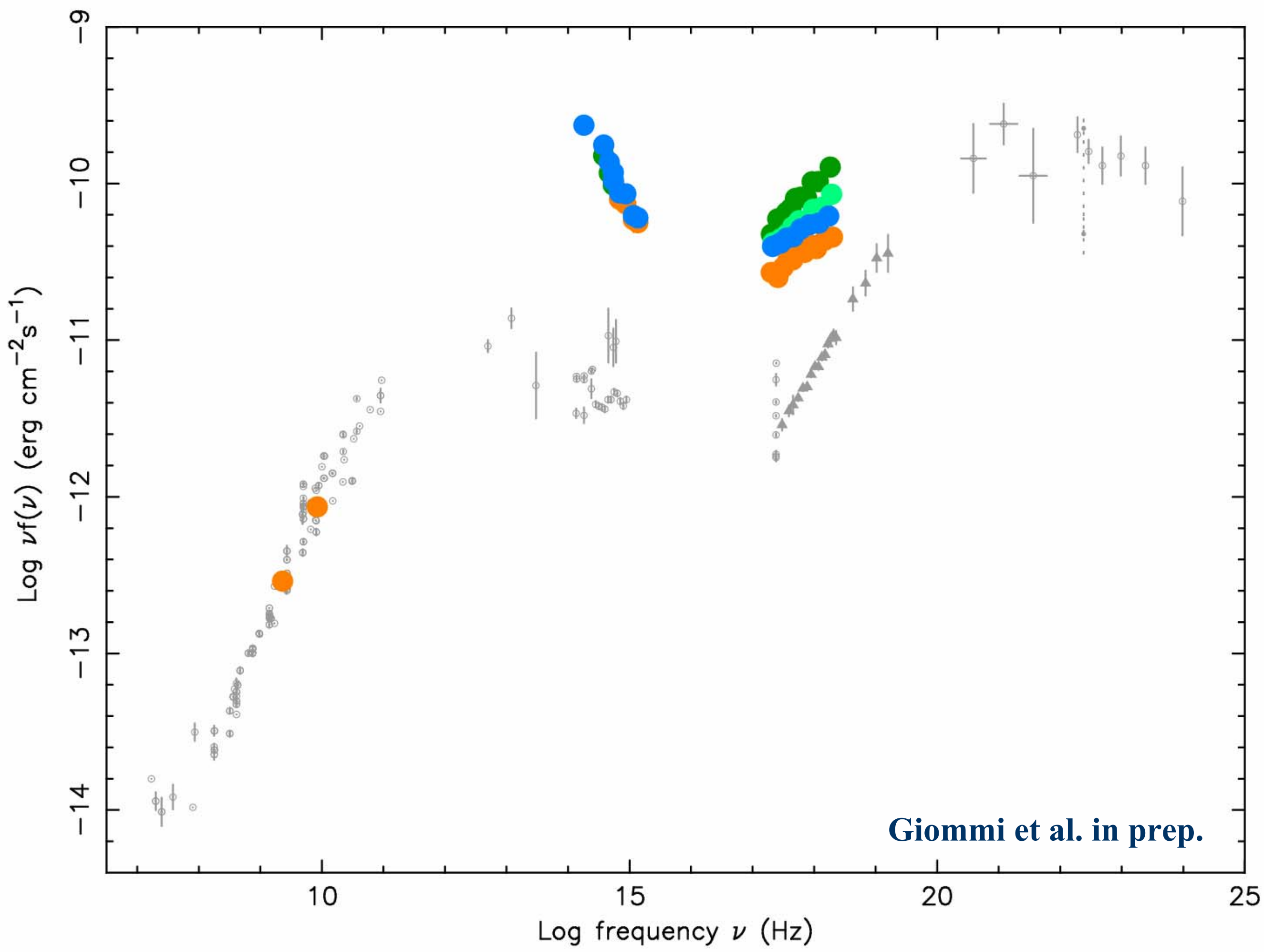

- "two-bump" general shape
- X-ray: factor 10-30 brighter than previously observed and factor 3 vaiability between epochs
- variability behaviour very different
- one-zone Synchrotron Self-Compton models too simple
- sim. multi-frequency observations in several bands important!

Spectral Evolution of 3C454.3 after Optical Outburst in May

(Krichbaum et al., Bonn+IRAM+SMA)

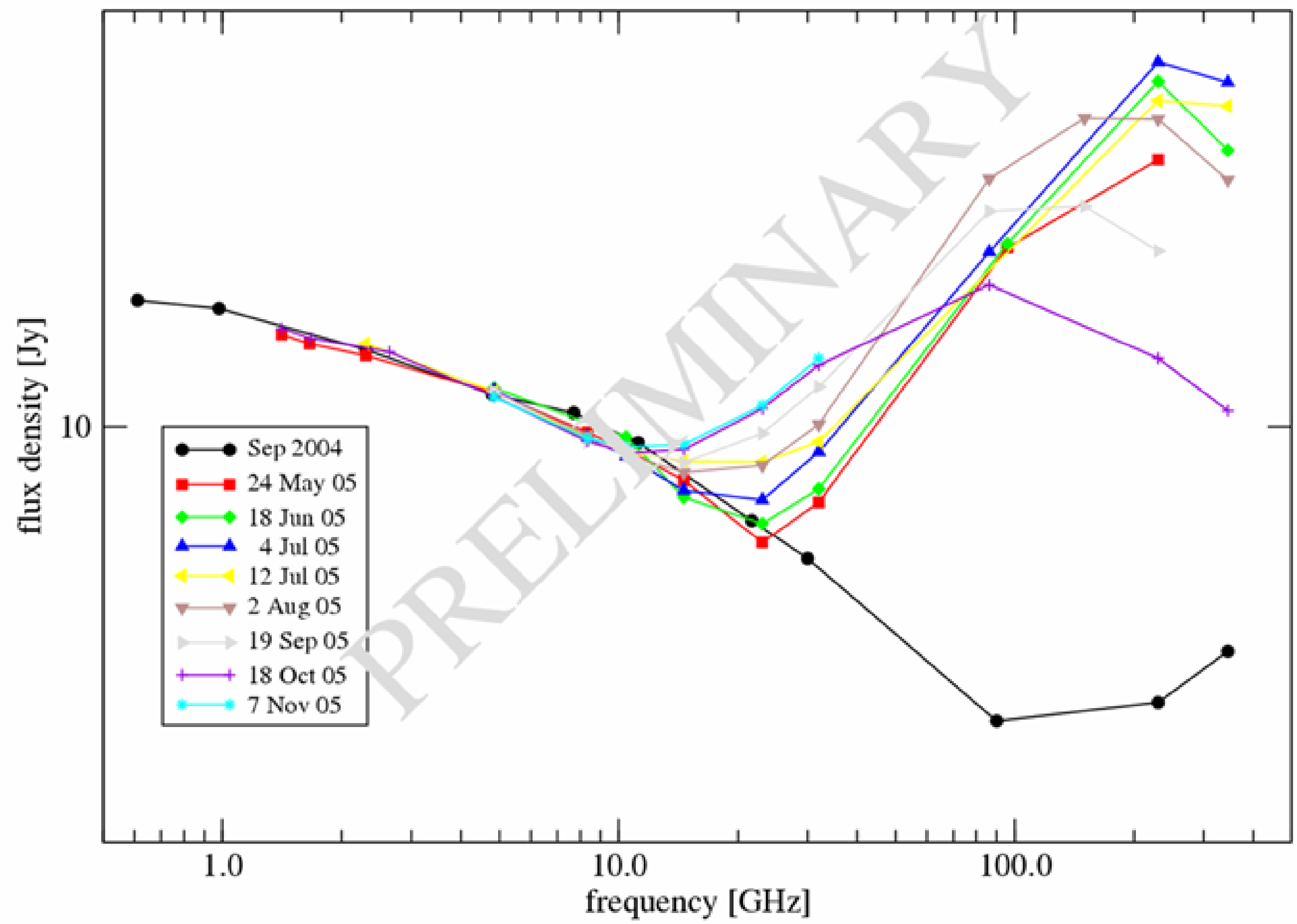

- **Thomas: radio-sub-mm observations during optical flare and beyond**
- **next 6 months**
- **EVPA changes at mm, but not much at cm wavelengths**
- **optical polarisation important (RM, B-Field/density of component)**

Outlook

- 3C454.3: a dramatic, historical outburst in May 2005
- spectral behaviour suggests
  - synchrotron peak below near-IR
  - geometrical origin of variations
- SWIFT data implies overall complex variability behaviour during flare
- future: detailed study of broad band behaviour putting all data sets together!!!

Where is the scattering screen?

- interstellar scintillation (ISS) “important process“
- what/where are the sights of scattering?
- direct detection yields new input for ISS models (D, electron density etc.)
- good example: IDV source 0954+658
  - ESEs and most likely a seasonal cycle
  - CO cloud at 100pc
  - screen: ionized surface (PDR) ?
  - CO clouds and PDRs are clumpy and turbulent
  - non-standard ISS theory (e.g. Boldyrev & Königl 2005)

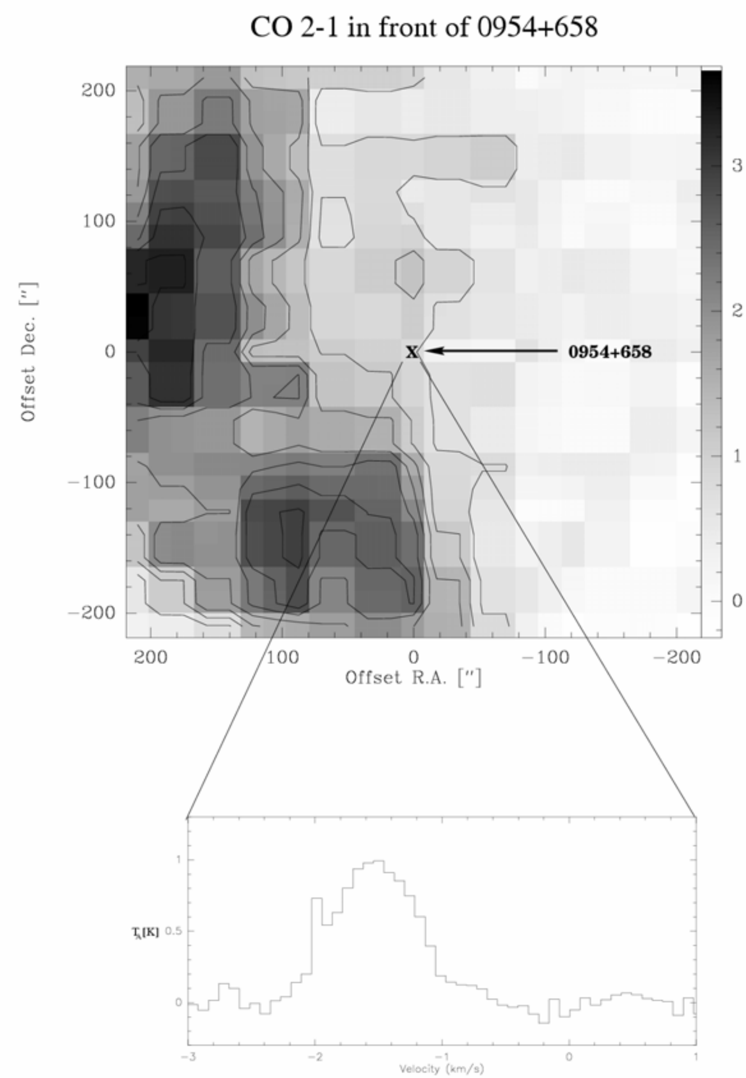

Where is the scattering screen?

- detection of [CII] 158 micron line

new approach: search for carbon recombination lines (carbon RRLs) in front of IDV/ESE sources with known CO clouds

→ **Effelsberg 8GHz: C90α and C91α**

High Energy Emission in the Jets of M 87 and Centaurus A

Łukasz Stawarz

Max-Planck-Institut für Kernphysik, Heidelberg, Germany

Obserwatorium Astronomiczne UJ, Kraków, Poland

ENIGMA Collaboration

Collaborators

Felix A. Aharonian *(MPIfK, Heidelberg, Germany)*

Philip G. Edwards *(ISAS, Sagamihara, Japan)*

Jun Kataoka *(TIT, Tokyo, Japan)*

Tanja Kneiske *(AU, Adelaide, Australia)*

Michał Ostrowski *(OA UJ, Kraków, Poland)*

Aneta Siemiginowska *(CfA, Cambridge, USA)*

Marek Sikora *(CAMK, Warszawa, Poland)*

Fumio Takahara *(OU, Osaka, Japan)*

Stefan Wagner *(MPIfA, Heidelberg, Germany*

Fanaroff & Riley Dichotomy

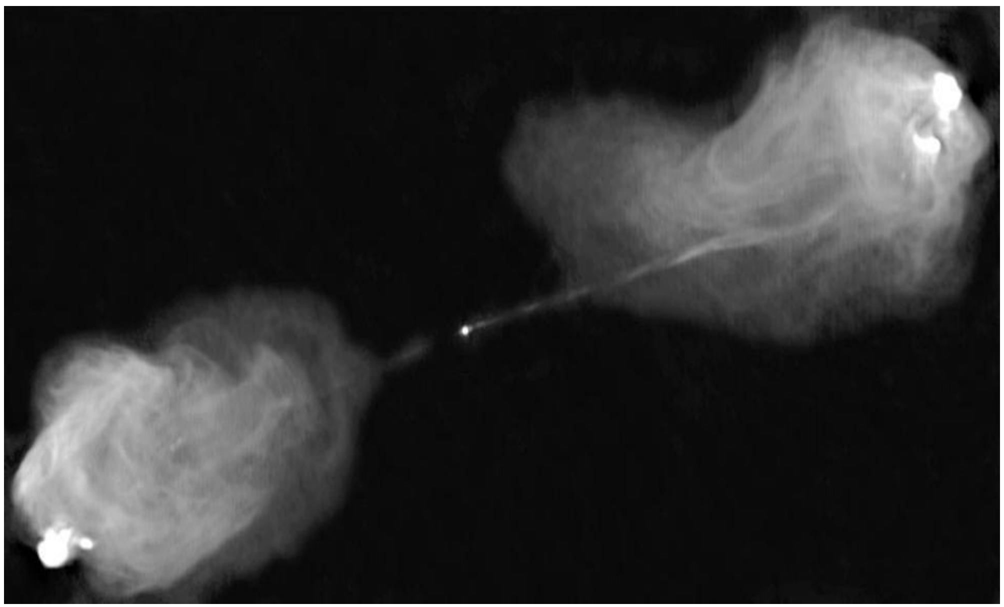

FR II (e.g., Cygnus A) and FR I (e.g., 3C 31) radio galaxies (*Fanaroff & Riley 1974, MNRAS, 167*):

- powerful $\leftrightarrow$ weak radio sources;
- edge-brightened $\leftrightarrow$ edge-darkened;
- one-sided jet & two hot-spots $\leftrightarrow$ two-sided jets & lacking hot-spots.

FR I Radio Galaxies

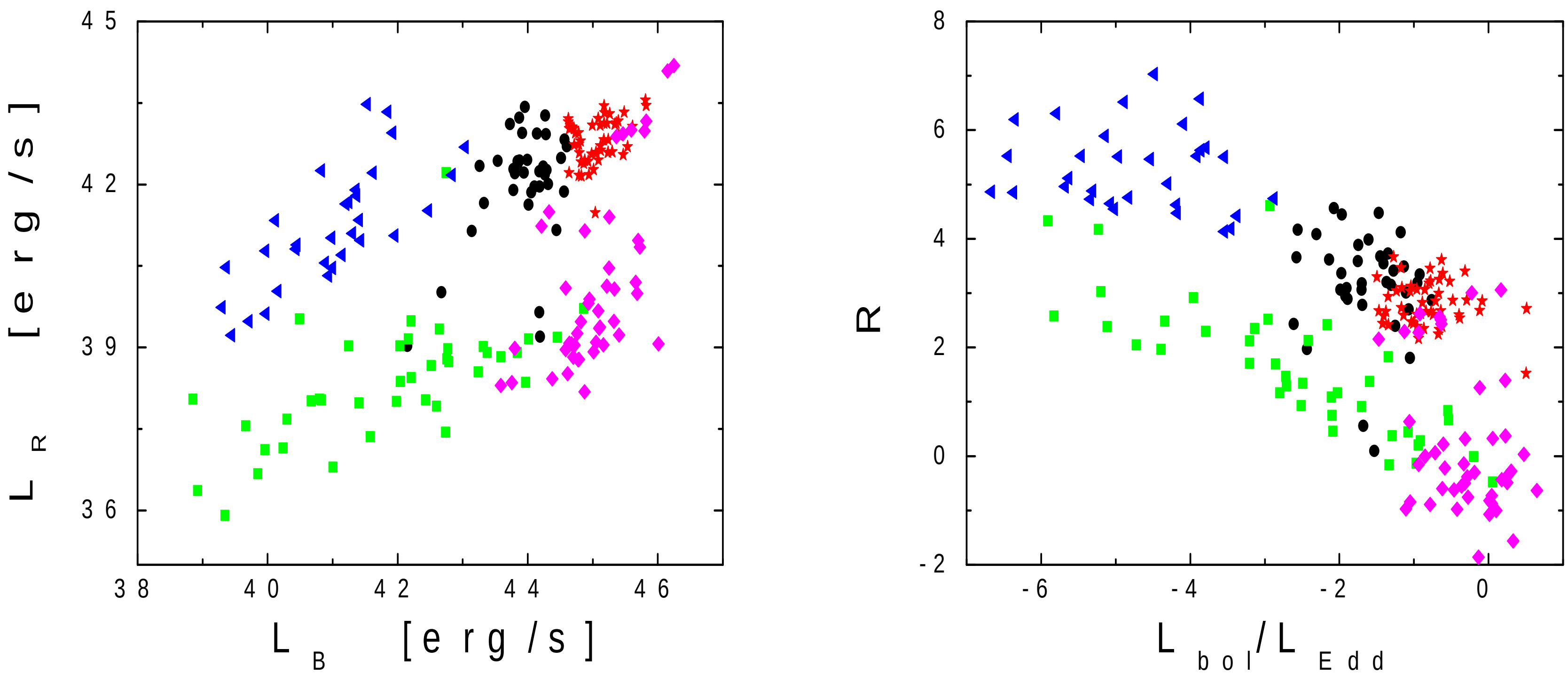

FR I Radio Galaxies compared with Broad-line Radio Galaxies and Quasars, Seyfert Galaxies and bright PG Quasars (*Sikora et al. 2006, in prep.*).

Large-Scale Radio Structure of M 87

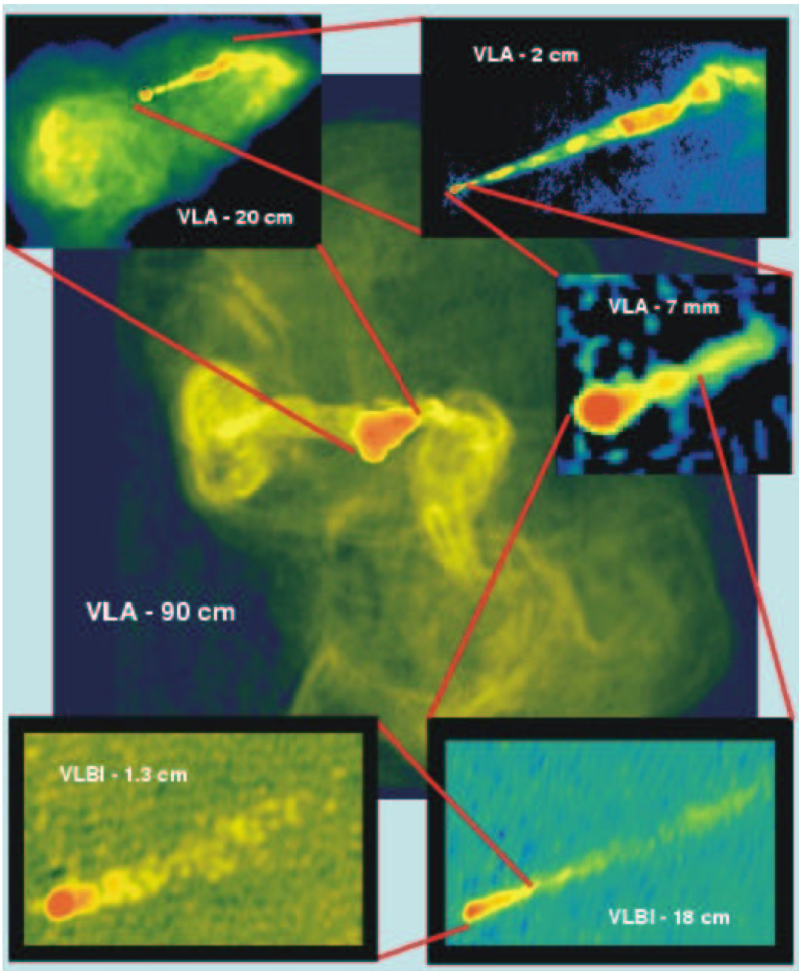

Amorphous large-scale radio structure of M 87 (*Owen et al. 2000, ApJ, 543*).

"buoyant bubbles of cosmic rays (inflated by an earlier nuclear active phase of the galaxy) rise through the cooling gas (...); bubbles uplift relatively cool X-ray-emitting gas from the central regions of the cooling flow to larger distances." (*Churazov et al. 2001, ApJ, 554*)

"the jet disrupts very close to the galactic core, but the plasma flow appears to continue in a much less ordered fashion, forming giant 'bubble' which has partly mixed with the ambient thermal plasma." (*Eilek et al. 2002, New AR, 46*)

X-ray Cluster Gas Around M 87

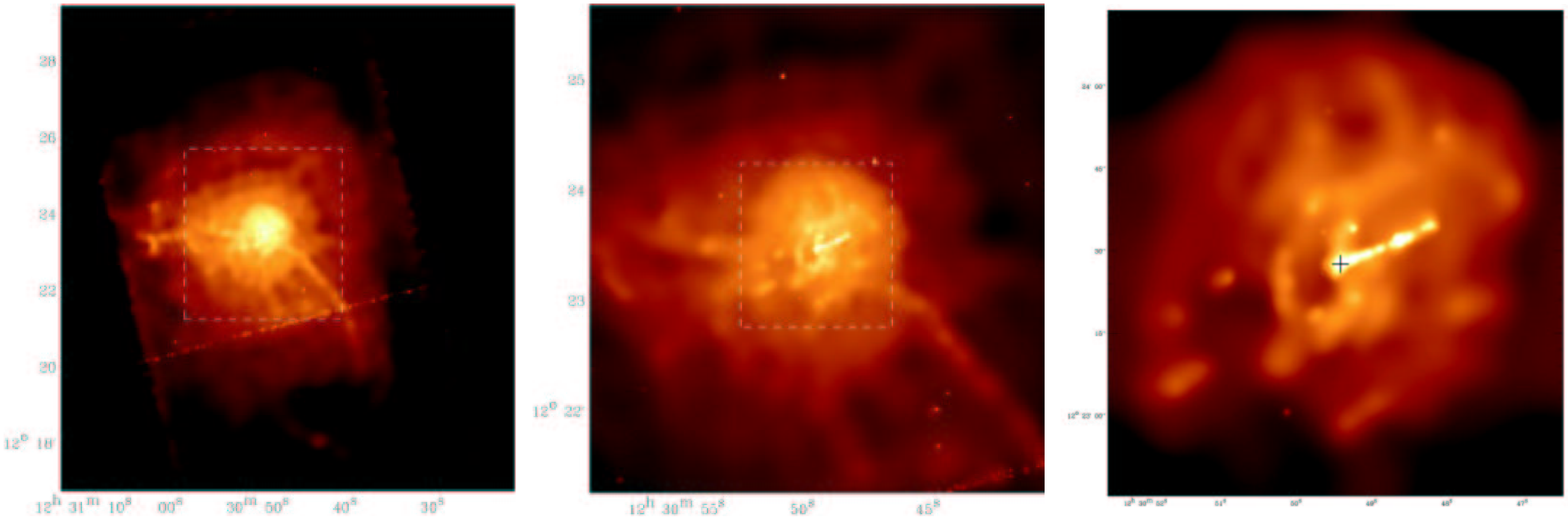

Cluster gas surrounding M 87 as observed in X-rays by the *Chandra X-ray Observatory*:

"The inner radio lobes are aligned with depressions in the X-ray surface brightness, and there is no evidence of shock heating in the X-ray emission immediately surrounding the inner radio lobes, suggesting that the radio plasma has gently pushed aside the X-rayemitting gas. (...) On larger scales the most striking feature is the X-ray arc running from the east, across the central regions of M87, and off to the southwest. The gas in the arc has at least two temperatures, with one component at the temperature of the ambient intracluster medium and a cooler component at ∼1 keV. The gas in the arcs is probably overpressured with respect to, and somewhat more metal-rich than, the ambient intracluster medium" (Young et al., 2002, ApJ, 579).

Synchrotron Emission of the M 87 Jet

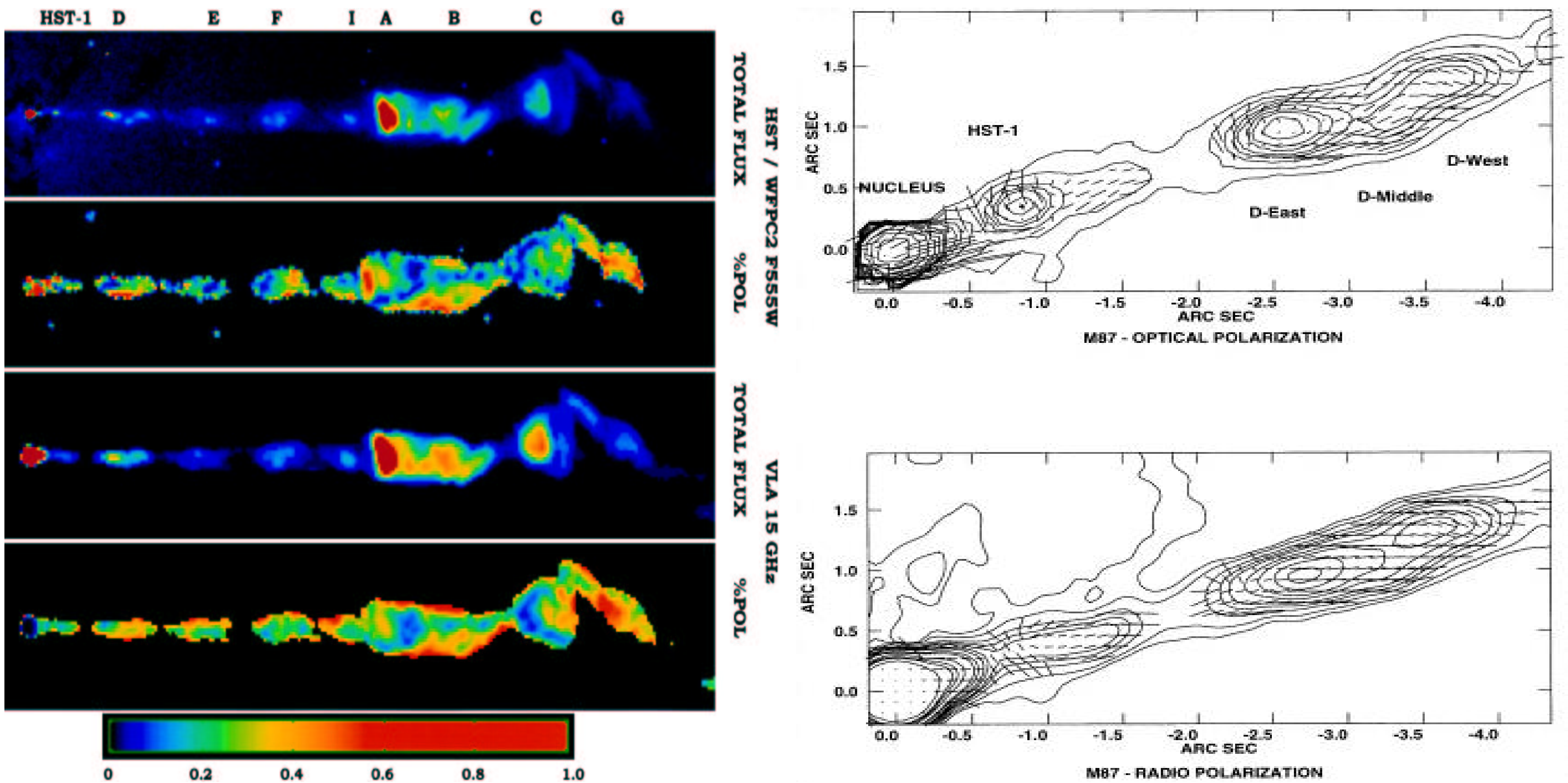

Radio and optical synchrotron emission of 2-kpc-long M 87 jet (*Perlman et al. 1999, AJ, 117*).

Spectral Profiles of the M 87 Jet

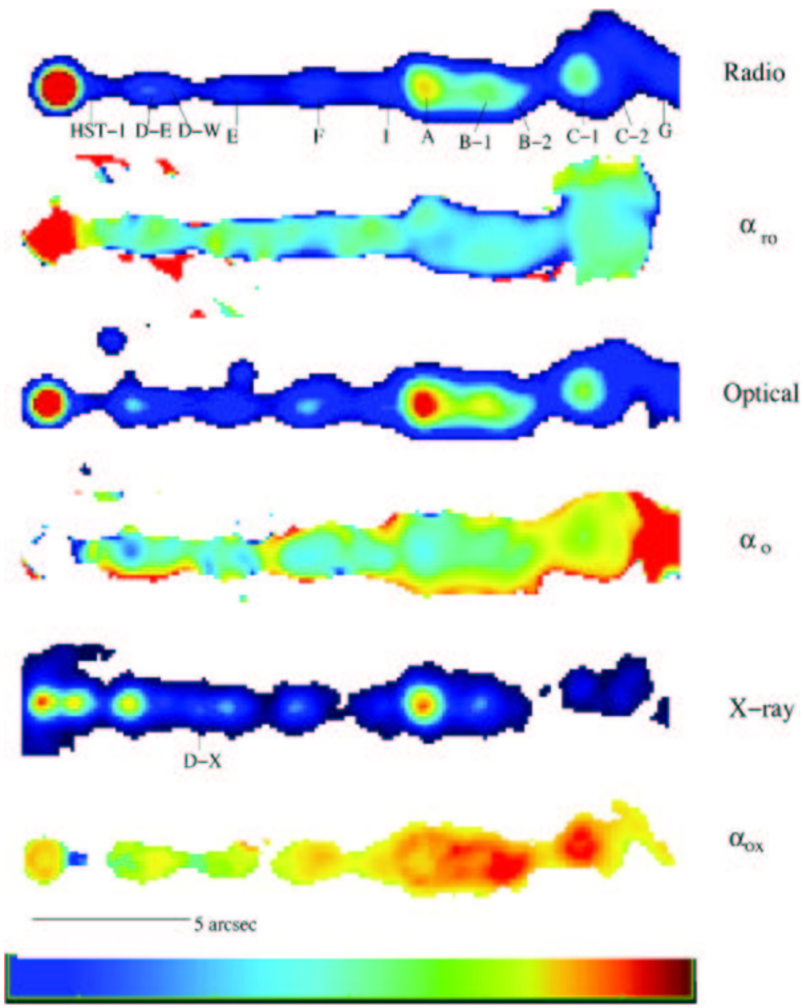

Images of the M87 jet
(*Perlman & Wilson, 2005, ApJ, 627*).

- Top: Radio (VLA 15 GHz)
- Second: Radio-optical spectral index
  0.85 (red) — 0.6 (blue)
- Third: Optical (HST F814W)
- Fourth: Optical spectral index
  1.5 (red) — 0.4 (blue)
- Fifth: X-rays (Chandra 0.3âĂŞ1.5 keV)
- Sixth: Optical-X-ray spectral index
  1.6 (red) — 0.9 (blue)

Large-Scale Radio Structure of Cen A

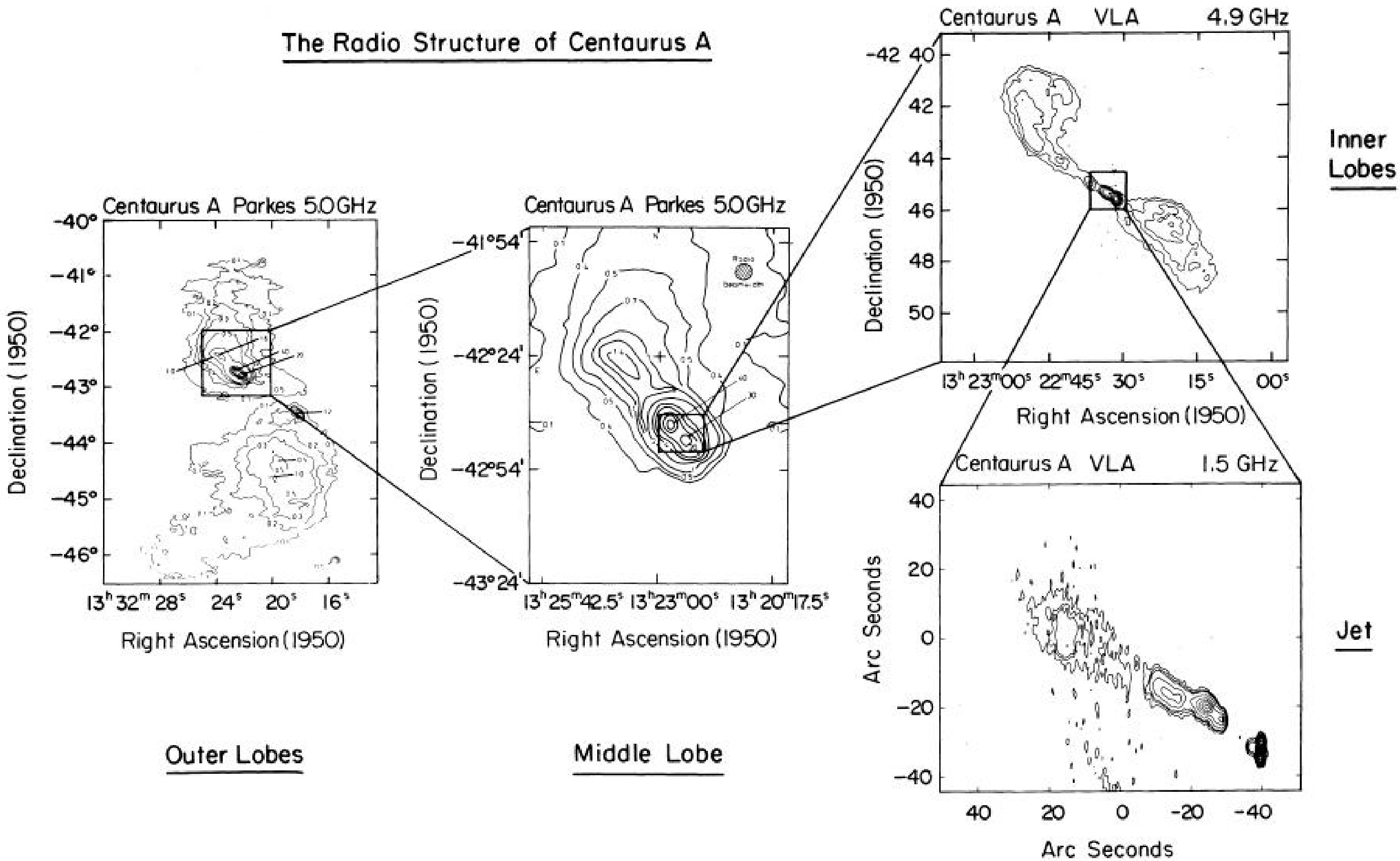

FIG. 11.—An illustration of the different scale sizes of radio structure in Cen A. The Parkes maps of the outer lobes and middle lobe were kindly provided by R. Ekers from a paper by Haynes, Cannon, and Ekers (1982). The inner lobes map is reproduced from Fig. 2, and the jet map is reproduced from Fig. 3.

Merger History of Cen A

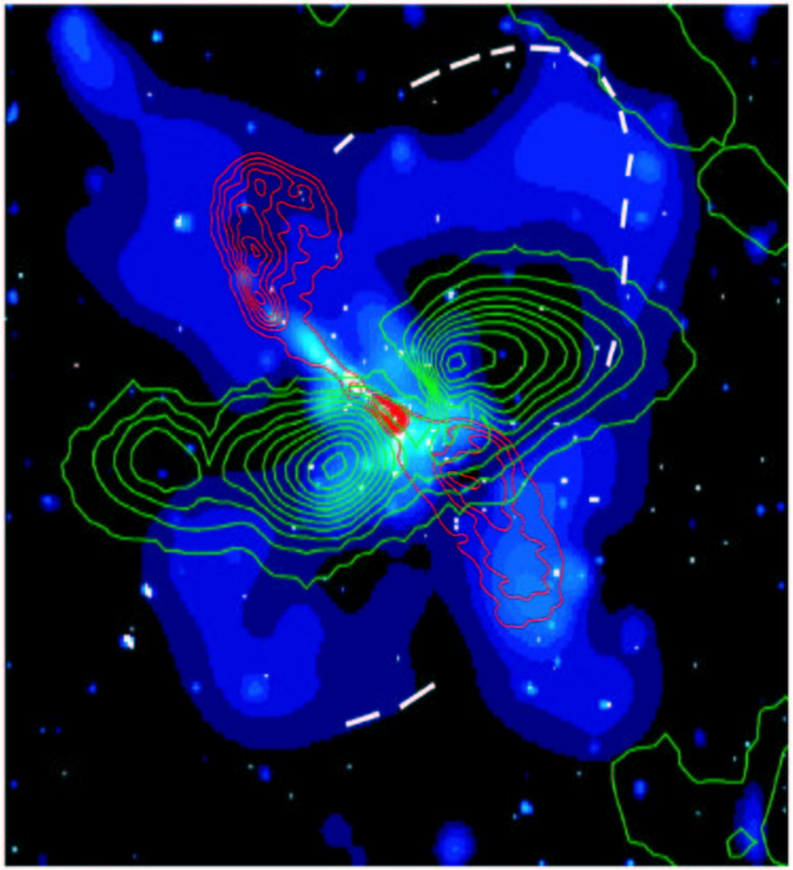

X-rays (blue), 21 cm radio continuum (red contours), 21 cm line H I (green contours) (*Karovska et al. 2002, ApJ, 577*).

$d = 3.4\,$Mpc, for which 1$''$ corresponds to 16 pc, and 1$'$ to 0.96 kpc.

Famous 'dark lane' pronounced within the host elliptical body, being in fact an edge-on disk of rotating metal-rich stars, nebulae, dust clouds, H II regions, OB associations, and supernova remnants, is most probably remnant of the merger with spiral galaxy, which happened some $10^8 - 10^9$ *years ago (see Israel 1998, ARA&A, 8).*

Radio and X-ray synchrotron jet in Cen A: a very complex jet morphology with filaments and diffuse sub-structured knots; limb-brightened radio and X-ray profiles; projected magnetic field parallel to the jet axis (see Schreier et al. 1979, 1981; Burns et al. 1983, Clarke et al. 1986, 1992; Kraft et al. 2002; Hardcastle et al. 2003).

X-ray Jet of Cen A

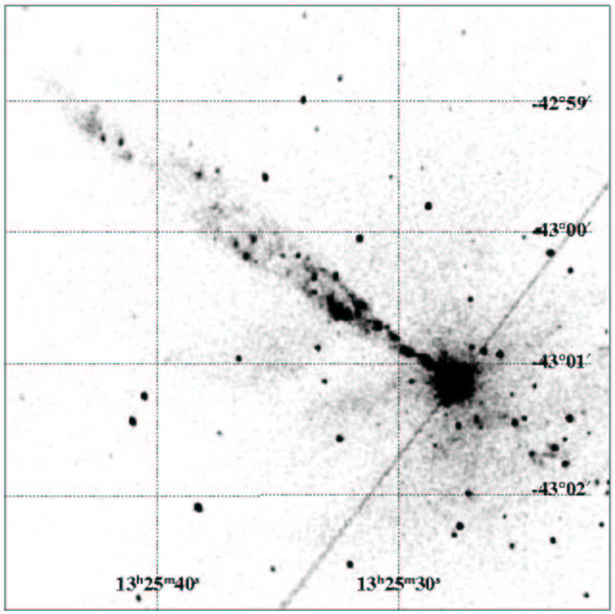

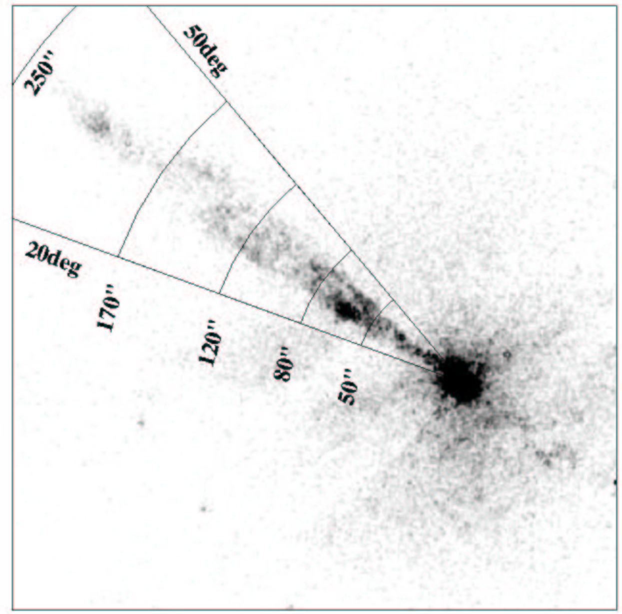

Left: *Chandra* 0.4–8.0 keV X-ray image of the Cen A jet. Archival data combined. The image is smoothed with a $\sigma = 0.5$ arcsec Gaussian. *Right:* The 0.4–8.0 keV X-ray image of the Cen A jet, after subtracting the point sources and filling in the blanks with values interpolated from surrounding background regions (*Kataoka et al. 2006, ApJ, submitted (astro-ph/0510661)*).

Longitudinal Profiles of the X-ray Jet in Cen A

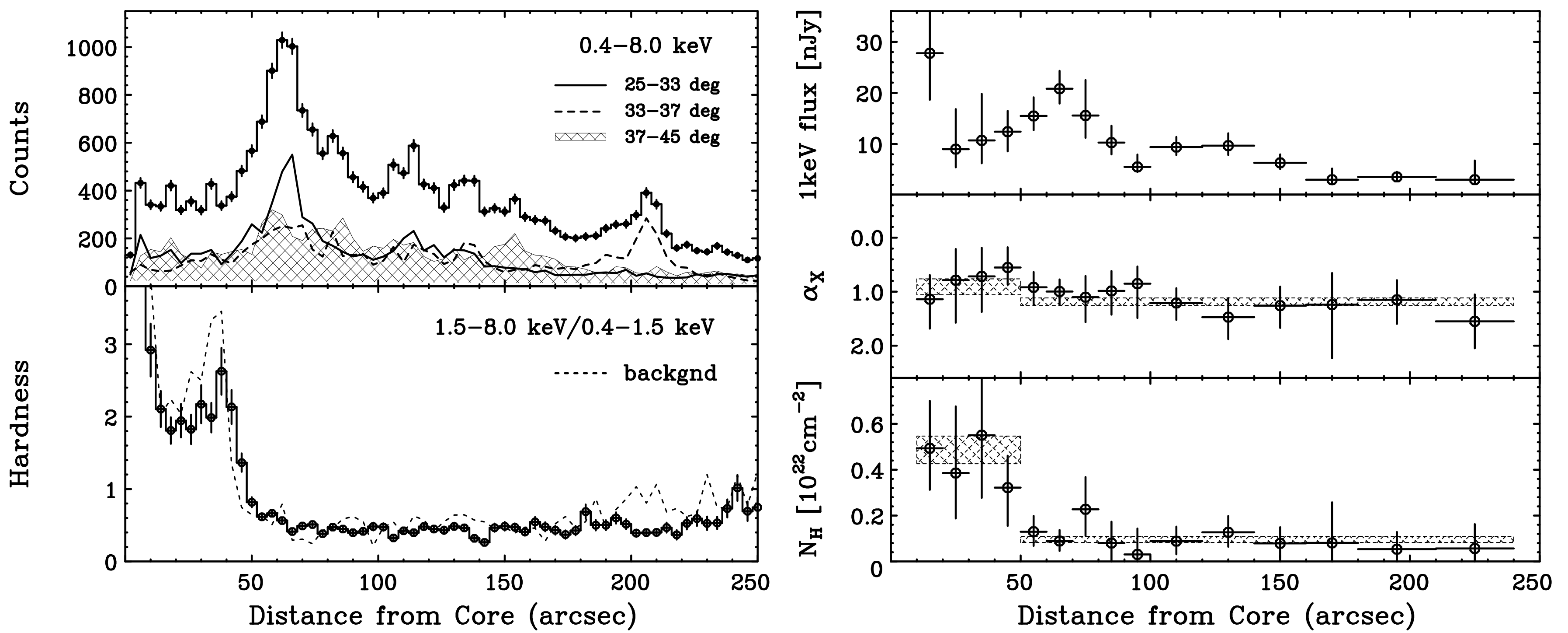

Left: The observed longitudinal X-ray intensity profile of the diffuse jet component in the 0.4−8.0 keV photon energy band *(top)*. Variation of the hardness ratio, defined as (0.4−1.5 keV)/(1.5−8.0 keV), along the main jet axis *(bottom)*. *Right:* Variation of the X-ray flux density measured at 1 keV (*top*), the X-ray energy spectral index $\alpha_{\rm X}$ (*middle*), and the absorbing column density $N_{\rm H}$ (*bottom*) of the diffuse emission along the jet. Hatched regions show the best-fit parameters and their $1\,\sigma$ uncertainties for the combined spectral fittings.

Transverse Profiles of the X-ray Jet in Cen A

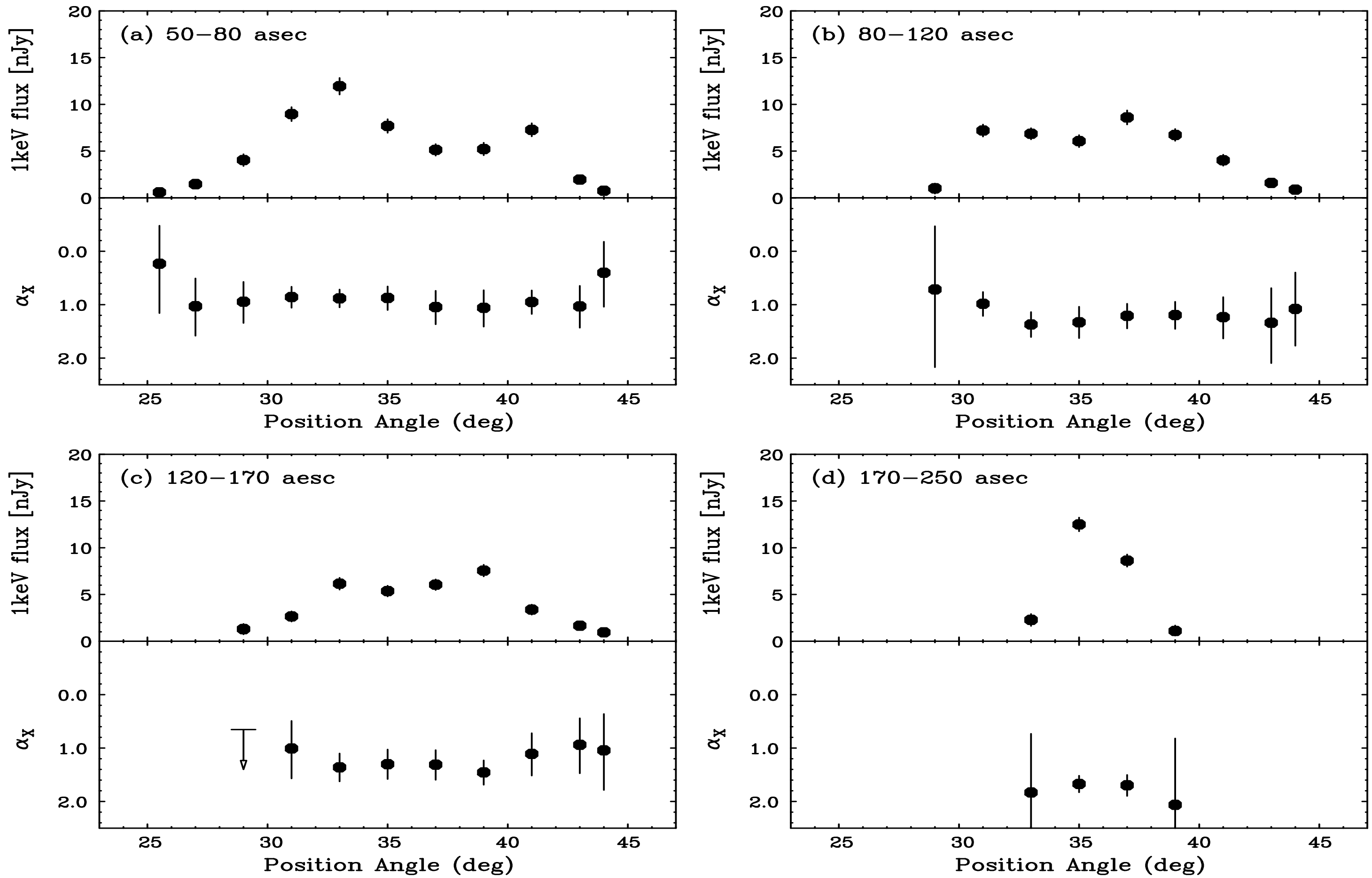

Variation of the X-ray intensity of the diffuse component measured at 1 keV (*top*), and the energy spectral index (*bottom*) across the jet (power-law + Galactic absorption).

Knots' Luminosity Function of the X-ray Jet in Cen A

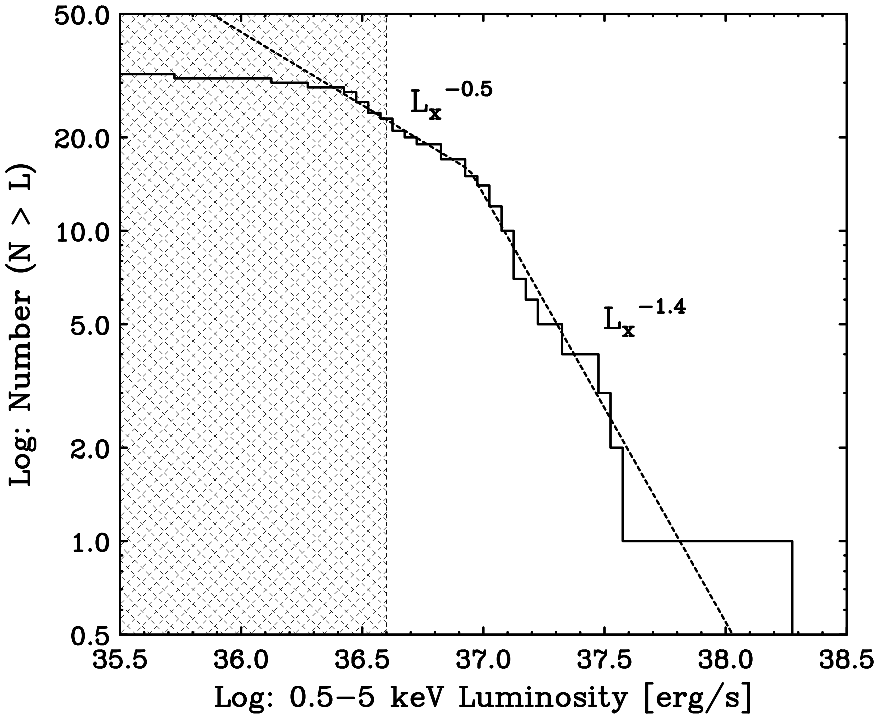

$N(> L_X) \propto L_X^{-\kappa}$
flattens significantly from κ = 1.4 to 0.5 below $L_{\rm brk} \simeq 9\times10^{36}$ erg s^{-1}.

Luminosity function of the X-ray knots. X-ray luminosity is the absorption corrected luminosity in the 0.5−5.0 keV band, assuming a power-law spectrum with energy spectral index α_X = 1.0 and N_H = 0.96×10^{21} cm^{-2}. The best fit broken power-law model, excluding the hatched region where our sample is incomplete and biased ($L_X \leq 4\times10^{36}$ erg s^{-1}), is also shown.

The total luminosity of the Cen A jet (i.e., the sum of the jet-knots and the unresolved diffuse emission) is 1.6×10^{39} erg s^{-1}. Integrating the LF down to any value of $L_{\rm min}$ gives $< 8.1\times10^{38}$ erg s^{-1} (which is only 25% larger than the sum of the *already resolved* jet-knots).

X-ray Jet of Cen A — Conclusions

- The X-ray jet emission remaining after substracting all the detected compact knots reveals a flat-topped intensity profile in the transverse jet direction, with the intensity peaking at the jet boundaries. $\boxed{\rightarrow}$ Sheared relativistic outflow (consistently with the observed parallel magnetic field structure and one-sideness of the jet).
- The extended component is most likely to be truly diffuse, rather than resulting from the pile-up of unresolved faint knots. $\boxed{\rightarrow}$ Continuous acceleration of the X-ray emitting electrons (the maximum propagation length of the jet electrons emitting 10 keV synchrotron photons within the 100 μG equipartition jet magnetic field is $l_{\rm rad} = c\,\Gamma\,t_{\rm rad} \sim 10$ pc for $\Gamma \sim 2$).
- The X-ray spectrum of the diffuse component uniform across and along the jet, with an X-ray energy spectral index of $\alpha_{\rm X} \approx 1$, similar to that observed in the compact knots. $\boxed{\rightarrow}$ 'Universal' electron energy distribution $n_{\rm e}(\gamma) \propto \gamma^{-s}$ characterized by the injection spectral index $s_{\rm in}$ = 2.1 (see *Young et al. 2005, ApJ, 626*) modified by the synchrotron losses up to $s = s_{\rm in} + 1$.
- Evidence for a possible spectral hardening at the outer sheath of the jet. $\boxed{\rightarrow}$ Synchrotron emission of the high-energy electrons which, in the outer sheath of the jet, lose energy predominantly due to inverse-Compton radiation in the Klein-Nishina regime (?)

A Role of the Boundary Shear Layers

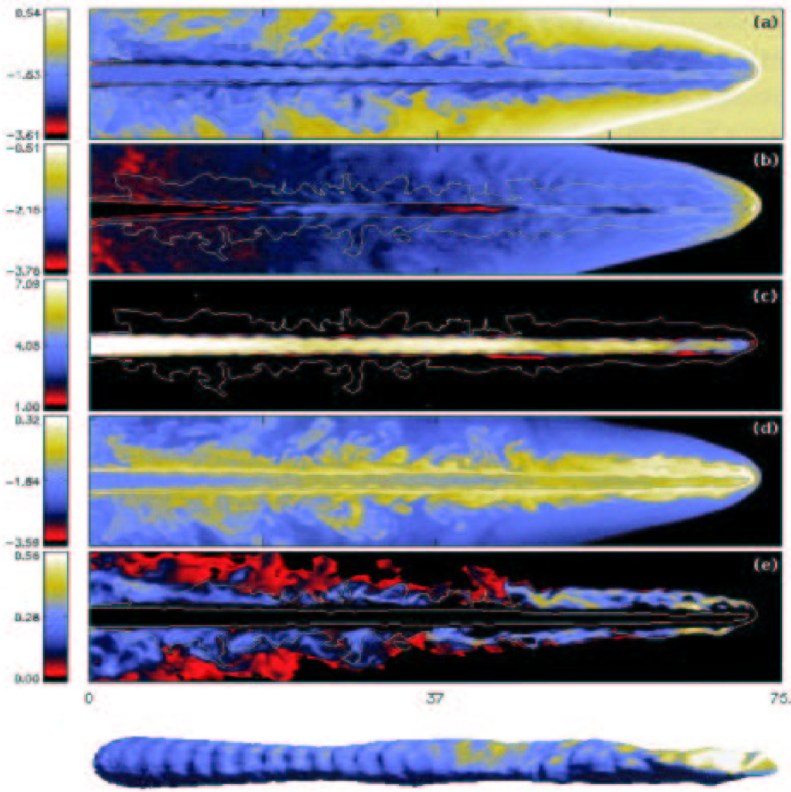

Aloy et al. 1999, ApJ, 523: 3D hydrodynamical simulations (FIG: (a) – the rest mass density; (b) – pressure; (c) – bulk Lorentz factor; (d) – specific internal energy).

X-ray emission of the large scale jets due to synchrotron radiation of ultrarelativistic electrons ($\gamma \sim 10^8$) accelerated continuously along the flows (*Stawarz & Ostrowski 2002, ApJ, 578*; *Stawarz et al. 2004, ApJ, 608*).

$$t_{\rm acc} \sim 5 \times 10^2 \, \gamma \text{ [s]}$$
$$t_{\rm esc} \sim 6 \times 10^{24} \, \gamma^{-1} \text{ [s]}$$
$$t_{\rm rad} \sim 8 \times 10^{18} \, \gamma^{-1} \text{ [s]}$$

i.e.

$$t_{\rm esc}/t_{\rm rad} \sim 10^6$$
$$t_{\rm acc} \sim t_{\rm rad} \Rightarrow \gamma_{\rm eq} \sim 10^8$$

(for the boundary shear layer acceleration see also *Rieger & Duffy 2004, ApJ, 617*, and references therein.)

Non-standard X-ray Spectra

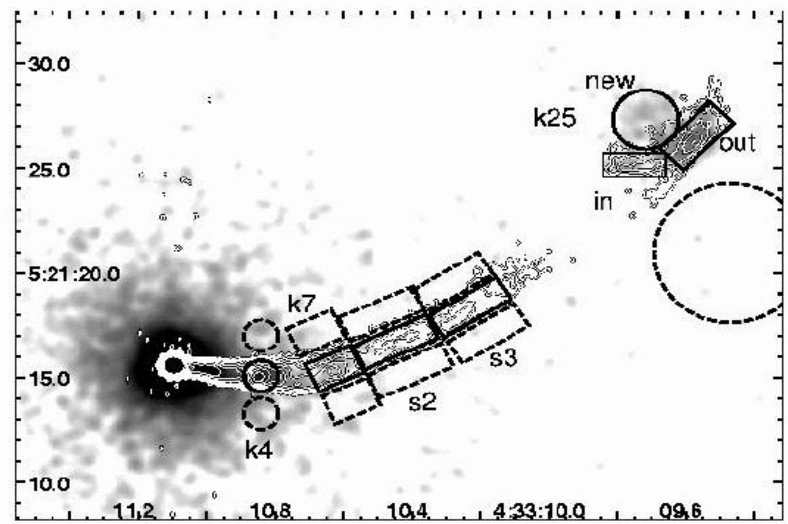

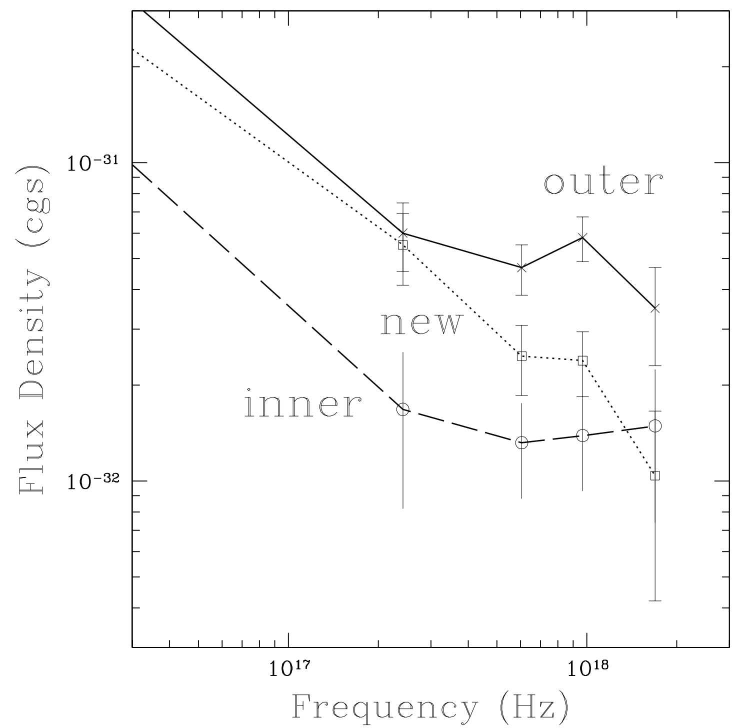

X-ray jet in 3C 120 radio galaxy: complex morphology, complex spectral behavior (*Harris et al. 2004, ApJ, 615*).

Non-standard Optical Spectra

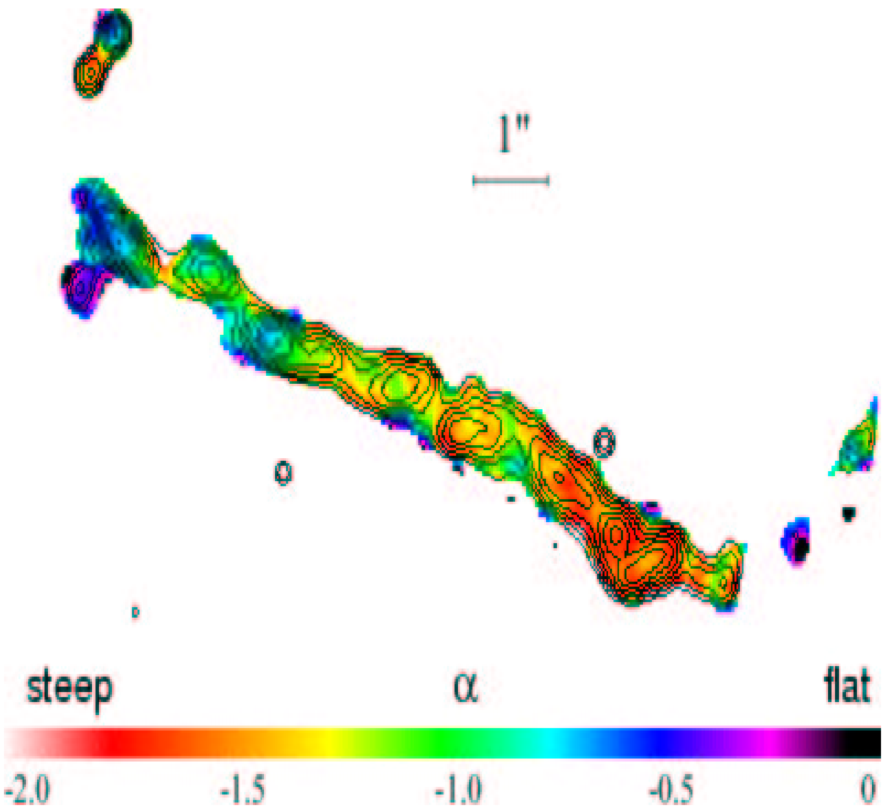

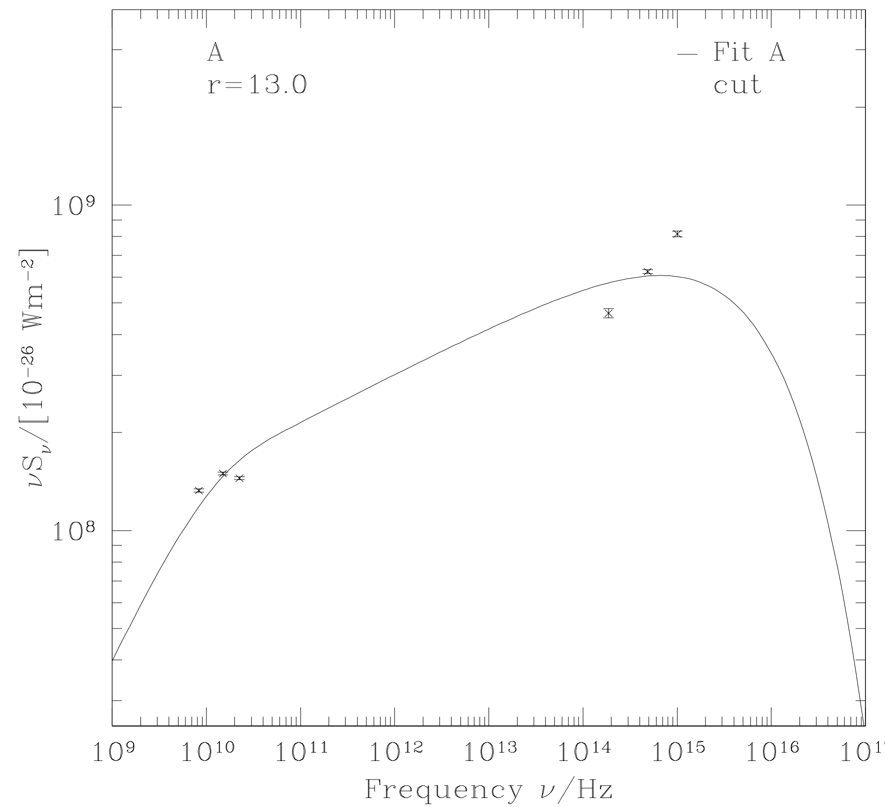

Optical jet in quasar 3C 273: unexpected character of the spectral changes along the jet, non-standard synchrotron spectra (*Jester et al. 2001, A&A, 447; 2002, A&A, 385; 2005, A&A, 431*). Here $f_\nu \propto \nu^\alpha$.

Synchrotron X-rays in All Large-Scale Jets?

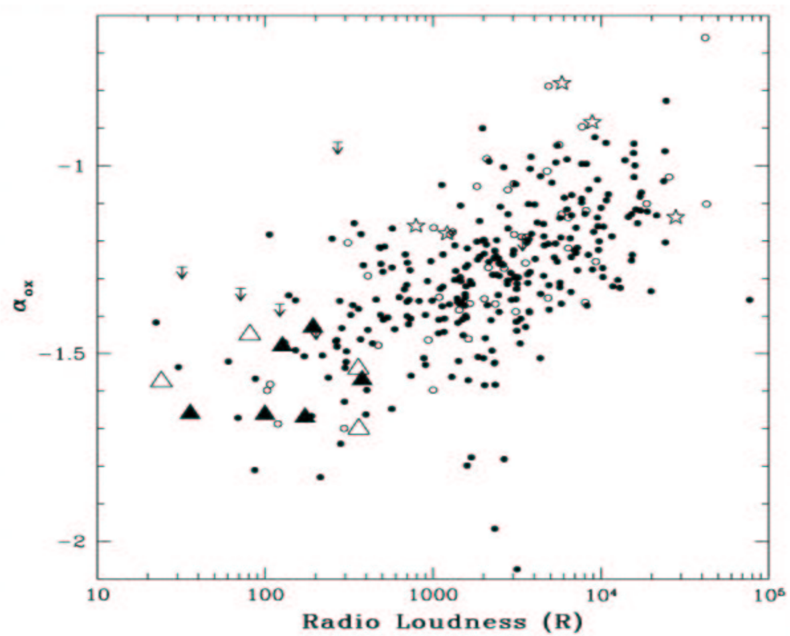

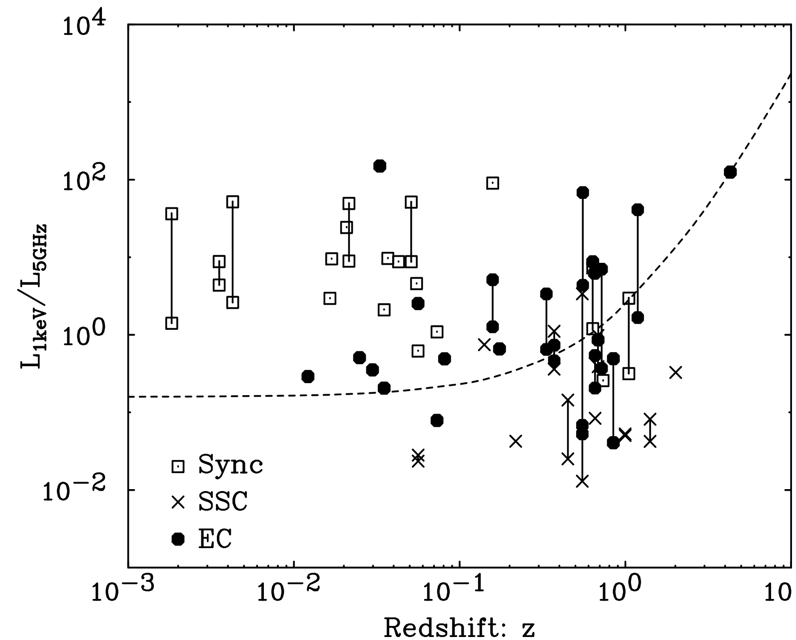

If the X-ray emission of powerful large-scale quasar jets is due to the IC/CMB process (*Tavecchio et al. 2000, ApJ, 544*; *Celotti et al. 2001, MNRAS, 321*), then due to $U_{\rm cmb} \propto (1+z)^4$ one should expect (*Schwartz 2002, ApJ, 569*):

- increase in the X-ray core luminosity with z ;
- $L_{\rm X}/L_{\rm R} \propto (1+z)^4$ for the large-scale jets.

THIS IS NOT THE CASE ! *Left*: *Bassett et al. 2004, AJ, 128*; *Right*: *Kataoka & Stawarz 2005, ApJ, 622*

VHE Electrons in the Jet of M 87

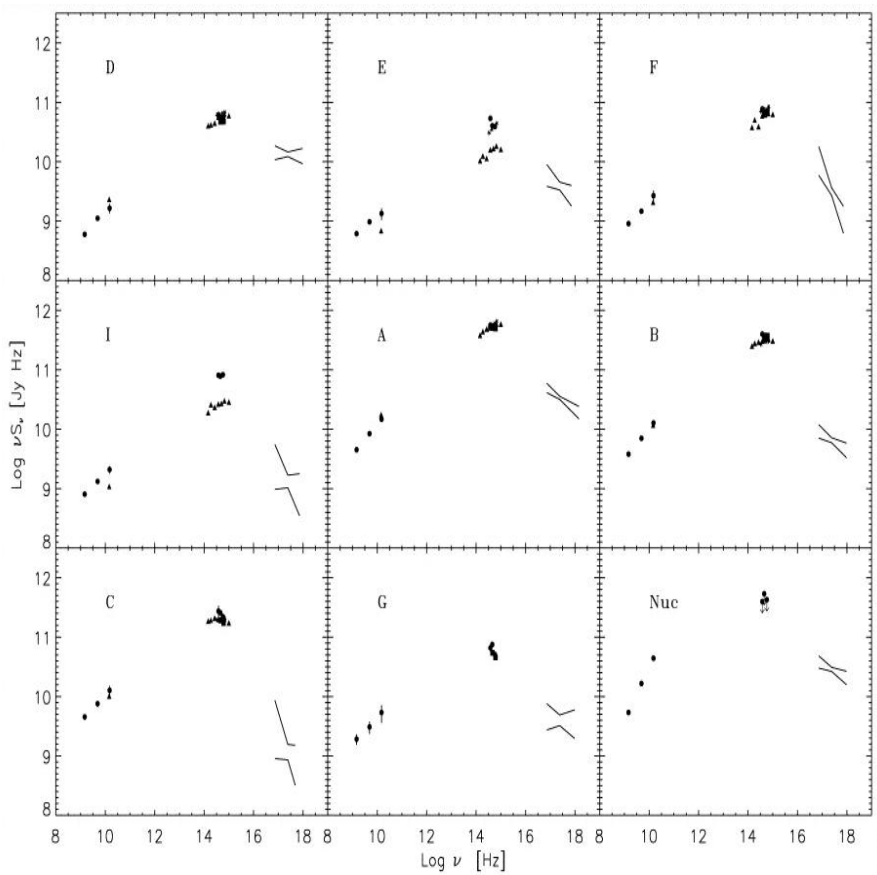

Synchrotron emission of the M 87 jet (*Wilson & Yang 2002, ApJ, 568*).

Let us reconctruct the comoving energy distribution of the electrons contributing to the observed emission of knot A, $n'_{\rm e} \equiv \int n'_{\rm e}(\gamma)\, d\gamma$, from the well-constrained synchrotron continuum, and find the expected inverse-Compton emission as a function of free parameters:

- the jet magnetic field B,
- the bulk Lorentz factor Γ,
- the jet viewing angle θ

including relativistic effects and Klein-Nishina regime (*Stawarz et al. 2003, ApJ, 597; 2005, ApJ, 626*).

Electron Energy Distribution in Knot A

We take the comoving electron energy distribution in a form

(1) $$n'_{\rm e}(\gamma) = K'_{\rm e}\,\gamma^{-p} \quad \text{for}\, \gamma \leq \gamma_{\rm br} \quad \text{and} \quad n'_{\rm e}(\gamma) = K'_{\rm e}\,\gamma_{\rm br}^{q}\gamma^{-(p+q)} \quad \text{for}\, \gamma > \gamma_{\rm br}$$

with $p = 2.3$ and $q = 1.6$. The electron break Lorentz factor,

(2) $$\gamma_{\rm br} = (4\pi\, m_{\rm e} c\, \nu_{\rm br}/e\,\delta\,B)^{1/2} \approx 2.7\times 10^{6}\,\delta^{-0.5}\,B_{-4}^{-0.5} \quad ,$$

corresponds to the observed synchrotron break frequency $\nu_{\rm br} = 10^{15}$ Hz for $B \equiv B_{-4}\,10^{-4}$G and Doppler factor δ. We normalize the number of electrons as

(3) $$[\nu L_{\nu}]_{\rm syn} = 4\pi\,\delta^{4}\,V'\,[\nu' j'_{\nu'}]_{\rm syn} \quad ,$$

where $V' = V_{obs}/\delta$ is the volume filled by those particles which are ‘seen’ at the given moment, and

(4) $$[\nu' j'_{\nu'}]_{\rm syn} = \frac{c\sigma_T}{48\pi^2}\,B^2\,[\gamma^3 n'_e(\gamma)]_{\gamma=(4\pi\, m_{\rm e} c\,\nu'/e\,B)^{1/2}} \quad ,$$

where $\nu' = \nu/\delta$. Hence, for a given observed synchrotron break luminosity $L_{\rm br} = 3\times 10^{41}$ erg s^{-1} one obtains $V' K'_{\rm e} = 1.8\times 10^{60}\,\delta^{-3.65}\,B_{-4}^{-1.65}$.

Host Galaxy Emission in M 87

We model the starlight emission of the host elliptical resulting from the evolved population of red giants in terms of a King profile

(5) $$j_{\rm star}(r) = j_0 \left[1 + \left(\frac{r}{r_{\rm c}}\right)^2\right]^{-3/2} \quad \text{for} \quad r < r_{\rm t} \quad ,$$

where r is the radius from the galactic center, $r_{\rm c}$ is the core radius for the galaxy, and $r_{\rm t}$ is the tidal radius ($\rho_{\rm L}(r) = 4\pi\, j_{\rm star}(r)$) in the I band given by *Lauer et al. 1992, AJ, 103*).

(6) $$I_{\rm star}(r,\kappa) = \int_0^{l_{\rm max}} j_{\rm star}\left(\sqrt{r^2 + l^2 + 2rl\kappa}\right)\, dl \quad ,$$

where $\zeta \equiv \cos^{-1}\kappa$ and the outer boundary of the host galaxy is

(7) $$l_{\rm max} = -r\kappa + \sqrt{r_{\rm t}^2 - r^2 + r^2\kappa^2} \quad .$$

Finally,

(8) $$U_{\rm star}(r) = \frac{2\pi}{c} \int_{-1}^{+1} I_{\rm star}(r,\kappa)\, d\kappa \quad .$$

Dominant Starlight Photon Field

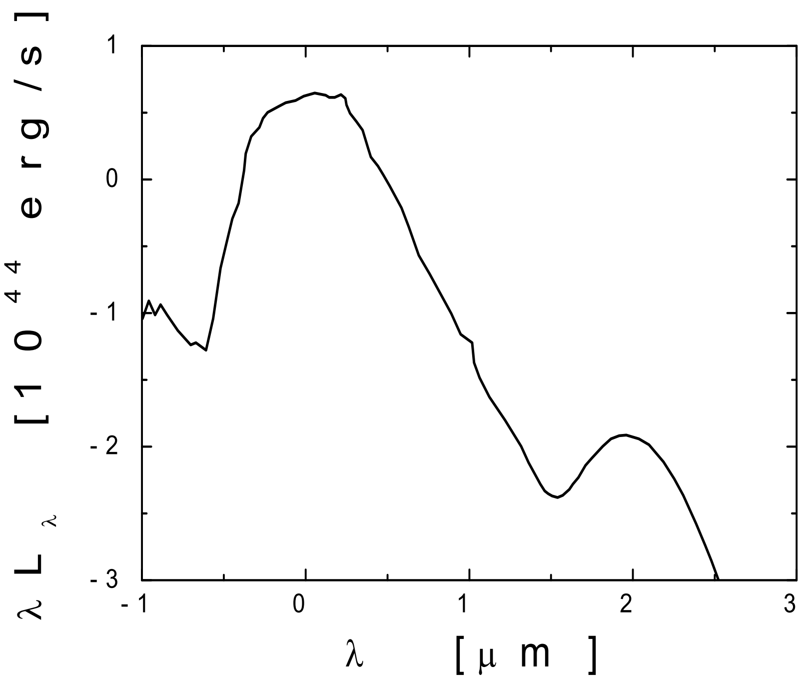

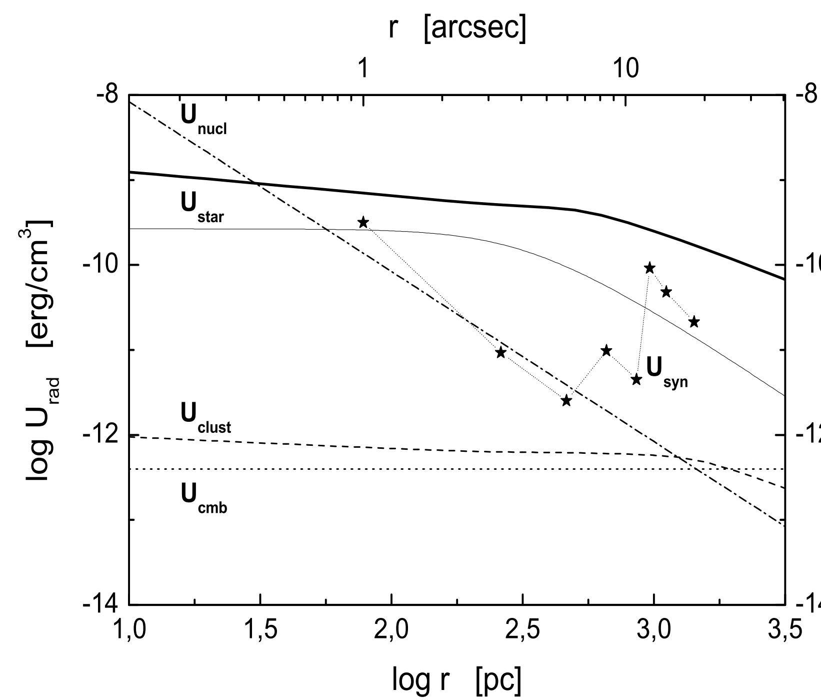

A template SED of a giant elliptical galaxy (*Silva et al. 1998, ApJ, 509*).

Radiation fields in M87 host galaxy along the jet (as measured by a stationary observer). $U_{\rm star}(1\,{\rm kpc}) \approx 10^{-10}$ erg cm^{-3} (safe lower limit).

Inverse-Comptont Emission of Knot A

The high-energy emissivity of knot A due to IC scattering on monoenergetic and mono-directional (in the jet rest frame) starlight photon field, including proper relativistic effects in the Klein-Nishina regime, can be found from the approximate expression given by *Aharonian & Atoyan (1981, Ap&SS, 79)* as

(9) $$[\nu' j'_{\nu'}]_{\rm ic} = \frac{c\,\sigma_{\rm T}}{4\pi}\,U_{\rm star}\,\nu_{\rm star}^{-2}\,\nu'^2 \int_{\gamma_0}^{\gamma_{\rm max}} \frac{n'_{\rm e}(\gamma)}{\gamma^2}\,f(\epsilon', \epsilon'_{\rm star}, \gamma, \mu')\,d\gamma \quad .$$

Here $\epsilon' \equiv h\,\nu'/m_{\rm e}c^2$, $\epsilon'_{\rm star} \equiv h\,\nu'_{\rm star}/m_{\rm e}c^2$, $\theta' \equiv \cos^{-1}\mu'$ is the scattering angle, and

(10) $$f(\epsilon', \epsilon'_{\rm star}, \gamma, \mu') = 1 + \frac{w'^2}{2(1-w')} - \frac{2w'}{v'(1-w')} + \frac{2w'^2}{v'^2(1-w')^2}$$

where $v' = 2(1-\mu')\,\epsilon'_{\rm star}\gamma$ and $w' = \epsilon'/\gamma$. The lower limit of the integral over γ is given by the condition $f \geq 0$. Hence, using the well known relativistic transformations $\epsilon'_{\rm star} = \epsilon_{\rm star}\Gamma$ (where Γ is a jet bulk Lorentz factor), $\epsilon' = \epsilon/\delta$, and $\mu' = (\mu - \beta)/(1 - \beta\mu)$, one can find the observed IC flux as

(11) $$[\nu S_\nu]_{\rm ic} = \frac{1}{d_{\rm L}^2}\,\delta^4\,V'\,[\nu' j'_{\nu'}]_{\rm ic} \quad .$$

VHE γ-Rays from M 87

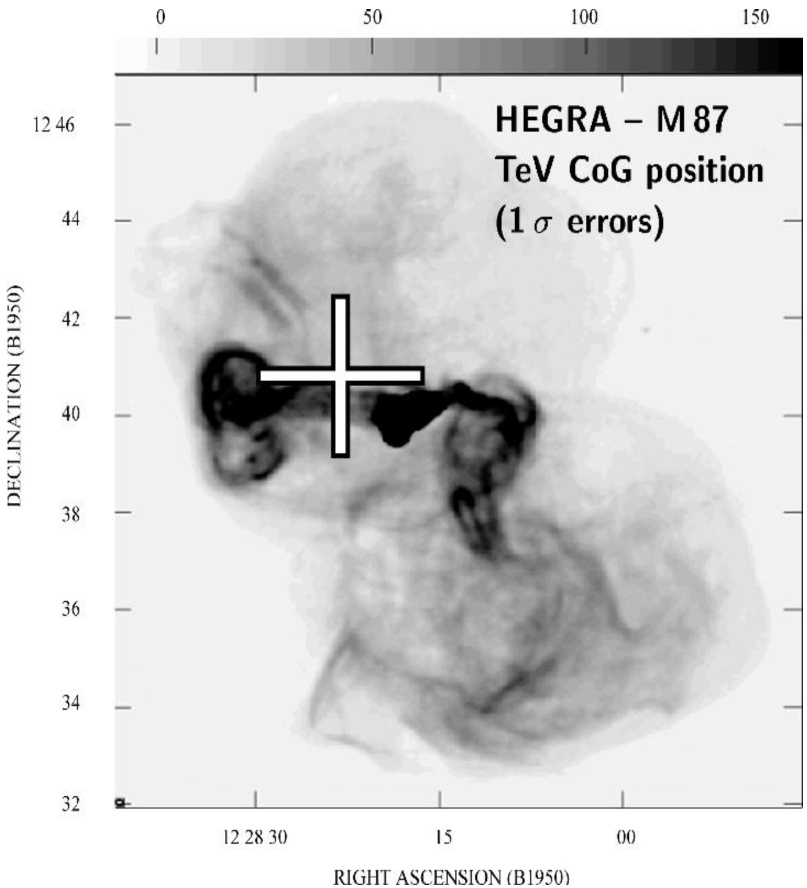

HEGRA detection of M 87 system (*Aharonian et al. 2003, A&A, 403*).

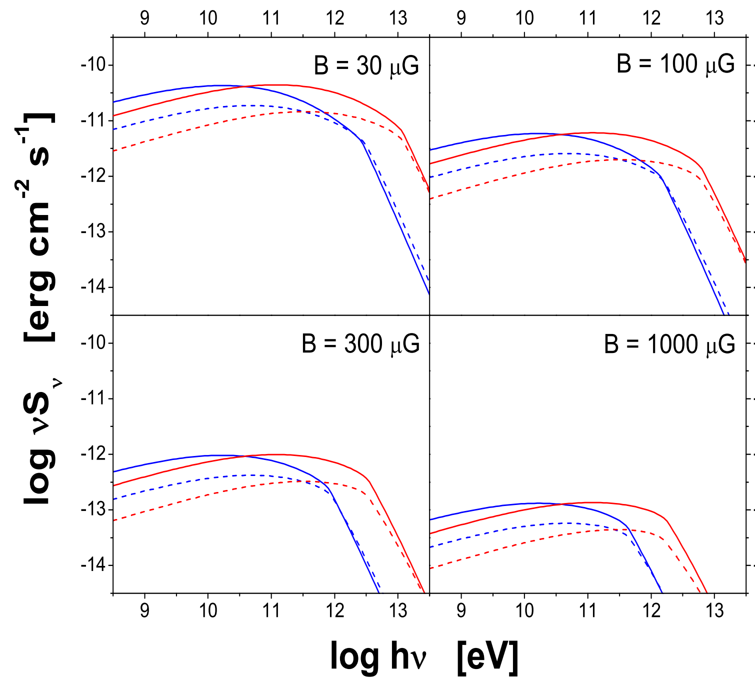

IC/STAR emission of knot A: for $\theta = 30^0$ and 20^0 (blue and red), $\Gamma = 5$ and 3 (solid and dashed) (*Stawarz et al. 2005, ApJ, 626*).

Knot A in the M 87 Jet — Strong Magnetic Field

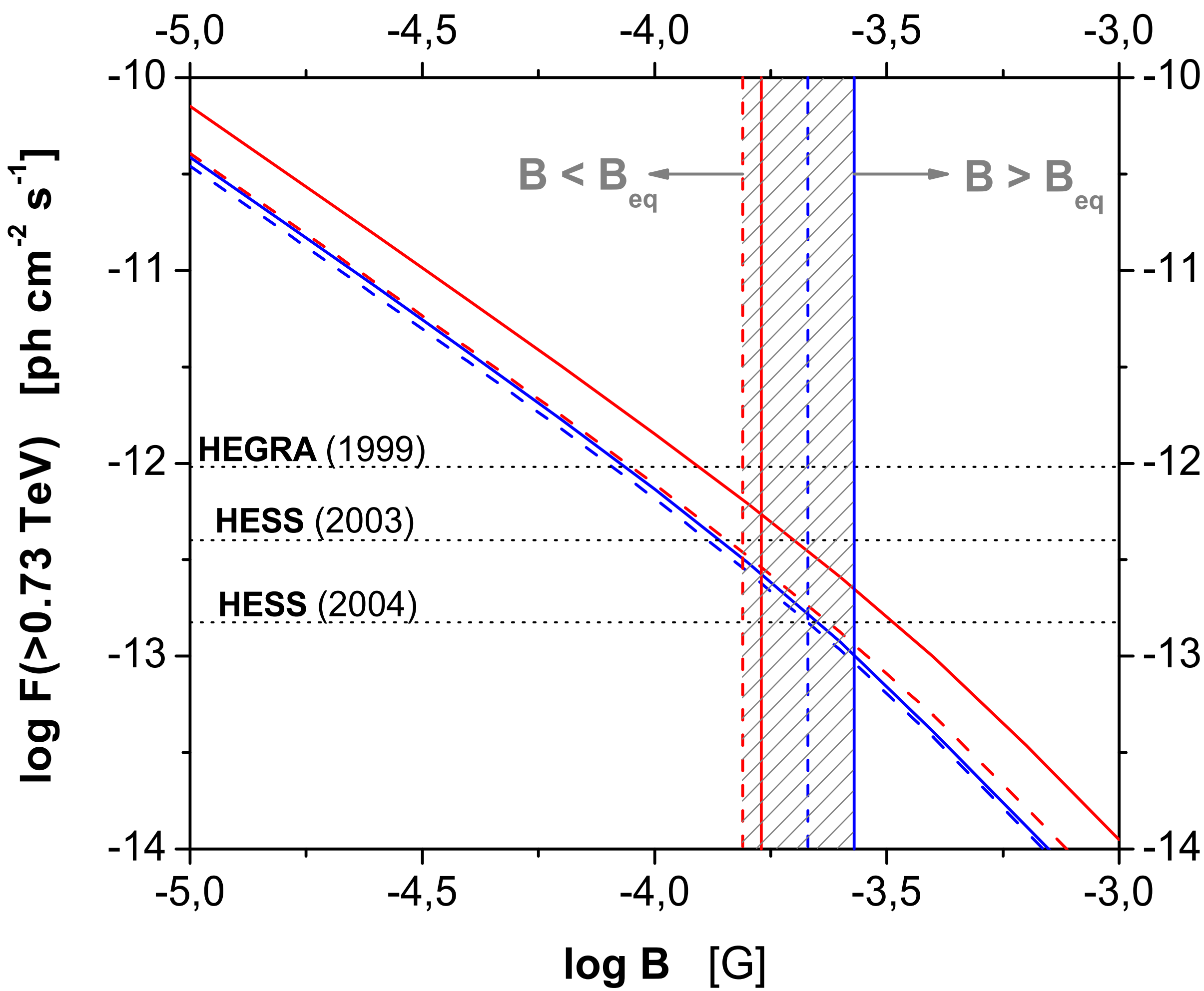

Contribution of FR I Jets to the γ-Ray Background

With the model for the Cosmic IR-to-UV Backround Radiation by *Kneiske et al. (2002, A&A, 386; 2004, A&A, 413)*, we compute the absorbed IC flux of the template FR I jet,

(12) $$S_\gamma(\varepsilon) = \frac{(1+z)\,L_\gamma\,[(1+z)\,\varepsilon]}{4\pi\,d_{\rm L}^2} \times \exp\left[-\tau_{\gamma\gamma}(\varepsilon,\,z)\right] \quad .$$

Template γ-ray spectrum constructed from the sample of 11 FR I jets detecetd by *Chandra*. γ-ray luminosity function for FR I sources constructed from *Willott et al. (2001, MNRAS, 322)*:

(13) $$\rho(L,\,z) \equiv \frac{dN}{dV\,d\log L} = \begin{cases} \rho_0 \left(\frac{L}{L_{\rm cr}}\right)^{-\alpha} \exp\left(\frac{-L}{L_{\rm cr}}\right) (1+z)^k & \text{for} \quad z < z_{\rm cr} \\ \rho_0 \left(\frac{L}{L_{\rm cr}}\right)^{-\alpha} \exp\left(\frac{-L}{L_{\rm cr}}\right) (1+z_{\rm cr})^k & \text{for} \quad z \geq z_{\rm cr} \end{cases}$$

Contribution to the EGRET γ-ray background evaluated as for the unresolved sources:

(14) $$[\varepsilon I_\gamma(\varepsilon)] = \frac{4\pi}{\Omega_{\rm EG}} \int_{z_{\rm min}}^{z_{\rm max}} \frac{dV}{d\Omega\,dz}\,dz \int_{L_\gamma^{\rm low}}^{L_\gamma^{\rm high}} \frac{\rho(L_\gamma,\,z)}{L_\gamma\,\ln 10}\,[\varepsilon S_\gamma(\varepsilon)]\,dL_\gamma$$

where $\Omega_{\rm EG} = 10.4$ is the solid angle covered by the survey, and $dV/d\Omega\,dz$ is the comoving volume element.

Template γ-Ray Spectra

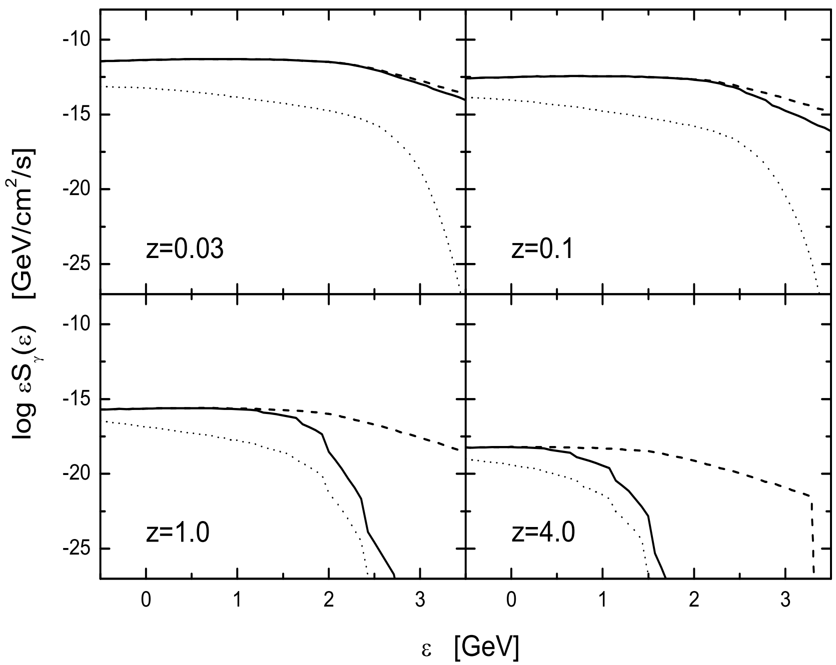

Template γ-ray spectra of kpc-scale FR I jet located at different redshifts for a total IC jet luminosity $L_\gamma = 10^{41}$ erg s^{-1}. Dashed lines indicate emission intrinsic to the source, thick solid lines correspond to the emission which would be measured by the observer located at $z = 0$ (with absorption/re-emission effects included), while dotted lines illustrate emission from the source's halo.

Note that $[\varepsilon I_\gamma(\varepsilon)] \propto B^{-2}$ (roughly!)

<u>*Stawarz et al. 2006, ApJ, in press (astro-ph/0507316)*</u>

$\rightarrow \quad B > 10\ \mu$G

FR I Jets — Strong Magnetic Fields (?)

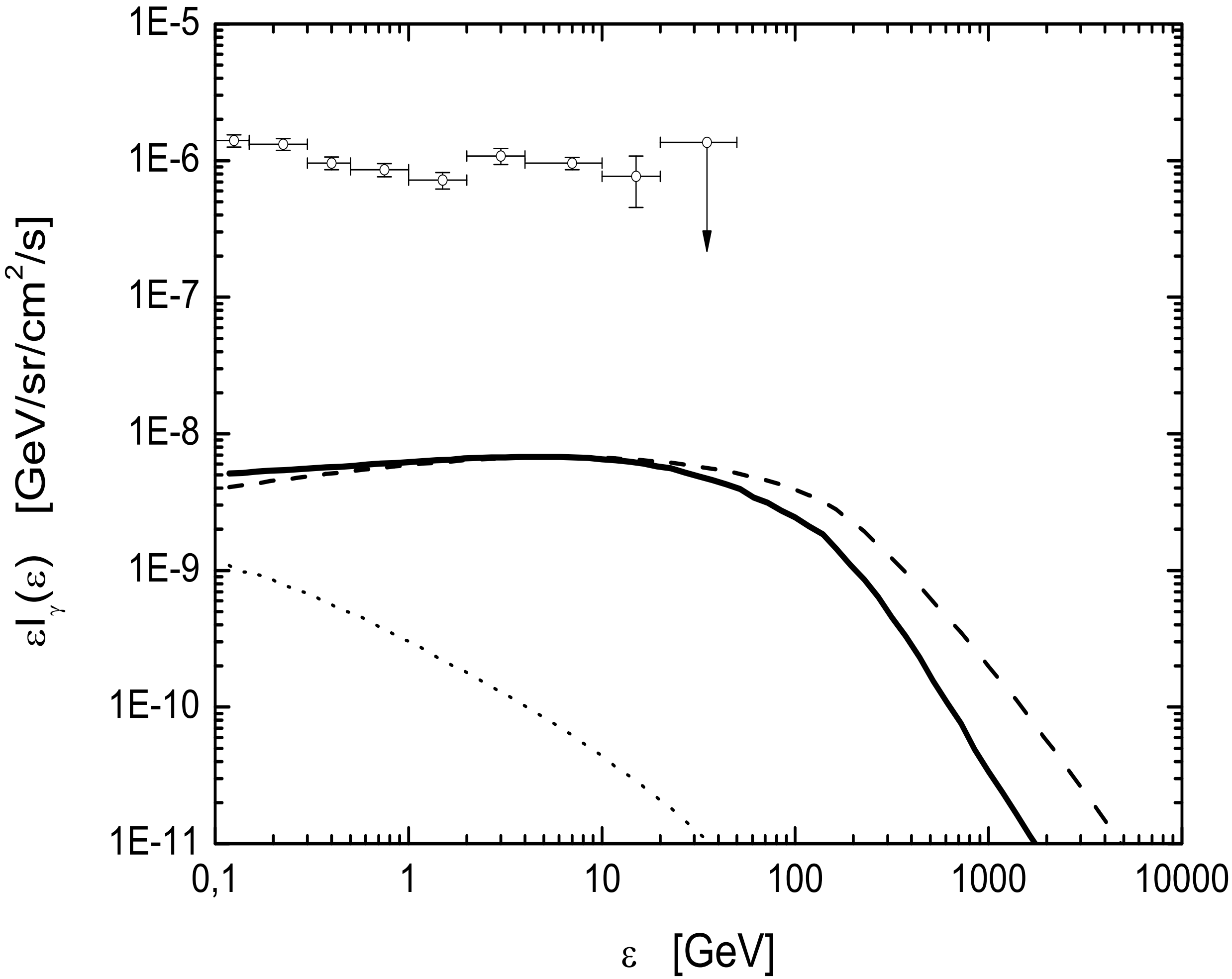

Variable VHE γ-Ray Emission of M 87

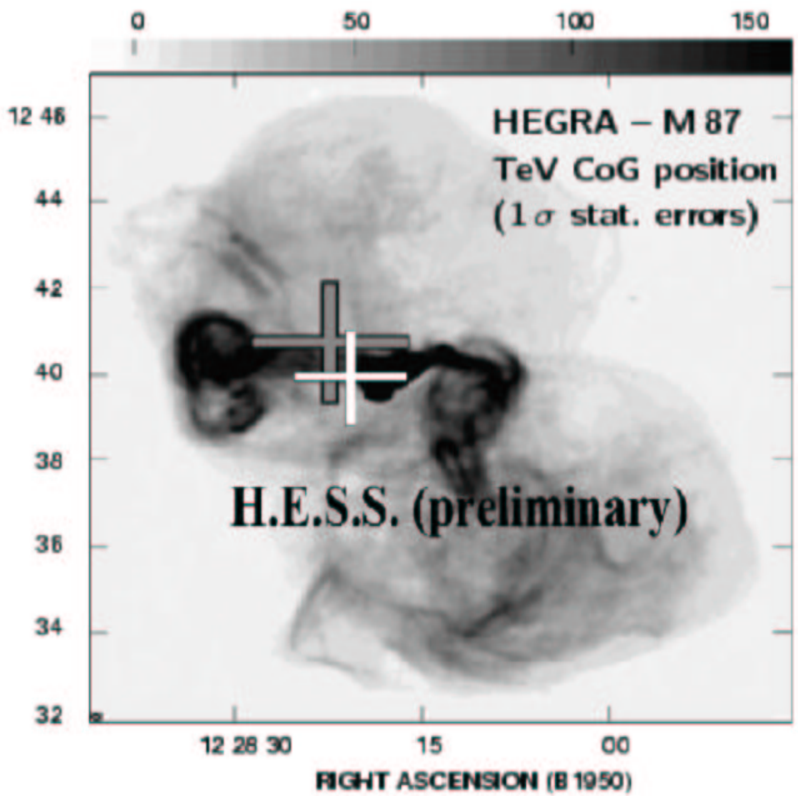

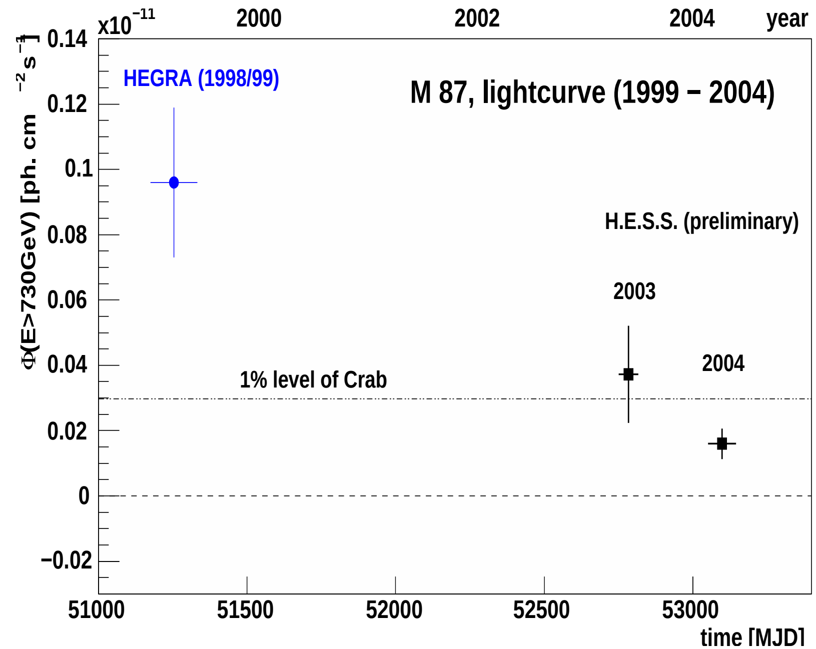

Detection of variable TeV emission of M 87 system by the *H.E.S.S.* Cherenkov Telescopes (*Beilicke et al. 2005, XXII Texas Symposium*).

Misaligned Synchrotron-Proton Blazar?

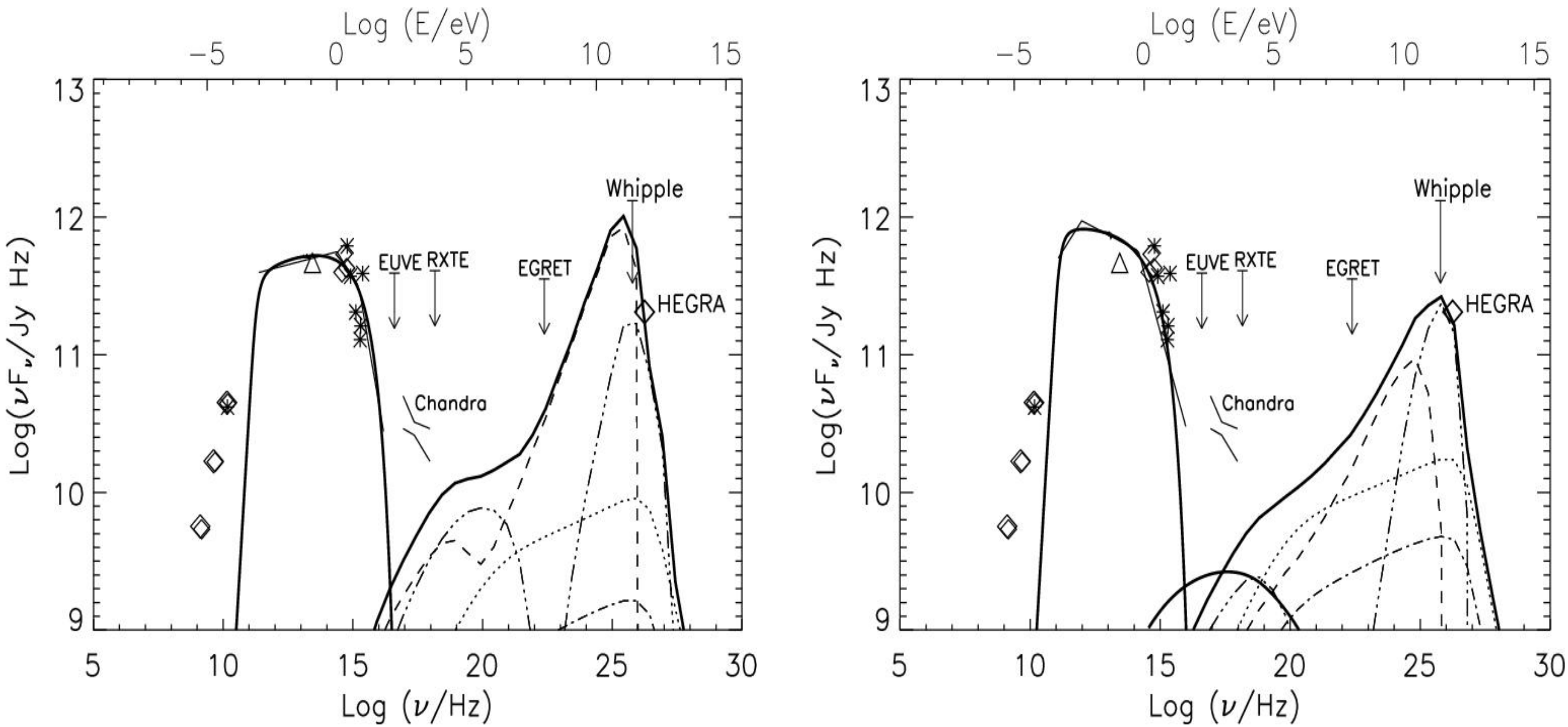

Hadronic processes in the inner portion of the jet (*Reimer et al. 2004, A&A, 419*).

<u>But what about the X-ray data?</u>

Structured Inner Jet?

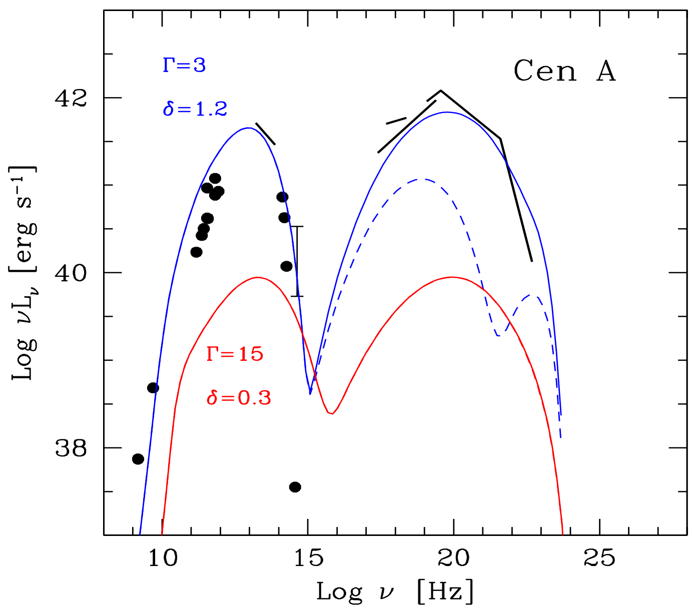

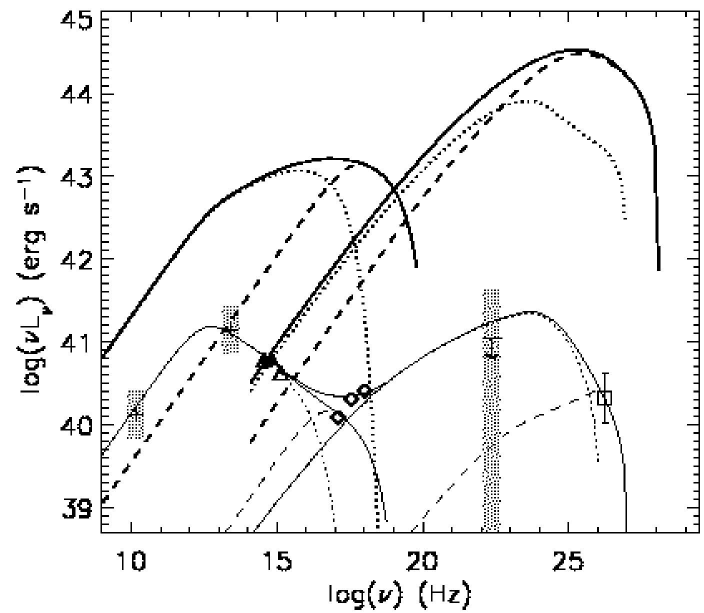

Relative enhancement of the radiation fields produced in the fast spine and the slower layer of the inner jet (*Ghisellini et al. 2005, A&A, 432*).

Crucial issue: jet velocity structure

Relative enhancement of the radiation fields produced in a different parts of the deccelerating flow (*Georganopoulos et al. 2005, ApJ, in press (astro-ph/0510783)*).

Crucial issue: jet velocity structure

The Most Inner Portions of the M 87 Jet

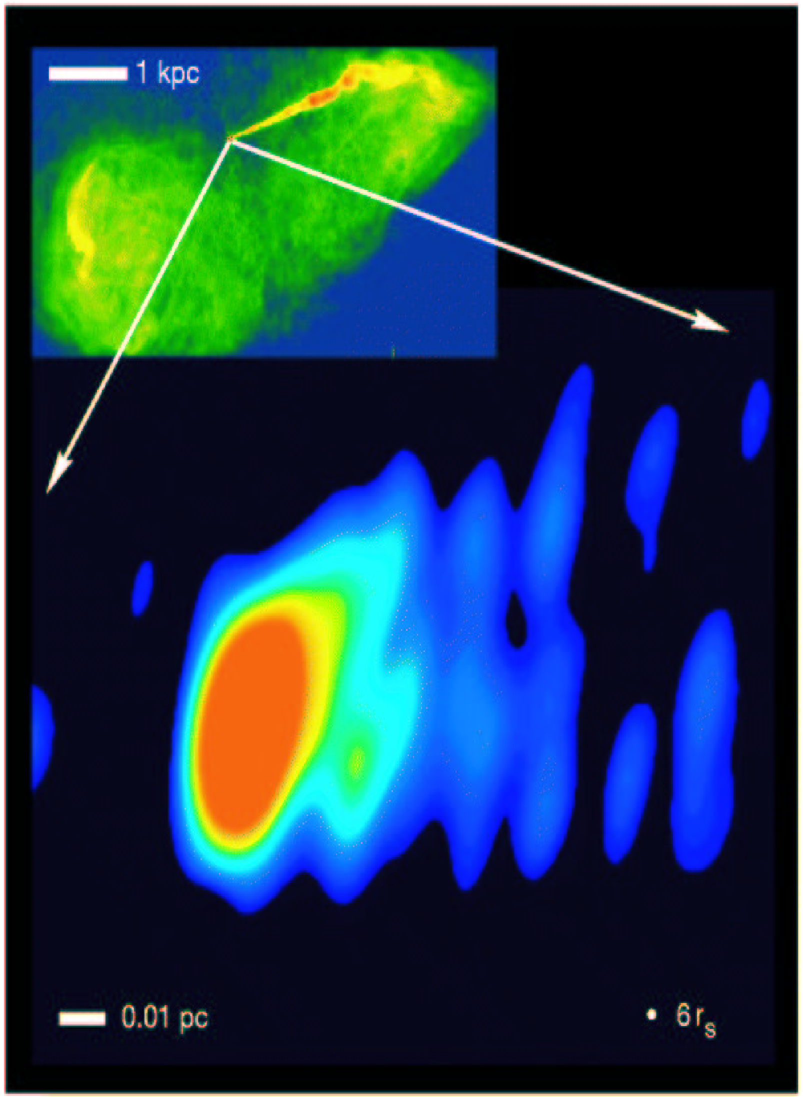

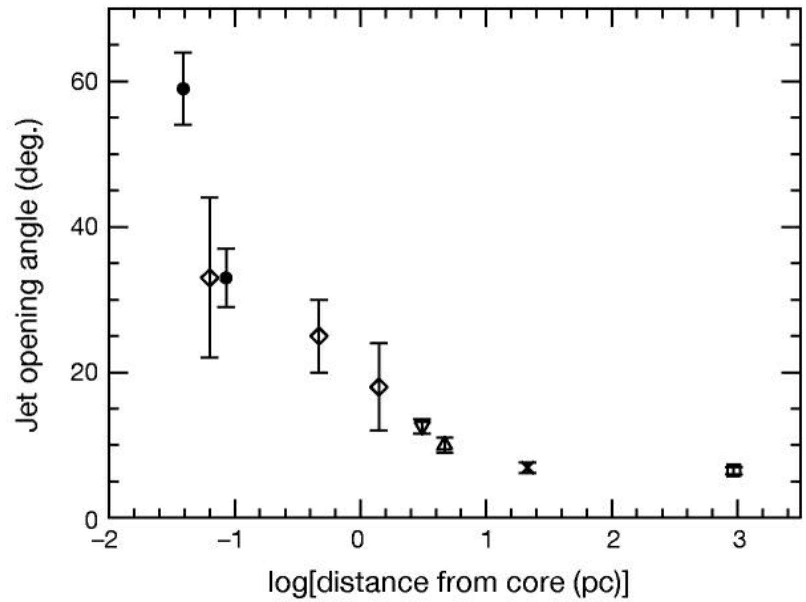

A very broad limb-brightened outflow on the scales < 0.5 mas; strong collimation at $\sim 100\ r_g$, continuing out to $\approx 3 \times 10^4\ r_g \approx 10$ pc (*Junor et al. 1999, Nature, 401*).

conversion:

$r_g = 3.85\ \mu$arcsec $= 0.3$ mpc

Elusive HST-1 knot of the M 87 Jet

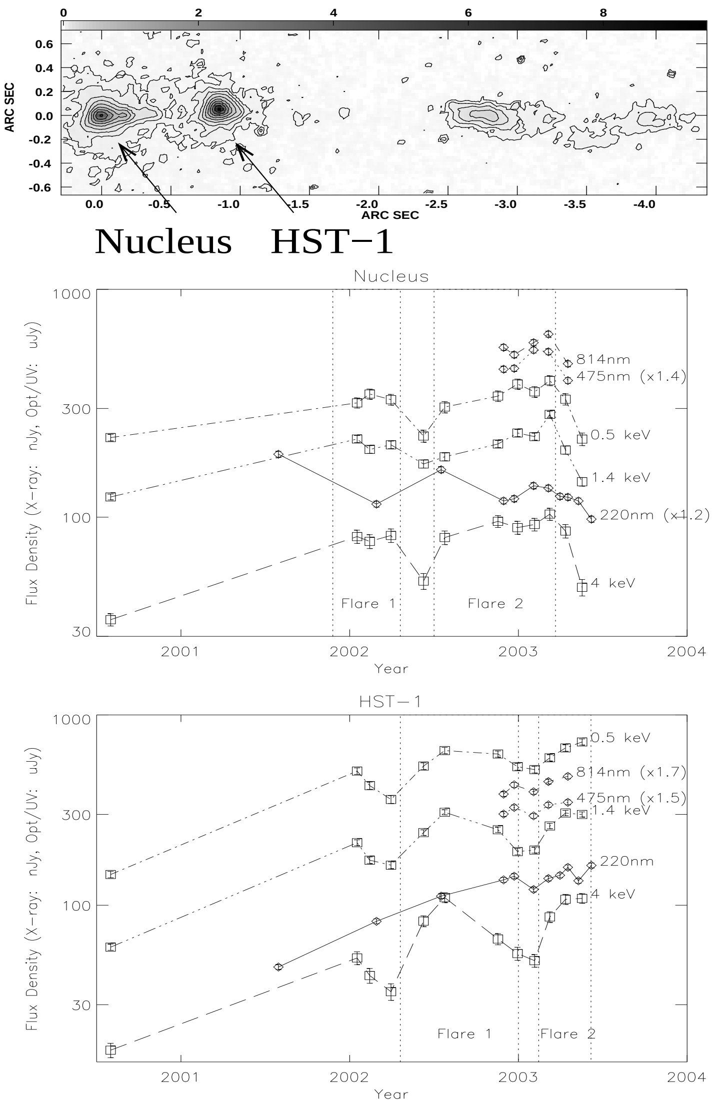

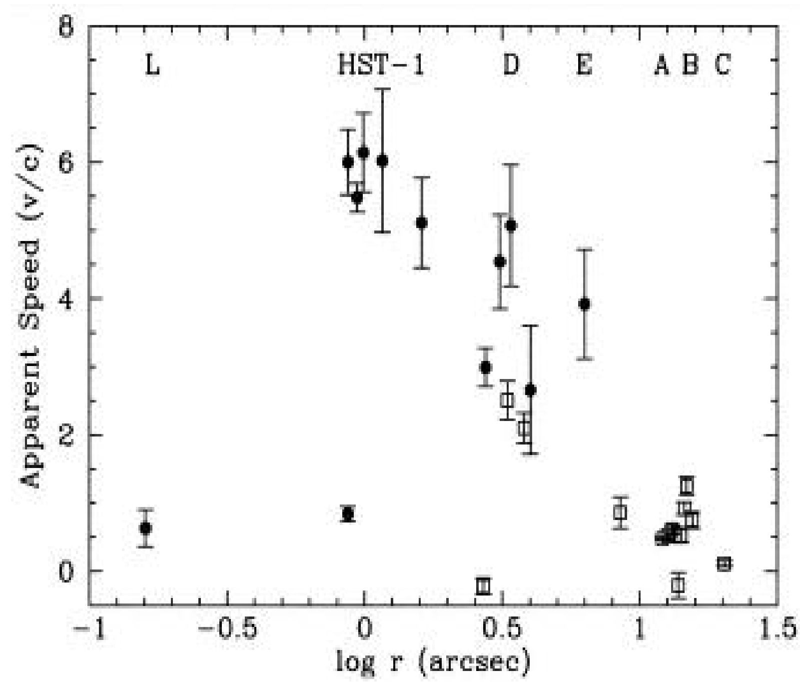

Left: X-ray and optical variable emission of the HST-1 knot (*Harris et al., 2003, ApJ, 586; Perlman et al. 2003, ApJ, 599*).

Right: Apparent velocities in M 87 jet (*Biretta et al. 1999, ApJ, 520* and references therein).

Instead of Conclusions

- Relativistic bulk velocities on kpc scales also for FR I sources:
  $\Gamma > 1$
- Presence of very high energy electrons:
  $E_{\rm e} >$ TeV
- Strong jet magnetic field:
  $B \geq B_{\rm eq}$ (?)
- Jet internal structure:
  spine + boundary shear layer morphology
  sub-structure of knot regions
  modulated/intermittent jet activity
  a role of the ambient medium
- Particle acceleration:
  localized processes in knots and hotspots
  processes acting continuously along the jet
  non-standard electron energy spectra

Cracow Jet Conference

CHALLENGES OF RELATIVISTIC JETS

25.06.2006 - 1.07.2006, Cracow, Poland

`http://www.oa.uj.edu.pl/2006jets/`

- **SOC:**
  A. Aharonian, M.C. Begelman, D. Gabuzda, D.E. Harris, J. Kirk, G. Madejski, M. Ostrowski, M. Sikora, Ł. Stawarz, F. Takahara
- **LOC:**
  M. Ostrowski, Ł. Stawarz
- **Invited Speakers:**
  F. Aharonian, J. Arons, M.C. Begelman, A. Bhattacharjee, G.V. Bicknell, K. Blundell, S.V. Bogovalov, A. Celotti, E. Churazov, L. Costamante, D. De Young, D. Eichler, R. Fender, D. Gabuzda, J.L. Gomez, J. Granot, M. Hardcastle, D.E. Harris, S. Heinz, M. Hoshino, S. Jester, J. Kataoka, J. Kirk, S.S. Komissarov, A. Konigl, D. Lazzati, Y.E. Lyubarsky, M. Lyutikov, J.P. Macquart, J.M. Marti, F. Mirabel, R. Moderski, J. Niemiec, M. Ostrowski, J.M. Paredes, V. Petrosian, L. Rudnick, M. Sikora, P. Slane, A. Spitkovsky, F. Takahara, G.B. Taylor, N. Vlahakis, J.F.C. Wardle, E.G. Zweibel,
  plus few more

Variability analysis of the IDV source 0954+658

N. Marchili, L. Fuhrmann,
T. P. Krichbaum, A. Witzel, A. Kraus

Introduction

- InterStellar Scintillation is thought to play an important role in the IDV phenomenon.
- The most recent ISS models expect an annual modulation in the variability time scales.
- 0954+658 is the second type II-IDV source showing strong evidences in favor of an annual modulation in the characteristic time scales.

A deepen discussion about all these topics, and information about the observations, the reduction and analysis of data can be found in Lars PhD thesis (Fuhrmann et al., in prep.)

The light curves

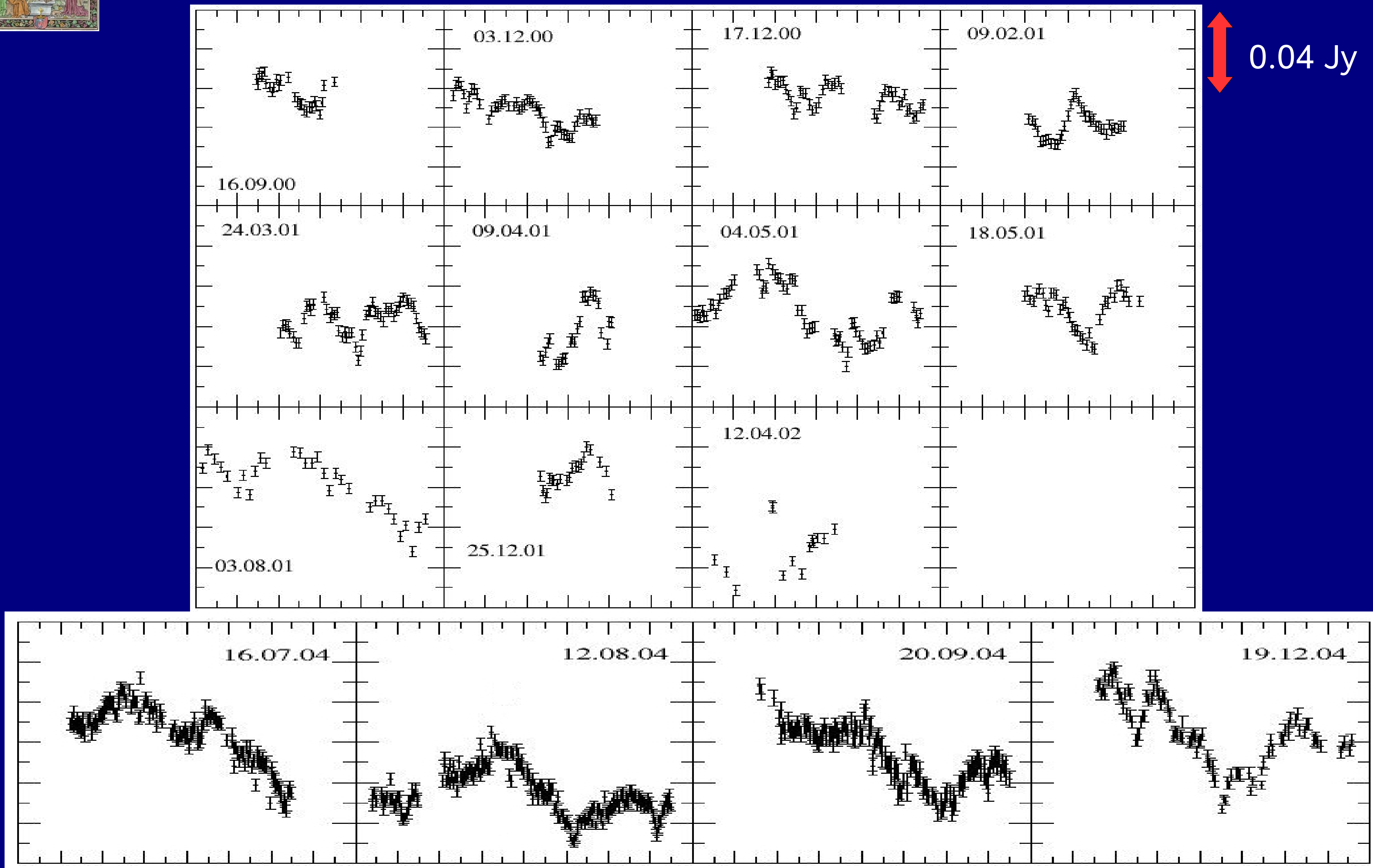

The light curves

Epoch	Duration (d)	Mean gap (h)
16.09.00	1.0	0.89
03.12.00	1.7	0.79
17.12.00	1.9	1.03
09.02.01	1.2	0.79
24.03.01	1.8	0.79
09.04.01	0.8	0.74
04.05.01	2.8	1.03
18.05.01	1.4	0.89
03.08.01	2.7	2.09
25.12.01	0.8	0.91
12.04.02	1.4	2.23
16.07.04	2.6	0.34
12.08.04	3.5	0.34
20.09.04	3.0	0.43
19.12.04	3.0	0.70

15 EPOCHS OF OBSERVATION WITH THE EFFELSBERG TELESCOPE

The duration of the observations varies between ~1 and 3.5 days

The mean gap in the data is ~0.8 h. There are two exceptions: the August 2001 and April 2002 monitoring campaigns (mean gap ~2 h)

SF analysis results

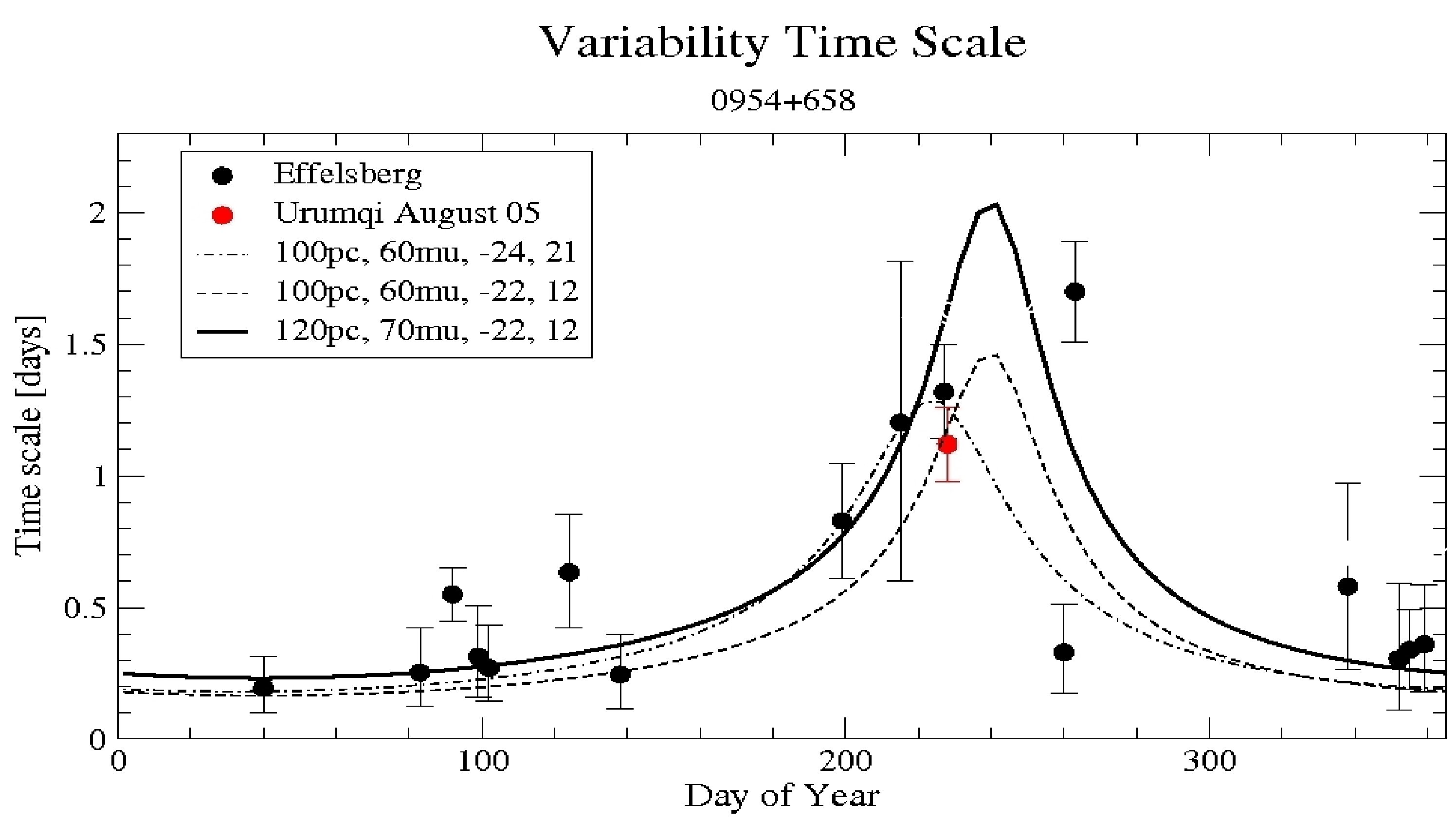

Results discussion

The August 01 observations

How important is the sampling in the SF evaluation of the characteristic time scales?

τ=1.2 d   τ=0.6 d

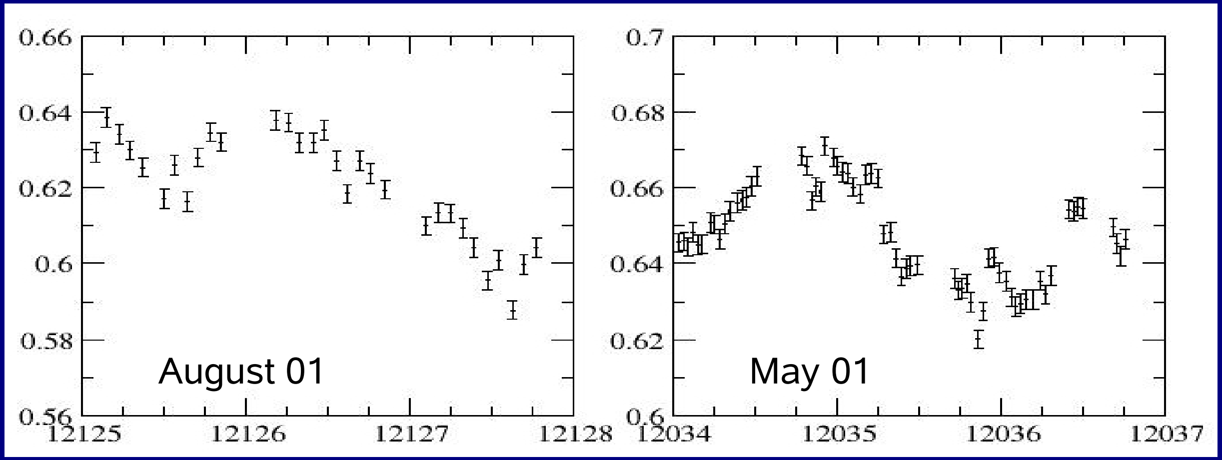

Results discussion

The August 01 observations

How important is the sampling in the SF evaluation of the characteristic time scales?

The results of SF analysis can be largely affected by sampling effects

τ=1.2 d

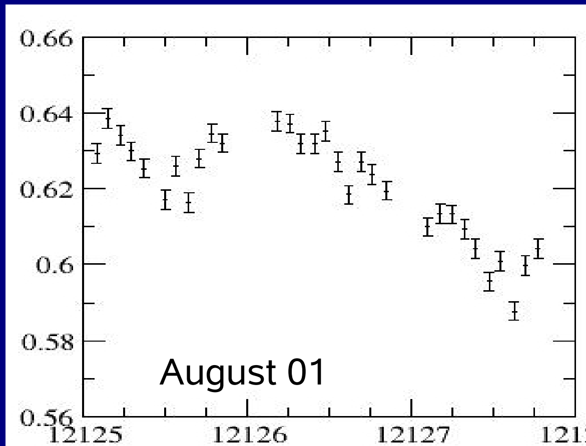

τ=0.6 d

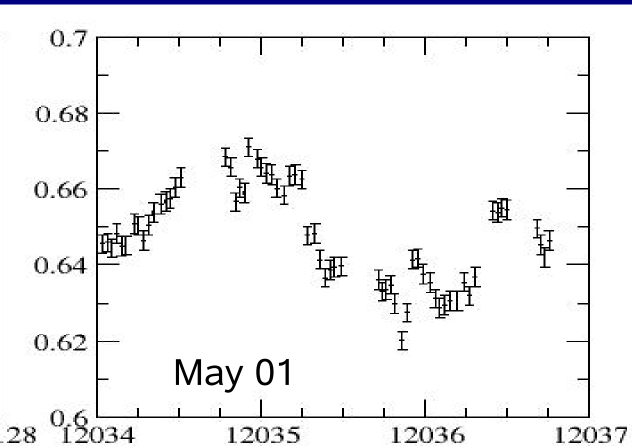

τ=1.0 d

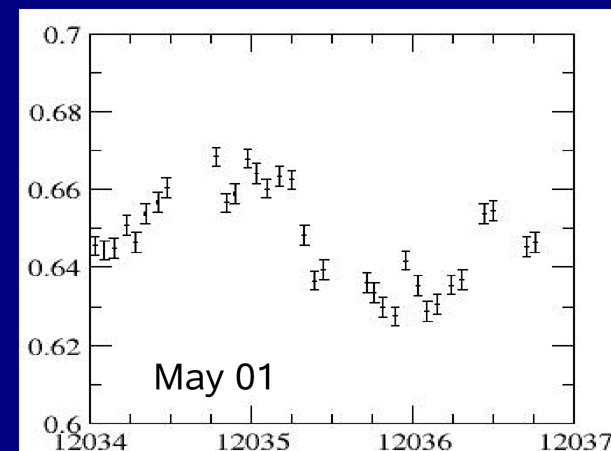

Results discussion

A visual inspection of the light curves

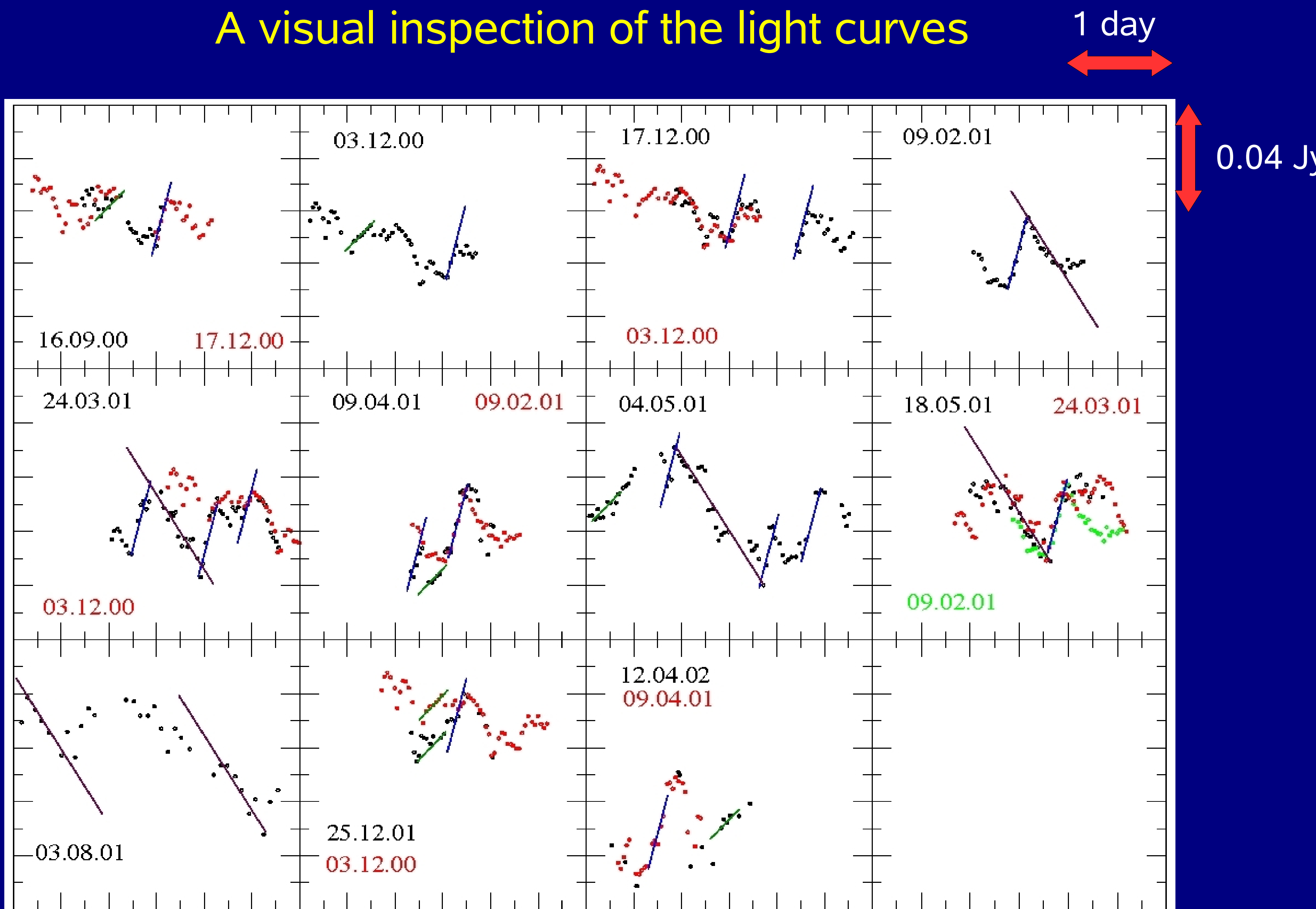

Results discussion

A visual inspection of the light curves

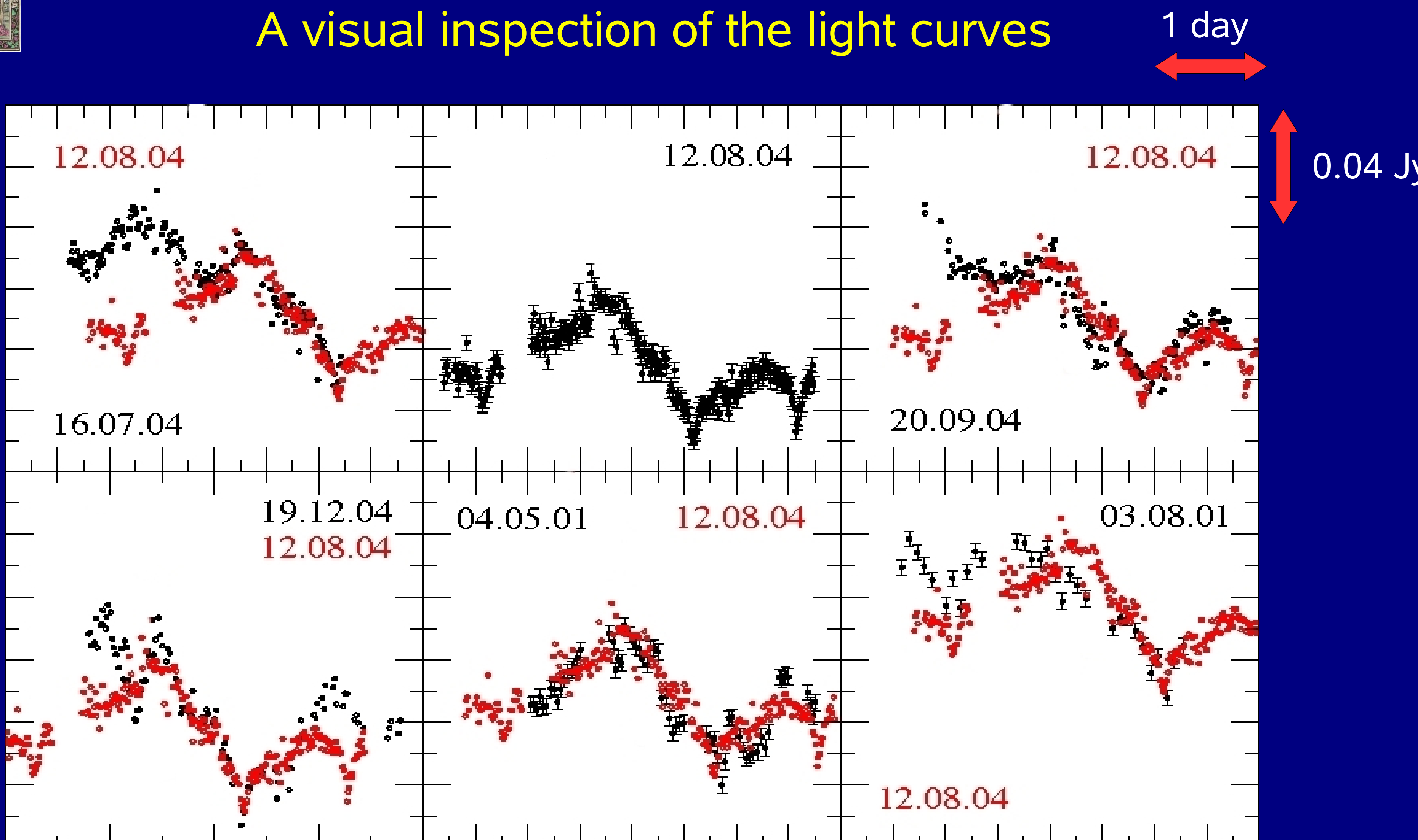

Results discussion

The superposition of the light curves shows important similarities

Characteristic time scales by Structure Function analysis

2004 observations

July 2004	~0.8 d
August 2004	~1.2 d
September 2004	~1.7 d
December 2004	~0.35 d

How to explain the large differences in SF results?

Which conclusions about the annual modulation model?

Some considerations about Structure Function

- In order to have comparable results for different light curves, the sampling should be almost the same

Possible solution: data resampling (interpolation, binning).

- More than one time scale is usually present in the light curves; SF depends also on the bin interval

All the time scales in the light curves have to be identified and quantified

- The time scales we are looking for are of the same order of the total length of the light curves! This reduces the statistical meaning of the results

Longer observational campaigns would be needed...

The 0954+658 characteristic time scales

The 2004 epochs show very similar features in different observational periods. These results seem not to confirm the annual modulation model.

On the other hand, the lengthening in the August 01 time scale is REAL. It is longer than the August 04 one of a factor ~1.4

Another question arise: both the monitoring campaigns have been performed in August!

THE PROBLEM OF THE ORIGIN OF IDV IN 0954+658 IS STILL OPEN

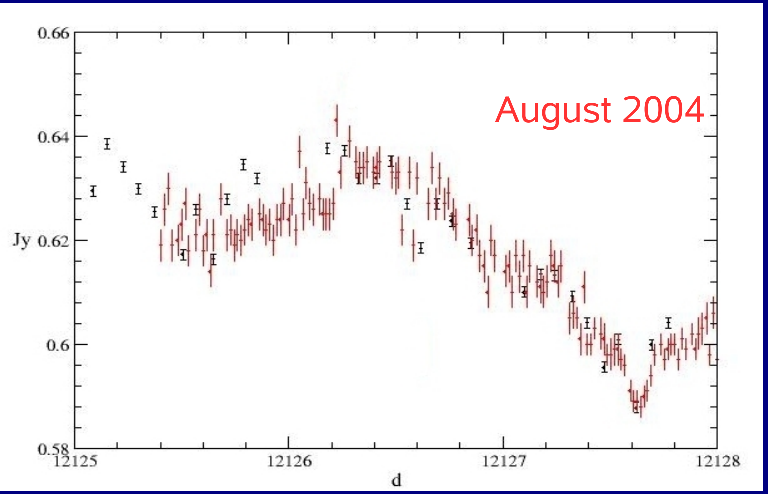

Developments

- Accurate study of the capability of the classical temporal analysis methods to find characteristic time scales in simple synthetic light curves

- Use of Wavelet analysis (mother wavelet: the “Mexican hat”)

December 04 Observations

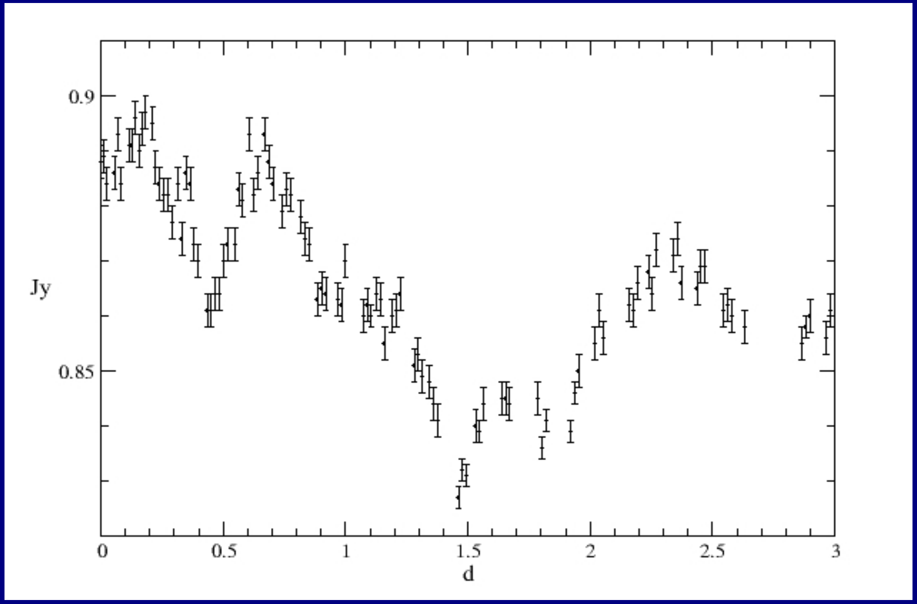

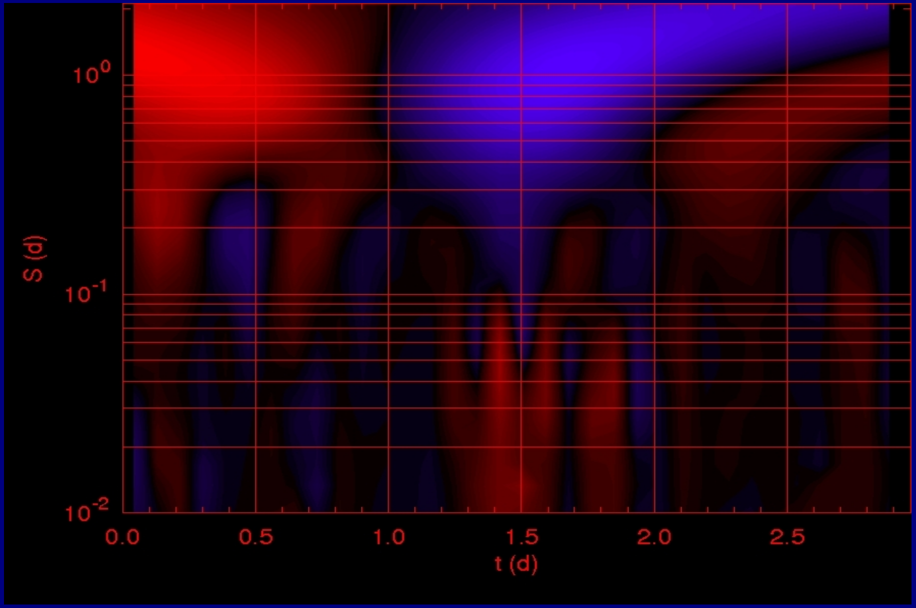

The QSO HE 1013-2136 (z = 0.785): Tracing the ULIRG-QSO connection towards large look-back times?

Jochen Heidt
LSW, Zentrum für Astronomie, Heidelberg
+
Klaus Jäger, MPIA Heidelberg
Matthias Dietrich, Ohio State University

Luminous QSOs @ low-z

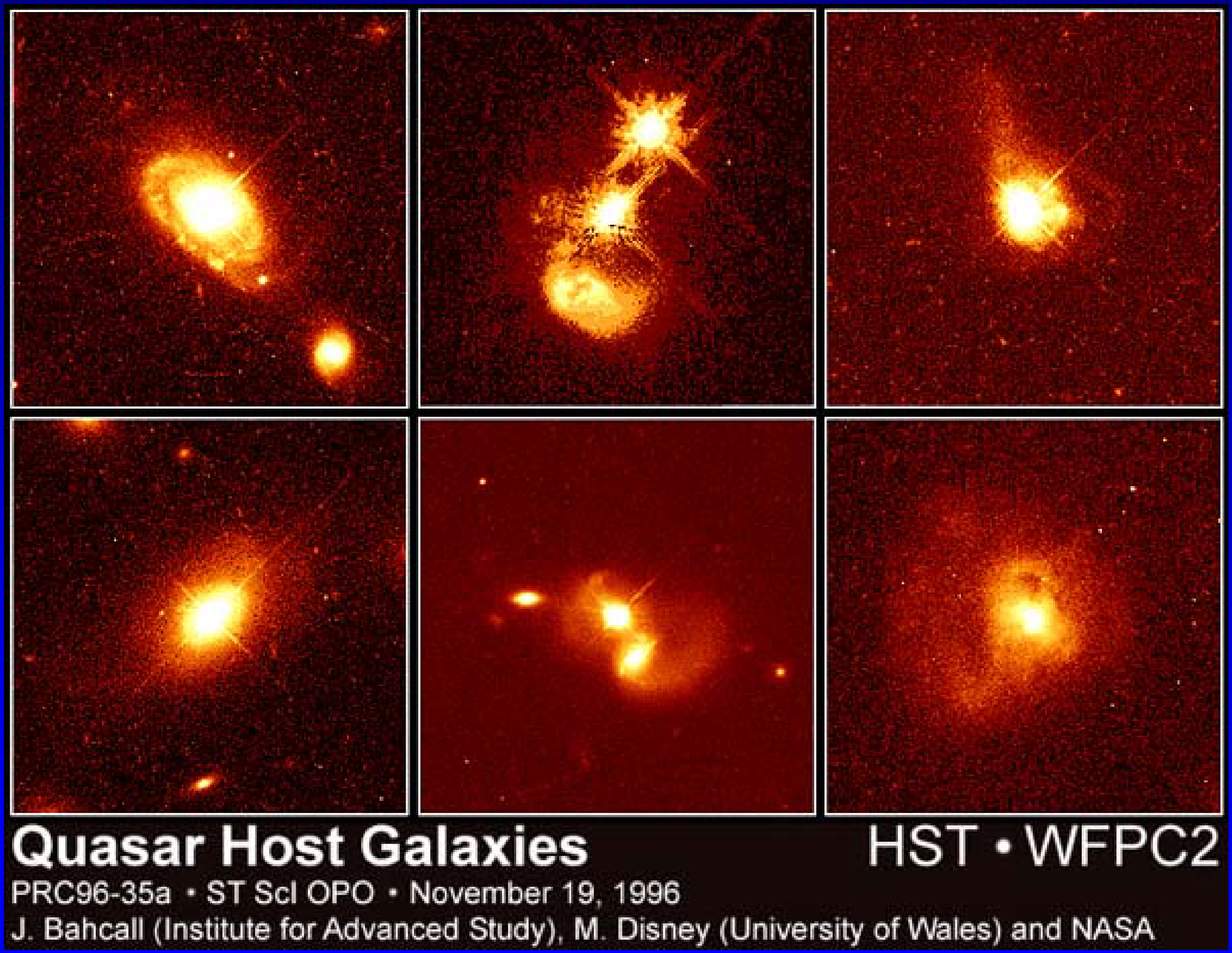

Many show signs of interaction, some of them are ULIRGs

How do the QSO/hosts form?

• QSOs found @ $z > 6$ → Black holes in their center must have been formed early, some AGN are switched on (or a couple of times)!

• most (all) massive galaxies have a black hole

• all type of luminous AGN have a bulge-dominated host (up to $z \sim 2$)

→ close connection

<u>Formation of host:</u>

→ Monolithic collapse @ high-z (4-5) + passive evolution thereafter

→ Accretion/merging of subunits → seen in radio galaxies at $z = 2\text{-}4$

→ Merging of 2 gas-rich galaxies to form a bulge-dominated galaxy (Toomre, Barnes, Naab...)

How do the QSO/hosts form?

- QSOs found @ $z > 6$ ➔ Black holes in their center must have been formed early, some AGN are switched on (or a couple of times)!
- most (all) massive galaxies have a black hole
- all type of luminous AGN have a bulge-dominated host (up to $z \sim 2$)

➔ close connection

Formation of host:

→ Monolithic collapse @ high-z (4-5) + passive evolution thereafter

→ Accretion/merging of subunits → seen in radio galaxies at $z = 2\text{-}4$

→ Merging of 2 gas-rich galaxies to form a bulge-dominated galaxy (Toomre, Barnes, Naab...)

Advanced explanation: ULIRG-QSO connection

Merging of (at least) 2 massive galaxies, at least one gas-rich, at least one with a BH

→ Strong burst of star formation →→ (UL)IRG

→ Provide fuel for AGN →→QSO starts (transition phase)

→ Once circumnuclear material (gas/dust) largely removed →→QSO

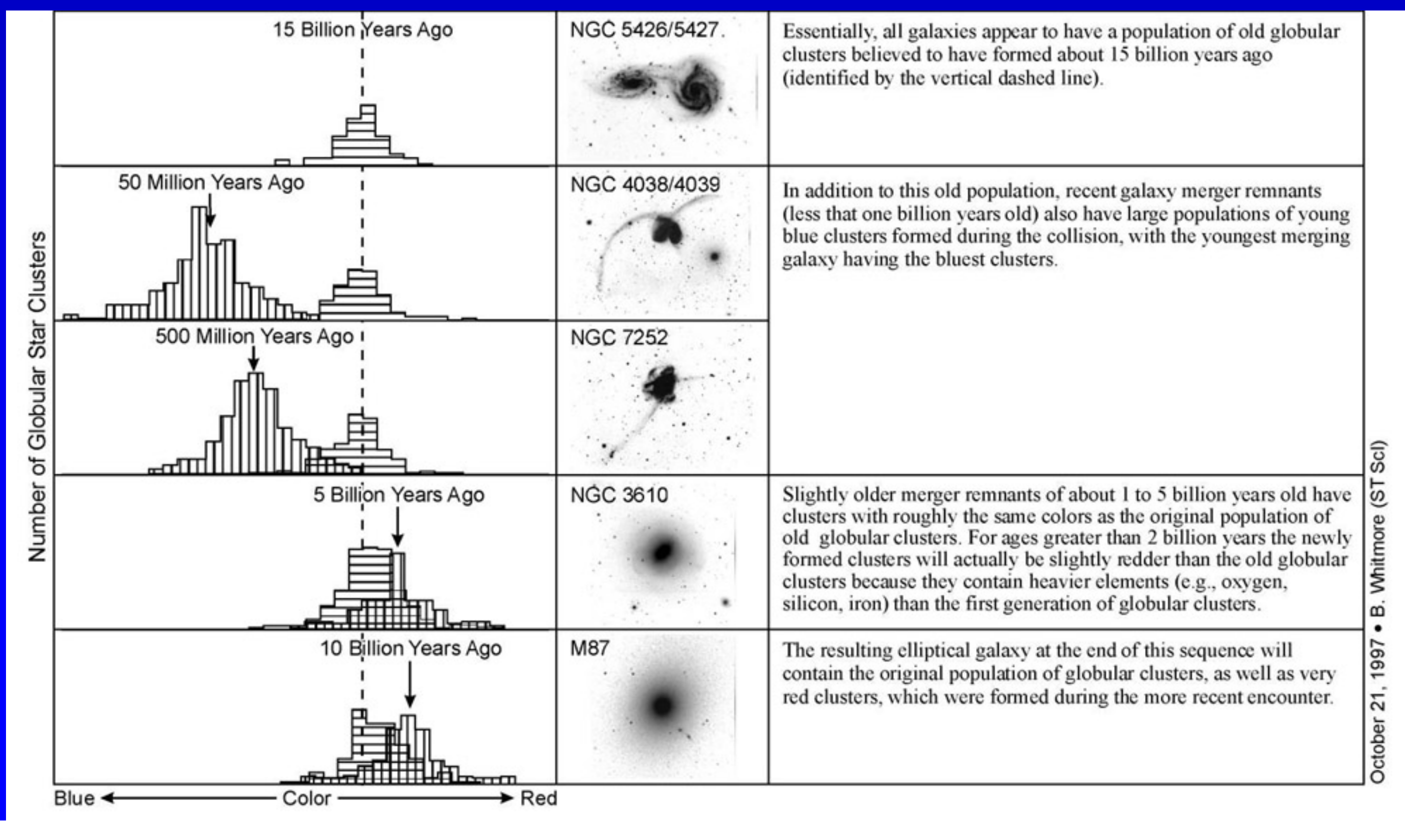

Time

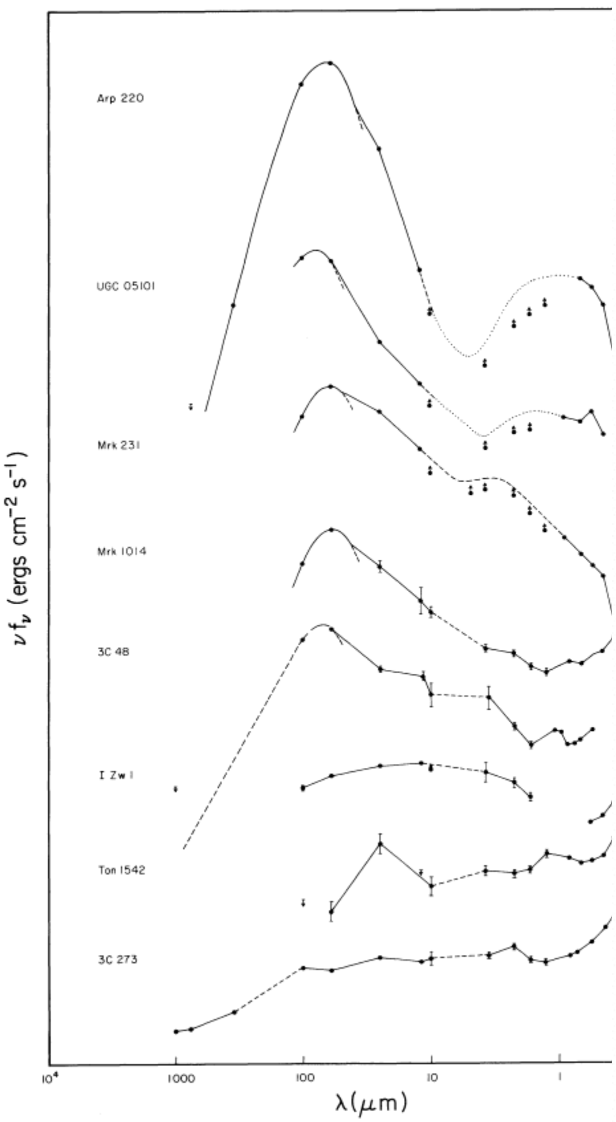

FIG. 17.—Spectral energy distributions for selected ultraluminous infrared galaxies and quasars which illustrate the pro
the infrared extreme objects like Arp 220 to the relatively unobscured quasars like Ton 1542 and 3C 273. Data for 3C 48 ar
and Miley (1985). For 3C 48 the dashed line connects the measured 100 μm data point to the highest frequency measureme
and near-infrared data for the other objects, as well as the *IRAS* data for Mrk 1014, are from Neugebauer *et al.* (1986, 1987a).

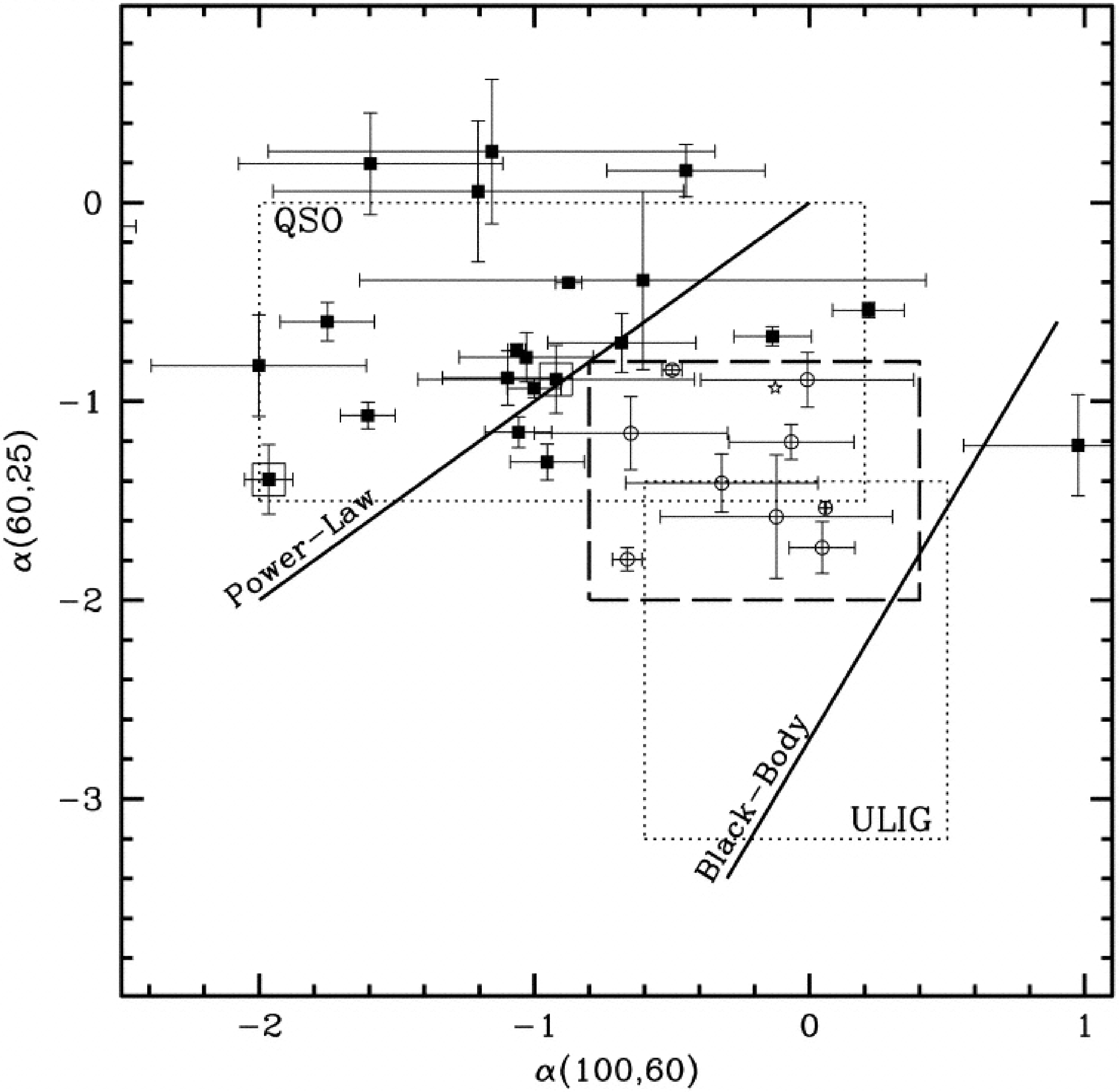

Advanced explanation: ULIRG-QSO connection

Merging of (at least) 2 massive galaxies, at least one gas-rich, at least one with a BH

➔ Strong burst of star formation ➔➔ (UL)IRG

➔ Provide fuel for AGN ➔➔QSO starts (transition phase)

➔Once cirumnuclear material (gas/dust) largely removed ➔➔QSO

...BUT: holds only for local Universe ($z < 0.2$ or so), but @ high-z?
(SFRD differs, interaction rate differs)

IRAS: not sufficiently deep (all-sky survey limit 0.5 Jy)

ISO: lots of data not yet available

Spitzer: finds more and more ULIRG candidates at high-z

6 ULIRGS at z < 0.1 and one QSO at z = 0.785

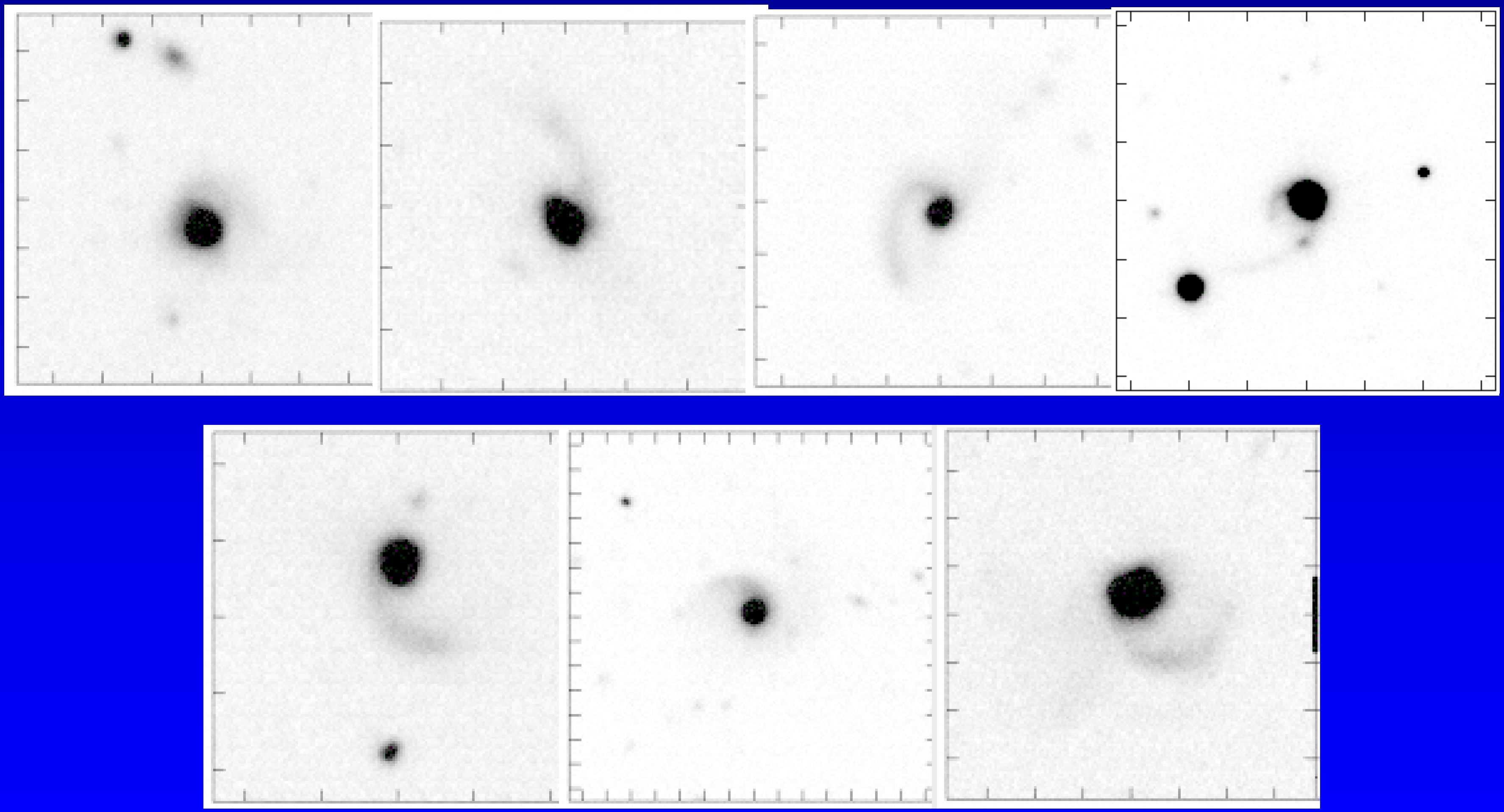

ULIRGs from Veilleux et al. (2002)

HE 1013-2136 (z = 0.785)

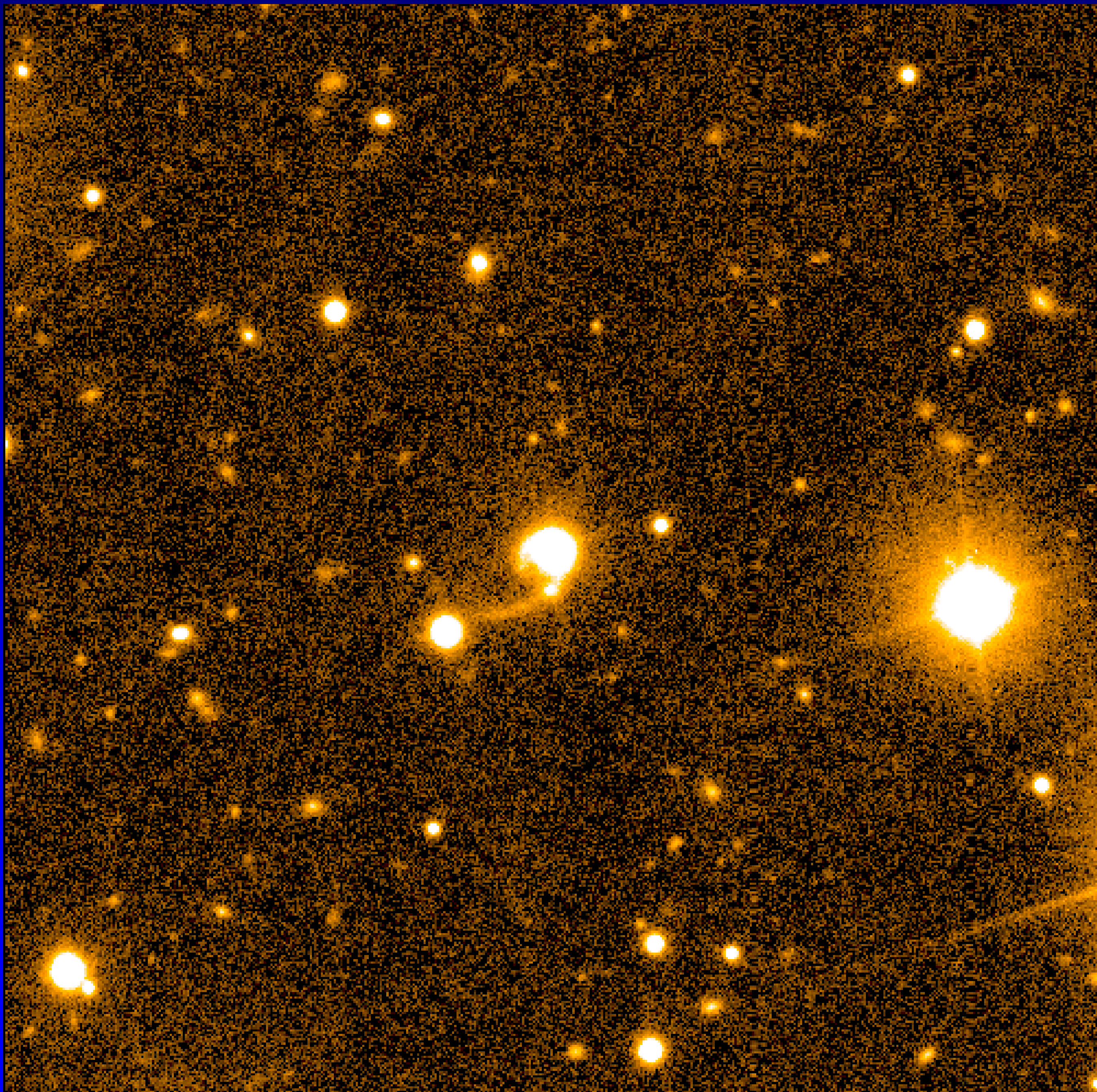

VLT + FORS

I-band, 30 min

0.65‘‘ FWHM

FOV: 1‘ • 1‘

HE 1013-2136, VLT, I-band, 30min, 0.65“ FWHM

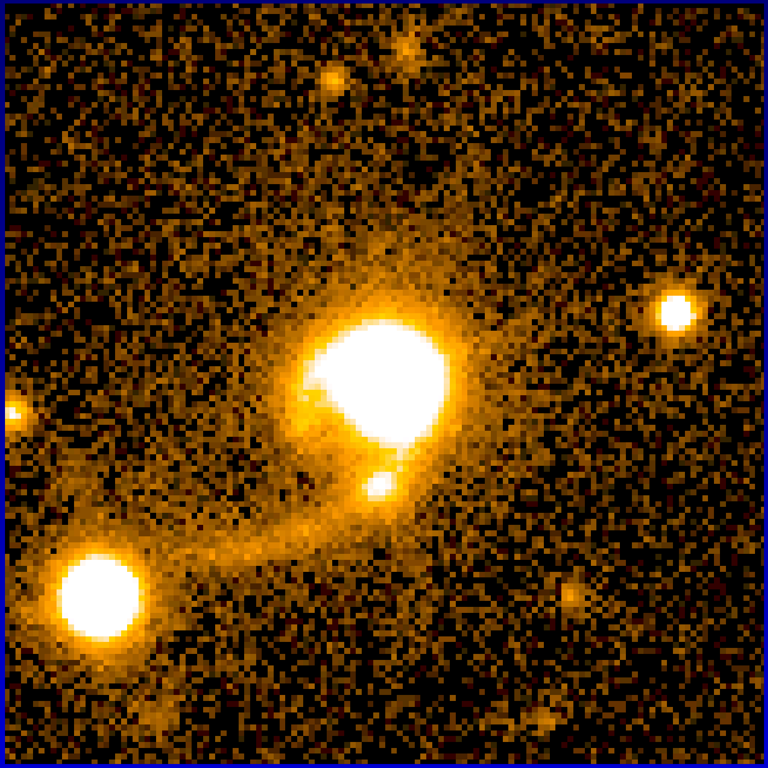

Original-image (25‘‘)

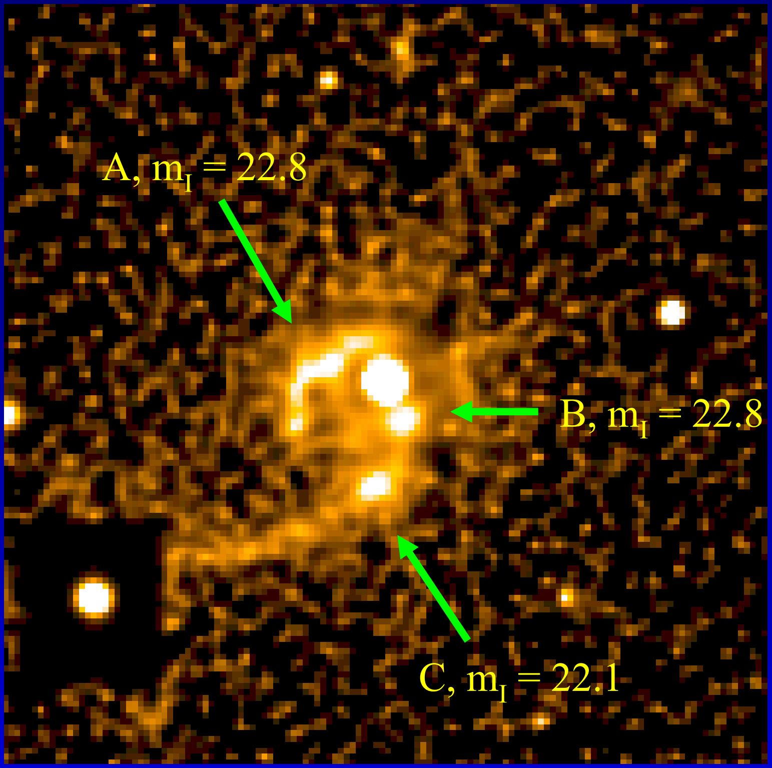

Deconvolved (Lucy 20 iterations)

2 tidal tails + several condensations, advanced merger (3:1)?

Tidal tails: 9“ (68 kpc) + 3.5“ (26 kpc) projected (conc. cosm.)

➔ Dynamical age ~ 220 + 90 Myrs (proj. vel. = 300 km/s)

Kondensations: between 1.4“ (11 kpc) and 3.6“ (27 kpc) from the core

Fitting procedure

core

(x,y,m)

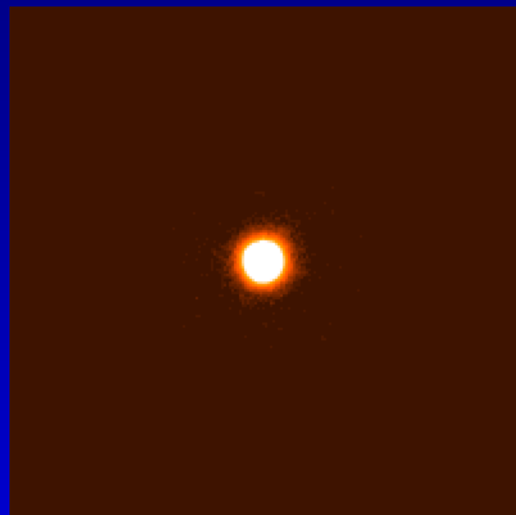

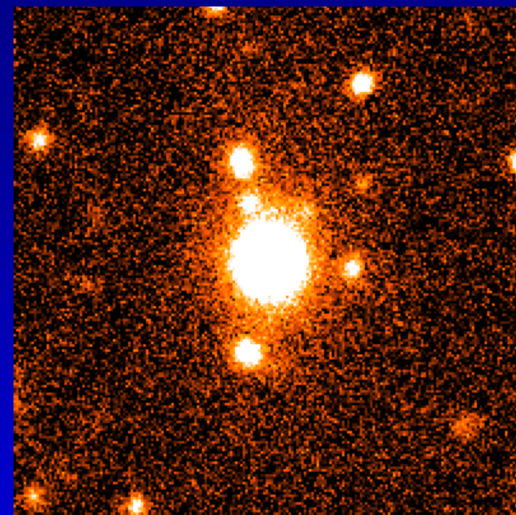

image

host galaxy

$(x,y,m,r_{eff},\varepsilon,PA,\beta)$

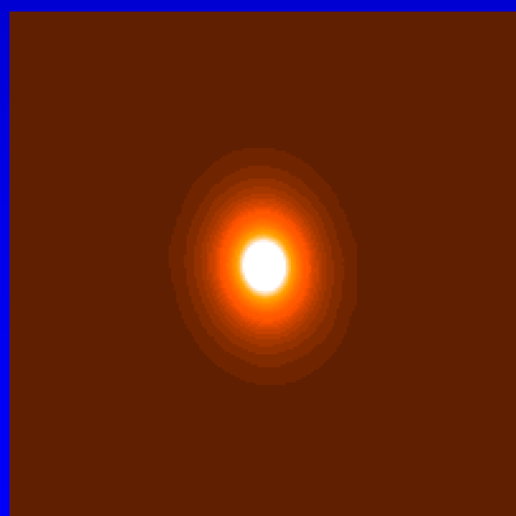

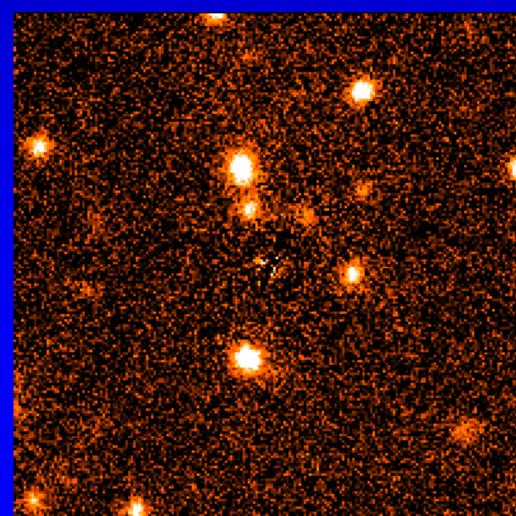

residuals

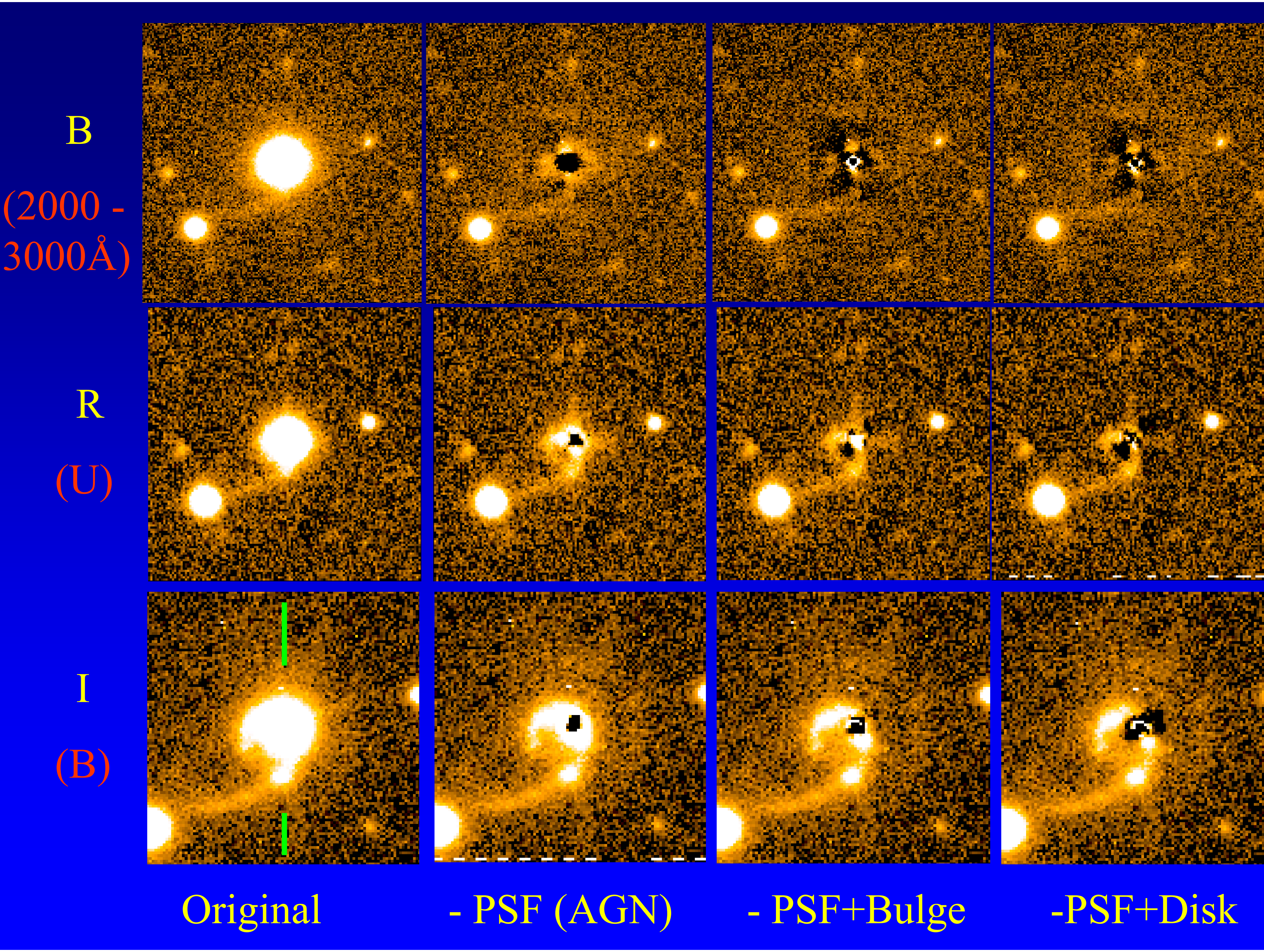

B
(2000 - 3000Å)
R
(U)
I
(B)
Original
- PSF (AGN)
- PSF+Bulge
-PSF+Disk

Restframe-spectrum QSO VLT+ESO 3.6m

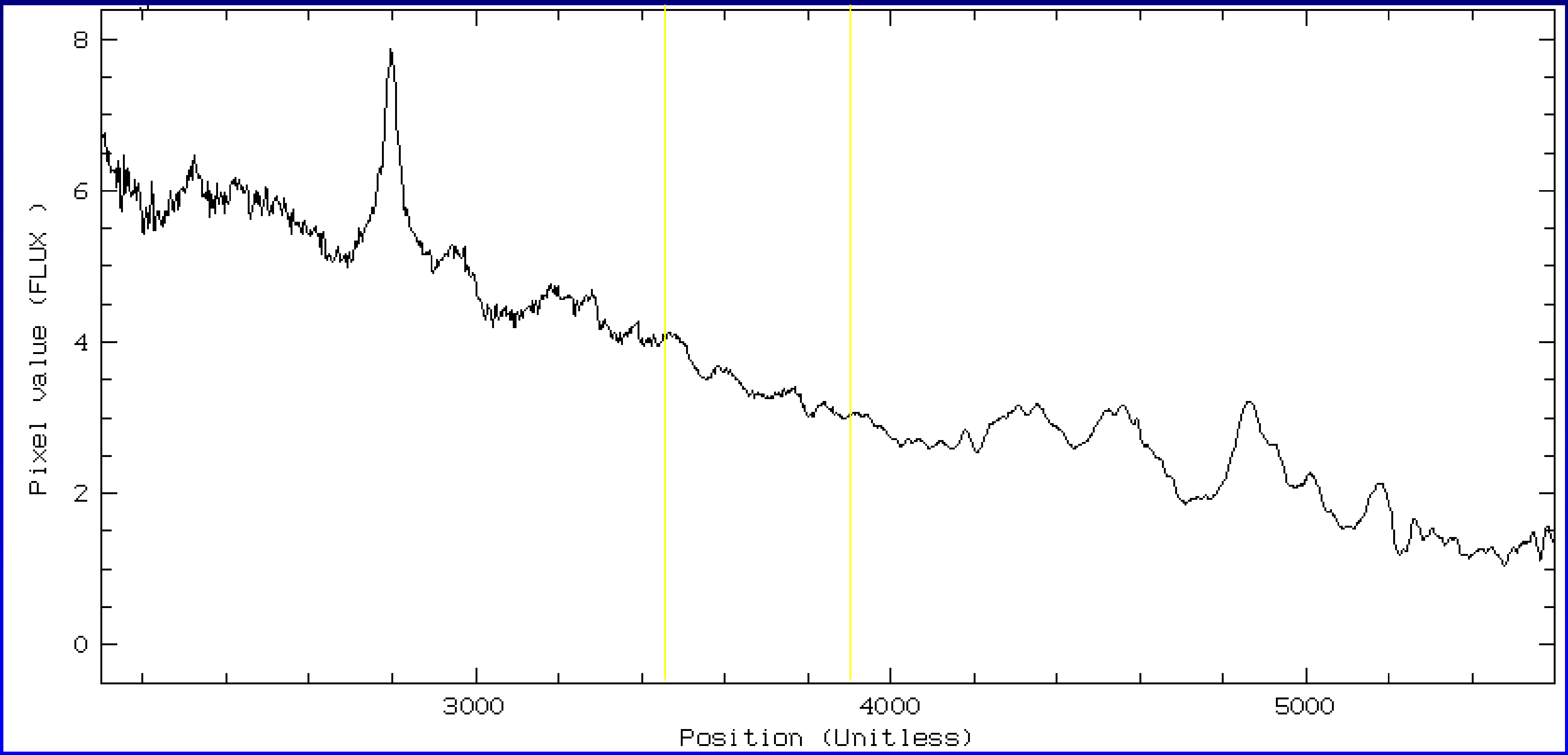

3.6m spectrum (Reimers et al. 1996),
Excellent overlap in common λ-range (3450-3890 Å)

Strong Mg II, Fe II, broad H_γ and H_β, but lack of [O II] and [O III]

Decomposition of QSO Spectrum

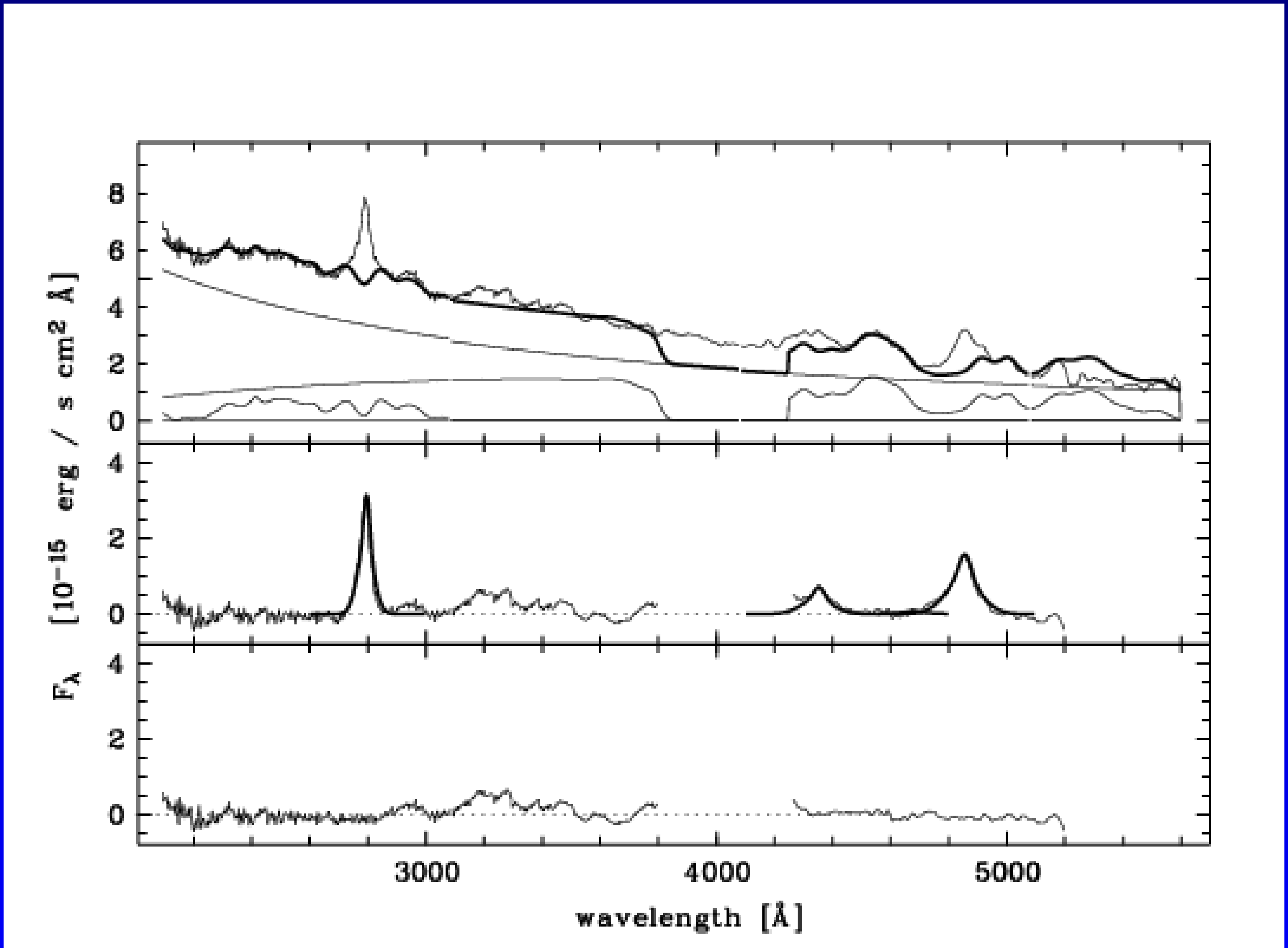

Contiuum,
Balmer continuum
Fe II UV + opt.

Mg II, H_γ, H_β

Residuals

Summary of properties

QSO-host from I-band:

➔ no galaxy-type preferred

➔ M_I = -25.8/-24.6 for ell/disk-typ host ➔ ~ 2-3 L^*

QSO-spectrum (m_I ~ 17 => M << - 23.5, J-K = 1.4, no IRAS detect):

➔ Mg II, H_γ, H_β broad, Fe II strong and broad (UV and opt)

➔ Fe II (UV) / Mg II = 2.6±0.5 (typical for QSOs)

➔ Mg II / H_β = 0.94±0.1 (low, typically 1.7-2.0)

➔ Fe II (opt) = 6 • Fe II (UV) ; [O II], [O III] absent/weak

➔➔ extreme Fe II emitter (typical for IR-bright QSO)

VLT spectrum of the southern companion C

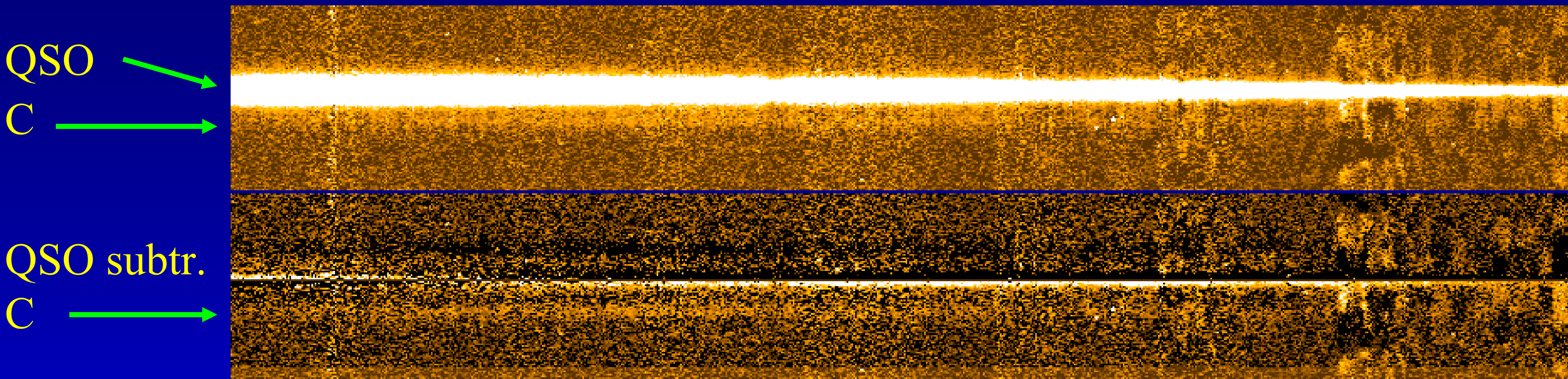

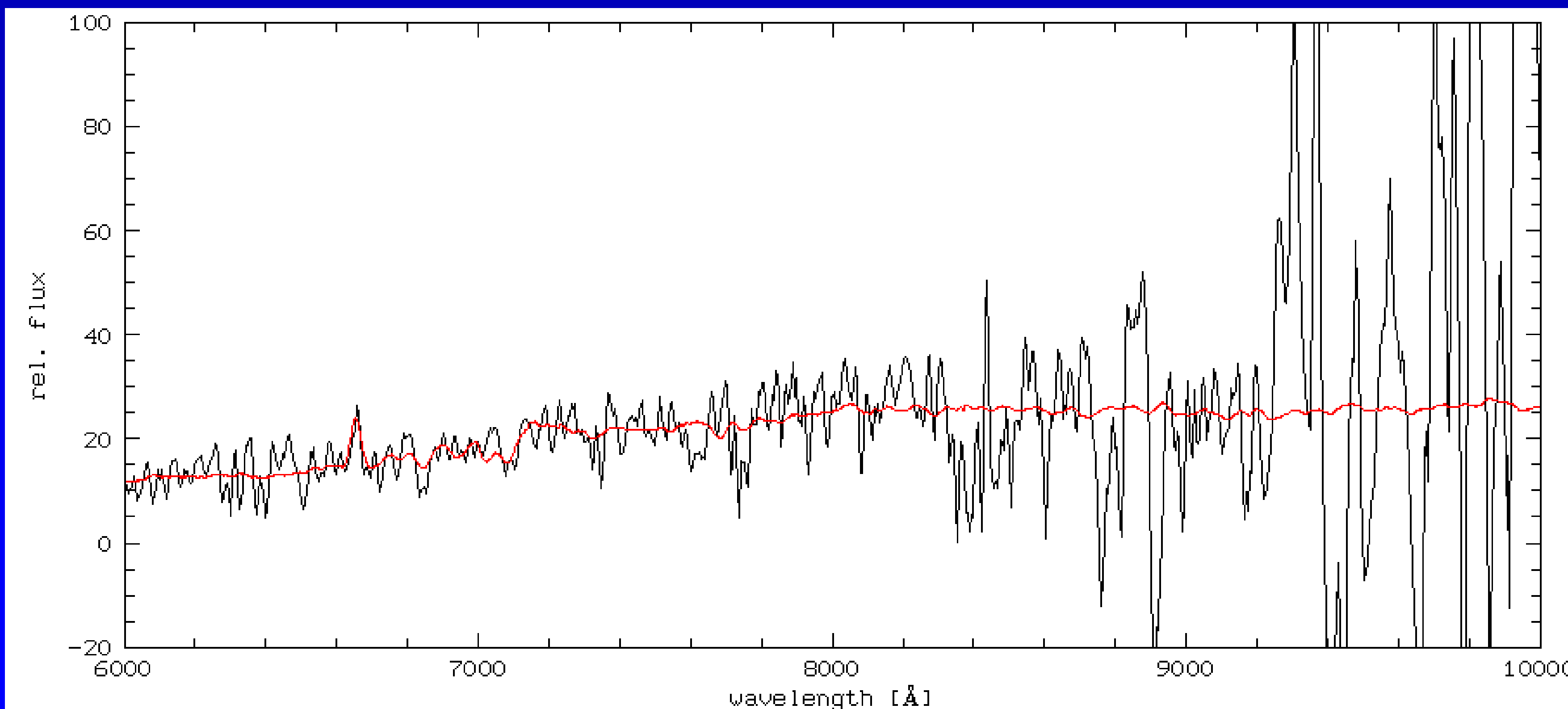

Evidence for early-type @ z = 0.785, but uncertain, no evidence for SB

Interpretation difficult ➔ could it be a transition QSO ?

➔ Comparison to a less distant transition QSO (PG 1700+518, z = 0.29)

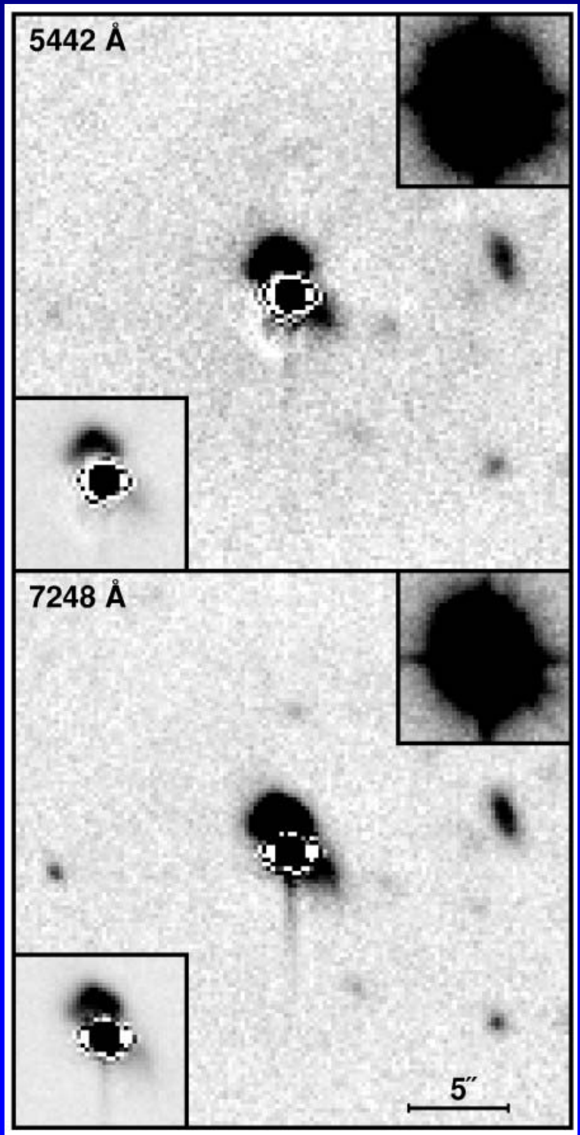

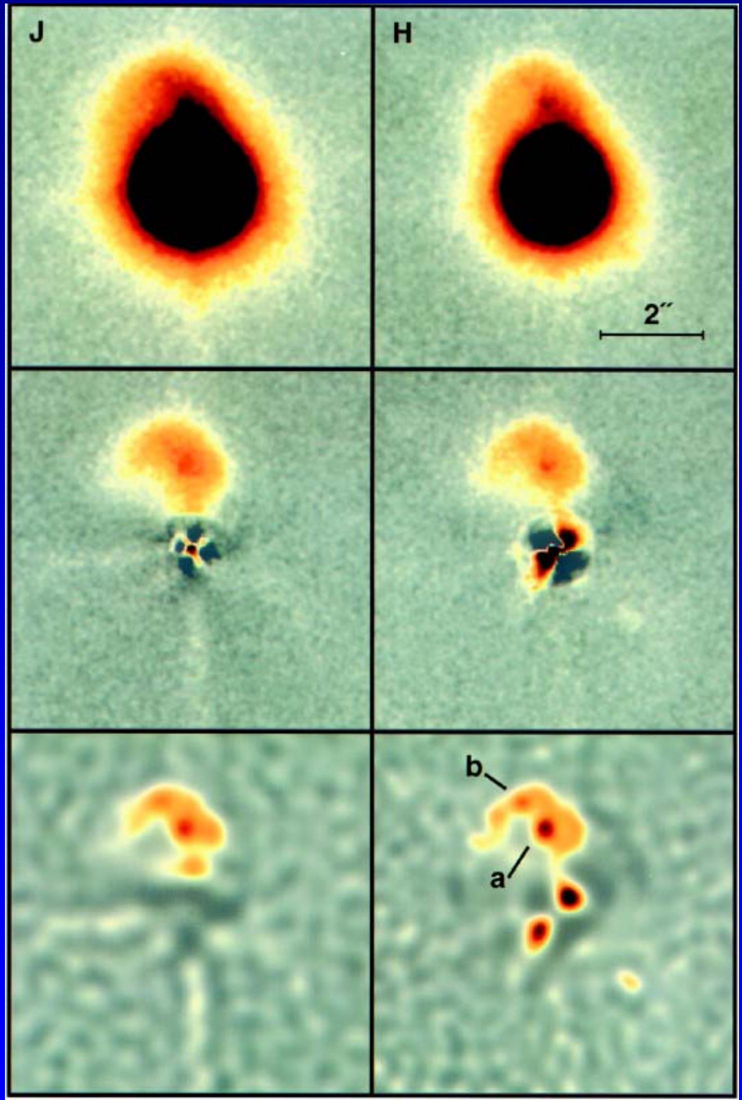

Stockton, Canalizo & Close (1998)

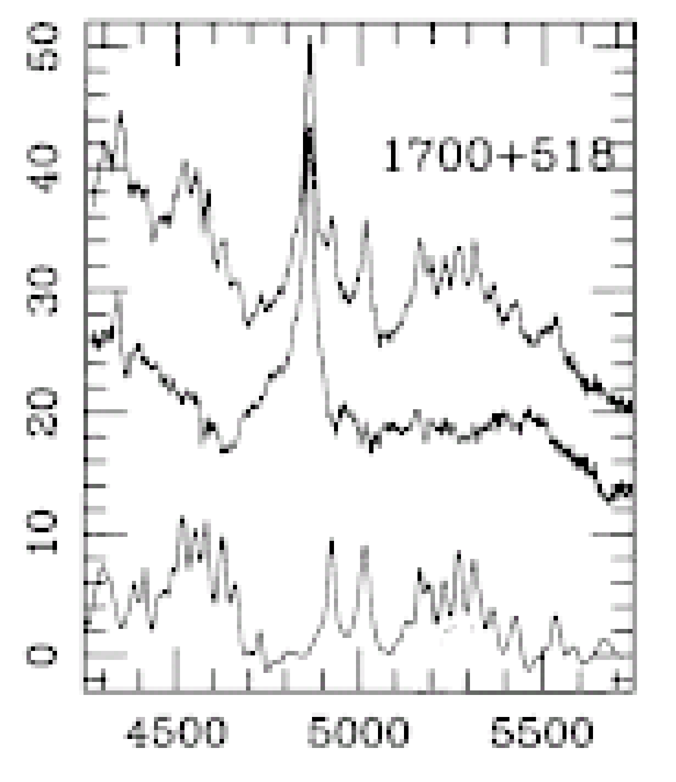

Boroson & Green (1992)

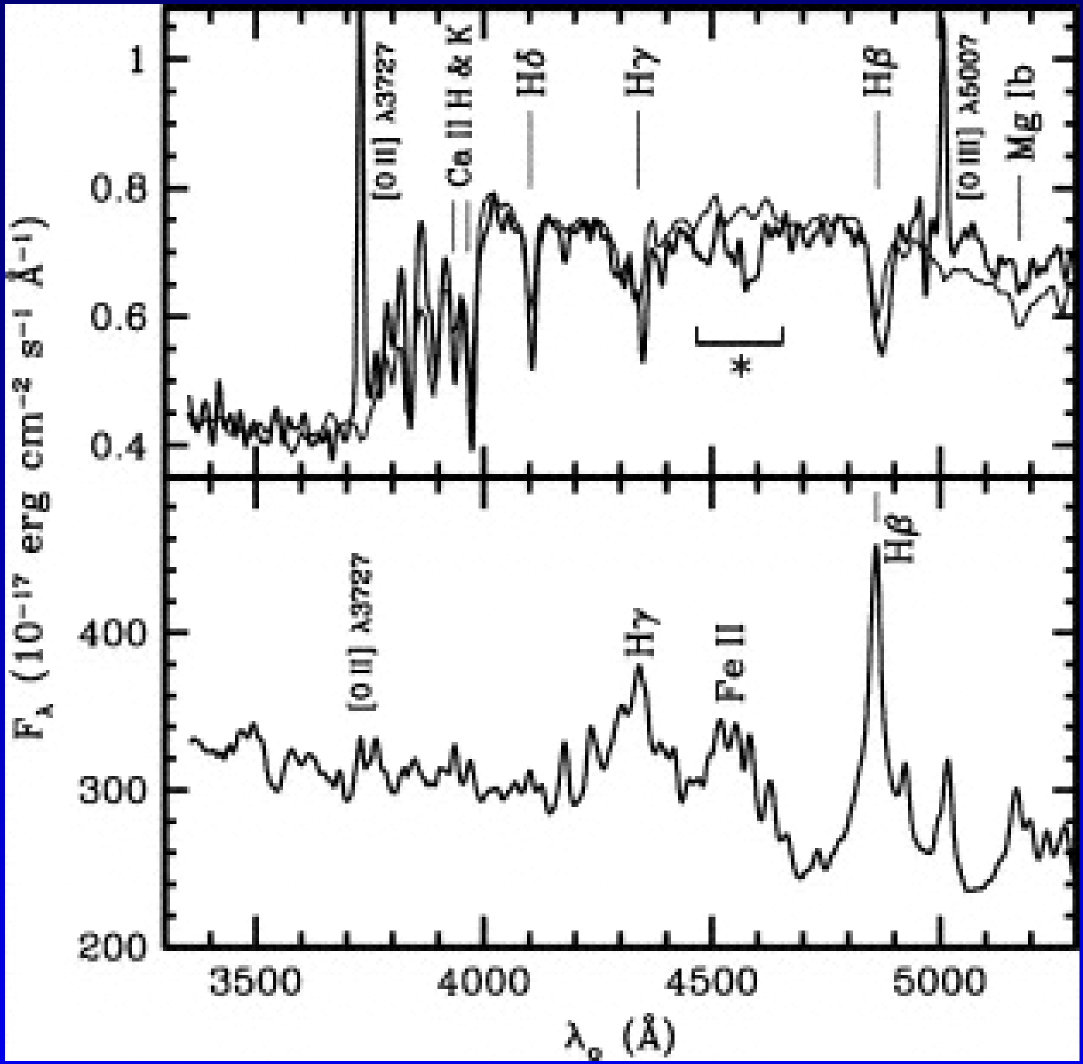

Canalizo & Stockton (1997)

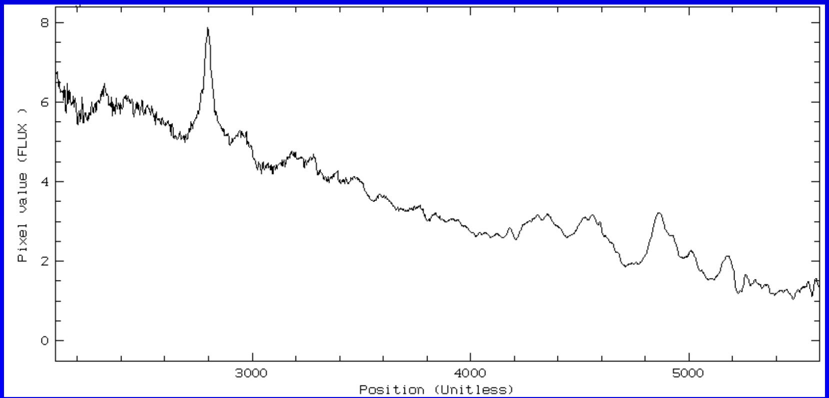

HE 1013-2136

Several similarities to PG 1700+518:

- ➔ Morphology: both strongly disturbed + nearby companion object, hosts have similar luminosities (2-3 L*)
- ➔ Spectra of QSOs: very similar, both are strong Fe II emitters
- ➔ Dynamical ages of tidal tails not too different (70 vs. 90/220 Myrs)
- ➔ Only (tentative) difference: Companion of HE 1013-2136 early type, but low S/N

Urgently required:

a) Spectral map of system

b) NIR-image to trace old stellar population

c) HST-image for morphology of host + substructure

d) IR-photometry: if a transition QSO (scaling from PG 1700+518) IR-fluxes (5-25 μm): 1-5 mJy easily done by Spitzer!

Several similarities to PG 1700+518:

➔ Morphology: both strongly disturbed + nearby companion object, hosts have similar luminosities (2-3 L*)

➔ Spectra of QSOs: very similar, both are strong Fe II emitters

➔ Dynamical ages of tidal tails not too different (70 vs. 90/220 Myrs)

➔ Only (tentative) difference: Companion of HE 1013-2136 early type, but low S/N

Urgently required:

a) Spectral map of system (VIMOS/IFU Apr.+ 2005) ➔ not done

b) NIR-image to trace old stellar population (H-band with ISAAC scheduled Apr.+ 2005) ➔ taken

c) HST-image for morphology of host + substructure ➔ killed

d) IR-photometry: if a transition QSO (scaling from PG 1700+518) IR-fluxes (5-25 μm): 1-5 mJy easily done by Spitzer! ➔ killed

HE1013-2136, VLT, H-band, 30min, 0.33" FWHM !!!

Restframe z

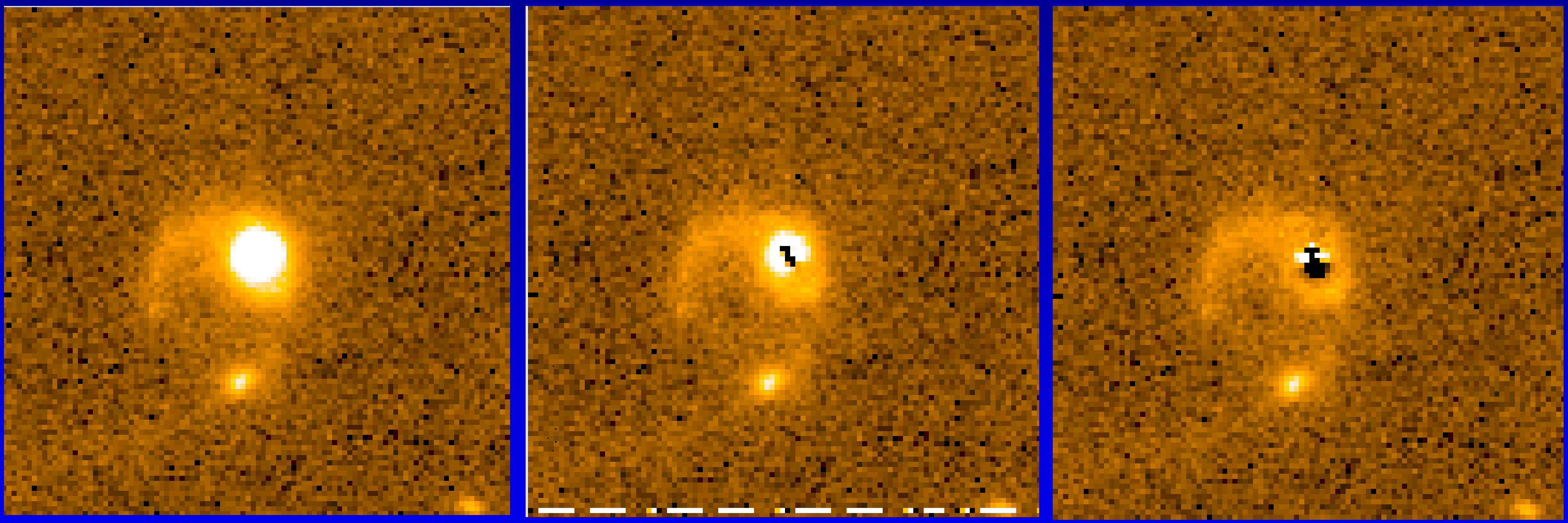

Original - AGN (PSF) - AGN (PSF) + Gal

HE1013-2136, Comparison I vs. H

I-band

H-band

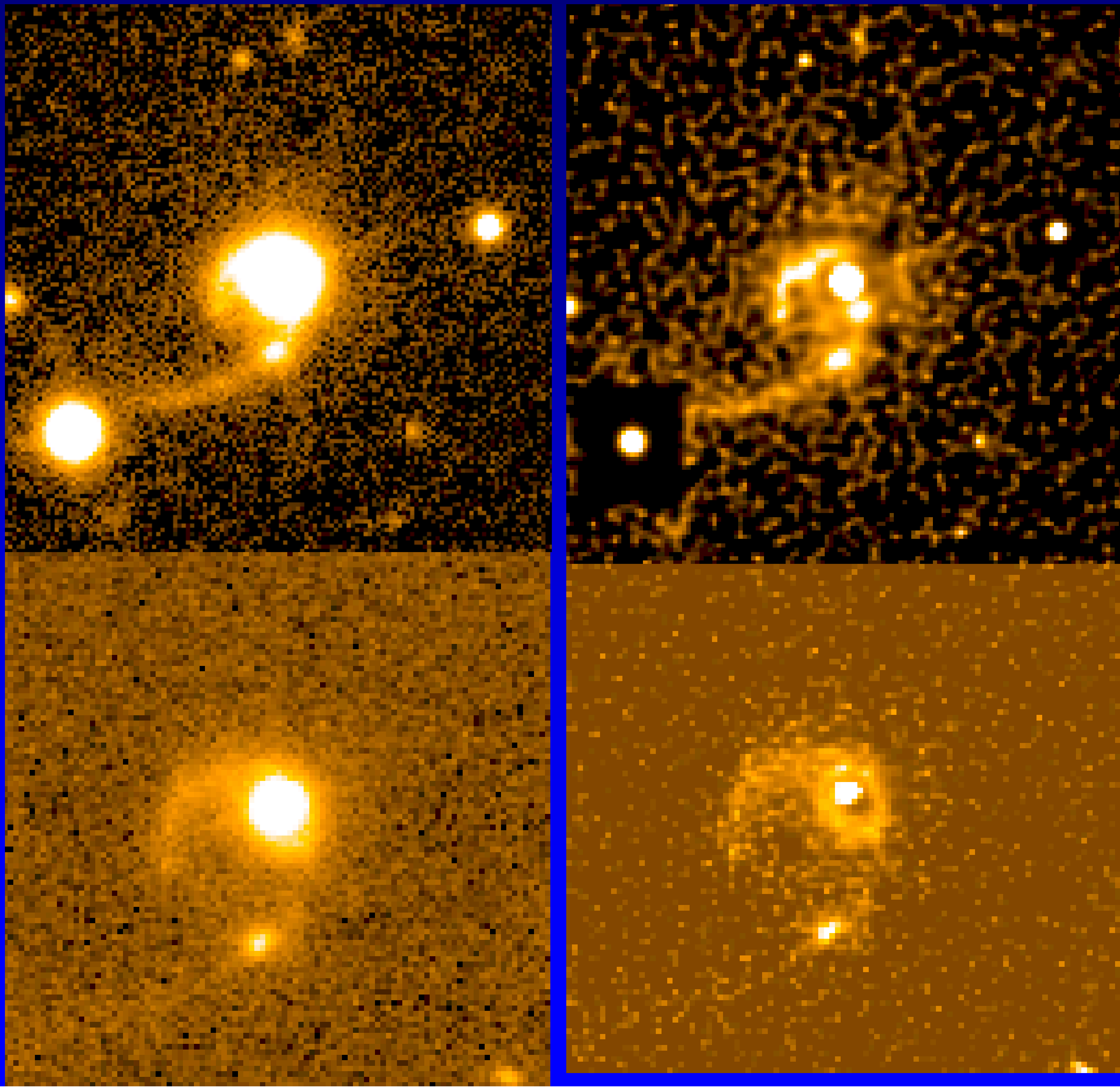

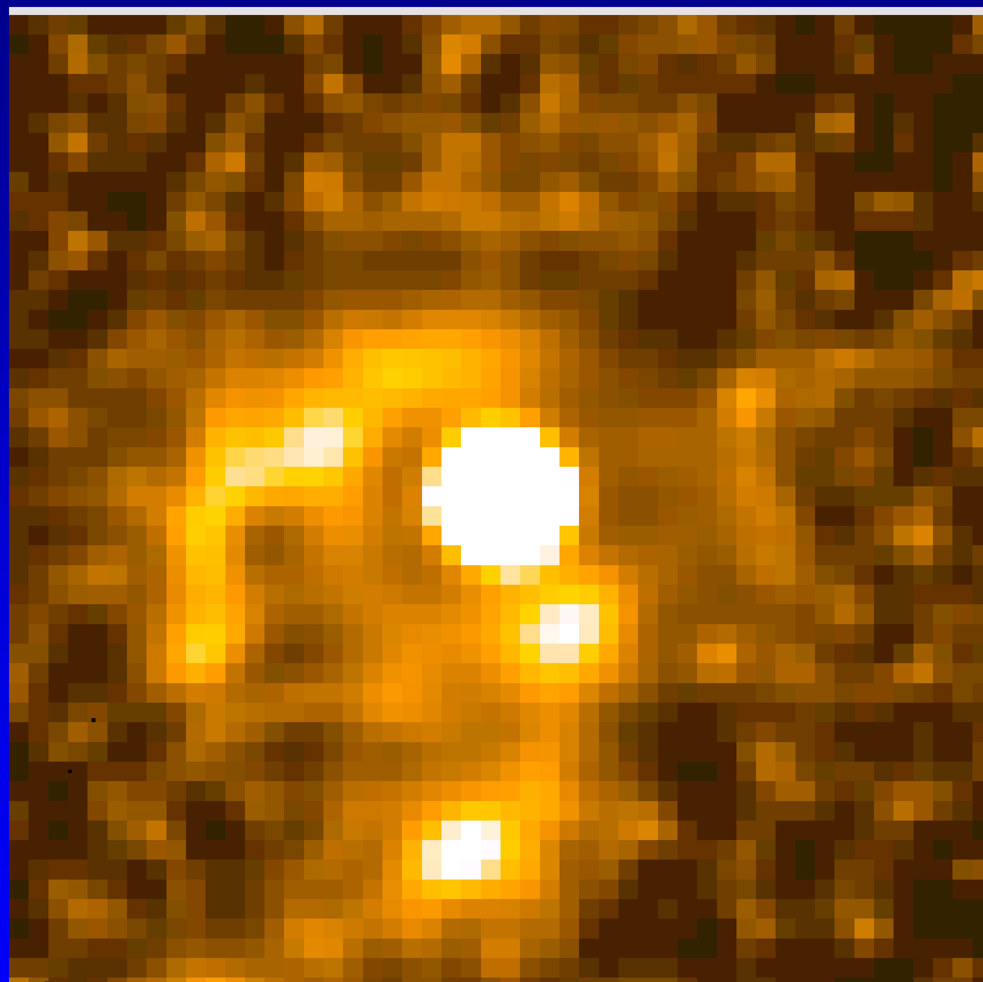

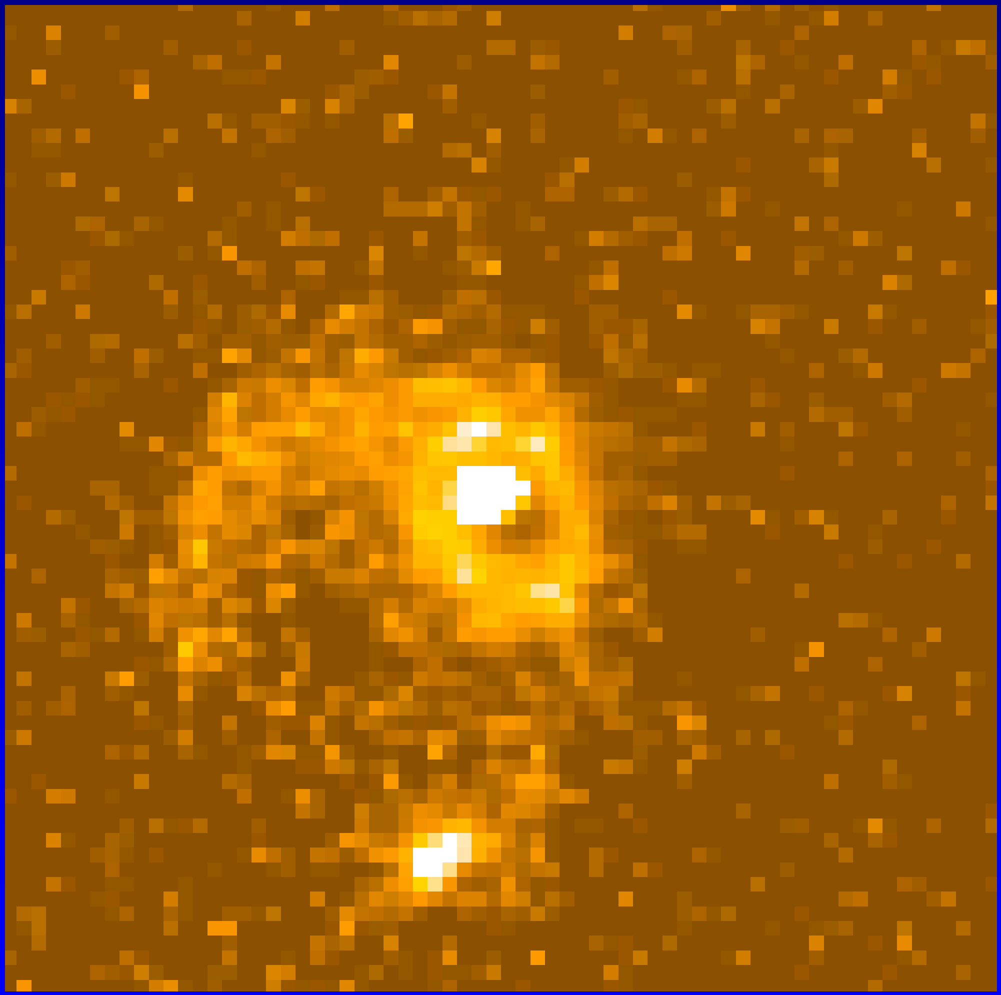

Speculation: Head-on collision of early-type? galaxy (Ntail) with disk-type galaxy + QSO (Stail)? Early type companion just projected?

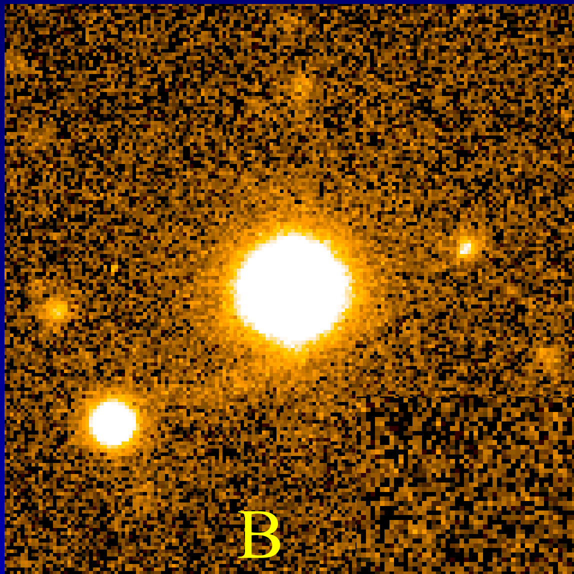

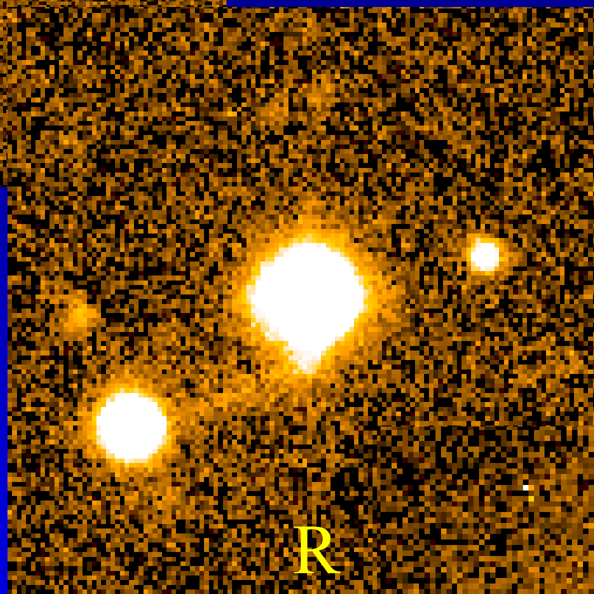

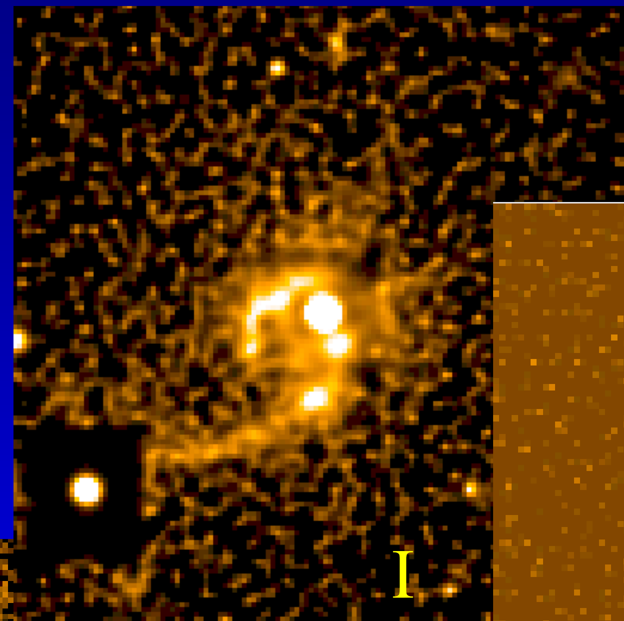

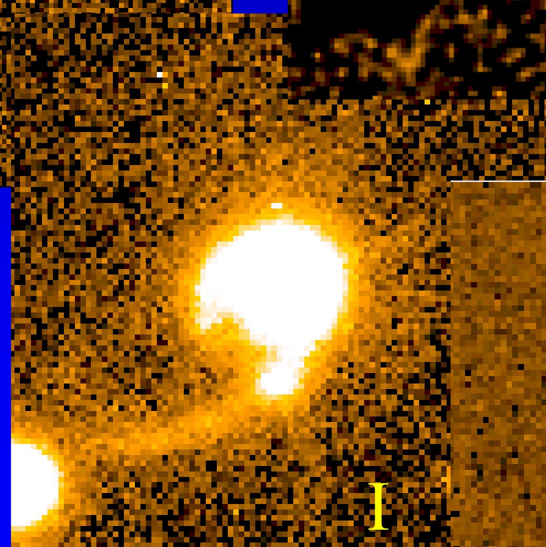

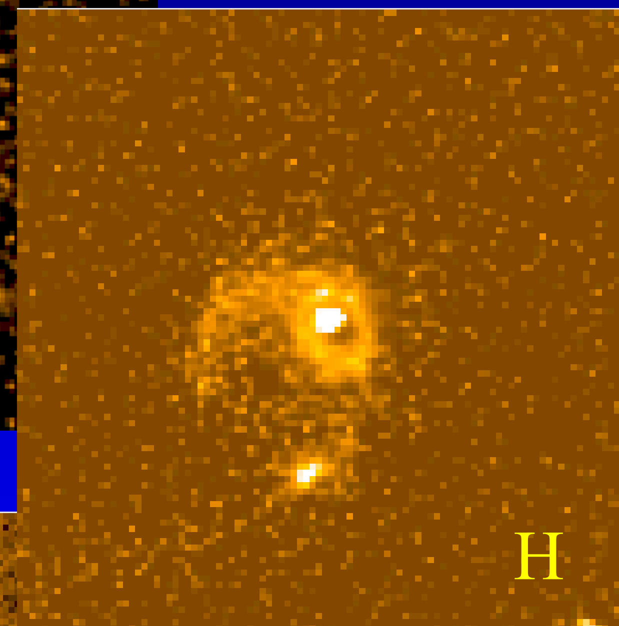

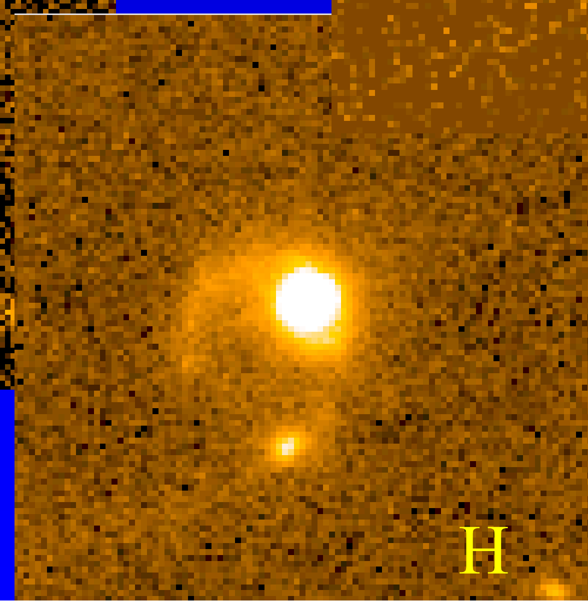

Southern tail → blue
Northern tail → red
Ringlike structure in H

Even more similarities to PG 1700+518:

- ➔ Morphology: both strongly disturbed + nearby companion object, hosts have similar luminosities (2-3 L*)
- ➔ Spectra of QSOs: very similar, both are strong Fe II emitters
- ➔ Dynamical ages of tidal tails not too different (70 vs. 90/220 Myrs)
- ➔ H-band image shows also ringlike structure as the H-band image of PG 1700+518 with HST (Hines et al. 1999)
- ➔ Only (tentative) difference: Companion of HE 1013-2136 early type, but could be projected

➔➔ Almost a twin to PG 1700+518

➔➔➔ HE 1013-2136 could indeed a transition QSO at ~ 7 Gyrs look-back time!!!